



TECHNISCHE
UNIVERSITÄT
WIEN
Vienna University of Technology

HABILITATIONSSCHRIFT

COMBINATORIAL ANALYSIS OF DIRECTED ACYCLIC GRAPHS, YOUNG TABLEAUX, AND LATTICE PATHS

Habilitationsschrift zur Erlangung der Lehrbefugnis für
Mathematik

eingereicht an der Technischen Universität Wien
Fakultät für Mathematik und Geoinformation

von

MICHAEL WALLNER
Rissaweggasse 2/85
A-1100 Wien

Wien, am 3. März 2022

Michael Wallner

COMBINATORIAL ANALYSIS OF DIRECTED ACYCLIC
GRAPHS, YOUNG TABLEAUX, AND LATTICE PATHS

MICHAEL WALLNER

Institute of Discrete Mathematics and Geometry
Faculty of Mathematics and Geoinformation
TU Wien

March 2022

Michael Wallner: *Combinatorial analysis of directed acyclic graphs, Young tableaux, and lattice paths*, March 2022

To Monika, Albert, and Birgit.

ABSTRACT

This habilitation thesis presents selected parts of my research in discrete mathematics and probability theory. Among the listed papers, [P1–P6, P17–P19, P21, P22, P26, P27] are part of or directly related to my PhD thesis and hence not included. Neither are [P16, P31–P33], since they are still under review.

Among the papers that are eligible to be included, I selected the nine papers [P8, P11–P15, P24, P28, P29] (marked in gray hereafter) since they give a very good overview of my work after my PhD on the three major objects of my research:

- directed acyclic graphs [P13, P24, P29]
- Young tableaux [P8, P15, P28]
- lattice paths [P11, P12, P14]

All these papers, except for [P24], were joint work with colleagues in the field. In all these projects it has been a great pleasure for me to work with brilliant people whom I value a lot. As is often the case in mathematical research, it is not possible to distinguish each individual contribution. However, I am happy to say that we discussed and developed everything together and always contributed equally to all parts.

ARTICLES THAT HAVE BEEN SUBMITTED TO JOURNALS AND ARE STILL UNDER REVIEW

[P33] **Phase transitions of composition schemes: Mittag-Leffler and mixed Poisson distributions** (with Cyril Banderier, Markus Kuba)
Annals of Applied Probability, 57 pages, submitted.
[arXiv:2103.03751](#)

[P32] **Walks avoiding a quadrant and the reflection principle** (with Mireille Bousquet-Mélou)
European Journal of Combinatorics, 48 pages, submitted.
[arXiv:2110.07633](#)

[P31] **On the critical exponents of generalized ballot sequences in three dimensions and large tandem walks**
Aequationes mathematicae, 11 pages, submitted.
[arXiv:2105.12155](#)

- [P30] **The binary digits of $n + t$** (with Lukas Spiegelhofer)
Annali della Scuola Normale Superiore di Pisa, Classe di Scienze, 27 pages, accepted.
[arXiv:2005.07167](https://arxiv.org/abs/2005.07167)
- [P29] **Compacted binary trees admit a stretched exponential** (with Andrew Elvey Price, Wenjie Fang)
Journal of Combinatorial Theory, Series A, 177, 105306, 40 pages, 2021.
[arXiv:1908.11181](https://arxiv.org/abs/1908.11181), [doi:10.1016/j.jcta.2020.105306](https://doi.org/10.1016/j.jcta.2020.105306)
- [P28] **Periodic Pólya Urns, the Density Method, and Asymptotics of Young Tableaux** (with Cyril Banderier, Philippe Marchal)
Annals of Probability, Volume 48, Number 4, 1921–1965, 2020.
[arXiv:1912.01035](https://arxiv.org/abs/1912.01035), [doi:10.1214/19-AOP1411](https://doi.org/10.1214/19-AOP1411)
- [P27] **Asymptotic Enumeration of Compacted Binary Trees of Bounded Right Height** (with Antoine Genitrini, Bernhard Gittenberger, Manuel Kauers)
Journal of Combinatorial Theory, Series A, Volume 172, 44 pages, 2020.
[arXiv:1703.10031](https://arxiv.org/abs/1703.10031), [doi:10.1016/j.jcta.2019.105177](https://doi.org/10.1016/j.jcta.2019.105177)
- [P26] **A half-normal distribution scheme for generating functions**
European Journal of Combinatorics, Volume 87, Article ID 103138, 21 pages, 2020.
[arXiv:1610.00541](https://arxiv.org/abs/1610.00541), [doi:10.1016/j.ejc.2020.103138](https://doi.org/10.1016/j.ejc.2020.103138)
- [P25] **Counting and sampling gene family evolutionary histories in the duplication-loss and duplication-loss-transfer models** (with Cedric Chauve, Yann Ponty)
Journal of Mathematical Biology, 80, pages 1353–1388, 2020.
[arXiv:1905.04971](https://arxiv.org/abs/1905.04971), [doi:10.1007/s00285-019-01465-x](https://doi.org/10.1007/s00285-019-01465-x)
- [P24] **A bijection of plane increasing trees with relaxed binary trees of right height at most one**
Theoretical Computer Science, Volume 755, pages 1–12, 2019.
[arXiv:1706.07163](https://arxiv.org/abs/1706.07163), [doi:10.1016/j.tcs.2018.06.053](https://doi.org/10.1016/j.tcs.2018.06.053)
- [P23] **The Tu–Deng conjecture holds almost surely** (with Lukas Spiegelhofer)
Electronic Journal of Combinatorics, Volume 26, no. 1, Paper 1.28, 28 pp., 2019.
[arXiv:1707.07945](https://arxiv.org/abs/1707.07945), [doi:10.37236/7178](https://doi.org/10.37236/7178)
- [P22] **On the shape of random Pólya structures** (with Bernhard Gittenberger, Emma Yu Jin)
Discrete Mathematics, Volume 341, Issue 4, pages 896–911, 2018.
[arXiv:1707.02144](https://arxiv.org/abs/1707.02144), [doi:10.1016/j.disc.2017.12.016](https://doi.org/10.1016/j.disc.2017.12.016)

- [P21] **Divisibility of binomial coefficients by powers of two** (with Lukas Spiegelhofer)
Journal of Number Theory, Volume 192, pages 221–239, 2018.
[arXiv:1710.10884](https://arxiv.org/abs/1710.10884), [doi:10.1016/j.jnt.2018.04.010](https://doi.org/10.1016/j.jnt.2018.04.010)
- [P20] **An explicit generating function arising in counting binomial coefficients divisible by powers of primes** (with Lukas Spiegelhofer)
Acta Arithmetica 181, 27–55, 2017.
[arXiv:1604.07089](https://arxiv.org/abs/1604.07089), [doi:10.4064/aa8524-6-2017](https://doi.org/10.4064/aa8524-6-2017)
- [P19] **Lattice paths with catastrophes** (with Cyril Banderier)
Discrete Mathematics & Theoretical Computer Science, Vol 19 no. 1, 2017.
[arXiv:1707.01931](https://arxiv.org/abs/1707.01931), [doi:10.23638/DMTCS-19-1-23](https://doi.org/10.23638/DMTCS-19-1-23)

ARTICLES PUBLISHED IN PEER-REVIEWED BOOKS

- [P18] **Explicit formulas for enumeration of lattice paths: basketball and the kernel method** (with Cyril Banderier, Christian Krattenthaler, Alan Krinik, Dmitry Kruchinin, Vladimir Kruchinin and David Nguyen)
Lattice Path Combinatorics and Applications, Developments in Mathematics, Springer-Verlag, Cham, pages 78–118, 2019.
[arXiv:1609.06473](https://arxiv.org/abs/1609.06473), [doi:10.1007/978-3-030-11102-1_6](https://doi.org/10.1007/978-3-030-11102-1_6)
- [P17] **The kernel method for lattice paths below a line of rational slope** (with Cyril Banderier)
Lattice Path Combinatorics and Applications, Developments in Mathematics, Springer, Springer-Verlag, Cham, pages 119–154, 2019.
[arXiv:1606.08412](https://arxiv.org/abs/1606.08412), [doi:10.1007/978-3-030-11102-1_7](https://doi.org/10.1007/978-3-030-11102-1_7)

ARTICLES SUBMITTED TO PEER-REVIEWED PROCEEDINGS

- [P16] **Enumeration of d -combining Tree-Child Networks** (with Yu-Sheng Chang, Michael Fuchs, Hexuan Liu, and Guan-Ru Yu)
AofA 2022, 12 pp., Philadelphia, submitted.
[https://dmg.tuwien.ac.at/mwallner/files/pub/\[Chang_etal\]-d-combining.pdf](https://dmg.tuwien.ac.at/mwallner/files/pub/[Chang_etal]-d-combining.pdf)

ARTICLES PUBLISHED IN PEER-REVIEWED PROCEEDINGS

- [P15] **Young tableaux with periodic walls: counting with the density method** (with Cyril Banderier)
SLC 85B.47, 12 pp., FPSAC 2021, Ramat Gan, 2021.
<https://www.mat.univie.ac.at/~slc/wpapers/FPSAC2021/47.html>

- [P14] **More models of walks avoiding a quadrant** (with Mireille Bousquet-Mélou)
LIPICs, Vol. 159 - AofA 2020, 8:1–8:14, Klagenfurt, 2020.
[doi:10.4230/LIPICs.AofA.2020.8](https://doi.org/10.4230/LIPICs.AofA.2020.8)
- [P13] **Asymptotics of minimal deterministic finite automata recognizing a finite binary language** (with Andrew Elvey Price, Wenjie Fang)
LIPICs, Vol. 159 - AofA 2020, 11:1–11:13, Klagenfurt, 2020.
[doi:10.4230/LIPICs.AofA.2020.11](https://doi.org/10.4230/LIPICs.AofA.2020.11)
- [P12] **Latticepathology and symmetric functions** (with Cyril Banderier, Marie-Louise Lackner)
LIPICs, Vol. 159 - AofA 2020, 2:1–2:16, Klagenfurt, 2020.
[doi:10.4230/LIPICs.AofA.2020.2](https://doi.org/10.4230/LIPICs.AofA.2020.2)
- [P11] **Combinatorics of nondeterministic walks of the Dyck and Motzkin type** (with Élie de Panafieu, Mohamed Lamine Lamali)
ANALCO 2019: 1–12, San Diego, 2019.
[arXiv:1812.06650](https://arxiv.org/abs/1812.06650), [doi:10.1137/1.9781611975505.1](https://doi.org/10.1137/1.9781611975505.1)
- [P10] **De la probabilité de creuser un tunnel** (with Élie de Panafieu, Mohamed Lamine Lamali)
AlgoTel 2019, Saint Laurent de la Cabrerisse, 2019.
[hal-02123269](https://hal.archives-ouvertes.fr/hal-02123269)
- [P9] **Periodic Pólya Urns and an Application to Young Tableaux** (with Cyril Banderier, Philippe Marchal)
LIPICs, Vol. 110 - AofA 2018, 11:1–11:13, Uppsala, 2018.
[arXiv:1806.03133](https://arxiv.org/abs/1806.03133), [doi:10.4230/LIPICs.Ao](https://doi.org/10.4230/LIPICs.Ao)
- [P8] **Rectangular Young tableaux with local decreases and the density method for uniform random generation** (with Cyril Banderier and Philippe Marchal)
CEUR Workshop Proc. 2113, GASCom 2018:60–68, Athens, 2018.
[arXiv:1805.09017](https://arxiv.org/abs/1805.09017)
- [P7] **Local time for lattice paths and the associated limit laws** (with Cyril Banderier)
CEUR Workshop Proc. 2113, GASCom 2018:69–78, Athens, 2018.
[arXiv:1805.09065](https://arxiv.org/abs/1805.09065)
- [P6] **Lattice paths with catastrophes** (with Cyril Banderier)
Electronic Notes in Discrete Mathematics, 59:131–146, GASCom 2016, La Marana, 2017.
[doi:10.1016/j.endm.2017.05.010](https://doi.org/10.1016/j.endm.2017.05.010)
- [P5] **A note on the scaling limits of random Pólya trees** (with Bernhard Gittenberger and Emma Yu Jin)
SIAM, ANALCO 85–93, Barcelona, 2017.
[arXiv:1606.08769](https://arxiv.org/abs/1606.08769), [doi:10.1137/1.9781611974775.8](https://doi.org/10.1137/1.9781611974775.8)

- [P4] **A half-normal distribution scheme for generating functions and the unexpected behavior of Motzkin paths**
AofA 2016, Krakow, Poland, pages 341–352, 2016.
[arXiv:1605.03046](https://arxiv.org/abs/1605.03046)
- [P3] **The reflection-absorption model for directed lattice paths** (with Cyril Banderier)
Vienna Young Scientists Symposium, Vienna, pages 98–99, 2016.
http://vss.tuwien.ac.at/fileadmin/t/vss/manuscript_VSS2016.pdf
- [P2] **Lattice paths of slope $2/5$** (with Cyril Banderier)
SIAM, ANALCO, San-Diego, pages 105–113, 2015.
[arXiv:1605.02967](https://arxiv.org/abs/1605.02967), [doi:10.1137/1.9781611973761.10](https://doi.org/10.1137/1.9781611973761.10)
- [P1] **Some reflections on directed lattice paths** (with Cyril Banderier)
AofA 2014, Paris, pages 25–36, 2014.
[arXiv:1605.01687](https://arxiv.org/abs/1605.01687)

THESES

- [T4] **Combinatorics of lattice paths and tree-like structures**
PhD thesis, TU Wien, Vienna, 2017.
[doi:10.34726/hss.2016.38100](https://doi.org/10.34726/hss.2016.38100)
- [T3] **Lattice path combinatorics**
Master's thesis, TU Wien, Vienna, 2013.
[doi:10.34726/hss.2013.21211](https://doi.org/10.34726/hss.2013.21211)
- [T2] **Algebraic multigrid methods for higher-order finite element discretization with parallelization**
Master's thesis, Brunel University, London, 2012.
https://dmg.tuwien.ac.at/mwallner/files/Dissertation_Brunel_Wallner.pdf
- [T1] **Polynome über endlichen Körpern**
Bachelor's thesis, TU Wien, 2011.
https://dmg.tuwien.ac.at/mwallner/files/Bachelor_TUW_Wallner.pdf

CONTENTS

1	INTRODUCTION	1
1.1	Notation and definitions	2
2	DIRECTED ACYCLIC GRAPHS	3
2.1	Introduction to compacted binary trees	3
2.2	Compacted binary trees admit a stretched exponential [P29]	6
2.3	Minimal binary deterministic finite automata [P13]	15
2.4	A bijection between increasing trees and relaxed binary trees [P24]	20
3	YOUNG TABLEAUX	29
3.1	Rectangular Young tableaux with local decreases [P8]	29
3.2	Young tableaux with periodic walls [P15]	37
3.3	Periodic Pólya urns, the density method and asymptotics of Young tableaux [P28]	44
4	LATTICE PATHS	63
4.1	Introduction and definitions	63
4.2	Latticepathology and symmetric functions [P12]	65
4.3	Combinatorics of nondeterministic walks [P11]	69
4.4	More models of walks avoiding a quadrant [P14]	78
	BIBLIOGRAPHY	85
A	Curriculum Vitae	99
B	TEACHING EXPERIENCE	109
B.1	Student feedback	111
C	PUBLISHED PAPERS	113
C.1	Compacted binary trees admit a stretched exponential [P29]	114
C.2	Asymptotics of Minimal Deterministic Finite Automata Recognizing a Finite Binary Language [P13]	154
C.3	A bijection of plane increasing trees with relaxed binary trees of right height at most one [P24]	167
C.4	Rectangular Young tableaux with local decreases and the density method for uniform random generation [P8]	179
C.5	Young tableaux with periodic walls: counting with the density method [P15]	188
C.6	Periodic Pólya urns, the density method and asymptotics of Young tableaux [P28]	200
C.7	Latticepathology and Symmetric Functions [P12]	245
C.8	Combinatorics of nondeterministic walks of the Dyck and Motzkin type [P11]	261
C.9	More Models of Walks Avoiding a Quadrant [P14]	273

This thesis belongs to the fields of enumerative and analytic combinatorics with special emphasis on the the large-scale behavior of *random discrete structures*, where we will focus on directed acyclic graphs, Young tableaux, and lattice paths. These objects appear in numerous scientific fields, ranging from computer science [117] to evolutionary biology [89] and from statistical mechanics [99] to queuing theory [81]. Our primary interest are *universal phenomena* in large random structures. Examples for such phenomena include specific terms in the asymptotic growth (e.g., $n^{-3/2}$ or $\mu^{n^{1/3}}$), families of limit laws (e.g., normal or Mittag-Leffler distributions), or necessary rescaling of random variables (e.g., X_n/\sqrt{n}). They describe the observation that many combinatorial structures are influenced by only a few global properties and do not depend on concrete and local details. This combinatorial analysis is the central theme of this thesis and will be presented in many new and old models of the three objects mentioned above. Thereby, we will answer some old conjectures, discover new (interdisciplinary) applications, and open the way for much further research.

From a technical point of view, before one can tackle the analysis of structures and limit laws, one has to solve the basic counting problem: How many objects of size n are there? There are several possible answers to this question, which all have different advantages and are also of different difficulty to obtain. First, a closed-form expression is probably most desirable, yet often quite complicated (if it even exists). Second, a recursive description gives a computational answer and allows, e.g., random generation. Third, an asymptotic answer helps to compare the growth rate and often fast approximate computation. Fourth, a generating function expression captures the nature (e.g., rational, algebraic, D-finite) and gives access to other solutions. In this thesis, we present solutions of all these types and use them in a next step to analyze the limiting objects.

In Chapter 2 we analyze two classes of directed acyclic graphs: compacted trees and minimal deterministic finite automata. For both classes we solve the asymptotic counting problem and we show the unexpected appearance of a stretched exponential μ^{n^σ} . Moreover, we present a bijective explanation of a surprisingly simple closed-form counting formula. In Chapter 3 we introduce the new class of Young tableaux with walls, in which the order constraints between certain cells are removed. We present bijections to trees and lattice paths, and introduce the density method, a method we developed for enumeration and random generation. This method also allows us to derive the

limit law of the south-east corner in large random triangular Young tableaux as well as of the composition of black and white balls in a new class of periodic Pólya urns. In Chapter 4 we present several new results on lattice paths and associated limit laws. First, we show new connections with symmetric functions. Second, we introduce a new variant of paths that model the encapsulation and decapsulation in networks. Third, we solve the two-dimensional counting problem of walks in non-convex cones and prove the D-finiteness of the underlying generating function. At the end, in Appendix A I include my CV and in Appendix B a summary of my teaching experience. Finally, since this thesis is cumulative, Appendix C contains the full manuscripts of the published papers this thesis draws from.

1.1 NOTATION AND DEFINITIONS

We let $\mathbb{N} = \{0, 1, 2, \dots\}$ denote the set of nonnegative integers, and \mathbb{N}_+ or \mathbb{Z}_+ the set of positive integers. Throughout this thesis, we assume that all random variables are defined on a common probability space whose measure is denoted by \mathbb{P} .

Let \mathbb{A} be a commutative ring and x an indeterminate. We denote by $\mathbb{A}[x]$ (resp. $\mathbb{A}[[x]]$) the ring of polynomials (resp. formal power series) in x with coefficients in \mathbb{A} . If \mathbb{A} is a field, then $\mathbb{A}(x)$ denotes the field of rational functions in x , and $\mathbb{A}((x))$ the field of Laurent series in x , i.e., series of the form $\sum_{n \geq n_0} a_n x^n$, with $n_0 \in \mathbb{Z}$ and $a_n \in \mathbb{A}$. The coefficient of x^n in a series $F(x)$ is denoted by $[x^n]F(x)$.

If \mathbb{A} is a field, a power series $F(x) \in \mathbb{A}[[x]]$ is *rational* if it is the ratio of two polynomials. It is *algebraic* (over $\mathbb{A}(x)$) if it satisfies a non-trivial polynomial equation $P(x, F(x)) = 0$ with coefficients in \mathbb{A} . It is *differentially finite* (or *D-finite*) if it satisfies a non-trivial linear differential equation with coefficients in $\mathbb{A}(x)$. It is *D-algebraic* if it satisfies a non-trivial *polynomial* differential equation $P(x, F(x), F'(x), \dots, F^{(k)}(x)) = 0$ with coefficients in $\mathbb{A}(x)$. For multivariate series, D-finiteness requires the existence of a differential equation *in each variable*. This hierarchy is summarized by the following sequence of strict inclusions:

$$\text{rational} \subset \text{algebraic} \subset \text{D-finite} \subset \text{D-algebraic}.$$

A sequence $(f_n)_{n \in \mathbb{N}}$ is called *P-recursive* if it satisfies a non-trivial linear recurrence with polynomial coefficients in n . This definition is equivalent to the power series $F(z) = \sum_{n \geq 0} f_n z^n$ being D-finite. Such functions and sequences are also sometimes called *holonomic*. D-finite functions satisfy many closure properties (sum, product, derivative, etc.) and they exist many efficient algorithms to manipulate them [34, 151] implemented in most computer algebra software. For more details on this important concept we refer to [27, 85, 113, 171].

2

DIRECTED ACYCLIC GRAPHS

2.1	Introduction to compacted binary trees	3
2.2	Compacted binary trees admit a stretched exponential [P29]	6
2.3	Minimal binary deterministic finite automata [P13]	15
2.4	A bijection between increasing trees and relaxed binary trees [P24]	20

Directed acyclic graphs are much studied and extensively used, for example in computer science [117] and evolutionary biology [89], yet many of their properties still remain unknown. Often not even the basic counting problem has been solved and only crude bounds exist. This chapter presents solutions for some of these problems and thereby shows my development since my PhD [T4] together with new collaborators and alone. We developed new tools, found links with other fields such as automata theory and phylogeny, and discovered a completely new and unexpected phenomenon: the appearance of a stretched exponential μ^{n^σ} in the asymptotics.

In Section 2.1, we introduce compacted binary trees, the main class of directed acyclic graphs we will work with, and recall previous results.

In Section 2.2, we solve the unbounded counting problem of compacted binary trees and show that they admit a stretched exponential. This answers an open question from [90], which was part of my PhD, and requires completely new tools such as bijections to special lattice paths, and the analysis of a class of two-variate recurrence relations.

In Section 2.3, we extend these methods and solve the counting problem of minimal deterministic finite automata. Again, this shows the appearance of a stretched exponential, which partly explains why this problem remained open for so long.

In Section 2.4, we solve another open problem from [90] by presenting a bijection between relaxed compacted binary trees and plane increasing trees. Additionally, we show how this bijection can be used to generate these objects uniformly at random.

2.1 INTRODUCTION TO COMPACTED BINARY TREES

Compacted binary trees are a special class of directed acyclic graphs that appear as a model for data structures in the compression of XML documents [39]; see Figure 1. Given a rooted binary tree of size n , its compacted form can be computed in expected and worst-case time

$\mathcal{O}(n)$ with expected compacted size $\Theta(n/\sqrt{\log n})$ [86]. Previously, together with Genitrini, Gittenberger, and Kauers, we solved the reversed question on the asymptotic number of compacted trees under certain height restrictions [90]; however the asymptotic number in the unrestricted case remained elusive. We also solved this problem for a simpler class of trees known as relaxed trees under the same height restrictions.

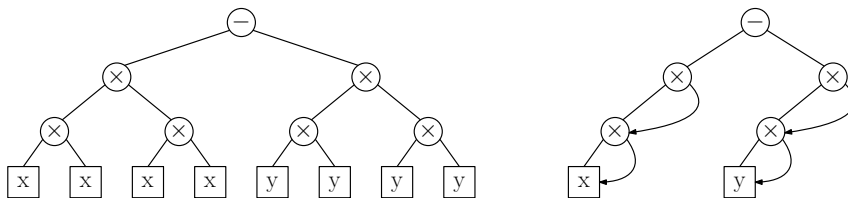


Figure 1: Example of a tree and its compacted tree associated with $x^4 - y^4$.

Before we define compacted and relaxed binary trees, let us recall some basic definitions. A *rooted tree* is a connected undirected acyclic graph with a distinguished node called the root. All trees in this chapter will be rooted and we omit this term in the future. The root introduces an order in the tree given by generations. The root is in generation 0. All neighbors of the root are in generation 1, and in general, nodes at distance k from the root are in generation k . For an arbitrary node of generation $k > 0$ its unique neighbor in generation $k - 1$ is called its *parent*. All other neighbors (which are necessarily in generation $k + 1$) are called its *children*. A tree is called *binary*, if all nodes have out-degree either 0 or 2 and all nodes other than the root have in-degree 1, while the root has in-degree 0. For each vertex with out-degree 2, the out-going edges are distinguished as a left edge and a right edge. Nodes with out-degree 0 are called *leaves*, and nodes with out-degree 2 are called *internal nodes*. The *size* of a tree is equal to the number of its internal nodes. For more details we refer to the excellent book [70].

Originally, compacted trees arose in a compression procedure in [86] which computes the number of unique fringe subtrees. Relaxed trees are then defined by relaxing the uniqueness condition. As we will not need this algorithmic point of view, we directly give the following definition adapted from [90, Definition 3.1 and Proposition 4.3].

Definition 2.1.1 (Relaxed binary tree). *A relaxed binary tree (or simply relaxed tree) of size n is a directed acyclic graph obtained from a binary tree with n internal nodes, called its spine, by keeping the left-most leaf and turning other leaves into pointers, with each one pointing to a node (internal ones or the left-most leaf) preceding it in postorder.*

The counting sequence $(r_n)_{n \in \mathbb{N}}$ of relaxed binary trees of size n starts as follows:

$$(r_n)_{n \in \mathbb{N}} = (1, 1, 3, 16, 127, 1363, 18628, 311250, 6173791, \dots).$$

It corresponds to [OEIS A082161](#) in the On-line Encyclopedia of Integer Sequences [167]. There, it first appeared as the counting sequence of the number of deterministic, completely defined, initially connected, acyclic automata with 2 inputs and n transient, unlabeled states and a unique absorbing state, yet without specified final states. This is a direct rephrasing of Definition 2.1.1 in the language of automata theory. Liskovets [131] provided (probably) the first recurrence relations ($C_2(n)$ used for r_n) and later Callan [52] showed that they are counted by determinants of Stirling cycle numbers. However, the asymptotics remained an open problem.

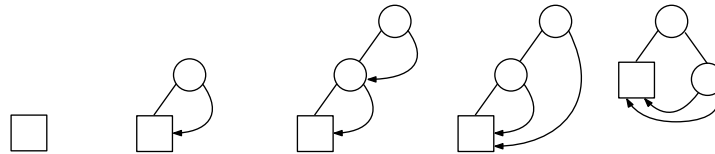


Figure 2: All relaxed (and also compacted) binary trees of size 0, 1, 2, where internal nodes are shown by circles and the unique leaf is drawn as a square.

Using the class of relaxed trees, it is then easy to define the set of compacted trees by requiring the uniqueness of subtrees.

Definition 2.1.2 (Compacted binary tree). *Given a relaxed binary tree, we associate to each node u a binary tree $B(u)$. We proceed by postorder. If u is the left-most leaf, we define $B(u) = u$. Otherwise, u has two children v, w , then $B(u)$ is the binary tree with $B(v)$ and $B(w)$ as left and right sub-trees, respectively.*

A compacted binary tree, or simply compacted tree of size n is a relaxed tree with $B(u) \neq B(v)$ (i.e., $B(u)$ not isomorphic to $B(v)$) for all pairs of distinct nodes u, v .

Figure 2 shows all relaxed (and compacted) trees of size $n = 0, 1, 2$ and Figure 3 gives the smallest relaxed tree that is not a compacted tree. The counting sequence $(c_n)_{n \in \mathbb{N}}$ of compacted binary trees of size n is [OEIS A254789](#) and starts as follows:

$$(c_n)_{n \in \mathbb{N}} = (1, 1, 3, 15, 111, 1119, 14487, 230943, 4395855, \dots).$$



Figure 3: (Left) The smallest relaxed binary tree that is not a compacted binary tree, as the two gray subtrees correspond to the same (classical) binary tree. (Right) A valid compacted binary tree of size 3 with the same spine.

2.2 COMPACTED BINARY TREES ADMIT A STRETCHED EXPONENTIAL [P29]

In this section, we present and summarize the results of [P29], in which we showed that the counting sequences $(c_n)_{n \in \mathbb{N}}$ of (unrestricted) compacted binary trees and $(r_n)_{n \in \mathbb{N}}$ of (unrestricted) relaxed binary trees both admit a stretched exponential:

Theorem 2.2.1. *The number of compacted and relaxed binary trees satisfy for $n \rightarrow \infty$*

$$c_n = \Theta\left(n! 4^n e^{3a_1 n^{1/3}} n^{3/4}\right) \quad \text{and}$$

$$r_n = \Theta\left(n! 4^n e^{3a_1 n^{1/3}} n\right),$$

where $a_1 \approx -2.338$ is the largest root of the Airy function $\text{Ai}(x)$ defined as the unique function satisfying $\text{Ai}''(x) = x\text{Ai}(x)$ and $\lim_{n \rightarrow \infty} \text{Ai}(x) = 0$.

We believe that there are constants γ_c and γ_r such that

$$c_n \sim \gamma_c n! 4^n e^{3a_1 n^{1/3}} n^{3/4} \quad \text{and} \quad r_n \sim \gamma_r n! 4^n e^{3a_1 n^{1/3}} n,$$

however, we have been unable to find the exact values of these constants or even prove their existence. Nevertheless, our empirical analysis yields what we believe to be very accurate estimates for γ_c and γ_r , namely $\gamma_c \approx 173.12670485$ and $\gamma_r \approx 166.95208957$.

The presence of a stretched exponential term in a sequence counting combinatorial objects is not common, although there are quite a few precedents. One simple example is that of *pushed Dyck paths*, where Dyck paths of maximum height h are given a weight y^{-h} for some $y > 1$. In this case McKay and Beaton determined the weighted number d_n of paths of length $2n$ up to and including the constant term to be asymptotically given by

$$d_n \sim Ay(y-1)(\log y)^{1/3} 4^n \exp\left(-C(\log y)^{2/3} n^{1/3}\right) n^{-5/6},$$

where $A = 2^{5/3} \pi^{5/6} / \sqrt{3}$ and $C = 3(\pi/2)^{2/3}$; see [96]. For the analogous problem of counting pushed self avoiding walks, Beaton et al. [24] gave a (non-rigorous) probabilistic argument for the presence of a stretched exponential of the form $e^{-cn^{3/7}}$ for some $c > 0$. In each of these cases, a stretched exponential appears as part of a compromise between the large height regime in which most paths occur and the small height regime in which the weight is maximized. We will see that a similar compromise occurs here.

Another situation in which stretched exponentials have appeared is in cogrowth sequences in groups [79], that is, paths on Cayley graphs which start and end at the same point. In particular, Revell [159] showed that in the lamplighter group the number c_n of these paths of length $2n$ behaves like

$$c_n \sim C 9^n \kappa^{n^{1/3}} n^{1/6}.$$

In the group $\mathbb{Z} \wr \mathbb{Z}$, Pittet and Saloff-Coste [155] showed that the asymptotics of the cogrowth series contains the slightly more complicated term $\kappa \sqrt{n \log n}$. Another example comes from the study of pattern avoiding permutations, where Conway, Guttmann, and Zinn-Justin [59, 60] have given compelling numerical evidence that the number p_n of 1324-avoiding permutations of length n behaves like

$$p_n \sim B \mu^n \mu_1^{\sqrt{n}} n^g,$$

with $\mu \approx 11.600$, $\mu_1 \approx 0.0400$, $g \approx -1.1$.

As seen by these examples, it is generally quite difficult to prove that a sequence has a stretched exponential in its asymptotics. Part of the difficulty is that a sequence which has a stretched exponential cannot be “very nice”. In particular, the generating function cannot be algebraic, and can only be D -finite if it has an irregular singularity [85].

Some explicit examples of D -finite generating functions with a stretched exponential are known; see, e.g., [179, 180, 181]. In these cases Wright uses a saddle-point method to prove the presence of the stretched exponential. To apply this method, one needs to meticulously check various analytic conditions on the generating function, or to bound related integrals in a delicate way. These tasks can be highly non-trivial and require a precise knowledge of the analytic properties of the generating function. For more detail on how to use the saddle-point method to prove stretched exponentials, and further examples; see [85, Chapter VIII].

In lieu of detailed information on the generating function, we find and analyze the following recurrence relation

$$r_{n,m} = r_{n,m-1} + (m+1)r_{n-1,m},$$

corresponding to a partial differential equation to which the saddle point method cannot be readily applied. The number of relaxed trees of size n is then $r_{n,n}$. We present a method that works directly with a transformed sequence $d_{n,k}$ and the respective recurrence relation. We find two explicit sequences $A_{n,k}$ and $B_{n,k}$ with the same asymptotic form, such that

$$A_{n,k} \leq d_{n,k} \leq B_{n,k}, \tag{1}$$

for all k and all n large enough. The idea is that $A_{n,k}$ and $B_{n,k}$ satisfy the recurrence of $d_{n,k}$ with the equalities replaced by inequalities, allowing us to prove (1) by induction. In order to find appropriate sequences $A_{n,k}$ and $B_{n,k}$, we start by performing a heuristic analysis to conjecture the asymptotic shape of $d_{n,k}$ for large n . We then prove that the required recursive inequalities hold for sufficiently large n using adapted Newton polygons.

The inductive step in the method described above requires that all coefficients in the recurrence be positive. This occurs in the case of

relaxed binary trees but not for compacted binary trees. In the latter case, we construct a sandwiching pair of sequences, each determined by a recurrence with positive coefficients, to which our method applies.

As an application, we use our results on relaxed and compacted trees to give new asymptotic upper and lower bounds for the number of minimal deterministic finite automata with n states recognizing a finite language on a binary alphabet. These automata are studied in the context of the complexity of regular languages; see [65, 66, 131]. To our knowledge no upper or lower bounds capturing even the exponential term had been proven for this problem. Our bounds are much more accurate, only differing by a polynomial factor, and thereby proving the presence of a stretched exponential term. We solved this asymptotic counting problem in [P13], which will be presented in Section 2.3.

In its simplest form, our method applies to two parameter linear recurrences with positive coefficients which may depend on both parameters. We expect, however, that our method could be adapted to handle a much wider range of recurrence relations, potentially involving more than two parameters, negative coefficients, and perhaps even some non-linear recurrences. Indeed, we have already seen that it can be adapted to at least one case involving negative coefficients, namely that of counting compacted binary trees.

2.2.1 A two-parameter recurrence relation

In [90, Theorem 5.1 and Corollary 5.4] the so-far most efficient recurrences are given for the number of compacted and relaxed binary trees, respectively. Computing the first n terms using these requires $\mathcal{O}(n^3)$ arithmetic operations. In this section, we give an alternative recurrence with only one auxiliary parameter (instead of two) other than the size n , which leads to an algorithm of arithmetic complexity $\mathcal{O}(n^2)$ to compute the first n terms of the sequence. The construction is motivated by the recent bijection [P24], which will be presented in Section 2.4.

As a corollary of Theorem 2.2.1, we directly get an estimate of the asymptotic proportion of compacted trees among relaxed trees:

$$\frac{c_n}{r_n} = \Theta(n^{-1/4}).$$

An analogous result for compacted and relaxed trees of bounded right height was shown in [90, Corollary 3.5]. The *right height* is the maximal number of right edges to internal nodes on a path in the spine from the root to a leaf. Let $c_{k,n}$ (resp. $r_{k,n}$) be the number of

compacted (resp. relaxed) trees of right height at most k . Then, [90, Corollary 3.5] states that for fixed k ,

$$\frac{c_{k,n}}{r_{k,n}} \sim \lambda_k n^{-\frac{1}{k+3} - (\frac{1}{4} - \frac{1}{k+3}) \frac{1}{\cos^2(\frac{\pi}{k+3})}} = o(n^{-1/4}),$$

for a constant λ_k independent of n . As $k \rightarrow \infty$, we see that the exponent of n approaches $-1/4$. It is thus not surprising that the exponent in the unbounded case is also $-1/4$.

2.2.1.1 Relaxed binary trees and horizontally decorated paths

For the subsequent construction, we need the following type of lattice paths.

Definition 2.2.2. A horizontally decorated path P is a lattice path starting from $(0,0)$ with steps $H = (1,0)$ and $V = (0,1)$ confined to the region $0 \leq y \leq x$, where each horizontal step H is decorated by a number in $\{1, \dots, k+1\}$ with k its y -coordinate. If P ends at (n,n) , we call it a horizontally decorated Dyck path.

We denote by \mathcal{D}_n the set of horizontally decorated Dyck paths of length $2n$.

Remark 2.2.3. Horizontally decorated Dyck paths can also be interpreted as classical Dyck paths, where below every horizontal step a box given by a unit square between the horizontal step and the line $y = -1$ is marked; see Figure 4. This gives an interpretation connecting these paths with the heights of Dyck paths, which we will exploit later. Independently, Callan gave in [52] a more general bijection in which he called the paths *column-marked subdiagonal paths*, and Bassino and Nicaud studied in [23] a variation when counting some automata, where the paths stay above the diagonal, which they called *k-Dyck boxed diagrams*.

Theorem 2.2.4. There exists a bijection **Dyck** between relaxed binary trees of size n and the set \mathcal{D}_n of horizontally decorated Dyck paths of length $2n$.

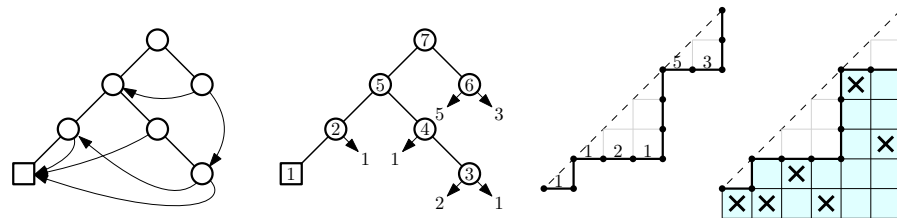


Figure 4: Example of the bijection **Dyck** between relaxed trees and horizontally decorated Dyck paths. It transforms internal nodes into vertical steps and pointers into horizontal steps.

We omit a precise description of the bijection here and refer to the example in Figure 4. In Section 2.3.2 we will describe a more general

version, which allows to count minimal deterministic finite automata. The following result gives the claimed algorithm with quadratic arithmetic complexity to count such paths, which can also be used as a precomputation step of an algorithm that randomly generates these paths using a linear number of arithmetic operations for each path. These algorithms are also applicable to relaxed binary trees via the bijection **Dyck**.

Proposition 2.2.5. *Let $r_{n,m}$ be the number of horizontally decorated paths ending at (n, m) . Then,*

$$\begin{aligned} r_{n,m} &= r_{n,m-1} + (m+1)r_{n-1,m}, & \text{for } n, m \geq 1 \text{ and } n \geq m, \\ r_{n,m} &= 0, & \text{for } n < m, \\ r_{n,0} &= 1, & \text{for } n \geq 0. \end{aligned}$$

The number of relaxed binary trees of size n is equal to $r_{n,n}$.

Remark 2.2.6 (Compacted trees of bounded right height). This restriction naturally translates relaxed binary trees of right height at most k from [90] into horizontally decorated Dyck paths of height at most $k+1$, where height is the maximal normal distance rescaled by $\sqrt{2}$ from a lattice point on the path to the diagonal. In other words, these paths are constrained to remain between the diagonal and a line translated to the right parallel to the diagonal by $k+1$ unit steps.

2.2.1.2 Compacted binary trees

Given a relaxed tree C , an internal node u is called a *cherry* if its children in the spine are both leaves and none of them is the left-most one. According to the discussion at the end of Section 4 in [90], the only obstacle for a relaxed tree to be a compacted tree is a cherry with badly chosen pointers.

Proposition 2.2.7. *A relaxed tree C is a compacted tree if and only if there are no two nodes $u \neq v$ in C which share the same left child u_ℓ and the same right child u_r . Moreover, if C is not a compacted tree, such a pair exists where v is a cherry and u precedes v in postorder.*

The restriction described in Proposition 2.2.7 has an analogue in the class of horizontally decorated paths: We label every step V with its final altitude plus one, which corresponds to its row number in the interpretation with marked boxes, and which also corresponds to the traversal/process order in postorder of its internal node in the relaxed tree; compare Figure 4. Note that each step H is already labeled. For any step S , let $\mathcal{L}(S)$ be its label. We associate to every step V a pair of integers (v_1, v_2) , which corresponds to the labels of its left and right children. First, let S' be the step before V and set $v_2 = \mathcal{L}(S')$. Next, draw a line from the ending point of V in the southwest direction parallel to the diagonal, and stop upon touching the path again. Let

S'' be the last step before V that ends on this line (if there is no such step, set $v_1 = 1$). Then set $v_1 = \mathcal{L}(S'')$.

Definition 2.2.8. A C-decorated path P is a horizontally decorated path where the decorations h_1 and h_2 of each pattern of consecutive steps HHV fulfill $(h_1, h_2) \neq (v_1, v_2)$ for all preceding steps V .

Proposition 2.2.9. The map **Dyck** bijectively sends the set of compacted trees of size n to the set of C-decorated Dyck paths of length $2n$.

The key observation for the counting result is that exactly one pair of labels (h_1, h_2) is avoided for each preceding step V of a consecutive pattern HHV . Applying this classification to the previous result we get a similar quadratic-time recurrence for compacted binary trees.

Proposition 2.2.10. Let $c_{n,m}$ be the number of C-decorated paths ending at (n, m) . Then,

$$\begin{aligned} c_{n,m} &= c_{n,m-1} + (m+1)c_{n-1,m} - (m-1)c_{n-2,m-1}, & \text{for } n \geq m \geq 1, \\ c_{n,m} &= 0, & \text{for } n < m, \\ c_{n,0} &= 1, & \text{for } n \geq 0. \end{aligned}$$

The number of compacted binary trees of size n is equal to $c_{n,n}$.

Note that one might also count the following simpler class which is in bijection with C-decorated paths, albeit without a natural bijection.

Definition 2.2.11. A H-decorated path P is a horizontally decorated path where the decorations h_1 and h_2 of each pattern of consecutive steps HHV fulfill $h_1 \neq h_2$ except for $h_1 = h_2 = 1$.

In terms of marked boxes, this constraint translates to the fact that, below the horizontal steps in each consecutive pattern HHV , the marks must be in different rows except possibly for the lowest one.

2.2.2 Heuristic analysis

In this section, we will explain briefly our heuristics and *ansatz* that are used to get the asymptotic behavior of r_n and c_n . These heuristics are closely related to the asymptotic behavior of Dyck paths and the Airy function.

2.2.2.1 An intuitive explanation of the stretched exponential

We can consider r_n as a weighted sum of Dyck paths, where each Dyck path P has a weight $w(P)$ that is the number of horizontally decorated Dyck paths that it gives rise to. There is thus a balance of the number of total paths and their weights for the weighted sum $r_{n,n}$. On the one hand, most paths have an (average) height of $\mathcal{O}(\sqrt{n})$ (i.e., mean distance to the diagonal). On the other hand, their weight is

maximal if their height is $\mathcal{O}(1)$, i.e., they are close to the diagonal. In other words, typical Dyck paths are numerous but with small weight, and Dyck paths atypically close to the diagonal are few but with enormous weight. The asymptotic behavior of the weighted sum of Dyck paths that we consider should be a result of a compromise between these two forces. We will now make this more explicit by analyzing Dyck paths with height approximately n^α for some $\alpha \in (0, 1/2)$.

Given a Dyck path P with steps $H = (1, 0)$ and $V = (0, 1)$ as in Definition 2.2.2, let m_i be the y -coordinate of the i th step H . The number of Dyck paths with m_i bounded uniformly satisfy the following property.

Proposition 2.2.12 ([121, Theorem 3.3]). *For a Dyck path P of length $2n$ chosen uniformly at random, let m_i be the y -coordinate of the i th step H . For $\alpha < 1/2$, we have*

$$\log \mathbb{P} \left(\max_{1 \leq i \leq n} (i - m_i) < n^\alpha \right) \sim -\pi^2 n^{1-2\alpha}.$$

Let $w(P)$ be the number of horizontally decorated Dyck paths whose unlabeled version is the Dyck path P . For a randomly chosen Dyck path P of length $2n$ with $i - m_i$ bounded uniformly by n^α , we heuristically expect most values of $i - m_i$ to be of the order $\Theta(n^\alpha)$, with i of order $\Theta(n)$. This leads to the following approximation:

$$\begin{aligned} \log \frac{w(P)}{n!} &= \sum_{1 \leq i \leq n} \log \left(\frac{m_i + 1}{i} \right) = \sum_{1 \leq i \leq n} \log \left(1 - \frac{i - m_i - 1}{i} \right) \\ &\approx cn \cdot \left(-\frac{n^\alpha}{n} \right) = -cn^\alpha. \end{aligned}$$

Here, $c > 0$ is some constant depending on α . This approximation is only heuristically justified and very hard to prove. The contribution of Dyck paths with $i - m_i$ uniformly bounded by n^α should thus roughly be $n!4^n \exp(-(1 + o(1))c'n^{p(\alpha)})$, with $p(\alpha) = \min(\alpha, 1 - 2\alpha)$ and $c' > 0$ a constant depending on α . Here, 4^n comes from the growth constant of Dyck paths. The function $p(\alpha)$ is minimal at $\alpha = 1/3$, which maximizes the contribution, leading to the following heuristic guess that the number of relaxed binary trees r_n should satisfy

$$\log \frac{r_n}{n!4^n} \underset{n \rightarrow \infty}{\sim} -an^{1/3},$$

for some constant $a > 0$. Furthermore, we anticipate that the main contribution should come from horizontally decorated Dyck paths with $i - m_i$ mostly of order $\Theta(n^{1/3})$. Since most such i 's should be of order $\Theta(n)$, we can even state the condition above as $x - y = \Theta(y^{1/3})$ for most endpoints (x, y) of horizontal steps. This heuristic is the starting point of our analysis.

2.2.2.2 Weighted Dyck meanders

The heuristics of the previous section suggest that the mean distance to the diagonal will play an important role. Therefore, we propose another model of lattice paths emphasizing this distance. A *Dyck meander* (or simply a *meander*) M is a lattice path consisting of up steps $U = (1, 1)$ and down steps $D = (1, -1)$ while never falling below $y = 0$. It is clear that Dyck paths of length $2n$ are in bijection with Dyck meanders of length $2n$ ending on $y = 0$ with the transcription $H \rightarrow U, V \rightarrow D$. This bijection can also be viewed geometrically as the linear transformation $x' = x + y, y' = x - y$. This transformation will simplify the following analysis. We can consider Dyck meanders as initial segments of Dyck paths.

Furthermore, we have seen that a rescaling by $n!$ seems practical. So we consider the following weight on steps U in a meander M . If U starts from (a, b) , then its weight is $(a - b + 2)/(a + b + 2)$, and the weight of M is the product of the weights of its steps U . Let $d_{n,m}$ denote the weighted sum of meanders ending at (n, m) . We get the following recurrence for $d_{n,m}$.

Proposition 2.2.13. *The weighted sum $d_{n,m}$ defined above for meanders ending at (n, m) satisfies the recurrence*

$$\begin{cases} d_{n,m} = \frac{n-m+2}{n+m}d_{n-1,m-1} + d_{n-1,m+1}, & \text{for } n > 0, m \geq 0, \\ d_{0,m} = 0, & \text{for } m > 0, \\ d_{n,-1} = 0, & \text{for } n \geq 0, \\ d_{0,0} = 1. \end{cases}$$

Corollary 2.2.14. *For integers m, n of the same parity, we have*

$$d_{n,m} = \frac{1}{((n+m)/2)!} r^{(n+m)/2, (n-m)/2}.$$

When m, n are not of the same parity, we have $d_{n,m} = 0$.

In particular, the number of relaxed trees of size n is given by $n!d_{2n,0}$.

For some simple cases of $d_{n,m}$, elementary computations show that $d_{n,m} = 0$ for $m > n$, $d_{n,n} = \frac{1}{n!}$, $d_{n,n-2} = \frac{2^{n-1}-1}{(n-1)!}$ and $d_{n,n-4} = \frac{7 \cdot 3^{n-3} - 2^n + 1}{2(n-2)!}$.

2.2.2.3 Analytic approximation of weighted Dyck meanders

The heuristic in Section 2.2.2.1 suggests that the main weight of $d_{n,m}$ comes from the region $m = \Theta(n^{1/3})$. It thus suggests an approximation of $d_{n,m}$ of the form

$$d_{n,m} \sim f(n^{-1/3}(m+1))h(n), \quad (2)$$

for some functions f and h , where we expect $h(n) \approx 2^n \rho^{n^{1/3}}$ for some ρ . The idea is that $h(n)$ describes how the total weight for a fixed

n grows, and $f(\kappa)$ describes the rescaled weight distribution in the main region $m = \Theta(n^{1/3})$.

Let $s(n)$ be the ratio $\frac{h(n)}{h(n-1)}$. Suppose that $m = \kappa n^{1/3} - 1$, the recurrence relation becomes

$$f(\kappa)s(n) = \frac{n - \kappa n^{1/3} + 3}{n + \kappa n^{1/3} - 1} f\left((n-1)^{-1/3}(\kappa n^{1/3} - 1)\right) + f\left((n-1)^{-1/3}(\kappa n^{1/3} + 1)\right). \quad (3)$$

Now, since we expect $h(n) \approx 2^n \rho^{n^{1/3}}$, we postulate that the ratio $s(n)$ behaves like

$$s(n) = 2 + cn^{-2/3} + O(n^{-1}), \quad (4)$$

and that $f(\kappa)$ is analytic. Using these assumptions, we can expand (3) as a Puiseux series in $1/n$. Moving all terms to the right-hand side yields

$$0 = ((c + 2\kappa)f(\kappa) - f''(\kappa)) n^{-2/3} + O(n^{-1}).$$

Solving the differential equation $(c + 2\kappa)f(\kappa) - f''(\kappa) = 0$ under the condition $f(\kappa) \rightarrow 0$ when $\kappa \rightarrow \infty$ yields the unique solution (up to multiplication by a constant)

$$f(\kappa) = b \text{Ai}\left(\frac{c + 2\kappa}{2^{2/3}}\right).$$

The condition on the behavior of $f(\kappa)$ near ∞ is motivated by the experimental observation that $d_{n,m}$ is quickly decaying for m close to n . We also insist that $f(0) = 0$ as $d_{n,-1} = 0$, which implies that $c = 2^{2/3}a_1$ where $a_1 \approx -2.338$ is the largest root of the Airy function $\text{Ai}(x)$; see [1, p. 450]. Now, using this conjectural value of c , it follows that (ignoring polynomial terms)

$$h(n) \approx 2^n \exp\left(3a_1(n/2)^{1/3}\right).$$

This suggests that the number of relaxed trees $r_n = n!d_{2n,0}$ satisfies

$$r_n \approx n!4^n \exp\left(3a_1n^{1/3}\right),$$

which is compatible with what we want to prove.

We observe that (3) can be expanded into a Puiseux series of $n^{1/3}$ by taking appropriate series expansions of $f(\kappa)$ and $s(n)$. Therefore, to refine the analysis above, it is natural to look at the expansion of $s(n)$ in (4) to more subdominant terms, and to postulate a more refined *ansatz* of $d_{n,m}$ than (2), probably as a series in $n^{1/3}$. Indeed, if we take

$$d_{n,m} \sim \left(f(n^{-1/3}(m+1)) + n^{-1/3}g(n^{-1/3}(m+1))\right) h(n)$$

and

$$s(n) = 2 + cn^{-2/3} + dn^{-1} + O(n^{-4/3}),$$

then using the same method we can reach the polynomial part of the asymptotic behavior of r_n as

$$r_n \approx n!4^n \exp\left(3a_1n^{1/3}\right)n.$$

In general, we can postulate

$$d_{n,m} \approx h(n) \sum_{j=0}^k f_j(n^{-1/3}(m+1))n^{-j/3},$$

and

$$s(n) = 2 + \gamma_2n^{-2/3} + \gamma_3n^{-1} + \dots + \gamma_kn^{-k/3} + o(n^{-k/3}).$$

The proof of our main result on relaxed binary trees is based on choosing the cutoff appropriately, and using perturbations of that truncation to bound r_n .

2.3 ASYMPTOTICS OF MINIMAL DETERMINISTIC FINITE AUTOMATA RECOGNIZING A FINITE BINARY LANGUAGE [P13]

In this section, we present the results of [P13], which extend the methods for counting relaxed and compacted trees from the previous Section 2.2. We show that the counting sequence $(m_{2,n})_{n \in \mathbb{N}}$ of minimal deterministic finite automata of size n recognizing a finite binary language admits a stretched exponential. Until now, the problem of counting these automata, even asymptotically, was widely open; see for example [65].

2.3.1 Counting minimal deterministic finite automata

A *deterministic finite automaton* (DFA) A is a 5-tuple $(\Sigma, Q, \delta, q_0, F)$, where Σ is a finite set of letters called the *alphabet*, Q is a finite set of states, $\delta : Q \times \Sigma \rightarrow Q$ is the *transition function*, q_0 is the *initial state*, and $F \subseteq Q$ is the set of *final states* (sometimes called *accept states*). States not in F are called *non-final* or *reject states*. A DFA can be represented by a directed graph with one vertex v_s for each state $s \in Q$, with the vertices corresponding to final states being highlighted, and for every transition $\delta(s, w) = \hat{s}$, there is an edge from s to \hat{s} labeled w (see Figure 5).

A word $w = w_1w_2 \dots w_\ell \in \Sigma^*$ is *accepted* by A if the sequence of states $(s_0, s_1, \dots, s_\ell) \in Q^{\ell+1}$ defined by $s_0 = q_0$ and $s_{i+1} = \delta(s_i, w_i)$ for $i = 0, \dots, \ell - 1$ ends with $s_\ell \in F$ a final state. The set of words

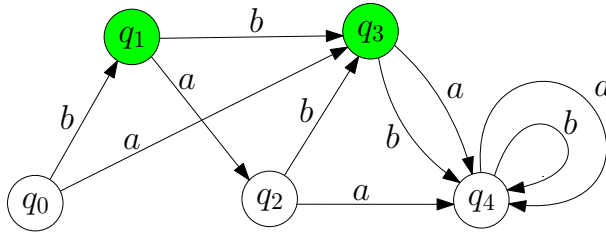


Figure 5: The unique minimal DFA for the language $\{a, b, bb, bab\}$. The initial state is q_0 , the final states are q_1 and q_3 , and the unique sink is q_4 .

accepted by A is called the *language* $\mathcal{L}(A)$ recognized by A . It is well-known that DFAs recognize exactly the set of regular languages. Note that every DFA recognizes a unique language, but a language can be recognized by several different DFAs. A DFA is called *minimal* if no DFA with fewer states recognizes the same language. The Myhill–Nerode Theorem states that every regular language is recognized by a unique minimal DFA (up to isomorphism) [97, Theorem 3.10]. For more details on automata see [97].

Since every regular language defines a unique minimal automaton, one may define the (space) complexity of the language to be the number of states in this corresponding automaton. Defining *space complexity* in this way, the number $m_{2,n}$ is simply the number of finite languages over a binary alphabet of space complexity $n + 1$.

The asymptotic proportion of minimal DFAs in the class of (not necessarily acyclic) automata was solved by Bassino, Nicaud, and Sportiello in [22], building on enumeration results by Korshunov [119, 120] and Bassino and Nicaud [23]. This result also exploits an underlying tree structure of the automata, but this tree structure comes from a different traversal than what we use. In that case, no stretched exponential appears in the asymptotic enumeration, and the minimal automata account for a constant fraction of all automata.

Now using our asymptotic results on compacted and relaxed trees from Section 2.2, we directly get the following new bounds on the asymptotic number of such automata, determining their asymptotics up to a polynomial multiplicative term.

Corollary 2.3.1. *Let $m_{2,n}$ be the number of minimal DFAs over a binary alphabet with n transient states (and a unique sink) that recognize a finite language. Then,*

$$2^{n-1}c_n \leq m_{2,n} \leq 2^{n-1}r_n.$$

As a consequence, there exist positive constants κ_1 and κ_2 such that

$$\kappa_1 n^{3/4} \leq \frac{m_{2,n}}{n! 8^n e^{3a_1 n^{1/3}}} \leq \kappa_2 n.$$

Extending the method for relaxed and compacted trees we will get the following result.

Theorem 2.3.2. *The number $m_{2,n}$ of non-isomorphic minimal DFAs on a binary alphabet recognizing a finite language with $n + 1$ states satisfies for $n \rightarrow \infty$*

$$m_{2,n} = \Theta \left(n! 8^n e^{3a_1 n^{1/3}} n^{7/8} \right),$$

where $a_1 \approx -2.338$ is the largest root of the Airy function.

This disproves the conjecture $m_{2,n} \sim K 2^{n-1} r_n$ for some $K > 0$ of Liskovets based on numerical data; see [131, Equation (16)].

Previously, Domaratzki derived in [64] the lower bound

$$m_{2,n} \geq \frac{(2n-1)!}{(n-1)!} c_1^{n-1},$$

with $c_1 \approx 1.0669467$, which implies the asymptotic bound $m_{2,n} \geq \frac{n!(4c_1)^n}{2c_1 \sqrt{\pi n}}$ (note that $m_{2,n} = f_2'(n+1)$ in his results). Furthermore, Domaratzki showed in [63] the upper bound

$$m_{2,n} \leq 2^{n-1} G_{2n+2},$$

where G_{2n} are the Genocchi numbers, which are defined by the series expansion of $\frac{2t}{e^t+1} = t + \sum_{n \geq 1} (-1)^n G_{2n} \frac{t^{2n}}{(2n)!}$. This then gives the asymptotic bound $m_{2,n} \leq 4(2n)! \left(\frac{2}{\pi^2}\right)^{n+1} n^2$, which is, however, much larger than the superexponential growth given by $n!$.

While not explicitly formulated in the literature, it is possible to bound the number of acyclic DFAs by general DFAs using the results by Korshunov [119, 120] (see also [23, Theorem 18]). Thereby, we get the upper bound

$$m_{2,n} = \mathcal{O} \left(n! (2e^2 \nu)^n \right),$$

where $\nu = \alpha^\alpha (1 + \alpha)^{1-\alpha} \approx 0.8359$ with α being the solution of $1 + x = x e^{2/(1+x)}$, and therefore $2e^2 \nu \approx 12.3531$, which is significantly larger than the actual exponential growth.

2.3.2 Recurrence relation

To derive a recurrence for automata recognizing a finite binary language, we need the following lemma. It builds on the result from [131, Lemma 2.3] (see also [97, Section 3.4]) and includes state uniqueness.

Lemma 2.3.3. *A DFA A is the minimal automaton for some finite language if and only if it has the following properties:*

1. *There is a unique sink s . That is, a state which is not a final state such that all transitions from s end at s that is, $\delta(s, w) = s$.*
2. *A is acyclic: the underlying directed graph has no cycles except for the loops at the sink.*

3. *A is initially connected: for any state p there exists a word $w \in \Sigma^*$ such that A reaches the state p upon reading w .*
4. *State uniqueness: there are no two distinct states q and q' with $\delta(q, a) = \delta(q', a)$ and $\delta(q, b) = \delta(q', b)$ such that both q and q' , or neither q nor q' , are accept states.*

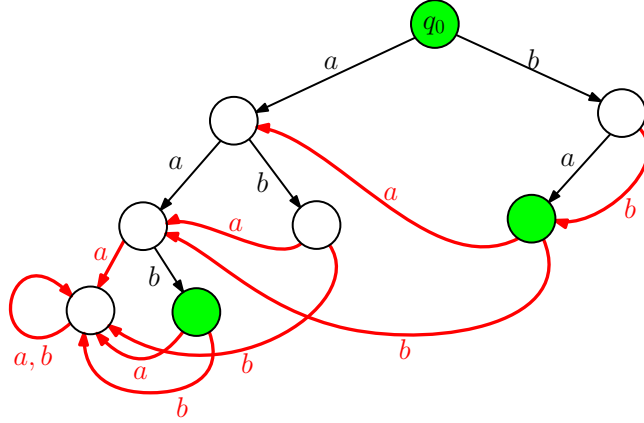


Figure 6: An acyclic DFA with its spanning subtree in black and all other edges in red. The initial state is q_0 and the final states are green.

Now consider two sets of DFAs: the set \mathfrak{F} of minimal DFAs recognizing finite languages, and the set \mathfrak{G} of acyclic and initially connected DFAs with a unique sink. By Lemma 2.3.3, \mathfrak{F} consists of precisely the automata in \mathfrak{G} that also satisfy state uniqueness.

Next, we transform DFAs in \mathfrak{G} into decorated lattice paths that we call *B-paths*. For a given $A \in \mathfrak{G}$, our first step is to construct a spanning subtree of A (excluding the sink) using a depth-first search (DFS) from the initial state q_0 as shown in Figure 6. This DFS is uniquely defined by taking edges marked by a before edges marked by b . Since A is initially connected, the tree obtained is a spanning tree.

Using the same DFS, we construct a path P starting at the point $(-1, 0)$ and illustrated by a blue line in Figure 7 as follows:

- Whenever the directed blue line around the tree in Figure 7 goes up we add a *vertical step* $V = (0, 1)$ to the path. We say that the state we just quit *corresponds* to this step.
- Whenever the directed blue line crosses an outgoing edge (including the edge leading to the sink), which is not part of the tree, we add a *horizontal step* $H = (1, 0)$.

The order of states corresponding to V -steps is called the *postorder* of states. It is clear that the first step of P is a H -step, and removing it from P gives a Dyck path under the main diagonal. We now decorate P with spots and crosses. Each step V is decorated by a green or white spot, according to whether the corresponding state is accepting or rejecting.

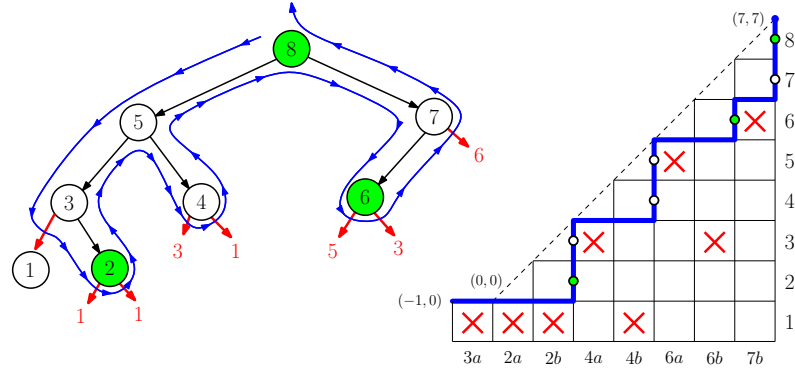


Figure 7: The transformation from an acyclic DFA to a B-path. In the DFA, the states are numbered in postorder and the outgoing external edges with the number of the states they point to.

Since A is acyclic, during the DFS, for an edge e pointing from the current state q to an already visited state q' , the state q' must not be an ancestor of q in the constructed tree, meaning that q' must either come before q in postorder or be the sink. In the former case, we put a cross in the cell at the intersection between the column of the H -step corresponding to e , and the row of the V -step corresponding to q' , while in the latter case we put the cross in the row below $y = 0$. Clearly the crosses are under P and above $y = -1$. We thus obtain a path B with decorations, which we call the B-path of the automaton A . Note that B-paths without spots and without the first H-step are horizontally decorated paths from Definition 2.2.2.

To characterize B-paths obtained from DFAs in \mathfrak{G} , we propose the following definition. An *automatic B-path* P of size n is defined as a lattice path consisting of up steps and horizontal steps from $(-1, 0)$ to (n, n) with decorations such that

- the first step is an H -step, and its removal leaves a Dyck path below the main diagonal;
- each H -step has a cross in its column between P and $y = -1$;
- every V -step has a white or green spot.

It is not difficult to see that automatic B-paths are in bijection with \mathfrak{G} , with the size preserved, since a B-path P obtained from a DFA $A \in \mathfrak{G}$ is clearly automatic, and the construction of B-paths can be easily reversed to obtain a DFA in \mathfrak{G} from an automatic B-path.

Now we examine automatic B-paths corresponding to DFAs in \mathfrak{F} . By definition, we only need to add state uniqueness. Given $A \in \mathfrak{G}$, let T be its depth-first search tree and B its corresponding automatic B-path. A state $q \in A$ is called a *cherry* if it is a leaf of T but not the sink. Seen on B , a cherry state corresponds to a sequence HHV of steps. We now propose a seemingly weaker notion of state uniqueness called *cherry-state uniqueness*, which is in fact equivalent in our case.

Lemma 2.3.4. *Suppose that $A \in \mathfrak{G}$, then A has state uniqueness if and only if it has cherry-state uniqueness, i.e., any two states q, q' such that q comes before q' in postorder, and q' is a cherry state, satisfy the conditions in the definition of state uniqueness.*

The big advantage of this characterization is that it transforms state uniqueness into a local property depending only on HHV steps. In other words, for paths ending at (n, m) we need to take paths ending at $(n - 2, m - 1)$ into account. With this last ingredient we get the following recursive description of automatic B -paths.

Proposition 2.3.5. *Let $b_{n,m}$ be the number of initial segments of automatic B -paths corresponding to DFAs in \mathfrak{F} ending at (n, m) . Then*

$$\begin{cases} b_{n,m} = 2b_{n,m-1} + (m+1)b_{n-1,m} - mb_{n-2,m-1}, & \text{for } n \geq m \geq 1, \\ b_{n,m} = 0, & \text{for } n < m, \\ b_{n,0} = 1, & \text{for } n \geq -1. \end{cases}$$

The number $m_{2,n}$ of minimal binary DFAs of size n recognizing a finite language is equal to $b_{n,n}$.

This recurrence relation can be directly used to compute all elements of the sequence $(m_{2,n})_{n \geq 0}$ up to size $n = N$ with $\mathcal{O}(N^2)$ arithmetic operations. The first few numbers of this sequence read

$$(m_{2,n})_{n \geq 0} = (1, 1, 6, 60, 900, 18480, 487560, 15824880, 612504240, \dots).$$

We have added it as sequence [OEIS A331120](#) in the Online Encyclopedia of Integer Sequences [167]. Previously, the first 7 elements were computed in [66, Section 6]. In addition, observe that this recurrence is very similar to the one of compacted binary trees in Proposition 2.2.10. Let us shortly discuss the differences and give combinatorial interpretations. Firstly, the factor 2 of $b_{n,m-1}$ corresponds to the fact that states are either accepting or not. Secondly, the factor m of $b_{n-2,m-1}$ corresponds to the fact that *all* previous states (in postorder) are removed, i.e. also the unique sink/leaf with label 1, which was ignored in the case of compacted trees as it has no children; compare Definitions 2.2.8 and 2.2.11.

2.4 A BIJECTION OF PLANE INCREASING TREES WITH RELAXED BINARY TREES OF RIGHT HEIGHT AT MOST ONE [P24]

In this section, we present the bijection from [P24] between relaxed binary trees of right height at most one shown in Figure 2 on page 5, and plane increasing trees shown in Figure 8. This solves an open problem of [90] about the miraculously simple counting formula given by the odd double factorials $(2n - 1)!! := (2n - 1)(2n - 3) \cdots 1$ for such trees with n nodes.

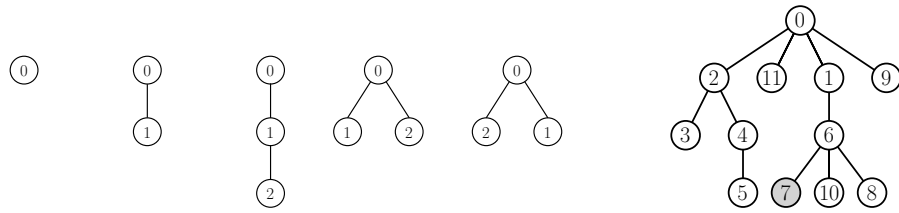


Figure 8: Left: All plane increasing trees of size 0, 1, 2. Right: An increasing tree of size 11 with young leaves 3, 5, 7 and maximal young leaf 7.

An *increasing tree* is a labeled rooted tree in which labels along any path from the root to the leaves are in increasing order. For notational convenience we label the nodes of a tree from 0 to n and define its size to be n . This concept was first introduced and intensively investigated by Bergeron, Flajolet, and Salvy [25]. These trees have found vast applications as data structures in computer science, as models in genealogy, and as representations of permutations, to name a few [70, 168].

Recall, that a tree is called *plane* (or *ordered*) if the children are equipped with a left-to-right order. For example the two trees in the center of Figure 8 whose roots have two children with labels 1 and 2 are considered to be different trees. This defines the classical family of rooted plane increasing trees, which can be generated uniformly at random by a growth process: start with the root and label 0. At step i there are $2i - 1$ possible places to insert node i . Choose one uniformly at random. Note that at a node with out-degree d there are $d + 1$ possible places to insert a new child. This idea is known as the Albert–Barabási model [2]. Note that this method gives a way to generate these trees uniformly at random in linear time.



Figure 9: Left: A compacted binary tree with right height 2. The labels give the level of the node. Right: The same tree rotated by 45 degrees. The unique leaf is marked by a square.

The second family we are interested in are relaxed trees from Definition 2.1.1. In Figure 2 we see all relaxed binary trees of size 0, 1, and 2. The *right height* is the maximal number of right edges (or right children) on all paths from the root to any leaf after deleting all pointers. The *level* of a node is the number of right edges on the path from the root to this node; see Figure 9. The asymptotic counting problem for relaxed (and the more restrictive class of compacted) binary trees of finite right height was solved in [90].

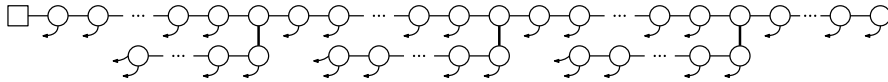


Figure 10: The structure of a relaxed binary tree with right height at most one. For clarity the pointers are only attached to their source. In a specific relaxed tree the pointers are fixed and point to specific nodes seen before the source node in postorder traversal.

The general structure of relaxed binary trees of right height at most one is shown in Figure 10. In [90, Theorem 7.3] it was shown that they admit the exponential generating function

$$R(z) = \frac{1}{\sqrt{1-2z}} = \sum_{n \geq 0} (2n-1)!! \frac{z^n}{n!}.$$

In other words, the number of relaxed binary trees of right height at most one of size n is equal to the number of increasing plane trees of size n and is equal to $(2n-1)!!$. These numbers count more than a dozen labeled objects (see OEIS A001147), yet the class of DAGs is to our knowledge the first not labeled one. Bijections appear repeatedly in the literature: See for example Janson [106] for a bijection between plane increasing trees and Stirling permutations, or Janson, Kuba, and Panholzer [108] for a bijection between plane increasing trees and ternary increasing trees.

2.4.1 Bijection

We will need the following concepts: A *branch node* is a node on level 0 without pointers to which a branch of nodes on level 1 is attached. We say that this is the branch node of the nodes in this branch. In the Figures 10 and 11 we see three branch nodes each. As before, a *cherry* is a node with 2 pointers and we will speak of relaxed trees always meaning relaxed binary trees. For a plane increasing tree \mathcal{T} we denote by \mathcal{T}_k the tree restricted to the labels $0, \dots, k$.

The bijection stated below is shown on an example in Figure 11. From top to bottom and left to right a relaxed binary tree of right height at most one is transformed into a plane increasing tree. Reversing these steps gives the inverse bijection.

Algorithm 1 presents a formal description of the transformation from relaxed binary trees to plane increasing trees. Let us start with an arbitrary relaxed binary tree of size n . First, we label the nodes from 0 to n according to an inorder traversal. We use v_i to reference the node with label i . In the labeling process we ignore pointers. Start at the leaf and label it with 0. Then, move to the parent. Whenever we see a node for the first time we attach a label incremented by one. If we meet a branch node we traverse its right branch starting from the cherry from left to right. Then we continue on level 0.

Algorithm 1 Relaxed binary tree $\mathcal{R} \rightarrow$ Plane Increasing Tree \mathcal{T}

```

1: Label nodes of  $\mathcal{R}$  inorder  $v_0, v_1, \dots, v_n$ 
2: For each cherry  $v_i$  move left pointer to  $v_{i-1}$   $\triangleright v_{i-1}$  is  $v_i$ 's branch
   node
3: For each node set  $p_i :=$  target of pointer of  $v_i$ 
4: if  $\text{level}(v_i) = 1$  and  $p_i = v_0$  then
5:    $p(v_i) :=$  Branch node of branch of  $v_i$ 
6: end if
7: Leaf  $v_0 \rightarrow$  Root of  $\mathcal{T}$ 
8: for  $i$  from 1 to  $n$  do
9:   if  $\text{level}(v_i) = 0$  then  $\triangleright$  Parent-pointer
10:    Attach  $v_i$  as first child to  $p_i$ 
11:   else  $\triangleright$  Sibling-pointer
12:    Attach  $v_i$  as direct sibling right of  $p_i$ 
13:   end if
14: end for

```

Next, we move the first (or left) pointer of each cherry v_i (which has to be on level 1) to v_{i-1} which is its branch node due to the previous labeling operation. This operation attaches to each node, except the leaf, a unique pointer.

Then, we separate the pointers into two sets: parent- and sibling-pointers. A *parent-pointer* is any pointer starting on level 0, and a *sibling-pointer* is any pointer starting on level 1. Next, every sibling-pointer that points to the leaf v_0 is changed to point to its branch node. This is shown for node 8 in Figure 11.

Finally, we consider the nodes in the order of their labels and build a plane increasing tree. The leaf with label 0 becomes the root. If the node has a parent-pointer, we attach it as a first child (very left) of the node it is pointing to. If the node has a sibling-pointer, we attach it as a direct sibling on the right of the node it is pointing to.

For the reverse bijection we need the notion of young leaves. A *young leaf* is a leaf without left sibling. A *maximal young leaf* is a young leaf with maximal label; see Figure 8 (see [53, Section 4.3] for a recurrence relation of plane increasing trees built on this parameter). Note that from the previous algorithm, the maximal young leaves are the nodes of level 0. Its formal description is given in Algorithm 2.

Let us start with an arbitrary plane increasing tree of size n . The tree is traversed iteratively in the order of its labels. The algorithm builds the relaxed tree and an auxiliary structure called the branch. At every step we either extend the tree or the branch, which is on some point attached as right child to a node at level 0. At the beginning this branch is empty.

For a label k we distinguish now two rules, depending on whether it is a maximal young leaf or not. First, if the current node k is a maximal young leaf of \mathcal{T}_k then attach the branch to the last node on

Algorithm 2 Plane Increasing Tree $\mathcal{T} \rightarrow$ Relaxed binary tree \mathcal{R}

```

1:  $\mathcal{B} := \emptyset$ 
2: for  $k$  from 0 to  $n$  do
3:   if  $v_k$  is a maximal young leaf in  $\mathcal{T}_k$  then
4:     Attach  $\mathcal{B}$  to current root and move its pointer to last node
     of  $\mathcal{B}$  as left pointer
5:     Attach  $v_k$  as new root with a pointer to the parent of  $v_k$  in
      $\mathcal{T}_k$ 
6:      $\mathcal{B} := \emptyset$ 
7:   else
8:     Attach  $v_k$  as root to  $\mathcal{B}$  with a pointer to the left sibling of
      $v_k$  in  $\mathcal{T}_k$ 
9:   end if
10: end for
11: Perform 4-5

```

level 0, move the pointer of this level 0 node as left pointer to the last node of the branch, and set the branch to be empty. Then, attach the node k as new root node on level 0. For the pointer apply the parent rule and set its pointer to the parent of node k in \mathcal{T}_k .

Second, if the current node is not a maximal young leaf of \mathcal{T}_k then attach the node k as new root to the branch. For the pointer the sibling rule applies: set the pointer to the direct left sibling of node k in \mathcal{T}_k . In the case that this is the current root at level 0, set the node to the leaf 0.

At the end attach the branch to the current root of level 0 and move its pointer to the last node in the branch as left pointer.

Theorem 2.4.1. *The procedure above is a bijection between relaxed binary trees of right height at most one of size n and plane increasing trees of size n . It maps nodes of level 0 to maximal young leaves in the growth process of the plane increasing tree.*

Corollary 2.4.2. *Relaxed binary trees of size n of right height at most one can be generated uniformly at random in linear time and with a linear amount of memory.*

Remark 2.4.3. It is possible to directly generate relaxed trees of size n by using a growth process with the ideas of Algorithm 2. At every point one decides to either attach a new root at level 0 or in the branch \mathcal{B} (which corresponds to level 1). In the first case one performs operations 4-6, and in the second case operation 8.

Note that generalizing this method with nested branches it may be used to generate relaxed binary trees with arbitrary or even without height restrictions. However, for the cases of right height larger than 1 this does not generate them uniformly at random.

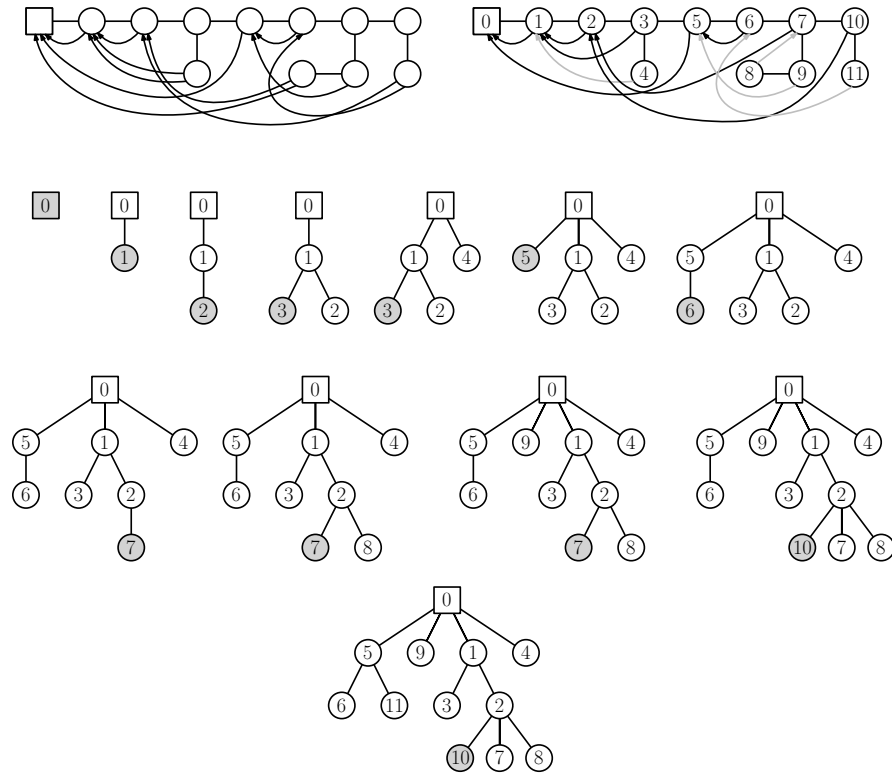


Figure 11: The bijection of Theorem 2.4.1 applied step by step. Parent-pointers are black, and sibling-pointers are gray. The leaf of the relaxed tree marked by a square is transformed into the root of the increasing plane tree. For the reverse bijection the maximal young leaves are shaded in gray.

Plane increasing trees are well-studied objects and many statistics exist on their parameters. This bijection transforms some of them into interesting quantities on relaxed binary trees of right height at most one. But vice versa it also leads to interesting results on plane increasing trees. In the next subsection we consider parameters which are easy to analyze on relaxed trees, and in the subsection thereafter we look at known results for plane increasing trees. For more details and an additional discussion of subclasses with many connections to the OEIS [167] see [P24].

2.4.2 Parameters of relaxed binary trees

From the bijection we have seen that the number of internal nodes on level 0 in relaxed binary trees of right height at most one is equal to the number of maximal young leaves in the growth process of a plane increasing tree. Using the theory from [90], it is now easy to analyze the number of nodes on level 0. Let X_n be the corresponding random variable in such a uniformly random tree of size n . Then, the following result follows using bivariate generating functions.

Theorem 2.4.4. *The standardized random variable*

$$\frac{X_n - \mu_1 n}{\sigma_1 \sqrt{n}},$$

with

$$\mu_1 = \frac{1}{2} + \frac{\log(n)}{4n} + \mathcal{O}\left(\frac{1}{n}\right) \quad \text{and} \quad \sigma_1^2 = \frac{1}{4} - \frac{\pi^2}{32n} + \mathcal{O}\left(\frac{1}{n^2}\right),$$

converges in law to a standard normal distribution $\mathcal{N}(0, 1)$.

Next, observe that a *branch* in a relaxed tree is a sequence of nodes on level 1. By the bijection these correspond to maximal young leaves, which are not immediately replaced in the growth process by a new young leaf in the next step. We call these *dominating young leaves*. Let Y_n be the random variable giving the number of branches of relaxed binary trees with right height at most one of size n drawn uniformly at random among all such trees of size n .

Theorem 2.4.5. *The standardized random variable*

$$\frac{Y_n - \mu_2 n}{\sigma_2 \sqrt{n}},$$

with

$$\mu_2 = \frac{1}{4} - \frac{1}{8n} + \mathcal{O}\left(\frac{1}{n^2}\right) \quad \text{and} \quad \sigma_2^2 = \frac{1}{16} + \frac{1}{32n} + \mathcal{O}\left(\frac{1}{n^2}\right),$$

converges in law to a standard normal distribution $\mathcal{N}(0, 1)$.

2.4.3 Parameters of plane increasing trees

Several parameters of plane increasing trees are well-understood. In order to understand their connection with respect to the stated bijection we introduce the concept of a *pointer-path*. This is a path following only pointers from an arbitrary node to the leaf 0 with two special rules: First, due to the transformation of the left cherry pointers to branch nodes, every internal node has exactly one outgoing pointer. Second, if a sibling-pointer points to the leaf it is interpreted as pointing to its branch node, compare node 8 in Figure 12. The length of a pointer-path is given by the number of parent-pointers in it. The results for our stated example are shown in Figure 12.

These pointer-paths also have an interpretation on the level of increasing trees. Starting from any node, one jumps to its left sibling as long as its label is decreasing. This corresponds to sibling-pointers. If this is not possible any more one moves up to its parent which corresponds to a parent-pointer. The length of the pointer-path is the depth of the node. In particular, this gives for every node a “maximal” decreasing sequence of labels encoded in the tree.

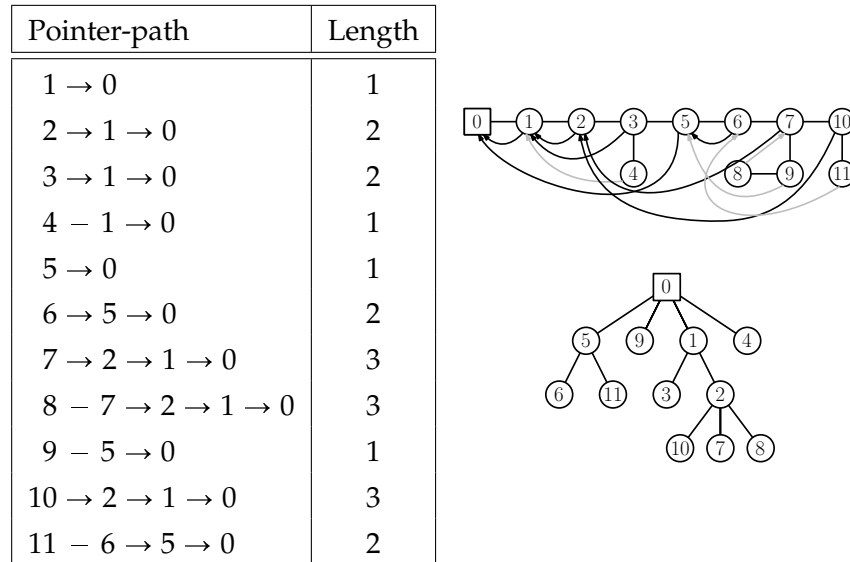


Figure 12: Pointer-paths of the example in Figure 11. Parent-pointers are marked by \rightarrow (or black arrows), sibling-pointers are marked by $-$ (or gray arrows).

There is rich literature on parameters of plane increasing trees; see, e.g., [25, 70, 108, 124, 135, 137, 153]. We have summarized four interesting parameters and their counterparts in relaxed binary trees of right height at most one in Table 1. In the first two cases the standardized random variables $\frac{X_n - \mathbb{E}X_n}{\sqrt{\text{Var}X_n}}$ converge in distribution to a standard normal distribution, whereas in the third case the normalized random variable $\frac{X_n}{\sqrt{2n}}$ converges in law to a standard Rayleigh distribution given by the density function $xe^{-x^2/2}$. For details on the distribution of the height see [70, Section 6.4] and [49, 69].

Plane incr. tree	Relaxed binary tree	$\mathbb{E}X_n$	$\mathbb{V}X_n$
Depth of node n [135]	Length pointer-path from node n	$\sim \frac{1}{2} \log n$	$\sim \frac{1}{2} \log n$
Number of leaves [137]	# nodes without ingoing parent-pointer	$= \frac{2}{3}n + \frac{1}{3}$	$= \frac{n}{9} + \frac{1}{18} - \frac{1/6}{2n+1}$
Root degree [25]	# pointer-paths of length 1	$\sim \sqrt{\pi n}$	$\sim (4 - \pi)n$
Height [70, 153]	Longest pointer-path	$\sim \frac{1}{2^s} \log n$	$= \mathcal{O}(1)$

Table 1: Parameters of plane increasing trees and the corresponding parameters in relaxed binary trees of right height at most one. The constant $s \approx 0.27846$ is the positive solution of $se^{s+1} = 1$.

3

YOUNG TABLEAUX

3.1	Rectangular Young tableaux with local decreases [P8] .	29
3.2	Young tableaux with periodic walls [P15]	37
3.3	Periodic Pólya urns, the density method and asymptotics of Young tableaux [P28]	44

The enumeration of Young tableaux is a subject I started after my PhD, working with my colleagues in France, Cyril Banderier and Phillipe Marchal. Most of the work was started during my time as a postdoc at the Université Sorbonne Paris Nord in 2017. All these results are fully independent of my PhD and demonstrate my ability to dive into new research areas.

In Section 3.1, we introduce the new model of Young tableaux with walls, in which some neighboring cells may not have to obey any order constraints. We present several bijections to trees and lattice paths, and we introduce the main tool of this chapter: the density method. We developed it to efficiently count and sample uniformly at random any given partially ordered set.

In Section 3.2, we present the solution of the enumeration problem for further families of Young tableaux with walls focusing on periodically repeating patterns using again the density method. We use these results to prove that the corresponding generating functions are either algebraic, hypergeometric, D-finite, or D-algebraic.

In Section 3.3, we introduce the new model of periodic Pólya urns and derive limit laws for its evolution. This urn model allows us to derive the limit law of the south-east corner in a random periodic triangular Young tableau, which we then use to analyze random surfaces arising from Young tableaux.

3.1 RECTANGULAR YOUNG TABLEAUX WITH LOCAL DECREASES AND THE DENSITY METHOD FOR UNIFORM RANDOM GENERATION [P8]

In this section, we present the results from [P8] and partly from [P15] on a generalization of Young tableaux. As predicted by Anatoly Vershik in [174], the twenty-first century should see a lot of challenges and advances on the links between probability theory and (algebraic) combinatorics. A key role is played here by Young tableaux, because of their ubiquity in representation theory [134] and in algebraic combinatorics, as well as their relevance in many other different fields; see, e.g., [173].

Definition 3.1.1 (Young tableau). *A Young tableau of size n is an array with columns of (weakly) decreasing height, in which each cell is labelled, and where the labels run from 1 to n and are strictly increasing along rows from left to right and columns from bottom to top.*

In other words, we use the French convention of drawing tableau. This basic definition is all we will need and we refer to [134] for more details. Our generalization is motivated by the following questions: What happens if we allow exceptionally some consecutive cells with decreasing labels? Does this variant lead to nice formulas if these local decreases are regularly placed? Is it related to other mathematical objects or theorems? How to generate them uniformly at random?

As illustrated in Figure 13, we put a bold red edge between the cells which are allowed to be decreasing. Therefore these two adjacent cells can have decreasing labels (like 19 and 12 in the top row of Figure 13, or 11 and 10 in the untrustable Fifth column), or as usual increasing labels (like 13 and 15 in the bottom row of Figure 13). We call these bold red edges “walls”.

7	18	19	12	21	20	17
2	6	8	9	10	14	16
1	3	4	5	11	13	15

Figure 13: We consider Young tableaux in which some pairs of (horizontally or vertically) consecutive cells are allowed to have decreasing labels. Such places where a decrease is allowed (but not compulsory) are drawn by a bold red edge, which we call a “wall”.

For Young tableaux of shape $n \times 2$ several cases lead directly to nice enumerative formulas for the total number of tableaux with $2n$ cells:

1. Walls everywhere: $(2n)!$
2. Horizontal walls everywhere: $\frac{(2n)!}{2^n}$
3. Horizontal walls everywhere in left column: $(2n - 1)!! = \frac{(2n)!}{2^n n!}$
4. Vertical walls everywhere: $\binom{2n}{n} = \frac{(2n)!}{(n!)^2}$
5. No walls: $\frac{1}{n+1} \binom{2n}{n} = \frac{(2n)!}{(n+1)(n!)^2}$

3.1.1 Young tableaux of shape $n \times 2$ and binary trees

We now consider Young tableaux of shape $n \times 2$, allowing some walls between their two columns; see Figure 14. They nicely illustrate the diversity of combinatorial objects which can be related to tableaux with walls. We will show two different bijections both proving the following enumeration result.

Theorem 3.1.2. *The number of $n \times 2$ Young tableaux with k vertical walls is equal to*

$$v_{n,k} = \frac{1}{n+1-k} \binom{n}{k} \binom{2n}{n}.$$

Let us present the bijection involved in proof of the previous theorem. It maps two-column Young tableaux of size $2n$ with k walls to Dyck paths without the positivity constraint of length $2n$ and k coloured down steps. These paths start at the origin, end on the x -axis and are composed out of up steps $(1, 1)$, and coloured down steps $(1, -1)$ which are either red or blue. Now, given an arbitrary two-column Young tableau, the m th step of the associated path is an up step if the entry m appears in the left column, while the m th step is a down step, if the m th entry appears in the right column. Furthermore, we associate colours to the down steps: If the m th down step is in a row with a wall we colour it red, and blue otherwise. Thus, $v_{n,k}$ counts the number of paths with exactly k red down steps, which we then count using the Chung–Feller Theorem [57].

As a simple consequence, we get the following result.

Corollary 3.1.3. *The average number of linear extensions of a random $n \times 2$ Young tableau with k walls, where the location of these walls is chosen uniformly at random, is*

$$\frac{1}{n+1-k} \binom{2n}{n}.$$

This gives us immediately the following limit law.

Theorem 3.1.4. *Let X_n be the random variable for the number of walls in a random $n \times 2$ Young tableau chosen uniformly at random. The rescaled random variable $\frac{X_n - n/2}{\sqrt{n/4}}$ converges to the standard normal distribution $\mathcal{N}(0, 1)$.*

The further analysis of these tableaux draws from [P15] and is included here as it nicely continues the analysis of $n \times 2$ tableaux. First, the following proposition gives a new combinatorial meaning to some entries in the OEIS [167], such as [OEIS A000108](#), [OEIS A000984](#), [OEIS A002457](#), [OEIS A002802](#), and [OEIS A020918](#).

Proposition 3.1.5. *The generating function of $n \times 2$ Young tableaux with k walls is equal to*

$$V_k(z) := \sum_{n \geq 0} v_{n,k} z^n = \frac{\text{Cat}(k-1) z^{k-1}}{(1-4z)^{(2k-1)/2}} \quad \text{with} \quad \text{Cat}(n) = \frac{1}{n+1} \binom{2n}{n}.$$

14	12
10	13
9	11
8	7
4	6
3	5
2	1

Figure 14: A $n \times 2$ Young tab. with walls.

The generating polynomial with respect to the number of walls is

$$v_n(u) := \sum_{k=0}^n v_{n,k} u^k = \text{Cat}(n)((1+u)^{n+1} - u^{n+1}). \tag{5}$$

It is noteworthy that $v_{n,k}$ is at the same time divisible by $\text{Cat}(n)$ and $\text{Cat}(k-1)$, and, obviously, (5) demands a simple combinatorial explanation. The following classical lemma will allow us to give a bijective explanation of all these facts. The key observation is that every element in the first column corresponds to an internal node and every element in the second column to a leaf.

Lemma 3.1.6. *Young tableaux of shape $n \times 2$ are in bijection with binary trees that have n internal nodes.*

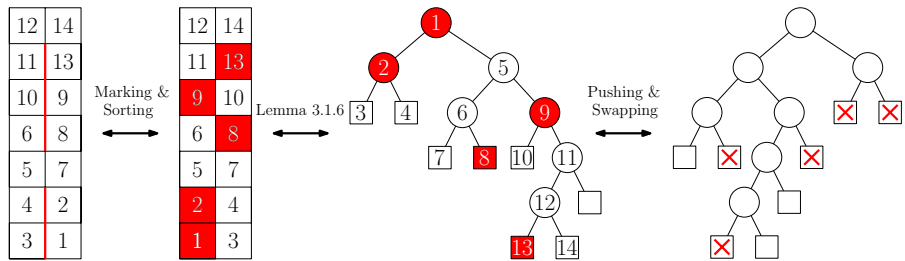


Figure 15: The bijection between $n \times 2$ Young tableaux with k walls and binary trees with k marked leaves from Theorem 3.1.7. Here $n = 14$ and $k = 5$.

The following bijection consists of (possibly) 3 steps and is shown on an example in Figure 15. First, we mark every entry in the second column that is in a row with a wall and remove the wall. Then, we sort each row to get a standard $n \times 2$ Young tableau (yet, with k markers).

Second, we transform this tableau together with its markers into a binary tree using Lemma 3.1.6. If no internal nodes are marked, then we are finished; yet if some internal nodes are marked, then we perform the following step.

Third, we inductively transform this binary tree into a binary tree with marked leaves. Start from the right-most leaf in the right branch of the root and move upwards. If an internal node is marked, push all markers to the leaves of the left subtree and thereafter swap the left and right subtree. Continue until you reach the root.

For the reverse bijection, we distinguish two cases: Either the right-most leaf is marked or not. If it is not marked we reverse only steps 1 and 2, while if it is marked, we reverse all three steps. Let us summarize this result in the following theorem.

Theorem 3.1.7. *Young tableaux of shape $n \times 2$ with k walls are in bijection with binary trees with n internal nodes and k marked leaves.*

3.1.2 Horizontal walls and the hook-length formula

The hook-length formula is a well-known formula to enumerate standard Young tableaux of a given shape (see, e.g., [134, 173]). What happens if we add walls in these tableaux? Let us first consider the case of a Young tableau of size n such that its walls cut the corresponding tableau into m disconnected parts without walls of size k_1, \dots, k_m (e.g., some walls form a full horizontal or vertical line). Then, the number of fillings of such a tableau is trivially:

$$\frac{n!}{k_1! \dots k_m!} \prod_{i=1}^m \text{HookLengthFormula}(\text{subtableau of size } k_i).$$

So in the remainder of this section, we focus on walls which are not trivially splitting the problem into subproblems: They are the only cases for which the enumeration (or the random generation) is indeed challenging.

We continue our study with families of Young tableaux of shape $m \times n$ having some local decreases at places indicated by horizontal walls in the left column. We will need the following lemma counting special fillings of Young tableaux.

Lemma 3.1.8. *The number of $n \times 2$ “Young tableaux” with 2λ cells filled with the numbers $1, 2, \dots, 2n$ for $n \geq \lambda$ such that (the number $2n$ is used and) all consecutive numbers between the minimum of the second column and $2n$ are used is equal to*

$$\binom{2n}{\lambda} - \binom{2n}{\lambda - 1}.$$

This result is the key ingredient to enumerate tableaux with horizontal walls.

Theorem 3.1.9. *The number of $n \times 2$ Young tableaux of size $2n$ with k walls in the first column at heights $0 < h_i < n$, $i = 1, \dots, k$ with $h_i < h_{i+1}$ is equal to*

$$\frac{1}{2n+1} \prod_{i=1}^{k+1} \binom{2h_i + 1}{h_i - h_{i-1}},$$

with $h_0 := 0$ and $h_{k+1} := n$.

Remark 3.1.10. Denoting consecutive relative distances of the walls by $\lambda_i := h_i - h_{i-1}$ for $i = 1, \dots, k+1$ the previous result can be stated as

$$\frac{1}{2n+1} \prod_{i=1}^{k+1} \binom{2(\lambda_1 + \dots + \lambda_i) + 1}{\lambda_i}.$$

Let us now also give the general formula for $n \times m$ Young tableaux with walls of lengths $m-1$ from columns 1 to $m-1$, i.e., a hole in

column m and nowhere else in a row with walls. Before we state the result, let us define for integers n, k the falling factorial $(n)_k := n(n-1) \cdots (n-k+1)$ and for integers n, m_1, \dots, m_k such that $n \geq m_1 + \dots + m_k$ the (shortened) multinomial coefficient $\binom{n}{m_1, m_2, \dots, m_k} := \frac{n!}{m_1! m_2! \cdots m_k! (n - m_1 - \dots - m_k)!}$.

Theorem 3.1.11. *The number of $n \times m$ Young tableaux of size mn with k walls from column 1 to $m-1$ at heights $0 < h_i < n$, $i = 1, \dots, k$ with $h_i < h_{i+1}$ is equal to*

$$\frac{(m-1)!}{(mn+m-1)_{m-1}} \left(\prod_{i=1}^{k+1} \prod_{j=1}^{m-2} \binom{\lambda_i+j}{j}^{-1} \right) \left(\prod_{i=1}^{k+1} \binom{m \sum_{\ell=1}^i \lambda_\ell + m - 1}{\lambda_i, \dots, \lambda_i} \right),$$

where $\lambda_i := h_i - h_{i-1}$ and the λ_i 's in the multinomial coefficients appear $m-1$ times.

As a special case, consider tableaux with walls between every row and a hole in the last column, i.e., $\lambda_i = 1$ for all i . This gives the general formula $\frac{(mn)!}{n!(m!)^n}$, for $n \times m$ tableaux; see [OEIS A001147](#) for $m = 2$ and [OEIS A025035](#) to [OEIS A025042](#) for the special cases $m = 3, \dots, 10$.

Now that we gave several examples of closed-form formulas enumerating some families of Young tableaux with local decreases, we go to harder families which do not necessarily lead to a closed-form result. However, we shall see that we have a generic method to get useful alternative formulas (based on recurrences), also leading to an efficient uniform random generation algorithm.

3.1.3 The density method, D-finiteness, random generation

In this section, we present a generic approach which allows us to enumerate and generate any shape involving some walls located at periodic positions. To keep it readable, we illustrate it with a specific example (without loss of generality).

So, we now illustrate the method on the case of a $2n \times 3$ tableau where we put walls on the right and on the left column at height $2k$ (for $1 \leq k \leq n-1$); see the leftmost tableau in [Figure 16](#). In order to have an easier description of the algorithm (and more compact formulas), we generate/enumerate first similar tableaux with an additional cell at the bottom of the middle column, see the middle tableau in [Figure 16](#): It is a polyomino Poly_n with $6n+1$ cells. There are trivially $(6n+1)!$ fillings of this polyomino with the numbers 1 to $6n+1$. Some of these fillings are additionally satisfying the classical constraints of Young tableaux (i.e., the labels are increasing in each row and each column), with some local decreases allowed between cells separated by a wall. Let f_n be the number of such constrained fillings.

To compute f_n we use a generic method which we call the *density method*. It relies on a geometric point of view of the problem: Let

$N := 6n + 1$ be the total number of cells and consider the hypercube $[0, 1]^N$ in which we associate to each coordinate a cell of Polyo_n . To almost every element $\alpha \in [0, 1]^N$ (more precisely, every element with all coordinates distinct) we can associate a filling of Polyo_n : Put 1 into the cell of Polyo_n corresponding to the smallest coordinate of α , 2 into the cell of Polyo_n corresponding to the second smallest coordinate of α and so on. In other words, if the j th coordinate of α is the i th biggest element, then we assign the value i to the cell j . This filling is not necessarily respecting all increasing constraints, but this operation is readily reversed by associating to every legitimate filling of Polyo_n a region of $[0, 1]^{6n+1}$ which corresponds to a polytope. The key observation now is that the volume of this polytope is equal to $1/N!$. Let \mathcal{P} be the set of all polytopes corresponding to correct fillings of Polyo_n (i.e., respecting the order constraints). Then, a uniformly random element \mathcal{P} corresponds to a uniformly random filling of Polyo_n . This \mathcal{P} is also known as the *order polytope* in poset theory.

What we call the density method is an appropriate combination of recurrences and integral representations of order polytope volumes in order to enumerate poset structures. For this reason, it could also be called the *polytope volume method*. Some ancestors of this natural idea can be found in [20, 29, 77, 149]. It should also be mentioned that several works by Stanley (see for example his nice survey [172]) contributed to propagating interest in this idea, e.g., in connection with variants of the enumeration of zig-zag permutations (permutations which have a periodic succession of rises and falls [4, 32]); this led to the articles [21, 133, 139]. Together with Philippe Marchal, we further developed this density method in [15, 16, 138, 140], as a way to analyse structures like permutations, trees, Young tableaux, all with additional order constraints on their labels.

Let us explain how the density method works. It requires two more ingredients. The first one is illustrated in Figure 16: It is a generic building block with 7 cells with names X, Y, Z, R, S, V, W . We put into each of these cells a number from $[0, 1]$, which we call x, y, z, r, s, v, w , respectively. The second ingredient is the sequence of polynomials $p_n(x)$, defined by the following recurrence:

$$p_{n+1}(z) = \int_0^z \int_x^z \int_0^y \int_r^z \int_z^1 \int_y^w p_n(v) dv dw ds dr dy dx,$$

with $p_0 = 1$. These nested integrals encode the full structure of the problem (i.e. all the inequalities): each integral corresponds to one cell, and the range corresponds to the inequalities. For example, the innermost integral with respect to v is associated with the cell V and the constraint that $Y < V < W$.

Let us now give a more algorithmic presentation of our method:

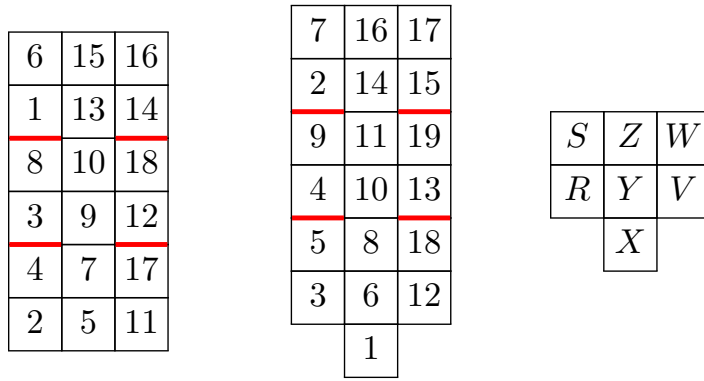


Figure 16: Left: A $2n \times 3$ Young tableau with walls. Centre: Our algorithm first generates a related labelled shape, Polyo_n , with one more cell in its bottom. (removing this cell and relabelling the remaining cells gives the left tableau). Right: The “building block” of 7 cells. Each polyomino Polyo_n is made of n overlapping building blocks.

Density method algorithm

- 1 *Initialization*: Order the building blocks from $k = n - 1$ (top) to $k = 0$ (bottom). Start with $k := n - 1$ and put into its cell Z a random number z with density $p_n(z) / \int_0^1 p_n(t) dt$. Repeat the following process until $k = 0$:
- 2 *Filling*: Put into the cells X, Y, R, S, V, W random numbers x, y, r, s, v, w with conditional density

$$g_{k,z}(x, y, r, s, v, w) := \frac{1}{p_{k+1}(z)} p_k(x) \mathbf{1}_{P_z},$$
 where $\mathbf{1}_{P_z}$ is the indicator function of the k th building block (with value z in cell Z):

$$\mathbf{1}_{P_z} := \mathbf{1}_{\{0 \leq x \leq y \leq z, 0 \leq r \leq y, r \leq s \leq z, z \leq w \leq 1, y \leq v \leq w\}}.$$
- 3 *Iteration*: Consider X as a the Z of the next building block. Set $k := k - 1$ and go to step 2.

Theorem 3.1.12. *The density method algorithm is a uniform random generation algorithm with quadratic time complexity and linear space complexity.*

Remark 3.1.13. If one wants to generate many diagrams and not just one, then it is valuable to make a precomputation phase computing and storing all the polynomials p_n . The rest of the algorithm is the same. For each new object generated, this is saving $O(n^2)$ time, to the price of $O(n^2)$ memory. The algorithm is globally still of quadratic time complexity (because of the evaluation at each step of $p_k(x)$, while $p_{k+1}(z)$ was already evaluated).

Remark 3.1.14. If one directly wants to generate $2n \times 3$ Young tableaux with decreases instead of our strange polyomino shapes Polyo_n , then one still uses the same relation between p_{n+1} and p_n but p_0 is not defined and p_1 has a more complicated form. Another way is to generate Polyo_n , and to reject all the ones not having a 1 in the bottom cell, then to remove this bottom cell and to relabel the remaining cells from 1 to $6n$ (see Figure 16). This still gives a fast algorithm of $O(n^2)$ time complexity (the only difference being the cost of the initial algorithm which is the multiplicative constant included in the big-O).

Using dynamic programming or clever backtracking algorithms allows hardly to compute the sequence f_n (the number of fillings of the diagram) for $n \geq 3$. In the same amount of time, the density method allows us to compute thousands of coefficients via the relation $f_n = (6n + 1)! \int_0^1 p_n(z)$, where the polynomial $p_n(z)$ is computed via the recurrence

$$p_{n+1}(z) = \int_0^z \frac{1}{24} (z-1)(x-z)(3x^3 - 7x^2z - xz^2 - z^3 - 2x^2 + 4xz + 4z^2)p_n(x) dx.$$

This gives the sequence

$$(f_n)_{n \geq 0} = (1, 12, 8550, 39235950, 629738299350, 26095645151941500, 2323497950101372223250, 392833430654718548673344250, 115375222087417545717234273063750, \dots).$$

As far as we know, there is no further simple expression for this sequence. This concludes our analysis of the model given by Figure 16.

We can additionally mention that the generating function associated to the sequence of polynomials $p_n(x)$ has a striking property:

Theorem 3.1.15. *The generating function $G(t, z) := \sum_{n \geq 0} p_n(z)t^n$ is D-finite in z .*

Note that $G(t, z)$ is D-finite in z , but in general not D-finite in t . When it is D-finite in t , our algorithm has a better complexity (namely, a $O(n^{3/2})$ time complexity), because it is then possible to evaluate $p_n(z)$ in time $O(\sqrt{n} \ln n)$ instead of $O(n)$; see [34, Chapter 15].

3.2 YOUNG TABLEAUX WITH PERIODIC WALLS: COUNTING WITH THE DENSITY METHOD [P15]

In the previous Section 3.1, we introduced rectangular Young tableaux with walls and explored their links with binary trees, hook-length-like formulas, and studied their uniform random generation. In this section, we present the results from [P15], and we will consider structures where the location of the walls obey some periodicity rules. This

will nicely illustrate the rich diversity of the corresponding generating functions and some of their unexpected closure properties. More precisely, let a tableau \mathcal{Y} with periodic walls be the concatenation (as shown in Figure 17) of n copies of a building block \mathcal{B} of cells (i.e., $\mathcal{Y} = \mathcal{B}^n$) and then filled with all integers from $\{1, \dots, |\mathcal{B}|n\}$ respecting the induced order constraints.

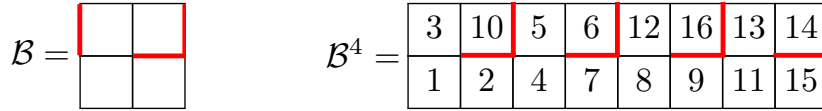


Figure 17: Left: example of a block \mathcal{B} of shape 2×2 . Right: a Young tableau with periodic walls at positions imposed by concatenations of \mathcal{B} .

Counting the number of linear extensions of a poset is known to be a hard problem; it was even proven to be #P-complete by Brightwell and Winkler [48]. The enumeration is even still #P-complete when restricted to posets of height 2; see Dittmer and Pak [62]. This enumeration challenge is also strongly connected to the question of uniform random generation. While there exist thousands of *ad hoc approaches* to generate combinatorial structures (see, e.g., [118, 148]), there are few *generic methods* for their uniform random generation: one could name rejection algorithms and Markov chain sampling [109], the recursive method [87, 148], generating trees [11], and Boltzmann sampling [72]. Another important method that we want to promote and to add to this list is the *density method*. We will again illustrate its power and its flexibility in this section by applying it to many different posets.

3.2.1 Jenga tableaux and the density method

The towers of the game Jenga inspired the following fruitful generalization of Young tableaux. Consider a column of n cells to which one attaches at row i , ℓ_i cells to the left and r_i cells to the right. The $N := n + \sum_i \ell_i + r_i$ cells of this structure are then filled with the integers 1 to N under the constraint that each row and the middle column have increasing labels, and each label appears only once; see Figure 18.

The density method is the key to enumerate such objects and was introduced in detail in Section 3.1.3. For our current problem, consider the generic building block of a row shown in Figure 18. It consists of the ℓ cells U_1, \dots, U_ℓ , the r cells V_1, \dots, V_r , one cell Z , and one cell X . To each of these cells we assign a random number from $[0, 1]$. Then, we define a sequence of polynomials $f_n(z)$ which encode the order constraints satisfied by these cells up to row n :

$$f_n(z) := \int_{z < v_1 < 1} \dots \int_{v_{r-1} < v_r < 1} \int_{0 < u_\ell < z} \dots \int_{0 < u_1 < u_2} \int_{0 < x < z} f_{n-1}(x) dx du_1 \dots dv_1.$$

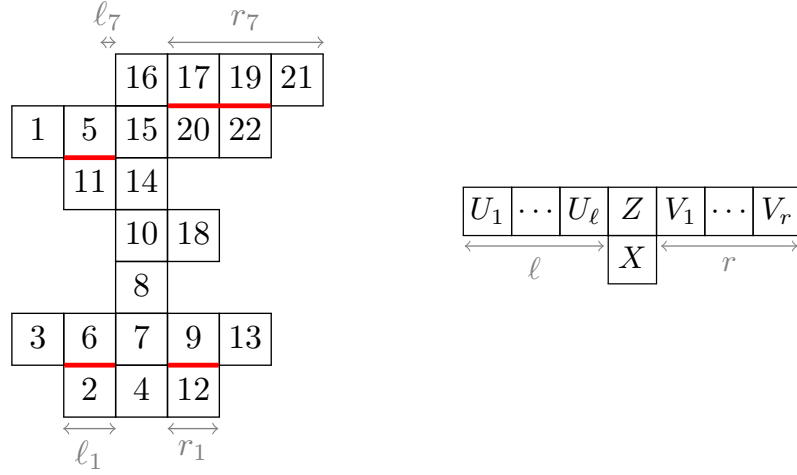


Figure 18: Left: a Jenga tableau with $n = 7$ rows and the left and right sub-sequences $(l_i)_{i=1}^7 = (1, 2, 0, 0, 1, 2, 0)$ and $(r_i)_{i=1}^7 = (1, 2, 0, 1, 0, 2, 3)$, respectively. Right: the building block used here in the density method to generate each row iteratively.

Now, the simple block structure of the rows leads to

$$f_n(z) = \frac{z^{\ell_n}(1-z)^{r_n}}{\ell_n!r_n!} \int_0^z f_{n-1}(x) dx,$$

$$f_1(z) := \frac{z^{\ell_1}(1-z)^{r_1}}{\ell_1!r_1!}.$$

The crucial observation is now the following: The value $\int_0^1 f_n(z) dz$ is equal to the volume of the order polytope \mathcal{P} associated to the correct fillings of \mathcal{Y}_n . Thus, $N! \int_0^1 f_n(z) dz$ is equal to the number of legitimate fillings. For more details see Section 3.1.3.

We thus get that the number y_n of Jenga tableaux with n rows is

$$y_n = \left(\sum_{i=1}^n (\ell_i + r_i + 1) \right)! \int_0^1 f_n(x) dx. \tag{6}$$

We now continue with some periodic patterns, that is if there exists an integer $p > 0$ such that $\ell_{i+p} = \ell_i$ and $r_{i+p} = r_i$ for all $i \geq 1$. The smallest such p is called the period. The simplest possible period is $p = 1$; this case leads to a noteworthy generating function.

Theorem 3.2.1 (D-finiteness of periodic Jenga tableaux with $p = 1$). *The bivariate generating function $F(t, z) = \sum_{n \geq 1} f_n(z)t^n$ is D-finite in t and z . Accordingly, the counting sequence $(y_n)_{n \geq 1}$ given by Equation (6) of Jenga tableaux with n rows is P-recursive.*

Note that set partitions of equal set sizes fall into the class of Theorem 3.2.1 as $\ell_i = m - 1$ and $r_i = 0$ for all $i \geq 0$. Let us also mention the following unexpected link.

As further examples of Jenga shapes, the density method also gives:

Proposition 3.2.2. For $r_i = 0$ for all $i \geq 1$ (see Figure 18), the number y_n of Jenga tableaux satisfies

$$y_n = \frac{(\sum_{i=1}^n (\ell_i + 1))!}{\prod_{i=1}^n \ell_i! (\sum_{j=1}^i (\ell_j + 1))}.$$

Specializing these tableaux to periodic cases leads to some hypergeometric formulas.

Proposition 3.2.3. Consider Jenga tableaux with period p , arbitrary left sequence $(\ell_i)_{i=0}^p$ and right sequence $(r_i)_{i=0}^p = (0, \dots, 0)$ (see Figure 18). Define $L := \sum_{i=1}^p \ell_i$. Then, the number y_n of such tableaux satisfies

$$y_{kp+m} = y_m \left(\frac{(L+p)^L}{\prod_{i=1}^p \ell_i!} \right)^k \prod_{\substack{j=1 \\ j \neq \ell_1 + \dots + \ell_i + i}}^{L+p} \frac{\Gamma\left(k + \frac{j+m}{L+p}\right)}{\Gamma\left(\frac{j+m}{L+p}\right)}.$$

Accordingly, the generating function of such tableaux is the sum of p hypergeometric functions.

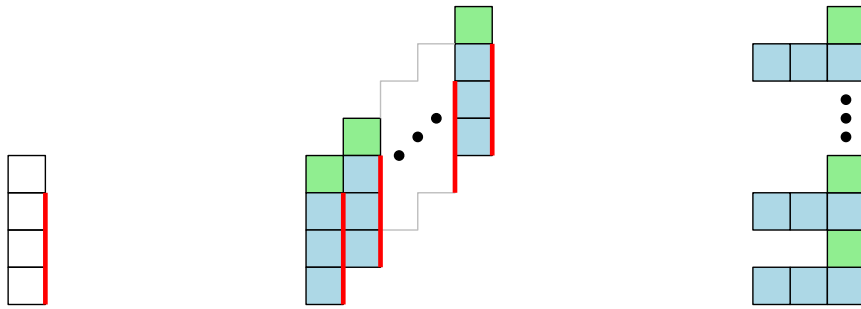


Figure 19: The building block of width 4 (left) is repeated k times and each time shifted up by one cell to form a Young tableau with periodic walls in a diagonal strip (centre). These tableaux are in bijection with periodic Jenga tableaux with period $p = 2$, left sequence $(\ell_i)_{i=1}^2 = (2, 0)$, and right sequence $(r_i)_{i=1}^2 = (0, 0)$ (right).

It is also possible to consider other shapes, such as skew Young tableaux. Finally, we give such an example and thus add walls to a model analysed in [20].

Proposition 3.2.4. Consider tableaux with periodic walls in a diagonal strip of width w between each column in all but the top cell; see Figure 19. Let $b_{w,n}$ be the number of such tableaux with n columns; one has

$$b_{w,n} = \left(\frac{w^{w-2}}{(w-2)!} \right)^n \prod_{j=1}^{w-2} \frac{\Gamma\left(n + \frac{j}{w}\right)}{\Gamma\left(\frac{j}{w}\right)}.$$

3.2.2 Some unusual asymptotics

The density method can also be used to count and generate objects which do not have simple counting formulas. We now present such a class, which is a priori quite simple, but which however leads to rather surprising asymptotics. Thus, this class illustrates well the non-intuitive asymptotic behaviour of our objects.

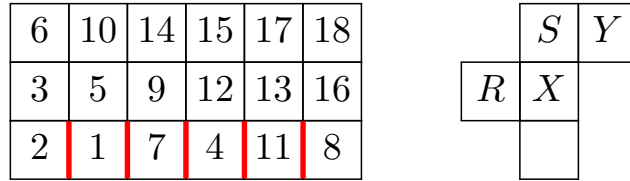


Figure 20: A $3 \times n$ Young tableau with walls in its first row, and the corresponding building block for each column used in the density method.

The increasing label constraints encoded in the building block of Figure 20 directly translate to the following densities

$$f_{n+1}(x, y) := x \int_0^x \int_x^y f_n(r, s) ds dr,$$

$$f_1(x, y) := x(y - x).$$

Then, the number of such tableaux is

$$a_n = (3n + 1)! \int_0^1 \int_0^y f_n(x, y) dx dy.$$

We multiply with $(3n + 1)!$ as the final shape includes a single cell Y on the top right with the maximum, which can therefore be simply removed to create a $3 \times n$ shape. This gives the sequence [OEIS A213863](#):

$$(a_n)_{n \geq 1} = (1, 7, 106, 2575, 87595, 3864040, 210455470, \dots).$$

It counts words where each letter ℓ of an n -ary alphabet occurs 3 times and for each prefix p one has $|p|_\ell = 0$ or $|p|_\ell \geq |p|_j$ for all $j > \ell$, where $|p|_\ell$ counts occurrences of ℓ in p . The bijection with our tableaux follows by mapping letters to columns; see [89] and [P16].

The following result is then obtained by using the methods introduced in Section 2.2.

Theorem 3.2.5. *The number a_n of Young tableaux of length n with shape given by Figure 20 has the following asymptotics*

$$a_n = \Theta \left(n! 12^n e^{a_1(3n)^{1/3}} n^{-2/3} \right),$$

where $a_1 \approx -2.338$ is the largest root of the Airy function of the first kind.

3.2.3 A classification of 2×2 periodic shapes

We now consider Young tableaux made of the concatenation of 2×2 blocks with walls; see Figure 17. This model is interesting as it leads to rather different natures of generating functions. Indeed, Table 2 hereafter summarizes the main results and groups them into four classes according to their counting sequences: simple products, algebraic, hypergeometric, or D-algebraic. Surprisingly, some of these sequences connect with classical combinatorial objects!

There are 6 possible non-trivial locations for walls in a 2×2 block (due to possible coincidences of the walls on the right when the blocks are concatenated). Thus, there are in total $2^6 = 64$ different types of building blocks. Most of these blocks come in pairs, as rotating a tableau by 180 degrees and reversing the labels gives a bijection.

First, one gets 40 blocks for which the walls create independent regions. This leads to 19 distinct sequences P_1 – P_{19} , all having a simple product formula.

Second, we consider the 4 blocks without vertical walls. They lead to 3 distinct sequences A_1 – A_3 , which all have an algebraic generating function. For A_1 and A_2 the proof uses a bijection to Dyck paths. For A_3 we decompose at the first wall that cannot be removed and get the recurrence $a_n = \text{Cat}(2n) + \sum_{i=1}^n \text{Cat}(2i-1)a_{n-i}$, which we then solve with generating functions.

Third, we consider 14 blocks with a uniquely determined minimum or maximum. They lead to 7 distinct sequences H_1 – H_7 , all hypergeometric. The models H_1 – H_5 are Jenga-like tableaux from Section 3.2.1 that satisfy $l_i = 0$ for all i . For the models H_6 and H_7 we use a recursive approach, decomposing with respect to the location of the unique minimum or maximum.

Fourth, there are three blocks which show a zig-zag-like pattern. By analogy to the known zig-zag permutations, we conjecture Z_2 and Z_3 to be non-D-finite. For Z_1 we are able to prove that the exponential generating function is D-algebraic, and not D-finite, i.e., it satisfies a non-linear differential equation and no linear one. For this purpose we use Carlitz' theory [55] of generalized alternating permutations.

A pleasant feature of the density method approach is that it is automatable. See <https://dmg.tuwien.ac.at/mwallner/Jenga/> for our Maple package dedicated to the enumeration of tableaux with walls.

In conclusion, we have seen that Young tableaux with walls are a rich model, leading (via the density method) to new varieties of recurrences, interesting *per se*, mixing finite differences and differential operators (challenging the current state of the art in computer algebra and holonomy theory!), and surprising asymptotics (challenging the current state of the art in analytic combinatorics!).

Class	Shape	Formula	Class	Shape	Formula	Class	Shape	Formula
P1		$4 \frac{(4n)!}{24^n}$	P6		$\frac{(4n)!}{6^n}$	P13		$6 \frac{(4n)!}{3^n}$
P2		$\frac{(4n)!}{12^n}$	P7		$3 \frac{(4n)!}{6^n}$	P14		$\frac{(4n)!}{2^n}$
P3		$3 \frac{(4n)!}{12^n}$	P8		$\frac{8}{5} (4n)! \left(\frac{5}{24}\right)^n$	P15		$2 \frac{(4n)!}{2^n}$
P4		$\frac{(4n)!}{8^n}$	P9		$\frac{(4n)!}{4^n}$	P16		$\frac{(4n)!}{(2n)!2^n}$
P5		$4 \frac{(4n)!}{8^n}$	P10		$2 \frac{(4n)!}{4^n}$	P17		$2 \frac{(4n)!}{(2n)!2^n}$
			P11		$4 \frac{(4n)!}{4^n}$	P18		$\frac{(4n)!}{(2n)!}$
			P12		$\frac{(4n)!}{3^n}$	P19		$(4n)!$

Class	Shape	Sequence	OEIS
A1		$\text{Cat}(2n) = \frac{1}{2n+1} \binom{4n}{2n}$	A048990
A2		$\binom{4n}{2n}$	A001448
A3		$2^{2n+1} \text{Cat}(n) - \text{Cat}(2n+1)$	A079489
H1		$\prod_{i=1}^n (4i-1)(4i-3)$	A101485
H2		$\prod_{i=1}^n (2i-1)(4i-1)$	A159605
H3		$2^{n+1} n! \prod_{i=1}^n (4i-3)$	$2^{n+1} \cdot \text{A084943}$
H4		$\binom{4n}{n} \prod_{i=1}^n (3i-1)$	$\binom{4n}{n} \cdot \text{A008544}$
H5		$\binom{4n}{n} \prod_{i=1}^n (3i-2)$	$\binom{4n}{n} \cdot \text{A007559}$
H6		$2^n n! \prod_{i=1}^n (4i-3)$	$n! \cdot \text{A084948}$
H7		$\prod_{i=1}^n (2i-1)(4i-1)$	A159605
Z1		$\frac{\cos(t/\sqrt{2})^2 + \cosh(t/\sqrt{2})^2}{2 \cos(t/\sqrt{2}) \cosh(t/\sqrt{2})}$	related to A211212
Z2		?	???
Z3		?	???

Table 2: The 64 different models of 2×2 blocks for tableaux with periodic walls grouped into 4 different classes: (P) simple products, (A) algebraic, (H) hypergeometric, (Z) zig-zag. The length n is equal to the number of repeated blocks. The model Z1 is D-algebraic and not D-finite, which is what we conjecture for the models Z2 and Z3.

3.3 PERIODIC PÓLYA URNS, THE DENSITY METHOD AND ASYMPTOTICS OF YOUNG TABLEAUX [P28]

In this section, we present the results of [P28]. We first introduce a new class of Pólya urns for which we solve the enumeration problem and derive limit laws for its evolution. Then, we show how this urn is connected to triangular Young tableaux and give some of the first results on its limit shape.

Pólya urns were introduced in a simplified version by George Pólya and his PhD student, Florian Eggenberger, in [75, 76, 156], with applications to disease spreading and conflagrations. They constitute a powerful model, which regularly finds new applications: see, for example, Rivest's recent work on auditing elections [160], or the analysis of deanonymization in Bitcoin's peer-to-peer network [80]. They are well-studied objects in combinatorial and probabilistic literature [9, 83, 136], because they offer fascinatingly rich links with numerous objects like random recursive trees, m -ary search trees, and branching random walks (see, e.g., [10, 56, 102, 103]).

In the *Pólya urn model*, one starts with an urn with b_0 black balls and w_0 white balls at time 0. At every discrete time step, one ball is drawn uniformly at random. After inspecting its colour, this ball is returned to the urn. If the ball is black, a black balls and b white balls are added; if the ball is white, c black balls and d white balls are added (where $a, b, c, d \in \mathbb{N}$ are nonnegative integers). This process can be described by the so-called *replacement matrix*:

$$M = \begin{pmatrix} a & b \\ c & d \end{pmatrix}, \quad a, b, c, d \in \mathbb{N}.$$

We call an urn *balanced* if $a + b = c + d$. In other words, in every step the same number of balls is added to the urn. This results in a deterministic number of balls after n steps: $b_0 + w_0 + (a + b)n$ balls. Let us now introduce a more general model.

Definition 3.3.1. *A periodic Pólya urn of period p with replacement matrices M_1, M_2, \dots, M_p is a variant of a Pólya urn in which the replacement matrix M_k is used at steps $np + k$. Such a model is called balanced if each of its replacement matrices is balanced.*

For $p = 1$, this model reduces to the classical model of Pólya urns with one replacement matrix.

Definition 3.3.2. *Let $p, \ell \in \mathbb{N}$. We call a Young-Pólya urn of period p and parameter ℓ the periodic Pólya urn of period p (with $b_0 \geq 1$ to avoid degenerate cases) and replacement matrices*

$$M_1 = M_2 = \dots = M_{p-1} = \begin{pmatrix} 1 & 0 \\ 0 & 1 \end{pmatrix} \text{ and } M_p = \begin{pmatrix} 1 & \ell \\ 0 & 1 + \ell \end{pmatrix}.$$

Example 3.3.3. Consider a Young–Pólya urn with parameters $p = 2$, $\ell = 1$, and initial conditions $b_0 = w_0 = 1$. The replacement matrices are $M_1 := \begin{pmatrix} 1 & 0 \\ 0 & 1 \end{pmatrix}$ for every odd and $M_2 := \begin{pmatrix} 1 & 1 \\ 0 & 2 \end{pmatrix}$ for every even step. For more details on this model see [14]. In the sequel, we will use it as a running example to explain our results.

Figure 21 illustrates the evolution of this urn. Each node of the tree corresponds to the current composition of the urn (number of black and white balls). At the beginning, one starts with $b_0 = 1$ black ball and $w_0 = 1$ white. In the first step, the matrix M_1 is used and leads to two different compositions. In the second step, matrix M_2 is used, in the third step, matrix M_1 is used again, in the fourth step, matrix M_2 , etc. Therefore, this leads to the following compositions: $(2, 1)$ and $(1, 2)$ at time 1, $(3, 2)$, $(2, 3)$ and $(1, 4)$ at time 2, $(4, 2)$, $(3, 3)$, $(2, 4)$ and $(1, 5)$ at time 3.

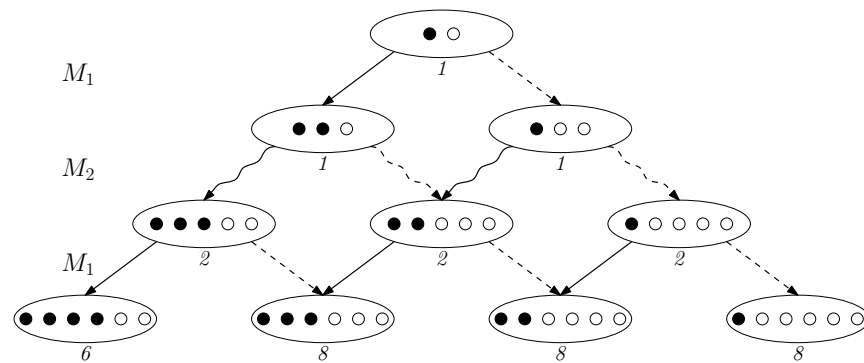


Figure 21: The evolution of the Young–Pólya urn with period $p = 2$ and parameter $\ell = 1$ with one initial black and one initial white ball. Black arrows mark that a black ball was drawn, dashed arrows mark that a white ball was drawn. Straight arrows indicate that the replacement matrix M_1 was used, curly arrows show that the replacement matrix M_2 was used. The number below each node is the number of possible transitions to reach this state.

In fact, each of these states may be reached in different ways, and such a sequence of transitions is called a *history*. (Some authors also call it a *scenario*, an *evolution*, or a *trajectory*.) Each history comes with weight one. Implicitly, they induce a probability measure on the states at step n . So, let B_n and W_n be random variables for the number of black and white balls after n steps, respectively. As our model is balanced, $B_n + W_n$ is a deterministic process, reflecting the identity

$$B_n + W_n = b_0 + w_0 + n + \ell \left\lfloor \frac{n}{p} \right\rfloor. \tag{7}$$

So, from now on, we concentrate our analysis on B_n .

3.3.1 The generalized gamma product distribution

For the classical model of a single balanced Pólya urn, the limit law of the random variable B_n is fully known and consists of a rich variety of distributions. To name a few, let us mention the uniform [82], the normal [10], and the beta and Mittag-Leffler distributions [102, 104]. Periodic Pólya urns lead to an even larger variety of distributions involving a product of *generalized gamma distributions* [170].

Definition 3.3.4. The *generalized gamma distribution* $\text{GenGamma}(\alpha, \beta)$ with real parameters $\alpha, \beta > 0$ is defined on $(0, +\infty)$ by the density function

$$f(t; \alpha, \beta) := \frac{\beta t^{\alpha-1} \exp(-t^\beta)}{\Gamma(\alpha/\beta)},$$

where Γ is the classical gamma function $\Gamma(z) := \int_0^\infty t^{z-1} \exp(-t) dt$.

Remark 3.3.5. Let $\Gamma(\alpha)$ be the gamma distribution¹ of parameter $\alpha > 0$, given on $(0, +\infty)$ by

$$g(t; \alpha) = \frac{t^{\alpha-1} \exp(-t)}{\Gamma(\alpha)}.$$

Then one has $\Gamma(\alpha) \stackrel{\mathcal{L}}{=} \text{GenGamma}(\alpha, 1)$ and, for $r > 0$, the distribution of the r th power of a random variable distributed like $\Gamma(\alpha)$ is

$$\Gamma(\alpha)^r \stackrel{\mathcal{L}}{=} \text{GenGamma}(\alpha/r, 1/r).$$

Our main results also include the *beta distribution* $\text{Beta}(p, q)$ with parameters $p, q > 0$. It is defined by the density $\frac{\Gamma(p+q)}{\Gamma(p)\Gamma(q)} x^{p-1} (1-x)^{q-1}$ on $[0, 1]$. We also introduce the convention that $\text{Beta}(p, q) = 1$ when either $p = 0$ or $q = 0$. The limit distribution of our urns is then expressed as a product of a beta and generalized gamma distributions.

Theorem 3.3.6 (Young–Pólya urns). *The renormalized distribution of black balls in a Young–Pólya urn of period p and parameter ℓ is asymptotically for $n \rightarrow \infty$ given by the following product of distributions:*

$$\frac{p^\delta}{p+\ell} \frac{B_n}{n^\delta} \xrightarrow{\mathcal{L}} \text{Beta}(b_0, w_0) \prod_{i=0}^{\ell-1} \text{GenGamma}(b_0 + w_0 + p + i, p + \ell), \quad (8)$$

with $\delta = p/(p + \ell)$, and $\text{Beta}(b_0, w_0) = 1$ when $w_0 = 0$.

Example 3.3.7. In the case of the Young–Pólya urn with $p = 2$, $\ell = 1$, and $w_0 = b_0 = 1$, one has $\delta = 2/3$. Thus, the previous result shows that the number of black balls converges in law to a generalized gamma distribution:

$$\frac{2^{2/3}}{3} \frac{B_n}{n^{2/3}} \xrightarrow{\mathcal{L}} \text{Unif}(0, 1) \cdot \text{GenGamma}(4, 3) = \text{GenGamma}(1, 3).$$

¹It is traditional to use the same letter for the Γ function and the Γ distribution. Some authors add a second parameter to the Γ distribution, which is set to 1 here.

An extension of the used methods then allows us to obtain the following much more general version.

Theorem 3.3.8 (Triangular balanced urns). *Let $p \geq 1$ and $\ell_1, \dots, \ell_p \geq 0$ be nonnegative integers. Consider a periodic Pólya urn of period p with replacement matrices M_1, \dots, M_p given by $M_j := \begin{pmatrix} 1 & \ell_j \\ 0 & 1 + \ell_j \end{pmatrix}$. Then the renormalized distribution of black balls is asymptotically for $n \rightarrow \infty$ given by the following product of distributions:*

$$\frac{p^\delta}{p+\ell} \frac{B_n}{n^\delta} \xrightarrow{\mathcal{L}} \text{Beta}(b_0, w_0) \prod_{\substack{i=1 \\ i \neq \ell_1 + \dots + \ell_j + j \\ \text{with } 1 \leq j \leq p-1}}^{p+\ell-1} \text{GenGamma}(b_0 + w_0 + i, p + \ell).$$

with $\ell = \ell_1 + \dots + \ell_p$, $\delta = p/(p + \ell)$, and $\text{Beta}(b_0, w_0) = 1$ when $w_0 = 0$.

In the sequel, we call this distribution the *generalized gamma product distribution* and denote it either by $\text{GenGammaProd}(p, \ell, b_0, w_0)$ or, in the more general case, by $\text{GenGammaProd}([\ell_1, \dots, \ell_p]; b_0, w_0)$. We will see in Section 3.3.4 that this distribution is characterized by its moments, which have a nice factorial shape given in Formula (12).

Example 3.3.9 (Staircase periodic Pólya urn). The number B_n of black balls in the Pólya urn of period 3 with replacement matrices

$$M_1 := \begin{pmatrix} 1 & 0 \\ 0 & 1 \end{pmatrix}, M_2 := \begin{pmatrix} 1 & 1 \\ 0 & 2 \end{pmatrix}, \text{ and } M_3 := \begin{pmatrix} 1 & 2 \\ 0 & 3 \end{pmatrix},$$

has the limit law $\text{GenGammaProd}([0, 1, 2]; b_0, w_0)$:

$$\frac{\sqrt{3}}{6} \frac{B_n}{\sqrt{n}} \xrightarrow{\mathcal{L}} \text{Beta}(b_0, w_0) \prod_{i=2,4,5} \text{GenGamma}(b_0 + w_0 + i, 6).$$

3.3.2 Connection with previous results

By [104, Theorem 1.3], the renormalization for the limit distribution of

B_n in an urn with replacement matrix $\begin{pmatrix} 1 & \ell \\ 0 & 1 + \ell \end{pmatrix}$ is equal to $n^{-1/(1+\ell)}$.

For $\ell = 0$ the limit distribution is the uniform distribution, whereas for $\ell = 1$ it is a Mittag-Leffler distribution (see [104, Example 3.1], [82, Example 7]), which simplifies to a half-normal distribution [177] when $b_0 = w_0 = 1$. Thus, using this replacement matrix periodically only every p th round and otherwise Pólya's replacement matrix with $\ell = 0$ changes the renormalization to $n^{-p/(p+\ell)}$.

The rescaling factor $n^{-\delta}$ with $\delta = p/(p + \ell)$ can also be obtained via a martingale computation. The true challenge is to get exact enumeration and the limit law. It is interesting that there exist other families

of urn models exhibiting the same rescaling factor, however, these alternative models lead to different limit laws.

A first natural alternative model consists in averaging the p replacement matrices. This gives a classical triangular Pólya urn satisfying

$$\frac{B_n}{n^\delta} \xrightarrow{\mathcal{L}} \mathfrak{B}, \quad (9)$$

where the distribution of \mathfrak{B} is, e.g., analysed by Flajolet et al. [82] via an analytic combinatorics approach, or by Janson [104] and Chauvin et al. [56] via a probabilistic approach relying on a continuous-time embedding introduced by Athreya and Karlin [8]. For example, averaging the Young–Pólya urn with $p = 2$, $\ell = 1$, and $b_0 = w_0 = 1$ leads

to the replacement matrix $\begin{pmatrix} 1 & 1/2 \\ 0 & 3/2 \end{pmatrix}$.

The corresponding classical urn model leads to a limit distribution with moments given, e.g., by Janson in [104, Theorem 1.7]:

$$\mathbb{E}(\mathfrak{B}^r) = \frac{\Gamma(4/3) r!}{\Gamma(2r/3 + 4/3)}.$$

Comparing these moments with the moments of our distribution (Equation (12) hereafter) proves that these two distributions are distinct. However, it is noteworthy that they have similar tails: we discuss this universality phenomenon in Section 3.3.24.

Another interesting alternative model, called multi-drawing Pólya urn model, consists in drawing multiple balls at once; see Lasmar et al. [129] or Kuba and Sulzbach [125]. Grouping p units of time into one drawing leads to a new replacement matrix. For example, for $p = 2$ and $\ell = 1$ we can approximate a Young–Pólya urn by an urn where at each unit of time 2 balls are drawn uniformly at random. If both of them are black we add 2 black balls and 1 white ball, if one is black and one is white we add 1 black and 2 white ball, and if both of them are white we add 3 white balls. Then the same convergence as in Equation (9) holds, yet again with a different limit distribution, as can be seen by comparing the means and variances; compare Kuba and Mahmoud [123, Theorem 1] with our Example 3.3.16.

Figure 22 shows that the distribution of B_n is spread. This is consistent with our result that the standard deviation and the mean $\mathbb{E}(B_n)$ (blue) have the same order of magnitude. Note that the same happens for classical urn models with replacement matrices being either M_1 or M_2 ; see [82, Figure 1]. In our case, the fluctuations around this mean are given by the generalized gamma product limit law from Equation (8). Previously, this distribution has appeared, e.g., in [107], as an instance of distributions with moments of gamma type (compare the supremum process of the Brownian motion); in [150], as distributions of processes on walks/trees/urns/preferential attachments in graphs; or in [116], as a generalization of several other distributions.

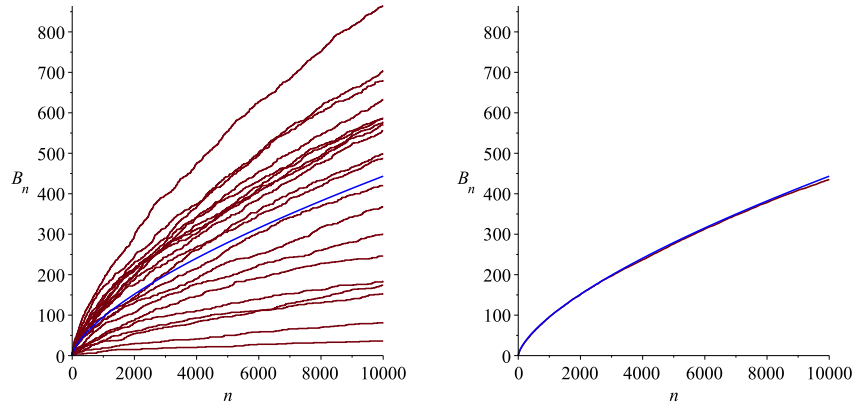


Figure 22: Left: 20 simulations (red) of the number B_n of black balls in the Young–Pólya urn with period $p = 2$ and parameter $\ell = 1$ with initially $b_0 = 1$ black and $w_0 = 1$ white balls, and the mean $\mathbb{E}(B_n)$ (blue). Right: the average (red) of the 20 simulations, fitting almost indistinguishably the limit curve $\mathbb{E}(B_n) = \Theta(n^{2/3})$ (blue).

3.3.3 A functional equation for periodic Pólya urns

3.3.3.1 Urn histories and differential operators

Let $h_{n,b,w}$ be the number of histories of a periodic Pólya urn after n steps with b black balls and w white balls, with an initial state of b_0 black and w_0 white balls. We define the polynomials

$$h_n(x, y) := \sum_{b,w \geq 0} h_{n,b,w} x^b y^w.$$

Note that these are indeed polynomials as there is just a finite number of histories after n steps. Due to the balanced urn model these polynomials are homogeneous. We collect all these histories in the trivariate exponential generating function

$$H(x, y, z) := \sum_{n \geq 0} h_n(x, y) \frac{z^n}{n!}.$$

Example 3.3.10. For the Young–Pólya urn with $p = 2$, $\ell = 1$, and $b_0 = w_0 = 1$ (compare Figure 21), we get for the first three terms

$$H(x, y, z) = xy + (xy^2 + x^2y)z + \left(2xy^4 + 2x^2y^3 + 2x^3y^2\right) \frac{z^2}{2} + \dots$$

The periodic nature of the problem motivates to split the number of histories into p residue classes. Let $H_0(x, y, z)$, $H_1(x, y, z)$, \dots , $H_{p-1}(x, y, z)$ be the generating functions of histories after $0, 1, \dots, p-1$ draws modulo p , respectively. In particular, we have

$$H_i(x, y, z) := \sum_{n \geq 0} h_{pn+i}(x, y) \frac{z^{pn+i}}{(pn+i)!},$$

for $i = 0, 1, \dots, p - 1$ such that

$$H(x, y, z) = H_0(x, y, z) + H_1(x, y, z) + \dots + H_{p-1}(x, y, z).$$

As our urns are balanced there is the deterministic link (7) between the number of black and white balls after n drawings. Thus it is natural to introduce the two shorthands

$$H(x, z) := H(x, 1, z) \quad \text{and} \quad H_i(x, z) := H_i(x, 1, z).$$

What is the nature of these functions? This is what we tackle now.

3.3.3.2 *D-finiteness of history generating functions*

The dynamics of urns are intrinsically related to *partial* differential equations (mixing ∂_x , ∂_y , and ∂_z); see, e.g., [83]. It is a nice surprise that it is also possible to describe their evolution in many cases with *ordinary* differential equations (i.e., involving only ∂_z).

Theorem 3.3.11 (Differential equations for histories). *The generating functions describing a Young–Pólya urn of period p and parameter ℓ with initially $s_0 = b_0 + w_0$ balls, where b_0 are black and w_0 are white, satisfy the following system of p partial differential equations:*

$$\begin{aligned} \partial_z H_{i+1}(x, z) = x(x-1)\partial_x H_i(x, z) + (1 + \ell/p)z\partial_z H_i(x, z) \\ + (s_0 - i\ell/p)H_i(x, z), \end{aligned} \tag{10}$$

for $i = 0, \dots, p - 1$ with $H_p(x, z) := H_0(x, z)$. Moreover, if any of the corresponding generating functions (ordinary, exponential, ordinary probability, or exponential probability) is *D-finite* in z , then all of them are *D-finite* in z .

Experimentally, in most cases a few terms suffice to guess a holonomic sequence in z . We believe that this sequence is always holonomic, yet we were not able to prove it in full generality.

Example 3.3.12. In the case of the Young–Pólya urn with $p = 2$, $\ell = 1$, and $b_0 = w_0 = 1$, the differential equations for histories (10) are

$$\begin{cases} \partial_z H_0(x, z) = x(x-1)\partial_x H_1(x, z) + \frac{3}{2}z\partial_z H_1(x, z) + \frac{3}{2}H_1(x, z), \\ \partial_z H_1(x, z) = x(x-1)\partial_x H_0(x, z) + \frac{3}{2}z\partial_z H_0(x, z) + 2H_0(x, z). \end{cases}$$

In addition to this system of **partial** differential equations, there exist also two **ordinary** linear differential equations in z for H_0 and H_1 , and therefore for their sum $H := H_0 + H_1$, the generating function of all histories.

Note that such *D-finite* equations lead under “generic” conditions to a Gaussian limit law; see [84, Theorem 7] and [85, Chapter IX.7]. It is interesting that these conditions are not fulfilled in our case. Thus, the model of periodic Pólya urns leads to an original analytic situation, which offers a new (non-Gaussian) limit law.

We thus need another strategy to determine the limit law, which we present now in the next section.

3.3.4 Moments of periodic Pólya urns

Let us introduce $m_r(n)$, the r th factorial moment of the distribution of black balls after n steps, i.e.

$$m_r(n) := \mathbb{E} (B_n(B_n - 1) \cdots (B_n - r + 1)).$$

Expressing them in terms of the generating function $H(x, z)$, we have

$$m_r(n) = \frac{[z^n] \frac{\partial^r}{\partial x^r} H(x, z) \Big|_{x=1}}{[z^n] H(1, z)}, \quad (11)$$

where $[z^n] \sum_n f_n z^n := f_n$ is the coefficient extraction operator. We will compute the sequences of the numerator and denominator separately.

3.3.4.1 Number of histories: a hypergeometric closed form

We show that $H(1, z)$ has a miraculous property which does not hold for $H(x, z)$: it is a sum of generalized hypergeometric functions [5].

Theorem 3.3.13 (Hypergeometric closed forms). *Let $h_n := n![z^n]H(1, z)$ be the number of histories after n steps in a Young–Pólya urn of period p and parameter ℓ with initially $s_0 = b_0 + w_0$ balls, where b_0 are black and w_0 are white. Then, for each i , $(h_{pm+i})_{m \in \mathbb{N}}$ is a hypergeometric sequence, satisfying*

$$h_{p(m+1)+i} = h_{pm+i} (p + \ell)^p \prod_{j=0}^{i-1} \left(m + 1 + \frac{s_0 + j}{p + \ell} \right) \prod_{j=i}^{p-1} \left(m + \frac{s_0 + j}{p + \ell} \right).$$

Example 3.3.14. For the Young–Pólya urn with $p = 2$, $\ell = 1$, and $b_0 = w_0 = 1$, one has for $h_n := n![z^n]H(1, z)$:

$$h_n = \begin{cases} 3^n \frac{\Gamma(\frac{n}{2}+1)\Gamma(\frac{n}{2}+\frac{2}{3})}{\Gamma(2/3)} & \text{if } n \text{ is even,} \\ 3^n \frac{\Gamma(\frac{n}{2}+\frac{1}{2})\Gamma(\frac{n}{2}+\frac{7}{6})}{\Gamma(2/3)} & \text{if } n \text{ is odd.} \end{cases}$$

Alternatively, this sequence satisfies $h(n+2) = \frac{3}{2}h(n+1) + \frac{1}{4}(9n^2 + 21n + 12)h(n)$. We added this sequence as [OEIS A293653](#) in the On-Line Encyclopedia of Integer Sequences [167]: 1, 2, 6, 30, 180, 1440, 12960, 142560, ... The exponential generating function can be written as the sum of two hypergeometric functions:

$$H(1, z) = {}_2F_1 \left(\left[\frac{2}{3}, 1 \right], \left[\frac{1}{2} \right], \left(\frac{3z}{2} \right)^2 \right) + 2z {}_2F_1 \left(\left[\frac{5}{3}, 1 \right], \left[\frac{3}{2} \right], \left(\frac{3z}{2} \right)^2 \right).$$

3.3.4.2 Method of moments

We proceed with the computation of the moments. By (11) we need to compute the derivatives of $H_i(x, z)$ with respect to x evaluated at $x = 1$. For this purpose we use the differential equations for histories (10). The key observation is that the derivative of $H_i(x, z)$ with respect

to x has a factor $(x - 1)$, which makes it possible to compute the derivatives iteratively by taking the r th derivative with respect to x and substituting $x = 1$. This leads to the following proposition.

Proposition 3.3.15. *The r th (factorial) moment of B_n (number of black balls after n draws in a Young–Pólya urn of period p and parameter ℓ with initially $s_0 = b_0 + w_0$ balls, b_0 black and w_0 white) satisfies ($\delta = \frac{p}{p+\ell}$)*

$$m_r(n) = \gamma_r n^{\delta r} \left(1 + \mathcal{O}\left(\frac{1}{n}\right) \right), \quad \text{with} \quad \gamma_r = \frac{b_0^{\bar{r}}}{p^{\delta r}} \prod_{j=0}^{r-1} \frac{\Gamma\left(\frac{s_0+j}{p+\ell}\right)}{\Gamma\left(\frac{s_0+r+j}{p+\ell}\right)}.$$

Example 3.3.16. For the Young–Pólya urn with $p = 2$, $\ell = 1$, and $b_0 = w_0 = 1$, we get for the mean and the variance of B_n

$$\begin{aligned} \mathbb{E}B_n &\sim \frac{3\sqrt{3}2^{1/3}\Gamma(2/3)^2}{4\pi}n^{2/3} \approx 0.9552 n^{2/3}, \\ \mathbb{V}B_n &\sim \frac{27}{8} \frac{\Gamma(2/3)^2 \left(3\Gamma(4/3) - \Gamma(2/3)^2\right)}{2^{1/3}\pi^2} n^{4/3} \approx 0.42068 n^{4/3}. \end{aligned}$$

Now we have all ingredients to use the method of moments to prove Theorem 3.3.6. The natural factors occurring in the constant γ_r of Proposition 3.3.15, may they be $1/\Gamma\left(\frac{s+r+j}{p+\ell}\right)$ or $(b_0^{\bar{r}})^{1/p}/\Gamma\left(\frac{s+r+j}{p+\ell}\right)$, do not satisfy the determinant/finite difference positivity tests for the Stieltjes/Hamburger/Hausdorff moment problems, therefore no continuous distribution has such moments; see [176]. However, the full product does correspond to moments of a distribution which is easier to identify if we start by transforming the constant γ_r by the Gauss multiplication formula of the gamma function; this gives

$$\begin{aligned} \gamma_r &= \frac{(p+\ell)^r}{p^{\delta r}} m_r, \quad \text{with} \\ m_r &:= \frac{\Gamma(b_0+r)\Gamma(s_0)}{\Gamma(b_0)\Gamma(s_0+r)} \prod_{j=0}^{\ell-1} \frac{\Gamma\left(\frac{s_0+r+p+j}{p+\ell}\right)}{\Gamma\left(\frac{s_0+p+j}{p+\ell}\right)}. \end{aligned} \quad (12)$$

Combining this result with the r th (factorial) moment $m_r(n)$ from Proposition 3.3.15, we see that the moments $\mathbb{E}(B_n^{*r})$ of the rescaled random variable $B_n^* := \frac{p^\delta}{p+\ell} \frac{B_n}{n^\delta}$ converge for $n \rightarrow \infty$ to the limit m_r , a simple formula involving the parameters (p, ℓ, b_0, w_0) of the model.

Now note that the following sum diverges (recall $0 \leq (1 - \delta) < 1$):

$$\sum_{r>0} m_r^{-1/(2r)} = C \sum_{r>0} r^{-(1-\delta)/2} (1 + o(1)) = +\infty.$$

Therefore, a result by Carleman (see [54, pp. 189–220]) implies that there exists a unique distribution \mathcal{D} with such moments m_r . Then, by Fréchet and Shohat [88, p. 536], B_n^* converges to \mathcal{D} . Finally, we identify the involved distributions and get Theorem 3.3.6.

In the next section, we will see what are the implications of our results for urns on an apparently unrelated topic: Young tableaux.

3.3.5 Periodic Young tableaux

Many results on the asymptotic shape of Young tableaux have been collected, but very few results are known on their asymptotic content when the shape is fixed (see, e.g., the works by Pittel and Romik, Angel et al., Marchal [6, 138, 154, 163], who have studied the distribution of the values of the cells in random rectangular or staircase Young tableaux, while the case of Young tableaux with a more general shape seems to be very intricate). It is therefore pleasant that our work on periodic Pólya urns allows us to get advances on the case of a triangular shape, with any rational slope.

Definition 3.3.17. For integers $n, \ell, p \geq 1$, a triangular Young tableau of parameters (ℓ, p, n) is a classical Young tableau with $N := p\ell n(n + 1)/2$ cells, with length $n\ell$, and height np such that the first ℓ columns have np cells, the next ℓ columns have $(n - 1)p$ cells, etc.; see Figure 23.

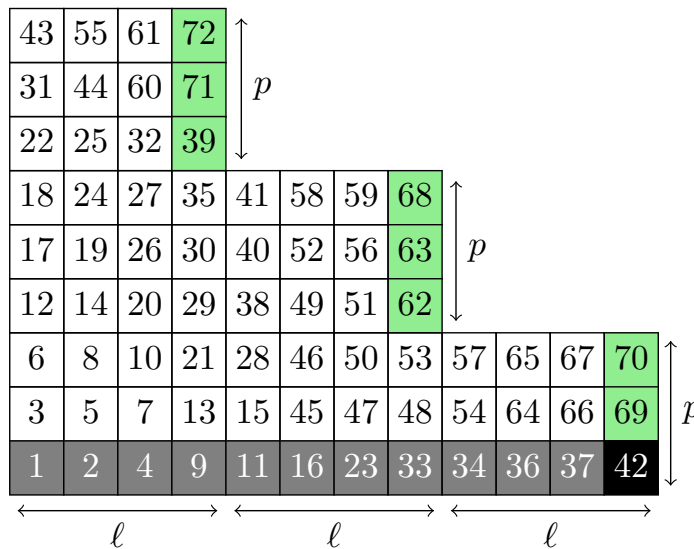


Figure 23: A triangular Young tableau (i.e., a given periodic shape). The south-east cell v (in black) of this Young tableau follows the same distribution we proved for urns (gen. gamma product dis.).

For such a tableau, we study the typical value of its south-east corner. It could be expected (e.g., via the Greene–Nijenhuis–Wilf hook walk algorithm for generating Young tableaux [95]) that the entries near the hypotenuse should be $N - o(N)$. Our result on periodic urns enables us to describe these $o(N)$ fluctuations including the right critical exponent and the limit law in the corner:

Theorem 3.3.18. Choose a uniform random triangular Young tableau of parameters (ℓ, p, n) and of size $N = p\ell n(n + 1)/2$ and put $\delta = p/(p + \ell)$. Let X_n be the entry of the south-east corner. Then $(N - X_n)/n^{1+\delta}$ converges in

law to the same limiting distribution as the number of black balls in the periodic Young–Pólya urn with initial conditions $b_0 = p$, $w_0 = \ell$ and with replacement matrices $M_1 = \cdots = M_{p-1} = \begin{pmatrix} 1 & 0 \\ 0 & 1 \end{pmatrix}$ and $M_p = \begin{pmatrix} 1 & \ell \\ 0 & 1 + \ell \end{pmatrix}$, that is, we have the convergence in law, as n goes to infinity, towards GenGammaProd (the distribution defined by Formula (8), page 46):

$$\frac{2}{p\ell} \frac{N - X_n}{n^{1+\delta}} \xrightarrow{\mathcal{L}} \text{GenGammaProd}(p, \ell, p, \ell).$$

Remark 3.3.19. If we replace the parameters (ℓ, p, n) by $(K\ell, Kp, n)$ for some integer $K > 1$, we are basically modelling the same triangle, yet the limit law is $\text{GenGammaProd}(Kp, K\ell, Kp, K\ell)$, which differs from $\text{GenGammaProd}(p, \ell, p, \ell)$. However, there is still some universality: the critical exponent δ remains the same and the limit laws are closely related in the sense that they have similar tails; see Section 3.3.6.2.

As in the case of Pólya urns, our result generalizes to a much bigger class of triangular Young tableaux: those with *any* periodic shape. Let us first specify what we mean by shape:

Definition 3.3.20 (The shape of a tableau²). *We say that a tableau has shape $\lambda_1^{i_1} \cdots \lambda_n^{i_n}$ (with $\lambda_1 > \cdots > \lambda_n$) if it has (from left to right) first i_1 columns of height λ_1 , etc., and ends with i_n columns of height λ_n .*

Moreover, let $b_0, w_0 > 0$. A tableau of shape $\lambda_1^{i_1} \cdots \lambda_n^{i_n}$ shifted by a block $b_0^{w_0}$ is a tableau of shape $(\lambda_1 + b_0)^{i_1} \cdots (\lambda_n + b_0)^{i_n} b_0^{w_0}$.

As an illustration, the tableau on the top of Figure 23 has shape $9^4 6^4 3^4$. Now we can define periodic tableaux.

Definition 3.3.21 (Periodic tableaux). *For any tuple of nonnegative integers (ℓ_1, \dots, ℓ_p) , a tableau with periodic pattern shape $(\ell_1, \dots, \ell_p; n)$ is a tableau with shape (recall Definition 3.3.20)*

$$\begin{aligned} & ((np)^{\ell_p} (np-1)^{\ell_{p-1}} \cdots (np-p+1)^{\ell_1}) \\ & \times (((n-1)p)^{\ell_p} \cdots ((n-1)p-p+1)^{\ell_1}) \times \cdots \times (p^{\ell_p} \cdots 1^{\ell_1}). \end{aligned}$$

A uniform random Young tableau with periodic pattern shape $(\ell_1, \dots, \ell_p; n)$ is a uniform random filling of a tableau with such a periodic pattern shape.

Let us put the previous pattern in words: we have a tableau made of n blocks, each of these blocks consisting of p smaller blocks of length ℓ_p, \dots, ℓ_1 , and the height decreases by 1 between each of these smaller blocks. This leads to a tableau length $(\ell_1 + \cdots + \ell_p)n$, which repeats periodically the same subshape along its hypotenuse.

Note that the triangular Young tableau of parameters (ℓ, p, n) from Definition 3.3.17 corresponds to Definition 3.3.21 for the $(p+1)$ -tuple $(0, \dots, 0, \ell; n)$.

We can now state the main theorem for periodic Young tableaux:

²Some authors define the shape of a tableau as its row lengths from bottom to top. Here we use the list of column lengths, as it directly gives the natural quantities to state our results in terms of trees and urns.

Theorem 3.3.22 (The distribution of the south-east entry in periodic Young tableaux). *Choose a uniform random Young tableau with periodic pattern shape $(\ell_1, \dots, \ell_p; n)$ shifted by a block $b_0^{w_0}$. Let N be its size, set $\ell := \ell_1 + \dots + \ell_p$ and $\delta := p/(p + \ell)$. Let X_n be the entry of the south-east corner. Then $(N - X_n)/n^{1+\delta}$ converges in law to the same limiting distribution as the number of black balls in the periodic Young–Pólya urn with initial conditions (b_0, w_0) and with replacement matrices $M_i = \begin{pmatrix} 1 & \ell_i \\ 0 & 1 + \ell_i \end{pmatrix}$:*

$$\frac{2}{p\ell} \frac{N - X_n}{n^{1+\delta}} \xrightarrow{\mathcal{L}} \text{Beta}(b_0, w_0) \prod_{\substack{i=1 \\ i \neq \ell_1 + \dots + \ell_j + j \\ \text{with } 1 \leq j \leq p-1}}^{p+\ell-1} \text{GenGamma}(b_0 + w_0 + i, p + \ell).$$

The proofs of these results build on the density method that we explained in the Sections 3.1 and 3.2. Let us now discuss some consequences of our results for the limit shapes of random Young tableaux.

3.3.6 Random Young tableaux and random surfaces

There is a vast and fascinating literature related to the asymptotics of Young tableaux when their shape is free, but the number of cells is going to infinity: it even originates from the considerations of Erdős, Szekeres, and Ulam on longest increasing subsequences in permutations (see [3, 163] for a nice presentation of these fascinating aspects). There, algebraic combinatorics and variational calculus appear to play a key rôle, as became obvious with the seminal works of Vershik and Kerov, Logan and Shepp [132, 175]. The asymptotics of Young tableaux when the shape is constrained is harder to handle, and this section tackles some of these aspects.

3.3.6.1 Random surfaces

Figure 24 illustrates some known results and some conjectures on “the continuous” limit of Young tableaux (see also the notion of continual Young tableaux in [115]). Let us now explain a little bit what is summarized by this figure, which, in fact, refers to different levels of renormalization in order to catch the right fluctuations. It should also be pinpointed that some results are established under the Plancherel distribution, while some others are established under the uniform distribution (like in the present work).

First, our Theorem 3.3.18 can be seen as a result on random surfaces arising from Young tableaux with a fixed shape. Let us be more specific. Consider a fixed rectangular triangle Tr where the size of the edges meeting at the right angle are p and q , respectively, where p and q are integers. One can approximate Tr by a sequence of triangular Young tableaux $(\mathcal{Y}_n)_{n \geq 0}$ from Definition 3.3.17, where the size of the sides meeting at the right angle are pn and qn .

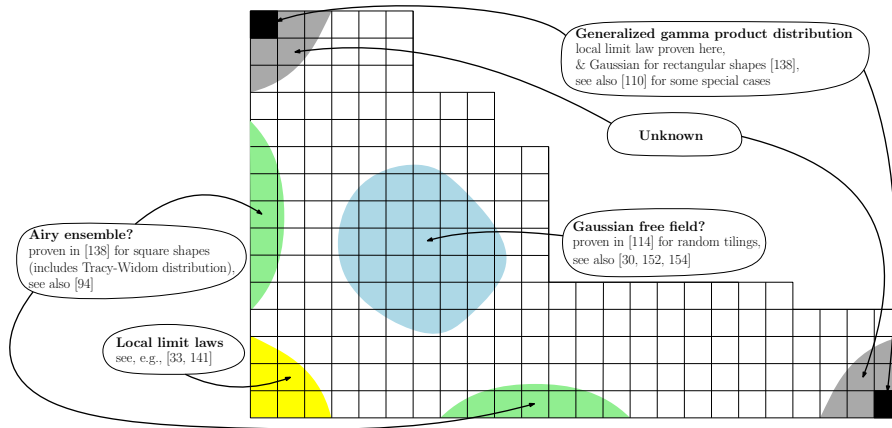


Figure 24: Known and conjectured limit laws of random Young tableaux.

For each of these tableaux, one can pick a random standard filling and one can interpret it as a random discretized surface. More precisely, if $0 \leq x \leq p$ and $0 \leq y \leq q$ are two reals and if the entry of the cell $(\lfloor xn \rfloor, \lfloor yn \rfloor)$ is z , then we set $f_n(x, y) := 2z/(pqn^2)$. Thereby, we construct a random function $f_n : \text{Tr} \rightarrow [0, 1]$ which is discontinuous but it is to be expected that, in the limit, the functions f_n converge in probability to a deterministic, continuous function f (see Figure 25). Intuitively, for every point (x, y) on the hypotenuse, one will have $f(x, y) = 1$ and this is the case in particular for the south-east corner, that is, the point $(p, 0)$. Then, one can view Theorem 3.3.18 as a result on the fluctuations of the random quantity $f_n(p, 0)$ away from its deterministic limit, which is 1.

As a matter of fact, the convergence of f_n to f has only been studied when the shape of the tableau is fixed. The convergence towards a limiting surface was first proven when the limit shape is a finite union of rectangles; see Biane [30]. There, the limiting surface can be interpreted in terms of characters of the symmetric group and free probability but this leads to complicated computations from which it is difficult to extract explicit expressions.

For rectangular Young tableaux, the limiting surface is described more precisely by Pittel and Romik [154]. A limiting surface also exists for staircase tableaux: it can be obtained by taking the limiting surface of a square tableau and cutting it along the diagonal; see [6, 130]. This idea does not work for *rectangular* (nonsquare) Young tableaux: if one cuts such tableaux along the diagonal, one *does not* get the limiting surface of triangular Young tableaux (the hypotenuse would have been the level line 1, but the diagonal is in fact not even a level line, as visible in Figure 25 and proven in [154]).

Apart from the particular cases mentioned above, convergence results for surfaces arising from Young tableau seem to be lacking. There are also very few results about the fluctuations away from

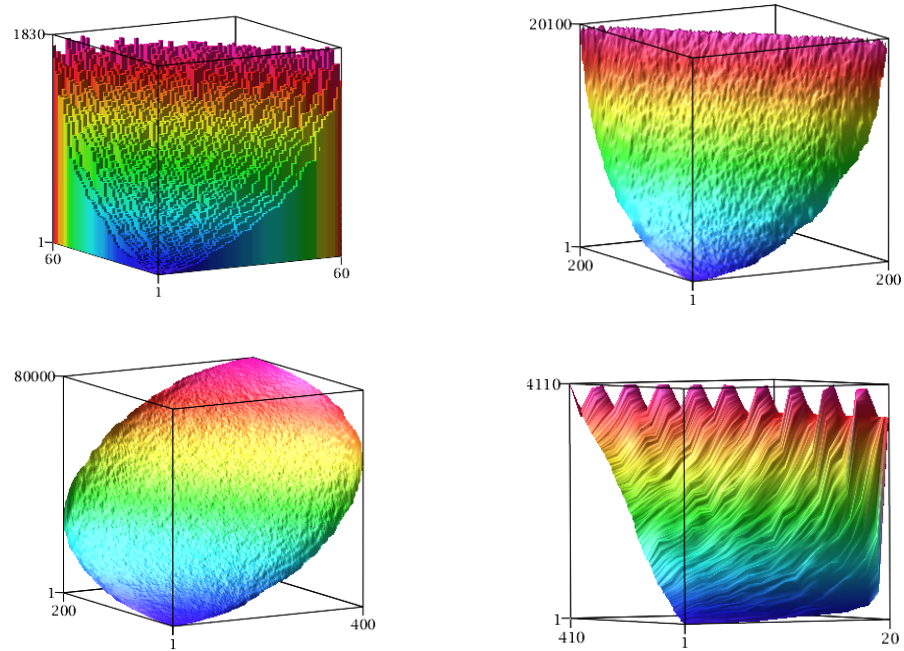


Figure 25: Random generation of Young tableaux, seen as random surfaces (the colours correspond to level lines). Top: triangular Young tableaux (size 60×60 , seen as histogram, and 200×200); Bottom: rectangular and triangular Young tableaux (400×200 and 410×20). The images are generated via our own Maple package available at <https://lipn.fr/~cb/YoungTableaux>, relying on a variant of the hook-length walk of [95].

the limiting surface. For rectangular shapes, these fluctuations were studied by Marchal [138]: they are Gaussian in the south-east and north-west corner, while the fluctuations on each edge follow a Tracy–Widom limit law, at least when the rectangle is a square (for general rectangles, there remain some technicalities, although the expected behaviour is the same). For staircase triangles, Gorin and Rahman [94] use a sorting network representation to obtain asymptotic formulas using double integrals. In particular, they find the limit law on the edge. Their approach may be generalizable to other triangular shapes. Also, instead of renormalized limits, one may be interested in local limits, there are then nice links with the famous jeu de taquin [169] and characters of symmetric groups [33].

There is another framework where random surfaces naturally arise, namely random tilings and related structures (see, e.g., [166]). Indeed, one can associate a height function with a tiling: this gives an interpretation as a surface. In this framework, there are results on the fluctuations of these surfaces, which are similar to the ones on Young tableaux. In the case of the Aztec diamond shape, Johansson and Nordenstam [110] proved that the fluctuations of the Arctic curve are related to eigenvalues of GUE minors (and are there-

fore Gaussian near the places where the curve is touching the edges, whereas they are Tracy–Widomian when the curve is far away from the edges). Note that this gives the same limit laws as for the Arctic curve of a TASEP jump process associated to rectangular Young tableaux [138, 162]. Similar results were also obtained for pyramid partitions [45, 46]. Moreover, in other models of lozenge tilings, it is proven that for some singular points, other limit laws appear: they are called cusp-Airy distributions, and are related to the Airy kernel [74]. It has to be noticed that, up to our knowledge, the generalized gamma distributions, which appear in our results, have not been found in the framework of random tilings.

A major challenge would be to capture the fluctuations of the surface in the interior of the domain. For Young tableaux, it is reasonable to conjecture that these fluctuations could be similar to those observed for random tilings: in this framework, Kenyon [114] and Petrov [152] proved that the fluctuations are given by the Gaussian free field (see also [51]).

Finally, a dual question would be: in which cell does a given entry lie in a random filling of the tableau? In the case of triangular shapes like ours, if we look at the largest entry, we get:

Proposition 3.3.23 (Location of the maximum). *Choose a uniform random triangular Young tableau of parameters (ℓ, p, n) (see Definition 3.3.17). Let $\text{Posi}_n \in \{1, \dots, \ell n\}$ be the x -coordinate of the cell containing the largest entry. Then one has*

$$\frac{\text{Posi}_n}{\ell n} \xrightarrow{\mathcal{L}} \text{Arcsine}(\delta), \quad \text{where } \delta := p/(p + \ell).$$

So, if we compare models with different p and ℓ , then the largest entry will have the tendency to be on the top of the hypotenuse when ℓ is much larger than p , while it will be on its bottom if p is much larger than ℓ (and on the bottom or the top with equally high probabilities when $p \approx \ell$); see Figure 25. This is in sharp contrast with the case of an $n \times n$ square tableau where, for $t \in (0, 1)$, the cell containing the entry tn^2 is asymptotically distributed according to the Wigner semicircle law on its level line; see [154]. We also refer to Romik [161] for further discussions on Young tableau landscapes and to Morales, Pak, and Panova [146] for recent results on skew-shaped tableaux.

3.3.6.2 From microscopic to macroscopic models: universality of the tails

What happens if we use different tableaux of parameters $(K\ell, Kp, n)$ for any “zoom factor” $K \in \mathbb{N}$, as shown in Figure 26? In the first case, we obtain the limit law $\text{GenGammaProd}(p, \ell, p, \ell)$ for the southeast corner, whereas in the second case, we get the different law $\text{GenGammaProd}(Kp, K\ell, Kp, K\ell)$.

In fact, we could even imagine more general periodic patterns as in Theorem 3.3.22 corresponding to the same macroscopic object. All

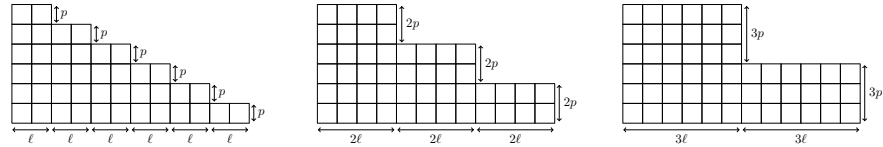


Figure 26: Different discrete models converge towards a tableau of slope $-p/\ell$. As usual for problems related to urns, many statistics have a sensibility to the initial conditions; it is therefore nice that some universality holds: the distributions (depending on p, ℓ , and the “zoom factor” K) of our statistics have similar tails compared to Mittag-Leffler distributions.

these models lead to different asymptotic distributions. However, we partially have some universal phenomenon in the sense that, although these limit distributions are different, they are closely related by the fact that their tails are similar to the tail of a Mittag-Leffler distribution.

Definition 3.3.24 (Similar tails). *One says that two random variables X and Y have similar tails and one writes $X \asymp Y$ if*

$$\frac{\log \frac{\mathbb{E}(X^r)}{\mathbb{E}(Y^r)}}{r} \rightarrow 0, \quad \text{as } r \rightarrow \infty.$$

This definition has the advantage to induce an equivalence relation between random variables which have moments of all orders: if X, Y are in the same equivalence class, then for every $\varepsilon \in (0, 1)$, for r large enough, one has

$$\mathbb{E}(((1 - \varepsilon)X)^r) \leq \mathbb{E}(Y^r) \leq \mathbb{E}(((1 + \varepsilon)X)^r).$$

In the following theorem, we give much finer asymptotics than the above bounds. Recall from, e.g., [93, page 8] that the *Mittag-Leffler distribution* $\text{ML}(\alpha, \beta)$ ($0 < \alpha < 1$ and $\beta > -\alpha$) is determined by its moments. Its r th moment has two equally useful closed forms:

$$m_{\text{ML},r} = \frac{\Gamma(\beta)\Gamma(\beta/\alpha + r)}{\Gamma(\beta/\alpha)\Gamma(\beta + \alpha r)} = \frac{\Gamma(\beta + 1)\Gamma(\beta/\alpha + r + 1)}{\Gamma(\beta/\alpha + 1)\Gamma(\beta + \alpha r + 1)}.$$

Theorem 3.3.25 (Similarity with the tail of a Mittag-Leffler distribution). *Let $X = \text{GenGammaProd}([\ell_1, \dots, \ell_p]; b_0, w_0)$ and put $\ell = \ell_1 + \dots + \ell_p$, $\delta = p/(\ell)$. Let $Y := \text{ML}(\delta, \beta)$ with $\beta > -\delta$. Then X and $\delta p^{\delta-1}Y$ have similar tails in the sense of Definition 3.3.24.*

Remark 3.3.26. The tails of this distribution are universal: they depend only on the slope δ and the period length p . They depend neither on the initial conditions b_0 and w_0 , nor on further details of the geometry of the periodic pattern (the ℓ_i 's).

One more universal property which holds for some families of urn distributions is that they possess sub-Gaussian tails, a notion introduced by Kahane in [111] (see also [125] for some urn models):

Definition 3.3.27 (Sub-Gaussian tails). *A random variable X has sub-Gaussian tails if there exist two constants $c, C > 0$, such that*

$$\mathbb{P}(|X| \geq t) \leq Ce^{-ct^2}, \quad t > 0.$$

Proposition 3.3.28. *The $\text{GenGammaProd}(p, \ell, b_0, w_0)$ distributions have sub-Gaussian tails if and only if $p \geq \ell$.*

Another useful notion which helps to gain insight into the limit of Young tableaux is the notion of a *level line*: let C_v be the curve separating the cells with an entry bigger than v and the cells with an entry smaller than v (and to get a continuous curve, one follows the border of the Young tableau if needed; see Figure 27).

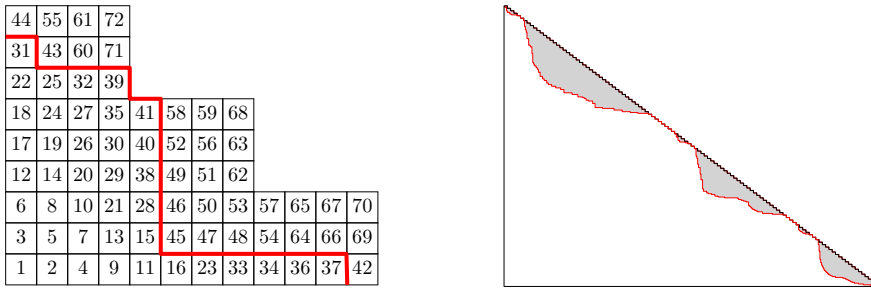


Figure 27: The level line (in red) of the south-east corner X_n : it separates all the entries smaller than X_n from the other ones. Left: one example with the level line of $X_n = 42$; right: the level line of X_n , for a very large Young tableau of size N of triangular shape. The area between this level line and the hypotenuse is the quantity $N - X_n$ from Theorem 3.3.22.

When $n \rightarrow \infty$, one may ask whether the level line C_{X_n} converges in distribution to some limiting random curve \mathcal{C} . If so, the limit laws we computed in Theorem 3.3.18 would give the (renormalized) area between the macroscopic curve \mathcal{C} and the hypotenuse. In particular, the law of \mathcal{C} would depend on the microscopic details of the model, since we find for the renormalized area a whole family of distributions $\text{GenGammaProd}(p, \ell, b_0, w_0)$ depending on 4 parameters. Besides, note that we could imagine even more general microscopic models for the same macroscopic triangle. For instance, for a slope -1 , starting from the south-east corner we could have a periodic pattern (1 step north, 2 steps west, 2 steps north, 1 step west). All shapes leading to the same slope are covered by Theorem 3.3.8 (see also Example 3.3.9), and our method then gives similar, but distinct, limit laws. Such models thus yield another limit law for the area, and thus another limiting random curve \mathcal{C} .

Note that the renormalized area between \mathcal{C} and the hypotenuse does not have the same distribution as the area below the positive part of a Brownian meander [105]. Funnily, Brownian motion theory is cocking a snook at us: another one of Janson's papers [107] studies the area below curves which are related to the Brownian supremum process and, here, one observes more similarities with our problem, as the moments of the corresponding distribution involve the gamma function. However, these moments grow faster than in the limit laws found in Theorem 3.3.18. It is widely open if there is some framework unifying all these points of view.

3.3.6.3 Factorizations of gamma distributions

With respect to the asymptotic landscape of random Young tableaux, let us add one last result: our results on the south-east corner directly imply similar results on the north-west corner. In particular, the critical exponent for the upper left corner is $1 - \delta$. In fact, it is a nice surprise that there is even more structure: any periodic pattern shape is naturally associated with a family of patterns such that the limit laws of the south-east corners of the corresponding Young tableaux are related to each other.

Let us describe the periodic pattern via a *shape path* $(i_1, j_1; \dots; i_m, j_m)$: it starts at the north-west corner of the tableau described by the pattern with i_1 right steps, followed by j_1 down steps, etc.; see Figure 28. Then its cyclic shift is defined by $(j_m, i_1; \dots; j_{m-1}, i_m)$. Furthermore, this notion is equivalent to Definition 3.3.21 of a periodic tableau via

$$(\ell_1, \dots, \ell_p) = (\underbrace{0, \dots, 0, j_m}_{i_m \text{ elements}}, \underbrace{0, \dots, 0, j_{m-1}, \dots, 0}_{i_{m-1} \text{ elements}}, \dots, \underbrace{0, \dots, 0, j_1}_{i_1 \text{ elements}}).$$

Then the *cyclic shift* is given by

$$(\ell'_1, \dots, \ell'_{p'}) := (\underbrace{0, \dots, 0, i_m}_{j_{m-1} \text{ elements}}, \dots, \underbrace{0, \dots, 0, i_2}_{j_1 \text{ elements}}, \underbrace{0, \dots, 0, i_1}_{j_m \text{ elements}}).$$

In particular we have $p' = \ell$ and $\ell' = p$. Appending now n copies of the shape path $(i_1, j_1; \dots; i_m, j_m)$ to each other corresponds to n repetitions of the pattern and, therefore, gives a periodic tableau.

Proposition 3.3.29. *Let (ℓ_1, \dots, ℓ_p) and $(\ell'_1, \dots, \ell'_{p'})$ be two sequences as defined above and let j_m be the smallest index such that $\ell_{j_m} > 0$. Let b_0, w_0 be two positive integers, and Y and Y' be independent random variables with respective distribution*

$$\begin{aligned} & \text{GenGammaProd}([\ell_1, \dots, \ell_p]; b_0, w_0) \quad \text{and} \\ & \text{GenGammaProd}([\ell'_1, \dots, \ell'_{p'}]; b_0 + w_0, j_m) \end{aligned}$$

from Theorem 3.3.8. Then we have the factorization

$$YY' \stackrel{\mathcal{L}}{=} \frac{1}{p + \ell} \Gamma(b_0). \tag{13}$$

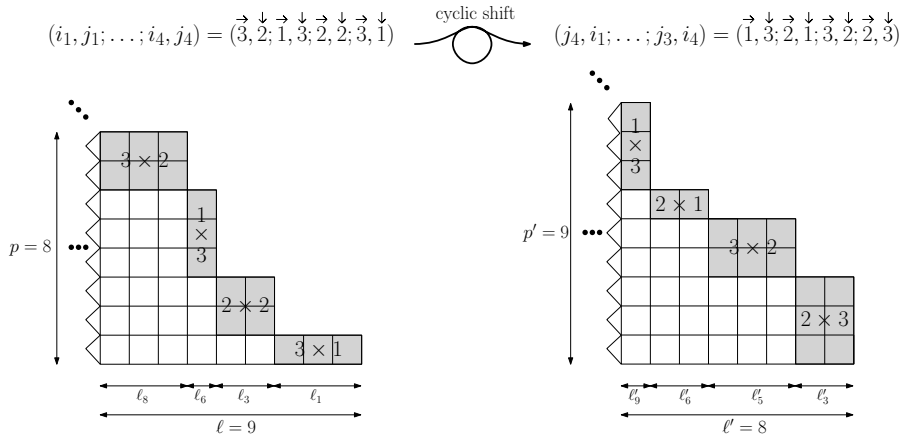


Figure 28: Example of a cyclic shift on a periodic pattern. On the left: one sees the shape path $(3,2;1,3;2,2;3,1)$, it corresponds to the pattern $(\ell_1, \dots, \ell_8) = (3,0,2,0,0,1,0,3)$ (as sequence of consecutive heights, from right to left). On the right: one sees its cyclic shift, which corresponds to the pattern $(\ell'_1, \dots, \ell'_9) = (0,0,2,0,3,2,0,0,1)$. In grey we see the size of the sub-rectangles described by the shape path, i.e., the k th rectangle has size $i_k \times j_k$.

Remark 3.3.30 (A duality between corners). One case of special interest is the case of Young tableaux having the mirror symmetry $(\ell_{j_m}, \dots, \ell_p) = (\ell_p, \dots, \ell_{j_m})$, where j_m is again the smallest index such that $\ell_{j_m} > 0$. Indeed, Y and Y' then correspond to the limit laws for the south-east (respectively north-west) corner of the same tableau. In this case, we can think of (13) as expressing a kind of duality between the corners of the tableau.

Similar factorizations of the exponential law, which is a particular case of the gamma distribution, have appeared recently in relation with functionals of Lévy processes, following [28]. These formulas are also some probabilistic echoes of identities satisfied by the gamma function.

4

LATTICE PATHS

4.1	Introduction and definitions	63
4.2	Latticepathology and symmetric functions [P12]	65
4.3	Combinatorics of nondeterministic walks [P11]	69
4.4	More models of walks avoiding a quadrant [P14]	78

The combinatorics of lattice paths has been a major theme of my research since my graduate studies. In my master’s thesis [T3] I surveyed three major breakthroughs in the theory of one-dimensional and two-dimensional walks. Then, in my PhD thesis [T4] I added my own humble contributions to the field of one-dimensional walks. Now, in the current habilitation thesis I want to present my developments since, which have led in completely new directions.

In Section 4.1, we introduce different models and definitions.

In Section 4.2, we present new links between one-dimensional walks and symmetric functions. We show that each of the fundamental families of symmetric polynomials (elementary, complete, and power sum homogeneous) corresponds to a lattice path generating function, which then allows the analysis of parameters and limit laws.

In Section 4.3, we analyze a new variant of one-dimensional walks arising in networking and queueing theory: the so-called “nondeterministic walks”. In such a model, the steps may consist of multiple paths explored in parallel. We derive closed forms for the generating functions and asymptotic counting formulas, which we then use to determine their nature.

In Section 4.4, we analyze a new two-dimensional model of walks confined to non-convex cones: the king model of all nearest neighbor steps confined to the three-quarter plane. We show that the generating function is D-finite and uncover an algebraicity phenomenon linking it with the well-understood walks confined to a quadrant.

4.1 INTRODUCTION AND DEFINITIONS

In recent years lattice paths have received a lot of attention in different fields, such as probability theory, computer science, biology, chemistry, physics, and much more [18, 42, 47, 73, 98, 101, 117, 122]. One reason for that is their versatility as models like, e.g., the up-to-date model of certain polymers in chemistry [100]. For more information and especially historical notes see [98, 122] and [T3, T4].

A key feature of lattice paths is their inherent recursive nature, governed by the predefined set of steps.

Definition 4.1.1 (Steps and lattice paths). A step set \mathcal{S} is a finite subset of \mathbb{Z}^d where $d \in \mathbb{Z}_+$ is called the dimension. The elements of \mathcal{S} are called steps or jumps. An n -step lattice path or walk w is a sequence $(j_1, \dots, j_n) \in \mathcal{S}^n$. Its length $|w|$ is the number n of jumps.

Let us focus now on dimension $d = 1$; these paths are also called *directed lattice paths*. Although such sequences are one-dimensional objects, it is often more insightful to embed them into two dimensions, by keeping track of the length in x -direction and of the height in y -direction. Indeed, (j_1, \dots, j_n) may be seen as a sequence of points $w = (w_0, w_1, \dots, w_n)$, where w_0 is the starting point and $w_i - w_{i-1} = (1, j_i)$ for $i = 1, \dots, n$. Unless otherwise specified, the starting point w_0 of these lattice paths is always the origin.

Let $\sigma_k := \sum_{i=1}^k j_i$ be the partial sum of the first k steps w . We define the *height* or *maximum* of w as $\max_k \sigma_k$, and the *final altitude* of w as σ_n . For example, the first walk in Table 3 has height 3 and final altitude 1. Table 3 also illustrates the following classical types of paths:

Definition 4.1.2 (Excursions, meanders, bridges). We define the following classes of one-dimensional lattice paths of length n :

- excursions satisfy $\sigma_k \geq 0$ for all $k = 1, \dots, n$ and $\sigma_n = 0$;
- meanders satisfy $\sigma_k \geq 0$ for all $k = 1, \dots, n$;
- bridges satisfy $\sigma_n = 0$.

In other words, excursions always stay weakly above the x -axis and end on it; meanders as well, but may end anywhere; and bridges only need to end on the x -axis, yet may cross it any number of times. Let $c := -\min \mathcal{S}$ be the maximal negative step, and $d := \max \mathcal{S}$ be the maximal positive step. To avoid trivial cases we assume $\min \mathcal{S} < 0 < \max \mathcal{S}$. Furthermore we associate to each step $i \in \mathcal{S}$ a weight s_i . They typically model probabilities $s_i \in \mathbb{R}_+$ or multiplicities $s_i \in \mathbb{Z}_+$. The weight of a lattice path is the product of the weights of its steps. Then we associate to this set of steps the following *step polynomial*:

$$S(u) = \sum_{i=-c}^d s_i u^i.$$

Banderier and Flajolet [12] showed that the generating functions of directed lattice paths can be expressed in terms of the roots of the *kernel equation*

$$1 - zS(u) = 0. \tag{14}$$

More precisely, this equation has $c + d$ solutions in u . The *small roots* $u_i(z)$, for $i = 1, \dots, c$, are the c solutions with the property $u_i(z) \sim 0$ for $z \sim 0$. The remaining d solutions are called *large roots* as they satisfy $|v_i(z)| \sim +\infty$ for $z \sim 0$. The generating functions of the classical types of lattice paths introduced above are shown in Table 3.

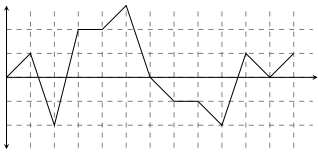
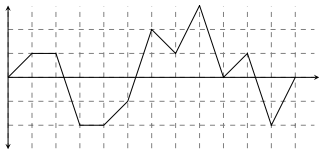
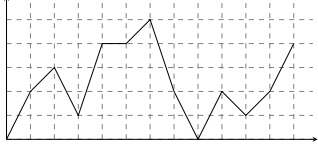
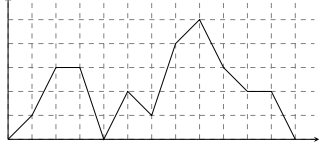
	ending anywhere	ending at 0
unconstr. (on \mathbb{Z})	 walk/path (\mathcal{W}) $W(z) = \frac{1}{1-zS(1)}$	 bridge (\mathcal{B}) $B(z) = z \sum_{i=1}^c \frac{u_i'(z)}{u_i(z)}$
constrained (on \mathbb{Z}_+)	 meander (\mathcal{M}) $M(z) = \frac{\prod_{i=1}^c (1-u_i(z))}{1-zS(1)}$	 excursion (\mathcal{E}) $E(z) = \frac{(-1)^{c-1}}{s-cz} \prod_{i=1}^c u_i(z)$

Table 3: Four types of paths: walks, bridges, meanders, and excursions, and the corresponding generating functions for directed lattice paths. The functions $u_i(z)$ for $i = 1, \dots, c$ are the roots of the kernel equation $1 - zS(u) = 0$ such that $\lim_{z \rightarrow 0} u_i(z) = 0$; see [12].

It should be stressed that the closed forms of Table 3 grant easy access to the asymptotics of all these classes of paths after the localization of the dominant singularities:

Lemma 4.1.3 (Radius of convergence of excursions, bridges, and meanders [12]). *The radius of convergence of excursions $E(z)$ and of bridges $B(z)$ is given by $\rho = 1/S(\tau)$, where τ is the smallest positive real number such that $S'(\tau) = 0$. For meanders $M(z)$, the radius depends on the drift $\delta := S'(1)$: It is ρ if $\delta < 0$ and it is $1/S(1)$ if $\delta \geq 0$.*

4.2 LATTICEPATHOLOGY AND SYMMETRIC FUNCTIONS [P12]

In this section, we present the results from [P12], focusing on the results about symmetric functions to remain consistent with the main theme of this thesis: universal properties such as asymptotics and limit laws. Note that in the mentioned paper additional result are derived on context-free grammar decompositions and on Spitzer and Wiener–Hopf identities. The properties of lattice paths may be analyzed in several different ways. Their recursive nature makes them amenable to context-free grammar techniques; their geometric nature makes them amenable to cut-and-paste bijections; their step-by-step construction makes them amenable to functional equations solvable by the kernel method; see, e.g., [7, 12, 17, 31, 37, 41, 42, 71, 122, 127, 143] for many applications of these ideas.

4.2.1 Lattice paths and symmetric functions

We now show that three fundamental classes of symmetric polynomials evaluated at the small roots $u_i(z)$ of the kernel (14) have a natural combinatorial interpretation in terms of directed lattice paths. We first recall the definitions of these symmetric polynomials (see, e.g., [171] for more on these objects).

Definition 4.2.1. *The complete homogeneous symmetric polynomials h_k of degree k in the d variables x_1, \dots, x_d are defined as*

$$h_k(x_1, \dots, x_d) = \sum_{1 \leq i_1 \leq \dots \leq i_k \leq d} x_{i_1} \cdots x_{i_k}.$$

The elementary homogeneous symmetric polynomials e_k of degree k in the d variables x_1, \dots, x_d are defined as

$$e_k(x_1, \dots, x_d) = \sum_{1 \leq i_1 < \dots < i_k \leq d} x_{i_1} \cdots x_{i_k}.$$

The power sum homogeneous symmetric polynomials p_k of degree k in the d variables x_1, \dots, x_d are defined as

$$p_k(x_1, \dots, x_d) = \sum_{i=1}^d x_i^k.$$

Many variants of directed lattice paths satisfy functional equations which are solvable by the kernel method and lead to formulas involving a quotient of Vandermonde-like determinants; see, e.g., Table 3 and [12]. It is thus natural that Schur polynomials intervene, they, e.g., play an important role for lattice paths in a strip; see [17, 37]. It is nice that the other symmetric polynomials also have a combinatorial interpretation, as presented in Table 4. All of them belong to the following class of lattice paths.

Definition 4.2.2. *A positive meander is a path from $\ell \geq 0$ to $k \geq 0$ staying strictly above the x -axis (and possibly touching it at one of its end points). The generating function is denoted by $M_{\ell,k}^+(z)$. Negative meanders are defined analogously, with the condition to stay strictly below the x -axis.*

In Table 4, we focus on positive meanders from 0 to k and from k to 0. Note that it suffices to consider the paths from 0 to k as by time-reversion they are mapped to each other. In particular, let $u_i(z)$ and $v_j(z)$ be the small and large roots of the initial model. Then, after time-reversion the small roots are $\frac{1}{v_j(z)}$ and the large roots are $\frac{1}{u_i(z)}$.

Theorem 4.2.3 (Generating function of positive meanders).

$$M_{0,k}^+(z) = h_k \left(\frac{1}{v_1(z)}, \dots, \frac{1}{v_d(z)} \right).$$

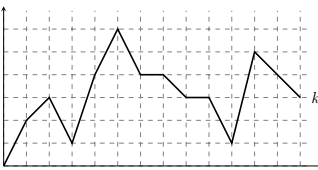
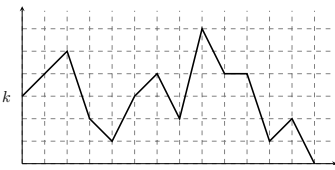
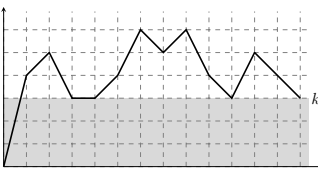
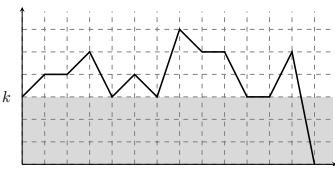
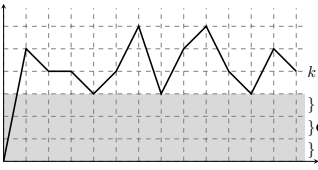
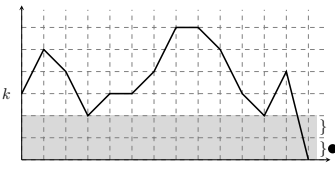
	from 0 to k	from k to 0
positive meander	 $M_{0,k}^+ = h_k \left(\frac{1}{v_1}, \dots, \frac{1}{v_d} \right)$	 $M_{k,0}^+ = h_k(u_1, \dots, u_c)$
positive meander avoiding $(0, k)$	 $M_{0,k}^{\geq} = (-1)^{k-1} e_k \left(\frac{1}{v_1}, \dots, \frac{1}{v_d} \right)$	 $M_{k,0}^{\geq} = (-1)^{k-1} e_k(u_1, \dots, u_c)$
positive meander marked below the minimum	 $M_{0,k}^\bullet = p_k \left(\frac{1}{v_1}, \dots, \frac{1}{v_d} \right)$	 $M_{k,0}^\bullet = p_k(u_1, \dots, u_c)$

Table 4: For clarity we omit the dependencies of each function on z . We show that the fundamental symmetric polynomials (of the complete homogeneous, elementary, and power sum type) are counting families of positive meanders (walks touching the x -axis only at one of the end points and staying always above the x -axis). The functions $v_j(z)$ for $j = 1, \dots, d$ are the roots of the kernel equation $1 - zS(u) = 0$ with $\lim_{z=0} |v_j(z)| = +\infty$, whereas the functions $u_i(z)$ for $i = 1, \dots, c$ are the roots such that $\lim_{z=0} u_i(z) = 0$.

This theorem gives a shorter proof of [12, Corollary 3]:

Corollary 4.2.4. *The generating function $M_k(z)$ of meanders ending at altitude k are given by*

$$\begin{aligned}
 M_k(z) &= E(z) h_k \left(\frac{1}{v_1(z)}, \dots, \frac{1}{v_d(z)} \right) \\
 &= \frac{1}{s_d z} \sum_{\ell=1}^d \left(\prod_{j \neq \ell} \frac{1}{v_j(z) - v_\ell(z)} \right) \frac{1}{v_\ell(z)^{k+1}}.
 \end{aligned}$$

The next class we consider is the one of elementary symmetric polynomials. These are associated to a decorated class of paths.

Definition 4.2.5. *A positive meander avoiding a strip of width k is a positive meander from 0 to k that always stays above any point of altitude $j < k$ except for its start point. The generating function is denoted by $M_{0,k}^{\geq}(z)$.*

Theorem 4.2.6 (Positive meanders avoiding the strip $[0, k]$).

$$M_{0,k}^{\geq}(z) = (-1)^{k-1} e_k \left(\frac{1}{v_1(z)}, \dots, \frac{1}{v_d(z)} \right).$$

We end our discussion with a third class of positive meanders.

Definition 4.2.7. A positive meanders marked below the minimum is a positive meander with an additional marker in $\{1, \dots, m\}$ where m is its minimal positive altitude. The generating function for such paths from 0 to k is denoted by $M_{0,k}^{\bullet}(z)$.

For example it is immediate that $M_{0,1}^{\bullet}(z) = M_{0,1}^{\geq}(z) = M_{0,1}^+(z)$ as the only restriction is to avoid the x -axis. Furthermore, $M_{0,0}^{\bullet}(z) = 0$ while $M_{0,0}^{\geq}(z) = M_{0,0}^+(z) = 1$.

Theorem 4.2.8 (Positive meanders marked below the minimum).

$$M_{0,k}^{\bullet}(z) = p_k \left(\frac{1}{v_1(z)}, \dots, \frac{1}{v_d(z)} \right).$$

4.2.2 Asymptotics and limit laws

We now use the closed forms of the generating functions to derive the asymptotics of the corresponding counting formulas. This allows us to revisit some limit laws in which the appearance of symmetric polynomials was so far unrecognized.

Here, we only consider *aperiodic* step sets \mathcal{S} , which are defined by $\gcd\{|i-j| : i, j \in \mathcal{S}\} = 1$. For the treatment of periodic step sets see [19]. Moreover, we focus on paths from k to 0, as the formulas are a bit simpler. The results for paths from 0 to k follow in an analogous fashion. The principal small branch $u_1(z)$ and the principal large branch $v_1(z)$ are defined by the property that they are real positive for z near $0+$ and meet at the dominant singularity $z = \rho$; see Lemma 4.1.3 and [12]. In particular, let τ be the structural constant determined by $S'(\tau) = 0$, $\tau > 0$. Then, $u_1(\rho) = v_1(\rho) = \tau$. In the next theorem we state the asymptotics of our three classes of positive meanders.

Theorem 4.2.9. Consider an aperiodic step set \mathcal{S} and the variants of paths from Table 4. The number of positive meanders from k to 0 of size n satisfies

$$[z^n] M_{k,0}^+(z) = \alpha_1 \frac{S(\tau)^n}{2\sqrt{\pi n^3}} \left(1 + \mathcal{O}\left(\frac{1}{n}\right) \right), \quad \alpha_1 = \frac{\partial e_k}{\partial x_1}(u_1(\rho), \dots, u_c(\rho)).$$

The number of positive meanders avoiding $(0, k)$ from k to 0 of size n satisfies

$$[z^n] M_{k,0}^{\geq}(z) = \alpha_2 \frac{S(\tau)^n}{2\sqrt{\pi n^3}} \left(1 + \mathcal{O}\left(\frac{1}{n}\right) \right), \quad \alpha_2 = \frac{\partial h_k}{\partial x_1}(u_1(\rho), \dots, u_c(\rho)).$$

The number of positive meanders marked below the minimum from k to 0 of size n satisfies

$$[z^n] M_{k,0}^{\bullet}(z) = \alpha_3 \frac{S(\tau)^n}{2\sqrt{\pi n^3}} \left(1 + \mathcal{O}\left(\frac{1}{n}\right) \right), \quad \alpha_3 = \frac{\partial p_k}{\partial x_1}(u_1(\rho), \dots, u_c(\rho)).$$

Many theorems leading to a Gaussian distribution require that a key quantity (let us call it σ) is nonzero. In [85], this nonzero assumption is called “variability condition”; see therein Theorem IX.8 (Quasi-power theorem), Theorem IX.9 (Meromorphic schema), Theorem IX.10 (Positive rational systems). Now, many lattice path statistics have a variance with an expansion $\sigma n + o(n)$, where σ is defined as in the following lemma, and is therefore nonzero.

Lemma 4.2.10 (Universal positivity of the variability condition). *For any Laurent series $S(u) = \sum_{i \geq -c} s_i u^i$, with $s_i \geq 0$ (at least two $s_i > 0$), one has $\sigma := S''(1)S(1) + S'(1)S(1) - S'(1)^2 > 0$.*

As a consequence, Lemma 4.2.10 guarantees that we can apply the quasi-power theorem [85, Theorem IX.8], and obtain a Gaussian limit theorem. This explains why many statistics related to lattice paths are Gaussian. For paths with positive or zero drift, it furnishes a Gaussian theorem, like, e.g., for statistics like the final altitude of meanders or for the height of walks. When the drift is negative, one gets some discrete limit laws of parameter given by our symmetric polynomial expressions:

Theorem 4.2.11 ([12, Theorem 6] and [178, Theorem 4.7]; negative drift cases). *Assume a negative drift $\delta = S'(1) < 0$ and let $\rho = 1/P(\tau)$ and $\rho_1 = 1/P(1)$.*

1. *Let X_n be the random variable of the final altitude of a meander of length n . Then, the limit law is discrete and given by*

$$\lim_{n \rightarrow \infty} \mathbb{P}(X_n = k) = (1 - \tau^{-1}) \frac{\sum_{i=0}^k \tau^{i-k} h_i(v_1(\rho)^{-1}, \dots, v_d(\rho)^{-1})}{\sum_{i \geq 0} h_i(v_1(\rho)^{-1}, \dots, v_d(\rho)^{-1})}.$$

2. *Let Y_n be the random variable of the height of a walk of length n . Then, the limit law is discrete and given by*

$$\lim_{n \rightarrow \infty} \mathbb{P}(Y_n = k) = \frac{h_k(v_1(\rho_1)^{-1}, \dots, v_d(\rho_1)^{-1})}{\sum_{i \geq 0} h_i(v_1(\rho_1)^{-1}, \dots, v_d(\rho_1)^{-1})}.$$

4.3 COMBINATORICS OF NONDETERMINISTIC WALKS OF THE DYCK AND MOTZKIN TYPE [P11]

In this section, we present the results from [P11] about a new application of lattice paths: the encapsulation of protocols over networks. To achieve this goal we generalize the class of lattice paths to so called *nondeterministic lattice paths*, or *N-walks*. In our context, this word does not mean “random”. Instead it is understood in the same sense as for automata and Turing machines. A process is nondeterministic if several branches are explored in parallel, and the process is said to end in an accepting state if one of those branches ends in an accepting state. Let us now give a precise definition of these walks.

Definition 4.3.1 (Nondeterministic walks). An N-step is a nonempty set of integers. Given an N-step set S , an N-walk w is a sequence of N-steps. Its length $|w|$ is equal to the number of its N-steps.

As for classical walks we always assume that they start at the origin and we distinguish different types.

Definition 4.3.2 (Types of N-walks). An N-walk $w = (w_1, \dots, w_n)$ and a classical walk $v = (v_1, \dots, v_n)$ are compatible if they have the same length n , the same starting point, and for each $1 \leq i \leq n$, the i th step is included in the i th N-step, i.e. $v_i \in w_i$. An N-bridge (resp. N-meander, resp. N-excursion) is an N-walk compatible with at least one bridge (resp. meander, resp. excursion).

The endpoints of classical walks are central to their analysis. We define their nondeterministic analogues.

Definition 4.3.3 (Reachable points). The reachable points of a general N-walk are the endpoints of all walks compatible with it. For N-meanders, the reachable points are defined as the set of endpoints of compatible meanders. In particular, all reachable endpoints of an N-meander are nonnegative. The minimum (resp. maximum) reachable point of an N-walk w is denoted by $\min(w)$ (resp. $\max(w)$). The minimum (resp. maximum) reachable point of an N-meander w is denoted by $\min^+(w)$ (resp. $\max^+(w)$).

The geometric realization of an N-walk is the sequence, for j from 0 to n , of its reachable points after j steps. Figure 29 illustrates the geometric realization of a walk $v = (2, -1, 0, 1)$ in (29a), of an N-walk $w = (\{2\}, \{-1, 1\}, \{-2, 0\}, \{0, 1, 2\})$ in (29b), and of the classical meanders compatible with w in (29c). Note that the walk v (highlighted in red) is compatible with the N-walk w .

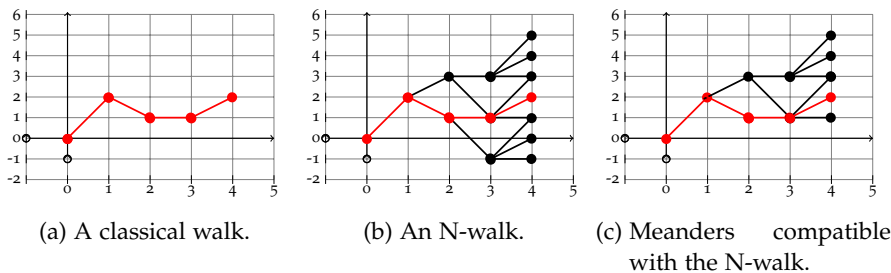


Figure 29: Geometric realization of a walk, an N-walk, and its compatible meanders.

Any set of weights, and in particular any probability distribution on the set of steps or N-steps, induces a probability distribution on walks or N-walks. The probability associated to the walk or N-walk $w = (w_1, \dots, w_n)$ is then the product $\prod_{i=1}^n \mathbb{P}(w_i)$ of the probabilities of its steps or N-steps.

4.3.1 Main results and models

Our main results are the analysis of the asymptotic number of non-deterministic walks of the *Dyck type* with step set

$$\{-1\}, \{1\}, \{-1, 1\}$$

and *Motzkin type* with step set

$$\{-1\}, \{0\}, \{1\}, \{-1, 0\}, \{-1, 1\}, \{0, 1\}, \{-1, 0, 1\}.$$

Table 5 shows the results for the unweighted case, where all weights are set equal to one. These results are derived using generating functions and singularity analysis. The reappearing phenomenon is the one of a simple dominating polar singularity arising from the large redundancy in the steps. The type of N-walk only influences the constant or the proportion among all N-walks. The lower order terms are exponentially smaller and of the square root type. These are much more influenced by the types. From a combinatorial point of view, we see a quite different behavior compared with classical paths. In particular, the limit probabilities for a Dyck N-walk of even length to be an N-bridge, an N-meander, or an N-excursion, are 1, 1/2, or 1/4, and for Motzkin N-walks 1, 3/4, or 9/16, resp., and thus do not tend to zero as it is the case for classical walks.

Next to the results on nondeterministic walks of Dyck and Motzkin type, we show the following result for arbitrary step sets.

Theorem 4.3.4. *For any N-step set S, the generating function of N-bridges is algebraic.*

Type	Dyck N-steps	Motzkin N-steps
N-Walk	3^n	7^n
N-Bridge	$3^n - \frac{2\sqrt{2}}{\sqrt{\pi}} \frac{8^{n/2}}{\sqrt{n}} + \mathcal{O}\left(\frac{8^{n/2}}{n^{3/2}}\right)$	$7^n - \sqrt{\frac{3}{\pi}} \frac{6^n}{\sqrt{n}} + \mathcal{O}\left(\frac{6^n}{n^{3/2}}\right)$
N-Meander	$\frac{3^n}{2} + \frac{6\sqrt{2}}{\sqrt{\pi}} \frac{8^{n/2}}{\sqrt{n^3}} + \mathcal{O}\left(\frac{8^{n/2}}{n^{5/2}}\right)$	$\frac{3}{4}7^n + \frac{3\sqrt{3}}{2\sqrt{\pi}} \frac{6^n}{\sqrt{n^3}} + \mathcal{O}\left(\frac{6^n}{n^{5/2}}\right)$
N-Excursion	$\frac{3^n}{4} + 4\sqrt{2} \frac{8^{n/2}}{\sqrt{\pi n^3}} + \mathcal{O}\left(\frac{8^{n/2}}{n^{5/2}}\right)$	$\frac{9}{16}7^n - \gamma \frac{6^n}{\sqrt{\pi n^3}} + \mathcal{O}\left(\frac{6^n}{n^{5/2}}\right)$

Table 5: Asymptotic number of nondeterministic unweighted (all weights equal to 1) Dyck and Motzkin N-walks with even number $n = 2k$ of steps. For odd number $n = 2k + 1$ of steps, the formulas for Motzkin N-steps stay the same, while the ones for Dyck N-steps partly change: N-Walk: 3^n ; N-Bridge and N-Excursion: 0; N-Meander: constant of $8^{n/2}/\sqrt{n^3}$ becomes $8/\sqrt{\pi}$. The constant $\gamma \approx 0.6183$ is the positive real solution of $1024\gamma^4 - 8019\gamma^2 + 2916 = 0$.

4.3.2 Motivation and related work

Let us start with a vivid motivation of the model using Russian dolls. Suppose we have a set of $n + 1$ people arranged in a line. There are three kinds of people. A person of the first kind is only able to put a received doll in a bigger one. A person of the second kind is only able to extract a smaller doll (if any) from a bigger one. If she receives the smallest doll, then she throws it away. Finally, a person of the third kind can either put a doll in a bigger one or extract a smaller doll if any. We want to know if it is possible for the last person to receive the smallest doll after it has been given to the first person and then, consecutively, handed from person to person while performing their respective operations. This is equivalent to asking if a given N-walk with each N-step in $\{\{1\}, \{-1\}, \{-1, 1\}\}$ is an N-excursion, i.e., if the N-walk is compatible with at least one excursion. The probabilistic version of this question is: What is the probability that the last person can receive the smallest doll according to some distribution on the set of people over the three kinds?

4.3.2.1 Networks and encapsulations

The original motivation of this work comes from networking. In a network, some nodes are able to encapsulate protocols (put a packet of a protocol inside a packet of another one), decapsulate protocols (extract a nested packet from another one), or perform any of these two operations. Additionally, most nodes are able to transmit packets as they receive them. A tunnel is a subpath starting with an encapsulation and ending with the corresponding decapsulation. Tunnels are very useful for achieving several goals in networking (e.g., interoperability: connecting IPv6 networks across IPv4 ones [182]; security and privacy: securing IP connections [165], establishing Virtual Private Networks [164], etc.). Moreover, tunnels can be nested to achieve several goals. Replacing the Russian dolls by packets, it is easy to see that an encapsulation can be modeled by a $\{1\}$ step, a decapsulation by a $\{-1\}$, and a passive transmission by a $\{0\}$ step.

Given a network with some nodes that are able to encapsulate or decapsulate protocols, a path from a sender to a receiver is *feasible* if it allows the latter to retrieve a packet exactly as dispatched by the sender. Computing the shortest feasible path between two nodes is polynomial [128] if cycles are allowed without restriction. In contrast, the problem is NP-hard if cycles are forbidden or arbitrarily limited. In [128], the algorithms are compared through worst-case complexity analysis and simulation. The simulation methodology for a fixed network topology is to make encapsulation (resp. decapsulation) capabilities available with some probability p and observe the processing time of the different algorithms. It would be interesting, for simulation purposes, to generate random networks with a given probability

of existence of a feasible path between two nodes. This work is the first step towards achieving this goal, since our results give the probability that any path is feasible (i.e., is a N-excursion) according to a probability distribution of encapsulation and decapsulation capabilities over the nodes.

4.3.2.2 Lattice paths

Nondeterministic walks naturally connect between lattice paths and branching processes. This is underlined by our usage of many well-established analytic and algebraic tools previously used to study lattice paths. In particular, those are the robustness of D-finite functions with respect to the Hadamard product, and the kernel method [12, 13, 19, 40, 85].

The N-walks are nondeterministic one-dimensional discrete walks. We will see that their generating functions require three variables: one marking the lowest point $\min(w)$ that can be reached by the N-walk w , another one marking the highest point $\max(w)$, and the last one marking its length $|w|$. Hence, they are also closely related to two-dimensional lattice paths, if we interpret $(\min(w), \max(w))$ as coordinates in the plane.

4.3.3 Dyck N-walks

The step set of classical Dyck paths is $\{-1, 1\}$. The N-step set of all nonempty subsets is

$$S = \{\{-1\}, \{1\}, \{-1, 1\}\},$$

and we call the corresponding N-walks *Dyck N-walks*. To every step we associate a weight or probability p_{-1} , p_1 , and $p_{-1,1}$, respectively.

Example 4.3.5 (Dyck N-walks). Let us consider the Dyck N-walk $w = (\{1\}, \{-1, 1\}, \{-1, 1\}, \{-1\})$. The sequence of its reachable points is $(\{0\}, \{1\}, \{0, 2\}, \{-1, 1, 3\}, \{-2, 0, 2\})$. There are 4 classical walks compatible with it:

Classical walk (steps)	Geometric realization (ordinates)
$(1, -1, -1, -1)$	$(0, 1, 0, -1, -2)$
$(1, -1, 1, -1)$	$(0, 1, 0, 1, 0)$
$(1, 1, -1, -1)$	$(0, 1, 2, 1, 0)$
$(1, 1, 1, -1)$	$(0, 1, 2, 3, 2)$

There are two bridges, which happen to be excursions. Thus, w is an N-bridge and an N-excursion.

The set of reachable points of a Dyck N-walk or N-meander has the following particular structure.

Lemma 4.3.6. *The reachable points of a Dyck N-walk w are*

$$\{\min(w) + 2i \mid 0 \leq \min(w) + 2i \leq \max(w)\},$$

where $\min(w)$, $\max(w)$, and the length of w have the same parity. The same result holds for Dyck N-meanders, with $\min(w)$ and $\max(w)$ replaced by $\min^+(w)$ and $\max^+(w)$ (see Definition 4.3.3).

We define the generating functions $D(x, y; t)$, $D^+(x, y; t)$, of Dyck N-walks and Dyck N-meanders as

$$\begin{aligned} & \sum_{\text{Dyck N-walk } w} \left(\prod_{s \in w} p_s \right) x^{\min(w)} y^{\max(w)} t^{|w|}, \\ & \sum_{\text{Dyck N-meander } w} \left(\prod_{s \in w} p_s \right) x^{\min^+(w)} y^{\max^+(w)} t^{|w|}. \end{aligned}$$

Note that by construction these are power series in t with Laurent polynomials in x and y , as each of the finitely many N-walks of length n has a finite minimum and maximum reachable point.

4.3.3.1 Dyck N-meanders and N-excursions

As a direct corollary of Lemma 4.3.6, all N-bridges and N-excursions have even length. The total number of Dyck N-bridges and Dyck N-excursions are then, respectively, given by

$$[x^{\leq 0} y^{\geq 0} t^{2n}] D(x, y; t) \quad \text{and} \quad D^+(0, 1; t),$$

where the nonpositive part extraction operator $[x^{\leq 0}]$ is defined as $[x^{\leq 0}] \sum_{k \in \mathbb{Z}} g_k x^k := \sum_{k \leq 0} g_k x^k$ (and analogously for $[y^{\geq 0}]$).

Proposition 4.3.7. *The generating function of Dyck N-meanders is characterized by the relation*

$$\begin{aligned} D^+(x, y; t) &= 1 + t(p_1 + p_{-1,1})xyD^+(0, 0; t) \\ &+ t(p_{-1}xy^{-1} + (p_1 + p_{-1,1})xy)(D^+(0, y; t) - D^+(0, 0; t)) \\ &+ t(p_{-1}x^{-1}y^{-1} + p_1xy + p_{-1,1}x^{-1}y)(D^+(x, y; t) - D^+(0, y; t)). \end{aligned}$$

Let us introduce the *min-max-change polynomial* $S(x, y)$ and the *kernel* $K(x, y)$ as

$$\begin{aligned} S(x, y) &:= \frac{p_{-1}}{xy} + p_1xy + p_{-1,1}\frac{y}{x}, \\ K(x, y) &:= xy(1 - tS(x, y)). \end{aligned}$$

The generating function of Dyck N-walks has now the compact form $1/(1 - tS(x, y))$. A key role in the following result on the closed form of Dyck N-meanders is played by $Y(t)$ and $X(y, t)$, the unique power

series solutions satisfying $K(1, Y(t)) = 0$, and $K(X(y, t), y) = 0$ which are given by

$$Y(t) = \frac{1 - \sqrt{1 - 4p_{-1}(p_1 + p_{-1,1})t^2}}{2(p_1 + p_{-1,1})t},$$

$$X(y, t) = \frac{1 - \sqrt{1 - 4p_1(p_{-1} + p_{-1,1}y^2)t^2}}{2p_1yt}.$$

Theorem 4.3.8. *The generating function $D^+(x, y; t)$ of Dyck N -meanders is algebraic of degree 4, and equal to*

$$\frac{x - X(y, t) \quad y - xY(t) - X(y, t)Y(t) + xyX(y, t)}{1 - X(y, t)^2 \quad xy(1 - tS(x, y))}.$$

The generating function of Dyck N -excursions is symmetric in p_{-1} and p_1 , and equal to

$$D^+(0, 1; t) = \frac{X(1, t) \quad 1 - X(1, t)Y(t)}{1 - X(1, t)^2 \quad (p_{-1} + p_{-1,1})t}.$$

With this result, we can easily answer the counting problem in which all weights are set equal to one.

Corollary 4.3.9. *For $p_{-1} = p_1 = p_{-1,1} = 1$ the generating function of unweighted Dyck N -meanders is*

$$D^+(1, 1, t) = -\frac{1 - 4t - \sqrt{1 - 8t^2}}{4t(1 - 3t)},$$

and their number $[t^n]D^+(1, 1, t)$ is asymptotically equal to

$$\frac{3^n}{2} + \left(3\sqrt{2}(1 + (-1)^n) + 4(1 - (-1)^n)\right) \frac{8^{n/2}}{\sqrt{\pi n^3}} + \mathcal{O}\left(\frac{8^{n/2}}{n^{5/2}}\right).$$

These N -walks are in bijection with walks in the first quadrant $\mathbb{Z}_{\geq 0}^2$ starting at $(0, 0)$ and consisting of steps $\{(-1, 0), (1, 0), (1, 1)\}$; see [OEIS A151281](#).

For $p_{-1} = p_1 = p_{-1,1} = 1$ the complete generating function of unweighted Dyck N -excursions is

$$D^+(0, 1, t) = \frac{1 - 8t^2 - (1 - 12t^2)\sqrt{1 - 8t^2}}{8t^2(1 - 9t^2)},$$

and their number $[t^n]D^+(0, 1, t)$ is asymptotically equal to

$$(1 + (-1)^n) \left(\frac{3^n}{8} + \sqrt{8} \frac{8^{n/2}}{\sqrt{\pi n^3}} + \mathcal{O}\left(\frac{8^{n/2}}{n^{5/2}}\right) \right).$$

We are now able to answer one of the starting questions from the networking motivation.

Theorem 4.3.10. *The probability for a random Dyck N -walk of length $2n$ to be an N -excursion has for $n \rightarrow \infty$ the following asymptotic form where the roles of p_{-1} and p_1 are interchangeable:*

- $\frac{(1-2p_1)(1-2p_{-1})}{(1-p_1)(1-p_{-1})} + \mathcal{O}\left(\frac{(4p_{-1}(1-p_{-1}))^n}{n^{3/2}}\right)$ if $0 < p_1 \leq p_{-1} < \frac{1}{2}$,
- $\frac{1-2p_1}{(1-p_1)\sqrt{\pi n}} + \mathcal{O}\left(\frac{1}{n^{3/2}}\right)$ if $0 < p_1 < \frac{1}{2}$ and $p_{-1} = \frac{1}{2}$,
- $\frac{1}{\sqrt{\pi n^3}} + \mathcal{O}\left(\frac{1}{n^{5/2}}\right)$ if $p_1 = p_{-1} = \frac{1}{2}$,
- $\mathcal{O}\left(\frac{(4p_{-1}(1-p_{-1}))^n}{n^{3/2}}\right)$ if $0 < p_1 < \frac{1}{2} < p_{-1} < 1$ and $p_{-1} + p_1 \leq 1$.

The (huge) formula for the constant in the last case can be made explicit in terms of p_{-1} and p_1 . However, it is of different shape for $p_{-1} + p_1 = 1$, and $p_{-1} + p_1 < 1$. In Figure 30 we compare the theoretical results with simulations for three different probability distributions. These nicely exemplify three of the four possible regimes.

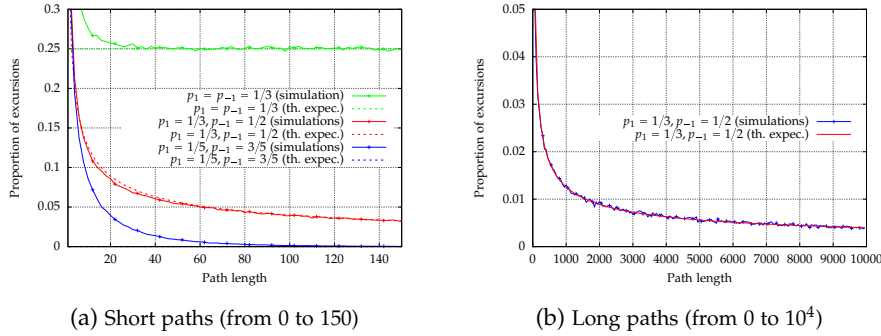


Figure 30: Comparison of theoretical expectation and averaged simulation (over 10^5 runs) of the proportion of Dyck N-excursions among Dyck N-walks.

4.3.3.2 Dyck N-bridges

We now turn our attention to Dyck N-bridges. Their generating function is defined as

$$B(x, y, t) = \sum_{n, k, \ell \geq 0} b_{2n, k, \ell} x^{-k} y^\ell t^{2n}.$$

Recall the following relation with all N-walks (note that bridges have to be of even length): $[t^{2n}]B(x, y, t) = [x^{\leq 0} y^{\geq 0} t^{2n}]D(x, y, t)$. In the following theorem we discover a great contrast to classical walks: nearly all N-walks are N-bridges.

Theorem 4.3.11. *The generating function of Dyck N-bridges $B(x, y, t)$ is algebraic of degree 4. For $p_{-1} = p_1 = p_{-1,1} = 1$ the generating function of unweighted Dyck N-bridges is algebraic of degree 2:*

$$B(1, 1, t) = \frac{1 - 6t^2}{\sqrt{1 - 8t^2(1 - 9t^2)'}}$$

and their number $[t^n]B(1, 1, t)$ is asymptotically equal to

$$\frac{1 + (-1)^n}{2} \left(3^n - \frac{2\sqrt{2}}{\sqrt{\pi}} \frac{8^{n/2}}{\sqrt{n}} + \mathcal{O}\left(\frac{8^{n/2}}{n^{3/2}}\right) \right).$$

4.3.4 Motzkin N-walks

The step set of classical Motzkin paths is $\{-1, 0, 1\}$. The N-step set of all nonempty subsets is

$$S = \{\{-1\}, \{0\}, \{1\}, \{-1, 0\}, \{-1, 1\}, \{0, 1\}, \{-1, 0, 1\}\},$$

and we call the corresponding N-walks *Motzkin N-walks*. A Motzkin N-walk w is said to be

- of type 1 if $\text{reach}(w) = \{\min(w), \min(w) + 2, \dots, \max(w)\}$,
- of type 2 if $\text{reach}(w) = \{\min(w), \min(w) + 1, \dots, \max(w)\}$ and $\max(w) - \min(w) \geq 1$.

The following proposition explains how these two types are sufficient to characterize the structure of Motzkin N-walks.

Proposition 4.3.12. *A Motzkin N-walk is of type 1 if and only if it consists only of the N-steps $\{-1\}$, $\{0\}$, $\{1\}$, and $\{-1, 1\}$. Otherwise, it is of type 2.*

The set of Motzkin N-walks of type 1 (resp. 2) is denoted by M_1 (resp. M_2), and their generating functions are defined as

$$M_1(x, y; t) = \sum_{w \in M_1} x^{\min(w)} y^{\max(w)} t^{|w|},$$

$$M_2(x, y; t) = \sum_{w \in M_2} x^{\min(w)} y^{\max(w)-1} t^{|w|}.$$

Theorem 4.3.13. *The generating functions $M_1(x, y, t)$ and $M_2(x, y, t)$ of Motzkin N-walks of type 1 and 2 are rational. The generating function of Motzkin N-bridges is algebraic and equal to*

$$[x \leq 0, y \geq 0] \left(\frac{M_1(x, y; t) + M_1(-x, y; t)}{2} + M_2(x, y; t) \right).$$

Remark 4.3.14. Using a computer algebra system it is easy to get closed forms and asymptotics for specific weights. We do not give these closed forms, as they are quite large and do not shed new light on the problem. It is however interesting to compute the asymptotic proportion of N-bridges among all N-walks. For example, when all weights are set to 1, it is equal to

$$1 - \sqrt{\frac{3}{\pi}} \frac{(6/7)^n}{\sqrt{n}} + \mathcal{O}\left(\frac{(6/7)^n}{n^{3/2}}\right).$$

Hence, again nearly all N-walks are N-bridges.

Next we consider Motzkin N-meanders and N-excursions.

Theorem 4.3.15. *The generating functions of Motzkin N-meanders and N-excursions are algebraic.*

Remark 4.3.16. We omit the technical construction of the generating functions and refer to [P11] for the full details. Instead, we state the simpler results for the unweighted case with $p_i = 1$ for all i . First, the generating function of N-meanders is algebraic of degree 2 and equal to

$$\frac{10t - 1 + \sqrt{(1+2t)(1-6t)}}{8t(1-7t)}.$$

Therefore, the total number of N-meanders is asymptotically equal to

$$\frac{3}{4}7^n + \frac{3\sqrt{3}}{2\sqrt{\pi}} \frac{6^n}{\sqrt{n^3}} + \mathcal{O}\left(\frac{6^n}{n^{5/2}}\right).$$

Second, the generating function of N-excursions is algebraic of degree 4. Their asymptotic number is

$$\frac{9}{16}7^n - \gamma \frac{6^n}{\sqrt{\pi n^3}} + \mathcal{O}\left(\frac{6^n}{n^{5/2}}\right),$$

where $\gamma \approx 0.6183$ is the positive real solution of $1024\gamma^4 - 8019\gamma^2 + 2916 = 0$. This means that for large n approximately 75% of all N-walks are N-meanders and 56.25% of all N-walks are N-excursions.

4.4 MORE MODELS OF WALKS AVOIDING A QUADRANT [P14]

In this section, we present the results from [P14] on a new model of walks confined to a non-convex cone. Over the last two decades, the enumeration of walks in the non-negative quadrant

$$\mathcal{Q} := \{(i, j) : i \geq 0 \text{ and } j \geq 0\}$$

has attracted a lot of attention and established its own scientific community with close to a hundred research papers; see, e.g., [40] and citing papers. One of its attractive features is the diversity of the used tools, such as algebra on formal power series [40, 144], bijective approaches [26, 58], computer algebra [35, 112], complex analysis [27, 157], probability theory [36, 61], and difference Galois theory [67]. Most of the attention has focused on walks *with small steps*, that is, taking their steps in a fixed subset \mathcal{S} of $\{-1, 0, 1\}^2 \setminus (0, 0)$. For each such step set \mathcal{S} (often called a *model* henceforth), one considers a trivariate generating function $Q(x, y; t)$ defined by

$$Q(x, y; t) = \sum_{n \geq 0} \sum_{i, j \in \mathcal{Q}} q_{i, j}(n) x^i y^j t^n, \quad (15)$$

where $q_{i, j}(n)$ is the number of quadrant walks with steps in \mathcal{S} , starting from $(0, 0)$, ending at (i, j) , and having in total n steps. For each \mathcal{S} , one now knows whether and where this series fits in the following classical hierarchy of series:

$$\text{rational} \subset \text{algebraic} \subset \text{D-finite} \subset \text{D-algebraic}.$$

Recall that a series (say $Q(x, y; t)$ in our case) is *rational* if it is the ratio of two polynomials, *algebraic* if it satisfies a polynomial equation (with coefficients that are polynomials in the variables), *D-finite* if it satisfies three *linear* differential equations (one in each variable), again with polynomial coefficients, and finally *D-algebraic* if it satisfies three *polynomial* differential equations. It has been known since the 1980s [91] that the generating function of walks confined to a half-plane is algebraic. This explains why $Q(x, y; t)$ is algebraic in some cases, for instance when $\mathcal{S} = \{\rightarrow, \uparrow, \leftarrow\}$: indeed, confining walks to the first quadrant is then equivalent to confining them to the right half-plane $i \geq 0$. It was shown in [40] that exactly 79 (essentially distinct) quadrant problems with small steps are *not* equivalent to any half-plane problem. One central result in the classification of these 79 models is that $Q(x, y; t)$ is D-finite if and only if a certain group, which is easy to construct from the step set \mathcal{S} , is finite [35, 36, 40, 126, 142, 145].

Since any strictly convex closed cone can be deformed into the first quadrant, the enumeration of walks confined to \mathcal{Q} captures all such counting problems (provided we consider all possible step sets \mathcal{S} , not only small steps). Similarly, any non-convex closed cone in two dimensions can be deformed into the three-quadrant plane

$$\mathcal{C} := \{(i, j) : i \geq 0 \text{ or } j \geq 0\}.$$

The enumeration of lattice paths confined to \mathcal{C} was initiated in 2016 by Bousquet-Mélou [38]. Therein, the two most natural models of walks were studied: *simple walks* with steps in $\{\rightarrow, \uparrow, \leftarrow, \downarrow\}$, and *diagonal walks* with steps in $\{\nearrow, \searrow, \swarrow, \nwarrow\}$. In both cases, the generating function

$$C(x, y; t) = \sum_{n \geq 0} \sum_{i, j \in \mathcal{C}} c_{i, j}(n) x^i y^j t^n$$

defined analogously to $Q(x, y; t)$ (see (15)) was proved to differ from the series

$$\frac{1}{3} \left(Q(x, y; t) - \frac{1}{x^2} Q\left(\frac{1}{x}, y; t\right) - \frac{1}{y^2} Q\left(x, \frac{1}{y}; t\right) \right) \quad (16)$$

by an *algebraic* one. In both cases, the underlying group is finite, hence $Q(x, y; t)$ is D-finite and $C(x, y; t)$ is D-finite as well.

It became then natural to explore more three-quadrant problems, in particular to understand whether the D-finiteness of $C(x, y; t)$ was again related to the finiteness of the associated group – at least for the 74 three-quadrant problems that are not equivalent to a half-plane problem; see Section 4.4.1. Using an asymptotic argument, Mustapha quickly proved that the 51 three-quadrant problems associated with an infinite group have, like their quadrant counterparts, a non-D-finite solution [147]. Regarding exact solutions, Raschel and Trotignon

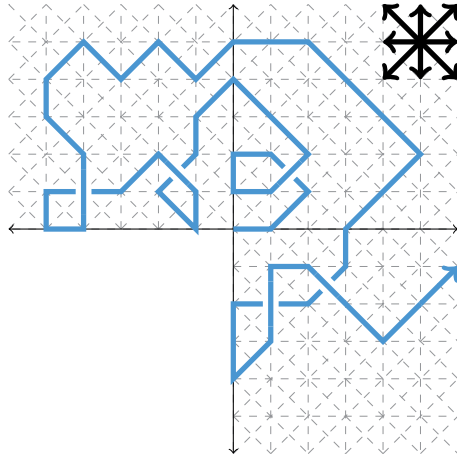


Figure 31: A king walk in the three-quadrant plane \mathcal{C} . The associated generating function is D-finite and transcendental (i.e., non-algebraic).

obtained in [158] sophisticated integral expressions for eight step sets. Four of them have a finite group (namely $\{\rightarrow, \uparrow, \leftarrow, \downarrow\}$, $\{\nearrow, \leftarrow, \downarrow\}$, $\{\rightarrow, \uparrow, \swarrow\}$, and $\{\rightarrow, \nearrow, \uparrow, \leftarrow, \swarrow, \downarrow\}$), and these expressions imply that they are D-finite (at least in x and y). In fact, the latter three are now known to be algebraic [44]. The other four have an infinite group and have been further studied by Dreyfus and Trotignon: one of them is D-algebraic, the other three are not [68]. Furthermore, the remarkable results of Budd [50] and Elvey Price [78] on the winding number of various families of plane walks provide explicit D-finite expressions for several generating functions of three-quadrant walks starting and ending close to the origin, in particular for step sets $\{\rightarrow, \nearrow, \leftarrow, \swarrow\}$ and $\{\rightarrow, \nwarrow, \leftarrow, \searrow\}$ in Budd's paper, as well as $\{\uparrow, \leftarrow, \searrow\}$ and $\{\rightarrow, \uparrow, \nwarrow, \leftarrow, \downarrow, \searrow\}$ in Elvey Price's. In both papers, when steps \nwarrow or \searrow are allowed, one includes in the enumeration walks using jumps from $(-1, 0)$ to $(0, -1)$ and vice-versa. Such jumps are forbidden in this section, but we show in [P32] that allowing them in king walks does not significantly modify the form of our results.

4.4.1 Interesting step sets

We fix a subset \mathcal{S} of $\{-1, 0, 1\}^2 \setminus \{(0, 0)\}$ and we want to count walks with steps in \mathcal{S} that start from the origin $(0, 0)$ of \mathbb{Z}^2 and remain in the cone $\mathcal{C} := \{(x, y) : x \geq 0 \text{ or } y \geq 0\}$. By this, we mean that not only must every vertex of the walk lie in \mathcal{C} , but also every edge: a walk containing a step from $(-1, 0)$ to $(0, -1)$ (or vice versa) is not considered as lying in \mathcal{C} . We often say for short that our walks *avoid the negative quadrant*. The *step polynomial* of \mathcal{S} is defined by

$$\begin{aligned} S(x, y) &= \sum_{(i,j) \in \mathcal{S}} x^i y^j \\ &= \bar{y}H_-(x) + H_0(x) + yH_+(x) = \bar{x}V_-(y) + V_0(y) + xV_+(y), \end{aligned}$$

for some Laurent polynomials H_-, H_0, H_+ and V_-, V_0, V_+ (of degree at most 1 and valuation at least -1) recording horizontal and vertical displacements, respectively. We denote by $C(x, y; t) \equiv C(x, y)$ the generating function of walks confined to \mathcal{C} , where the variable t records the length of the walk, and x and y the coordinates of its endpoints:

$$C(x, y) = \sum_{(i,j) \in \mathcal{C}} \sum_{n \geq 0} c_{i,j}(n) x^i y^j t^n = \sum_{(i,j) \in \mathcal{C}} x^i y^j C_{i,j}(t).$$

Here, $c_{i,j}(n)$ is the number of walks of length n that go from $(0, 0)$ to (i, j) and that are confined to \mathcal{C} .

As in the quadrant case [40], we can decrease the number of step sets that are worth being considered thanks to a few simple observations (*a priori*, there are 2^8 of them):

- As the cone \mathcal{C} (as well as the quarter plane \mathcal{Q}) is x/y -symmetric, the counting problems defined by \mathcal{S} and by its mirror image $\bar{\mathcal{S}} := \{(j, i) : (i, j) \in \mathcal{S}\}$ are equivalent; the associated generating functions are related by $\bar{C}(x, y) = C(y, x)$.
- If all steps of \mathcal{S} are contained in the right half-plane $\{(i, j) : i \geq 0\}$, then *all* walks with steps in \mathcal{S} lie in \mathcal{C} , and the series $C(x, y) = 1/(1 - tS(x, y))$ is simply rational. The series $Q(x, y)$ is known to be algebraic in this case [12, 41, 71, 91].
- If all steps of \mathcal{S} are contained in the left half-plane $\{(i, j) : i \leq 0\}$, then confining a walk to \mathcal{C} is equivalent to confining it to the upper half-plane: the associated generating function is then algebraic, and so is $Q(x, y)$.
- If all steps of \mathcal{S} lie (weakly) above the first diagonal ($i = j$), then confining a walk to \mathcal{C} is again equivalent to confining it to the upper half-plane: the associated generating function is then algebraic, and so is $Q(x, y)$.
- If all steps of \mathcal{S} lie (weakly) above the second diagonal ($i + j = 0$), then all walks with steps in \mathcal{S} lie in \mathcal{C} , and $C(x, y) = 1/(1 - tS(x, y))$ is simply rational. In this case however, the series $Q(x, y)$ is not at all trivial [40, 145]. Such step sets are sometimes called *singular* in the framework of quadrant walks.
- Finally, if all steps of \mathcal{S} lie (weakly) below the second diagonal, then a walk confined to \mathcal{C} moves for a while along the second diagonal, and then either stops there or leaves it into the NW or SE quadrant using a South, South-West, or West step. It cannot leave the chosen quadrant anymore and behaves therein like a half-plane walk. By polishing this observation, one can prove that $C(x, y)$ is algebraic (while $Q(x, y) = 1$).

By combining these arguments, one finds that there are 74 essentially distinct models of walks avoiding the negative quadrant that are worth studying: the 79 models considered for quadrant walks (see [40, Tables 1–4]) except the 5 “singular” models for which all steps of \mathcal{S} lie weakly above the diagonal $i + j = 0$.¹

4.4.2 The king walks

We enrich the collection of completely solved cases with the the so-called *king walks*, which take their steps from $\{\rightarrow, \nearrow, \uparrow, \nwarrow, \leftarrow, \swarrow, \downarrow, \searrow\}$; see Figure 31. This is again a finite group model, and the series $Q(x, y; t)$ is a well-understood D-finite series [40]. Here we determine $C(x, y; t)$, and show that the *algebraicity phenomenon* of [38] persists: the series $C(x, y; t)$ differs from the linear combination (16) by an algebraic series, this time of degree 216. For the simple and diagonal walks of [38] this algebraic series was of degree 72 “only”. The generating function $C_{i,j}$ of walks ending at a prescribed position (i, j) differs from a series of the form $\pm Q_{k,\ell}/3$ by an algebraic series of degree at most 24 (while this degree was bounded by 8 in the models of [38]).

Moreover, we expect a similar property to hold (with variations on the above linear combination of the series Q) for the 7 step sets of Figure 32, related to reflection groups, and for which the quadrant problem can be solved using the reflection principle [92]. However, we also expect the effective solution of these models to be extremely challenging in computational terms, mostly, because the relevant algebraic series have very large degree. This is illustrated by our main theorem below. There, and in the sequel, we use the shorthand $\bar{x} = 1/x$, $\bar{y} = 1/y$, and omit in the notation the dependencies on t , writing for instance $Q(x, y)$ instead of $Q(x, y; t)$.

Theorem 4.4.1. *Take the step set $\{-1, 0, 1\}^2 \setminus \{(0, 0)\}$ and let $Q(x, y)$ be the generating function of lattice walks starting from $(0, 0)$ that are confined to the first quadrant \mathcal{Q} (this series is D-finite and given in [40]). Then, the generating function of walks starting from $(0, 0)$, confined to \mathcal{C} , and ending in the first quadrant (resp. at a negative abscissa) is*

$$\frac{1}{3}Q(x, y) + P(x, y), \quad (\text{resp. } -\frac{\bar{x}^2}{3}Q(\bar{x}, y) + \bar{x}M(\bar{x}, y)), \quad (17)$$

where $P(x, y)$ and $M(x, y)$ are algebraic of degree 216 over $\mathbb{Q}(x, y, t)$. Of course, the generating function of walks ending at a negative ordinate follows, using the x/y -symmetry.

The series P is expressed in terms of M by:

$$P(x, y) = \bar{x}(M(x, y) - M(0, y)) + \bar{y}(M(y, x) - M(0, x)), \quad (18)$$

¹This corrects two typos in [43, Section 2.1], where 51 distinct models as well as 56 quadrant models were wrongly mentioned.

and M is defined by the following equation:

$$\begin{aligned}
 K(x, y) (2M(x, y) - M(0, y)) &= \frac{2x}{3} - 2t\bar{y}(x + 1 + \bar{x})M(x, 0) \\
 &+ t\bar{y}(y + 1 + \bar{y})M(y, 0) + t(x - \bar{x})(y + 1 + \bar{y})M(0, y) \quad (19) \\
 &- t(1 + \bar{y}^2 - 2\bar{x}\bar{y})M(0, 0) - t\bar{y}M_x(0, 0),
 \end{aligned}$$

where $K(x, y) = 1 - t(x + xy + y + \bar{x}y + \bar{x} + \bar{x}\bar{y} + \bar{y} + x\bar{y})$. The specializations $M(x, 0)$ and $M(0, y)$ are algebraic each of degree 72 over $\mathbb{Q}(x, t)$ and $\mathbb{Q}(y, t)$, respectively, and $M(0, 0)$ and $M_x(0, 0)$ have degree 24 over $\mathbb{Q}(t)$.

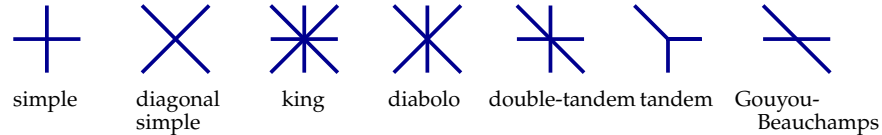


Figure 32: The seven step sets to which the strategy of this section should apply. The first two are solved in [38], the third one in this section.

We have moreover a complete algebraic description of all the series needed to reconstruct $P(x, y)$ and $M(x, y)$ from (18) and (19), namely the univariate series $M(0, 0)$ and $M_x(0, 0)$, and the bivariate series $M(x, 0)$ and $M(0, y)$. In particular, both univariate series lie in the extension of $\mathbb{Q}(t)$ (the field of rational functions in t) generated in 3 steps as follows: first, $u = t + t^2 + \mathcal{O}(t^3)$ is the only series in t satisfying

$$(1 - 3u)^3(1 + u)t^2 + (1 + 18u^2 - 27u^4)t - u = 0,$$

then $v = t + 3t^2 + \mathcal{O}(t^3)$ is the only series with constant term zero satisfying

$$(1 + 3v - v^3)u - v(v^2 + v + 1) = 0,$$

and finally

$$w = \sqrt{1 + 4v - 4v^3 - 4v^4} = 1 + 2t + 4t^2 + \mathcal{O}(t^3).$$

Schematically, $\mathbb{Q}(t) \xrightarrow{4} \mathbb{Q}(t, u) \xrightarrow{3} \mathbb{Q}(t, v) \xrightarrow{2} \mathbb{Q}(t, w)$. Of particular interest is the series $M(0, 0)$: by (17), this is also the series $C_{-1,0}$ that counts by the length walks in \mathcal{C} ending at $(-1, 0)$. It is algebraic, as conjectured in [158], and given by

$$\begin{aligned}
 M(0, 0) = C_{-1,0} &= \frac{1}{2t} \left(\frac{w(1 + 2v)}{1 + 4v - 2v^3} - 1 \right) \\
 &= t + 2t^2 + 17t^3 + 80t^4 + 536t^5 + \mathcal{O}(t^6).
 \end{aligned}$$

Once the series $C(x, y)$ is determined, we are able to derive detailed asymptotic results, which refine general universal results of Denisov and Wachtel [61] and Mustapha [147] (who obtained the following estimates up to a multiplicative factor).

Corollary 4.4.2. *The number $c_{0,0}(n)$ of n -step king walks confined to \mathcal{C} and ending at the origin, and the number $c(n)$ of walks of \mathcal{C} ending anywhere satisfy for $n \rightarrow \infty$:*

$$c_{0,0}(n) \sim \left(\frac{2^{29}K}{3^7}\right)^{1/3} \frac{\Gamma(2/3)}{\pi} \frac{8^n}{n^{5/3}},$$

$$c(n) \sim \left(\frac{2^{32}K}{3^7}\right)^{1/6} \frac{1}{\Gamma(2/3)} \frac{8^n}{n^{1/3}},$$

where K is the unique real root of $101^6K^3 - 601275603K^2 + 92811K - 1$.

BIBLIOGRAPHY

- [1] M. Abramowitz and I. A. Stegun. *Handbook of Mathematical Functions With Formulas, Graphs, and Mathematical Tables*, volume 55. U.S. Government Printing Office, Washington, D.C., 1964. Tenth Printing, December 1972.
- [2] R. Albert and A.-L. Barabási. Statistical mechanics of complex networks. *Reviews of Modern Physics*, 74(1):47–97, Jan. 2002.
- [3] D. Aldous and P. Diaconis. Longest increasing subsequences: from patience sorting to the Baik-Deift-Johansson theorem. *Bull. Amer. Math. Soc. (N.S.)*, 36(4):413–432, 1999.
- [4] D. André. Sur les permutations alternées. *Journal de mathématiques pures et appliquées*, 7:167–184, 1881. Long version of several articles by André in 1879.
- [5] G. E. Andrews, R. Askey, and R. Roy. *Special Functions*, volume 71 of *Encyclopedia of Mathematics and its Applications*. Cambridge University Press, 1999.
- [6] O. Angel, A. E. Holroyd, D. Romik, and B. Virág. Random sorting networks. *Adv. Math.*, 215(2):839–868, 2007.
- [7] A. Asinowski, A. Bacher, C. Banderier, and B. Gittenberger. Analytic combinatorics of lattice paths with forbidden patterns: enumerative aspects. In *LATA'18*, volume 10792 of *Lecture Notes in Comput. Sci.*, pages 195–206. Springer, 2018.
- [8] K. B. Athreya and S. Karlin. Embedding of urn schemes into continuous time Markov branching processes and related limit theorems. *Ann. Math. Statist.*, 39:1801–1817, 1968.
- [9] K. B. Athreya and P. E. Ney. *Branching processes*. Dover Publications, 2004. Reprint of the 1972 original.
- [10] A. Bagchi and A. K. Pal. Asymptotic normality in the generalized Pólya-Eggenberger urn model, with an application to computer data structures. *SIAM J. Algebraic Discrete Methods*, 6(3):394–405, 1985.
- [11] C. Banderier, M. Bousquet-Mélou, A. Denise, P. Flajolet, D. Gardy, and D. Gouyou-Beauchamps. Generating functions for generating trees. *Discrete Math.*, 246(1-3):29–55, 2002.
- [12] C. Banderier and P. Flajolet. Basic analytic combinatorics of directed lattice paths. *Theoret. Comput. Sci.*, 281(1-2):37–80, 2002.

- [13] C. Banderier, C. Krattenthaler, A. Krinik, D. Kruchinin, V. Kruchinin, D. Nguyen, and M. Wallner. *Explicit Formulas for Enumeration of Lattice Paths: Basketball and the Kernel Method*, volume 58 of *Dev. in Mathematics*, pages 78–118. Springer, 2019.
- [14] C. Banderier, P. Marchal, and M. Wallner. Periodic Pólya Urns and an Application to Young Tableaux. In *AofA 2018*, volume 110 of *Leibniz International Proceedings in Informatics (LIPIcs)*, pages 11.1–11.13, 2018.
- [15] C. Banderier, P. Marchal, and M. Wallner. Rectangular Young tableaux with local decreases and the density method for uniform random generation. In *GASCom 2018, CEUR Workshop Proceedings*, volume 2113, pages 60–68, 2018.
- [16] C. Banderier, P. Marchal, and M. Wallner. Periodic Pólya urns, the density method and asymptotics of Young tableaux. *Ann. Probab.*, 48(4):1921–1965, 2020.
- [17] C. Banderier and P. Nicodème. Bounded discrete walks. *Discrete Math. Theor. Comput. Sci.*, AM:35–48, 2010.
- [18] C. Banderier and M. Wallner. Lattice paths with catastrophes. *Discrete Mathematics & Theoretical Computer Science*, Vol 19 no. 1, Sept. 2017. Full version.
- [19] C. Banderier and M. Wallner. *The Kernel Method for Lattice Paths Below a Line of Rational Slope*, volume 58 of *Dev. in Mathematics*, pages 119–154. Springer, 2019.
- [20] Y. Baryshnikov and D. Romik. Enumeration formulas for Young tableaux in a diagonal strip. *Israel J. Math.*, 178:157–186, 2010.
- [21] N. Basset. Counting and generating permutations in regular classes. *Algorithmica*, 76(4):989–1034, 2016.
- [22] F. Bassino, J. David, and A. Sportiello. Asymptotic enumeration of minimal automata. In *STACS 2012*, volume 14 of *LIPIcs. Leibniz Int. Proc. Inform.*, pages 88–99. Schloss Dagstuhl. Leibniz-Zent. Inform., Wadern, 2012.
- [23] F. Bassino and C. Nicaud. Enumeration and random generation of accessible automata. *Theoret. Comput. Sci.*, 381(1-3):86–104, 2007.
- [24] N. R. Beaton, A. J. Guttmann, I. Jensen, and G. F. Lawler. Compressed self-avoiding walks, bridges and polygons. *Journal of Physics A: Mathematical and Theoretical*, 48(45):454001, oct 2015.

- [25] F. Bergeron, P. Flajolet, and B. Salvy. Varieties of increasing trees. In *CAAP '92 (Rennes, 1992)*, volume 581 of *Lecture Notes in Computer Science*, pages 24–48. Springer Berlin Heidelberg, 1992.
- [26] O. Bernardi. Bijective counting of Kreweras walks and loopless triangulations. *J. Combin. Theory Ser. A*, 114(5):931–956, 2007.
- [27] O. Bernardi, M. Bousquet-Mélou, and K. Raschel. Counting quadrant walks via Tutte’s invariant method. *Combin. Theory*, 1, 2021.
- [28] J. Bertoin and M. Yor. On subordinators, self-similar Markov processes and some factorizations of the exponential variable. *Electron. Comm. Probab.*, 6:95–106, 2001.
- [29] F. Beukers, J. A. C. Kolk, and E. Calabi. Sums of generalized harmonic series and volumes. *Nieuw Arch. Wiskd., IV. Ser.*, 11(3):217–224, 1993.
- [30] P. Biane. Representations of symmetric groups and free probability. *Adv. Math.*, 138(1):126–181, 1998.
- [31] O. Bodini and Y. Ponty. Multi-dimensional Boltzmann sampling of languages. *Discrete Math. Theor. Comput. Sci. Proc.*, AM:49–63, 2010.
- [32] M. Bóna. *Combinatorics of permutations*. Chapman & Hall/CRC, 2004.
- [33] A. Borodin and G. Olshanski. *Representations of the Infinite Symmetric Group*, volume 160 of *Cambridge Studies in Advanced Mathematics*. Cambridge University Press, Cambridge, 2017.
- [34] A. Bostan, F. Chyzak, M. Giusti, R. Lebreton, G. Lecerf, B. Salvy, and É. Schost. *Algorithmes Efficaces en Calcul Formel*. Self-publishing, Aug. 2017.
- [35] A. Bostan and M. Kauers. The complete generating function for Gessel walks is algebraic. *Proc. Amer. Math. Soc.*, 138(9):3063–3078, 2010.
- [36] A. Bostan, K. Raschel, and B. Salvy. Non-D-finite excursions in the quarter plane. *J. Combin. Theory Ser. A*, 121:45–63, 2014.
- [37] M. Bousquet-Mélou. Discrete excursions. *Sém. Lothar. Combin.*, 57:23 pp., 2008.
- [38] M. Bousquet-Mélou. Square lattice walks avoiding a quadrant. *Journal of Combinatorial Theory, Series A*, 144:37 – 79, 2016.

- [39] M. Bousquet-Mélou, M. Lohrey, S. Maneth, and E. Noeth. XML compression via directed acyclic graphs. *Theory of Computing Systems*, 57(4):1322–1371, 2015.
- [40] M. Bousquet-Mélou and M. Mishna. Walks with small steps in the quarter plane. In *Algorithmic probability and combinatorics*, volume 520 of *Contemp. Math.*, pages 1–39. Amer. Math. Soc., Providence, RI, 2010.
- [41] M. Bousquet-Mélou and M. Petkovšek. Linear recurrences with constant coefficients: the multivariate case. *Discrete Math.*, 225(1-3):51–75, 2000.
- [42] M. Bousquet-Mélou and Y. Ponty. Culminating paths. *Discrete Math. Theor. Comput. Sci.*, 10(2):125–152, 2008.
- [43] M. Bousquet-Mélou and M. Wallner. More Models of Walks Avoiding a Quadrant. In *AofA 2020*, volume 159 of *LIPICs*, pages 8:1–8:14, Dagstuhl, Germany, 2020.
- [44] M. Bousquet-Mélou. Enumeration of three-quadrant walks via invariants: some diagonally symmetric models. *arXiv*, pages 1–56, 2021.
- [45] C. Boutillier, J. Bouttier, G. Chapuy, S. Corteel, and S. Ramasamy. Dimers on rail yard graphs. *Ann. Inst. Henri Poincaré D*, 4(4):479–539, 2017.
- [46] J. Bouttier, G. Chapuy, and S. Corteel. From Aztec diamonds to pyramids: steep tilings. *Trans. Amer. Math. Soc.*, 369(8):5921–5959, 2017.
- [47] R. Brak, G. K. Iliev, and T. Prellberg. An infinite family of adsorption models and restricted Lukasiewicz paths. *J. Stat. Phys.*, 145(3):669–685, 2011.
- [48] G. Brightwell and P. Winkler. Counting linear extensions. *Order*, 8(3):225–242, 1991. A preliminary version appeared in the proceedings of STOC’91.
- [49] N. Broutin, L. Devroye, E. McLeish, and M. de la Salle. The height of increasing trees. *Random Structures Algorithms*, 32(4):494–518, 2008.
- [50] T. Budd. Winding of simple walks on the square lattice. *J. Combin. Theory Ser. A*, 172:105191, 59, 2020.
- [51] A. Bufetov and V. Gorin. Fourier transform on high-dimensional unitary groups with applications to random tilings. *Duke Math. J.*, 168(13):2559–2649, 2019.

- [52] D. Callan. A determinant of Stirling cycle numbers counts unlabeled acyclic single-source automata. *Discrete Math. Theor. Comput. Sci.*, 10(2):77–86, 2008.
- [53] D. Callan. A combinatorial survey of identities for the double factorial. *arXiv*, 2009.
- [54] T. Carleman. *Sur les équations intégrales singulières à noyau réel et symétrique*. Uppsala Universitets Årsskrift, 1923.
- [55] L. Carlitz. Permutations with prescribed pattern. *Math. Nachr.*, 58:31–53, 1973.
- [56] B. Chauvin, C. Mailler, and N. Pouyanne. Smoothing equations for large Pólya urns. *J. Theoret. Probab.*, 28(3):923–957, 2015.
- [57] K. L. Chung and W. Feller. On fluctuations in coin-tossing. *Proc. Nat. Acad. Sci. U. S. A.*, 35:605–608, 1949.
- [58] F. Chyzak and K. Yeats. Bijections between Łukasiewicz walks and generalized tandem walks. *Electron. J. Combin.*, 27(2):Paper 2.3, 46 pp., 2020.
- [59] A. R. Conway and A. J. Guttmann. On 1324-avoiding permutations. *Adv. in Appl. Math.*, 64:50–69, 2015.
- [60] A. R. Conway, A. J. Guttmann, and P. Zinn-Justin. 1324-avoiding permutations revisited. *Adv. in Appl. Math.*, 96:312–333, 2018.
- [61] D. Denisov and V. Wachtel. Random walks in cones. *Ann. Probab.*, 43(3):992–1044, 2015.
- [62] S. Dittmer and I. Pak. Counting linear extensions of restricted posets. *Electron. J. Combin.*, 27(4):Paper No. 4.48, 13, 2020.
- [63] M. Domaratzki. Combinatorial interpretations of a generalization of the Genocchi numbers. *J. Integer Seq.*, 7(3):Article 04.3.6, 11, 2004.
- [64] M. Domaratzki. Improved bounds on the number of automata accepting finite languages. *Internat. J. Found. Comput. Sci.*, 15(1):143–161, 2004. Computing and Combinatorics Conference—COCOON’02.
- [65] M. Domaratzki. Enumeration of formal languages. *Bulletin of the EATCS*, 89:117–133, 2006.
- [66] M. Domaratzki, D. Kisman, and J. Shallit. On the number of distinct languages accepted by finite automata with n states. *J. Autom. Lang. Comb.*, 7(4):469–486, 2002.

- [67] T. Dreyfus, C. Hardouin, J. Roques, and M. F. Singer. On the nature of the generating series of walks in the quarter plane. *Invent. Math.*, 213(1):139–203, 2018.
- [68] T. Dreyfus and A. Trotignon. On the Nature of Four Models of Symmetric Walks Avoiding a Quadrant. *Ann. Comb.*, 25(3):617–644, 2021.
- [69] M. Drmota. The height of increasing trees. *Annals of Combinatorics*, 12(4):373–402, 2009.
- [70] M. Drmota. *Random trees: an interplay between combinatorics and probability*. Springer Science & Business Media, 2009.
- [71] P. Duchon. On the enumeration and generation of generalized Dyck words. *Discrete Math.*, 225(1-3):121–135, 2000.
- [72] P. Duchon, P. Flajolet, G. Louchard, and G. Schaeffer. Random sampling from Boltzmann principles. In *Automata, languages and programming. Proceedings of ICALP 2002.*, pages 501–513. Springer, 2002.
- [73] H. Duminił-Copin and S. Smirnov. The connective constant of the honeycomb lattice equals $\sqrt{2 + \sqrt{2}}$. *Ann. of Math. (2)*, 175(3):1653–1665, 2012.
- [74] E. Duse, K. Johansson, and A. Metcalfe. The cusp-Airy process. *Electron. J. Probab.*, 21:Paper No. 57, 50, 2016.
- [75] F. Eggenberger and G. Pólya. Über die Statistik verketteter Vorgänge. *Z. Angew. Math. Mech.*, 3:279–290, 1923.
- [76] F. Eggenberger and G. Pólya. Sur l’interprétation de certaines courbes de fréquence. *C. R. Acad. Sc.*, 187:870–872, 1928.
- [77] N. D. Elkies. On the sums $\sum_{k=-\infty}^{\infty} (4k + 1)^{-n}$. *Amer. Math. Monthly*, 110(7):561–573, 2003.
- [78] A. Elvey Price. Counting lattice walks by winding angle. *Sém. Lothar. Combin.*, 84B:Art. 43, 12 pp., 2020.
- [79] A. Elvey Price and A. J. Guttmann. Numerical studies of Thompson’s group F and related groups. *Internat. J. Algebra Comput.*, 29(2):179–243, 2019.
- [80] G. Fanti and P. Viswanath. Deanonymization in the Bitcoin P2P Network. *Proceedings of the 31st Conference on Neural Information Processing Systems*, 2017.
- [81] W. Feller. *An introduction to probability theory and its applications. Vol. I*. Third edition. John Wiley & Sons, 1968.

- [82] P. Flajolet, P. Dumas, and V. Puyhaubert. Some exactly solvable models of urn process theory. *Discrete Math. Theor. Comput. Sci. Proc.*, AG:59–118, 2006.
- [83] P. Flajolet, J. Gabarró, and H. Pekari. Analytic urns. *Ann. Probab.*, 33(3):1200–1233, 2005.
- [84] P. Flajolet and T. Lafforgue. Search costs in quadrees and singularity perturbation asymptotics. *Discrete Comput. Geom.*, 12(2):151–175, 1994.
- [85] P. Flajolet and R. Sedgewick. *Analytic Combinatorics*. Cambridge University Press, 2009.
- [86] P. Flajolet, P. Sipala, and J.-M. Steyaert. Analytic variations on the common subexpression problem. In *Automata, languages and programming*, pages 220–234. Springer, 1990.
- [87] P. Flajolet, P. Zimmerman, and B. Van Cutsem. A calculus for the random generation of labelled combinatorial structures. *Theoret. Comput. Sci.*, 132(1-2):1–35, 1994.
- [88] M. Fréchet and J. Shohat. A proof of the generalized second-limit theorem in the theory of probability. *Trans. Amer. Math. Soc.*, 33(2):533–543, 1931.
- [89] M. Fuchs, G.-R. Yu, and L. Zhang. On the asymptotic growth of the number of tree-child networks. *European J. Combin.*, 93:Paper No. 103278, 20, 2021.
- [90] A. Genitrini, B. Gittenberger, M. Kauers, and M. Wallner. Asymptotic enumeration of compacted binary trees of bounded right height. *J. Combin. Theory Ser. A*, 172:105177, 49, 2020.
- [91] I. Gessel. A factorization for formal Laurent series and lattice path enumeration. *J. Combin. Theory Ser. A*, 28(3):321–337, 1980.
- [92] I. M. Gessel and D. Zeilberger. Random walk in a Weyl chamber. *Proc. Amer. Math. Soc.*, 115(1):27–31, 1992.
- [93] C. Goldschmidt and B. Haas. A line-breaking construction of the stable trees. *Electron. J. Probab.*, 20:no. 16, 24, 2015.
- [94] V. Gorin and M. Rahman. Random sorting networks: local statistics via random matrix laws. *Probability Theory and Related Fields*, 175:45–96, 2019.
- [95] C. Greene, A. Nijenhuis, and H. S. Wilf. Another probabilistic method in the theory of Young tableaux. *J. Comb. Theory, Ser. A*, 37:127–135, 1984.

- [96] A. J. Guttmann. Analysis of series expansions for non-algebraic singularities. *Journal of Physics A: Mathematical and Theoretical*, 48(4):045209, 2015.
- [97] J. E. Hopcroft and J. D. Ullman. *Introduction to automata theory, languages, and computation*. Addison-Wesley Publishing Co., Reading, Mass., 1979. Addison-Wesley Series in Computer Science.
- [98] K. Humphreys. A history and a survey of lattice path enumeration. *J. Statist. Plann. Inference*, 140(8):2237–2254, 2010.
- [99] E. J. Janse van Rensburg. Square lattice directed paths adsorbing on the line $y = qx$. *Journal of Statistical Mechanics: Theory and Experiment*, 2005(09):P09010, 2005.
- [100] E. J. Janse van Rensburg, T. Prellberg, and A. Rechnitzer. Partially directed paths in a wedge. *J. Combin. Theory Ser. A*, 115(4):623–650, 2008.
- [101] E. J. Janse van Rensburg and A. Rechnitzer. Adsorbing and collapsing directed animals. *J. Statist. Phys.*, 105(1-2):49–91, 2001.
- [102] S. Janson. Functional limit theorems for multitype branching processes and generalized Pólya urns. *Stochastic Process. Appl.*, 110(2):177–245, 2004.
- [103] S. Janson. Asymptotic degree distribution in random recursive trees. *Random Structures Algorithms*, 26(1-2):69–83, 2005.
- [104] S. Janson. Limit theorems for triangular urn schemes. *Probab. Theory Related Fields*, 134(3):417–452, 2006.
- [105] S. Janson. Brownian excursion area, Wright’s constants in graph enumeration, and other Brownian areas. *Probab. Surv.*, 4:80–145, 2007.
- [106] S. Janson. Plane recursive trees, Stirling permutations and an urn model. In *Fifth Colloquium on Mathematics and Computer Science*, Discrete Math. Theor. Comput. Sci. Proc., AI, pages 541–547. Assoc. Discrete Math. Theor. Comput. Sci., Nancy, 2008.
- [107] S. Janson. Moments of Gamma type and the Brownian supremum process area. *Probab. Surv.*, 7:1–52, 2010. With addendum on pages 207–208.
- [108] S. Janson, M. Kuba, and A. Panholzer. Generalized Stirling permutations, families of increasing trees and urn models. *J. Combin. Theory Ser. A*, 118(1):94–114, 2011.
- [109] M. Jerrum. *Counting, Sampling and Integrating: Algorithms and Complexity*. Birkhäuser, 2003.

- [110] K. Johansson and E. Nordenstam. Eigenvalues of GUE minors. *Electron. J. Probab.*, 11:1342–1371, 2007. See also the erratum in [Electron. J. Probab. (2007), vol. 12, pp. 1048–1051].
- [111] J.-P. Kahane. Propriétés locales des fonctions à séries de Fourier aléatoires. *Studia Math.*, 19:1–25, 1960.
- [112] M. Kauers, C. Koutschan, and D. Zeilberger. Proof of Ira Gessel’s lattice path conjecture. *Proc. Natl. Acad. Sci. USA*, 106(28):11502–11505, 2009.
- [113] M. Kauers and P. Paule. *The concrete tetrahedron*. Texts and Monographs in Symbolic Computation. Springer, 2011. Symbolic sums, recurrence equations, generating functions, asymptotic estimates.
- [114] R. Kenyon. Dominos and the Gaussian free field. *Ann. Probab.*, 29(3):1128–1137, 2001.
- [115] S. V. Kerov. Transition probabilities of continual Young diagrams and the Markov moment problem. *Funct. Anal. Appl.*, 27(2):104–117, 1993.
- [116] M. Khodabin and A. Ahmadabadi. Some properties of generalized gamma distribution. *Math. Sci. Q. J.*, 4(1):9–27, 2010.
- [117] D. E. Knuth. *The art of computer programming. Vol. 1: Fundamental algorithms*. Addison-Wesley, 1968.
- [118] D. E. Knuth. *The Art of Computer Programming. Volume 4A. Combinatorial Algorithms, Part 1*. Addison-Wesley, 2011.
- [119] A. D. Korshunov. Enumeration of finite automata. *Problemy Kibernet.*, 34:5–82, 1978. (In Russian).
- [120] A. D. Korshunov. On the number of nonisomorphic strongly connected finite automata. *Elektron. Informationsverarb. Kybernet.*, 22(9):459–462, 1986.
- [121] T. Kousha. Asymptotic behavior and the moderate deviation principle for the maximum of a Dyck path. *Statist. Probab. Lett.*, 82(2):340–347, 2012.
- [122] C. Krattenthaler. Lattice path enumeration. In *Handbook of enumerative combinatorics*, Discrete Math. Appl. (Boca Raton), pages 589–678. CRC Press, Boca Raton, FL, 2015.
- [123] M. Kuba and H. M. Mahmoud. Two-colour balanced affine urn models with multiple drawings I: central limit theorems. *arXiv*, 2015.

- [124] M. Kuba and A. Panholzer. On the degree distribution of the nodes in increasing trees. *Journal of Combinatorial Theory, Series A*, 114(4):597–618, may 2007.
- [125] M. Kuba and H. Sulzbach. On martingale tail sums in affine two-color urn models with multiple drawings. *J. Appl. Probab.*, 54(1):96–117, 2017.
- [126] I. Kurkova and K. Raschel. On the functions counting walks with small steps in the quarter plane. *Publications mathématiques de l’IHÉS*, 116(1):69–114, 2012.
- [127] J. Labelle and Y.-N. Yeh. Generalized Dyck paths. *Discrete Math.*, 82(1):1–6, 1990.
- [128] M. L. Lamali, N. Fergani, J. Cohen, and H. Pouyllau. Path computation in multi-layer networks: Complexity and algorithms. In *IEEE INFOCOM 2016, San Francisco, CA, USA, April 10-14, 2016*, pages 1–9, 2016.
- [129] N. Lasmar, C. Mailler, and O. Selmi. Multiple drawing multi-colour urns by stochastic approximation. *J. Appl. Probab.*, 55(1):254–281, 2018.
- [130] S. Linusson, S. Potka, and R. Sulzgruber. On random shifted standard Young tableaux and 132-avoiding sorting networks. *arXiv*, 2018.
- [131] V. A. Liskovets. Exact enumeration of acyclic deterministic automata. *Discrete Applied Mathematics*, 154(3):537–551, 2006.
- [132] B. F. Logan and L. A. Shepp. A variational problem for random Young tableaux. *Advances in Math.*, 26(2):206–222, 1977.
- [133] J.-M. Luck. On the frequencies of patterns of rises and falls. *Physica A*, 407:252–275, 2014.
- [134] I. G. Macdonald. *Symmetric functions and Hall polynomials*. Oxford Classic Texts in the Physical Sciences. The Clarendon Press, Oxford University Press, second edition, 2015.
- [135] H. M. Mahmoud. Distances in random plane-oriented recursive trees. *Journal of Computational and Applied Mathematics*, 41(1-2):237–245, aug 1992. Asymptotic methods in analysis and combinatorics.
- [136] H. M. Mahmoud. *Pólya urn models*. CRC Press, 2009.
- [137] H. M. Mahmoud, R. T. Smythe, and J. Szymański. On the structure of random plane-oriented recursive trees and their branches. *Random Structures Algorithms*, 4(2):151–176, 1993.

- [138] P. Marchal. Rectangular Young tableaux and the Jacobi ensemble. *Discrete Math. Theor. Comput. Sci. Proceedings*, BC:839–850, 2016.
- [139] P. Marchal. The density method and permutations with a prescribed descent set. In *GASCom 2018, CEUR Workshop Proceedings. Vol. 2113.*, pages 179–186, 2018.
- [140] P. Marchal. Permutations with a prescribed descent set. In *GASCom 2018, CEUR Workshop Proceedings*, volume 2113, pages 179–186, 2018.
- [141] B. D. McKay, J. Morse, and H. S. Wilf. The distributions of the entries of Young tableaux. *J. Combin. Theory Ser. A*, 97(1):117–128, 2002.
- [142] S. Melczer and M. Mishna. Singularity analysis via the iterated kernel method. *Combin. Probab. Comput.*, 23(5):861–888, 2014.
- [143] D. Merlini, D. G. Rogers, R. Sprugnoli, and C. Verri. Underdiagonal lattice paths with unrestricted steps. *Discrete Appl. Math.*, 91(1-3):197–213, 1999.
- [144] M. Mishna. Classifying lattice walks restricted to the quarter plane. *J. Combin. Theory Ser. A*, 116(2):460–477, 2009.
- [145] M. Mishna and A. Rechnitzer. Two non-holonomic lattice walks in the quarter plane. *Theoret. Comput. Sci.*, 410(38-40):3616–3630, 2009.
- [146] A. H. Morales, I. Pak, and G. Panova. Hook formulas for skew shapes III. Multivariate and product formulas. *arXiv*, 2017.
- [147] S. Mustapha. Non-D-finite walks in a three-quadrant cone. *Ann. Comb.*, 23(1):143–158, 2019.
- [148] A. Nijenhuis and H. S. Wilf. *Combinatorial algorithms*. Academic Press, Inc. [Harcourt Brace Jovanovich, Publishers], New York-London, second edition, 1978.
- [149] I. Pak. Hook length formula and geometric combinatorics. *Sém. Lothar. Combin.*, 46:Art. B46f, 13, 2001.
- [150] E. A. Peköz, A. Röllin, and N. Ross. Generalized gamma approximation with rates for urns, walks and trees. *Ann. Probab.*, 44(3):1776–1816, 2016.
- [151] M. Petkovsek, H. S. Wilf, and D. Zeilberger. *A = B*. AK Peters, 1996.
- [152] L. Petrov. Asymptotics of uniformly random lozenge tilings of polygons. Gaussian free field. *Ann. Probab.*, 43(1):1–43, 2015.

- [153] B. Pittel. Note on the heights of random recursive trees and random m -ary search trees. *Random Structures Algorithms*, 5(2):337–347, 1994.
- [154] B. Pittel and D. Romik. Limit shapes for random square Young tableaux. *Adv. Appl. Math.*, 38(2):164–209, 2007.
- [155] C. Pittet and L. Saloff-Coste. On random walks on wreath products. *Ann. Probab.*, 30(2):948–977, 2002.
- [156] G. Pólya. Sur quelques points de la théorie des probabilités. *Annales de l'Institut Henri Poincaré*, 1:117–161, 1930.
- [157] K. Raschel. Counting walks in a quadrant: a unified approach via boundary value problems. *J. Eur. Math. Soc. (JEMS)*, 14(3):749–777, 2012.
- [158] K. Raschel and A. Trotignon. On Walks Avoiding a Quadrant. *Electron. J. Combin.*, 26(3):Paper 3, 31, 2019.
- [159] D. Revelle. Heat kernel asymptotics on the lamplighter group. *Electronic Communications in Probability*, 8:142–154, 2003.
- [160] R. L. Rivest. Bayesian tabulation audits: Explained and extended. *arXiv*, 2018.
- [161] D. Romik. Explicit formulas for hook walks on continual Young diagrams. *Adv. in Appl. Math.*, 32(4):625–654, 2004.
- [162] D. Romik. Arctic circles, domino tilings and square Young tableaux. *Ann. Probab.*, 40(2):611–647, 2012.
- [163] D. Romik. *The Surprising Mathematics of Longest Increasing Subsequences*. Institute of Mathematical Statistics Textbooks. Cambridge University Press, 2015.
- [164] E. Rosen, I. Wijnands, Y. Cai, and A. Boers. RFC7582 - multicast virtual private network (mvpn): Using bidirectional p-tunnels, 2015.
- [165] K. Seo and S. Kent. RFC4301 - security architecture for the internet protocol, 2005.
- [166] S. Sheffield. Random Surfaces. *Astérisque*, 304, 2005.
- [167] N. J. A. Sloane. The On-Line Encyclopedia of Integer Sequences (OEIS). <http://oeis.org>.
- [168] R. T. Smythe and H. M. Mahmoud. A survey of recursive trees. *Theory of Probability and Mathematical Statistics*, 51:1–27, 1994.
- [169] P. Śniady. Robinson–Schensted–Knuth algorithm, jeu de taquin, and Kerov–Vershik measures on infinite tableaux. *SIAM J. Discrete Math.*, 28(2):598–630, 2014.

- [170] E. W. Stacy. A generalization of the gamma distribution. *Ann. Math. Statist.*, 33:1187–1192, 1962.
- [171] R. P. Stanley. *Enumerative combinatorics. Vol. 2*, volume 62 of *Cambridge Studies in Advanced Mathematics*. Cambridge University Press, Cambridge, 1999.
- [172] R. P. Stanley. A survey of alternating permutations. In *Combinatorics and graphs*, pages 165–196. American Mathematical Society (AMS), 2010.
- [173] R. P. Stanley. *Enumerative combinatorics. Volume 1*, volume 49 of *Cambridge Studies in Advanced Mathematics*. Cambridge University Press, Cambridge, second edition, 2011.
- [174] A. M. Vershik. Randomization of algebra and algebraization of probability. In B. Engquist and W. Schmid, editors, *Mathematics unlimited—2001 and beyond.*, pages 1157–1166. Springer, 2001.
- [175] A. M. Vershik and S. V. Kerov. Asymptotic behavior of the Plancherel measure of the symmetric group and the limit form of Young tableaux. *Dokl. Akad. Nauk SSSR*, 233(6):1024–1027, 1977.
- [176] H. S. Wall. *Analytic Theory of Continued Fractions*. D. Van Nostrand Company, 1948. (See also the reprint by Chelsea in 1967).
- [177] M. Wallner. A half-normal distribution scheme for generating functions and the unexpected behavior of Motzkin paths. In *AofA 2016*, pages 341–352, 2016.
- [178] M. Wallner. A half-normal distribution scheme for generating functions. *European J. Combin.*, 87:103138, 21, 2020.
- [179] E. M. Wright. The coefficients of a certain power series. *J. London Math. Soc.*, 7(4):256–262, 1932.
- [180] E. M. Wright. On the coefficients of power series having exponential singularities. *J. London Math. Soc.*, 8(1):71–79, 1933.
- [181] E. M. Wright. On the coefficients of power series having exponential singularities. II. *J. London Math. Soc.*, 24:304–309, 1949.
- [182] P. Wu, Y. Cui, J. Wu, J. Liu, and C. Metz. Transition from IPv4 to IPv6: A state-of-the-art survey. *IEEE Communications Surveys & Tutorials*, 15(3):1407–1424, 2013.

Michael Wallner

Curriculum Vitae

Rissaweggasse 2/85
1100 Wien

✉ michael.wallner@tuwien.ac.at
ORCID orcid.org/0000-0001-8581-449X
📄 dmg.tuwien.ac.at/mwallner



Personal

Date of birth December 3rd, 1987 (34 years) in Oberwart
Citizenship Austria
Family status married (2017), 1 son (2020), 1 daughter (2021)

Education

- 11/2013–01/2017 **PhD in Mathematics**, *TU Wien*, Austria, Analytic combinatorics, discrete mathematics, lattice paths, compacted trees.
Dissertation: „Combinatorics of Lattice Paths and Tree-like Objects“ supervised by Prof. Dr. Bernhard Gittenberger
Promotio sub auspiciis presidentis rei publicae (Graduation with highest national distinction), awarded on 05/12/2017 by the Austrian president Dr. Alexander Van der Bellen
- 09/2011–09/2012 **Master of Science (MSc)**, *Brunel University London*, United Kingdom, Computational Mathematics with Modelling.
Focus: FEM- and BEM-Methods for PDEs, Variational Calculus, Perturbation Theory, Integral Equations, Monte Carlo Methods for Asset Pricing
Thesis Title: “Algebraic Multigrid Methods for Higher-Order Finite Element Discretization with Parallelization” supervised by Prof. Dr. Matthias Maischak
Graduated with highest distinction
- 07/2011–10/2013 **Master of Science (Dipl.-Ing.)**, *TU Wien*, Austria, Technical Mathematics in the Computer Sciences.
Focus: Discrete Mathematics, Calculus, Algebra, IT Security, Cryptography, Programming
Thesis Title: “Lattice Path Combinatorics” supervised by Prof. Dr. Michael Drmota
Graduated with highest distinction
- 10/2008–07/2011 **Bachelor of Science (BSc)**, *TU Wien*, Austria, Technical Mathematics in the Computer Sciences.
Thesis Title: “Polynomials over finite fields” supervised by Prof. Dr. Michael Drmota
Graduated with highest distinction
- 07/2007–01/2008 **Military service**, *Medic*, Austria.
- 09/2002–06/2007 **HTL Pinkafeld, Abteilung EDV und Organisation**, Austria.
Austrian Matura passed with distinction

PhD thesis at TU Wien

- Title *Combinatorics of Lattice Paths and Tree-like Objects*
- Supervisor Prof. Dr. Bernhard Gittenberger, TU Wien
- Description The thesis is concerned with the enumerative and asymptotic analysis of directed lattice paths and tree-like structures. In the first part, several new models for lattice paths are introduced and some of their characterizing parameters, such as the number of returns to zero, or their average height and final altitude are analyzed. In the second part, enumerative and asymptotic results on compacted binary trees are solved. Such trees are a special class of directed acyclic graphs arising from a compressing method.
- TU Wien The TU Wien is one of the main universities in Vienna, Austria. It has more than 28 000 students enrolled in 18 bachelor’s, 33 master’s, and 3 PhD programs; it has 8 faculties and about 5 000 staff members (3 800 academics). The university’s teaching and research focuses on computer science, quantum physics, engineering, and natural sciences. For more information see www.tuwien.at.

Academic work experience

- Since 02/2020 **Postdoc and PI (FWF J 4162 and P 34142)**, *TU Wien, Institute of Discrete Mathematics and Geometry, Vienna*, 1 year return phase of FWF J 4162; FWF Stand-Alone Project P 34142.
- 01/2021–03/2021 **Paternity leave.**
- 02/2018–01/2020 **Postdoc as Erwin Schrödinger Fellow (FWF J 4162)**, *Université de Bordeaux, Laboratoire Bordelais de Recherche en Informatique (LaBRI), Bordeaux.*
- 09/2017–12/2017 **Postdoc**, *Université Paris 13, Laboratoire d'Informatique de Paris Nord (LIPN), Paris.*
- 05/2017–07/2017 **Postdoc**, *Academia Sinica, Institute of Statistical Science, Taipei.*
- 02/2017–04/2017 **Postdoc**, *TU Wien, Institute of Discrete Mathematics and Geometry, Vienna.*
- 09/2015–01/2017 **External lecturer**, *FH Campus Wien - University of Applied Sciences, Vienna.*
Small group tutoring in "Calculus 1" for electrical engineering students.
- 11/2013–04/2017 **Graduate teaching and research assistant**, *TU Wien, Institute of Discrete Mathematics and Geometry, Vienna.*
Research in FWF project SFB F50-03; teaching and teaching administration in computer science BSc courses.
- 10/2012–01/2013 **Undergraduate teaching assistant**, *TU Wien, Institute of Analysis and Scientific Computing, Vienna.*
Small group tutoring in numerical mathematics.

Grants

- 04/2021–07/2024 FWF Stand-Alone Project P 34142 *Stretched exponentials and beyond*, Principal investigator, 400k€
- 02/2018–03/2021 FWF Erwin Schrödinger-Fellowship J 4162 *Combinatorial and probabilistic study of higher dimensional lattice paths and tree-like structures*, Principal investigator, 157k€
- 12/2017–12/2019 Exzellenzstipendium für sub auspiciis Praesidentis Promovierende (Scholarship of excellence), 9k€
- 2012–2013 TUtheTOP Excellence programme at TU Wien
- 2011–2012 Erasmus Scholarship Brunel University London
- 2011 Julius-Raab-Stipendium
- 2010 Athens Programme, Leuven, Belgium
- 2009–2013 Leistungsstipendium der TU Wien (Excellence scholarship; 5 years in a row)

Teaching

All courses were taught in German and were exercise classes (German: Übungen).

FH Campus Wien - University of Applied Sciences

2016/2017 Analysis 1

2015/2016 Analysis 1

TU Wien

2021/2022 Discrete Mathematics

2015/2016 Discrete Methods, Analysis for Computer Science

2014/2015 Discrete Methods, Analysis for Computer Science, Algebra and Discrete Mathematics

2013/2014 Discrete Methods, Algebra and Discrete Mathematics

2012/2013 Numerical Analysis

Lecture

2015 Invited course "An Invitation to Analytic Combinatorics and Lattice Path Counting", 3rd ALEA in Europe Young Researchers' Workshop, University of Bath, UK

Student supervision

- Since 09/2021 PhD student Manosij Ghosh Dastidar in my FWF Project P 34142 (co-supervised with Bernhard Gittenberger)

Research areas

My main interest lies within (analytic) combinatorics, with an emphasis both on exact and asymptotic results for the enumeration of labeled and unlabeled structures and on probabilistic limit laws for combinatorial parameters. In line with this interest, my main focus areas are lattice paths and tree-like structures, but I am also interested in finding other applications of combinatorial and probabilistic tools.

Discrete objects	Random walks, trees and tree-like objects (phylogenetic networks, DFAs, DAGs), Young tableaux
Limit laws	Enumeration, generating functions, probability distributions, random generation
Applications	Biology, queueing theory, number theory, computer science

Scientific activity

Publications	28 published (peer-reviewed), 1 accepted, 4 submitted; see Section Publications.
Talks	57 talks and 3 poster presentations at international events; see Sections Talks and Posters.
Reviews	Article reviewing for international journals and conferences: <ul style="list-style-type: none">○ Journal of Combinatorial Theory, Series A○ Electronic Journal of Combinatorics○ Annals of Combinatorics○ Discrete Mathematics○ Discrete Mathematics and Theoretical Computer Science○ Journal of Integer Sequences○ Séminaire Lotharingien de Combinatoire○ Online Journal of Analytic Combinatorics○ Proceedings of Formal Power Series and Algebraic Combinatorics (FPSAC)○ Proceedings of the International Meeting on Probabilistic, Combinatorial and Asymptotic Methods for the Analysis of Algorithms (AofA)○ Proceedings of the International Conference on Lattice Path Combinatorics & Applications○ Birkhäuser Science Lecture Notes in Applied and Numerical Harmonic Analysis series○ Mathematical Reviews (https://mathscinet.ams.org)○ Zentralblatt (https://zbmath.org)

Computer skills

Programming	Java, C++, Fortran, Matlab, Maple
Database	Oracle, MySQL, SAP
Network	Cisco CCNA-Education
Publishing	Latex, Microsoft Office, LibreOffice, HTML

Languages

German	Mother tongue
English	Proficiency (C2)
Hungarian	Independent user (B1)
French	Basic user (A2)

Interests

Guitar	17 years of attending the music school Oberwart, member of different ensembles, participation at several concerts, longterm member of the church ensemble Unterwart
Climbing	Member of Alpenverein Edelweiss (Austrian climbing society)
Other	Hiking, skiing, gym, board games, books

Esteem factors

- 2022 Organizing committee member of *Computational Logic and Applications*, Vienna, Austria
- 2021 Organizing committee member of *Lattice Path Combinatorics and Interactions*, Luminy, France
- 2020 Program committee member of *Computational Logic and Applications*, online
- 2020 Scientific and organizing committee member of *L'École de Jeunes Chercheurs en Informatique Mathématique (EJCIM2020)*, Bordeaux, France and online
- 2017 Organizing committee member of *ALEA in Europe Workshop*, Vienna, Austria
- 2017 Organizing committee member of the *European Conference on Combinatorics, Graph Theory and Applications*, Vienna, Austria
- 2016 Organizing committee member of the *4th ALEA in Europe Young Researcher's Workshop*, Vienna, Austria
- 2015 Organizing committee member of *AofA 2015*, Strobl, Austria
- 2014–today Administrator of the website of the seminar of the Arbeitsgemeinschaft Diskrete Mathematik, TU Wien, Austria
- 2013–2017 Teaching support at the Institute of Discrete Mathematics and Geometry, TU Wien, Austria
- 2011–2012 Student representative of “Computational Mathematics with Modelling” at Brunel University London, UK
- 2007 Team leader during final year project “Vienna Online Diabetes Education” at HTBL Pinkafeld, First prize at school competition “Jugend Innovativ”, category ICT
- 2007 Quality management technician after ISO 9001
- 2005 Driving license category B (Austria)

Popularization

- Since 2020 Member of the TUForMath team; responsible for interactions between mathematics and biology and school excursions in the Natural History Museum Vienna.
- 05/2021 Public lecture at TUForMath: *Das 1x1 des evolutinären Stammbaums (German)*, TU Wien, Austria, 06/05/2021.
- 09/2019 Newspaper article *Analysen von Algorithmen und Ahnenbäume* about my life in Bordeaux appeared in “*Die Presse*”, 13/09/2019.
- 08/2019 Magazine article *Pfade und Bäume in Bordeaux* about my experiences as a Schrödinger-Fellow in Bordeaux, *scilog-Magazin des Wissenschaftsfonds FWF*, 07/08/2019.
- 12/2018 Talk at the 7th Weihnachtskolloquium: *Asymptotic Enumeration of Compacted Binary Trees*, TU Wien, Austria, 21/12/2018.

Major research achievements

- (1) Asymptotic enumeration of **phylogenetic networks** and other **minimal DFAs** using the Airy function
- (2) Counting and sampling gene families in phylogenetic **duplication-loss-transfer models**
- (3) Analyzing typical shapes of **periodic Young tableaux** and **periodic Pólya urns**
- (4) Solving lattice path models including a conjecture by Donald Knuth on the asymptotics of **periodic LPs**

Publications

The major research achievements and most important publications are marked by their respective number.

Peer-reviewed papers journals

- submitted⁽⁴⁾ *Phase transitions of composition schemes: Mittag-Leffler and mixed Poisson distributions* with Cyril Banderier, Markus Kuba, *Annals of Applied Probability*, 57 pages, preprint available at arxiv.org/abs/2103.03751.
- submitted⁽⁴⁾ *Walks avoiding a quadrant and the reflection principle* with Mireille Bousquet-Mélou, *European Journal of Combinatorics*, 48 pages, preprint available at arxiv.org/abs/2110.07633.

- submitted *On the critical exponents of generalized ballot sequences in three dimensions and large tandem walks*
Aequationes mathematicae, 11 pages, preprint available at arxiv.org/abs/2105.12155.
- accepted *The binary digits of $n + t$*
with Lukas Spiegelhofer, Annali della Scuola Normale Superiore di Pisa, Classe di Scienze, 27 pages,
preprint available at arxiv.org/abs/2005.07167.
- 2021⁽¹⁾ *Compacted binary trees admit a stretched exponential*
with Andrew Elvey Price, Wenjie Fang, Journal of Combinatorial Theory, Series A, 177 (2021), 105306,
40 pages (Citations: 1), preprint available at arxiv.org/abs/1908.11181.
- 2020⁽³⁾ *Periodic Pólya Urns, the Density Method, and Asymptotics of Young Tableaux*
with Cyril Banderier, Philippe Marchal, Annals of Probability, Volume 48, Number 4 (2020), 1921–1965
(Citations: 1), preprint available at arxiv.org/abs/1912.01035.
- 2020⁽¹⁾ *Asymptotic Enumeration of Compacted Binary Trees of Bounded Right Height*
with Antoine Genitrini, Bernhard Gittenberger, Manuel Kauers, Journal of Combinatorial Theory, Series A,
Volume 172, May 2020, 44 pages (Citations: 3), preprint available at arxiv.org/abs/1703.10031.
- 2020⁽⁴⁾ *A half-normal distribution scheme for generating functions*
European Journal of Combinatorics, Volume 87, Article ID 103138, 21 pages, June 2020 (Citations: 4),
preprint available at arxiv.org/abs/1610.00541.
- 2020⁽²⁾ *Counting and sampling gene family evolutionary histories in the duplication-loss and duplication-loss-transfer models*
with Cedric Chauve, Yann Ponty, Journal of Mathematical Biology, 80, pages 1353–1388(2020), preprint
available at arxiv.org/abs/1905.04971.
- 2019 *A bijection of plane increasing trees with relaxed binary trees of right height at most one*
Theoretical Computer Science, Volume 755, 10 January 2019, pages 1–12 (Citations: 3), preprint available
at arxiv.org/abs/1706.07163.
- 2019 *The Tu–Deng conjecture holds almost surely*
with Lukas Spiegelhofer, Electronic Journal of Combinatorics, Volume 26 (2019), no. 1, Paper 1.28,
28 pp. (Citations: 2), preprint available at arxiv.org/abs/1707.07945.
- 2018 *On the shape of random Pólya structures*
with Bernhard Gittenberger, Emma Yu Jin, Discrete Mathematics, Volume 341, Issue 4, April 2018,
pages 896–911 (Citations: 1), preprint available at arxiv.org/abs/1707.02144.
- 2018 *Divisibility of binomial coefficients by powers of two*
with Lukas Spiegelhofer, Journal of Number Theory, Volume 192, November 2018, pages 221–239
(Citations: 2), preprint available at arxiv.org/abs/1710.10884.
- 2017 *An explicit generating function arising in counting binomial coefficients divisible by powers of primes*
with Lukas Spiegelhofer, Acta Arithmetica 181 (2017), 27–55 (Citations: 5), preprint available at
arxiv.org/abs/1604.07089.
- 2017 *Lattice paths with catastrophes*
with Cyril Banderier, Discrete Mathematics & Theoretical Computer Science, September 29, 2017,
Vol 19 no. 1 (Citations: 6), preprint available at arxiv.org/abs/1707.01931.

Peer-reviewed papers in books

- 2019 *Explicit formulas for enumeration of lattice paths: basketball and the kernel method*
with Cyril Banderier, Christian Krattenthaler, Alan Krinik, Dmitry Kruchinin, Vladimir Kruchinin and
David Nguyen, Lattice Path Combinatorics and Applications, Developments in Mathematics, Springer-
Verlag, Cham, 2019, pages 78–118 (Citations: 5), preprint available at arxiv.org/abs/1609.06473.
- 2019⁽⁴⁾ *The kernel method for lattice paths below a line of rational slope*
with Cyril Banderier, Lattice Path Combinatorics and Applications, Developments in Mathematics,
Springer, Springer-Verlag, Cham, 2019, pages 119–154 (Citations: 3), preprint available at arxiv.org/abs/1606.08412.

Peer-reviewed papers in proceedings

- submitted⁽¹⁾ *Enumeration of d -combining Tree-Child Networks*
with Yu-Sheng Chang, Michael Fuchs, Hexuan Liu, and Guan-Ru Yu, AofA2022, 12 pp., Philadelphia.
- 2021⁽³⁾ *Young tableaux with periodic walls: counting with the density method*
with Cyril Banderier, SLC 85B.47, 12 pp., FPSAC2021, Ramat Gan.
- 2020⁽⁴⁾ *More models of walks avoiding a quadrant*
with Mireille Bousquet-Mélou, LIPIcs, Vol. 159 - Aofa 2020, 8:1–8:14, Klagenfurt (Citations: 1).
- 2020⁽¹⁾ *Asymptotics of minimal deterministic finite automata recognizing a finite binary language*
with Andrew Elvey Price, Wenjie Fang, LIPIcs, Vol. 159 - Aofa 2020, 11:1–11:13, Klagenfurt.
- 2020 *Latticepathology and symmetric functions (extended abstract)*
with Cyril Banderier, Marie-Louise Lackner, LIPIcs, Vol. 159 - Aofa 2020, 2:1–2:16, Klagenfurt.
- 2019⁽⁴⁾ *Combinatorics of nondeterministic walks of the Dyck and Motzkin type*
with Élie de Panafieu, Mohamed Lamine Lamali, ANALCO 2019: 1–12, San Diego, 2019, preprint available at arxiv.org/abs/1812.06650.
- 2019 *De la probabilité de creuser un tunnel*
with Élie de Panafieu, Mohamed Lamine Lamali, AlgoTel 2019, Saint Laurent de la Cabrerisse, 2019, preprint available at HAL 02123269v1.
- 2018⁽³⁾ *Periodic Pólya Urns and an Application to Young Tableaux*
with Cyril Banderier, Philippe Marchal, LIPIcs, Vol. 110 - Aofa 2018, 11:1-11:13, 2018, Uppsala (Citations: 1), preprint available at arxiv.org/abs/1806.03133.
- 2018 *Rectangular Young tableaux with local decreases and the density method for uniform random generation*
with Cyril Banderier and Philippe Marchal, CEUR Workshop Proceedings 2113, GASCom 2018:60–68, Athens, 2018, preprint available at arxiv.org/abs/1805.09017.
- 2018 *Local time for lattice paths and the associated limit laws*
with Cyril Banderier, CEUR Workshop Proceedings 2113, GASCom 2018:69–78, Athens, 2018, preprint available at arxiv.org/abs/1805.09065.
- 2017 *Lattice paths with catastrophes*
with Cyril Banderier, Electronic Notes in Discrete Mathematics, 59:131-146, GASCom 2016, La Marana (Citations: 2).
- 2017 *A note on the scaling limits of random Pólya trees*
with Bernhard Gittenberger and Emma Yu Jin, ANALCO 85–93, Barcelona, 2017, preprint available at arxiv.org/abs/1606.08769.
- 2016⁽⁴⁾ *A half-normal distribution scheme for generating functions and the unexpected behavior of Motzkin paths*
AofA 2016, Krakow, Poland, pages 341–352 (Citations: 1), preprint available at arxiv.org/abs/1605.03046.
- 2016 *The reflection-absorption model for directed lattice paths*
with Cyril Banderier, Vienna Young Scientists Symposium, Vienna, pages 98–99.
- 2015⁽⁴⁾ *Lattice paths of slope $2/5$ (Citations: 3)*
with Cyril Banderier, ANALCO, San-Diego, pages 105–113, preprint available at arxiv.org/abs/1605.02967.
- 2014 *Some reflections on directed lattice paths*
with Cyril Banderier, AofA 2014, Paris, pages 25–36 (Citations: 2), preprint available at arxiv.org/abs/1605.01687.

Theses

- 2017 *Combinatorics of lattice paths and tree-like structures*
PhD thesis, TU Wien, Vienna.
- 2013 *Lattice path combinatorics*
Master's thesis, TU Wien, Vienna.
- 2012 *Algebraic multigrid methods for higher-order finite element discretization with parallelization*
Master's thesis, Brunel University, London.

2011 *Polynome über endlichen Körpern*
Bachelor's thesis, TU Wien.

Talks

All events are links leading to the respective venues. Invited talks are marked with a "*", international conferences by "I".

- 57 *Phase transitions of composition schemes: Mittag-Leffler and mixed Poisson distributions*, Probability, Statistics and Combinatorics Seminar, Online/Uppsala University, Sweden, February 2022.
- 56 *Young Tableaux with Periodic Walls: Counting with the Density Method*, Arbeitsgemeinschaft Diskrete Mathematik, Online/TU Wien, Austria, January 2022.
- 55 *Young Tableaux with Periodic Walls: Counting with the Density Method*, Seminar Combinatoire et interactions, Online/Bordeaux, France, November 2021.
- 54^I *Compacted binary trees and minimal automata admit stretched exponentials*, DMV-ÖMG Jahrestagung 2021, Passau (Online), September 2021.
- 53 *More Models of Walks Avoiding a Quadrant*, SFB In-person Meeting, Linz, Austria, August 2021.
- 52^{I*} *Stretched exponentials and beyond*, 32nd International Conference on Probabilistic, Combinatorial and Asymptotic Methods for the Analysis of Algorithms (AofA 2021), Online/Klagenfurt, Austria, June 2021.
- 51^{*I} *Compacted binary trees and minimal automata admit stretched exponentials*, CanaDAM 2021, Online, Canada, May 2021.
- 50^{*I} *More Models of Walks Avoiding a Quadrant*, CanaDAM 2021, Online, Canada, May 2021.
- 49^{*} *Das 1x1 des evolutinären Stammbaums (German)*, public lecture for a general audience held online at TUForMath, TU Wien (Online), Austria, May 2021.
- 48 *Periodic Pólya urns and asymptotics of Young tableaux*, Arbeitsgemeinschaft Diskrete Mathematik, TU Wien, Austria, March 2021.
- 47 *Compacted binary trees and minimal automata admit stretched exponentials*, Arbeitsgemeinschaft Diskrete Mathematik, TU Wien, Austria, January 2021.
- 46^I *Compacted binary trees admit stretched exponentials*, Computational Logic and Applications (CLA 2020), online, October 2020.
- 45^I *Latticepathology and Symmetric Functions*, 31st International Conference on Probabilistic, Combinatorial and Asymptotic Methods for the Analysis of Algorithms (AofA 2020), online, October 2020.
- 44^I *More Models of Walks Avoiding a Quadrant*, 31st International Conference on Probabilistic, Combinatorial and Asymptotic Methods for the Analysis of Algorithms (AofA 2020), online, October 2020.
- 43 *Periodic Pólya urns and asymptotics of Young tableaux*, Plateau Saclay Combinatorics Seminar, online and Paris, France, June 2020.
- 42 *Stretched exponentials for compacted binary trees and a class of minimal automata*, Séminaire d'algorithmique, UPEM, Paris, France, January 2020.
- 41 *Compacted binary trees admit a stretched exponential*, Seminar Combinatoire Énumérative et Algébrique, LaBRI, Bordeaux, France, December 2019.
- 40^I *Counting and Sampling Gene Families Evolutionary Histories*, 5th Algorithmic and Enumerative Combinatorics Summer School 2019, Hagenberg, Austria, July 2019.
- 39^I *Periodic Pólya urns and an application to Young tableaux*, SIAM Algebraic Combinatorics Conference, Bern, Switzerland, July 2019.
- 38^I *Asymptotic Enumeration of Compacted Binary Trees with Height Restrictions*, 30th International Conference on Probabilistic, Combinatorial and Asymptotic Methods for the Analysis of Algorithms (AofA 2019), CIRM, Marseille, France, July 2019.
- 37 *Counting and Sampling Gene Families Evolutionary Histories*, Seminar Combinatoire Énumérative et Algébrique, LaBRI, Bordeaux, France, April 2019.
- 36^{*I} *Periodic Pólya Urns and Asymptotics of Triangular Young tableaux*, Journées de combinatoire de Bordeaux, LaBRI, Bordeaux, France, February 2019.

- 35 *Periodic Pólya Urns and Asymptotics of Triangular Young tableaux*, Séminaires de Probabilités-Statistiques, Université de Versailles Saint-Quentin-en-Yvelines, Versailles, France, February 2019.
- 34*^I *Limit laws for lattice paths with catastrophes*, Joint Mathematics Meetings 2019, Baltimore, USA, January 2019.
- 33^I *A bijection of plane increasing trees with bounded relaxed binary trees*, 4th Algorithmic and Enumerative Combinatorics Summer School 2018, Hagenberg, Austria, July 2018.
- 32^I *Periodic Pólya urns and an application to Young tableaux*, 29th International Conference on Probabilistic, Combinatorial and Asymptotic Methods for the Analysis of Algorithms (AofA 2018), Uppsala, Sweden, June 2018.
- 31 *Periodic Pólya urns and an application to Young tableaux*, Seminar Combinatoire Énumérative et Algébrique, LaBRI, Bordeaux, France, June 2018.
- 30^I *Asymptotic Enumeration of Compacted Binary Trees with Height Restrictions*, Computational Logic and Applications, Sorbonne University, Paris, France, May 2018.
- 29*^I *Periodic Pólya urns and an application to Young tableaux*, Journée MathStic - Combinatoire, probabilités, et physique, LIPN, Paris, France, May 2018.
- 28^I *A bijection of plane increasing trees with bounded relaxed binary trees*, Journées ALEA, CIRM, Marseille, France, March 2018.
- 27 *Asymptotic Enumeration of Compacted Binary Trees with Height Restrictions*, Seminar of the Combinatoire Énumérative et Algébrique, LaBRI, Bordeaux, France, February 2018.
- 26* *Half-normal lattice paths*, PhD Seminars Mathematics, Ghent University, Belgium, December 2017.
- 25 *Asymptotic Enumeration of Compacted Binary Trees with Height Restrictions*, Seminar "Computations and Proofs", INRIA, France, December 2017.
- 24 *Lattice paths with catastrophes: limit laws and random generation*, Séminaire de Probabilités et Théorie Ergodique, Université de Tours, France, November 2017.
- 23 *Limit laws for lattice paths with catastrophes*, séminaire de combinatoire, LIPN, Paris, France, September 2017.
- 22 *An introduction to lattice path counting (with catastrophes)*, PostDoc Seminar, Institute of Statistical Science, Academia Sinica, Taiwan, July 2017.
- 21 *Limit laws for lattice paths with catastrophes*, Seminar on Combinatorics, Institute of Mathematics, Academia Sinica, Taiwan, July 2017.
- 20 *The kernel method for lattice paths below a line of rational slope*, Algo@ISS-AS Seminar, Institute of Statistical Science, Academia Sinica, Taiwan, June 2017.
- 19^I *A note on the scaling limits of random Pólya trees*, Analytic Algorithmics and Combinatorics (ANALCO), Barcelona, Spain, January 2017.
- 18 *Compacted binary trees*, SFB F50 Algorithmic and Enumerative Combinatorics status seminar, Strobl, Austria, November 2016.
- 17 *A note on the scaling limits of random Pólya trees*, Arbeitsgemeinschaft Diskrete Mathematik, TU Wien, Austria, November 2016.
- 16^I *Lattice paths with catastrophes*, 77th Séminaire Lotharingien de combinatoire (SLC77), Strobl, Austria, September 2016.
- 15*^I *A half-normal distribution scheme for generating functions*, Asymptotic Analysis of Algorithms & Combinatorial Structures (A3CS), Paris, France, September 2016.
- 14^I *A half-normal distribution scheme for generating functions and the unexpected behavior of Motzkin paths*, 27th International Conference on Probabilistic, Combinatorial and Asymptotic Methods for the Analysis of Algorithms (AofA 2016), Kraków, Poland, July 2016.
- 13*^I *Lattice paths below a line of rational slope*, Final conférence of the MADACA project, Domaine de Chalès, France, June 2016.
- 12 *A half-normal distribution scheme for generating functions*, Arbeitsgemeinschaft Diskrete Mathematik, TU Wien, Austria, June 2016.
- 11*^I *An Invitation to Analytic Combinatorics and Lattice Path Counting*, ALEA in Europe Young Researchers' Workshop, University of Bath, Bath, UK, December 2015.

- 10 *Counting compacted trees*, SFB F50 Algorithmic and Enumerative Combinatorics status seminar, Strobl, Austria, December 2015.
- 9 *Why and when does the half-normal distribution appear in combinatorics?*, Séminaire de combinatoire, LIPN, Paris, France, September 2015.
- 8^I *A half-normal limit distribution scheme and applications to lattice paths*, 8th International Conference on Lattice Path Combinatorics & Applications, Cal Poly Pomona, USA, August 2015.
- 7* *The extension of a Rayleigh limiting distribution scheme*, SFB workshop on Lattice Walks, Hagenberg, Austria, May 2015.
- 6^I *Lattice paths of slope 2/5*, Analytic Algorithmics and Combinatorics (ANALCO), San Diego, USA, January 2015.
- 5 *Lattice paths of slope 2/5*, SFB F50 Algorithmic and Enumerative Combinatorics status seminar, Strobl, Austria, December 2014.
- 4 *Lattice paths of slope 2/5 – Solving a problem of Knuth*, Arbeitsgemeinschaft Diskrete Mathematik, TU Wien, Austria, November 2014.
- 3 *Some (more) reflections on lattice paths*, Probability seminar of the Université Francois Rabelais, Tours, France, September 2014.
- 2^I *Some reflections on lattice paths*, 25th International Conference on Probabilistic, Combinatorial and Asymptotic Methods for the Analysis of Algorithms (AofA 2014), Paris, France, June 2014.
- 1 *Some reflections on directed lattice paths*, Arbeitsgemeinschaft Diskrete Mathematik, TU Wien, Austria, May 2014.

Poster presentations

- 3 *Young Tableaux with Periodic Walls: Counting with the Density Method*, 33rd International Conference on Formal Power Series and Algebraic Combinatorics (FPSAC 2021), Online/Ramat-Gan, Israel, January 2022.
- 2 *Latticepathology and symmetric functions*, Lattice Paths, Combinatorics and Interactions, Online/CIRM, Marseille, France, July 2021.
- 1 *The reflection-absorption model for directed lattice paths*, VIENNA young SCIENTISTS SYMPOSIUM (VSS16), Vienna, Austria, June 2016.

Coauthors

- 1 Cyril Banderier, Université Sorbonne Paris Nord, France,
<https://lipn.univ-paris13.fr/~banderier/>
- 2 Mireille Bousquet-Mélou, Université de Bordeaux, France,
<https://www.labri.fr/perso/bousquet/>
- 3 Yu-Sheng Chang, National Chengchi University, Taipei, Taiwan,
<https://web.math.nccu.edu.tw/mfuchs/>
- 4 Cedric Chauve, Simon Fraser University, Canada,
<http://www.cecm.sfu.ca/~cchauve/>
- 5 Élie de Panafieu, Bell Labs, Paris, France,
<https://www.lincs.fr/people/elie-de-panafieu/>
- 6 Andrew Elvey Price, Université de Bordeaux, France,
<https://www.idpoisson.fr/elveyprice/en/>
- 7 Wenjie Fang, Université Paris-Est Marne-la-Vallée, France,
<http://igm.univ-mlv.fr/~wfang/>
- 8 Michael Fuchs, National Chengchi University, Taipei, Taiwan,
<https://web.math.nccu.edu.tw/mfuchs/>
- 9 Antoine Genitrini, Sorbonne Université, France,
<https://www-apr.lip6.fr/~genitrini/>
- 10 Bernhard Gittenberger, TU Wien, Austria,
<https://dmg.tuwien.ac.at/bgitten/>

- 11 Emma Yu Jin, Universität Wien, Austria,
<https://sites.google.com/site/schatzjin/>
- 12 Manuel Kauers, Johannes Kepler Universität, Austria,
<http://kauers.de/>
- 13 Christian Krattenthaler, Universität Wien, Austria,
<https://www.mat.univie.ac.at/~kratt/>
- 14 Alan Krinik, California State Polytechnic University, Pomona, USA,
https://www.researchgate.net/profile/Alan_Krinik
- 15 Dmitry Kruchinin, Tomsk State University, Russia,
https://www.researchgate.net/profile/Dmitry_Kruchinin
- 16 Vladimir Kruchinin, Tomsk State University, Russia,
https://www.researchgate.net/profile/Vladimir_Kruchinin3
- 17 Markus Kuba, FH-Technikum Wien, Austria,
<https://dmg.tuwien.ac.at/kuba/>
- 18 Marie-Louise Lackner, TU Wien, Austria,
<http://marielouise.lackner.xyz/>
- 19 Mohamed Lamine Lamali, Université de Bordeaux, France,
<http://www.labri.fr/perso/mlamali/>
- 20 Liu Hexuan, National Chengchi University, Taipei, Taiwan,
<https://web.math.nccu.edu.tw/mfuchs/>
- 21 Philippe Marchal, Université Sorbonne Paris Nord, France,
<https://www.math.univ-paris13.fr/~marchal/>
- 22 David T. Nguyen, UC Santa Barbara, USA,
<http://web.math.ucsb.edu/~dnguyen/>
- 23 Yann Ponty, École Polytechnique, France,
<http://www.lix.polytechnique.fr/~ponty/>
- 24 Lukas Spiegelhofer, Montanuniversität Leoben, Austria,
<http://dmg.tuwien.ac.at/spiegelhofer/>
- 25 Yu Guan-Ru, National Kaohsiung Normal University, Taiwan,
<https://sites.google.com/site/guanryu0127/>

B

TEACHING EXPERIENCE

I have acquired teaching experience at TU Wien, FH Campus Wien¹, and as invited speaker at international conferences. Already during my master's degree I gained experience as a teaching assistant (TA) and later in my PhD as a university assistant coordinating up to 10 TAs at a time for more than 400 students. These courses were aimed at mathematicians, computer scientists, and electrical engineers at the bachelor's and master's levels. Between 2017 and 2020 I was working abroad as a postdoc on different research projects, yet without any teaching duties.

Table 6 gives a detailed summary of my experience in teaching and the supervision of teaching assistants. I have gathered considerable experience in teaching exercise classes (German: Übungen) and I have recently started to be responsible for lectures as well. In the last winter term 2021, I co-taught the lecture Discrete Mathematics for master's students in computer science at TU Wien together with Bernhard Gittenberger. In the upcoming summer term 2022, I will co-teach the lecture and exercise class Discrete Methods (German: Diskrete Methoden) for master's students in mathematics at TU Wien again together with Bernhard Gittenberger. In the following years, I plan to teach at least one lecture per term, as I really enjoy the personal contact with students.

Additionally, I have taught a mini-course for PhD students with the title “**An Invitation to Analytic Combinatorics and Lattice Path Counting**” at the ALEA in Europe Young Researchers' Workshop² at the University of Bath, UK, 2015 and repeatedly substituted lectures in Analysis for Computer Science, Algebra and Discrete Mathematics, Discrete Methods, and Analysis for Electronics.

For more details I refer to my CV in Appendix A.

¹FH Campus Wien (University of applied sciences): <https://www.fh-campuswien.ac.at/en/studies/study-courses/detail/angewandte-elektronik-bachelor.html>

²<http://people.bath.ac.uk/cdm37/AE-YRW.html>

Year	University	Course	Hours	Level	Students
2021/22	TU Wien	Discrete Mathematics	60	MSc	58
2016/17	FH Campus	Analysis 1	65	BSc	33
2015/16	FH Campus	Analysis 1	65	BSc	34
2015/16	TU Wien	Discrete Methods	24	MSc	17
2015/16	TU Wien	Analysis for Computer Science	36	BSc	40
2014/15	TU Wien	Discrete Methods	24	MSc	30
2014/15	TU Wien	Analysis for Computer Science	36	BSc	40
2014/15	TU Wien	Algebra and Discrete Mathematics	36	BSc	42
2013/14	TU Wien	Discrete Methods	20	MSc	24
2013/14	TU Wien	Algebra and Discrete Mathematics	140	BSc	188
2012/13	TU Wien	Numerical Analysis	60	MSc	18

Year	University	Course	Groups	Level	TAs/Students
2015/16	TU Wien	Analysis for Computer Science	3	BSc	5/171
2014/15	TU Wien	Analysis for Computer Science	3	BSc	2/96
2014/15	TU Wien	Algebra and Discrete Mathematics	8	BSc	10/437
2013/14	TU Wien	Analysis for Computer Science	2	BSc	2/79
2013/14	TU Wien	Algebra and Discrete Mathematics	8	BSc	7/318

Table 6: Teaching experience and supervision of teaching assistants (TAs).

B.1 STUDENT FEEDBACK

In the following I state the totality of the feedback that was given to me by students after the end of each course through the anonymous evaluation survey in TISS (TU Wien Information Systems & Services). This feedback is left in the original form and hence mostly in German, as nearly all course were taught in German.

Diskrete Methoden

Kommentare: Besonders gut gefallen hat mir...

- » Die Beispiele waren immer auf den aktuellen Vorlesungsstoff abgestimmt. Der Umgang mit den Studierenden war sehr respektvoll und freundlich.
- » Bekanntgabe zu Beginn der Übung, wer welche Aufgabe vorrechnet.
- » Das entspannte Verhältnis zwischen Übungsleiter und Kursteilnehmern, sowie die Hilfsbereitschaft und Erklärungen des Übungsleiters (Wallner).

Kommentare: Wallner, Michael; Univ.Ass. Dipl.-Ing.

- » Michael hat die Übung sehr angenehm und fair gestaltet.

Kommentare: Wallner, Michael; Univ.Ass. Dipl.-Ing.

- » Sehr netter Übungsleiter; hat auch geholfen, wenn auch mal was nicht ganz gestimmt hat; am Anfang der UE-Einheit wurden gleich für jedes Beispiel diejenigen an die Tafel geschrieben, die dazu dann drankommen -> das nahm die Anspannung weg und man konnte sich aufs wesentliche konzentrieren

Kommentare: Wallner, Michael; Projektass.(FWF) Dipl.-Ing.

- » Sehr angenehme Atmosphäre in der Übung.

Kommentare: Besonders gut gefallen hat mir...

- » ...die freundliche und kollegiale Art des Übungsleiters Wallner. Hilfreich fand ich auch, dass nach Beispielen oft alternative Lösungswege angesprochen wurden. Sehr angenehmes Klima, danke!

Algebra und Diskrete Mathematik

Kommentare: Besonders gut gefallen hat mir...

- » Super Tutor in der Übungsgruppe (Mo 10:30), sehr freundlich, hat alles super erklärt und alle fragen beantwortet. habe von ihm sehr viel gelernt
- » Das lockere Auftreten des Vortragenden (Wallner)! Man hat sich sehr wohl | gefühlt in den Übungen

Kommentare: Besonders gut gefallen hat mir...

- » Herr Wallner war sehr bemüht und es wurde sehr auf die Fragen der Studierenden eingegangen.
- » Der Umgang zwischen Vortragendem (Wallner Michael) und Studierenden.

Analysis

Kommentare: Besonders gut gefallen hat mir...

- » ...die Kompetenz von Herrn Wallner in der Übung. Sehr respektvoller Umgang mit den Studenten, wenn mal jemand kurz auf der "Leitung stand" konnte er durch gezieltes Fragen dem Studenten einen "Schubs" in die richtige Richtung geben, sodass dieser fortsetzen konnte. Sehr inspirierend.

Kommentare: Der Umgang zwischen Lehrenden und Studierenden war respektvoll.

- » Mein Tutor, Michael Wallner, war herausragend.

Kommentare: Ich habe die Lehrveranstaltung gerne besucht.

- » Mein Dank an den Herrn Michael Wallner

Kommentare: Zum Fragebogen habe ich folgende Anregungen...

- » Das Feedback bezieht sich ausschließlich auf die Übung von Michael Wallner. Ich möchte seine hervorragende Fähigkeit komplexe Inhalte zu vermitteln herausstellen. Dazu hat er das noch mit einer sehr sympathischen Art getan und sich Zeit für uns genommen - mit Gesprächen nach der Übung und kurzfristigen Sprechstunden um Unklarheiten auszuräumen. Vielen Dank dafür!

Numerische Mathematik

Kommentare: Wallner, Michael

- » Unser Tutor, Michael Wallner, war sehr engagiert und hilfsbereit. Das Klima in der Übung war wirklich angenehm. Ich kann auf eine mustergültige Übung zurückblicken!
- » War sehr engagiert und auch außerhalb der Übungszeiten stets für Fragen erreichbar.
- » Du bist toll! Danke für die viele Hilfe. Mit dir kann man sehr gut arbeiten :)
- » Es war eine großartige Übung. Ich habe viel gelernt, auch viel Arbeit, aber mindestens genauso viel Freude an den Projekten gehabt. Danke für die erstklassige Betreuung!

Discrete Mathematics

Kommentare: Wallner, Michael; Projektass.(FWF) Dipl.-Ing. Dr.techn. MSc

- » Mr Wallner really took to time to ensure every student had understood the exercise
- » der Versuch des Hr. Wallner ein grundlegendes Verständnis zu geben bei komplexen Fragestellungen
- » Mr. Wallners efforts to make sure everyone presented enough and to answer all our questions. Just in general his energy and enthusiasm made me like the course.

C

PUBLISHED PAPERS

c.1	Compacted binary trees admit a stretched exponential [P29]	114
c.2	Asymptotics of Minimal Deterministic Finite Automata Recognizing a Finite Binary Language [P13]	154
c.3	A bijection of plane increasing trees with relaxed binary trees of right height at most one [P24]	167
c.4	Rectangular Young tableaux with local decreases and the density method for uniform random generation [P8]	179
c.5	Young tableaux with periodic walls: counting with the density method [P15]	188
c.6	Periodic Pólya urns, the density method and asymptotics of Young tableaux [P28]	200
c.7	Latticepathology and Symmetric Functions [P12]	245
c.8	Combinatorics of nondeterministic walks of the Dyck and Motzkin type [P11]	261
c.9	More Models of Walks Avoiding a Quadrant [P14]	273

This chapter contains all papers included in this thesis as originally published.



Contents lists available at ScienceDirect

Journal of Combinatorial Theory,
Series Awww.elsevier.com/locate/jcta

Compacted binary trees admit a stretched exponential

Andrew Elvey Price^{a,1}, Wenjie Fang^{b,2}, Michael Wallner^{a,c,*,3}^a *Laboratoire Bordelais de Recherche en Informatique, UMR 5800, Université de Bordeaux, 351 Cours de la Libération, 33405 Talence Cedex, France*^b *Laboratoire d'Informatique Gaspard-Monge, UMR 8049, Université Gustave-Eiffel, CNRS, ESIEE Paris, 5 Boulevard Descartes, 77454 Marne-la-Vallée, France*^c *Institute of Discrete Mathematics and Geometry, TU Wien, Wiedner Hauptstraße 8–10, 1040 Wien, Austria*

ARTICLE INFO

Article history:

Received 3 December 2019

Received in revised form 2 July 2020

Accepted 3 August 2020

Available online xxxx

*Keywords:*Airy function
Asymptotics
Bijection
Compacted trees
Directed acyclic graphs
Dyck paths
Finite languages
Minimal automata
Stretched exponential

ABSTRACT

A compacted binary tree is a directed acyclic graph encoding a binary tree in which common subtrees are factored and shared, such that they are represented only once. We show that the number of compacted binary trees of size n grows asymptotically like

$$\Theta\left(n! 4^n e^{3a_1 n^{1/3}} n^{3/4}\right),$$

where $a_1 \approx -2.338$ is the largest root of the Airy function. Our method involves a new two parameter recurrence which yields an algorithm of quadratic arithmetic complexity for computing the number of compacted trees up to a given size. We use empirical methods to estimate the values of all terms defined by the recurrence, then we prove by induction

* Corresponding author.

E-mail addresses: andrew.elvey@univ-tours.fr (A. Elvey Price), wenjie.fang@u-pem.fr (W. Fang), michael.wallner@tuwien.ac.at (M. Wallner).

URLs: <http://igm.univ-mlv.fr/~wfang/> (W. Fang), <https://dmg.tuwien.ac.at/mwallner/> (M. Wallner).

¹ Andrew Elvey Price was supported by the European Research Council (ERC) in the European Union's Horizon 2020 research and innovation programme, under the Grant Agreement No. 759702.

² Wenjie Fang was supported by the Austrian Science Fund (FWF) grant P 27290 and I 2309-N35 as a postdoctoral fellow at TU Graz, during which part of the work was done.

³ Michael Wallner was supported by the Erwin Schrödinger Fellowship of the Austrian Science Fund (FWF): J 4162-N35.

<https://doi.org/10.1016/j.jcta.2020.105306>

0097-3165/© 2020 Elsevier Inc. All rights reserved.

that these estimates are sufficiently accurate for large n to determine the asymptotic form. Our results also lead to new bounds on the number of minimal finite automata recognizing a finite language on a binary alphabet. As a consequence, these also exhibit a stretched exponential.

© 2020 Elsevier Inc. All rights reserved.

1. Introduction

Compacted binary trees are a special class of directed acyclic graphs that appear as a model for data structures in the compression of XML documents [5]. Given a rooted binary tree of size n , its compacted form can be computed in expected and worst-case time $\mathcal{O}(n)$ with expected compacted size $\Theta(n/\sqrt{\log n})$ [16]. Recently, Genitrini, Gittenberger, Kauers, and Wallner solved the reversed question on the asymptotic number of compacted trees under certain height restrictions [17]; however the asymptotic number in the unrestricted case remained elusive. They also solved this problem for a simpler class of trees known as relaxed trees under the same height restrictions. In this paper we show that the counting sequences $(c_n)_{n \in \mathbb{N}}$ of (unrestricted) compacted binary trees and $(r_n)_{n \in \mathbb{N}}$ of (unrestricted) relaxed binary trees both admit a stretched exponential:

Theorem 1.1. *The number of compacted and relaxed binary trees satisfy for $n \rightarrow \infty$*

$$c_n = \Theta\left(n! 4^n e^{3a_1 n^{1/3}} n^{3/4}\right) \quad \text{and} \quad r_n = \Theta\left(n! 4^n e^{3a_1 n^{1/3}} n\right),$$

where $a_1 \approx -2.338$ is the largest root of the Airy function $\text{Ai}(x)$ defined as the unique function satisfying $\text{Ai}''(x) = x\text{Ai}(x)$ and $\lim_{n \rightarrow \infty} \text{Ai}(x) = 0$.

We believe that there are constants γ_c and γ_r such that

$$c_n \sim \gamma_c n! 4^n e^{3a_1 n^{1/3}} n^{3/4} \quad \text{and} \quad r_n \sim \gamma_r n! 4^n e^{3a_1 n^{1/3}} n,$$

however, we have been unable to find the exact values of these constants or even prove their existence. Nevertheless, our empirical analysis yields what we believe to be very accurate estimates for γ_c and γ_r , namely $\gamma_c \approx 173.12670485$ and $\gamma_r \approx 166.95208957$.

The presence of a stretched exponential term in a sequence counting combinatorial objects is not common, although there are quite a few precedents. One simple example is that of *pushed Dyck paths*, where Dyck paths of maximum height h are given a weight y^{-h} for some $y > 1$. In this case McKay and Beaton determined the weighted number d_n of paths of length $2n$ up to and including the constant term to be asymptotically given by

$$d_n \sim Ay(y-1)(\log y)^{1/3} 4^n \exp\left(-C(\log y)^{2/3} n^{1/3}\right) n^{-5/6},$$

where $A = 2^{5/3}\pi^{5/6}/\sqrt{3}$ and $C = 3(\pi/2)^{2/3}$; see [18]. For the analogous problem of counting pushed self avoiding walks, Beaton et al. [4] gave a (non-rigorous) probabilistic argument for the presence of a stretched exponential of the form $e^{-cn^{3/7}}$ for some $c > 0$. In each of these cases, a stretched exponential appears as part of a compromise between the large height regime in which most paths occur and the small height regime in which the weight is maximized. We will see that a similar compromise occurs in this paper. Another situation in which stretched exponentials have appeared is in cogrowth sequences in groups [14], that is, paths on Cayley graphs which start and end at the same point. In particular, Revelle [25] showed that in the lamplighter group the number c_n of these paths of length $2n$ behaves like

$$c_n \sim C 9^n \kappa^{n^{1/3}} n^{1/6}.$$

In the group $\mathbb{Z} \wr \mathbb{Z}$, Pittet and Saloff-Coste showed that the asymptotics of the cogrowth series contains the slightly more complicated term $\kappa^{\sqrt{n \log n}}$ [24]. Another example comes from the study of pattern avoiding permutations, where Conway, Guttmann, and Zinn-Justin [7,8] have given compelling numerical evidence that the number p_n of 1324-avoiding permutations of length n behaves like

$$p_n \sim B \mu^n \mu_1^{\sqrt{n}} n^g,$$

with $\mu \approx 11.600$, $\mu_1 \approx 0.0400$, $g \approx -1.1$.

As seen by these examples, it is generally quite difficult to prove that a sequence has a stretched exponential in its asymptotics. Part of the difficulty is that a sequence which has a stretched exponential cannot be “very nice”. In particular, the generating function cannot be algebraic, and can only be D -finite if it has an irregular singularity [15].

Some explicit examples of D -finite generating series with a stretched exponential are known; see e.g. [28–30]. In these cases Wright uses a saddle-point method to prove the presence of the stretched exponential. To apply this method, one needs to meticulously check various analytic conditions on the generating function, or to bound related integrals in a delicate way. These tasks can be highly non-trivial and require a precise knowledge of the analytic properties of the generating function. For more detail on how to use the saddle-point method to prove stretched exponentials, and further examples, see [15, Chapter VIII].

In lieu of detailed information on the generating function, we find and analyze the following recurrence relation

$$r_{n,m} = r_{n,m-1} + (m+1)r_{n-1,m},$$

corresponding to a partial differential equation to which the saddle point method cannot be readily applied. The number of relaxed trees of size n is then $r_{n,n}$. We present a method that works directly with a transformed sequence $d_{n,k}$ and the respective recur-

rence relation. We find two explicit sequences $A_{n,k}$ and $B_{n,k}$ with the same asymptotic form, such that

$$A_{n,k} \leq d_{n,k} \leq B_{n,k}, \quad (1)$$

for all k and all n large enough. The idea is that $A_{n,k}$ and $B_{n,k}$ satisfy the recurrence of $d_{n,k}$ with the equalities replaced by inequalities, allowing us to prove (1) by induction. In order to find appropriate sequences $A_{n,k}$ and $B_{n,k}$, we start by performing a heuristic analysis to conjecture the asymptotic shape of $d_{n,k}$ for large n . We then prove that the required recursive inequalities hold for sufficiently large n using adapted Newton polygons.

The inductive step in the method described above requires that all coefficients in the recurrence be positive. This occurs in the case of relaxed binary trees but not for compacted binary trees. In the latter case, we construct a sandwiching pair of sequences, each determined by a recurrence with positive coefficients, to which our method applies.

As an application, we use our results on relaxed and compacted trees to give new asymptotic upper and lower bounds for the number of minimal deterministic finite automata with n states recognizing a finite language on a binary alphabet. These automata are studied in the context of the complexity of regular languages; see [11,12,23]. To our knowledge no upper or lower bounds capturing even the exponential term had been proven for this problem. Our bounds are much more accurate, only differing by a polynomial factor, and thereby proving the presence of a stretched exponential term.

As a further extension of our method, some preliminary results show that our approach can be generalized to a k -ary version of compacted trees, which in turn settles the enumeration of minimal finite automata recognizing finite languages for an arbitrary alphabet. A follow-up paper in this direction is underway.

In its simplest form, our method applies to two parameter linear recurrences with positive coefficients which may depend on both parameters. We expect, however, that our method could be adapted to handle a much wider range of recurrence relations, potentially involving more than two parameters, negative coefficients and perhaps even some non-linear recurrences. Indeed, we have already seen that it can be adapted to at least one case involving negative coefficients, namely that of counting compacted binary trees.

Plan of the article In Section 2 we introduce compacted binary trees and the related relaxed binary trees, and then derive a bijection to Dyck paths with weights on their horizontal steps. In Section 3 we show a heuristic method of how to conjecture the asymptotics and in particular the appearance of a stretched exponential term. Building on these heuristics, we prove exponentially and polynomially tight bounds for the recurrence of relaxed binary trees in Section 4 and of compacted binary trees in Section 5. In Section 6 we show how our results lead to new bounds on minimal acyclic automata on a binary alphabet.

2. A two-parameter recurrence relation

Originally, compacted binary trees arose in a compression procedure in [16] which computes the number of unique fringe subtrees. Relaxed binary trees are then defined by relaxing the uniqueness conditions on compacted binary trees. As we will not need this algorithmic point of view, we directly give the following definition adapted from [17, Definition 3.1 and Proposition 4.3].

Before we define compacted and relaxed binary trees, let us recall some basic definitions. A *rooted binary tree* is a plane directed connected graph with a distinguished node called the root, in which all nodes have out-degree either 0 or 2 and all nodes other than the root have in-degree 1, while the root has in-degree 0. For each vertex with out-degree 2, the out-going edges are distinguished as a left edge and a right edge. Nodes with out-degree 0 are called *leaves*, and nodes with out-degree 2 are called *internal nodes*. All trees in this paper will be rooted and we omit this term in the future.

Definition 2.1 (*Relaxed binary tree*). A *relaxed binary tree* (or simply *relaxed tree*) of size n is a directed acyclic graph obtained from a binary tree with n internal nodes, called its *spine*, by keeping the left-most leaf and turning other leaves into pointers, with each one pointing to a node (internal ones or the left-most leaf) preceding it in postorder.

The counting sequence $(r_n)_{n \in \mathbb{N}}$ of relaxed binary trees of size n starts as follows:

$$(r_n)_{n \in \mathbb{N}} = (1, 1, 3, 16, 127, 1363, 18628, 311250, 6173791, 142190703, \dots).$$

It corresponds to [OEIS A082161](https://oeis.org/A082161) in the On-line Encyclopedia of Integer Sequences.⁴ There, it first appeared as the counting sequence of the number of deterministic, completely defined, initially connected, acyclic automata with 2 inputs and n transient, unlabeled states and a unique absorbing state, yet without specified final states. This is a direct rephrasing of Definition 2.1 in the language of automata theory; for more details see Section 6. Liskovets [23] provided (probably) the first recurrence relations ($C_2(n)$ used for r_n) and later Callan [6] showed that they are counted by determinants of Stirling cycle numbers. However, the asymptotics remained an open problem, which we will solve in the present paper.

Using the class of relaxed trees, it is then easy to define the set of compacted trees by requiring the uniqueness of subtrees.

Definition 2.2 (*Compacted binary tree*). Given a relaxed tree, to each node u we can associate a binary tree $B(u)$. We proceed by postorder. If u is the left-most leaf, we define $B(u) = u$. Otherwise, u has two children v, w , then $B(u)$ is the binary tree with $B(v)$ and $B(w)$ as left and right sub-trees, respectively. A *compacted binary tree*, or

⁴ <https://oeis.org>.

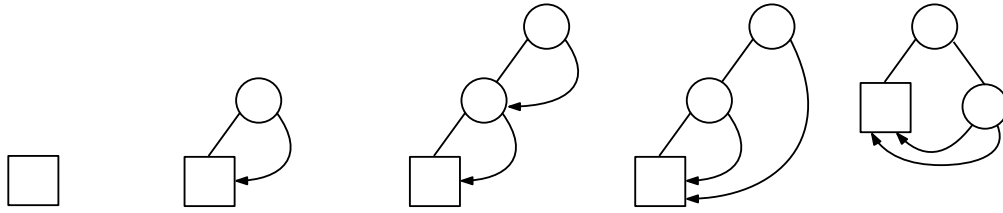


Fig. 1. All relaxed (and also compacted) binary trees of size 0, 1, 2, where internal nodes are shown by circles and the unique leaf is drawn as a square.



Fig. 2. (Left) The smallest relaxed binary tree that is not a compacted binary tree, as the two gray subtrees correspond to the same (classical) binary tree. (Right) A valid compacted binary tree of size 3 with the same spine.

simply *compacted tree* of size n is a relaxed tree with $B(u) \neq B(v)$ (i.e., $B(u)$ not isomorphic to $B(v)$) for all pairs of distinct nodes u, v .

Fig. 1 shows all relaxed (and compacted) trees of size $n = 0, 1, 2$ and Fig. 2 gives the smallest relaxed tree that is not a compacted tree. The counting sequence $(c_n)_{n \in \mathbb{N}}$ of compacted binary trees of size n is [OEIS A254789](#) and starts as follows:

$$(c_n)_{n \in \mathbb{N}} = (1, 1, 3, 15, 111, 1119, 14487, 230943, 4395855, 97608831, \dots).$$

In [17, Theorem 5.1 and Corollary 5.4] the so-far most efficient recurrences are given for the number of compacted and relaxed binary trees, respectively. Computing the first n terms using these requires $\mathcal{O}(n^3)$ arithmetic operations. In this section we give an alternative recurrence with only one auxiliary parameter (instead of two) other than the size n , which leads to an algorithm of arithmetic complexity $\mathcal{O}(n^2)$ to compute the first n terms of the sequence. The construction is motivated by the recent bijection [26].

As a corollary of our main result Theorem 1.1, we directly get an estimate of the asymptotic proportion of compacted trees among relaxed trees:

$$\frac{c_n}{r_n} = \Theta(n^{-1/4}).$$

An analogous result for compacted and relaxed trees of bounded right height was shown in [17, Corollary 3.5]. The right height is the maximal number of right edges to internal nodes on a path in the spine from the root to a leaf. Let $c_{k,n}$ (resp. $r_{k,n}$) be the number of compacted (resp. relaxed) trees of right height at most k . Then, for fixed k ,

$$\frac{c_{k,n}}{r_{k,n}} \sim \lambda_k n^{-\frac{1}{k+3} - \left(\frac{1}{4} - \frac{1}{k+3}\right) \frac{1}{\cos^2\left(\frac{1}{k+3}\right)}} = o\left(n^{-1/4}\right),$$

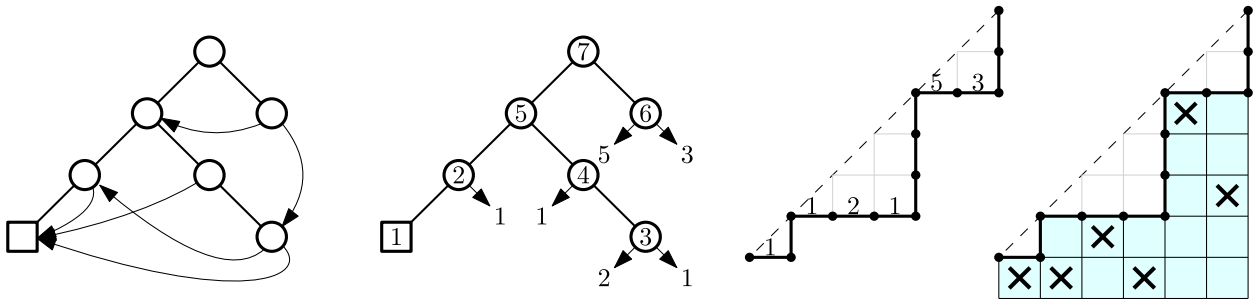


Fig. 3. Example of the bijection **Dyck** between relaxed trees and horizontally decorated Dyck paths. It transforms internal nodes into vertical steps and pointers into horizontal steps.

for a constant λ_k independent of n . As $k \rightarrow \infty$, we see that the exponent of n approaches $-1/4$. It is thus not surprising that the exponent in the unbounded case is also $-1/4$.

2.1. Relaxed binary trees and horizontally decorated paths

For the subsequent construction, we need the following type of lattice paths.

Definition 2.3. A horizontally decorated path P is a lattice path starting from $(0, 0)$ with steps $H = (1, 0)$ and $V = (0, 1)$ confined to the region $0 \leq y \leq x$, where each horizontal step H is decorated by a number in $\{1, \dots, k + 1\}$ with k its y -coordinate. If P ends at (n, n) , we call it a horizontally decorated Dyck path.

We denote by \mathcal{D}_n the set of horizontally decorated Dyck paths of length $2n$.

Remark 2.4. Horizontally decorated Dyck paths can also be interpreted as classical Dyck paths, where below every horizontal step a box given by a unit square between the horizontal step and the line $y = -1$ is marked, see Fig. 3. This gives an interpretation connecting these paths with the heights of Dyck paths, which we will exploit later. Independently, Callan gave in [6] a more general bijection in which he called the paths *column-marked subdiagonal paths*, and Bassino and Nicaud studied in [3] a variation when counting some automata, where the paths stay *above* the diagonal, which they called *k-Dyck boxed diagrams*.

Theorem 2.5. There exists a bijection **Dyck** between relaxed binary trees of size n and the set \mathcal{D}_n of horizontally decorated Dyck paths of length $2n$.

Proof. Let C be a relaxed binary tree of size n , and C_* its spine. For convenience, we identify the internal nodes in C and C_* , and pointers in C with leaves (not the left-most one) in C_* .

We now give a recursive procedure transforming C into a horizontally decorated Dyck path P . First, we take C_* and label its internal nodes *and the left-most leaf* in postorder from 1 to $n + 1$. Next, we define the following function **Path** that transforms C_* into

a lattice path in H and V . Given a binary tree T , it either consists of two sub-trees (T_1, T_2) , or it is a leaf ε . We thus define **Path** recursively by

$$\mathbf{Path}((T_1, T_2)) = \mathbf{Path}(T_1)\mathbf{Path}(T_2)V, \quad \mathbf{Path}(\varepsilon) = H.$$

It is clear that $\mathbf{Path}(C_*)$ starts with H for the left-most leaf. Let P_0 be $\mathbf{Path}(C_*)$ with its starting H removed. Note that **Path** performs a postorder traversal on C_* where leaves are matched with H and internal nodes with V . Then, $\mathbf{Path}(C_*)$ ends at $(n+1, n)$ and stays always strictly below $y = x$ because every binary (sub-)tree has one more leaf than internal nodes, and each initial segment of $\mathbf{Path}(C_*)$ corresponds to a collection of subtrees of C_* . Hence, P_0 is a Dyck path. Observe that the i -th step V in P_0 corresponds to the $(i+1)$ -st node in postorder, as the left-most leaf is labeled 1. Finally, for each step H in P_0 , we label it by the label of the internal node (or the left-most leaf) to which its corresponding leaf in C_* points in C . We thus obtain a Dyck path P with labels on the horizontal steps, and we define $\mathbf{Dyck}(C_*) = P$.

We have seen that the Dyck path P_0 is in bijection with the spine C_* . To see that the labeling condition on horizontally decorated Dyck paths is equivalent to the condition on relaxed binary trees, we take a pointer p pointing to a node u with label ℓ that corresponds to a step H with a certain coordinate k . By construction of the Dyck path, p comes after u in postorder if and only if the step H from p comes after the step V from u , which is equivalent to $\ell \leq k+1$, as the node with label 1 is the left-most leaf and is not recorded as a step H . We thus have the equivalence of the two conditions, so **Dyck** is indeed a bijection as claimed. \square

The following result gives the claimed algorithm with quadratic arithmetic complexity to count such paths, which can also be used as a precomputation step of an algorithm that randomly generates these paths using a linear number of arithmetic operations for each path. These algorithms are also applicable to relaxed binary trees via the bijection **Dyck**.

Proposition 2.6. *Let $r_{n,m}$ be the number of horizontally decorated paths ending at (n, m) . Then,*

$$\begin{aligned} r_{n,m} &= r_{n,m-1} + (m+1)r_{n-1,m}, & \text{for } n, m \geq 1 \text{ and } n \geq m, \\ r_{n,m} &= 0, & \text{for } n < m, \\ r_{n,0} &= 1, & \text{for } n \geq 0. \end{aligned}$$

The number of relaxed binary trees of size n is equal to $r_{n,n}$.

Proof. Let us start with the boundary conditions. First of all, no such path is allowed to cross the diagonal $y = x$, thus $r_{n,m} = 0$ for $n < m$. Second, the paths consisting only

of horizontal steps stay at altitude 0 and admit therefore just one possible label for each step, i.e., $r_{n,0} = 1$ for $n \geq 0$.

For the recursion we consider how a path can jump to (n, m) . It either uses a step V from $(n, m - 1)$ or it uses a step H from $(n - 1, m)$. In the second case, there are $m + 1$ possible decorations as the path is currently at altitude m . \square

Remark 2.7 (*Compacted trees of bounded right height*). This restriction naturally translates relaxed binary trees of right height at most k from [17] into horizontally decorated Dyck paths of height at most $k + 1$, where height is the maximal normal distance rescaled by $\sqrt{2}$ from a lattice point on the path to the diagonal. In other words, these paths are constrained to remain between the diagonal and a line translated to the right parallel to the diagonal by $k + 1$ unit steps.

2.2. Compacted binary trees

Given a relaxed tree C , an internal node u is called a *cherry* if its children in the spine are both leaves and none of them is the left-most one. According to the discussion at the end of Section 4 in [17], the only obstacle for a relaxed tree to be a compacted tree is a cherry with badly chosen pointers. For the convenience of the reader, we now recall and formalize this observation in the following proposition.

Proposition 2.8. *A relaxed tree C is a compacted tree if and only if there are no two nodes $u \neq v$ in C which share the same left child u_ℓ and the same right child u_r . Moreover, if C is not a compacted tree, such a pair exists where v is a cherry and u precedes v in postorder.*

Proof. The “only if” part follows directly from Definition 2.2. We now focus on the “if” part. Suppose that C is not a compacted tree, which means there is at least a pair of internal nodes u, v such that u precedes v and $B(u) = B(v)$, with $B(u)$ defined in Definition 2.2. Now we want to show that there is one such pair with v being a cherry. We take such a pair (u, v) . If v is a cherry, the claim holds. Otherwise, without loss of generality, we suppose that the left child v' of v is not a leaf. Let u_ℓ be the left child of u . If u_ℓ is an internal node, we take $u' = u_\ell$. Otherwise, we take u' to be the internal node pointed to by u_ℓ . By definition, we have $B(u') = B(v')$, and clearly u' precedes v' in postorder. We thus obtain a new pair with the same conditions but of greater depth in the spine. However, since the spine has finite depth, this process cannot continue forever. As it only stops when v is a cherry, we have the existence of such a pair (u, v) with v a cherry. \square

The restriction described in Proposition 2.8 has an analogue in the class of horizontally decorated paths: We label every step V with its final altitude plus one, which corresponds to its row number in the interpretation with marked boxes, and which also corresponds to

the traversal/process order in postorder of its internal node in the relaxed tree; compare Fig. 3. Recall that each step H is already labeled. For any step S , let $\mathcal{L}(S)$ be its label. We associate to every step V a pair of integers (v_1, v_2) , which correspond to the labels of its left and right children. First, let S' be the step before V and set $v_2 = \mathcal{L}(S')$. Next, draw a line from the ending point of V in the southwest direction parallel to the diagonal, and stop upon touching the path again. Let S'' be the last step before V that ends on this line (if there is no such step, set $v_1 = 1$). Then set $v_1 = \mathcal{L}(S'')$.

Definition 2.9. A *C-decorated path* P is a horizontally decorated path where the decorations h_1 and h_2 of each pattern of consecutive steps HHV fulfill $(h_1, h_2) \neq (v_1, v_2)$ for all preceding steps V .

Proposition 2.10. *The map **Dyck** bijectively sends the set of compacted trees of size n to the set of C-decorated Dyck paths of length $2n$.*

Proof. Recall from Theorem 2.5 that the map **Dyck** is a bijection sending relaxed trees of size n to the set of horizontally decorated Dyck paths of size $2n$. C-decorated paths are defined precisely so that their corresponding relaxed trees satisfy the condition of Proposition 2.8. Therefore, **Dyck** forms a bijection between C-decorated paths and compacted trees. \square

The key observation for the counting result is that exactly one pair of labels (h_1, h_2) is avoided for each preceding step V of a consecutive pattern HHV . Applying this classification to the previous result we get a similar quadratic-time recurrence for compacted binary trees.

Proposition 2.11. *Let $c_{n,m}$ be the number of C-decorated paths ending at (n, m) . Then,*

$$\begin{aligned} c_{n,m} &= c_{n,m-1} + (m+1)c_{n-1,m} - (m-1)c_{n-2,m-1}, & \text{for } n \geq m \geq 1, \\ c_{n,m} &= 0, & \text{for } n < m, \\ c_{n,0} &= 1, & \text{for } n \geq 0. \end{aligned}$$

The number of compacted binary trees of size n is equal to $c_{n,n}$.

Proof. In the first case, the term $(m+1)c_{n-1,m}$ counts the paths ending with a H -step while $c_{n,m-1} - (m-1)c_{n-2,m-1}$ counts the paths ending with a V -step. The term $-(m-1)c_{n-2,m-1}$ occurs because, for each C-decorated path ending at $(n-2, m-1)$, there are exactly $m-1$ paths formed by adding an additional HHV that are not C-decorated paths. \square

Note that one might also count the following simpler class which is in bijection with C-decorated paths, albeit without a natural bijection.

Definition 2.12. A *H-decorated path* P is a horizontally decorated path where the decorations h_1 and h_2 of each pattern of consecutive steps HHV fulfill $h_1 \neq h_2$ except for $h_1 = h_2 = 1$.

In terms of marked boxes, this constraint translates to the fact that, below the horizontal steps in each consecutive pattern HHV , the marks must be in different rows except possibly for the lowest one.

3. Heuristic analysis

In this section, we will explain briefly some heuristics and an *ansatz* that we will apply later to get the asymptotic behavior of r_n and c_n . These heuristics are closely related to the asymptotic behavior of Dyck paths and the Airy function.

3.1. An intuitive explanation of the stretched exponential

We can consider r_n as a weighted sum of Dyck paths, where each Dyck path P has a weight $w(P)$ that is the number of horizontally decorated Dyck paths that it gives rise to. There is thus a balance of the number of total paths and their weights for the weighted sum $r_{n,n}$. On the one hand, most paths have an (average) height of $\mathcal{O}(\sqrt{n})$ (i.e., mean distance to the diagonal). On the other hand, their weight is maximal if their height is $\mathcal{O}(1)$, i.e., they are close to the diagonal. In other words, typical Dyck paths are numerous but with small weight, and Dyck paths atypically close to the diagonal are few but with enormous weight. The asymptotic behavior of the weighted sum of Dyck paths that we consider should be a result of a compromise between these two forces. We will now make this more explicit by analyzing Dyck paths with height approximately n^α for some $\alpha \in (0, 1/2)$.

Given a Dyck path P with steps $H = (1, 0)$ and $V = (0, 1)$ as in Definition 2.3, let m_i be the y -coordinate of the i -th step H . The number of Dyck paths with m_i bounded uniformly satisfy the following property.

Proposition 3.1 ([22, Theorem 3.3]). *For a Dyck path P of length $2n$ chosen uniformly at random, let m_i be the y -coordinate of the i -th step H . For $\alpha < 1/2$, we have*

$$\log \mathbb{P} \left(\max_{1 \leq i \leq n} (i - m_i) < n^\alpha \right) \sim -\pi^2 n^{1-2\alpha}.$$

Let $w(P)$ the number of horizontally decorated Dyck paths whose unlabeled version is the Dyck path P . For a randomly chosen Dyck path P of length $2n$ with $i - m_i$ bounded uniformly by n^α , we heuristically expect most values of $i - m_i$ to be of the order $\Theta(n^\alpha)$, with i of order $\Theta(n)$. This leads to the following approximation:

$$\log \frac{w(P)}{n!} = \sum_{1 \leq i \leq n} \log \left(\frac{m_i + 1}{i} \right) = \sum_{1 \leq i \leq n} \log \left(1 - \frac{i - m_i - 1}{i} \right) \approx cn \cdot \left(-\frac{n^\alpha}{n} \right) = -cn^\alpha.$$

Here, $c > 0$ is some constant depending on α . This approximation is only heuristically justified and very hard to prove. The contribution of Dyck paths with $i - m_i$ uniformly bounded by n^α should thus roughly be $n!4^n \exp(-(1 + o(1))c'n^{p(\alpha)})$, with $p(\alpha) = \min(\alpha, 1 - 2\alpha)$ and $c' > 0$ a constant depending on α . Here, 4^n comes from the growth constant of Dyck paths. The function $p(\alpha)$ is minimal at $\alpha = 1/3$, which maximizes the contribution, leading to the following heuristic guess that the number of relaxed binary trees r_n should satisfy

$$\log \frac{r_n}{n!4^n} \underset{n \rightarrow \infty}{\sim} -an^{1/3},$$

for some constant $a > 0$. Furthermore, we anticipate that the main contribution should come from horizontally decorated Dyck paths with $i - m_i$ mostly of order $\Theta(n^{1/3})$. Since most such i 's should be of order $\Theta(n)$, we can even state the condition above as $x - y = \Theta(y^{1/3})$ for most endpoints (x, y) of horizontal steps. This heuristic is the starting point of our analysis.

3.2. Weighted Dyck meanders

The heuristics of the previous section suggest that the mean distance to the diagonal will play an important role. Therefore, we propose another model of lattice paths emphasizing this distance. A *Dyck meander* (or simply a *meander*) M is a lattice path consisting of up steps $U = (1, 1)$ and down steps $D = (1, -1)$ while never falling below $y = 0$. It is clear that Dyck paths of length $2n$ are in bijection with Dyck meanders of length $2n$ ending on $y = 0$ with the transcription $H \rightarrow U, V \rightarrow D$. This bijection can also be viewed geometrically as the linear transformation $x' = x + y, y' = x - y$. This transformation will simplify the following analysis. We can consider Dyck meanders as initial segments of Dyck paths.

Furthermore, we have seen that a rescaling by $n!$ seems practical. So we consider the following weight on steps U in a meander M . If U starts from (a, b) , then its weight is $(a - b + 2)/(a + b + 2)$, and the weight of M is the product of the weights of its steps U . Let $d_{n,m}$ denote the weighted sum of meanders ending at (n, m) . We get the following recurrence for $d_{n,m}$.

Proposition 3.2. *The weighted sum $d_{n,m}$ defined above for meanders ending at (n, m) satisfies the recurrence*

$$\begin{cases} d_{n,m} = \frac{n-m+2}{n+m} d_{n-1,m-1} + d_{n-1,m+1}, & \text{for } n > 0, m \geq 0, \\ d_{0,m} = 0, & \text{for } m > 0, \\ d_{n,-1} = 0, & \text{for } n \geq 0, \\ d_{0,0} = 1. \end{cases} \quad (2)$$

Proof. We concentrate on the first case, as the boundary cases follow directly from the definition of meanders. Given a meander ending at (n, m) with $n > 0$, the last step may be an up step or a down step. The contribution of the former case is $\frac{n-m+2}{n+m}d_{n-1,m-1}$, with the weight of the last up step taken into account. The contribution of the latter case is simply $d_{n-1,m+1}$. We thus get the claimed recurrence. \square

Corollary 3.3. *For integers m, n of the same parity, we have*

$$d_{n,m} = \frac{1}{((n+m)/2)!} r_{(n+m)/2, (n-m)/2}.$$

When m, n are not of the same parity, we have $d_{n,m} = 0$.

In particular, the number of relaxed trees of size n is given by $n!d_{2n,0}$.

Proof. It is clear that meanders can only end on points (n, m) for n, m of the same parity. In this case, it suffices to compare Proposition 2.6 with Proposition 3.2 under the proposed equality. \square

For some simple cases of $d_{n,m}$, elementary computations show that $d_{n,m} = 0$ for $m > n$, $d_{n,n} = \frac{1}{n!}$, $d_{n,n-2} = \frac{2^{n-1}-1}{(n-1)!}$ and $d_{n,n-4} = \frac{7 \cdot 3^{n-3} - 2^n + 1}{2(n-2)!}$.

3.3. Analytic approximation of weighted Dyck meanders

The heuristic in Section 3.1 suggests that the main weight of $d_{n,m}$ comes from the region $m = \Theta(n^{1/3})$. It thus suggests an approximation of $d_{n,m}$ of the form

$$d_{n,m} \sim f(n^{-1/3}(m+1))h(n), \tag{3}$$

for some functions f and h , where we expect $h(n) \approx 2^n \rho^{n^{1/3}}$ for some ρ . The idea is that $h(n)$ describes how the total weight for a fixed n grows, and $f(\kappa)$ describes the rescaled weight distribution in the main region $m = \Theta(n^{1/3})$.

Let $s(n)$ be the ratio $\frac{h(n)}{h(n-1)}$. Suppose that $m = \kappa n^{1/3} - 1$, the recurrence becomes

$$f(\kappa)s(n) = \frac{n - \kappa n^{1/3} + 3}{n + \kappa n^{1/3} - 1} f\left(\frac{\kappa n^{1/3} - 1}{(n-1)^{1/3}}\right) + f\left(\frac{\kappa n^{1/3} + 1}{(n-1)^{1/3}}\right). \tag{4}$$

Now, since we expect $h(n) \approx 2^n \rho^{n^{1/3}}$, we postulate that the ratio $s(n)$ behaves like

$$s(n) = 2 + cn^{-2/3} + O(n^{-1}), \tag{5}$$

and that $f(\kappa)$ is analytic. Using these assumptions, we can expand (4) as a Puiseux series in $1/n$. Moving all terms to the right-hand side yields

$$0 = ((c + 2\kappa)f(\kappa) - f''(\kappa))n^{-2/3} + O(n^{-1}).$$

Solving the differential equation $(c + 2\kappa)f(\kappa) - f''(\kappa) = 0$ under the condition $f(\kappa) \rightarrow 0$ when $\kappa \rightarrow \infty$ yields the unique solution (up to multiplication by a constant)

$$f(\kappa) = b\text{Ai}\left(\frac{c + 2\kappa}{2^{2/3}}\right). \tag{6}$$

The condition on the behavior of $f(\kappa)$ near ∞ is motivated by the experimental observation that $d_{n,m}$ is quickly decaying for m close to n . We also insist that $f(0) = 0$ as $d_{n,-1} = 0$, which implies that $c = 2^{2/3}a_1$ where $a_1 \approx -2.338$ is the first root of the Airy function $\text{Ai}(x)$, i.e. the largest one as all roots are on the real negative axis; see [1, p. 450]. Now, using this conjectural value of c , it follows that (ignoring polynomial terms)

$$h(n) \approx 2^n \exp\left(3a_1(n/2)^{1/3}\right).$$

This suggests that the number of relaxed trees $r_n = n!d_{2n,0}$ behaves like

$$r_n \approx n!4^n \exp\left(3a_1n^{1/3}\right),$$

which is compatible with what we want to prove.

We observe that (4) can be expanded into a Puiseux series of $n^{1/3}$ by taking appropriate series expansions of $f(\kappa)$ and $s(n)$. Hence, to refine the analysis above, it is natural to look at the expansion of $s(n)$ in (5) to more subdominant terms, and to postulate a more refined *ansatz* of $d_{n,m}$ than (3), probably as a series in $n^{1/3}$. Indeed, if we take

$$d_{n,m} \sim \left(f(n^{-1/3}(m + 1)) + n^{-1/3}g(n^{-1/3}(m + 1))\right) h(n)$$

and

$$s(n) = 2 + cn^{-2/3} + dn^{-1} + O(n^{-4/3}),$$

then using the same method we can reach the polynomial part of the asymptotic behavior of r_n as

$$r_n \approx n!4^n \exp\left(3a_1n^{1/3}\right) n.$$

In general, we can postulate

$$d_{n,m} \approx h(n) \sum_{j=0}^k f_j(n^{-1/3}(m + 1))n^{-j/3},$$

and

$$s(n) = 2 + \gamma_2n^{-2/3} + \gamma_3n^{-1} + \dots + \gamma_kn^{-k/3} + o(n^{-k/3}).$$

The proof of our main result on relaxed binary trees is based on choosing the cutoff appropriately, and using perturbations of that truncation to bound r_n .

3.4. Discussion on the constants

One of the first steps in our method involves taking ratios $h(n)/h(n - 1)$ (or equivalently r_n/r_{n-1}) of successive terms. From the leading asymptotic behavior of these ratios we can deduce the exact asymptotic form up to the constant term. Unfortunately, however, this method makes it impossible to exactly determine the constant term γ_r . In this section we give estimates of the constant terms: we believe that there are constants $\gamma_r \approx 166.95208957$ and $\gamma_c \approx 173.12670485$ such that

$$c_n \sim \gamma_c n! 4^n e^{3a_1 n^{1/3}} n^{3/4} \quad \text{and} \quad r_n \sim \gamma_r n! 4^n e^{3a_1 n^{1/3}} n.$$

Based on the analysis in Section 3.3, we expect the ratios r_n/r_{n-1} to behave like

$$\frac{r_n}{r_{n-1}} = \sum_{j=0}^{k-1} \beta_j n^{1-j/3} + \mathcal{O}(n^{1-k/3}),$$

for any positive integer k , with the sequence β_0, β_1, \dots beginning with the terms $4, 0, 4a_1, 4$. This is equivalent to the existence of a sequence $\delta_0, \delta_1, \dots$ such that r_n behaves like

$$r_n = n! 4^n \exp(3a_1 n^{1/3}) n \left(\sum_{j=0}^{k-1} \delta_j n^{-j/3} + \mathcal{O}(n^{-k/3}) \right),$$

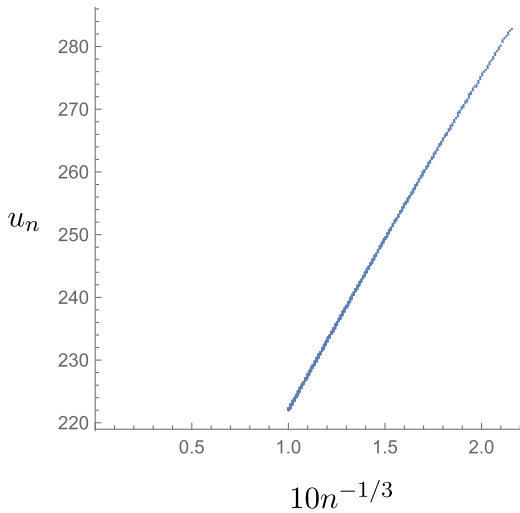
for any positive integer k . In this equation, $\delta_0 = \gamma_r$ is the constant term that we aim to approximate. A simple way to approximate γ_r is to write

$$u_n = \frac{r_n}{n! 4^n \exp(3a_1 n^{1/3}) n}.$$

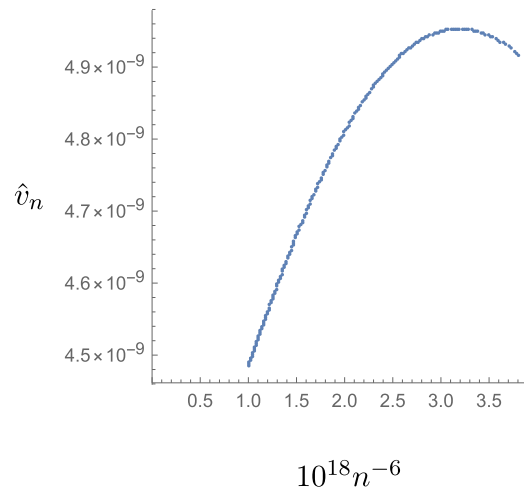
Then the graph of the values of u_n plotted against $10n^{-1/3}$ (because n is close to 1000) should be roughly linear (see Fig. 4a), and the point where it crosses the y -axis can be taken as an approximation for γ_r . This yields $\gamma_r \approx 160$. We get a more precise estimate as follows: Fix k to be some positive integer. Then, for each n , consider the integers $m \in [n, n + k)$. For each such m we expect the equation

$$u_m \approx \sum_{j=0}^{k-1} \delta_j m^{-j/3}$$

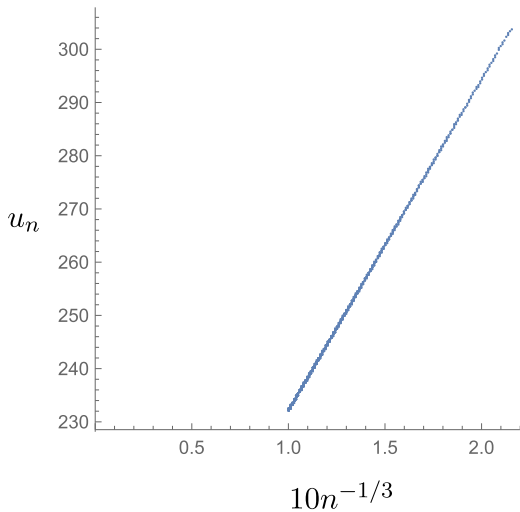
to be approximately true. We then solve this system of equations for $\delta_0, \dots, \delta_{k-1}$ as though the equations were exact, using known, exact values of u_m . This yields approximations for $\delta_0, \dots, \delta_{k-1}$. Denote the approximation thus obtained for $\delta_0 = \gamma_r$



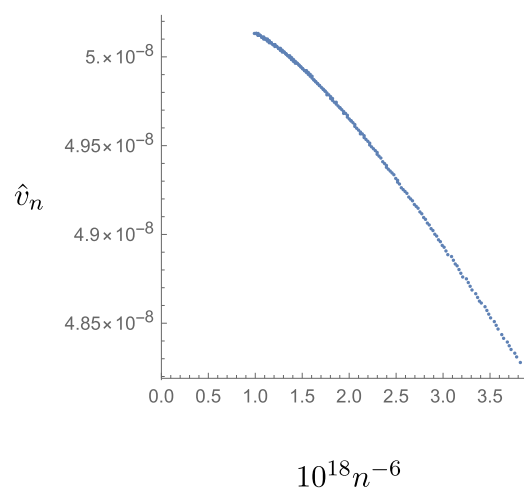
(a) Plot of u_n vs. $10n^{-1/3}$ for approximating the constant term γ_r of relaxed trees.



(b) Plot of $\hat{v}_n = v_n - 166.95208957$ vs. $10^{18}n^{-6}$, where v_n approximates the constant term γ_r for relaxed trees.



(c) Plot of u_n vs. $10n^{-1/3}$ for approximating the constant term γ_c of compacted trees.



(d) Plot of $\hat{v}_n = v_n - 173.1267048$ vs. $10^{18}n^{-6}$, where v_n approximates the constant term γ_c of compacted trees.

Fig. 4. Plots for $800 \leq n \leq 1000$ visualizing the numerical approximation of the leading constants γ_r and γ_c of relaxed and compacted trees, respectively. Note that the scalings on the x -axes with $10n^{-1/3}$ and $10^{18}n^{-6}$ are chosen because n is close to 1000.

by v_n . Note that this is equivalent to writing v_n as a weighted sum of the numbers u_m , which cancels the terms $n^{-j/3}$ for $1 \leq j < k$. For example, if $k = 2$ then $v_n = ((n+1)^{1/3}u_n - n^{1/3}u_{n+1})/((n+1)^{1/3} - n^{1/3})$. Hence, if our assumptions are correct then $v_n = \gamma_r + \mathcal{O}(n^{-k/3})$. Taking $k = 18$ and plotting v_n against $10^{18}n^{-6}$ (because n is close to 1000) as in Fig. 4b yields the approximation $\gamma_r \approx 166.95208957$, where we expect the quoted digits to be correct. In Figs. 4c and 4d we show a similar analysis of the counting sequence for compacted trees, yielding the approximation $\gamma_c \approx 173.12670485$.

4. Proof of stretched exponential for relaxed trees

In this section we prove upper and lower bounds for the number of relaxed trees. These bounds differ only in the constant term, so they completely determine both the stretched exponential factor and the polynomial factor in the asymptotic number of relaxed trees for large n .

Recall from Corollary 3.3 that the number of relaxed trees r_n of size n is given by $r_n = n!d_{2n,0}$, where the terms $d_{n,m}$ are given by the recurrence relation (2) which we repeat here for the convenience of the reader:

$$\begin{cases} d_{n,m} = \frac{n-m+2}{n+m}d_{n-1,m-1} + d_{n-1,m+1}, & \text{for } n > 0, m \geq 0, \\ d_{0,m} = 0, & \text{for } m > 0, \\ d_{n,-1} = 0, & \text{for } n \geq 0, \\ d_{0,0} = 1. \end{cases}$$

Our proofs of the upper and lower bounds for relaxed trees come from more general bounds for the numbers $d_{n,m}$, which we prove by induction. Suppose that $(X_{n,m})_{n \geq m \geq 0}$ and $(s_n)_{n \geq 1}$ are sequences of non-negative real numbers satisfying

$$X_{n,m}s_n \leq \frac{n-m+2}{n+m}X_{n-1,m-1} + X_{n-1,m+1}, \tag{7}$$

for all sufficiently large n and all integers $m \in [0, n]$. We define the sequence $(h_n)_{n \geq 0}$ by $h_0 = 1$ and $h_n = s_n h_{n-1}$. By induction on n , for some constant b_0 , the following inequality holds for all sufficiently large n and all $m \geq 0$:

$$\begin{aligned} X_{n,m}h_n &\stackrel{(7)}{\leq} \frac{n-m+2}{n+m}X_{n-1,m-1}h_{n-1} + X_{n-1,m+1}h_{n-1} \\ &\stackrel{\text{(IS)}}{\leq} \frac{n-m+2}{n+m}b_0d_{n-1,m-1} + b_0d_{n-1,m+1} \\ &\stackrel{(2)}{=} b_0d_{n,m}. \end{aligned} \tag{8}$$

Here (IS) marks the ‘‘Induction Step’’. Similarly, if we can show the opposite of (7), it will imply that

$$X_{n,m}h_n \geq b_1 \cdot d_{n,m},$$

for all sufficiently large n and all integers $m \in [0, n]$.

Comparing to the heuristic analysis in Section 3.3, we see that $X_{n,m}$ acts as the function $f(\kappa)$, and s_n as $s(n)$. Therefore, we should expect $X_{n,m}$ to be close to (6), and s_n to be a slight deviation of (5).

In Lemma 4.2 we will prove that certain explicit sequences $\tilde{X}_{n,m}$ and \tilde{s}_n satisfy (7), which will lead to a lower bound on the numbers $d_{n,m}$. Similarly, in Lemma 4.4 we will

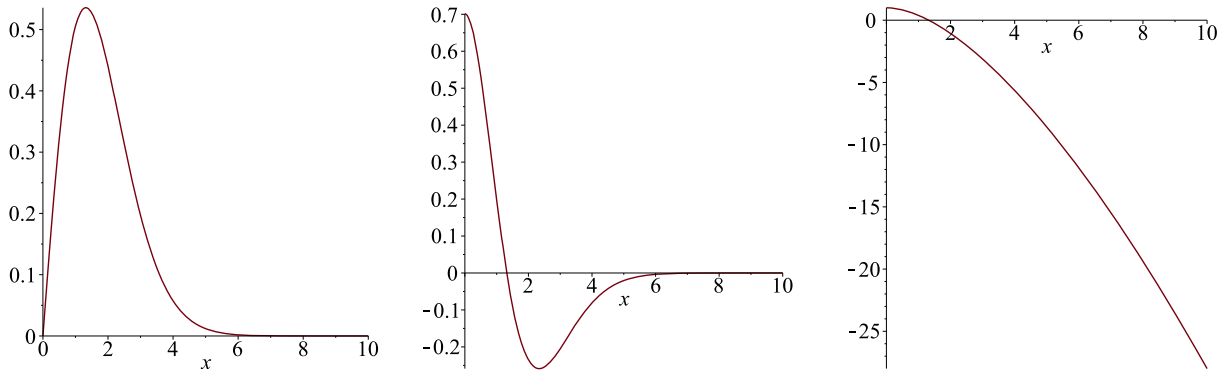


Fig. 5. (Left) The Airy function $\text{Ai}(a_1 + x)$, (Centre) its derivative $\text{Ai}'(a_1 + x)$, and (Right) the quotient $\Phi(x) = x \frac{\text{Ai}'(a_1 + x)}{\text{Ai}(a_1 + x)}$ on the positive real line.

show that other explicit sequences $\hat{X}_{n,m}$ and \hat{s}_n satisfy the opposite of (7), which therefore yields an upper bound on the numbers $d_{n,m}$. Together, these two bounds determine the exact asymptotic form of the numbers $d_{2n,0}$ up to the constant term.

In order to prove these bounds with the explicit expressions of $X_{n,m}$ and s_n , we will consider the difference between the right- and the left-hand side of (7). Then we will show that this difference is non-negative. We start by expanding the involved Airy function and its derivative in the neighborhood of an appropriate point α , leading to a sum of the form

$$p_{n,m} \text{Ai}(\alpha) + p'_{n,m} \text{Ai}'(\alpha),$$

where $p_{n,m}$ and $p'_{n,m}$ can be expressed as Puiseux series in n whose coefficients are fractional polynomials in m . By looking at the “Newton polygon” of these Puiseux series, we can pick out the dominant term at different regimes of n and m , leading to a proof of (7) (or the reverse direction).

The following Lemma summarizes some elementary results on the relation between the Airy function Ai and its derivative Ai' . We will use these results in Lemmas 4.2 and 4.4 to bound the subsequently defined auxiliary sequence $\tilde{X}_{n,m}$.

Lemma 4.1. *The functions*

$$\Phi(x) = x \frac{\text{Ai}'(a_1 + x)}{\text{Ai}(a_1 + x)} \quad \text{and} \quad \Psi(x) = \frac{\text{Ai}'(a_1 + x)}{\text{Ai}(a_1 + x)}$$

are infinitely differentiable and monotonically decreasing on $x > 0$ with $\Phi(0) = 1$.

Proof. First, by l’Hospital’s rule it is easy to see that $\Phi(0) = 1$. Second, as a_1 is the largest root of $\text{Ai}(x)$, the functions $\Phi(x)$ and $\Psi(x)$ are infinitely differentiable as compositions of differentiable functions. It remains to prove the monotonicity; see Fig. 5. A local expansion at $x = 0$ shows that the functions are initially decreasing. The same holds for large x due to the approximation $\text{Ai}(x) \sim \frac{\exp(-\frac{2}{3}x^{3/2})}{2\sqrt{\pi}x^{1/4}}$, see [1, Equation 10.5.49], giving

$$\Psi(x) \sim -\sqrt{a_1 + x}, \tag{9}$$

for $x \rightarrow \infty$. We will show that $\Phi'(x)$ and $\Psi'(x)$ are always negative for $x > 0$. Note that $\Phi(x)$ and $\Psi(x)$ will change sign only once at $x_0 \approx 0.91$.

We present the following argument for the monotonicity of $\Phi(x)$. Assume that there exists an x_+ such that $\Phi'(x_+) > 0$. Then, as $\Phi(x)$ is initially and finally decreasing, there must exist $y_1 < x_+ < y_2$ such that $\Phi'(y_1) = \Phi'(y_2) = 0$ and $\Phi''(y_1) \geq 0 \geq \Phi''(y_2)$.

The second derivatives are equal to

$$\Phi''(x) = 2a_1 + 3x - \frac{2}{x}\Phi(x)\Phi'(x).$$

These lead to $2a_1 + 3y_1 \geq 0 \geq 2a_1 + 3y_2$, thus also the contradiction $y_1 \geq y_2$. The argument for the monotonicity of $\Psi(x)$ is analogous, except that the second derivative is now

$$\Psi''(x) = 1 - 2\Psi(x)\Psi'(x),$$

leading to the contradiction $\Psi''(y_1) = \Psi''(y_2) = 1$. \square

Later we will use the value x_0 which is the unique root of $\Phi(x)$ and $\Psi(x)$ to determine the dominant term in the expansion of our series in $\text{Ai}(x)$ and $\text{Ai}'(x)$.

4.1. Lower bound

Lemma 4.2. *For all $n, m \geq 0$ let*

$$\begin{aligned} \tilde{X}_{n,m} &:= \left(1 - \frac{2m^2}{3n} + \frac{m}{2n}\right) \text{Ai}\left(a_1 + \frac{2^{1/3}(m+1)}{n^{1/3}}\right) && \text{and} \\ \tilde{s}_n &:= 2 + \frac{2^{2/3}a_1}{n^{2/3}} + \frac{8}{3n} - \frac{1}{n^{7/6}}. \end{aligned}$$

Then, for any $\varepsilon > 0$, there exists an \tilde{n}_0 such that

$$\tilde{X}_{n,m}\tilde{s}_n \leq \frac{n-m+2}{n+m}\tilde{X}_{n-1,m-1} + \tilde{X}_{n-1,m+1}, \tag{10}$$

for all $n \geq \tilde{n}_0$ and for all $0 \leq m < n^{2/3-\varepsilon}$.

Proof. First, define the following sequence

$$P_{n,m} := -Z_{n,m}s_n + \frac{n-m+2}{n+m}Z_{n-1,m-1} + Z_{n-1,m+1},$$

where

$$s_n := \sigma_0 + \frac{\sigma_1}{n^{1/3}} + \frac{\sigma_2}{n^{2/3}} + \frac{\sigma_3}{n} + \frac{\sigma_4}{n^{7/6}},$$

$$Z_{n,m} := \left(1 + \frac{\tau_2 m^2 + \tau_1 m}{n}\right) \text{Ai}\left(a_1 + \frac{2^{1/3}(m+1)}{n^{1/3}}\right),$$

with $\sigma_i, \tau_j \in \mathbb{R}$. Then the inequality (10) is equivalent to $P_{n,m} \geq 0$ with $\sigma_0 = 2, \sigma_1 = 0, \sigma_2 = 2^{2/3}a_1, \sigma_3 = 8/3,$ and $\sigma_4 = -1$ as well as $\tau_0 = 0, \tau_1 = 1/2,$ and $\tau_2 = -2/3$. Next, we expand $\text{Ai}(z)$ in a neighborhood of

$$\alpha = a_1 + \frac{2^{1/3}m}{n^{1/3}}, \tag{11}$$

and we get the following expansion

$$P_{n,m} = p_{n,m} \text{Ai}(\alpha) + p'_{n,m} \text{Ai}'(\alpha),$$

where $p_{n,m}$ and $p'_{n,m}$ are functions of m and n^{-1} and may be expanded as power series in $n^{-1/6}$ with coefficients polynomial in m . As long as $n > 1$ and $n > m$, this series converges absolutely because the Airy function is entire and so all functions expanded are analytic in the region defined by $|n| > 1$ and $|n| > |m|$.

As a first step we compute the possible range of the powers in m and n . We will start by showing that $[m^i n^j]P_{n,m} = 0$ for $i + j > 1, i, j \in \mathbb{Q}$. The expansions of the three involved Airy functions only give terms of the form $\mathcal{O}(m^j n^{-j} (n^{-1/3})^k) \text{Ai}^{(k)}(\alpha)$, with $j, k \geq 0$. Due to the differential equation $\text{Ai}''(\alpha) = \alpha \text{Ai}(\alpha)$, the term $\text{Ai}^{(k)}(\alpha)$ takes the form $\mathcal{O}(\alpha^{\lfloor k/2 \rfloor}) \text{Ai}(\alpha) + \mathcal{O}(\alpha^{\lfloor (k-1)/2 \rfloor}) \text{Ai}'(\alpha)$. Hence, all terms in the expansion of the Airy function are of the form $\mathcal{O}(m^j n^{-j}) \text{Ai}(\alpha)$ or $\mathcal{O}(m^j n^{-j-1/3}) \text{Ai}'(\alpha)$ for some $j \geq 0$. Due to the factor $m^2 n^{-1}$ in the definition of $\tilde{X}_{n,m}$, this implies that $[m^i n^j]P_{n,m} = 0$ for $i + j > 1$. Additionally, it also implies that the coefficients of $\text{Ai}'(\alpha)$ are equal to 0 for $i + j > 2/3$.

Next, we strengthen this result by choosing suitable values σ_i for $0 \leq i \leq 4$ in the definition of s_n in order to eliminate more initial coefficients. Then, we will show that the remaining terms satisfy $P_{n,m} \geq 0$. We performed this tedious task in Maple and we refer to the accompanying worksheet [27] for more details. The results are summarized in Fig. 6 where the initial non-zero coefficients are shown. A diamond at (i, j) is drawn if and only if the coefficient $[m^i n^j]P_{n,m}$ is non-zero. It is an empty diamond if the given choice of σ_i and τ_j makes it disappear, whereas it is a solid diamond if it remains non-zero. The convex hull is formed by the following three lines

$$L_1 : j = -\frac{7}{6} - \frac{7i}{18},$$

$$L_2 : j = -\frac{1}{3} - \frac{2i}{3},$$

$$L_3 : j = 1 - i.$$

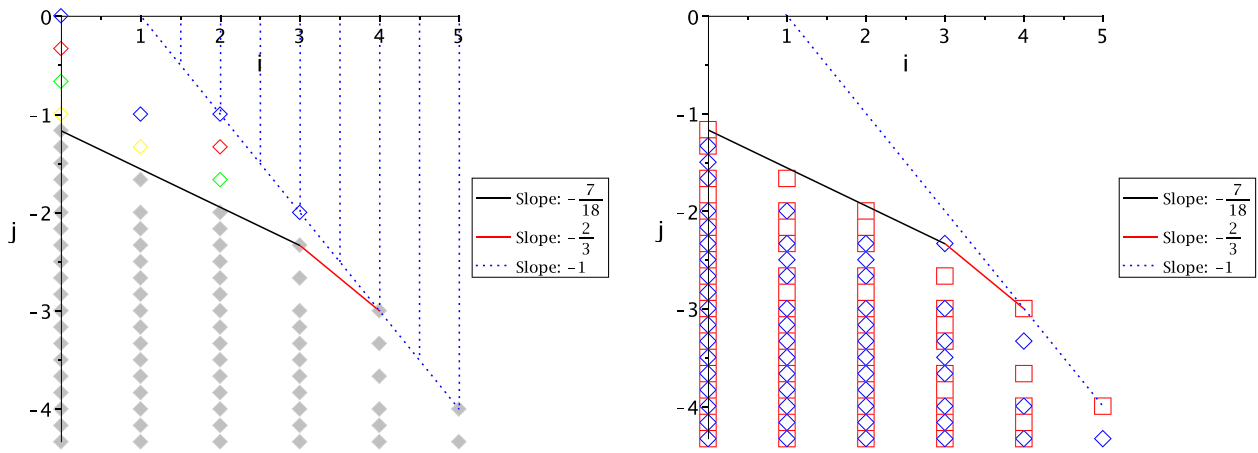


Fig. 6. (Left) Non-zero coefficients of $P_{n,m} = \sum a_{i,j} m^i n^j$ shown by diamonds for $s_n := \sigma_0 + \frac{\sigma_1}{n^{1/3}} + \frac{\sigma_2}{n^{2/3}} + \frac{\sigma_3}{n} + \frac{\sigma_4}{n^{7/6}}$ and $Z_{n,m} := \left(1 + \frac{\tau_2 m^2 + \tau_1 m}{n}\right) \text{Ai}\left(a_1 + \frac{2^{1/3}(m+1)}{n^{1/3}}\right)$. There are no terms in the blue dashed area. The blue terms vanish for $\sigma_0 = 2$, the red terms vanish for $\sigma_1 = 0$, the green terms vanish for $\sigma_2 = 2^{2/3}a_1$, and the yellow terms vanish for $\sigma_3 = 8/3$ and $\tau_2 = -2/3$. The black and red lines represent the two parts L_1 and L_2 , respectively, of the convex hull. (Right) The solid gray diamonds are decomposed into the coefficients $p_{n,m}$ of $\text{Ai}(\alpha)$ (red boxes) and $p'_{n,m}$ of $\text{Ai}'(\alpha)$ (blue diamonds). (For interpretation of the colors in the figure(s), the reader is referred to the web version of this article.)

Next, we distinguish between the contributions arising from $p_{n,m}$ and $p'_{n,m}$. The expansions for n tending to infinity start as follows, where the elements on the convex hull are written in color:

$$\begin{aligned}
 P_{n,m} = & \text{Ai}(\alpha) \left(-\frac{\sigma_4}{n^{7/6}} - \frac{2^{5/3}a_1 m}{3n^{5/3}} - \frac{41m^2}{9n^2} - \frac{2^{8/3}a_1 m^3}{3n^{8/3}} - \frac{34m^4}{9n^3} - \frac{62m^5}{135n^4} + \dots \right) + \\
 & \text{Ai}'(\alpha) \left(\frac{2^{1/3}(2\tau_1 - 1)}{n^{4/3}} + \frac{2^{1/3}}{n^{3/2}} - \frac{8a_1 m}{9n^2} + \frac{2^{1/3}(24\tau_1 - 31)m^2}{9n^{7/3}} - \frac{2^{13/3}m^3}{9n^{7/3}} \right. \\
 & \quad \left. - 5\frac{2^{5/3}m^4}{9n^{10/3}} - 89\frac{2^{4/3}m^5}{135n^{13/3}} + \dots \right).
 \end{aligned}$$

We now choose $\sigma_4 = -1$ which leads to a positive term $\text{Ai}(\alpha)n^{-7/6}$ and set $\tau_1 = 1/2$ to eliminate the term of order $n^{-4/3}$ from the convex hull (it is replaced by $\frac{2^{1/3}}{n^{3/2}}$). Then, the non-zero coefficients are shown in Fig. 7. Next, for fixed (large) n we prove that for all m the dominant contributions in $P_{n,m}$ are positive. Therefore, we consider three different regimes. Let x_0 be the unique positive root of $\Psi(x)$ from Lemma 4.1.

1. Consider the range of small values of m given by $m \leq x_0(n/2)^{1/3}$. In this range $\text{Ai}(\alpha)$ and $\text{Ai}'(\alpha)$ are both positive. Moreover, the (red) coefficients of $\text{Ai}(\alpha)$ are dominated by $n^{-7/6}$ for large n , while the (blue) coefficients of $\text{Ai}'(\alpha)$ apart from the term $\nu = -\frac{2^{13/3}m^3}{9n^{7/3}}\text{Ai}'(\alpha)$ are dominated by $\frac{2^{1/3}}{n^{3/2}}$. By Lemma 4.1 we have

$$\frac{2^{1/3}m}{n^{1/3}}\text{Ai}'(\alpha) - \text{Ai}(\alpha) < 0.$$

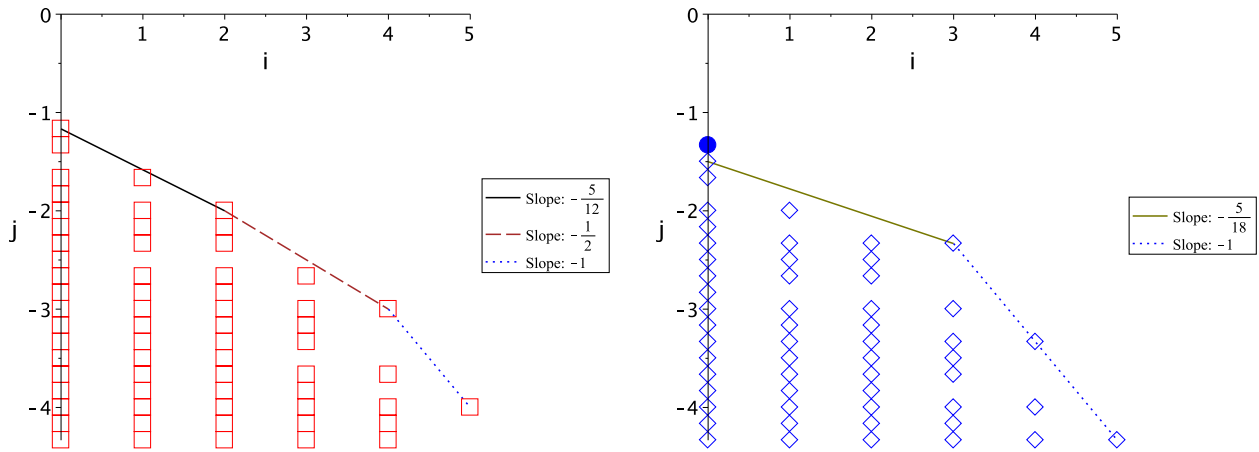


Fig. 7. Non-zero coefficients $p_{n,m} = \sum \tilde{a}_{i,j} m^i n^j$ (red, left) and $p'_{n,m} = \sum \tilde{a}'_{i,j} m^i n^j$ (blue, right) of the expansion (11) for $P_{n,m}$. The coefficient of $n^{-4/3}$ in the right picture depicted as a solid blue circle disappears for $\tau_1 = 1/2$.

Hence, $\nu > -\frac{16m^2}{9n^2} \text{Ai}(\alpha)$, and it can therefore be treated as if it belonged to the coefficients of $\text{Ai}(\alpha)$. Thus, as the dominating terms are positive, there exists some N_0 such that $P_{n,m} > 0$ whenever $n > N_0$ and $m \leq x_0(n/2)^{1/3}$.

2. Next, consider the central range $x_0(n/2)^{1/3} < m \leq n^{7/18}$. Here, we have $\text{Ai}'(\alpha) < 0$. On the one hand, as seen in the left part of Fig. 7, the (red) coefficients of $\text{Ai}(\alpha)$ are still dominated by $n^{-7/6}$ (which holds up to $m = \Theta(n^{5/12})$). On the other hand, in this range the term $\nu = -\frac{2^{13/3}m^3}{9n^{7/3}} \text{Ai}'(\alpha)$ dominates all other (blue) coefficients of $\text{Ai}'(\alpha)$ (due to $\tau_1 = 1/2$). Since $\nu > 0$ in this range, this implies that there exists some (sufficiently large) N_1 such that $P_{n,m} > 0$ whenever $n > N_1$ and $x_0(n/2)^{1/3} < m \leq n^{7/18}$.
3. Finally, consider the range of large values $n^{7/18} < m < n^{2/3-\epsilon}$. By the reasoning on $\Psi(x)$ in Lemma 4.1 we see that $-\text{Ai}'(\alpha) > \text{Ai}(\alpha) > 0$. Therefore, the (blue) term ν dominates all of the (red) terms of $\text{Ai}(\alpha)$ as well as all other (blue) terms of $\text{Ai}'(\alpha)$. Hence there exists some N_2 such that $P_{n,m} > 0$ whenever $n > N_2$ and $n^{7/18} < m < n^{2/3-\epsilon}$.

Choosing $\tilde{n}_0 = \max\{N_0, N_1, N_2\}$ completes the proof. \square

Remark 4.3. The previous result could be strengthened to hold up to $m \leq n^{1-\epsilon}$ by (9) as will be shown in the proof of Lemma 4.4. However, we will not need this result in the sequel.

Now, to complete the lower bound we define the sequence $X_{n,m} := \max\{\tilde{X}_{n,m}, 0\}$, i.e.,

$$X_{n,m} := \begin{cases} \tilde{X}_{n,m}, & \text{if } m < \frac{\sqrt{96n+9}+3}{8}, \\ 0, & \text{if } m \geq \frac{\sqrt{96n+9}+3}{8}. \end{cases}$$

Then, in the first case we get the following inequality for all sufficiently large n

$$X_{n,m}\tilde{s}_n \leq \frac{n-m+2}{n+m}\tilde{X}_{n-1,m-1} + \tilde{X}_{n-1,m+1} \leq \frac{n-m+2}{n+m}X_{n-1,m-1} + X_{n-1,m+1},$$

using Lemma 4.2 with $\varepsilon = \frac{1}{12}$. Note that we could choose any $\varepsilon \in (0, \frac{1}{6})$, as we just need $n^{2/3-\varepsilon} > \frac{\sqrt{96n+9}+3}{8}$ for large n . In the second case we have

$$X_{n,m}\tilde{s}_n = 0 \leq \frac{n-m+2}{n+m}X_{n-1,m-1} + X_{n-1,m+1}.$$

Finally, we write $\tilde{h}_n = \tilde{s}_n\tilde{h}_{n-1}$ and we deduce by induction that $d_{n,m} \geq b\tilde{h}_nX_{n,m}$ for some constant $b > 0$, all sufficiently large n and all $m \in [0, n]$. In particular, it follows from (8) that the number $r_n = n!d_{2n,0}$ of relaxed trees of size n is bounded below by

$$r_n \geq \gamma n!4^n e^{3a_1n^{1/3}} n, \tag{12}$$

for some constant $\gamma > 0$. In the next section we will show an upper bound with the same asymptotic form, but with a different constant γ .

4.2. Upper bound

Next, we consider a similar auxiliary sequence $\hat{X}_{n,m}$ which will give rise to an upper bound on the number of relaxed binary trees.

Lemma 4.4. *Choose $\eta > 2/9$ fixed and for all $n, m \geq 0$ let*

$$\begin{aligned} \hat{X}_{n,m} &:= \left(1 - \frac{2m^2}{3n} + \frac{m}{2n} + \eta \frac{m^4}{n^2}\right) \text{Ai} \left(a_1 + \frac{2^{1/3}(m+1)}{n^{1/3}}\right) \quad \text{and} \\ \hat{s}_n &:= 2 + \frac{2^{2/3}a_1}{n^{2/3}} + \frac{8}{3n} + \frac{1}{n^{7/6}}. \end{aligned}$$

Then, for any $\varepsilon > 0$, there exists a constant \hat{n}_0 such that

$$\hat{X}_{n,m}\hat{s}_n \geq \frac{n-m+2}{n+m}\hat{X}_{n-1,m-1} + \hat{X}_{n-1,m+1}, \tag{13}$$

for all $n \geq \hat{n}_0$ and all $0 \leq m < n^{1-\varepsilon}$.

Proof. The proof follows the same lines as that of Lemma 4.2. Therefore we only focus on the needed modifications. As a first step we define the following sequence

$$Q_{n,m} := \hat{X}_{n,m}\hat{s}_n - \frac{n-m+2}{n+m}\hat{X}_{n-1,m-1} - \hat{X}_{n-1,m+1}.$$

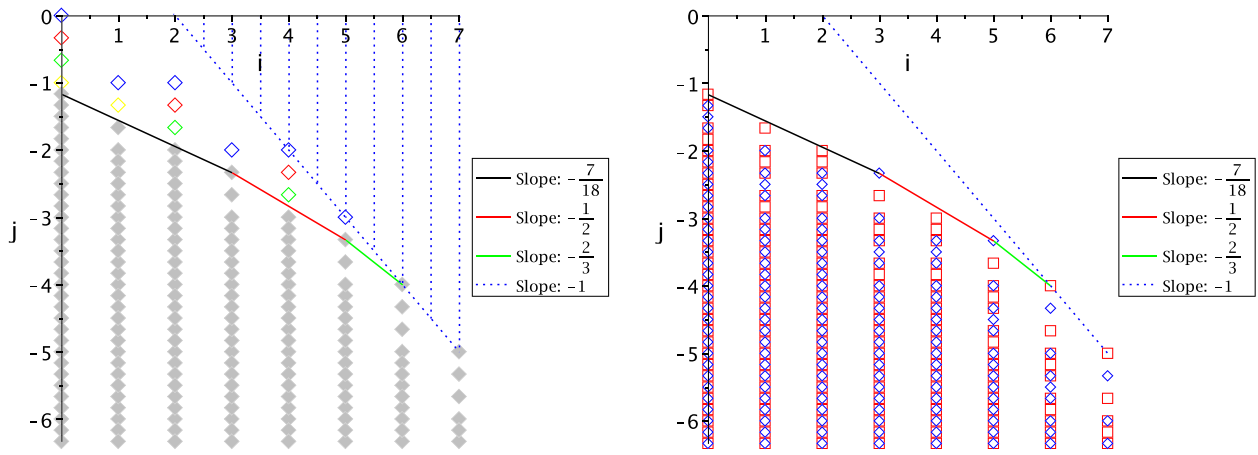


Fig. 8. (Left) Non-zero coefficients of $Q_{n,m} = \sum b_{i,j} m^i n^j$ shown in solid gray diamonds for $s_n := \sigma_0 + \frac{\sigma_1}{n^{1/3}} + \frac{\sigma_2}{n^{2/3}} + \frac{\sigma_3}{n} + \frac{\sigma_4}{n^{7/6}}$ and $X_{n,m} := \left(1 + \frac{\tau_2 m^2 + \tau_1 m}{n} + \eta \frac{m^4}{n^2}\right) \text{Ai}\left(a_1 + \frac{2^{1/3}(m+1)}{n^{1/3}}\right)$. There are no terms in the blue dashed area. The blue terms vanish for $\sigma_0 = 2$, the red terms vanish for $\sigma_1 = 0$, the green terms vanish for $\sigma_2 = 2^{2/3}a_1$, and the yellow term vanishes for $\sigma_3 = 8/3$ and $\tau_2 = -2/3$. The black, red, and green lines represent the three parts \hat{L}_1, \hat{L}_2 and \hat{L}_3 , respectively, of the convex hull. (Right) The solid gray diamonds are decomposed into the coefficients $q_{n,m}$ of $\text{Ai}(\alpha)$ (red boxes) and $q'_{n,m}$ of $\text{Ai}'(\alpha)$ (blue diamonds).

Then the inequality (13) is equivalent to $Q_{n,m} \geq 0$. Again, we expand $\text{Ai}(z)$ in a neighborhood of $\alpha = a_1 + \frac{2^{1/3}m}{n^{1/3}}$, and we get (see [27] for more details)

$$Q_{n,m} = q_{n,m} \text{Ai}(\alpha) + q'_{n,m} \text{Ai}'(\alpha),$$

where $q_{n,m}$ and $q'_{n,m}$ are functions of m and n^{-1} and may again be expanded as power series in $n^{-1/6}$ with coefficients polynomial in m . Now, it is easy to see that $[m^i n^j]Q_{n,m} = 0$ for $i + j > 2$, where the shift by 1 compared to the lower bound is due to the factor $\eta m^4 n^{-2}$. The initial non-zero coefficients are shown in Fig. 8. The four lines (black, red, green, blue) of the convex hull are

$$\begin{aligned} \hat{L}_1 : j &= -\frac{7}{6} - \frac{7i}{18}, \\ \hat{L}_2 : j &= -\frac{5}{6} - \frac{i}{2}, \\ \hat{L}_3 : j &= -\frac{2i}{3}, \\ \hat{L}_4 : j &= 2 - i. \end{aligned}$$

Next, we distinguish between the contributions arising from $q_{n,m}$ and $q'_{n,m}$. The non-zero coefficients are shown in Fig. 9. The expansions for n tending to infinity start as follows, where the elements on the convex hull are written in color.

$$\begin{aligned} Q_{n,m} = \text{Ai}(\alpha) &\left(\frac{\sigma_4}{n^{7/6}} + \frac{2^{5/3}a_1 m}{3n^{5/3}} + \frac{m^2(41 - 108\eta)}{9n^2} + \frac{2^{8/3}a_1 m^3(1 - 6\eta)}{3n^{8/3}} \right. \\ &\left. + \frac{2m^4(17 - 132\eta)}{9n^3} - \frac{2^{5/3}a_1 m^5 \eta}{n^{11/3}} - \frac{17m^6 \eta}{3n^4} - \frac{31m^7 \eta}{45n^5} + \dots \right) + \end{aligned}$$

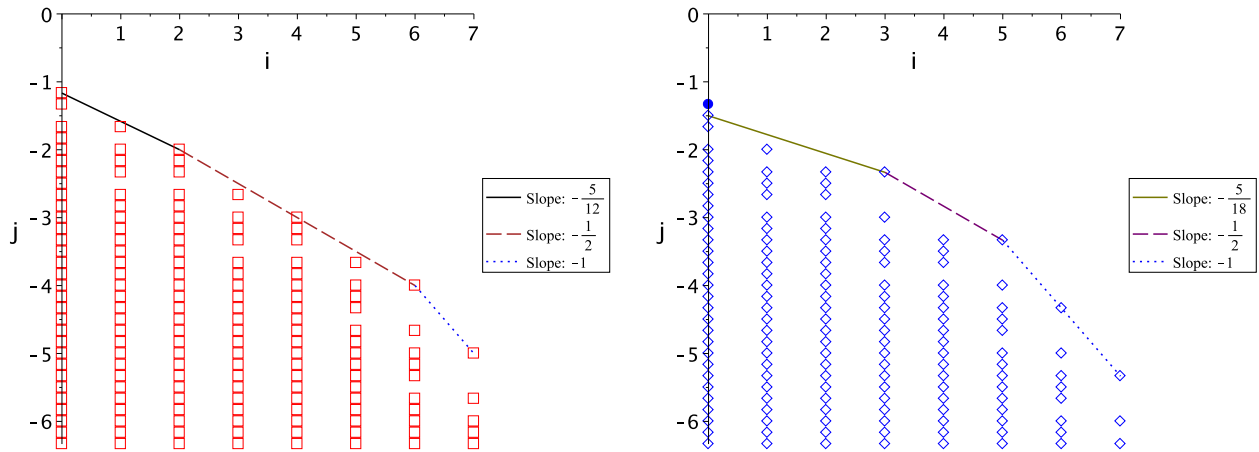


Fig. 9. Non-zero coefficients $q_{k,l} = \sum \tilde{b}_{i,j} m^i n^j$ (red, left) and $q'_{k,\ell} = \sum \tilde{b}'_{i,j} m^i n^j$ (blue, right) of the expansion for $Q_{n,m}$. The coefficient of $n^{-4/3}$ in the right picture depicted as a solid blue circle disappears for $\tau_1 = 1/2$.

$$\begin{aligned}
 \text{Ai}'(\alpha) & \left(\frac{2^{1/3}}{n^{3/2}} + \frac{8a_1 m}{9n^2} + \frac{2^{1/3} m^2 (19 - 108\eta)}{9n^{7/3}} + \frac{2^{10/3} m^3 (2 - 9\eta)}{9n^{7/3}} \right. \\
 & \left. + \frac{5m^4 2^{1/3} (2 - 27\eta)}{9n^{10/3}} - \frac{2^{10/3} m^5 \eta}{3n^{10/3}} - \frac{5m^6 2^{1/3} \eta}{3n^{13/3}} - \frac{89m^7 2^{1/3} \eta}{45n^{16/3}} + \dots \right).
 \end{aligned}$$

Let x_0 be again the unique positive root of $\Psi(x)$ from Lemma 4.1. In order to prove that $Q_{n,m} \geq 0$ for $m \leq n^{1-\epsilon}$, we consider the following four regions:

1. $m \leq x_0(n/2)^{1/3}$,
2. $x_0(n/2)^{1/3} < m \leq n^{7/18}$,
3. $n^{7/18} < m \leq n^{1/2}$,
4. $n^{1/2} < m \leq n^{1-\epsilon}$.

Recall that in the proof that $P_{n,m} \geq 0$ in Lemma 4.2, we considered almost the same first 3 regions, except that in that case the upper bound on the third region was slightly larger ($n^{2/3-\epsilon}$). So the main difference here is the addition of the fourth region, which is required for this lemma to apply up to $m = n^{1-\epsilon}$.

The treatments of the first 3 regions are analogous to those in Lemma 4.2 except for 2 minor changes. First, in the second and third regime we include the additional variable η to make the dominant term $\frac{2^{10/3} m^3 (2-9\eta)}{9n^{7/3}} \text{Ai}'(\alpha)$ positive. Second, in the third regime an additional dominant term $-\frac{2^{10/3} m^5 \eta}{3n^{10/3}} \text{Ai}'(\alpha)$ appears for $m = \Theta(n^{1/2})$ which is positive anyway.

Finally, in the fourth regime, the aforementioned term $-\frac{2^{10/3} m^5 \eta}{3n^{10/3}} \text{Ai}'(\alpha)$ is positive and dominates all other blue terms. However, the dominant red term is $-\frac{17m^6 \eta}{3n^4} \text{Ai}(z)$, which is negative, so it suffices to show that this is dominated by the blue term. Indeed, due to (9) we know that as $m/n^{1/3}$ tends to infinity, $\text{Ai}'(\alpha) \sim -2^{1/6} \frac{m^{1/2}}{n^{1/6}} \text{Ai}(\alpha)$. Hence, the blue term $-\frac{2^{10/3} m^5 \eta}{3n^{10/3}} \text{Ai}'(\alpha)$ dominates in this entire region $n^{1/2} < m \leq n^{1-\epsilon}$. \square

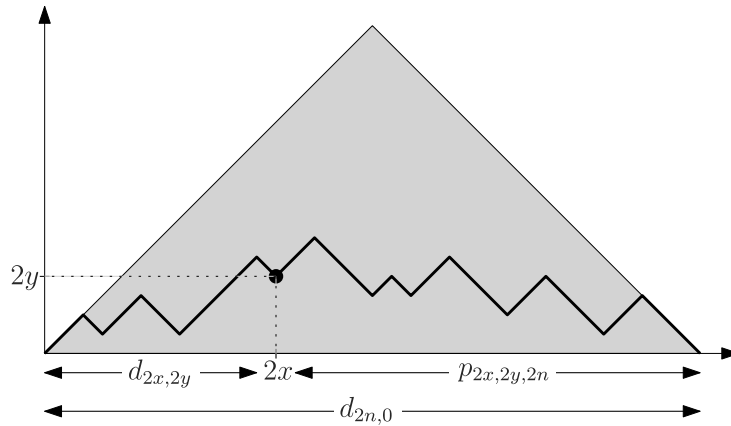


Fig. 10. Proportion of weighted Dyck paths of length $2n$ passing through the point $(2x, 2y)$ showing one example path contributing to $s_{x,y,n}$.

To finish the proof of the upper bound, we will choose some constant $N > 0$ and define a sequence $\tilde{d}_{n,m}$ by the same rules as $d_{n,m}$ except that $\tilde{d}_{n,m} = 0$ whenever $m > n^{3/4}$ and $n > N$. Then, writing $\hat{h}_n = \hat{s}_n \hat{h}_{n-1}$, we can use the lemma above to show by induction that the numbers $\tilde{d}_{n,m}$ satisfy the inequality.

$$b_0 \tilde{d}_{n,m} \leq \hat{h}_n X_{n,m},$$

for some constant b_0 and all sufficiently large n ; compare (8). In particular, the numbers $\tilde{d}_{2n,0}$ are bounded above by

$$\tilde{d}_{2n,0} \leq \gamma 4^n e^{3a_1 n^{1/3}} n,$$

for some constant $\gamma > 0$. The rest of this section is dedicated to proving that there is some choice of N such that $\tilde{d}_{2n,0} \geq d_{2n,0}/2$ for all n .

In order to finish our proof of the upper bound for the numbers $d_{2n,0}$, we will use the interpretation of these numbers as weighted Dyck paths, described in Section 3.2. It will be useful to have an upper bound on the number of these paths which pass through a certain point $(2x, 2y)$ as a proportion of the total weighted number of paths. Let $p_{\ell,m,2n}$ denote the weighted number of paths from (ℓ, m) to $(2n, 0)$; see Fig. 10. Then the proportion $s_{x,y,n}$ of the $d_{2n,0}$ weighted Dyck paths that pass through $(2x, 2y)$ is

$$s_{x,y,n} = \frac{d_{2x,2y} p_{2x,2y,2n}}{d_{2n,0}}.$$

The following lemma yields an upper bound on the number $p_{2x,2y,2n}$.

Lemma 4.5. *The numbers $p_{\ell,m,2n}$ satisfy the inequality*

$$\frac{p_{\ell,j,2n}}{j+1} \geq \frac{p_{\ell,k,2n}}{k+1},$$

for integers $0 \leq j < k \leq \ell \leq 2n$ satisfying $2 \mid k - j$.

Proof. First we note that the numbers $p_{\ell,m,2n}$ are determined by the recurrence relation

$$p_{\ell,m,2n} = p_{\ell+1,m-1,2n} + \frac{\ell - m + 2}{\ell + m + 2} p_{\ell+1,m+1,2n}$$

along with the initial conditions $p_{2n,m,2n} = \delta_{m,0}$ and $p_{l,-1,2n} = 0$. We will now prove the statement of the lemma by reverse induction on ℓ . Our base case is $\ell = 2n$, for which the inequality clearly holds. For the inductive step, we assume that the inequality holds for $\ell + 1$ and all m , and we will prove that it holds for ℓ . It suffices to prove that for $m \geq 1$ the following inequality holds

$$\frac{p_{\ell,m-1,2n}}{m} - \frac{p_{\ell,m+1,2n}}{m+2} \geq 0.$$

Let L denote the left-hand side of this inequality. Using the recurrence relation, we can rewrite L as

$$L = \frac{p_{\ell+1,m-2,2n}}{m} + \frac{(\ell - m + 3)p_{\ell+1,m,2n}}{(\ell + m + 1)m} - \frac{p_{\ell+1,m,2n}}{m+2} - \frac{(\ell - m + 1)p_{\ell+1,m+2,2n}}{(\ell + m + 3)(m+2)}.$$

Now, by the inductive assumption we get the inequalities $p_{\ell+1,m+2,2n} \leq \frac{m+3}{m+1} p_{\ell+1,m,2n}$ and $p_{\ell+1,m-2,2n} \geq \frac{m-1}{m+1} p_{\ell+1,m,2n}$, where the latter even holds for $m = 1$ as then both sides are 0. It follows that

$$\begin{aligned} L &\geq \frac{(m-1)p_{\ell+1,m,2n}}{(m+1)m} + \frac{(\ell - m + 3)p_{\ell+1,m,2n}}{(\ell + m + 1)m} - \frac{p_{\ell+1,m,2n}}{m+2} \\ &\quad - \frac{(m+3)(\ell - m + 1)p_{\ell+1,m,2n}}{(m+1)(\ell + m + 3)(m+2)} \\ &= \frac{4(3 + m + \ell + m\ell)p_{\ell+1,m,2n}}{m(m+2)(1 + m + \ell)(3 + m + \ell)} \geq 0 \end{aligned}$$

as desired. This completes the induction, which proves the inequality for $\ell \in [0, 2n]$. We refer to the accompanying worksheet [27] for more details. \square

In particular, it follows from this lemma that

$$p_{2x,2y,2n} \leq (2y + 1)p_{2x,0,2n}.$$

Moreover, note that the proportion $s_{x,0,n}$ of weighted paths passing through $(2x, 0)$ satisfies $s_{x,0,n} \leq 1$. Hence, the proportion $s_{x,y,n}$ satisfies

$$s_{x,y,n} = \frac{p_{2x,2y,2n}d_{2x,2y}}{d_{2n,0}} \leq \frac{(2y + 1)p_{2x,0,2n}d_{2x,2y}}{d_{2n,0}s_{x,0,n}} = (2y + 1)\frac{d_{2x,2y}}{d_{2x,0}}. \tag{14}$$

From the lower bound (12) we have

$$d_{2x,0} \geq \gamma 4^x e^{3a_1 x^{1/3}} x,$$

so we now desire an upper bound for $d_{2x,2y}$. It will suffice to use the upper bound

$$d_{2x,2y} \leq \binom{2x}{x+y},$$

which holds because the right-hand side is the number of (unweighted) paths from $(0, 0)$ to $(2x, 2y)$, and all weights on our weighted paths are smaller than 1. We are now ready to prove the following lemma

Lemma 4.6. *For all $\varepsilon > 0$ there exists a constant $N_\varepsilon > 0$ with the following property: Recall that $d_{n,m}$ is the weighted number of paths ending at (n, m) . Let $\tilde{d}_{n,m}$ be the number of these paths such that no intermediate point $(2x, 2y)$ on the path satisfies $x > N_\varepsilon$ and $y > x^{3/4}$. Then $d_{2n,0} \leq (1 + \varepsilon)\tilde{d}_{2n,0}$ for all $n > 0$.*

Proof. We can rewrite the desired inequality as

$$1 - \frac{\tilde{d}_{2n,0}}{d_{2n,0}} \leq \frac{\varepsilon}{1 + \varepsilon}.$$

Note that the left-hand side is equal to the proportion of weighted paths with at least one intermediate point $(2x, 2y)$ satisfying $x > N_\varepsilon$ and $y > x^{3/4}$. The proportion $s_{x,y,n}$ of weighted paths which go through any such point $(2x, 2y)$ is bounded above by

$$\begin{aligned} s_{x,y,n} &\stackrel{(14)}{\leq} (2y + 1) \frac{d_{2x,2y}}{d_{2x,0}} \\ &\stackrel{(12)}{\leq} \frac{2y + 1}{\gamma 4^x e^{3a_1 x^{1/3}} x} \binom{2x}{x+y} \\ &\leq \gamma^{-1} 4^{-x} e^{-3a_1 x^{1/3}} x^{-1} \frac{(2y + 1)\Gamma(2x + 1)}{\Gamma(x + x^{3/4} + 1)\Gamma(x - x^{3/4} + 1)}. \end{aligned}$$

The right-hand side of this inequality behaves like

$$\Theta \left(e^{-x^{1/2} + \mathcal{O}(x^{1/3})} \right) \tag{15}$$

for large x . Hence, there is some constant c such that

$$s_{x,y,n} \leq c \cdot 2^{-x^{1/2}}$$

for all x, y, n satisfying $y > x^{3/4}$. Now, the proportion $1 - \tilde{d}_{2n,0}/d_{2n,0}$ of weighted paths passing through at least one point $(2x, 2y)$ is no greater than the sum of the proportions of paths going through each such point. Hence

$$1 - \frac{\tilde{d}_{2n,0}}{d_{2n,0}} \leq \sum_{x \geq N_\epsilon + 1} \sum_{x \geq y > x^{3/4}} s_{x,y,n} \leq \sum_{x \geq N_\epsilon + 1} \sum_{x \geq y > x^{3/4}} c \cdot 2^{-x^{1/2}} \leq \sum_{x \geq N_\epsilon + 1} cx \cdot 2^{-x^{1/2}}.$$

The sum on the right converges to a value less than $\epsilon/(1 + \epsilon)$ for sufficiently large N_ϵ . This completes the proof of the lemma. \square

Remark 4.7. Choosing $y > x^\beta$ instead of $y > x^{3/4}$ one can show that (15) behaves like $\mathcal{O}\left(e^{-x^{2\beta-1}-3a_1x^{1/3}}\right)$. Hence, any $\beta > 2/3$ gives the same result, yet $\beta = 2/3$ is not sufficient.

Finally, we define $\tilde{d}_{n,m}$ as in Lemma 4.6 with some fixed $\epsilon > 0$. Then it follows from Lemma 4.4 that there is some constant $\gamma' > 0$ such that

$$\tilde{d}_{2n,0} \leq \gamma' 4^n e^{3a_1 n^{1/3}} n,$$

for all n . Hence

$$r_n = n! d_{2n,0} \leq 2\gamma' n! 4^n e^{3a_1 n^{1/3}} n,$$

completing the proof of the upper bound. We have now proven upper and lower bounds for the number r_n of relaxed trees, which differ only in the constant term. Therefore,

$$r_n = \Theta\left(n! 4^n e^{3a_1 n^{1/3}} n\right).$$

5. Proof of stretched exponential for compacted trees

We will now deal with compacted binary trees, whose recurrence as in Proposition 2.11 has negative terms. We start by transforming the terms $c_{n,m}$ counting compacted trees to a sequence $e_{n,m}$ using the equation

$$e_{n,m} = \frac{1}{((n+m)/2)!} c_{(n+m)/2, (n-m)/2},$$

for $n - m$ even. Then, the terms $e_{n,m}$ are determined by the recurrence

$$\begin{cases} e_{n,m} = \frac{n-m+2}{n+m} e_{n-1,m-1} + e_{n-1,m+1} - \frac{2(n-m-2)}{(n+m)(n+m-2)} e_{n-3,m-1}, & \text{for } n \geq m > 0, \\ e_{n,m} = e_{n-1,m+1}, & \text{for } n > 0, m = 0, \\ e_{n,m} = 1, & \text{for } n = m = 0, \\ e_{n,m} = 0, & \text{for } m > n, \end{cases}$$

and the number of compacted trees of size n is equal to $n! e_{2n,0}$.

The method that we applied to (2) in the relaxed case does not directly apply to this recurrence, as there is a negative term on the right-hand side. We solve this problem using the following lemma:

Lemma 5.1. For $n \geq 3$ and $n > m \geq 0$, the term $e_{n,m}$ for compacted binary trees is bounded below by

$$L_e = \frac{n - m + 2}{n + m} e_{n-1,m-1} + \frac{n - m - 2}{n - m} e_{n-1,m+1} + \frac{n - m - 4}{n - m - 2} \left(\frac{2}{n - m} e_{n-2,m+2} + \frac{2}{n + m} e_{n-3,m+1} \right)$$

and bounded above by

$$U_e = \frac{n - m + 2}{n + m} e_{n-1,m-1} + \frac{n - m - 2}{n - m} e_{n-1,m+1} + \frac{2}{n - m} e_{n-2,m+2} + \frac{2}{n + m} e_{n-3,m+1} + \frac{4}{(n + m)(n + m - 2)} e_{n-3,m-1}.$$

That is, $L_e \leq e_{n,m} \leq U_e$. Furthermore, $U_e \leq U_d \leq d_{n,m}$ where U_d is defined by the same expression as U_e but with each e replaced by d .

Proof. We start with the upper bound of $e_{n,m}$. In order to prove that, we will compute successively stronger upper bounds. We start with the trivial upper bound

$$e_{n,m} \leq \frac{n - m + 2}{n + m} e_{n-1,m-1} + e_{n-1,m+1}. \tag{16}$$

Applying this bound to $e_{n-1,m+1}$ then $e_{n-2,m}$ we find that

$$e_{n-1,m+1} \leq \frac{n - m}{n + m} \left(\frac{n - m}{n + m - 2} e_{n-3,m-1} + e_{n-3,m+1} \right) + e_{n-2,m+2}. \tag{17}$$

Adding $2/(n - m)$ times this inequality to the defining equation of $e_{n,m}$ yields

$$e_{n,m} \leq \frac{n - m + 2}{n + m} e_{n-1,m-1} + \frac{n - m - 2}{n - m} e_{n-1,m+1} + \frac{2}{n - m} e_{n-2,m+2} + \frac{2}{n + m} e_{n-3,m+1} + \frac{4}{(n + m)(n + m - 2)} e_{n-3,m-1}.$$

Now we will prove that $U_d \leq d_{n,m}$. Note that the first two inequalities (16) and (17) in this proof become equalities when each e is replaced by d . Adding $2/(n - m)$ times the latter (now) equality (17) to the defining equation (2) of $d_{n,m}$ yields

$$U_d = d_{n,m} - \frac{2(n - m - 2)}{(n + m)(n + m - 2)} d_{n-3,m-1} \leq d_{n,m}.$$

We then see that $e_{n,m} \leq U_e \leq U_d \leq d_{n,m}$ through induction on n .

For the lower bound on $e_{n,m}$, we start with the inequality

$$e_{n,m} \geq \frac{n-m+2}{n+m} e_{n-1,m-1}. \tag{18}$$

This is clear for $m = 0$, and for $m \geq n$ it is an equality. We can then deduce this inequality (18) for all n, m using induction: Assume that the statement is true for all $n < N$ and all $m \in [0, n]$. Then, for $m \in [1, n-2]$ and $n = N$, we have

$$\frac{1}{n-m} e_{n-1,m+1} \geq \frac{1}{n+m} e_{n-2,m} > \frac{n-m-2}{(n+m)(n+m-2)} e_{n-3,m-1}.$$

Hence,

$$\begin{aligned} e_{n,m} &= \frac{n-m+2}{n+m} e_{n-1,m-1} + e_{n-1,m+1} - \frac{2(n-m-2)}{(n+m)(n+m-2)} e_{n-3,m-1} \\ &\geq \frac{n-m+2}{n+m} e_{n-1,m-1} + \left(1 - \frac{2}{n-m}\right) e_{n-1,m+1}. \\ &\geq \frac{n-m+2}{n+m} e_{n-1,m-1}. \end{aligned}$$

This completes the induction. Moreover, it shows that

$$e_{n,m} \geq \frac{n-m+2}{n+m} e_{n-1,m-1} + \left(1 - \frac{2}{n-m}\right) e_{n-1,m+1}, \tag{19}$$

for $m \in [1, n-2]$. It is easy to see that this stronger inequality (19) also holds for $m = 0$ and $m \geq n$. Applying (19) to $e_{n-1,m+1}$ then $e_{n-2,m}$ yields

$$\begin{aligned} \frac{1}{n-m} e_{n-1,m+1} &\geq \frac{1}{n+m} e_{n-2,m} + \frac{n-m-4}{(n-m)(n-m-2)} e_{n-2,m+2} \\ &\geq \frac{1}{n+m} \left(\frac{n-m}{n+m-2} e_{n-3,m-1} + \frac{n-m-4}{n-m-2} e_{n-3,m+1} \right) \\ &\quad + \frac{n-m-4}{(n-m)(n-m-2)} e_{n-2,m+2}. \end{aligned}$$

Finally, combining this with the inequality

$$e_{n,m} \geq \frac{n-m+2}{n+m} e_{n-1,m-1} + e_{n-1,m+1} - \frac{2(n-m)}{(n+m)(n+m-2)} e_{n-3,m-1}$$

yields the desired result. \square

The advantage of the bounds in the lemma above is that all terms are positive, so we can derive the asymptotics using the same techniques as for relaxed binary trees. Note that the behavior stays the same in the process of deriving the Newton polygons and leads to the same pictures as shown in Figs. 6 and 7.

5.1. Lower bound

The following result is analogous to Lemma 4.2.

Lemma 5.2. For all $n, m \geq 0$ let

$$\tilde{Y}_{n,m} := \left(1 - \frac{2m^2}{3n} + \frac{m}{4n}\right) \text{Ai} \left(a_1 + \frac{2^{1/3}(m+1)}{n^{1/3}}\right) \quad \text{and}$$

$$\tilde{s}_n := 2 + \frac{2^{2/3}a_1}{n^{2/3}} + \frac{13}{6n} - \frac{1}{n^{7/6}}.$$

Then, for any $\varepsilon > 0$, there exists a constant \tilde{n}_0 such that

$$\begin{aligned} \tilde{Y}_{n,m} \tilde{s}_n \tilde{s}_{n-1} \tilde{s}_{n-2} &\leq \frac{n-m+2}{n+m} \tilde{Y}_{n-1,m-1} \tilde{s}_{n-1} \tilde{s}_{n-2} + \frac{n-m-2}{n-m} \tilde{Y}_{n-1,m+1} \tilde{s}_{n-1} \tilde{s}_{n-2} \\ &+ \frac{n-m-4}{n-m-2} \left(\frac{2}{n-m} \tilde{Y}_{n-2,m+2} \tilde{s}_{n-2} + \frac{2}{n+m} \tilde{Y}_{n-3,m+1} \right), \end{aligned}$$

for all $n \geq \tilde{n}_0$ and all $0 \leq m < n^{2/3-\varepsilon}$.

Proof. The proof is analogous to the case of relaxed trees. In this case, the expansions for $n \rightarrow \infty$ start as follows, where the elements on the convex hull are written in color:

$$\begin{aligned} P_{n,m} = \text{Ai}(\alpha) &\left(-\frac{4\sigma_4}{n^{7/6}} - \frac{2^{11/3}a_1m}{3n^{5/3}} - \frac{164m^2}{9n^2} - \frac{2^{14/3}a_1m^3}{3n^{8/3}} - \frac{136m^4}{9n^3} - \frac{248m^5}{135n^4} + \dots \right) + \\ \text{Ai}'(\alpha) &\left(\frac{2^{7/3}}{n^{3/2}} - \frac{32a_1m}{9n^2} - 7\frac{2^{13/3}m^2}{9n^{7/3}} - \frac{2^{19/3}m^3}{9n^{7/3}} - \frac{5m^4 2^{10/3}}{9n^{10/3}} - \frac{89m^5 2^{10/3}}{135n^{13/3}} + \dots \right). \end{aligned}$$

In this expansion we choose $\sigma_4 = -1$, which leads to a positive term $\text{Ai}(\alpha)n^{-7/6}$, and we also choose $\tau_1 = 1/4$ (instead of $1/2$ in the relaxed trees case), which kills the leading coefficient of $\text{Ai}'(\alpha)2^{4/3}(4\tau_1 - 1)n^{-4/3}$ for small $m = o(n^{1/3})$. Then, the behavior and thus the pictures are identical to the case of relaxed trees shown in Figs. 6 and 7. Hence, the proof follows exactly the same lines as that Lemma 4.2. \square

As in the relaxed case, we define a sequence $Y_{n,m} := \max\{\tilde{Y}_{n,m}, 0\}$, i.e.,

$$Y_{n,m} := \begin{cases} \tilde{Y}_{n,m}, & \text{if } m < \frac{\sqrt{384n+9}+3}{16}, \\ 0, & \text{if } m \geq \frac{\sqrt{384n+9}+3}{16}. \end{cases}$$

Then defining $\tilde{h}_n = \tilde{s}_n \tilde{h}_{n-1}$, we get by induction

$$e_{n,m} \geq \kappa_0 \tilde{h}_n Y_{n,m},$$

for some $\kappa_0 > 0$. In particular, it follows that the number $c_n = n!e_{2n,0}$ of compacted trees of size n is bounded below by

$$c_n \geq \gamma n!4^n e^{3a_1 n^{1/3}} n^{3/4}, \tag{20}$$

for some constant $\gamma > 0$. In the next section we will show an upper bound with the same asymptotic form, but with a different constant γ .

5.2. Upper bound

The following result is analogous to Lemma 4.4.

Lemma 5.3. *Choose $\eta > 2/9$ fixed and for all $n, m \geq 0$ let*

$$\hat{Y}_{n,m} := \left(1 - \frac{2m^2}{3n} + \frac{m}{4n} + \eta \frac{m^4}{n^2}\right) \text{Ai}\left(a_1 + \frac{2^{1/3}(m+1)}{n^{1/3}}\right) \quad \text{and}$$

$$\hat{s}_n := 2 + \frac{2^{2/3}a_1}{n^{2/3}} + \frac{13}{6n} + \frac{1}{n^{7/6}}.$$

Then, for any $\varepsilon > 0$, there exists a constant \hat{n}_0 such that

$$\begin{aligned} \hat{Y}_{n,m} \hat{s}_n \hat{s}_{n-1} \hat{s}_{n-2} &\geq \frac{n-m+2}{n+m} \hat{Y}_{n-1,m-1} \hat{s}_{n-1} \hat{s}_{n-2} + \frac{n-m-2}{n-m} \hat{Y}_{n-1,m+1} \hat{s}_{n-1} \hat{s}_{n-2} \\ &\quad + \frac{2}{n-m} \hat{Y}_{n-2,m+2} \hat{s}_{n-2} \\ &\quad + \frac{2}{n+m} \hat{Y}_{n-3,m+1} + \frac{4}{(n+m)(n+m-2)} \hat{Y}_{n-3,m-1}, \end{aligned}$$

for all $n \geq \hat{n}_0$ and all $0 \leq m < n^{1-\varepsilon}$.

Proof. The proof is again analogous to the case of relaxed trees. In this case, the expansions for $n \rightarrow \infty$ start as follows, where the elements on the convex hull are written in color:

$$\begin{aligned} Q_{n,m} = \text{Ai}(\alpha) &\left(\frac{4\sigma_4}{n^{7/6}} + \frac{2^{11/3}a_1 m}{3n^{5/3}} + \frac{4m^2(41-108\eta)}{9n^2} + \frac{2^{14/3}a_1 m^3(1-6\eta)}{3n^{8/3}} \right. \\ &\quad \left. + \frac{8m^4(17-132\eta)}{9n^3} - \frac{2^{11/3}a_1 m^5 \eta}{n^{11/3}} - \frac{68m^6 \eta}{3n^4} - \frac{124m^7 \eta}{45n^5} + \dots \right) + \\ \text{Ai}'(\alpha) &\left(\frac{2^{7/3}}{n^{3/2}} + \frac{32a_1 m}{9n^2} + \frac{2^{13/3}m^2(7-27\eta)}{9n^{7/3}} + \frac{2^{16/3}m^3(2-9\eta)}{9n^{7/3}} \right. \\ &\quad \left. + \frac{2^{4/3}m^4(20-279\eta)}{9n^{10/3}} - \frac{2^{16/3}m^5 \eta}{3n^{10/3}} - \frac{5m^6 2^{7/3} \eta}{3n^{13/3}} - \frac{89m^7 2^{7/3} \eta}{45n^{16/3}} + \dots \right). \end{aligned}$$

In this expansion we choose $\sigma_4 = 1$, which leads to a positive term $\text{Ai}(\alpha)n^{-7/6}$, and again $\tau_1 = 1/4$. Then, the behavior and therefore the pictures are identical to the case of relaxed trees shown in the Figs. 8 and 9; see the proof of Lemma 4.4 for more details. \square

As in the relaxed tree case, the inequality of Lemma 5.3 is only proven for $m < n^{1-\varepsilon}$, so we need to do more work to handle the $m \geq n^{1-\varepsilon}$ case and deduce the desired upper bound. In order to use the lemma, we define a new sequence $\hat{e}_{n,m}$ by the recurrence relation

$$\left\{ \begin{array}{l} \hat{e}_{n,m} = \frac{n-m+2}{n+m}\hat{e}_{n-1,m-1} + \frac{n-m-2}{n-m}\hat{e}_{n-1,m+1} \\ \quad + \frac{2}{n-m}\hat{e}_{n-2,m+2} + \frac{2}{n+m}\hat{e}_{n-3,m+1} \\ \quad + \frac{4}{(n+m)(n+m-2)}\hat{e}_{n-3,m-1}, \quad \text{for } n \geq 3, n > m \geq 0, \\ \hat{e}_{n,m} = e_{n,m}, \quad \text{otherwise.} \end{array} \right.$$

Then it follows from Lemma 5.1 that $e_{n,m} \leq \hat{e}_{n,m} \leq d_{n,m}$ for all n, m , as $\hat{e}_{n,m}$ share the same recurrence as U_d in Lemma 5.1. Now consider some large $N > 0$, to be determined later, and define a second sequence $\tilde{e}_{n,m}$ by the same rules as $\hat{e}_{n,m}$ except that $\tilde{e}_{n,m} = 0$ whenever $m > n^{3/4}$ and $n > N$. Then, using Lemma 5.3 and defining $\hat{h}_n = \hat{s}_n \hat{h}_{n-1}$, we can show by induction that there is some constant κ_1 such that

$$\tilde{e}_{n,m} \leq \kappa_1 \hat{h}_n \hat{Y}_{n,m}.$$

It follows that there is some constant $\gamma' > 0$ such that

$$\tilde{e}_{2n,0} \leq \gamma' 4^n e^{3a_1 n^{1/3}} n^{3/4}.$$

Hence, it suffices to prove that there is some choice of N and some constant $\varepsilon > 0$ such that $\hat{e}_{2n,0} \leq (1 + \varepsilon)\tilde{e}_{2n,0}$ for all n . Therefore, we first define a class \mathcal{C} of weighted paths with the step set $\{(1, 1), (1, -1), (2, -2), (3, -1), (3, 1)\}$ and weights corresponding to the recurrence defining $\hat{e}_{n,m}$. Then $\hat{e}_{n,m}$ is the weighted number of paths $p \in \mathcal{C}$ from $(0, 0)$ to (n, m) . We start with the following lemma, which is analogous to Lemma 4.5.

Lemma 5.4. *Let $q_{\ell,m,2n}$ denote the weighted number of paths $p \in \mathcal{C}$ from (ℓ, m) to $(2n, 0)$. Then the numbers $q_{\ell,m,2n}$ satisfy the inequality*

$$\frac{q_{\ell,j,2n}}{j+1} \geq \frac{q_{\ell,k,2n}}{k+1},$$

for integers $0 \leq j < k \leq \ell \leq 2n$ satisfying $2|k - j$ and $n \geq 10$.

Proof. The proof is along the same lines as the proof of Lemma 4.5. As in that case, it suffices to prove that

$$\frac{q_{\ell,m-1,2n}}{m} - \frac{q_{\ell,m+1,2n}}{m+2} \geq 0, \tag{21}$$

for all $m \geq 1$. We proceed by reverse induction on ℓ , with base case $\ell = 2n$. For the inductive step, note that q satisfies the following recurrence for $\ell < 2n$:

$$\begin{cases} q_{\ell,m,2n} = 0, & \text{for } m < 0, \\ q_{\ell,m,2n} = \frac{\ell-m}{\ell-m+2}q_{\ell+1,m-1,2n} + \frac{\ell-m+2}{\ell+m+2}q_{\ell+1,m+1,2n} \\ \quad + \frac{2}{\ell-m+4}q_{\ell+2,m-2,2n} + \frac{2}{\ell+m+2}q_{\ell+3,m-1,2n} \\ \quad + \frac{4}{(\ell+m+4)(\ell+m+2)}q_{\ell+3,m+1,2n}, & \text{for } m \geq 0. \end{cases}$$

Now in order to prove (21), we expand the left-hand side $L(\ell, m, n)$ using the recurrence relation above. For $m \geq 2$, we use the inductive assumption, which says that (21) holds for all larger values of ℓ and all m , to show that

$$L(\ell, m, n) \geq R_1(\ell, m)q_{\ell+1,m,2n} + R_2(\ell, m)q_{\ell+2,m-1,2n} + R_3(\ell, m)q_{\ell+3,m-2,2n},$$

for some explicit rational functions R_1, R_2 and R_3 . Due to the nature of the functions R_1, R_2 and R_3 , we can prove that the right-hand side above is positive using the inequalities

$$q_{\ell+1,m,2n} \geq \frac{\ell - m + 1}{\ell - m + 3}q_{\ell+2,m-1,2n} \quad \text{and} \quad q_{\ell+2,m-1,2n} \geq \frac{\ell - m + 3}{\ell - m + 5}q_{\ell+3,m-2,2n},$$

which follow directly from the recurrence relation. The case $m = 1$ is similar, though we instead find

$$L(\ell, 1, n) \geq \tilde{R}_1(\ell)q_{\ell+1,1,2n} + \tilde{R}_2(\ell)q_{\ell+2,0,2n} + \tilde{R}_3(\ell)q_{\ell+3,1,2n},$$

and we prove that the right hand side is positive using the inequalities

$$q_{\ell+1,1,2n} \geq \frac{\ell}{\ell + 2}q_{\ell+2,0,2n} \quad \text{and} \quad q_{\ell+2,0,2n} \geq q_{\ell+3,1,2n},$$

which follow directly from the recurrence relation. We refer the accompanying worksheet [27] for more details. \square

Now, among the $\hat{e}_{2n,0}$ weighted paths starting at $(0,0)$ and ending at $(2n,0)$, the proportion of those passing through some point $(2x, 2y)$ is

$$\begin{aligned} \frac{\hat{e}_{2x,2y}q_{2x,2y,2n}}{\hat{e}_{2n,0}} &\leq \frac{\hat{e}_{2x,2y}q_{2x,2y,2n}}{\hat{e}_{2x,0}q_{2x,0,2n}} \leq (2y + 1)\frac{\hat{e}_{2x,2y}}{\hat{e}_{2x,0}} \leq (2y + 1)\frac{d_{2x,2y}}{e_{2x,0}} \\ &\leq \frac{2y + 1}{\gamma 4^x e^{3a_1 x^{1/3}} x^{3/4}} \binom{2x}{x + y}. \end{aligned}$$

We used the fact that $\hat{e}_{2x,2y} \leq d_{2x,2y}$ which we proved inductively using Lemma 5.1, and we also used the lower bound (20) for $e_{2x,0}$. We can finish in exactly the same way as in Lemma 4.6 for relaxed trees, thereby showing that there is some choice for N such that $\hat{e}_{2n,0} \leq 2\tilde{e}_{2n,0}$ for all n .

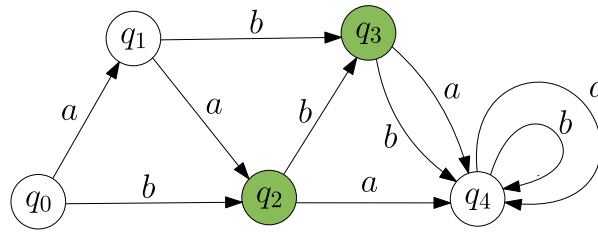


Fig. 11. The unique minimal DFA with 5 states for the language $\{aa, aab, ab, b, bb\}$. Here, q_0 is the initial state, q_2 and q_3 are the final states, and q_4 is the unique dead state.

Recall that $e_{2n,0} \leq \hat{e}_{2n,0}$ and there is some constant κ_1 such that $\tilde{e}_{n,m} \leq \kappa_1 \hat{h}_n \hat{Y}_{n,m}$. This implies that

$$c_n = n!c_{2n,0} \leq 2\kappa_1 n! \hat{h}_{2n} \hat{Y}_{2n,0}.$$

The right-hand side behaves asymptotically like $\Theta(n!4^n e^{3a_1 n^{1/3}} n^{3/4})$, hence there is some constant γ'' such that

$$c_n \leq \gamma'' n!4^n e^{3a_1 n^{1/3}} n^{3/4},$$

for all n . This completes the upper bound. Indeed, since we have now proven both the upper and lower bounds, which differ only in the constant term, they imply that

$$c_n = \Theta\left(n!4^n e^{3a_1 n^{1/3}} n^{3/4}\right).$$

6. Minimal finite automata

In this section we use the results on compacted and relaxed trees to give bounds on the enumeration of a certain class of deterministic finite automata considered in [11,12,23]. We start with some basic definitions of automata.

A *deterministic finite automaton* (DFA) A is a 5-tuple $(\Sigma, Q, \delta, q_0, F)$, where Σ is a finite set of letters called the *alphabet*, Q is a finite set of states, $\delta : Q \times \Sigma \rightarrow Q$ is the *transition function*, q_0 is the *initial state*, and $F \subseteq Q$ is the set of *final states* (sometimes called *accept states*). A DFA can be represented by a directed graph with one vertex v_s for each state $s \in Q$, with the vertices corresponding to final states being highlighted, and for every transition $\delta(s, w) = \hat{s}$, there is an edge from s to \hat{s} labeled w (see Fig. 11).

A word $w = w_1 w_2 \cdots w_n \in \Sigma^*$ is *accepted* by A if the sequence of states $(s_0, s_1, \dots, s_n) \in Q^{n+1}$ defined by $s_0 = q_0$ and $s_{i+1} = \delta(s_i, w_i)$ for $i = 0, \dots, n - 1$ ends with $s_n \in F$ a final state. The set of words accepted by A is called the *language* $\mathcal{L}(A)$ recognized by A . It is well-known that DFAs recognize exactly the set of regular languages. Note that every DFA recognizes a unique language, but a language can be recognized by several different DFAs. A DFA is called *minimal* if no DFA with fewer states recognizes the same language. The Myhill-Nerode Theorem states that every regular language is recognized by a unique minimal DFA (up to isomorphism) [19, Theorem 3.10]. For more details on automata see [19].

Since every regular language defines a unique minimal automaton, one can define the complexity of the language to be the number of states in the corresponding automaton. More precisely, this is an interpretation for the space complexity of the language.

The asymptotic proportion of minimal DFAs in the class of (not necessarily acyclic) automata was solved by Bassino, Nicaud, and Sportiello in [2], building on enumeration results by Korshunov [20,21] and Bassino and Nicaud [3]. This result also exploits an underlying tree structure of the automata, but this tree structure comes from a different traversal than what we use. In that case, no stretched exponential appears in the asymptotic enumeration, and the minimal automata account for a constant fraction of all automata.

The analogous problem in the restricted case of automata that recognize a finite language is widely open (see for example [11]). This corresponds to counting finite languages by their space complexity. To show the relation between these automata and compacted and relaxed trees, we need the following lemma from [23, Lemma 2.3] or [19, Section 3.4]. For the convenience of the reader, we include a proof of one direction here.

Lemma 6.1. *A DFA A is the minimal automaton for some finite language if and only if it has the following properties:*

- *There is a unique sink s . That is, a state which is not a final state and with all transitions from s end at s that is, $\delta(s, w) = s$.*
- *A is acyclic: the corresponding directed graph has no cycles except for the loops at the dead state.*
- *A is initially connected: for any state p there exists a word $w \in \Sigma^*$ such that A reaches the state p upon reading w .*
- *A is reduced: for any two different states q, q' , the two automata with initial state q and q' recognize different languages.*

Proof. We will show one direction of this proof: that a minimal automaton has the four properties. For a proof of the reverse direction see e.g. [23, Lemma 2.3] or [19, Section 3.4].

If A is minimal but not reduced then there are two states q and q' from which the same language is recognized. These two states can be merged into a single state without changing the language, contradicting the minimality of A . This implies that there is at most one state q from which the empty language is recognized. Moreover, such a state must exist for the language to be finite. This state q must therefore be the unique sink.

The fact the A is acyclic follows immediately from the fact that A recognizes a finite language. Finally, if we remove from A all states p that cannot be reached, the language accepted by the automaton will not be changed, so by the minimality of A , there must be no such states and A must be initially connected. \square

We note here one consequence of this lemma: since the automaton is acyclic, there must be some state q other than the sink s such that all transitions from q end at s .

Then since the automaton is reduced, there must be only one such state q , and it must be an accept state.

Now using our asymptotic results on compacted and relaxed trees, we give the following new bounds on the asymptotic number of such automata, determining their asymptotics up to a polynomial multiplicative term.

Theorem 6.2. *Let $m_{2,n}$ be the number of minimal DFAs over a binary alphabet with n transient states (and a unique sink) that recognize a finite language. Then,*

$$2^{n-1}c_n \leq m_{2,n} \leq 2^{n-1}r_n.$$

As a consequence, there exist positive constants κ_1 and κ_2 such that

$$\kappa_1 n^{3/4} \leq \frac{m_{2,n}}{n!8^n e^{3a_1 n^{1/3}}} \leq \kappa_2 n.$$

Proof. By the lemma above, a compacted tree \mathcal{C} can be transformed into an automaton A that recognizes a finite language over the alphabet $\{a, b\}$ as follows: The states of the automaton A correspond to the internal nodes and the leaf of \mathcal{C} . The initial state corresponds to the root, and at each state, the transition after reading a (resp. b) is given by the left (resp. right) child or pointer in \mathcal{C} . The leaf is designated as the unique sink, and we can choose any subset of internal nodes as final states, with the condition that the unique node with two pointers to the sink is always a final state.

To prove the minimality of such automata, we just need to check the four conditions of Lemma 6.1. The fact that A is acyclic and has a unique sink follow immediately from the fact the \mathcal{C} is a DAG. Then A is initially connected because \mathcal{C} has a unique source. Now we will show that A is reduced. For any state q in A , let $\mathcal{L}(q)$ denote the language recognized by the automaton with initial state q . Now suppose that A is not reduced and let q and q' be different states of A satisfying $\mathcal{L}(q) = \mathcal{L}(q')$. We also assume that amongst all such pairs (q, q') , the length of the longest word in $\mathcal{L}(q)$ is minimized. Since the unique node with both pointers to the sink is a final state, the language $\mathcal{L}(q)$ can only be empty if q and q' are both the final state, which is impossible. Since $\mathcal{L}(q) = \mathcal{L}(q')$ we must have $\mathcal{L}(\delta(q, a)) = \mathcal{L}(\delta(q', a))$ and $\mathcal{L}(\delta(q, b)) = \mathcal{L}(\delta(q', b))$. Then, the minimality condition on the language $\mathcal{L}(q)$ implies that $\delta(q, a) = \delta(q', a)$ and $\delta(q, b) = \delta(q', b)$. But this means that the node u and v in \mathcal{C} corresponding to q and q' have the same left child and the same right child, contradicting the fact that \mathcal{C} is compacted. This completes the proof that A is reduced.

Hence, each of the 2^{n-1} subsets of the remaining states (not the sink and not the node with two pointers to the sink) gives a valid minimal automaton of size n .

Applying the same construction to relaxed trees gives an upper bound, as every minimal automaton, after forgetting which states are final, corresponds by construction to a relaxed tree. Note that this observation has already been made in [23, Equation (1)], yet the asymptotics was not known. \square

Using the methods of the present work, the authors showed in a companion paper [13] that

$$m_{2,n} = \Theta \left(n! 8^n e^{3a_1 n^{1/3}} n^{7/8} \right).$$

To our knowledge, our results give the best known bounds on the asymptotic number of minimal DFAs on a binary alphabet recognizing a finite language. Note that they disprove the conjecture $m_{2,n} \sim K 2^{n-1} r_n$ for some $K > 0$ of Liskovets based on numerical data; see [23, Equation (16)]. Previously, Domaratzki derived in [10] the lower bound

$$m_{2,n} \geq \frac{(2n-1)!}{(n-1)!} c_1^{n-1},$$

with $c_1 \approx 1.0669467$, which implies the asymptotic bound $m_{2,n} \geq \frac{n!(4c_1)^n}{2c_1\sqrt{\pi n}}$ (note that $m_{2,n} = f'_2(n+1)$ in his results). Furthermore, Domaratzki showed in [9] the upper bound

$$m_{2,n} \leq 2^{n-1} G_{2n+2},$$

where G_{2n} are the Genocchi numbers defined by $\frac{2t}{e^t+1} = t + \sum_{n \geq 1} (-1)^n G_{2n} \frac{t^{2n}}{(2n)!}$. This gives the asymptotic bound $m_{2,n} \leq 4(2n)! \left(\frac{2}{\pi^2}\right)^{n+1} n^2$. This bound, however, is much larger than the superexponential growth given by $n!$ in our upper bound. While not explicitly formulated in the literature, it is possible to bound the acyclic DFAs by general DFAs using the results by Korshunov [20,21] (see also [3, Theorem 18]). Thereby, we get the upper bound

$$m_{2,n} = \mathcal{O} \left(n!(2e^2\nu)^n \right),$$

where $\nu = \alpha^\alpha(1+\alpha)^{1-\alpha} \approx 0.8359$ with α being the solution of $1+x = xe^{2/(1+x)}$, and therefore $2e^2\nu \approx 12.3531$, which is significantly larger than the exponential growth in our upper bound.

Acknowledgments

We would like to thank Tony Guttmann for sending us calculations on the asymptotic form of pushed Dyck paths. More generally, we thank him, Cyril Banderier and Andrea Sportiello for interesting discussions on the presence of a stretched exponential. We want to thank the anonymous referees for their detailed comments which improved the presentation of this work.

References

[1] M. Abramowitz, I.A. Stegun, *Handbook of Mathematical Functions with Formulas, Graphs, and Mathematical Tables*, National Bureau of Standards Applied Mathematics Series, vol. 55, 1964, For sale by the Superintendent of Documents, U.S. Government Printing Office, Washington, D.C.

- [2] F. Bassino, J. David, A. Sportiello, Asymptotic enumeration of minimal automata, in: 29th International Symposium on Theoretical Aspects of Computer Science, in: LIPIcs. Leibniz Int. Proc. Inform., vol. 14, Schloss Dagstuhl. Leibniz-Zent. Inform., Wadern, 2012, pp. 88–99.
- [3] F. Bassino, C. Nicaud, Enumeration and random generation of accessible automata, *Theor. Comput. Sci.* 381 (1–3) (2007) 86–104.
- [4] N.R. Beaton, A.J. Guttmann, I. Jensen, G.F. Lawler, Compressed self-avoiding walks, bridges and polygons, *J. Phys. A* 48 (45) (Oct. 2015) 454001.
- [5] M. Bousquet-Mélou, M. Lohrey, S. Maneth, E. Noeth, XML compression via directed acyclic graphs, *Theory Comput. Syst.* 57 (4) (2015) 1322–1371.
- [6] D. Callan, A determinant of Stirling cycle numbers counts unlabeled acyclic single-source automata, *Discrete Math. Theor. Comput. Sci.* 10 (2) (2008) 77–86.
- [7] A.R. Conway, A.J. Guttmann, On 1324-avoiding permutations, *Adv. Appl. Math.* 64 (2015) 50–69.
- [8] A.R. Conway, A.J. Guttmann, P. Zinn-Justin, 1324-avoiding permutations revisited, *Adv. Appl. Math.* 96 (2018) 312–333.
- [9] M. Domaratzki, Combinatorial interpretations of a generalization of the Genocchi numbers, *J. Integer Seq.* 7 (3) (2004) 11, Article 04.3.6.
- [10] M. Domaratzki, Improved bounds on the number of automata accepting finite languages, in: Computing and Combinatorics Conference, COCOON’02, *Int. J. Found. Comput. Sci.* 15 (1) (2004) 143–161.
- [11] M. Domaratzki, Enumeration of formal languages, *Bull. Eur. Assoc. Theor. Comput. Sci.* 89 (2006) 117–133.
- [12] M. Domaratzki, D. Kisman, J. Shallit, On the number of distinct languages accepted by finite automata with n states, *J. Autom. Lang. Comb.* 7 (4) (2002) 469–486.
- [13] A. Elvey Price, W. Fang, M. Wallner, Asymptotics of minimal deterministic finite automata recognizing a finite binary language, in: AofA 2020, in: LIPIcs, vol. 159, Schloss Dagstuhl–Leibniz-Zentrum für Informatik, 2020, pp. 11:1–11:13.
- [14] A. Elvey Price, A.J. Guttmann, Numerical studies of Thompson’s group F and related groups, *Int. J. Algebra Comput.* 29 (2) (2019) 179–243.
- [15] P. Flajolet, R. Sedgewick, *Analytic Combinatorics*, Cambridge University Press, Cambridge, 2009.
- [16] P. Flajolet, P. Sipala, J.-M. Steyaert, Analytic variations on the common subexpression problem, in: Automata, Languages and Programming, Coventry, 1990, in: *Lecture Notes in Comput. Sci.*, vol. 443, Springer, New York, 1990, pp. 220–234.
- [17] A. Genitrini, B. Gittenberger, M. Kauers, M. Wallner, Asymptotic enumeration of compacted binary trees of bounded right height, *J. Comb. Theory, Ser. A* 172 (2020) 105177, arXiv:1703.10031.
- [18] A.J. Guttmann, Analysis of series expansions for non-algebraic singularities, *J. Phys. A* 48 (4) (2015) 045209.
- [19] J.E. Hopcroft, J.D. Ullman, *Introduction to Automata Theory, Languages, and Computation*, Addison-Wesley Series in Computer Science, Addison-Wesley Publishing Co., Reading, Mass., 1979.
- [20] A.D. Korshunov, Enumeration of finite automata, *Probl. Kibern.* 34 (1978) 5–82 (In Russian).
- [21] A.D. Korshunov, On the number of nonisomorphic strongly connected finite automata, *Elektron. Inf.verarb. Kybern.* 22 (9) (1986) 459–462.
- [22] T. Kousha, Asymptotic behavior and the moderate deviation principle for the maximum of a Dyck path, *Stat. Probab. Lett.* 82 (2) (2012) 340–347.
- [23] V.A. Liskovets, Exact enumeration of acyclic deterministic automata, *Discrete Appl. Math.* 154 (3) (2006) 537–551.
- [24] C. Pittet, L. Saloff-Coste, On random walks on wreath products, *Ann. Probab.* 30 (2) (2002) 948–977.
- [25] D. Revelle, Heat kernel asymptotics on the lamplighter group, *Electron. Commun. Probab.* 8 (2003) 142–154.
- [26] M. Wallner, A bijection of plane increasing trees with relaxed binary trees of right height at most one, *Theor. Comput. Sci.* 755 (2019) 1–12.
- [27] M. Wallner, <http://dmg.tuwien.ac.at/mwallner>, 2020.
- [28] E.M. Wright, The coefficients of a certain power series, *J. Lond. Math. Soc.* 7 (4) (1932) 256–262.
- [29] E.M. Wright, On the coefficients of power series having exponential singularities, *J. Lond. Math. Soc.* 8 (1) (1933) 71–79.
- [30] E.M. Wright, On the coefficients of power series having exponential singularities. II, *J. Lond. Math. Soc.* 24 (1949) 304–309.

Asymptotics of Minimal Deterministic Finite Automata Recognizing a Finite Binary Language

Andrew Elvey Price 

Université de Bordeaux, Laboratoire Bordelais de Recherche en Informatique, UMR 5800,
351 Cours de la Libération, 33405 Talence Cedex, France
Université de Tours, Institut Denis Poisson, UMR 7013, Parc de Grandmont, 37200 Tours, France
<https://www.idpoisson.fr/elveyprice/en/>
andrew.elvey@univ-tours.fr

Wenjie Fang 

Laboratoire d'Informatique Gaspard-Monge, UMR 8049, Université Gustave Eiffel, CNRS,
ESIEE Paris, 77454 Marne-la-Vallée, France
<http://igm.univ-mlv.fr/~wfang/>
wenjie.fang@u-pem.fr

Michael Wallner 

Université de Bordeaux, Laboratoire Bordelais de Recherche en Informatique, UMR 5800,
351 Cours de la Libération, 33405 Talence Cedex, France
TU Wien, Institute for Discrete Mathematics and Geometry,
Wiedner Hauptstrasse 8–10, 1040 Wien, Austria
<https://dmg.tuwien.ac.at/mwallner/>
michael.wallner@tuwien.ac.at

Abstract

We show that the number of minimal deterministic finite automata with $n + 1$ states recognizing a finite binary language grows asymptotically for $n \rightarrow \infty$ like

$$\Theta\left(n! 8^n e^{3a_1 n^{1/3}} n^{7/8}\right),$$

where $a_1 \approx -2.338$ is the largest root of the Airy function. For this purpose, we use a new asymptotic enumeration method proposed by the same authors in a recent preprint (2019). We first derive a new two-parameter recurrence relation for the number of such automata up to a given size. Using this result, we prove by induction tight bounds that are sufficiently accurate for large n to determine the asymptotic form using adapted Netwon polygons.

2012 ACM Subject Classification Theory of computation \rightarrow Regular languages; Mathematics of computing \rightarrow Enumeration; Mathematics of computing \rightarrow Generating functions

Keywords and phrases Airy function, asymptotics, directed acyclic graphs, Dyck paths, bijection, stretched exponential, compacted trees, minimal automata, finite languages

Digital Object Identifier 10.4230/LIPIcs.AofA.2020.11

Related Version The companion paper “Compacted binary trees admit a stretched exponential” by the same authors is available at arXiv:1908.11181.

Funding *Andrew Elvey Price*: European Research Council (ERC) in the European Union’s Horizon 2020 research and innovation programme, under the Grant Agreement No. 759702.

Wenjie Fang: *Recherche en esprit libre, i.e.*, not supported by fundings with precise predefined goals.

Michael Wallner: Erwin Schrödinger Fellowship of the Austrian Science Fund (FWF): J 4162-N35.

Acknowledgements We would like to thank Cyril Banderier, Tony Guttman, and Andrea Sportiello for interesting discussions on the presence of a stretched exponential. We also thank our referees for their careful reading and helpful comments.



© Andrew Elvey Price, Wenjie Fang, and Michael Wallner;
licensed under Creative Commons License CC-BY

31st International Conference on Probabilistic, Combinatorial and Asymptotic Methods for the Analysis of Algorithms (AofA 2020).

Editors: Michael Drmota and Clemens Heuberger; Article No. 11; pp. 11:1–11:13



Leibniz International Proceedings in Informatics

Schloss Dagstuhl – Leibniz-Zentrum für Informatik, Dagstuhl Publishing, Germany

1 Introduction

A *deterministic finite automaton* (DFA) A is a 5-tuple $(\Sigma, Q, \delta, q_0, F)$, where Σ is a finite set of letters called the *alphabet*, Q is a finite set of states, $\delta : Q \times \Sigma \rightarrow Q$ is the *transition function*, q_0 is the *initial state*, and $F \subseteq Q$ is the set of *final states* (sometimes called *accept states*). States not in F are called *non-final* or *reject states*. A DFA can be represented by a directed graph with one vertex v_s for each state $s \in Q$, with the vertices corresponding to final states being highlighted, and for every transition $\delta(s, w) = \hat{s}$, there is an edge from s to \hat{s} labeled w (see Figure 1).

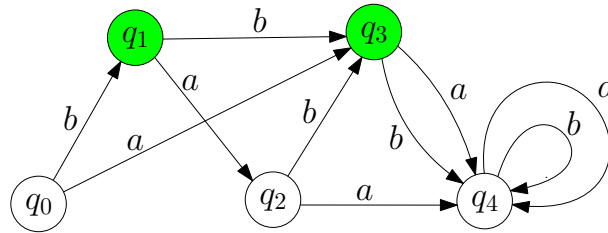


Figure 1 The unique minimal DFA for the language $\{a, b, bab, bb\}$. Here, q_0 is the initial state, q_1 and q_3 are the final states, and q_4 is the unique sink.

A word $w = w_1w_2 \dots w_\ell \in \Sigma^*$ is *accepted* by A if the sequence of states $(s_0, s_1, \dots, s_\ell) \in Q^{\ell+1}$ defined by $s_0 = q_0$ and $s_{i+1} = \delta(s_i, w_i)$ for $i = 0, \dots, \ell - 1$ ends with $s_\ell \in F$ a final state. The set of words accepted by A is called the *language* $\mathcal{L}(A)$ recognized by A . It is well-known that DFAs recognize exactly the set of regular languages. Note that every DFA recognizes a unique language, but a language can be recognized by several different DFAs. A DFA is called *minimal* if no DFA with fewer states recognizes the same language. The Myhill-Nerode Theorem states that every regular language is recognized by a unique minimal DFA (up to isomorphism) [8, Theorem 3.10]. For more details on automata see [8].

In this paper we show that the counting sequence $(m_{2,n})_{n \in \mathbb{N}}$ of minimal DFAs of size n recognizing a finite binary language admits a stretched exponential. Until now, the problem of counting these automata, even asymptotically, was widely open, see for example [4].

► Theorem 1. *The number $m_{2,n}$ of non-isomorphic minimal DFAs on a binary alphabet recognizing a finite language with $n + 1$ states satisfies for $n \rightarrow \infty$*

$$m_{2,n} = \Theta \left(n! 8^n e^{3a_1 n^{1/3}} n^{7/8} \right),$$

where $a_1 \approx -2.338$ is the largest root of the Airy function.

Since every regular language defines a unique minimal automaton, one may define the (space) complexity of the language to be the number of states in this corresponding automaton. Defining *space complexity* in this way, the number $m_{2,n}$ is simply the number of finite languages over a binary alphabet of space complexity $n + 1$.

In the recent paper [6] we showed lower and upper asymptotic bounds on $m_{2,n}$ by first establishing a connection between automata counted by $m_{2,n}$ and classes of directed acyclic graphs (DAGs) and then solving their asymptotic enumeration problem. In particular, we proved that

$$2^{n-1} c_n \leq m_{2,n} \leq 2^{n-1} r_n, \tag{1}$$

where c_n is the number of compacted and r_n the number of relaxed binary trees of size n . These appear naturally in the compression of XML documents [3, 7]. In the same paper, we showed that as $n \rightarrow \infty$,

$$c_n = \Theta\left(n! 4^n e^{3a_1 n^{1/3}} n^{3/4}\right) \quad \text{and} \quad r_n = \Theta\left(n! 4^n e^{3a_1 n^{1/3}} n\right),$$

leading to asymptotic lower and upper bounds on $m_{2,n}$. The results of the present work arise as a further application of the general method from [6] for proving the appearance of such stretched exponentials. They showcase the strength of our method, and we expect that our method may be applied to yet other combinatorial objects governed by similar recurrences.

The asymptotic proportion of general minimal DFAs (not necessarily recognizing a *finite* language) was solved by Bassino, Nicaud, and Sportiello in [1], building on enumeration results by Korshunov [9, 10] and Bassino and Nicaud [2]. The result in [1] also exploits an underlying tree structure of the related automata, but from a different traversal than what we use. In that case, no stretched exponential appears in the asymptotic enumeration, and the minimal automata account for a constant fraction of all automata.

2 Recurrence relation

To derive a recurrence for automata recognizing a finite language, we need the following lemma. In the following, we only consider automata on the binary alphabet $\{a, b\}$.

► **Lemma 2** ([11, Lemma 2.3], [8, Section 3.4]). *A DFA A is the minimal automaton for some finite language if and only if it has the following properties:*

- (a) *There is a unique sink s . That is, a state which is not a final state such that all transitions from s end at s that is, $\delta(s, w) = s$.*
- (b) *A is acyclic: the underlying directed graph has no cycles except for the loops at the sink.*
- (c) *A is initially connected: for any state p there exists a word $w \in \Sigma^*$ such that A reaches the state p upon reading w .*
- (d) *A is reduced: for any two different states q, q' , the two automata with initial state q and q' recognize different languages.*

Next, we identify a property that can replace the one of being *reduced*.

► **Lemma 3.** *An acyclic, initially connected DFA A with a unique sink is reduced if and only if it satisfies the following condition:*

- (d') *State uniqueness: there are no two distinct states q and q' with $\delta(q, a) = \delta(q', a)$ and $\delta(q, b) = \delta(q', b)$ such that both q and q' , or neither q nor q' , are accept states.*

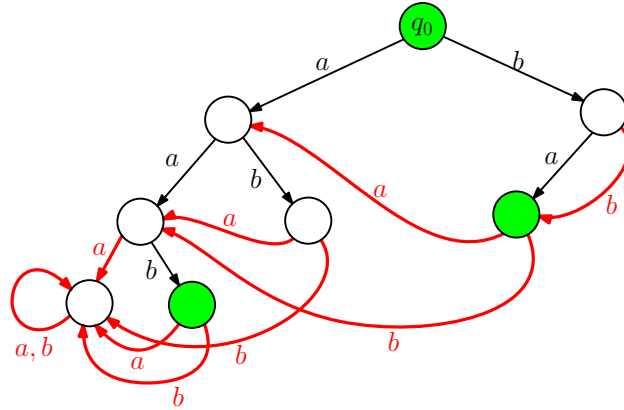
Proof. By definition, being reduced implies state uniqueness. Now suppose that A is not reduced while state uniqueness holds. Then there are two states $q \neq q'$ in A such that the two automata with initial state q and q' recognize the same language L . As A is acyclic, L is finite. We define the weight of L to be $\sum_{w \in L} (|w| + 1)$, and we pick q, q' such that the weight of L is minimal.

Suppose that L is not empty. By the state uniqueness, we must have $\delta(q, a) \neq \delta(q', a)$ or $\delta(q, b) \neq \delta(q', b)$. Without loss of generality, suppose that $r = \delta(q, a) \neq \delta(q', a) = r'$. The two automata with initial state r and r' recognize the same language $a^{-1}L = \{w \mid aw \in L\}$. Since the weights of $a^{-1}L$ are strictly less than that of L , we have r and r' violating the minimality of the weight of L . Therefore, L must be empty.

Since L is empty, q and q' are both rejecting. They cannot both be the sink as the sink is unique. Suppose that q is not the sink. Then due to state uniqueness, among $\delta(q, a)$ and $\delta(q, b)$ there is at least one state q_1 that is not the sink. As L is empty, q_1 is also rejecting.

11:4 Asymptotics of Minimal DFAs Recognizing a Finite Binary Language

We can then replace q with q_1 and perform the same argument to q_1 and q' , repeating *ad infinitum*. This creates an infinite sequence of states without repetition since A is acyclic. This is impossible as A is a DFA. Therefore, the existence of q and q' is impossible, meaning that A is reduced. We thus have the desired equivalence. ◀



■ **Figure 2** An acyclic DFA with its spanning subtree in black and all other edges in red. The initial state is q_0 and the final states are colored green.

We now consider two sets of DFAs: the set \mathfrak{F} of minimal DFAs recognizing finite languages, and the set \mathfrak{G} of acyclic and initially connected DFAs with a unique sink. From Lemmas 2 and 3, \mathfrak{F} consists of precisely the automata in \mathfrak{G} that also possess the state uniqueness.

In order to derive our recurrence, we first transform DFAs in \mathfrak{G} into decorated lattice paths that we call *B-paths*. For a given $A \in \mathfrak{G}$, our first step is to construct a spanning subtree of A (excluding the sink) using a depth-first search (*DFS* hereinafter) from the initial state q_0 as shown in Figure 2. This DFS is uniquely defined by taking edges marked by a before edges marked by b . Since A is initially connected, the tree obtained is a spanning tree.

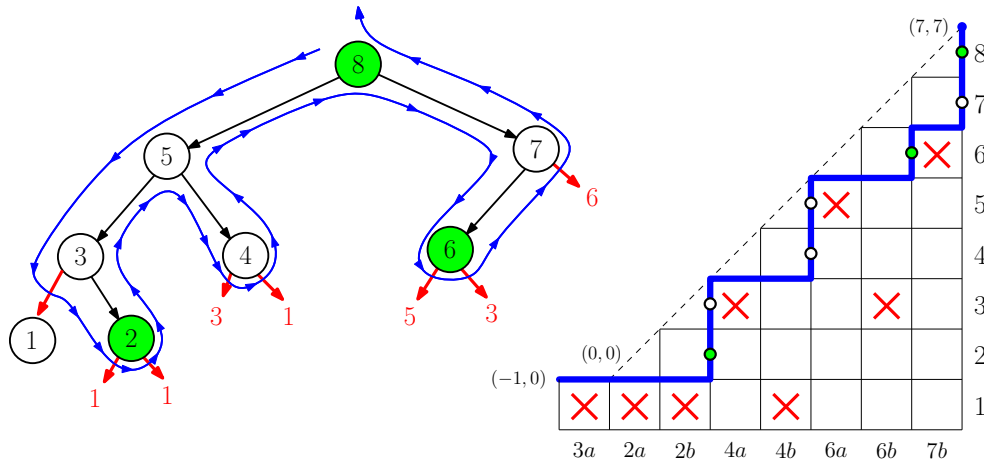
Using the same DFS, we construct a path P starting at the point $(-1, 0)$ and illustrated by a blue line in Figure 3 as follows:

- Whenever the directed blue line around the tree in Figure 3 goes up we add a *vertical step* $V = (0, 1)$ to the path. We say that the state we just quit *corresponds* to this step.
- Whenever the directed blue line crosses an outgoing edge (including the edge leading to the sink), which is not part of the tree, we add a *horizontal step* $H = (1, 0)$.

The order of states corresponding to V -steps is called the *postorder* of states. It is clear that the first step of P is a H -step, and removing it from P gives a Dyck path under the main diagonal. We now decorate P with spots and crosses. Each step V is decorated by a green or white spot, according to whether the corresponding state is accepting or rejecting.

Since A is acyclic, during the DFS, for an edge e pointing from the current state q to an already visited state q' , the state q' must not be an ancestor of q in the constructed tree, meaning that q' must either come before q in postorder or be the sink. In the former case, we put a cross in the cell at the intersection between the column of the H -step corresponding to e , and the row of the V -step corresponding to q' , while in the latter case we put the cross in the row just below $y = 0$. Clearly the crosses are under P and above $y = -1$. We thus obtain a path B with decorations, and we say that B is the *B-path* of the automaton A .

To characterize *B-paths* obtained from DFAs in \mathfrak{G} , we propose the following definition. An *automatic B-path* P of size n is defined as a lattice path consisting of up steps and horizontal steps from $(-1, 0)$ to (n, n) with decorations such that



■ **Figure 3** The transformation from an acyclic DFA to a B-path. In the DFA, the states are numbered in order of their corresponding up steps and we have labelled each outgoing edge not in the tree with the number of the state it points to.

- The first step is an H -step, and its removal leaves a Dyck path below the main diagonal;
- Each H -step has a cross in its column, under P and above $y = -1$.
- Every V -step has a white or green spot.

It is not difficult to see that automatic B-paths are in bijection with \mathfrak{G} , with the size preserved, since a B-path P obtained from a DFA $A \in \mathfrak{G}$ is clearly automatic, and the construction of B-paths can be easily reversed to obtain a DFA in \mathfrak{G} from an automatic B-path.

Now we examine automatic B-paths corresponding to DFAs in \mathfrak{F} . By definition, we only need to take the state uniqueness into account. Given $A \in \mathfrak{G}$, let T be its depth-first search tree and B its corresponding automatic B-path. A state $q \in A$ is called a *cherry* if it is a leaf of T but not the sink. Seen on B , a cherry state corresponds to a sequence HHV of steps. We now propose a seemingly weaker notion of state uniqueness called *cherry-state uniqueness*, which is in fact equivalent in our case.

► **Lemma 4.** *Suppose that $A \in \mathfrak{G}$, then A has state uniqueness if and only if it has cherry-state uniqueness, i.e., any two states q, q' such that q comes before q' in postorder, and q' is a cherry state, satisfy the conditions in the definition of state uniqueness.*

Proof. State uniqueness clearly implies cherry-state uniqueness. For the other direction, let T be the DFS tree of A . Suppose that we have two states $q \neq q'$ such that $\delta(q, a) = \delta(q', a)$ and $\delta(q, b) = \delta(q', b)$. We suppose that q precedes q' in postorder. It is clear that q' is not an ancestor of q , but q is also not an ancestor of q' , or else q would have a transition to itself or to one of its ancestors, which is impossible as A is acyclic. This implies that both $\delta(q, a)$ and $\delta(q, b)$ come before q in postorder, so neither $\delta(q, a)$ nor $\delta(q, b)$ can be a child of q' . Hence, q' is a cherry. Therefore, cherry-state uniqueness implies state uniqueness. ◀

We now try to construct step by step automatic B-paths corresponding to DFAs in \mathfrak{F} . We denote by $B_{n,m}$ the set of prefixes ending at (n, m) of such paths. We always start by an H -step from $(-1, 0)$, thus there is exactly one path in $B_{0,0}$. Suppose that we have constructed all automatic B-paths ending at $0 \leq m' \leq m$ and $m' \leq n' \leq n$ except for (n, m) , and we now construct paths in $B_{n,m}$. First, from any path in $B_{n-1,m}$, we can construct a path $P \in B_{n,m}$ by adding an H -step at height m with a cross, and there are $(m + 1)$

11:6 Asymptotics of Minimal DFAs Recognizing a Finite Binary Language

possibilities for the cross. Second, from any path in $B_{n,m-1}$, we can construct a path P by adding a V -step with a spot that can be green or white. Such a path P ends in a V -step, thus it is different from paths in the first case. However, it may not be in $B_{n,m}$, because it may end in HHV with H -steps at height $m-1$. In such a case it corresponds to a cherry state that violates the cherry-state uniqueness. Such paths violating the condition for \mathfrak{F} are all constructed by adding HHV at the end of paths in $B_{n-2,m-1}$, then adding crosses for the last two H -steps to make the corresponding cherry state “copy” one of the m states preceding it in postorder. Excluding such paths, we obtain all the paths in $B_{n,m}$. In this way, we construct all automatic B -paths corresponding to DFAs in \mathfrak{F} . This construction can be translated into the following recurrence.

► **Proposition 5.** *Let $b_{n,m}$ be the number of initial segments of automatic B -paths corresponding to DFAs in \mathfrak{F} ending at (n,m) . Then*

$$\begin{cases} b_{n,m} = 2b_{n,m-1} + (m+1)b_{n-1,m} - mb_{n-2,m-1}, & \text{for } n \geq m \geq 1, \\ b_{n,m} = 0, & \text{for } n < m, \\ b_{n,0} = 1, & \text{for } n \geq -1. \end{cases}$$

The number $m_{2,n}$ of minimal binary DFAs of size n recognizing a finite language is equal to $b_{n,n}$.

This recurrence relation can be directly used to compute all elements of the sequence $(m_{2,n})_{n \geq 0}$ up to size $n = N$ with $\mathcal{O}(N^2)$ arithmetic operations. The first few numbers of this sequence read

$$(m_{2,n})_{n \geq 0} = (1, 1, 6, 60, 900, 18480, 487560, 15824880, 612504240, 27619664640, \dots).$$

We have added it as sequence OEIS A331120 in the Online Encyclopedia of Integer Sequences¹. Previously, the first 7 elements were computed in [5, Section 6].

3 A stretched exponential appears

We now perform an asymptotic analysis of the numbers $m_{2,n}$ using the recurrence derived in the previous section. As a first step we define an auxiliary sequence, which simplifies the subsequent analysis by absorbing the leading exponential behaviour:

$$\begin{aligned} \tilde{b}_{n,m} &= \frac{b_{n,m}}{2^{m-1}}, & \text{for } m \geq 1, \\ \tilde{b}_{n,0} &= b_{n,0} = 1. \end{aligned}$$

This gives

$$\begin{cases} \tilde{b}_{n,m} = \tilde{b}_{n,m-1} + (m+1)\tilde{b}_{n-1,m} - \frac{m}{2}\tilde{b}_{n-2,m-1}, & \text{for } n \geq m > 1, \\ \tilde{b}_{n,m} = 0, & \text{for } n < m, \\ \tilde{b}_{n,0} = 1, & \text{for } n \geq -1. \end{cases}$$

Next, we transform the sequence $(\tilde{b}_{n,m})_{0 \leq m \leq n}$ into a sequence $(e_{n,m})_{\substack{0 \leq m \leq n \\ n-m \text{ even}}}$ using

$$e_{n,m} = \frac{1}{((n+m)/2)!} \tilde{b}_{(n+m)/2, (n-m)/2},$$

¹ <https://oeis.org>

(note that $e_{n,m}$ is only defined when $n - m$ is even). Then, the terms $e_{n,m}$ are determined by the following recurrence for $n, m \geq 1$

$$\begin{cases} e_{n,m} = \frac{n-m+2}{n+m}e_{n-1,m-1} + e_{n-1,m+1} - \frac{n-m}{(n+m)(n+m-2)}e_{n-3,m-1}, & \text{for } n \geq m \geq 0, \\ e_{0,0} = 1, \\ e_{n,m} = 0, \\ e_{n,-1} = 0, \end{cases} \quad \begin{matrix} \\ \\ \text{for } n < m, \\ \text{for } n \geq -1. \end{matrix}$$

The number of minimal DFAs of size n is equal to $n!2^{n-1}e_{2n,0}$. Now, for some simple cases of $e_{n,m}$, elementary computations show that $e_{n,n} = \frac{1}{n!}$, $e_{n,n-2} = \frac{2^{n-1}-1}{(n-1)!}$, and $e_{n,n-4} = \frac{3^{n-2}-3 \cdot 2^{n-3}}{(n-2)!}$. Comparing the recurrence above with the one of compacted binary trees given in [6, Section 5] for $e_{n,m}$, we notice only two differences:

1. a slightly different factor $\frac{2(n-m-2)}{(n+m)(n+m-2)}$ of $e_{n-3,m-1}$ and
2. no special cases for $n \geq m > n - 3$.

Therefore, we are anticipating the same method to be applicable. The very basic idea is that we will prove lower and upper bounds which differ only in the constant term. This method requires that the recurrence involves only non-negative terms on the right-hand side. As in the case of compacted binary trees, we solve this problem by finding suitable upper and lower bounds given in the subsequent Lemma. We omit its technical proof as it follows exactly the same lines as [6, Lemma 5.1].

► **Lemma 6.** *For $n - 3 \geq m \geq 2$, the term $e_{n,m}$ is bounded below by*

$$L_e = \frac{n-m+2}{n+m}e_{n-1,m-1} + \frac{n-m-1}{n-m}e_{n-1,m+1} + \frac{n-m-3}{n-m-2} \left(\frac{1}{n-m}e_{n-2,m+2} + \frac{1}{n+m}e_{n-3,m+1} \right)$$

and for $n \geq 5, n > m \geq 0$ bounded above by

$$U_e = \frac{n-m+2}{n+m}e_{n-1,m-1} + \frac{n-m-1}{n-m}e_{n-1,m+1} + \frac{1}{n-m}e_{n-2,m+2} + \frac{1}{n+m}e_{n-3,m+1}.$$

That is, $L_e(n, m) \leq e_{n,m} \leq U_e(n, m)$.

3.1 Lower bound

The following technical Lemma is at the heart of the following inductive proof of the lower bound. It links the recurrence of $e_{n,m}$ (or rather its lower bound L_e) with two explicit sequences \tilde{s}_n and $\tilde{X}_{n,m}$ involving the Airy function, shifted to its right-most root a_1 .

► **Lemma 7.** *For all $n, m \geq 0$ let*

$$\begin{aligned} \tilde{X}_{n,m} &:= \left(1 - \frac{2m^2}{3n} + \frac{3m}{8n} \right) \text{Ai} \left(a_1 + \frac{2^{1/3}(m+1)}{n^{1/3}} \right) \quad \text{and} \\ \tilde{s}_n &:= 2 + \frac{2^{2/3}a_1}{n^{2/3}} + \frac{29}{12n} - \frac{1}{n^{7/6}}. \end{aligned}$$

Then, for any $\varepsilon > 0$, there exists a constant \tilde{n}_0 such that

$$\begin{aligned} \tilde{X}_{n,m}\tilde{s}_n\tilde{s}_{n-1}\tilde{s}_{n-2} &\leq \frac{n-m+2}{n+m}\tilde{X}_{n-1,m-1}\tilde{s}_{n-1}\tilde{s}_{n-2} + \frac{n-m-1}{n-m}\tilde{X}_{n-1,m+1}\tilde{s}_{n-1}\tilde{s}_{n-2} \\ &\quad + \frac{n-m-3}{n-m-2} \left(\frac{1}{n-m}\tilde{X}_{n-2,m+2}\tilde{s}_{n-2} + \frac{1}{n+m}\tilde{X}_{n-3,m+1} \right), \end{aligned}$$

for all $n \geq \tilde{n}_0$ and all $0 \leq m < n^{2/3-\varepsilon}$.

Let us show how this Lemma is used before stating its actual proof. First, we define the sequence $X_{n,m} := \max\{\tilde{X}_{n,m}, 0\}$ (note that the factor $1 - \frac{2m^2}{3n} + \frac{3m}{8n}$ is negative for large m). Then, using Lemma 7 we have

$$X_{n,m}\tilde{s}_n\tilde{s}_{n-1}\tilde{s}_{n-2} \leq \frac{n-m+2}{n+m}X_{n-1,m-1}\tilde{s}_{n-1}\tilde{s}_{n-2} + \frac{n-m-1}{n-m}X_{n-1,m+1}\tilde{s}_{n-1}\tilde{s}_{n-2} \\ + \frac{n-m-3}{n-m-2} \left(\frac{1}{n-m}X_{n-2,m+2}\tilde{s}_{n-2} + \frac{1}{n+m}X_{n-3,m+1} \right),$$

for n large enough and all $m \leq n$. Finally, we define the sequence \tilde{h}_n such that $\tilde{h}_n = \tilde{s}_n\tilde{h}_{n-1}$ for $n > 0$ and set $\tilde{h}_0 = \tilde{s}_0$. Then we deduce by induction that $e_{n,m} \geq b_0\tilde{h}_n X_{n,m}$ for some constant $b_0 > 0$, all sufficiently large n , and all $m \in [0, n]$:

$$b_0X_{n,m}\tilde{h}_n \leq \frac{n-m+2}{n+m}e_{n-1,m-1} + \frac{n-m-1}{n-m}e_{n-1,m+1} + \frac{n-m-3}{n-m-2} \left(\frac{e_{n-2,m+2}}{n-m} + \frac{e_{n-3,m+1}}{n+m} \right) \\ \leq e_{n,m},$$

where the first inequality follows by induction and the second one by Lemma 6 for $m \leq n-3$. For $m > n-3$ and n large enough the inequality holds trivially as $X_{n,m} = 0$. Therefore,

$$m_{2,n} = n!2^{n-1}e_{2n,0} \\ \geq b_0n!2^{n-1}\tilde{h}_{2n}X_{2n,0} \\ \geq b_0n!2^{n-1} \prod_{i=1}^{2n} \left(2 + \frac{2^{2/3}a_1}{i^{2/3}} + \frac{29}{12i} - \frac{1}{i^{7/6}} \right) \text{Ai} \left(a_1 + \frac{1}{n^{1/3}} \right) \\ \geq \gamma_L n!8^n e^{3a_1n^{1/3}} n^{7/8}, \quad (2)$$

for some constant $\gamma_L > 0$.

► **Remark 8.** Let us compare the result of Lemma 7 to the respective results for compacted and relaxed binary trees to which this method was applied first. Recall the lower and upper bounds (1) which are tight up to the constant and the polynomial term. Indeed, the corresponding results [6, Lemmas 4.2 and 5.2] possess a very similar structure: First, in $\tilde{X}_{n,m}$ the only difference is in the factor $\frac{3m}{8n}$ which is $\frac{m}{2n}$ for relaxed trees and $\frac{m}{4n}$ for compacted trees. The purpose of this term is of technical nature as it simplifies the Newton polygon method, yet it has no influence on the final asymptotics; compare Figure 5. Second, in \tilde{s}_n the only difference is in the term $\frac{29}{12n}$ which is $\frac{8}{3n}$ for relaxed trees and $\frac{13}{6n}$ for compacted trees. Now this term influences the polynomial factor in the asymptotics (compare with [6, Section 3.3]). More generally, whenever the third term in the expansion of \tilde{s}_n has the form $\frac{\alpha}{n}$, we get in the enumeration a polynomial factor with exponent $\frac{\alpha}{2} - \frac{1}{3}$. Finally, the similarity in all other terms of the expansion for \tilde{s}_n and $\tilde{X}_{n,m}$ is responsible for the fact that $m_{2,n}$ and the families of trees enumerated in [6] have the same exponential growth, as well as the same stretched-exponential behaviour.

Proof (Lemma 7). The proof follows nearly verbatim [6, Lemma 4.2], so we will only introduce the main idea, omitting the technical details. Note that all (often tedious) computations are available in the accompanying Maple worksheet [12].

We start by defining the following sequence

$$P_{n,m} := -Z_{n,m}s_n s_{n-1} s_{n-2} \\ + \frac{n-m+2}{n+m}Z_{n-1,m-1}s_{n-1}s_{n-2} + \frac{n-m-1}{n-m}Z_{n-1,m+1}s_{n-1}s_{n-2} \\ + \frac{n-m-3}{n-m-2} \left(\frac{1}{n-m}Z_{n-2,m+2}s_{n-2} + \frac{1}{n+m}Z_{n-3,m+1} \right),$$

where

$$s_n := \sigma_0 + \frac{\sigma_1}{n^{1/3}} + \frac{\sigma_2}{n^{2/3}} + \frac{\sigma_3}{n} + \frac{\sigma_4}{n^{7/6}},$$

$$Z_{n,m} := \left(1 + \frac{\tau_2 m^2 + \tau_1 m}{n}\right) \text{Ai}\left(a_1 + \frac{2^{1/3}(m+1)}{n^{1/3}}\right),$$

with $\sigma_i, \tau_j \in \mathbb{R}$. Then the inequality is equivalent to $P_{n,m} \geq 0$ with $\sigma_0 = 2$, $\sigma_1 = 0$, $\sigma_2 = 2^{2/3}a_1$, $\sigma_3 = 29/12$, and $\sigma_4 = -1$ as well as $\tau_1 = 3/8$ and $\tau_2 = -2/3$. Next, we expand $\text{Ai}(z)$ in a neighborhood of

$$\alpha = a_1 + \frac{2^{1/3}m}{n^{1/3}}, \tag{3}$$

and we get

$$P_{n,m} = p_{n,m} \text{Ai}(\alpha) + p'_{n,m} \text{Ai}'(\alpha),$$

where $p_{n,m}$ and $p'_{n,m}$ are functions of m and n^{-1} and may be expanded as power series in $n^{-1/6}$ with coefficients polynomial in m . We will see that, as long as $n > 1$ and $n > m$, this series converges absolutely because the Airy function is entire and so all the functions for which we need to perform a bivariate expansion (in n and m) are indeed analytic in the region defined by $|n| > 1$ and $|m| < |n|^{2/3-\epsilon}$.

Now we proceed with the technical analysis, which is only performed on a superficial level here. The first step is to show that $[m^i n^j]P_{n,m} = 0$ for $i + j > 1$, $i, j \in \mathbb{Q}$. Then, as a second step, we strengthen this result by choosing suitable values σ_i for $0 \leq i \leq 4$ in the definition of s_n in order to eliminate more terms. The results are summarized in Figure 4 where the initial non-zero coefficients are shown. A diamond at (i, j) is drawn if and only if the coefficient $[m^i n^j]P_{n,m}$ is non-zero for generic values of σ and τ . It is an empty diamond if the given choice of σ_i and τ_j makes it vanish, whereas it is a solid diamond if it remains non-zero. The convex hull is formed by the following three lines

$$L_1 : j = -\frac{7}{6} - \frac{7i}{18}, \quad L_2 : j = -\frac{1}{3} - \frac{2i}{3}, \quad L_3 : j = 1 - i.$$

From now on, we distinguish between the contributions arising from $p_{n,m}$ and $p'_{n,m}$. The non-zero coefficients are shown in Figure 5. For technical reasons we choose at this point $\tau_1 = 8/3$ and thereby reduce the slope of the convex hull of the non-zero coefficients of $p'_{n,m}$. The expansions for n tending to infinity start as follows, where the elements on the convex hull are written in color:

$$P_{n,m} = \text{Ai}(\alpha) \left(-\frac{4\sigma_4}{n^{7/6}} - \frac{2^{11/3}a_1 m}{3n^{5/3}} - \frac{164m^2}{9n^2} - \frac{2^{14/3}a_1 m^3}{3n^{8/3}} - \frac{136m^4}{9n^3} - \frac{248m^5}{135n^4} + \dots \right) +$$

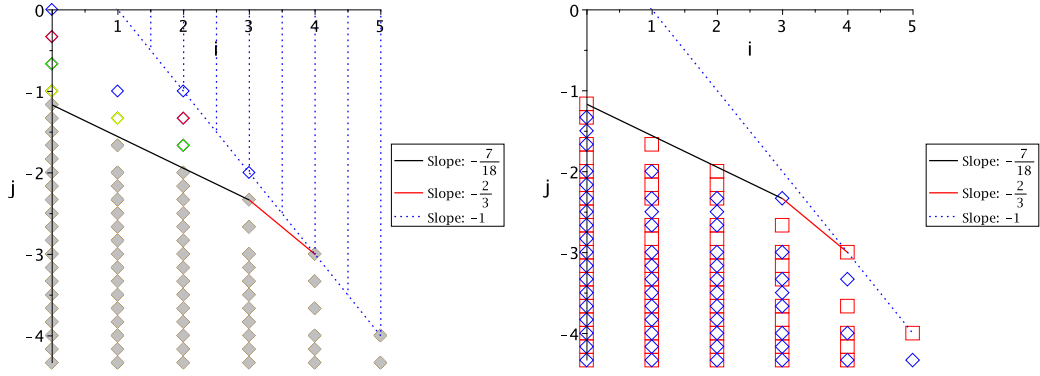
$$\text{Ai}'(\alpha) \left(\frac{2^{1/3}(8\tau_1 - 3)}{n^{4/3}} + \frac{2^{7/3}}{n^{3/2}} - \frac{32a_1 m}{9n^2} + \frac{2^{4/3}m^2(48\tau_1 - 65)}{9n^{7/3}} - \frac{2^{19/3}m^3}{9n^{7/3}} \right.$$

$$\left. - 5\frac{2^{10/3}m^4}{9n^{10/3}} - 89\frac{2^{10/3}m^5}{135n^{13/3}} + \dots \right).$$

We now choose $\sigma_4 = -1$ which leads to a positive term $\text{Ai}(\alpha)n^{-7/6}$. Next, for fixed (large) n we prove that for all m the dominant contributions in $P_{n,m}$ are positive. Motivated by Figures 4 and 5, we consider three different regimes: $m \leq Cn^{1/3}$, $Cn^{1/3} < m \leq n^{7/18}$, and $n^{7/18} < m < n^{2/3-\epsilon}$ for a suitable constant $C > 0$. We end the proof by showing that there exists an $N > 0$ such that all terms are positive for $n > N$ and all $m < n^{2/3}$. ◀

In the next section we will show an upper bound with the same asymptotic form, but with a different constant γ_U .

11:10 Asymptotics of Minimal DFAs Recognizing a Finite Binary Language



■ **Figure 4** (Left) Non-zero coefficients of $P_{n,m} = \sum a_{i,j} m^i n^j$ shown by diamonds for $s_n := \sigma_0 + \frac{\sigma_1}{n^{1/3}} + \frac{\sigma_2}{n^{2/3}} + \frac{\sigma_3}{n} + \frac{\sigma_4}{n^{7/6}}$ and $Z_{n,m} := \left(1 + \frac{\tau_2 m^2 + \tau_1 m}{n}\right) \text{Ai}\left(a_1 + \frac{2^{1/3}(m+1)}{n^{1/3}}\right)$. There are no terms in the blue dashed area. The blue terms vanish for $\sigma_0 = 2$, the red terms vanish for $\sigma_1 = 0$, the green terms vanish for $\sigma_2 = 2^{2/3}a_1$, and the yellow terms vanish for $\sigma_3 = 29/12$ and $\tau_2 = -2/3$. The black and red lines represent the two parts L_1 and L_2 , respectively, of the convex hull. (Right) The solid gray diamonds are decomposed into the coefficients $p_{n,m}$ of $\text{Ai}(\alpha)$ (red boxes) and $p'_{n,m}$ of $\text{Ai}'(\alpha)$ (blue diamonds).

3.2 Upper bound

The following lemma links as in the case of the lower bound $e_{n,m}$ (and its upper bound U_e) with two explicit sequences \hat{s}_n and $\hat{X}_{n,m}$ involving again the Airy function.

► **Lemma 9.** Choose $\eta > 2/9$ fixed and for all $n, m \geq 0$ let

$$\hat{X}_{n,m} := \left(1 - \frac{2m^2}{3n} + \frac{3m}{8n} + \eta \frac{m^4}{n^2}\right) \text{Ai}\left(a_1 + \frac{2^{1/3}(m+1)}{n^{1/3}}\right) \quad \text{and}$$

$$\hat{s}_n := 2 + \frac{2^{2/3}a_1}{n^{2/3}} + \frac{29}{12n} + \frac{1}{n^{7/6}}.$$

Then, for any $\varepsilon > 0$, there exists a constant \hat{n}_0 such that

$$\hat{X}_{n,m} \hat{s}_n \hat{s}_{n-1} \hat{s}_{n-2} \geq \frac{n-m+2}{n+m} \hat{X}_{n-1,m-1} \tilde{s}_{n-1} \tilde{s}_{n-2} + \frac{n-m-1}{n-m} \hat{X}_{n-1,m+1} \tilde{s}_{n-1} \tilde{s}_{n-2} \quad (4)$$

$$+ \frac{1}{n-m} \hat{X}_{n-2,m+2} \tilde{s}_{n-2} + \frac{1}{n+m} \hat{X}_{n-3,m+1},$$

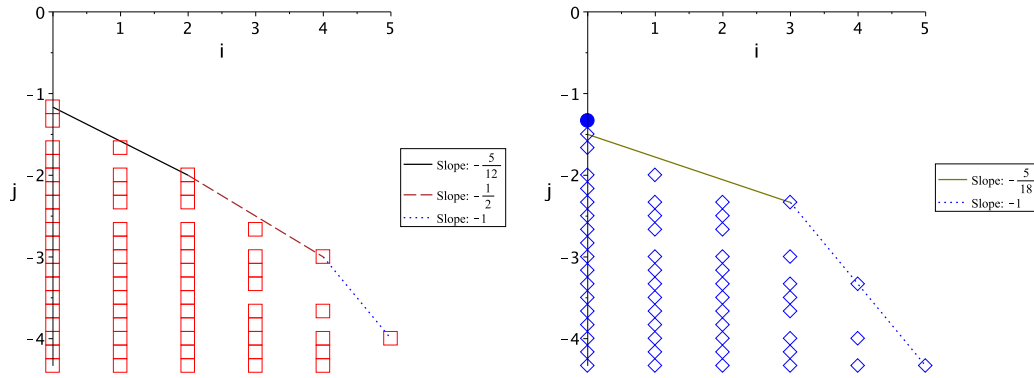
for all $n \geq \hat{n}_0$ and all $0 \leq m < n^{1-\varepsilon}$.

Proof (Sketch). The proof follows the same lines as that of Lemma 7, so we will only elucidate the required modifications. As a first step we define the following sequence

$$Q_{n,m} := \hat{X}_{n,m} \hat{s}_n \hat{s}_{n-1} \hat{s}_{n-2} - \frac{n-m+2}{n+m} \hat{X}_{n-1,m-1} \tilde{s}_{n-1} \tilde{s}_{n-2} - \frac{n-m-1}{n-m} \hat{X}_{n-1,m+1} \tilde{s}_{n-1} \tilde{s}_{n-2}$$

$$- \frac{1}{n-m} \hat{X}_{n-2,m+2} \tilde{s}_{n-2} - \frac{1}{n+m} \hat{X}_{n-3,m+1}.$$

Then the inequality is equivalent to $Q_{n,m} \geq 0$. Again, we expand $\text{Ai}(z)$ in a neighborhood of $\alpha = a_1 + \frac{2^{1/3}m}{n^{1/3}}$, and we get the following expansion (see the accompanying Maple worksheet [12] for full details). As before, the elements on the convex hull are written in color.



■ **Figure 5** Non-zero coefficients $p_{n,m} = \sum \tilde{a}_{i,j} m^i n^j$ (red) and $p'_{n,m} = \sum \tilde{a}'_{i,j} m^i n^j$ (blue) of the expansion (3) for $P_{n,m}$. The coefficient of $n^{-4/3}$ in the right picture depicted as a solid blue circle disappears for $\tau_1 = 3/8$.

$$\begin{aligned}
 Q_{n,m} = & \text{Ai}(\alpha) \left(\frac{4}{n^{7/6}} + \frac{2^{11/3} a_1 m}{3n^{5/3}} + \frac{4m^2(41 - 108\eta)}{9n^2} + \frac{2^{14/3} a_1 m^3(1 - 6\eta)}{3n^{8/3}} \right. \\
 & \left. + \frac{8m^4(17 - 132\eta)}{9n^3} - \frac{2^{11/3} a_1 m^5 \eta}{n^{11/3}} - \frac{68m^6 \eta}{3n^4} - \frac{124m^7 \eta}{45n^5} + \dots \right) + \\
 & \text{Ai}'(\alpha) \left(\frac{2^{7/3}}{n^{3/2}} + \frac{32a_1 m}{9n^2} + \frac{2^{4/3} m^2(47 - 216\eta)}{9n^{7/3}} + \frac{2^{16/3} m^3(2 - 9\eta)}{9n^{7/3}} \right. \\
 & \left. + \frac{2^{1/3} m^4(40 - 549\eta)}{9n^{10/3}} - \frac{2^{16/3} m^5 \eta}{3n^{10/3}} - \frac{5m^6 2^{7/3} \eta}{3n^{13/3}} - \frac{89m^7 2^{7/3} \eta}{45n^{16/3}} + \dots \right).
 \end{aligned}$$

Then we can finish in the same way as in the proof of Lemma 7. For the full details we refer to the proofs of [6, Lemma 4.4 and 5.3] which explains how to deal with the new cases required in the treatment of the upper bound (that happen to be analogous for the sequence at hand here, and the ones in that paper). Note that even the final convex hull in the Newton polygons is the same. ◀

The idea is now similar to the lower bound, yet a bit more intricate: We want to find an auxiliary sequence $(\tilde{e}_{n,m})_{n,m \geq 0}$ satisfying $e_{n,m} \leq C\tilde{e}_{n,m}$ for some constant $C > 0$, all n large, and all $m \leq n$ such that

$$\tilde{e}_{n,m} \leq \kappa_1 \hat{h}_n \hat{X}_{n,m}, \tag{5}$$

where the sequence $(\hat{h}_n)_{n \geq 1}$ is defined by $\hat{h}_n = \hat{s}_n \hat{h}_{n-1}$. As shown in (2), this implies that there is a constant $\gamma_U > 0$ such that

$$\tilde{e}_{2n,0} \leq \gamma_U 4^n e^{3a_1 n^{1/3}} n^{7/8}.$$

Now, in order to find such a sequence we use Lemma 6 and state the following definition for $(\tilde{e}_{n,m})_{n,m \geq 0}$:

$$\begin{cases} \tilde{e}_{n,m} = \frac{n-m+2}{n+m} \tilde{e}_{n-1,m-1} + \frac{n-m-1}{n-m} \tilde{e}_{n-1,m+1} \\ \quad + \frac{1}{n-m} \tilde{e}_{n-2,m+2} + \frac{1}{n+m} \tilde{e}_{n-3,m+1}, & \text{for } n \geq 5, n^{3/4} > m \geq 0, \\ \tilde{e}_{n,m} = e_{n,m}, & \text{for } n < 5, n \geq m \geq 0, \\ \tilde{e}_{n,m} = 0, & \text{otherwise.} \end{cases} \tag{6}$$

11:12 Asymptotics of Minimal DFAs Recognizing a Finite Binary Language

There are several ideas in the choice of the sequence (6) which we want to explain now. Firstly, in order to prove (5), the sequence has to be zero for large values of m . We achieve this by cutting off the values for $m > n^{3/4}$. Secondly, it has to have positive coefficients, because then we can prove (5) by induction as it was done in the lower bound. Thirdly, it has to be an upper bound of $e_{n,m}$, i.e., $e_{n,m} \leq C\hat{e}_{n,m}$ for all n, m . Due to the cut off for $m > n^{3/4}$ this is, of course, impossible, so we introduce a second auxiliary sequence $(\hat{e}_{n,m})_{n,m \geq 0}$ with the same rules as (6) yet with no cut off, i.e., the recurrence holds for $n \geq 5$ and $n > m \geq 0$. Then, by Lemma 6 we have $e_{n,m} \leq \hat{e}_{n,m}$ for all n, m .

Hence, it remains to prove that there is a choice of N and a constant $C > 0$ such that

$$\hat{e}_{2n,0} \leq C\tilde{e}_{2n,0}$$

for all $n > N$. As a first step, we define a class \mathcal{C} of weighted paths with the step set $\mathcal{S} := \{(1, 1), (1, -1), (2, -2), (3, -1)\}$ and weights corresponding to the recurrence defining $\hat{e}_{n,m}$. Then $\hat{e}_{n,m}$ can be interpreted as the weighted enumeration of paths $p_0 p_1 \dots p_k \in \mathcal{C}$ ($p_i \in \mathbb{Z}^2$) from p_0 to $p_k = (n, m)$ such that $p_{i+1} - p_i \in \mathcal{S}$ for $0 \leq i \leq k-1$, with the additional initial condition that $p_0 = (u_0, v_0)$ and $p_1 = (u_1, v_1)$ satisfy $v_0 \leq u_0 < 5 \leq u_1$. In other words, the first jump $p_1 - p_0$ has to exit $\mathcal{I} := \{(i, j) : i < 5\}$. The weight given to each path in this enumeration is e_{u_0, v_0}

► **Lemma 10.** *Let $q_{\ell, m, 2n}$ denote the weighted number of paths $p \in \mathcal{C}$ from (ℓ, m) to $(2n, 0)$. Then the numbers $q_{\ell, m, 2n}$ satisfy the inequality*

$$\frac{q_{\ell, j, 2n}}{j+1} \geq \frac{q_{\ell, k, 2n}}{k+1},$$

for integers $0 \leq j < k \leq \ell \leq 2n$ satisfying $2|k - j$ and $n \geq 10$.

Proof (Sketch). Reversing the steps in (6) we see that q satisfies the following recurrence for $\ell < 2n$:

$$\begin{cases} q_{\ell, m, 2n} = 0, & \text{for } m < 0, \\ q_{\ell, m, 2n} = \frac{\ell-m+1}{\ell-m+2} q_{\ell+1, m-1, 2n} + \frac{\ell-m+2}{\ell+m+2} q_{\ell+1, m+1, 2n} \\ \quad + \frac{1}{\ell-m+4} q_{\ell+2, m-2, 2n} + \frac{1}{\ell+m+2} q_{\ell+3, m-1, 2n} & \text{for } m \geq 0. \end{cases}$$

Then we follow nearly verbatim the lines of the proof of [6, Lemma 5.4]. For more details we refer to the accompanying Maple worksheet [12]. ◀

The last ingredient we will need is that

$$\hat{e}_{2x, 2y} \leq d_{2x, 2y} \leq \binom{2x}{x+y},$$

where the sequence $d_{x,y}$ corresponds to the weighted number of Dyck meanders of length x ending at y ; see [6, Proposition 3.2]. The first inequality is proved by induction using the recurrence relations of $\hat{e}_{x,y}$ and $d_{x,y}$. The second inequality is proved in [6], yet simply a consequence of the fact that $\binom{2x}{x+y}$ is the (unweighted) number of Dyck meanders from $(0, 0)$ to $(2x, 2y)$, while the weights of weighted Dyck meanders are always smaller than 1.

Finally, among the $\hat{e}_{2n,0}$ weighted paths ending at $(2n, 0)$, the proportion of those passing through some point $(2x, 2y)$ is

$$\frac{\hat{e}_{2x, 2y} q_{2x, 2y, 2n}}{\hat{e}_{2n, 0}} \leq \frac{\hat{e}_{2x, 2y} q_{2x, 2y, 2n}}{\hat{e}_{2x, 0} q_{2x, 0, 2n}} \leq (2y+1) \frac{\hat{e}_{2x, 2y}}{\hat{e}_{2x, 0}} \leq \frac{2y+1}{\gamma_{\mathbb{L}} 4^x e^{3a_1 x^{1/3}} x^{3/4}} \binom{2x}{x+y}.$$

In the last inequality we used Lemma 10 as well as $e_{n,m} \leq \hat{e}_{n,m}$ and the lower bound (2) for $\hat{e}_{2x,0}$. Hence, we can use the same ideas as used in [6, Lemma 4.6] to show that there is some choice for N such that $\hat{e}_{2n,0} \leq 2\tilde{e}_{2n,0}$ for all n .

This proves the missing link and ends the proof of Theorem 1.

To conclude, we observe that all arguments in Section 2 can be extended to any finite alphabet of any size at least 2. Our analysis may also be extended to this more general case, but this remains a work in progress.

References

- 1 Frédérique Bassino, Julien David, and Andrea Sportiello. Asymptotic enumeration of minimal automata. In *29th International Symposium on Theoretical Aspects of Computer Science*, volume 14 of *LIPICs. Leibniz Int. Proc. Inform.*, pages 88–99. Schloss Dagstuhl. Leibniz-Zent. Inform., Wadern, 2012. doi:10.4230/LIPICs.STACS.2012.88.
- 2 Frédérique Bassino and Cyril Nicaud. Enumeration and random generation of accessible automata. *Theoret. Comput. Sci.*, 381(1-3):86–104, 2007. doi:10.1016/j.tcs.2007.04.001.
- 3 Mireille Bousquet-Mélou, Markus Lohrey, Sebastian Maneth, and Eric Noeth. XML compression via directed acyclic graphs. *Theory Comput. Syst.*, 57(4):1322–1371, 2015. doi:10.1007/s00224-014-9544-x.
- 4 Michael Domaratzki. Enumeration of formal languages. *Bull. Eur. Assoc. Theor. Comput. Sci. EATCS*, 89:117–133, 2006. URL: <http://eatcs.org/images/bulletin/beatcs89.pdf>.
- 5 Michael Domaratzki, Derek Kisman, and Jeffrey Shallit. On the number of distinct languages accepted by finite automata with n states. *J. Autom. Lang. Comb.*, 7(4):469–486, 2002. URL: <https://cs.uwaterloo.ca/~shallit/Papers/enum.ps>.
- 6 Andrew Elvey Price, Wenjie Fang, and Michael Wallner. Compacted binary trees admit a stretched exponential, 2019. arXiv:1908.11181.
- 7 Antoine Genitrini, Bernhard Gittenberger, Manuel Kauers, and Michael Wallner. Asymptotic enumeration of compacted binary trees of bounded right height. *J. Combin. Theory Ser. A*, 172:105177, 2020. doi:10.1016/j.jcta.2019.105177.
- 8 John E. Hopcroft and Jeffrey D. Ullman. *Introduction to automata theory, languages, and computation*. Addison-Wesley Publishing Co., Reading, Mass., 1979. Addison-Wesley Series in Computer Science.
- 9 Aleksej D. Korshunov. Enumeration of finite automata. *Problemy Kibernet.*, 34:5–82, 1978. (In Russian).
- 10 Aleksej D. Korshunov. On the number of nonisomorphic strongly connected finite automata. *Elektron. Informationsverarb. Kybernet.*, 22(9):459–462, 1986.
- 11 Valery A Liskovets. Exact enumeration of acyclic deterministic automata. *Discrete Appl. Math.*, 154(3):537–551, 2006. doi:10.1016/j.dam.2005.06.009.
- 12 Michael Wallner. Personal website, 2020. URL: <http://dmg.tuwien.ac.at/mwallner>.



A bijection of plane increasing trees with relaxed binary trees of right height at most one [☆]



Michael Wallner

Institute of Statistical Science, Academia Sinica, 128 Academia Road, Nankang, Taipei 11529, Taiwan

ARTICLE INFO

Article history:

Received 30 June 2017
 Received in revised form 27 March 2018
 Accepted 30 June 2018
 Available online 5 July 2018
 Communicated by T. Calamoneri

Keywords:

Bijection
 Directed acyclic graphs
 Increasing trees
 Fibonacci numbers
 Analytic combinatorics
 Limit laws
 Random generation

ABSTRACT

Plane increasing trees are rooted labeled trees embedded into the plane such that the sequence of labels is increasing on any branch starting at the root. Relaxed binary trees are a subclass of unlabeled directed acyclic graphs. We construct a bijection between these two combinatorial objects and study the therefrom arising connections of certain parameters. Furthermore, we show central limit theorems for two statistics on leaves. We end the study by considering more than 20 subclasses and their bijective counterparts. Many of these subclasses are enumerated by known counting sequences, and thus enrich their combinatorial interpretation.

© 2018 Elsevier B.V. All rights reserved.

1. Introduction

This paper provides a bijection between a class of directed acyclic graphs (DAGs) shown in Fig. 1, and plane increasing trees shown in Fig. 2. The number of elements with n nodes is given by the odd double factorials (OEIS A001147 [18]) $(2n-1)!! := (2n-1)(2n-3)\cdots 3\cdot 1$.

We start with some basic definitions. For more details we refer to the excellent book [7]. A *rooted tree* of size n is a connected undirected acyclic graph with $n+1$ nodes, n edges, and a distinguished node called the root. All trees appearing in this paper will have a root and we will shortly speak only of trees. The root introduces an order in the tree given by generations. The root is in generation 0. All neighbors of the root are in generation 1, and in general, nodes at distance k from the root are in generation k . For an arbitrary node of generation $k > 0$ its unique neighbor in generation $k-1$ is called its *parent*. All other neighbors (which are necessarily in generation $k+1$) are called its *children*.

An *increasing tree* is a labeled rooted tree in which labels along any path from the root to the leaves are in increasing order. For notational convenience we label the nodes of a tree from 0 to n and define its size to be n . This concept was first introduced and intensively investigated by Bergeron, Flajolet, and Salvy [2]. These trees have found vast applications as data structures in computer science, as models in genealogy, and as representations of permutations, to name a few [7,19].

A tree is called *plane* (or sometimes also *ordered*) if the children are equipped with a left-to-right order. In other words, trees with a different order of the children, are considered to be different trees. For example the two trees in the center of Fig. 2 whose roots have two children with labels 1 and 2 are considered to be different trees.

[☆] This research was partially supported by the Austrian Science Fund (FWF) grant SFB F50-03.

E-mail address: michael.wallner@tuwien.ac.at.

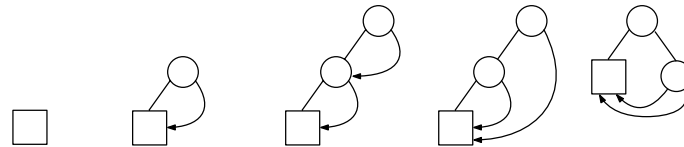


Fig. 1. All relaxed binary trees of size 0, 1, 2. Internal nodes are depicted by circles, the unique leaf is depicted by a square. Note that in general these are not trees as there appear directed and undirected edges.

This defines the classical family of rooted plane increasing trees, which can be generated uniformly at random by a growth process: start with the root and label 0. At step i there are $2i - 1$ possible places to insert node i . Choose one uniformly at random. Note that at a node with out-degree d there are $d + 1$ possible places to insert a new child. This idea is known as the Albert–Barabási model [1]. Note that this method gives a way to generate these trees uniformly at random in linear time.

The *degree* of a node is the number of its neighbors, whereas the *out-degree* is the number of its children. Nodes of degree 1 (and therefore out-degree 0) are called *leaves* or *external nodes*. All other nodes are called *internal nodes*. A *young leaf* is a leaf without left sibling. A *maximal young leaf* is a young leaf with maximal label, see Fig. 2 (see [5, Section 4.3] for a recurrence relation of plane increasing trees built on this parameter).

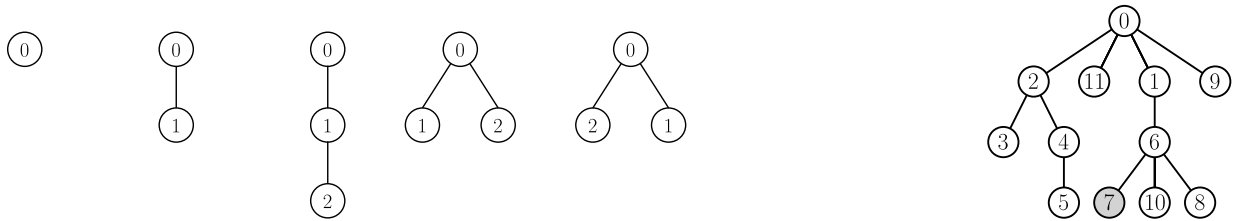


Fig. 2. Left: All plane increasing trees of size 0, 1, 2. Right: An increasing tree of size 11 with the young leaves 3, 5, 7 and the maximal young leaf 7.

The second family we are interested in are the less known compacted and relaxed trees. Let us start with their origin and give a definition thereafter.

In computer science trees are a widely used data structures. Yet real world data often contain vast amount of redundant information. A strategy to save memory is to store every distinct subtree only once and to mark repeated appearances. This concept finds applications in the efficient storage of XML documents [3], and the design and analysis of algorithms and compilers [8]. The gain in memory was studied by Flajolet, Sipala, and Steyaert in [9]. The corresponding procedure defines a subclass of DAGs, called *compacted trees*, which are in bijection with the original trees, see [9,10]. The characterizing property of the generated structure is the uniqueness of each subtree which in the end brings savings in memory.

We will not need a precise definition of compacted trees, but of a related class, the one of relaxed binary trees. These appear when the uniqueness condition of subtrees is neglected. Let us give a precise definition of this class.

A *relaxed tree* of size n is a directed acyclic graph with n internal nodes, one leaf, n internal edges, and n pointers which is rooted at an internal node. It is constructed from a tree of size n , where the first leaf in a postorder traversal is kept and all other leaves are replaced by pointers. These may point to any node that has already been visited in a postorder traversal. It is called *binary* if it was constructed from a binary tree. All relaxed trees considered in this paper will be relaxed binary trees

In Fig. 1 we see all relaxed binary trees of size 0, 1, and 2. Note that for this small sizes all relaxed binary trees are also compacted binary trees. However, for size 3 there are 16 relaxed binary trees and only 15 compacted binary trees.

The *right height* is the maximal number of right edges (or right children) on all paths from the root to any leaf after deleting all pointers. The *level* of a node is the number of right edges on the path from the root to this node, see Fig. 3.

The asymptotic counting problem for relaxed (and the more restrictive class of compacted) binary trees when restricted to being of finite right height was solved in [10].



Fig. 3. Left: A compacted binary tree with right height 2. The labels give the level of the node. Right: The same tree rotated by 45 degrees. The unique leaf is marked by a square.

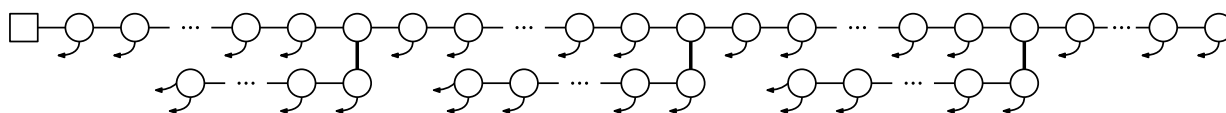


Fig. 4. The structure of a relaxed binary tree with right height at most one. For clarity the pointers are only attached to their source. Note that for a specific relaxed tree the pointers are fixed and point to specific nodes seen before the source node in postorder traversal.

The general structure of relaxed binary trees of right height at most one is shown in Fig. 4. In [10, Theorem 7.3] it was shown that they admit the exponential generating function

$$R(z) = \frac{1}{\sqrt{1-2z}} = \sum_{n \geq 0} (2n-1)!! \frac{z^n}{n!}. \quad (1)$$

In other words, the number of relaxed binary trees of right height at most one of size n is equal to the number of increasing plane trees of size n and is equal to $(2n-1)!!$. These numbers count more than a dozen labeled objects (see OEIS A001147), yet the class of DAGs is to our knowledge the first not labeled one. Bijections appear repeatedly in the literature in order to relate properties of different objects to each other. See for example Janson [11] for a bijection between plane increasing trees and Stirling permutations, or Janson, Kuba, and Panholzer [12] for a bijection between plane increasing trees and ternary increasing trees.

Plan of this article. First, in Section 2, we present our main contribution: a bijection between relaxed binary trees of right height at most one and plane increasing trees. As a corollary we get a uniform random sampling algorithm for relaxed binary trees of size n of right height at most one requiring $\mathcal{O}(n)$ steps and $\mathcal{O}(n)$ memory. In Section 3, we consider the bijection from the point of view of relaxed trees. We investigate the number of elements on level 0 and the number of branches (or, equivalently, leaves on level 1), and map them to parameters of plane increasing trees. Additionally, we show that they admit a central limit theorem. In Section 4, we analyze the bijection from the point of view of plane increasing trees. We collect known results and relate them to relaxed trees. Finally, in Section 5, we investigate more than 20 subclasses of the relaxed trees under consideration. We derive their generating functions and relate their counting sequences to known and unknown ones of the OEIS. Thereby we find new interpretations of sequences and discover unexpected connections to Fibonacci numbers.

2. Bijection

We will need the following concepts: A *branch node* is a node on level 0 without pointers to which a branch of nodes on level 1 is attached. We say that this is the branch node of the nodes in this branch. In the Figs. 4 and 5 we see three branch nodes each. A *cherry* is a node with 2 pointers. For a plane increasing tree \mathcal{T} we denote by \mathcal{T}_k the tree restricted to the labels $0, \dots, k$. For notational convenience, we will speak of relaxed trees always meaning relaxed binary trees.

Algorithm 1 Relaxed binary tree $\mathcal{R} \rightarrow$ Plane Increasing Tree \mathcal{T} .

```

1: Label nodes of  $\mathcal{R}$  in order  $v_0, v_1, \dots, v_n$ 
2: For each cherry  $v_i$  move left pointer to  $v_{i-1}$  ▷  $v_{i-1}$  is  $v_i$ 's branch node
3: For each node set  $p_i :=$  target of pointer of  $v_i$ 
4: if  $\text{level}(v_i) = 1$  and  $p_i = v_0$  then
5:    $p(v_i) :=$  Branch node of branch of  $v_i$ 
6: end if
7: Leaf  $v_0 \rightarrow$  Root of  $\mathcal{T}$ 
8: for  $i$  from 1 to  $n$  do
9:   if  $\text{level}(v_i) = 0$  then ▷ Parent-pointer
10:    Attach  $v_i$  as first child to  $p_i$ 
11:   else ▷ Sibling-pointer
12:    Attach  $v_i$  as direct sibling right of  $p_i$ 
13:   end if
14: end for

```

The bijection stated below is shown on an example in Fig. 5. From top to bottom and left to right a relaxed binary tree of right height at most one is transformed into a plane increasing tree. Reversing these steps gives the inverse bijection.

Algorithm 1 presents a formal description of the transformation from relaxed binary trees to plane increasing trees. Let us start with an arbitrary relaxed binary tree of size n . First, we label the nodes from 0 to n according to an in-order traversal. We use v_i to reference the node with label i . In the labeling process we ignore pointers. Start at the leaf and label it with 0. Then, move to the parent. Whenever we see a node for the first time we attach a label incremented by one. If we meet a branch node we traverse its right branch starting from the cherry from left to right. Then we continue on level 0.

Next, we move the first (or left) pointer of each cherry v_i (which has to be on level 1) to v_{i-1} which is its branch node due to the previous labeling operation. This operation attaches to each node, except the leaf, a unique pointer.

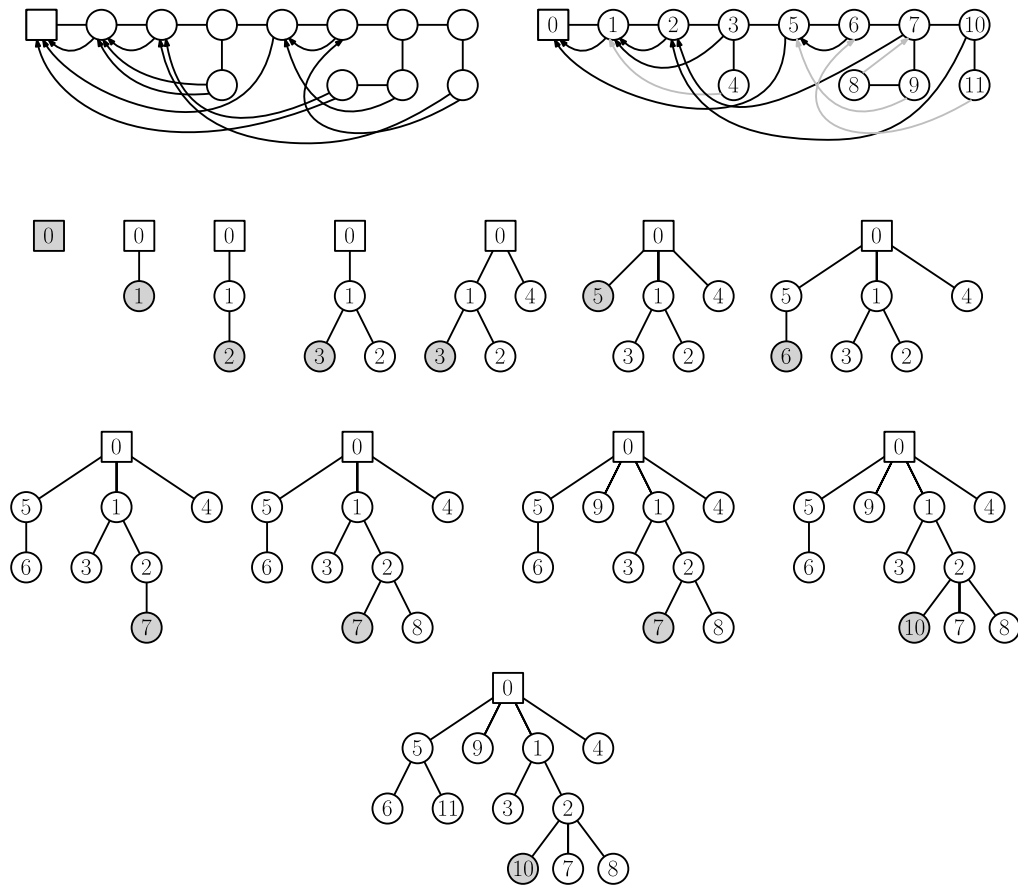


Fig. 5. The bijection applied step by step. Parent-pointers are black, and sibling-pointers are gray. The leaf of the relaxed tree marked by a square is transformed into the root of the increasing plane tree. For the reverse bijection the maximal young leaves are shaded in gray.

Then, we separate the pointers into two sets: parent- and sibling-pointers. A *parent-pointer* is any pointer starting on level 0, and a *sibling-pointer* is any pointer starting on level 1.

Moreover, every sibling-pointer that points to the leaf v_0 is changed to point to its branch node. This is shown for node 8 in Fig. 5.

Finally, we consider the nodes in the order of their labels and build a plane increasing tree. The leaf with label 0 becomes the root. If the node has a parent-pointer, we attach it as a first child (very left) of the node it is pointing to. If the node has a sibling-pointer, we attach it as a direct sibling on the right of the node it is pointing to.

Algorithm 2 Plane Increasing Tree $\mathcal{T} \rightarrow$ Relaxed binary tree \mathcal{R} .

```

1:  $\mathcal{B} := \emptyset$ 
2: for  $k$  from 0 to  $n$  do
3:   if  $v_k$  is a maximal young leaf in  $\mathcal{T}_k$  then
4:     Attach  $\mathcal{B}$  to current root and move its pointer to last node of  $\mathcal{B}$  as left pointer
5:     Attach  $v_k$  as new root with a pointer to the parent of  $v_k$  in  $\mathcal{T}_k$ 
6:      $\mathcal{B} := \emptyset$ 
7:   else
8:     Attach  $v_k$  as root to  $\mathcal{B}$  with a pointer to the left sibling of  $v_k$  in  $\mathcal{T}_k$ 
9:   end if
10: end for
11: Perform 4-5

```

For the reverse bijection we need the notion of young leaves from the introduction. Note that from the previous algorithm, the maximal young leaves are the nodes of level 0. Its formal description is given in Algorithm 2.

Let us start with an arbitrary plane increasing tree of size n . The tree is traversed iteratively in the order of its labels. The algorithm builds the relaxed tree and an auxiliary structure called the branch. At every step we either extend the tree or the branch, which is on some point attached as right child to a node at level 0. At the beginning this branch is empty.

For a label k one of the following two rules applies: First, if the current node k is a maximal young leaf of \mathcal{T}_k then attach the branch to the last node on level 0, move the pointer of this level 0 node as left pointer to the last node of the branch, and set the branch to be empty. Then, attach the node k as new root node on level 0. For the pointer the parent rule applies: set its pointer to the parent of node k in \mathcal{T}_k .

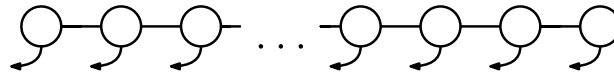


Fig. 6. The generic structure of a sequence of nodes. Note that the last left edge, which is omitted here, could either be an internal edge or a pointer.

Second, if the current node is not a maximal young leaf of \mathcal{T}_k then attach the node k as new root to the branch. For the pointer the sibling rule applies: set the pointer to the direct left sibling of node k in \mathcal{T}_k . In the case that this is the current root at level 0, set the node to the leaf 0.

At the end attach the branch to the current root of level 0 and move its pointer to the last node in the branch as left pointer.

Theorem 2.1. *The procedure above is a bijection between relaxed binary trees of right height at most one of size n and plane increasing trees of size n . It maps nodes of level 0 to maximal young leaves in the growth process of the plane increasing tree.*

Proof. The procedure uniquely transforms relaxed binary trees of right height at most one of size n into plane increasing trees of size n and vice versa.

The main observation is the following: On the one hand, when inserting a node into \mathcal{T}_k there are $k + 1$ places to insert it as maximal young leaf and k not to. On the other hand, when inserting a new node into the relaxed binary tree of size k there are $k + 1$ possibilities for the pointer if the node becomes a new root on level 0, while there are only k possibilities for the pointer if it becomes a new root in the branch. The latter holds, as the pointer cannot point to its (later) branch node. Thus, maximal young leaves correspond to level 0 nodes and non-maximal leaves to level 1 nodes. \square

Corollary 2.2. *Relaxed binary trees of size n of right height at most one can be generated uniformly at random in linear time and with a linear amount of memory.*

Proof. The growth process mentioned in the introduction can be used to generate a rooted increasing tree of size n in linear time using a linear amount of memory (compare with the Albert–Barabási model [1]). Then, Algorithm 2 transforms this tree into a relaxed binary tree of size n with right height at most one in n steps. \square

Remark 2.3. Note that it is possible to directly generate the relaxed tree of size n by using a growth process for relaxed trees with the ideas of Algorithm 2. Basically, at every point one decides to either attach a new root at level 0 or in the branch \mathcal{B} (which corresponds to level 1). In the first case one performs operations 4–6, and in the second case operation 8.

We want to point out that generalizing this method with nested branches it may be used to generate relaxed binary trees with arbitrary or even without height restrictions. However, for the cases of right height larger than 1 this does not generate them uniformly at random.

Plane increasing trees are well-studied objects and many statistics exist on their parameters. This bijection transforms some of them into interesting quantities on relaxed binary trees of right height at most one. But vice versa it also leads to interesting results on plane increasing trees. In the next section we consider parameters which are easy to analyze on relaxed trees, and in the section thereafter we look at known results for plane increasing trees.

3. Parameters of relaxed binary trees

We will use the bivariate generating function $R(z, u) = \sum_{n,k \geq 0} r_{nk} \frac{z^n}{n!} u^k$ with $r_{nk} \geq 0$. It is connected to the original generating function by $R(z, 1) = R(z)$. In particular, for fixed n the sequence $(r_{nk})_{k \geq 0}$ refines the number r_n , and we have $\sum_{k \geq 0} r_{nk} = r_n$. The bivariate generating function $R(z, u)$ will be constructed from the functional equation of $R(z)$ by marking a parameter of interest by an additional variable u . For more details of this concept we refer to the excellent book [8].

In the sequel we will repeatedly talk about a *sequence of nodes*. This is the (sub-)graph given by a set of internal nodes whose left children are always internal nodes (except maybe the last one) and whose right children are always pointers. Its generic structure is shown in Fig. 6.

Let us therefore briefly revisit the combinatorial construction of $R(z)$ given in [10, Corollary 7.2 and Theorem 7.3]. For more details we refer to the deduction in there. The functional equation is equal to

$$R(z) = \frac{1}{1-z} + \frac{1}{1-z} \int \frac{1}{1-z} z(zR(z))' dz. \tag{2}$$

The first term corresponds to the last sequence of nodes on level 0 after the last branch node. It can be interpreted as the initial value or boundary case of the combinatorial construction. The factor in front of the integral represents a sequence of nodes on level 0 between branch nodes. The integral creates a branch node. The factor $\frac{1}{1-z}$ under the integral creates the nodes of a branch on level 1 except the final cherry. Finally, the operator $z(zR(z))'$ creates the cherry of the branch.

Solving this equation, by for example solving the equivalent differential equation, gives the representation of $R(z)$ in (1). In the next subsections we will use this equation by marking certain parameters in order to deduce information on their distribution. For more information on this concept see e.g., [8,20]. We start with the number of elements on level 0.

3.1. Number of elements on level 0 and number of maximal young leaves

Let r_{nk} be the number of relaxed binary trees of right height at most one with k internal nodes on level 0. This is also equal to the number of maximal young leaves in the growth process of a plane increasing tree. Then, the bivariate generating function $R(z, u) = \sum_{n,k \geq 0} r_{nk} \frac{z^n}{n!} u^k$ can be computed from the functional equation (2) by marking nodes on level 0. This gives

$$R(z, u) = \frac{1}{1 - uz} + \frac{u}{1 - uz} \int \frac{z}{1 - z} \frac{\partial}{\partial z} (zR(z, u)) dz,$$

which is then solved to give

$$R(z, u) = \frac{1}{(1 - (1 + u)z)^{\frac{1}{1+u}}}.$$

Let X_n be the random variable of the number of internal nodes on level 0 of relaxed binary trees with right height at most one drawn uniformly at random among all such trees of size n . Then, we have

$$\mathbb{P}(X_n = k) = \frac{[z^n u^k]R(z, u)}{[z^n]R(z, 1)}.$$

Theorem 3.1. *The standardized random variable*

$$\frac{X_n - \mu_1 n}{\sigma_1 \sqrt{n}}, \quad \text{with} \quad \mu_1 = \frac{1}{2} + \frac{\log(n)}{4n} + \mathcal{O}\left(\frac{1}{n}\right) \quad \text{and} \quad \sigma_1^2 = \frac{1}{4} - \frac{\pi^2}{32n} + \mathcal{O}\left(\frac{1}{n^2}\right),$$

converges in law to a standard normal distribution $\mathcal{N}(0, 1)$.

Proof. The result follows from [17, Theorem 4.2] (see also [8, Theorem IX.13]), a generalized quasi-powers scheme for bivariate generating functions. The necessary form is proved by the saddle-point method [8, Chapter VIII]. \square

3.2. Number of branches and number of dominating young leaves

Recall that a *branch* in a relaxed tree is a sequence of nodes on level 1. By the bijection these correspond to maximal young leaves, which are not immediately replaced in the growth process by a new young leaf in the next step. We call these *dominating young leaves*. Let s_{nk} be the number of relaxed binary trees of right height at most one with k branches. Then, the bivariate generating function $S(z, u) = \sum_{n,k \geq 0} s_{nk} \frac{z^n}{n!} u^k$ can be computed in a similar way as done in Section 3.1 by marking only the branch node given by the integral. We get

$$S(z, u) = \frac{1}{\sqrt{1 - 2z + (1 - u)z^2}}.$$

Let Y_n be the random variable giving the number of branches of relaxed binary trees with right height at most one of size n drawn uniformly at random among all such trees of size n :

$$\mathbb{P}(Y_n = k) = \frac{[z^n u^k]S(z, u)}{[z^n]S(z, 1)}.$$

Theorem 3.2. *The standardized random variable*

$$\frac{Y_n - \mu_2 n}{\sigma_2 \sqrt{n}}, \quad \text{with} \quad \mu_2 = \frac{1}{4} - \frac{1}{8n} + \mathcal{O}\left(\frac{1}{n^2}\right) \quad \text{and} \quad \sigma_2^2 = \frac{1}{16} + \frac{1}{32n} + \mathcal{O}\left(\frac{1}{n^2}\right),$$

converges in law to a standard normal distribution $\mathcal{N}(0, 1)$.

Proof. The result follows the same lines as the one of Theorem 3.1. \square

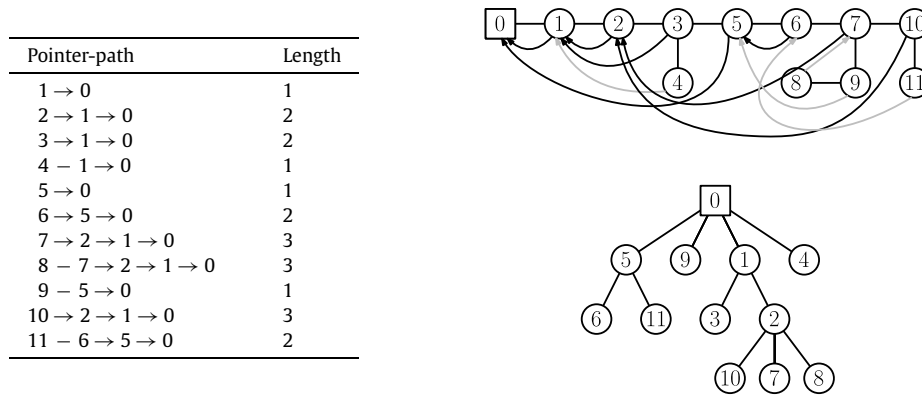


Fig. 7. Pointer-paths of the example in Fig. 5. Parent-pointers are marked by \rightarrow (or black arrows), sibling-pointers are marked by $-$ (or gray arrows).

Table 1

Parameters of plane increasing trees and the corresponding parameters in relaxed binary trees of right height at most one. The constant $s \approx 0.27846$ is the positive solution of $se^{s+1} = 1$.

Plane increasing tree	Relaxed binary tree	$\mathbb{E}X_n$	$\mathbb{V}X_n$
Depth of node n [14]	Length of pointer-path from node n	$\frac{1}{2} \log n + \mathcal{O}(1)$	$\frac{1}{2} \log n + \mathcal{O}(1)$
Number of leaves [15]	Number of nodes without ingoing parent-pointer	$\frac{2}{3}n + \frac{1}{3}$	$\frac{n}{9} + \frac{1}{18} - \frac{1}{6(2n+1)}$
Root degree [2]	Number of pointer-paths of length 1	$\sqrt{\pi n} + \mathcal{O}(1)$	$(4 - \pi)n + \mathcal{O}(1)$
Height [7,16]	Longest pointer-path	$\frac{1}{2s} \log n + o(\log n)$	$\mathcal{O}(1)$

4. Parameters of plane increasing trees

Several parameters of plane increasing trees are well-understood. In order to understand their connection with respect to the stated bijection we introduce the concept of a *pointer-path*. This is a path following only pointers from an arbitrary node to the leaf 0 with two special rules: First, due to the transformation of the left cherry pointers to branch nodes, every internal node has exactly one outgoing pointer. Second, if a sibling-pointer points to the leaf it is interpreted as pointing to its branch node, compare node 8 in Fig. 7. The length of a pointer-path is given by the number of parent-pointers in it. The results for our stated example are shown in Fig. 7.

These pointer-paths also have an interpretation on the level of increasing trees. Starting from any node, one jumps to its left sibling as long as its label is decreasing. This corresponds to sibling-pointers. If this is not possible any more one moves up to its parent which corresponds to a parent-pointer. The length of the pointer-path is the depth of the node. In particular, this gives for every node a “maximal” decreasing sequence of labels encoded in the tree.

There is rich literature on parameters of plane increasing trees, see e.g. [2,7,12–16]. We have summarized four interesting parameters and their counterparts in relaxed binary trees of right height at most one in Table 1. In the first two cases the standardized random variables $\frac{X_n - \mathbb{E}X_n}{\sqrt{\mathbb{V}X_n}}$ converge in distribution to a standard normal distribution, whereas in the third case the normalized random variable $\frac{X_n}{\sqrt{2n}}$ converges in law to a standard Rayleigh distribution given by the density function $xe^{-x^2/2}$. For details on the distribution of the height see [7, Section 6.4] and [4,6].

Remark 4.1. The Rayleigh distribution in the third case follows directly from the closed form of the number of increasing trees of size n and root degree k given by

$$k \cdot \frac{(2n - 3 - k)!}{2^{n-1-k}(n - 1 - k)!}.$$

This was derived in [2, Corollary 5], with a small typo of a missing factor k .

A final interesting parameter is the distribution of out-degrees. Similar to the root degree, the out-degree of a node i corresponds to the number of pointer-paths of length 1 ending with a parent-pointer in i . Note that by definition all pointer-paths ending in 0 end with a parent-pointer. Let λ_d be the limiting probability that a random node has out-degree d . Then, in [2] it was shown that

$$\lambda_d = \frac{4}{(d + 1)(d + 2)(d + 3)}.$$

Thus, the probability that a random node has no ingoing parent-pointer is $\frac{2}{3}$, conforming the proportion of number of leaves above. The probability for one ingoing parent-pointer is $\frac{1}{6}$. The case $\lambda_2 = \frac{1}{15}$ corresponds to either two parent-pointers

whose source nodes do not have sibling-pointers, or one parent-pointer whose source node has exactly one sibling-pointer and this source node has no sibling-pointer.

5. Subclasses

At the end we want to consider some subclasses of relaxed binary trees of right height at most one. We will show connections with certain sequences in the OEIS [18] and solve some open conjectures therein. This adds new combinatorial interpretations to several of them. We start with subclasses that have no initial and/or final sequence of nodes.

5.1. Variations of the initial and final sequences

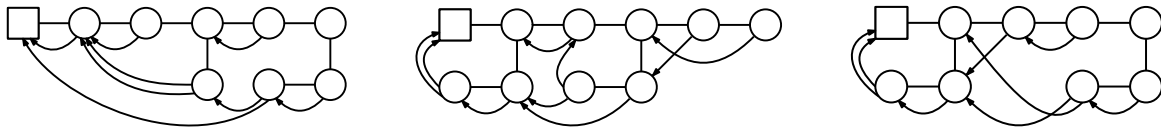


Fig. 8. Left: Subclass \mathcal{R}_1 without initial sequence; Center: \mathcal{R}_2 without final sequence; Right: \mathcal{R}_3 without initial and final sequence.

First, we consider the case of an empty initial sequence, see Fig. 8. In other words all such relaxed trees start with a branch node. By [10, Proposition 6.4] a multiplication by $1 - z$ of the generating function $R(z)$ gives the generating function of this class:

$$\begin{aligned} R_1(z) &:= \frac{1-z}{\sqrt{1-2z}} = 1 + \sum_{n \geq 2} (n-1)(2n-3)!! \frac{z^n}{n!} \\ &= 1 + \frac{z^2}{2!} + 6 \frac{z^3}{3!} + 45 \frac{z^4}{4!} + 420 \frac{z^5}{5!} + 4725 \frac{z^6}{6!} + \dots \end{aligned}$$

The sequence of coefficients is [OEIS A001879](#) and counts the number of descents in all fixed-point-free involutions of $\{1, 2, \dots, 2(n-1)\}$ (we have a shift of minus two). Comparing these numbers to the total number $(2n-1)!!$ of relaxed binary trees of right height at most one, we see that for large n half of all trees fall into this class.

The bijection transforms this class into the one of plane increasing trees where the leaf with the highest label is not a maximal young leaf, except for the tree of size 0. Considering these trees we can give an alternative proof of the counting sequence $(n-1)(2n-3)!!$, $n \geq 2$: There are $(2n-3)!!$ trees of size $n-1$ in which we may insert the leaf with label n at $n-1$ out of the $2n-1$ possible places in order not to create a maximal young leaf.

Second, we consider the related subclass of relaxed binary trees of right height at most one where the final sequence on level 0 after the last branch node consists of only a single leaf, see Fig. 8. If there is no branch node then only the leaf belongs to this class. From the explanations at the beginning of Section 3 we know that the final sequence corresponds to the first term $\frac{1}{1-z}$ in the functional equation (2). Thus, omitting this one and solving the corresponding equation gives the generating function

$$\begin{aligned} R_2(z) &:= \frac{1}{3\sqrt{1-2z}} + \frac{2}{3} - \frac{z}{3} = \sum_{n \geq 0} \frac{(2n-1)!!}{3} \frac{z^n}{n!} \\ &= 1 + \frac{z^2}{2!} + 5 \frac{z^3}{3!} + 35 \frac{z^4}{4!} + 315 \frac{z^5}{5!} + 3465 \frac{z^6}{6!} + \dots \end{aligned}$$

This sequence is [OEIS A051577](#) and has no combinatorial interpretation so far. Note that for the second derivative we have $R_2''(z) = (1-2z)^{-5/2}$. We see that exactly one third of all trees have an empty final sequence.

Trees of this class correspond to plane increasing trees where node 2 is at depth 1 and right of node 1. As above, we can give an alternative proof of the counting sequence. In particular, after 2 steps of the growth process we have a tree with root 0 and a single child 1. Among the three possible places to insert node 2 only one puts it right of node 1. Inserting more nodes will not change the relative position of nodes 1 and 2 at depth 1.

As a third class, we look at the combination of the last two classes. It is given by

$$R_3(z) := (1-z)(R_2(z)-1) + 1 = 1 + \frac{z^2}{2!} + 2 \frac{z^3}{3!} + 15 \frac{z^4}{4!} + 140 \frac{z^5}{5!} + 1575 \frac{z^6}{6!} + \dots$$

The sequence of coefficients gives the new entry [OEIS A288950](#).

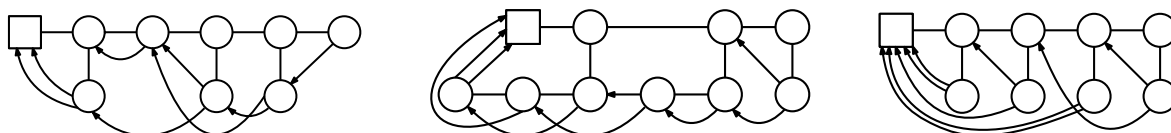


Fig. 9. Left: Subclass \mathcal{R}_4 with at most one node per branch (i.e., on level 1); Center: \mathcal{R}_5 without sequences on level 0; Right: \mathcal{R}_6 is the intersection of \mathcal{R}_4 and \mathcal{R}_5 .

5.2. Trees without sequences – connections with Fibonacci numbers

Fourth, let us consider relaxed trees where every sequence on level 1 consists of only one element, see Fig. 9. Adapting the functional equation (2) we see that the corresponding generating function $R_4(z)$ satisfies

$$R_4(z) = \frac{1}{1-z} + \frac{1}{1-z} \int z(zR(z))' dz, \tag{3}$$

because the factor $\frac{1}{1-z}$ under the integral would create these sequences. Solving this equation with e.g., a computer algebra system like Maple gives

$$\begin{aligned} R_4(z) &= \frac{\exp\left(\frac{1}{\sqrt{5}} \operatorname{artanh}\left(\frac{\sqrt{5}z}{2-z}\right)\right)}{\sqrt{1-z-z^2}} = \frac{1}{\sqrt{1-z-z^2}} \left(\frac{\sqrt{5}+1+2z}{\sqrt{5}-1-2z}\right)^{\frac{\sqrt{5}}{10}} \\ &= 1 + z + 3\frac{z^2}{2!} + 13\frac{z^3}{3!} + 79\frac{z^4}{4!} + 603\frac{z^5}{5!} + 5593\frac{z^6}{6!} + \dots \end{aligned}$$

The second expression is computed by the expression of the artanh function in terms of logarithms. This sequence is [OEIS A213527](#). It implies a different representation.

Lemma 5.1. Let F_n be the n -th Fibonacci number, given by $F_0 = 0$, $F_1 = 1$ and $F_n = F_{n-1} + F_{n-2}$ for $n \geq 2$. Then, we have

$$R_4(z) = \exp\left(\sum_{n \geq 1} \frac{F_{n+1}z^n}{n}\right) = \frac{1}{1-z-z^2} \exp\left(-\sum_{n \geq 1} \frac{F_{n-1}z^n}{n}\right).$$

Proof. On the one hand we differentiate $G(z) := \sum_{n \geq 1} \frac{F_{n+1}z^n}{n}$ and get $G'(z) = \frac{1+z}{1-z-z^2}$. On the other hand we get from (3) that the logarithmic derivative of $R_4(z)$ is also equal to the same expression. Comparing the initial conditions we deduce that $R_4(z) = \exp(G(z))$.

For the second expression note that $F_{n-1} + F_{n+1} = L_n$ which is the n -th Lucas number, [OEIS A000032](#). They are defined by $L_0 = 2$, $L_1 = 1$ and $L_n = L_{n-1} + L_{n-2}$ for $n \geq 2$. Furthermore, integrating the known representation $\sum_{n \geq 0} L_{n+1}z^n = \frac{1+2z}{1-z-z^2}$ gives $\sum_{n \geq 1} \frac{L_n z^n}{n} = \log\left(\frac{1}{1-z-z^2}\right)$. This proves the claim. \square

These relaxed trees correspond bijectively to plane increasing trees where during the growth process never two non-maximal young leaves are inserted after each other. In other words, if k was not a maximal young leaf, then $k+1$ has to be one.

Finally, note that adding constraints like not allowing an initial sequence, not allowing a final sequence, and the combination of both does not lead to any known sequences in the OEIS nor to nice expressions for the generating functions.

As a fifth class, we consider the conjugate class with no sequences between branch nodes on level 0, see Fig. 9. These objects are strongly related to the previous ones. We get

$$\begin{aligned} R_5(z) &= \frac{\exp\left(-\frac{1}{\sqrt{5}} \operatorname{artanh}\left(\frac{\sqrt{5}z}{2-z}\right)\right)}{\sqrt{1-z-z^2}} = \frac{1}{\sqrt{1-z-z^2}} \left(\frac{\sqrt{5}-1-2z}{\sqrt{5}+1+2z}\right)^{\frac{\sqrt{5}}{10}} \\ &= 1 + \frac{z^2}{2!} + 2\frac{z^3}{3!} + 15\frac{z^4}{4!} + 92\frac{z^5}{5!} + 835\frac{z^6}{6!} + \dots \end{aligned}$$

This sequence was so far not known in the OEIS. It is now given by [OEIS A288952](#).

Lemma 5.2. Let F_n be the Fibonacci number defined as in Lemma 5.1. Then, we have

$$R_5(z) = \exp\left(-\sum_{n \geq 1} \frac{F_{n-1}z^n}{n}\right).$$

Proof. From the closed-form expressions we get the relation $R_4(z)R_5(z) = \frac{1}{1-z-z^2}$. Together with the second representation of $R_4(z)$ in Lemma 5.1 this proves the claim. \square

The corresponding plane increasing trees are such that a maximal young leaf has to be followed by a non-maximal young leaf.

Sixth, let us consider a further restriction of the previous class by also not allowing any sequences on level 0, see Fig. 9. This class can be considered maximal with respect to its branches per node. Its functional equation is obtained from (3) by replacing both terms $\frac{1}{1-z}$ by 1. Then, we get

$$R_6(z) := \frac{1}{\sqrt{1-z^2}} = \sum_{n \geq 0} ((2n-1)!!)^2 \frac{z^{2n}}{(2n)!}$$

$$= 1 + \frac{z^2}{2!} + 9 \frac{z^4}{4!} + 225 \frac{z^6}{6!} + 11025 \frac{z^8}{8!} + \dots$$

This sequence is [OEIS A177145](#). We have $R_6(z) = \sum_{n \geq 0} r_{6,n} \frac{z^n}{n!} = \arcsin'(z)$. Here it is easy to derive the counting formula directly: The only element of size 0 is the leaf, $r_{6,0} = 1$. To an element of size $2n$ (which has to be even), we append a branch node connected with a node on level 1 which has two pointers. These may point to all elements of the existing tree which gives $(2n+1)^2$ possibilities. This gives $r_{6,2n+2} = (2n+1)^2 \cdot r_{6,2n}$.

From the previous consideration it is easy to identify the corresponding plane increasing trees. Their growth process consists of alternating insertions of maximal and non-maximal young leaves.

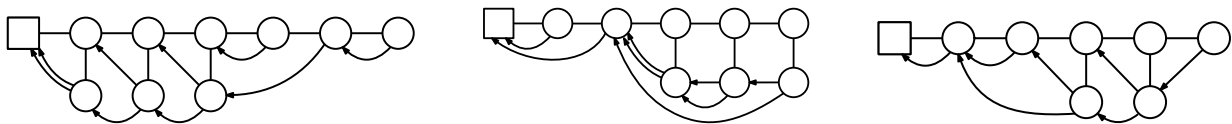


Fig. 10. Left: Subclass \mathcal{R}_7 is like \mathcal{R}_6 with a possible initial sequence on level 0; Center: \mathcal{R}_8 is like \mathcal{R}_6 with a possible final sequence on level 0; Right: \mathcal{R}_9 is like \mathcal{R}_6 with a possible initial and final sequence on level 0.

Seventh, we consider a variation of the previous class by allowing an initial sequence on level 0, see Fig. 10. This corresponds to a multiplication of $R_6(z)$ by $\frac{1}{1-z}$ and we get

$$R_7(z) := \frac{1}{1-z} \frac{1}{\sqrt{1-z^2}} = 1 + z + 3 \frac{z^2}{2!} + 9 \frac{z^3}{3!} + 45 \frac{z^4}{4!} + 225 \frac{z^5}{5!} + 1575 \frac{z^6}{6!} + \dots$$

This sequence is [OEIS A000246](#) and counts the number of permutations in the symmetric group S_n that have odd order. The equivalent class of plane increasing trees is like the previous one except that we allow a sequence of maximal young leaves at the end of the growth process. In other words the consecutive labels k, \dots, n may be maximal young leaves.

Eighth, we consider the analogous variation of allowing a sequence only at the end of level 0, see Fig. 10. The generating function $R_8(z)$ of this class is obtained by omitting only the factor $\frac{1}{1-z}$ in front of the integral in (3). This gives

$$R_8(z) := \frac{1}{3\sqrt{1-z^2}} - \frac{z-2}{3(1-z)^2} = 1 + z + 3 \frac{z^2}{2!} + 10 \frac{z^3}{3!} + 51 \frac{z^4}{4!} + 280 \frac{z^5}{5!} + 1995 \frac{z^6}{6!} + \dots$$

This sequence gives rise to the new entry [OEIS A288953](#). Again, the equivalent plane increasing trees are like the one of case 6 but with a possible sequence of maximal young leaves at the beginning of the growth process, i.e., the consecutive labels $1, \dots, k$ may be maximal young leaves.

Ninth, we consider the combination of the previous two, i.e., allowing sequences at the beginning and at the end only on level 0, see Fig. 10. This gives

$$R_9(z) := \frac{1}{3(1-z)\sqrt{1-z^2}} + \frac{3z^3 - z^2 - 2z + 2}{3(1+z)(1-z)^3}$$

$$= 1 + z + 3 \frac{z^2}{2!} + 13 \frac{z^3}{3!} + 79 \frac{z^4}{4!} + 555 \frac{z^5}{5!} + 4605 \frac{z^6}{6!} + \dots$$

This sequence corresponds to the new entry [OEIS A288954](#). The corresponding plane increasing trees may have consecutive nodes of maximal young leaves $1, \dots, k$ at the beginning and ℓ, \dots, n at the end. Otherwise maximal and non-maximal leaves alternate.

Table 2

Variations of case 10 where each cherry has only one pointer. The comment “Long” marks generating functions which do not have a closed form or are too long to state. The sequence A316666 is a new entry.

Subclass	EGF	Sequence	OEIS
One cherry pointer	$\exp\left(\frac{z}{1-z}\right)$	1, 1, 3, 13, 73, 501, 4051, ...	A000262
No final sequence	Long	1, 0, 1, 5, 29, 201, 1631, ...	A201203
No initial sequence	$(1-z)\exp\left(\frac{z}{1-z}\right)$	1, 0, 1, 4, 21, 136, 1045, ...	A052852
No sequence on level 0	$\frac{e^{-z}}{1-z}$	1, 0, 1, 2, 9, 44, 265, 1854, ...	A000166
No sequence on level 1	$\frac{e^{-z}}{(1-z)^2}$	1, 1, 3, 11, 53, 309, 2119, ...	A000255
+ no initial sequence	$\frac{e^{-z}}{1-z}$	1, 0, 1, 2, 9, 44, 265, 1854, ...	A000166
+ no final sequence	$\frac{3e^{-z}+z-2}{(1-z)^2}$	1, 0, 1, 3, 15, 87, 597, 4701, ...	A316666
+ no initial and final seq.	$\frac{3e^{-z}-z^2}{1-z} - 2$	1, 0, 1, 0, 3, 12, 75, 522, ...	A176408
No seq. on level 0 and 1	$e^{\frac{z}{2}}$	1, 0, 1, 0, 3, 0, 15, 0, 105, 0, ...	A123023
+ initial sequence	$\frac{e^{\frac{z}{2}}}{1-z}$	1, 1, 3, 9, 39, 195, 1185, ...	A130905
+ final sequence	Long	1, 1, 3, 8, 33, 152, 885, 5952, ...	–
+ initial and final seq.	Long	1, 1, 3, 11, 53, 297, 1947, ...	–

5.3. Simplifying the pointer structure

Tenth, consider the adaption of relaxed trees where both pointers of a cherry are forced to point to the same node (or alternatively the second one is fixed). The corresponding generating function $R_{10}(z)$ satisfies a functional equation given by (2) where $(zR(z))'$ is replaced by $R(z)$. The reason is that at the end of the sequence on level 1 we create only one pointer and let the second one point to the same place. Thus, this subclass is best pictured as the one where cherries have just one pointer. This gives

$$R_{10}(z) := \exp\left(\frac{1}{1-z}\right) = 1 + z + 3\frac{z^2}{2!} + 13\frac{z^3}{3!} + 73\frac{z^4}{4!} + 501\frac{z^5}{5!} + 4051\frac{z^6}{6!} + \dots$$

This sequence is [OEIS A000262](#) and counts the number of sets of lists and many other combinatorial objects.

There are many interpretations of the corresponding plane increasing trees. For example a non-maximal young leaf following a maximal young leaf has to be inserted immediately right of it. Or alternatively, as last child of the root. In particular the place of this non-maximal leaf can be chosen uniformly for the class and is fully determined.

Obviously the same subclasses as before can be considered for this class. The 11 additional results are summarized in Table 2.

6. Conclusion

In this paper we provided a bijection between relaxed binary trees (a subclass of directed acyclic graphs arising in the compactification of binary trees) with plane increasing trees. With the latter being well-studied objects, we had access to a vast amount of results on shape parameters which gave us interesting results on the class of relaxed binary trees. Vice versa we were also able to study new parameters on plane increasing trees, by the corresponding parameters on relaxed binary trees. Furthermore, this bijection gave a way to generate relaxed binary trees of size n of right height at most 1 uniformly at random in linear time using a linear amount of memory. Finally, we considered more than 20 subclasses and showed that most of them also enumerate other combinatorial structures. We want to point out that in many cases these are the first non labeled structures.

Acknowledgement

We want to thank the anonymous referee for the detailed comments which significantly improved the presentation of this work.

References

- [1] R. Albert, A.-L. Barabási, Statistical mechanics of complex networks, *Rev. Modern Phys.* 74 (1) (Jan. 2002) 47–97.
- [2] F. Bergeron, P. Flajolet, B. Salvy, Varieties of increasing trees, in: CAAP '92, Rennes, 1992, in: *Lecture Notes in Computer Science*, vol. 581, Springer, Berlin Heidelberg, 1992, pp. 24–48.
- [3] M. Bousquet-Mélou, M. Lohrey, S. Maneth, E. Noeth, XML compression via directed acyclic graphs, *Theory Comput. Syst.* 57 (4) (2015) 1322–1371.
- [4] N. Broutin, L. Devroye, E. McLeish, M. de la Salle, The height of increasing trees, *Random Structures Algorithms* 32 (4) (2008) 494–518.
- [5] D. Callan, A combinatorial survey of identities for the double factorial, ArXiv preprint, arXiv:0906.1317, 2009, <http://arxiv.org/abs/0906.1317>.

- [6] M. Drmota, The height of increasing trees, *Ann. Comb.* 12 (4) (Mar 2009) 373–402.
- [7] M. Drmota, *Random Trees: An Interplay Between Combinatorics and Probability*, Springer Science & Business Media, 2009.
- [8] P. Flajolet, R. Sedgewick, *Analytic Combinatorics*, Cambridge University Press, 2009.
- [9] P. Flajolet, P. Sipala, J.-M. Steyaert, Analytic variations on the common subexpression problem, in: *Automata, Languages and Programming*, in: *Lecture Notes in Computer Science*, vol. 443, Springer, 1990, pp. 220–234.
- [10] A. Genitrini, B. Gittenberger, M. Kauers, M. Wallner, Asymptotic enumeration of compacted binary trees of bounded right height, ArXiv preprint, arXiv:1703.10031, 2017, <http://arxiv.org/abs/1703.10031>.
- [11] S. Janson, Plane recursive trees, Stirling permutations and an urn model, in: *Fifth Colloquium on Mathematics and Computer Science*, Nancy, in: *Discrete Math. Theor. Comput. Sci. Proc., AI, Assoc. Discrete Math. Theor. Comput. Sci.*, 2008, pp. 541–547.
- [12] S. Janson, M. Kuba, A. Panholzer, Generalized Stirling permutations, families of increasing trees and urn models, *J. Combin. Theory Ser. A* 118 (1) (Jan. 2011) 94–114.
- [13] M. Kuba, A. Panholzer, On the degree distribution of the nodes in increasing trees, *J. Combin. Theory Ser. A* 114 (4) (May 2007) 597–618.
- [14] H.M. Mahmoud, Distances in random plane-oriented recursive trees, in: *Asymptotic Methods in Analysis and Combinatorics*, *J. Comput. Appl. Math.* 41 (1–2) (aug 1992) 237–245.
- [15] H.M. Mahmoud, R.T. Smythe, J. Szymański, On the structure of random plane-oriented recursive trees and their branches, *Random Structures Algorithms* 4 (2) (1993) 151–176.
- [16] B. Pittel, Note on the heights of random recursive trees and random m -ary search trees, *Random Structures Algorithms* 5 (2) (1994) 337–347.
- [17] V.N. Sachkov, *Probabilistic Methods in Combinatorial Analysis*, *Encyclopedia of Mathematics and its Applications*, vol. 56, Cambridge University Press, Cambridge, 1997, Translated from the Russian, Revised by the author.
- [18] N.J.A. Sloane, The on-line encyclopedia of integer sequences (OEIS), <http://oeis.org>.
- [19] R.T. Smythe, H.M. Mahmoud, A survey of recursive trees, *Theory Probab. Math. Statist.* 51 (1994) 1–27.
- [20] M. Wallner, A half-normal distribution scheme for generating functions, ArXiv preprint, arXiv:1610.00541, 2016, <http://arxiv.org/abs/1610.00541>.

Rectangular Young tableaux with local decreases and the density method for uniform random generation

Cyril Banderier
LIPN (UMR CNRS 7030)
Université de Paris Nord, France
<http://lipn.univ-paris13.fr/~banderier/>

Philippe Marchal
LAGA (UMR CNRS 7539)
Université de Paris Nord, France
<https://www.math.univ-paris13.fr/~marchal>

Michael Wallner
LaBRI (UMR CNRS 5800)
Université de Bordeaux, France
<http://dmg.tuwien.ac.at/mwallner/>

Abstract

In this article, we consider a generalization of Young tableaux in which we allow some consecutive pairs of cells with decreasing labels. We show that this leads to a rich variety of combinatorial formulas, which suggest that these new objects could be related to deeper structures, similarly to the ubiquitous Young tableaux. Our methods rely on variants of hook-length type formulas, and also on a new efficient generic method (which we call the density method) which allows not only to generate constrained combinatorial objects, but also to enumerate them. We also investigate some repercussions of this method on the D-finiteness of the generating functions of combinatorial objects encoded by linear extension diagrams, and give a limit law result for the average number of local decreases.

Copyright © by the paper's authors. Copying permitted for private and academic purposes.

In: L. Ferrari, M. Vamvakari (eds.): Proceedings of the GASCom 2018 Workshop, Athens, Greece, 18–20 June 2018, published at <http://ceur-ws.org>

1 Introduction

As predicted by Anatoly Vershik in [Ver01], the 21st century should see a lot of challenges and advances on the links of probability theory with (algebraic) combinatorics. A key role is played here by Young tableaux, because of their ubiquity in representation theory [Mac15] and in algebraic combinatorics, as well as their relevance in many other different fields (see e.g. [Sta11]).

Young tableaux are tableaux with n cells labelled from 1 to n , with the additional constraint that these labels increase among each row and each column (starting from the lower left cell). Here we consider the following variant: What happens if we allow exceptionally some consecutive cells with decreasing labels? Does this variant lead to nice formulas if these local decreases are regularly placed? Is it related to other mathematical objects or theorems? How to generate them? This article gives some answers to these questions.

As illustrated in Figure 1, we put a bold red edge between the cells which are allowed to be decreasing. Therefore these two adjacent cells can have decreasing labels (like 19 and 12 in the top row of Figure 1, or 11 and 10 in the untrustable Fifth column), or as usual increasing labels (like 13 and 15 in the bottom row of Figure 1). We call these bold red edges “walls”.

7	18	19	12	21	20	17
2	6	8	9	10	14	16
1	3	4	5	11	13	15

Figure 1: We consider Young tableaux in which some pairs of (horizontally or vertically) consecutive cells are allowed to have decreasing labels. Such places where a decrease is allowed (but not compulsory) are drawn by a bold red edge, which we call a “wall”.

For Young tableaux of shape¹ $n \times 2$ several cases lead directly to nice enumerative formulas for the total number of specific tableaux with $2n$ cells:

1. Walls everywhere: $(2n)!$
2. Horizontal walls everywhere: $\frac{(2n)!}{2^n}$
3. Horizontal walls everywhere in left (or right) column: $(2n - 1)!! = \frac{(2n)!}{2^n n!}$
4. Vertical walls everywhere: $\binom{2n}{n} = \frac{(2n)!}{(n!)^2}$
5. No walls: $\frac{1}{n+1} \binom{2n}{n} = \frac{(2n)!}{(n+1)(n!)^2}$

In this article we are interested in the enumeration and the generation of Young tableaux (of different rectangular shapes) with such local decreases, and we investigate to which other mathematical notions they are related. Section 2 focuses on the case of horizontal walls: We give a link with the Chung–Feller Theorem, binomial numbers and a Gaussian limit law. Section 3 focuses on the case of vertical walls: We give a link with hook-length type formulas. Section 4 presents a generic method, which allows us to enumerate many variants of Young tableaux (or more generally, linear extensions of posets), and which also offers an efficient uniform random generation algorithm, and links with D-finiteness.

¹We will refer to “ $n \times m$ Young tableaux”, or “Young tableaux of shape $n \times m$ ”, for rectangular Young tableaux with n rows and m columns. They are trivially in bijection with $m \times n$ Young tableaux.

2 Vertical walls, Chung–Feller and binomial numbers

In this section we consider a family of Young tableaux having some local decreases at places indicated by vertical walls, see Figure 2.

Theorem 2.1. *The number of $n \times 2$ Young tableaux with k vertical walls is equal to*

$$v_{n,k} = \frac{1}{n+1-k} \binom{n}{k} \binom{2n}{n}.$$

Proof. We apply a bijection between two-column Young tableaux of size $2n$ with k walls and Dyck paths without the positivity constraint of length $2n$ and k coloured down steps. These paths start at the origin, end on the x -axis and are composed out of up steps $(1, 1)$, and coloured down steps $(1, -1)$ which are either red or blue.

Given an arbitrary two-column Young tableau, the m -th step of the associated path is an up step if the entry m appears in the left column, while the m -th step is a down step, if the m -th entry appears in the right column. Furthermore, we associate colours to the down steps: If the m -th down step is in a row with a wall we colour it red, and blue otherwise.

Thus, $v_{n,k}$ counts the number of paths with exactly k red down steps. Note that the down steps of a path below the x -axis are always red because a wall has to be involved, yet above the x -axis down steps can have any colour. We decompose paths with k coloured down steps with respect to the number of steps which are below the x -axis. By the Chung–Feller Theorem [CF49] (see also [Che08] for a bijective proof) the number of Dyck paths of length $2n$ with i down steps below the x -axis is independent of i and equal to the Catalan number $\text{Cat}_n = \frac{1}{n+1} \binom{2n}{n}$. When i steps are below the x -axis we have to colour $k - i$ of the remaining $n - i$ steps above the x -axis red. This gives

$$v_{n,k} = \sum_{i=0}^k \binom{n-i}{k-i} \text{Cat}_n = \binom{n+1}{k} \text{Cat}_n,$$

and the claim follows. \square

As a simple consequence, we get the following result.

Corollary 2.2. *The average number of linear extensions of a random $n \times 2$ Young tableau with k walls, where the location of these walls is chosen uniformly at random, is*

$$\frac{1}{n+1-k} \binom{2n}{n}.$$

Proof. In a two-column Young tableau of size $2n$ we have $\binom{n}{k}$ possibilities to add k walls. \square

We now conclude this section with a limit law result.

Theorem 2.3. *Let X_n be the random variable for the number of walls in a random $n \times 2$ Young tableau chosen uniformly at random. The rescaled random variable $\frac{X_n - n/2}{\sqrt{n/4}}$ converges to the standard normal distribution $\mathcal{N}(0, 1)$.*

Proof. We see that the total number of two-column Young tableaux of size n with walls is equal to

$$\sum_{k=0}^n v_{n,k} = \text{Cat}_n (2^{n+1} - 1).$$

Then, the previous results show that

$$\mathbb{P}(X_n = k) = \binom{n+1}{k} \frac{1}{2^{n+1} - 1},$$

which is a slight variation of a binomial distribution with parameters $n+1$ and probability $1/2$. By the well-known convergence of the rescaled binomial distribution to a normal distribution the claim holds (see e.g. [FS09]). \square

14	12
10	13
9	11
8	7
4	6
3	5
2	1

Figure 2: Example of one of our $n \times 2$ Young tableaux with walls.

3 Horizontal walls and the hook-length formula

The hook-length formula is a well-known formula to enumerate standard Young tableaux of a given shape (see e.g. [Mac15, Sta11]). What happens if we add walls in these tableaux? Let us first consider the case of a Young tableau of size n such that its walls cut the corresponding tableau into m disconnected parts without walls of size k_1, \dots, k_m (e.g., some walls form a full horizontal or vertical line). Then, the number of fillings of such a tableau is trivially:

$$\frac{n!}{k_1! \dots k_m!} \prod_{i=1}^m \text{HookLengthFormula}(\text{subtableau of size } k_i).$$

So in the rest of article, we focus on walls which are not trivially splitting the problem into subproblems: They are the only cases for which the enumeration (or the random generation) is indeed challenging.

We continue our study with families of Young tableaux of shape $m \times n$ having some local decreases at places indicated by horizontal walls in the left column. We will need the following lemma counting special fillings of Young tableaux.

Lemma 3.1. *The number of $n \times 2$ “Young tableaux” with 2λ cells filled with the numbers $1, 2, \dots, 2n$ for $n \geq \lambda$ such that (the number $2n$ is used and) all consecutive numbers between the minimum of the second column and $2n$ are used is equal to*

$$\binom{2n}{\lambda} - \binom{2n}{\lambda-1}. \quad (1)$$

Proof. The constraint on the maximum implies that all not used numbers are smaller than the number in the bottom right cell. Therefore it is legitimate to add these numbers to the tableaux. In particular, we create a standard Young tableau of shape $(\lambda, 2n - \lambda)$ (i.e., the first column has λ cells and the second one $2n - \lambda$) which is in bijection with the previous tableau.

Next we build a bijection between standard Young tableaux of shape $(\lambda, 2n - \lambda)$ and Dyck paths with up steps $(1, 1)$ and down steps $(1, -1)$ starting at $(0, 2(n - \lambda))$, always staying above the x -axis and ending on the x -axis after $2n$ steps. In particular, if the number i appears in the left column, the i -th step is an up step, and if it appears in the right column, the i -th step is a down step.

Finally, note that these paths can be counted using the reflection principle [And87]. In particular, there are $\binom{2n}{\lambda}$ possible paths from $(0, 2(n - \lambda))$ to $(2n, 0)$. Yet, $\binom{2n}{\lambda-1}$ “bad” paths cross the x -axis at some point. This can be seen, by cutting such a path at the first time it reaches altitude -1 . The remaining path is reflecting along the horizontal line $y = -1$ giving a path ending at $(2n, -2)$. It is easy to see that this is a bijection between bad paths from $(0, 2(n - \lambda))$ to $(2n, 0)$ and all paths from $(0, 2(n - \lambda))$ to $(2n, -2)$. The latter is obviously counted by $\binom{2n}{\lambda-1}$, as $\lambda - 1$ of the $2n$ steps have to be up steps. \square

Theorem 3.2. *The number of $n \times 2$ Young tableaux of size $2n$ with k walls in the first column at heights $0 < h_i < n$, $i = 1, \dots, k$ with $h_i < h_{i+1}$ is equal to*

$$\frac{1}{2n+1} \prod_{i=1}^{k+1} \binom{2h_i+1}{h_i-h_{i-1}},$$

with $h_0 := 0$ and $h_{k+1} := n$.

Remark 3.3. Denoting consecutive relative distances of the walls by $\lambda_i := h_i - h_{i-1}$ for $i = 1, \dots, k+1$ the previous result can also be stated as

$$\frac{1}{2n+1} \prod_{i=1}^{k+1} \binom{2(\lambda_1 + \dots + \lambda_i) + 1}{\lambda_i}.$$

Proof. We will show this result by induction on the number of walls k . For $k = 0$ the result is clear as we are counting two-column standard Young tableaux which are counted by Catalan numbers (for a proof see also Lemma 3.1 with $\lambda = n$).

Next, assume the formula has been shown for $k - 1$ walls and arbitrary n . Choose a proper filling with k walls and cut the tableau at the last wall at height h_k into two parts. The top part is a Young tableau with $2(n - h_k)$

elements and no walls, yet labels between 1 and $2n$. Furthermore, it has the constraint that all numbers larger than the element in the bottom right cell have to be present. This is due to the fact that all elements in lower cells must be smaller. In other words, these are the objects of Lemma 3.1 and counted by (1).

The bottom part is a Young tableau with $k - 1$ walls and $2h_k$ elements (after proper relabelling). By our induction hypothesis this number is equal to

$$\frac{1}{2h_k + 1} \prod_{i=1}^k \binom{2h_i + 1}{h_i - h_{i-1}}.$$

As a final step, we rewrite Formula (1) into

$$\frac{2(n - \lambda) + 1}{2n + 1} \binom{2n + 1}{\lambda},$$

and set $\lambda := n - h_k$. Multiplying the last two expressions then shows the claim. \square

Remark 3.4. Note that so far we have not found a direct combinatorial interpretation of this formula. However, note that in general $\binom{2n+1}{\lambda}$ does not have to be divisible by $2n + 1$.

Let us now also give the general formula for $n \times m$ Young tableaux with walls of lengths $m - 1$ from columns 1 to $m - 1$, i.e., a hole in column m and nowhere else in a row with walls. Before we state the result, let us define for integers n, k the falling factorial $(n)_k := n(n - 1) \cdots (n - k + 1)$ and for integers n, m_1, \dots, m_k such that $n \geq m_1 + \dots + m_k$ the (shortened) multinomial coefficient² $\binom{n}{m_1, m_2, \dots, m_k} := \frac{n!}{m_1! m_2! \cdots m_k! (n - m_1 - \dots - m_k)!}$.

Theorem 3.5. *The number of $n \times m$ Young tableaux of size mn with k walls from column 1 to $m - 1$ at heights $0 < h_i < n$, $i = 1, \dots, k$ with $h_i < h_{i+1}$ is equal to*

$$\frac{(m - 1)!}{(mn + m - 1)_{m-1}} \left(\prod_{i=1}^{k+1} \prod_{j=1}^{m-2} \binom{\lambda_i + j - 1}{j} \right) \binom{m(\lambda_1 + \dots + \lambda_k) + m - 1}{\lambda_1, \dots, \lambda_k},$$

where $\lambda_i := h_i - h_{i-1}$ and the λ_i 's in the multinomial coefficients appear $m - 1$ times.

Proof (Sketch). First derive an extension of Lemma 3.1 proved by the hook-length formula and then compute the product. Note that this gives a telescoping factor, giving the first factor. \square

Just as one more example, here is a more explicit example of what it gives.

Corollary 3.6. *The number of $n \times 4$ Young tableaux with k walls from column 1 to 3 at heights $0 < h_i < n$, $i = 1, \dots, k$ with $h_i < h_{i+1}$ is equal to*

$$\frac{6}{(4n + 3)(4n + 2)(4n + 1)} \left(\prod_{i=1}^{k+1} \frac{2}{(\lambda_i + 1)^2 (\lambda_i + 2)} \right) \binom{4(\lambda_1 + \dots + \lambda_k) + 3}{\lambda_1, \lambda_1, \lambda_1},$$

with $\lambda_i := h_i - h_{i-1}$.

Let us consider some other special cases. For example, consider tableaux with walls between every row and a hole in the last column. For this case we set $\lambda_i = 1$ for all i . This gives the general formula $\frac{(mn)!}{n!(m!)^n}$, for $n \times m$ tableaux, see OEIS A001147 for $m = 2$ and OEIS A025035 to OEIS A025042 for the special cases $m = 3, \dots, 10$.

Now that we gave several examples of closed-form formulas enumerating some families of Young tableaux with local decreases, we go to harder families which do not necessarily lead to a closed-form result. However, we shall see that we have a generic method to get useful alternative formulas (based on recurrences), also leading to an efficient uniform random generation algorithm.

²In the literature, one more often finds the notation $\binom{n}{m_1, m_2, \dots, m_k, n - m_1 - \dots - m_k} := \frac{n!}{m_1! m_2! \cdots m_k! (n - m_1 - \dots - m_k)!}$. But we opted in this article for a more suitable notation to the eyes of our readers!

4 The density method, D-finiteness, random generation

In this section, we present a generic approach which allows us to enumerate and generate any shape involving some walls located at periodic positions. To keep it readable, we illustrate it with a specific example (without loss of generality).

So, we now illustrate the method on the case of a $2n \times 3$ tableau where we put walls on the right and on the left column at height $2k$ (for $1 \leq k \leq n-1$), see the leftmost tableau in Figure 3. In order to have an easier description of the algorithm (and more compact formulas), we generate/enumerate first similar tableaux with an additional cell at the bottom of the middle column, see the middle tableau in Figure 3: It is a polyomino Polyo_n with $6n+1$ cells. There are trivially $(6n+1)!$ fillings of this polyomino with the numbers 1 to $6n+1$. Some of these fillings are additionally satisfying the classical constraints of Young tableaux (i.e., the labels are increasing in each row and each column), with some local decreases allowed between cells separated by a wall (as shown with bold red edges in Figure 3). Let f_n be the number of such constrained fillings.

To compute f_n we use a generic method which we call the *density method*, which we introduced and used in [Mar18, Mar16, BMW18]. It relies on a geometric point of view of the problem: Consider the hypercube $[0, 1]^{6n+1}$ and associate to each coordinate a cell of Polyo_n . To almost every element α of $[0, 1]^{6n+1}$ (more precisely, every element with all coordinates distinct) we can associate a filling of Polyo_n : Put 1 into the cell of Polyo_n corresponding to the smallest coordinate of α , 2 into the cell of Polyo_n corresponding to the second smallest coordinate of α and so on. The reverse operation associates to every filling of Polyo_n a region of $[0, 1]^{6n+1}$ (which is actually a polytope). We call \mathcal{P} the set of all polytopes corresponding to correct fillings of Polyo_n (i.e., respecting the order constraints). This \mathcal{P} is also known as the “order polytope” in poset theory.

Let us explain how the density method works. It requires two more ingredients. The first one is illustrated in Figure 3: It is a generic building block with 7 cells with names X, Y, Z, R, S, V, W. We put into each of these cells a number from $[0, 1]$, which we call x, y, z, r, s, v, w , respectively. The second ingredient is the sequence of polynomials $p_n(x)$, defined by the following recurrence (which in fact encodes the full structure of the problem, building block after building block):

$$p_{n+1}(z) = \int_0^z \int_x^z \int_0^y \int_r^z \int_z^1 \int_y^w p_n(v) dv dw ds dr dy dx, \quad \text{with } p_0 = 1. \quad (2)$$

The fact that this sequence of nested integrals encodes the full structure of the problem (i.e. all the inequalities) is better stressed with the following writing:

$$p_{n+1}(z) = \int_{0 < x < z} \int_{x < y < z} \int_{0 < r < y} \int_{r < s < z} \int_{z < w < 1} \int_{y < v < w} p_n(v) dv dw ds dr dy dx, \quad \text{with } p_0 = 1. \quad (3)$$

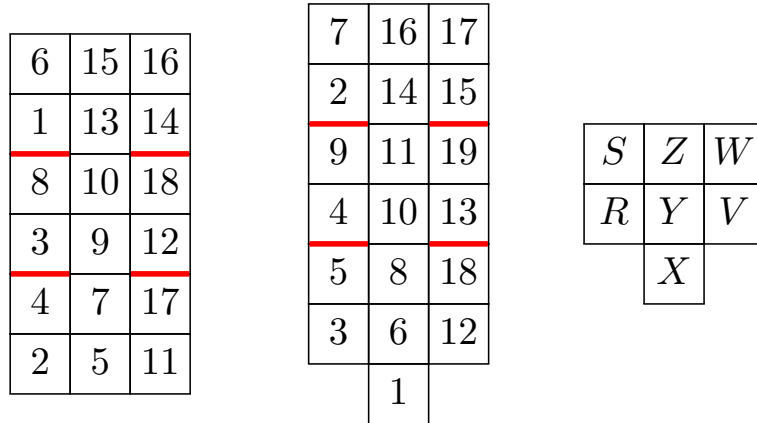


Figure 3: **Left:** A $2n \times 3$ Young tableau with walls. **Centre:** Our algorithm first generates a related labelled shape, Polyo_n , with one more cell in its bottom (removing this cell and relabelling the remaining cells gives the left tableau). **Right:** The “building block” of 7 cells. Each polyomino Polyo_n is made of the overlapping of n such building blocks.

Let us now give a more algorithmic presentation of our method:

Density method algorithm

1 Initialization: We order the building blocks from $k = n - 1$ (the top one) to $k = 0$ (the bottom one). We start with the value $k := n - 1$, i.e. the building block from the top. Put into its cell Z a random number z with density $p_n(z)/\int_0^1 p_n(t) dt$. We repeat the following process until $k = 0$:

2 Filling: Now that Z is known, put into the cells X, Y, R, S, V, W random numbers x, y, r, s, v, w with conditional density

$$g_{k,z}(x, y, r, s, v, w) := \frac{1}{p_{k+1}(z)} p_k(x) \mathbf{1}_{\mathcal{P}_z},$$

where $\mathbf{1}_{\mathcal{P}_z}$ is the indicator function of the k -th building block (with value z in cell Z):

$$\mathbf{1}_{\mathcal{P}_z} := \mathbf{1}_{\{0 \leq x \leq y \leq z, 0 \leq r \leq y, r \leq s \leq z, z \leq w \leq 1, y \leq v \leq w\}}.$$

3 Iteration: Consider X as the Z of the next building block. Set $k := k - 1$ and go to step 2.

Next we prove that this algorithm generates Young tableaux with walls uniformly and determine its cost.

Theorem 4.1. *The density method algorithm is a uniform random generation algorithm with quadratic time complexity and linear space complexity.*

Proof. Let us indeed prove that the algorithm gives a random element of our set of polytopes \mathcal{P} with the uniform measure. Our algorithm yields a $(6n + 1)$ -tuple $\mathbf{x} := (x_j, y_i, r_i, s_i, v_i, w_i, 0 \leq j \leq n, 0 \leq i \leq n - 1)$ whose density is the product of the conditional densities:

$$\frac{p_n(x_n)}{\int_0^1 p_n(t) dt} \prod_{i=1}^n g_{n-i, x_{n-i+1}}(x_{n-i}, y_{n-i}, r_{n-i}, s_{n-i}, v_{n-i}, w_{n-i}) \tag{4}$$

The crucial point is that this product is telescopic and equal to

$$\frac{p_n(x_n)}{\int_0^1 p_n(t) dt} \prod_{k=0}^{n-1} \frac{p_k(x_k) \mathbf{1}_{\mathcal{P}_{x_k}}}{p_{k+1}(x_{k+1})} = \frac{p_0(x_0) \mathbf{1}_{\mathcal{P}}}{\int_0^1 p_n(t) dt} = \frac{\mathbf{1}_{\mathcal{P}}}{\int_0^1 p_n(t) dt} \quad (\text{as } p_0 = 1), \tag{5}$$

where $\mathbf{1}_{\mathcal{P}_{x_k}}$ is as in the algorithm above the indicator function of the k -th block (where the local variables x, y, r, s, v, w, z of the algorithm are now $x_k, y_k, r_k, s_k, v_k, w_k, z_k$) and where the product $\mathbf{1}_{\mathcal{P}}$ of these indicator functions is the indicator function of the full polytope (with n blocks): $\mathbf{1}_{\mathcal{P}} = \prod_{k=0}^{n-1} \mathbf{1}_{\mathcal{P}_{x_k}}$.

Therefore, this density is constant on our set \mathcal{P} of polytopes and zero elsewhere, which is exactly what we wanted. The fact that it is a density implies that its integral is 1, whence

$$\int_{[0,1]^{6n+1}} \mathbf{1}_{\mathcal{P}} d\mathbf{x} = \int_0^1 p_n(t) dt. \tag{6}$$

Now if we choose a random uniform element in $[0, 1]^{6n+1}$, the probability that it belongs to our set \mathcal{P} of polytopes is

$$\int_{[0,1]^{6n+1}} \mathbf{1}_{\mathcal{P}} d\mathbf{x}. \tag{7}$$

But due to the reasoning above, this is also the probability that a random uniform filling of our building block is correct (i.e., respects the order constraints). Thus this probability is given by $\int_0^1 p_n(t) dt / (6n + 1)!$.

This implies that $f_n = (6n + 1)! \int_0^1 p_n(t) dt$.

Finally, as each step relies on the computation and the evaluation of the associated polynomial $p_n(z)$ (of degree proportional to n), this gives a quadratic time complexity, and takes linear space. \square

Remark 4.2. If one wants to generate many diagrams and not just one, then it is valuable to make a precomputation phase computing and storing all the polynomials p_n . The rest of the algorithm is the same. For each new object generated, this is saving $O(n^2)$ time, to the price of $O(n^2)$ memory. The algorithm is globally still of quadratic time complexity (because of the evaluation at each step of $p_k(x)$, while $p_{k+1}(z)$ was already evaluated).

Remark 4.3. If one directly wants to generate $2n \times 3$ Young tableaux with decreases instead of our strange polyomino shapes Polyo_n , then one still uses the same relation between p_{n+1} and p_n but p_0 is not defined and p_1 has a more complicated form. Another way is to generate Polyo_n , and to reject all the ones not having a 1 in the bottom cell, then to remove this bottom cell and to relabel the remaining cells from 1 to $6n$ (see Figure 3). This still gives a fast algorithm of $O(n^2)$ time complexity (the only difference being the cost of the initial algorithm which is the multiplicative constant included in the big-O).

Using dynamic programming or clever backtracking algorithms allows hardly to compute the sequence f_n (the number of fillings of the diagram) for $n \geq 3$. In the same amount of time, the density method allows us to compute thousands of coefficients via the relation $f_n = (6n + 1)! \int_0^1 p_n(z)$, where the polynomial $p_n(z)$ is computed via the recurrence

$$p_{n+1}(z) = \int_0^z \frac{1}{24}(z-1)(x-z)(3x^3 - 7x^2z - xz^2 - z^3 - 2x^2 + 4xz + 4z^2)p_n(x) dx. \quad (8)$$

This gives the sequence $\{f_n\}_{n \geq 0}$:

{1, 12, 8550, 39235950, 629738299350, 26095645151941500, 2323497950101372223250, 392833430654718548673344250, 115375222087417545717234273063750, 55038140590519890608190921051205837500, 40460077456664688766902540022810130044068750, 4393840235884118464495128448703896167747914784375, ... }.

As far as we know, there is no further simple expression for this sequence. This concludes our analysis of the model given by Figure 3.

We can additionally mention that the generating function associated to the sequence of polynomials $p_n(x)$ has a striking property:

Theorem 4.4. *The generating function $G(t, z) := \sum_{n \geq 0} p_n(z)t^n$ is D-finite³ in z .*

Proof. The general scheme (whenever one has one hole between the walls) is

$$p_{n+1}(z) = \int_0^z Q(x, z)p_n(x) dx, \quad (9)$$

where Q is a polynomial in x and z , given by $Q(x, z) := \int_{\mathcal{P}_z} 1$. The fact that there is just one hole between the walls guarantees that all the other variables encoding the faces of the polytope \mathcal{P}_z will disappear in this integration. Let d be the degree of Q in z , applying $\frac{\partial^{d+1}}{\partial z^{d+1}}$ to both sides of Formula 9 leads to a relation between the $(d+1)$ -st derivative of p_{n+1} and the first $(d+1)$ derivatives of p_n . Multiplying this new relation by t^{n+1} and summing over $n \geq 0$ leads to the D-finite equation for $G(t, z)$. \square

Note that $G(t, z)$ is D-finite in z , but is (in general) not D-finite in t . When it is D-finite in t , our algorithm has a better complexity (namely, a $O(n^{3/2})$ time complexity), because it is then possible to evaluate $p_n(z)$ in time $O(\sqrt{n} \ln n)$ instead of $O(n)$. See [BCGLSS17, Chapter 15] for more details on these complexity issues.

5 Conclusion

We presented a new way to enumerate and generate Young tableaux with local decreases (and, more generally, linear extensions of posets). Our approach is different from the classical way to generate Young tableaux (e.g. via the Greene–Nijenhuis–Wilf algorithm, see [GNW84]), which relies on the existence of an enumeration by a simple product formula (given by the hook-length formula). As there is no such simple product formula for the more general cases we considered here, such an approach cannot work anymore. Obviously, in order to generate these objects, there is the alternative to use some naive “brute-force-like” methods (like e.g. dynamic programming with backtracking). However this leads to an exponential time algorithm. The density method which we presented here is the only method we are aware of which leads to a quadratic cost uniform random generation algorithm.

³A function $F(z)$ is D-finite if it satisfies a linear differential equation, with polynomial coefficients in z . See e.g. [FS09] for their role in enumeration and asymptotics of combinatorial structures.

It would be a full project to examine many more families of Young tableaux with local decreases, to check which ones lead to nice generating functions, to give bijections, and so on. This article presented three different approaches to handle them: bijections, hook-length-like formulas, and the density method. Let us emphasize again that the last one is of great generality. We will give more examples in the long version of this article.

Acknowledgements

This work was initiated during the postdoctoral position of Michael Wallner at the University of Paris Nord, in September-December 2017, thanks a MathStic funding. The subsequent part of this collaboration was funded by the Erwin Schrödinger Fellowship of the Austrian Science Fund (FWF): J 4162-N35.

References

- [And87] D. André. Solution directe du problème résolu par M. Bertrand. *Comptes Rendus de l'Académie des Sciences*, 105:436–437, 1887.
- [BMW18] C. Banderier, P. Marchal and M. Wallner. Periodic Pólya urns and an application to Young tableaux. *To appear in Proceedings of the 29th International Conference on Probabilistic, Combinatorial and Asymptotic Methods for the Analysis of Algorithms (AofA 2018), Uppsala, 2018*, pp. 1–12, 2018.
- [BCGLSS17] A. Bostan, F. Chyzak, M. Giusti, R. Lebreton, G. Lecerf, B. Salvy and É. Schost. *Algorithmes Efficaces en Calcul Formel*. Frédéric Chyzak (auto-édit.), Palaiseau, September 2017, 686 pp. Printed by CreateSpace.
- [Che08] Y.-M. Chen. The Chung–Feller theorem revisited. *Discrete Mathematics*, 308(7):1328–1329, 2008.
- [CF49] K. L. Chung and W. Feller. On fluctuations in coin-tossing. *Proceedings of the National Academy of Sciences of the United States of America*, 35:605–608, 1949.
- [FS09] P. Flajolet and R. Sedgewick. *Analytic Combinatorics*. Cambridge University Press, 2009.
- [GNW84] C. Greene, A. Nijenhuis and H. S. Wilf. Another probabilistic method in the theory of Young tableaux. *Journal of Combinatorial Theory Series A*, 37:127–135, 1984.
- [Mac15] I. G. Macdonald. *Symmetric functions and Hall polynomials*. Oxford Classic Texts in the Physical Sciences. The Clarendon Press, Oxford University Press, second edition, 2015.
- [Mar16] P. Marchal. Rectangular Young tableaux and the Jacobi ensemble. *Discrete Mathematics and Theoretical Computer Science Proceedings*, BC:839–850, 2016.
- [Mar18] P. Marchal. Permutations with a prescribed descent set. *This Proceedings Volume*, 2018.
- [Sta11] R. P. Stanley. *Enumerative combinatorics. Volume 1*. Cambridge University Press, 2nd edition, 2011.
- [Ver01] A. M. Vershik. Randomization of Algebra and Algebraization of Probability. In: B. Engquist, W. Schmid (Eds.): *Mathematics unlimited—2001 and beyond.*, pp. 1157–1166. Springer, 2001.

Young tableaux with periodic walls: counting with the density method

Cyril Banderier^{*1} and Michael Wallner^{†2}

¹LIPN, University Sorbonne Paris Nord, Villetaneuse, France

²Institute of Discrete Mathematics and Geometry, TU Wien, Vienna, Austria

Abstract. We consider a generalization of Young tableaux in which we allow some consecutive pairs of cells with decreasing labels, conveniently visualized by a "wall" between the corresponding cells. Some shapes can be enumerated by variants of hook-length type formulas. We focus on families of tableaux (like the so-called "Jenga tableaux") having some periodic shapes, for which the generating functions are harder to obtain. We get some interesting new classes of recurrences, and a surprisingly rich zoo of generating functions (algebraic, hypergeometric, D-finite, differentially-algebraic). Some patterns lead to nice bijections with trees, lattice paths, or permutations. Our approach relies on the density method, a powerful way to perform both random generation and enumeration of linear extensions of posets.

Keywords: Young tableaux, analytic combinatorics, generating functions, D-finite functions, hypergeometric functions, differentially-algebraic functions, random generation, density method, linear extensions of posets

1 Introduction

Counting the number of linear extensions of a poset is known to be a hard problem; it was even proven to be #P-complete by Brightwell and Winkler [9]. The enumeration is even still #P-complete when restricted to posets of height 2; see Dittmer and Pak [11]. This enumeration challenge is also strongly connected to the question of uniform random generation. While there exist thousands of *ad hoc approaches* to generate combinatorial structures (see, e.g., [18, 22]), there are few *generic methods* for their uniform random generation: one could name rejection algorithms and Markov chain sampling [17], the recursive method [15, 22], generating trees [2], and Boltzmann sampling [12]. Another important method that we want to promote and to add to this list is the *density method*. We will illustrate its power and its flexibility in this article by applying it to many different posets.

^{*}<https://lipn.fr/~banderier>

 <https://orcid.org/0000-0003-0755-3022>

[†]<https://dmg.tuwien.ac.at/mwallner/>

 <https://orcid.org/0000-0001-8581-449X>

Michael Wallner was supported by the Austrian Science Fund (FWF): J 4162 and P 34142.

What we call the density method is an appropriate combination of recurrences and integral representations of order polytope volumes in order to enumerate poset structures. For this reason, as suggested by one referee, it could also be called the *polytope volume method*. Some ancestors of this natural idea can be found in [5, 7, 13, 23]. It should also be mentioned that several works by Stanley (see for example his nice survey [26]) contributed to propagating interest in this idea, e.g., in connection with variants of the enumeration of zig-zag permutations (permutations which have a periodic succession of rises and falls [1, 8]); this led to the articles [6, 19, 21]. Together with Philippe Marchal, we further developed this density method in [3, 4], as a way to analyse structures like permutations, trees, Young tableaux, all with additional order constraints on their labels.

In this article, we consider a generalization of Young tableaux by allowing two consecutive cells to have decreasing values. We put a bold red edge between the cells which are allowed (but not imposed) to be decreasing (we call these edges "walls"), and consider structures where the location of the walls obey some periodicity rules. More precisely, let a tableau \mathcal{Y} with periodic walls be the concatenation (as shown in Figure 1) of n copies of a building block \mathcal{B} of cells (i.e., $\mathcal{Y} = \mathcal{B}^n$) and then filled with all integers from $\{1, \dots, |\mathcal{B}|n\}$ respecting the induced order constraints.

$$\mathcal{B} = \begin{array}{|c|c|} \hline & \\ \hline & \\ \hline \end{array} \quad \mathcal{B}^4 = \begin{array}{|c|c|c|c|c|c|c|c|} \hline 3 & 10 & 5 & 6 & 12 & 16 & 13 & 14 \\ \hline 1 & 2 & 4 & 7 & 8 & 9 & 11 & 15 \\ \hline \end{array}$$

Figure 1: Left: example of a block \mathcal{B} of shape 2×2 . Right: a Young tableau with periodic walls at positions imposed by concatenations of \mathcal{B} .

13	14	16	17	19	20	21	25	27
11	2	10	12	15	18	6	23	26
4	1	8	5	7	9	3	22	24
←→			←→			←→		
λ_1			λ_2			λ_3		

Some of these tableaux are in bijection with other combinatorial structures. Just to give a small example, if all the λ_i 's = 1, the tableaux on the left are in bijection with partitions of $\{1, \dots, 3n\}$ into n sets of size 3.

In [3], we introduced rectangular Young tableaux with walls and explored their links with hook-length-like formulas, the Chung–Feller theorem, and studied their uniform random generation. In this article, we introduce other several families of tableaux with periodic walls to illustrate the rich diversity of the corresponding generating functions, and some of their unexpected closure properties.

Plan of the article. In Section 2, we consider the class of Young tableaux of shape $n \times 2$, where adding walls enrich known bijections with trees and lattice paths. In Section 3, we use the density method to enumerate certain poset structures (the new Jenga tableaux), which lead to unexpected closed forms, and sometimes to D-finite generating functions. In Section 4, we show that some simple classes of Young tableaux with periodic walls lead to complicated asymptotic formulas. In Section 5, we characterize (except for two cases) Young tableaux with periodic walls built of 2×2 blocks with respect to the nature of their counting sequences: simple product, algebraic, hypergeometric, or D-algebraic.

2 Young tableaux of shape $n \times 2$ and binary trees

In this section, just to illustrate a little bit more the diversity of combinatorial objects which can be related to tableaux with walls, we consider Young tableaux of shape $n \times 2$, allowing some walls between their two columns and map them bijectively to leaf-marked binary trees; see Figure 2. The following proposition gives a new combinatorial meaning to several OEIS¹ entries, such as A000108, A000984, A002457, A002802, and A020918.

Proposition 2.1. *The generating function of $n \times 2$ Young tableaux with k walls is equal to*

$$V_k(z) := \sum_{n \geq 0} v_{n,k} z^n = \frac{\text{Cat}(k-1) z^{k-1}}{(1-4z)^{(2k-1)/2}} \quad \text{where} \quad \text{Cat}(n) = \frac{1}{n+1} \binom{2n}{n},$$

and the corresponding generating polynomial with respect to the number of walls is

$$v_n(u) := \sum_{k=0}^n v_{n,k} u^k = \text{Cat}(n) ((1+u)^{n+1} - u^{n+1}). \quad (2.1)$$

Proof. In [3, Theorem 2.1], using a link with Dyck paths and the Chung–Feller theorem, we proved that the number $v_{n,k}$ of $n \times 2$ Young tableaux with k vertical walls is equal to

$$v_{n,k} = \frac{1}{n+1-k} \binom{n}{k} \binom{2n}{n}.$$

The formula for $v_n(u)$ follows by summing $v_{n,k}$ with respect to n . What is more, a simple rewriting shows that $v_{n,k} = \frac{(n)_{k-1}}{k!} \binom{2n}{n}$ for $k \geq 1$. This shows

$$\sum_{n \geq 0} v_{n,k} z^n = \sum_{n \geq k-1} \frac{(n)_{k-1}}{k!} \binom{2n}{n} z^n = \frac{z^{k-1}}{k!} \frac{d^{k-1}}{dz^{k-1}} \sum_{n \geq 0} \binom{2n}{n} z^n = \frac{z^{k-1}}{k!} \frac{d^{k-1}}{dz^{k-1}} \frac{1}{\sqrt{1-4z}}. \quad \square$$

It is noteworthy that $v_{n,k}$ is at the same time divisible by $\text{Cat}(n)$ and $\text{Cat}(k-1)$, and, obviously, (2.1) demands a simple combinatorial explanation. The following classical lemma will allow us to give a bijective explanation of all these facts.

Lemma 2.2. *Young tableaux of shape $n \times 2$ are in bijection with binary trees that have n internal nodes.*

Proof. The key observation is that every element in the first column corresponds to an internal node and every element in the second column to a leaf. For the bijection we iterate through the cells in increasing order. We start with an internal node for the entry 1. Depending on the column of m , we add an internal node or a leaf to the next available empty position in depth-first order. At the end, we add a leaf to the left-most branch of the root. \square

¹OEIS stands for the On-Line Encyclopedia of Integer Sequences, accessible via <https://oeis.org>.

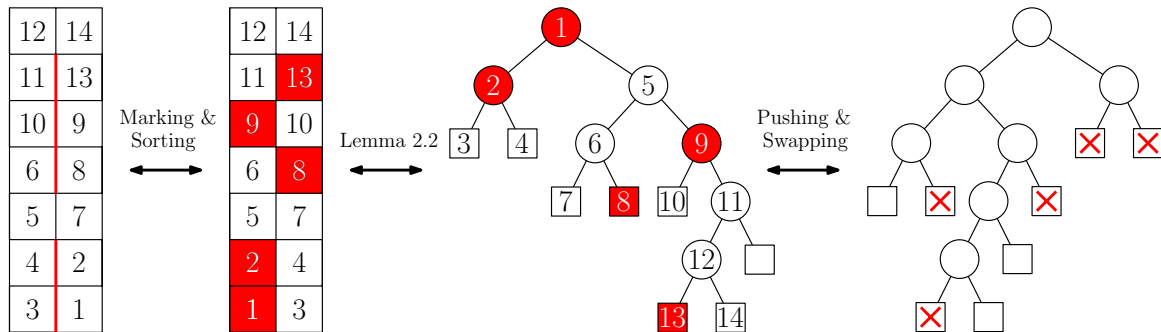


Figure 2: The bijection between $n \times 2$ Young tableaux with k walls and binary trees with k marked leaves from Theorem 2.3. Here $n = 14$ and $k = 5$.

Theorem 2.3. *Young tableaux of shape $n \times 2$ with k walls are in bijection with binary trees with n internal nodes and k marked leaves.*

Proof. The following bijection consists of (possibly) 3 steps and is shown on an example in Figure 2. First, we mark every entry in the second column that is in a row with a wall and remove the wall. Then, we sort each row to get a standard $n \times 2$ Young tableau (yet, with k markers).

Second, we transform this tableau together with its markers into a binary tree using Lemma 2.2. If no internal nodes are marked, then we are finished; yet if some internal nodes are marked, then we perform the following step.

Third, we inductively transform the binary tree with markers into a binary tree with marked leaves. Observe that if an internal node on the right-most branch of the root is marked, all internal nodes in the left subtree are marked as well, but no leaf. Vice versa, if in such a subtree at least one leaf is marked, no internal node is marked. This follows from the depth-first traversal of Lemma 2.2 as we only append a new internal node to the right-most branch of the root if the subtableau corresponding to the previous nodes is a valid Young tableau. Now, start from the right-most leaf in the right branch of the root and move upwards to the root. If an internal node is marked, push all markers to the leaves of the left subtree and thereafter swap the left and right subtree. Continue until you reach the root.

For the reverse bijection, we distinguish two cases: Either the right-most leaf is marked or not. If it is not marked we reverse only steps 1 and 2, while if it is marked, we reverse all three steps. \square

In the next section, we introduce the main tool of this article: the density method. We apply it on different variants of tableaux with walls, leading here to unexpectedly well-structured generating functions (e.g., hypergeometric or D-finite).

3 Jenga tableaux and the density method

The towers of the game Jenga² inspired the following fruitful generalization of Young tableaux. Consider a column of n cells to which one attaches at row i , ℓ_i cells to the left and r_i cells to the right. The $N := n + \sum_i \ell_i + r_i$ cells of this structure are then filled with the integers 1 to N under the constraint that each row and the middle column have increasing labels, and each label appears only once; see Figure 3.

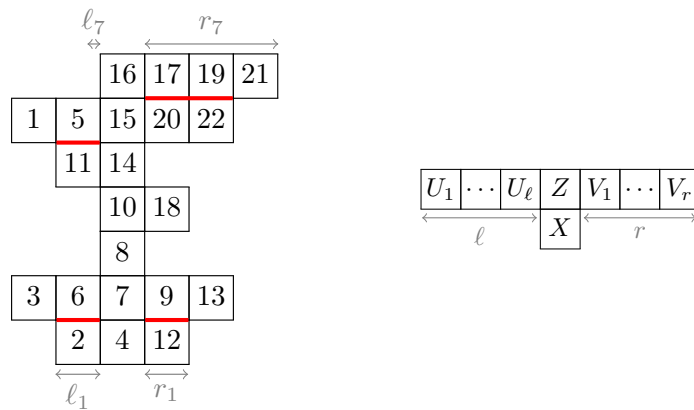


Figure 3: Left: a Jenga tableau with $n = 7$ rows and the left and right subsequences $(\ell_i)_{i=1}^7 = (1, 2, 0, 0, 1, 2, 0)$ and $(r_i)_{i=1}^7 = (1, 2, 0, 1, 0, 2, 3)$, respectively. Right: the building block used here in the density method to generate each row iteratively.

The density method is the key to enumerate such objects. We used it in [4, 20, 21] for other classes of tableaux. Let us sketch its principle on the example of Jenga tableaux.

The density method builds on a geometric interpretation of the problem. Consider an N -tuple α (with non-equal coordinates) that is an element of the hypercube $[0, 1]^N$. Then, we associate to each of these N coordinates one of the N cells of \mathcal{Y} : if the j th coordinate of α is the i th biggest element, then we assign the value i to the cell j . This filling is not (yet) respecting all increasing constraints, but this operation is readily reversed by associating to every legitimate filling of \mathcal{Y} a region of $[0, 1]^N$ which corresponds to a polytope. The key observation now is that the volume of this polytope is equal to $1/N!$. Let \mathcal{P} be the set of all polytopes corresponding to correct fillings of \mathcal{Y} . Then, a uniformly random element \mathcal{P} corresponds to a uniformly random filling of \mathcal{Y} . Note that \mathcal{P} is also known as the “order polytope” in poset theory.

We build now on this geometric viewpoint and describe how the density method works. Consider the generic building block of a row shown in Figure 3. It consists of the ℓ cells U_1, \dots, U_ℓ , the r cells V_1, \dots, V_r , one cell Z , and one cell X . To each of these cells we assign a random number from $[0, 1]$. Then, we define a sequence of polynomials $f_n(z)$ which encode the order constraints satisfied by these cells up to row n :

²“Jenga!” means “Construct!” in Swahili. It is the name of a game created by Leslie Scott for his children in the 70s in which one dismantles block by block a tower of small wooden building blocks.

$$f_n(z) := \int_{z < v_1 < 1} \dots \int_{v_{r-1} < v_r < 1} \int_{0 < u_\ell < z} \dots \int_{0 < u_1 < u_2} \int_{0 < x < z} f_{n-1}(x) dx du_1 \dots du_\ell dv_r \dots dv_1.$$

Now the simple block structure of each row leads to the following simplification

$$f_n(z) = \frac{z^{\ell_n}(1-z)^{r_n}}{\ell_n!r_n!} \int_0^z f_{n-1}(x) dx \quad \text{and} \quad f_1(z) := \frac{z^{\ell_1}(1-z)^{r_1}}{\ell_1!r_1!}. \quad (3.1)$$

The crucial observation is now the following: The value $\int_0^1 f_n(z) dz$ is equal to the volume of the order polytope \mathcal{P} associated to the correct fillings of \mathcal{Y}_n . Thus, $N! \int_0^1 f_n(z) dz$ is equal to the number of legitimate fillings. For more details see [4].

We thus get that the number y_n of Jenga tableaux with n rows is

$$y_n = \left(\sum_{i=1}^n (\ell_i + r_i + 1) \right)! \int_0^1 f_n(x) dx. \quad (3.2)$$

We now continue with some periodic patterns, that is if there exists an integer $p > 0$ such that $\ell_{i+p} = \ell_i$ and $r_{i+p} = r_i$ for all $i \geq 1$. The smallest such p is called the period. The simplest possible period is $p = 1$; this case leads to a noteworthy generating function.

Theorem 3.1 (D-finiteness of periodic Jenga tableaux with $p = 1$). *The bivariate generating function $F(t, z) = \sum_{n \geq 1} f_n(z) t^n$ is D-finite in t and z . Accordingly, the counting sequence $(y_n)_{n \geq 1}$ given by Equation (3.2) of Jenga tableaux with n rows is P-recursive.*

Proof. In [3, Theorem 4.4] it was shown that $F(t, z)$ is D-finite in z for any periodic pattern with one hole. For the D-finiteness in t we use the density relations (3.1) and obtain

$$F(t, z) = t f_1(z) \exp \left(t \int_0^z f_1(u) du \right). \quad (3.3)$$

Then, taking the derivative with respect to t , we get that $F(t, z)$ is also D-finite in t :

$$t F_t(t, z) - \left(1 + t \int_0^z f_1(u) du \right) F(t, z) = 0.$$

Hence, by closure properties (Hadamard product and integration; see, e.g., [25]), the corresponding sequence $(y_n)_{n \geq 1}$ of Jenga tableaux with n rows is P-recursive. \square

Note that set partitions of equal set sizes fall into the class of Theorem 3.1 as $\ell_i = m - 1$ and $r_i = 0$ for all $i \geq 0$. Let us also mention the following unexpected link.

Remark 3.2 (Link with Sheffer sequences). *Considering the series expansion of $F(t, z)$ in z instead of t , Equation (3.3) shows that we have here some variant of Borel transform³ of Sheffer sequences. Sheffer sequences are sequences of polynomials $\hat{f}_n(t)$ having an exponential generating function of shape $\sum_{n=0}^{\infty} \hat{f}_n(t) \frac{z^n}{n!} = A(z) \exp(tB(z))$. They play an important rôle in umbral calculus; see [24] and [25, Exercise 5.37].*

³The Borel transform (or the “inverse Laplace transform”) of a sequence (a_n) is the sequence $(a_n/n!)$.

As further examples of Jenga shapes, the density method also gives:

Proposition 3.3. For $r_i = 0$ for all $i \geq 1$ (see Figure 3), the number y_n of Jenga tableaux satisfies

$$y_n = \frac{(\sum_{i=1}^n (\ell_i + 1))!}{\prod_{i=1}^n \ell_i! (\sum_{j=1}^i (\ell_j + 1))}.$$

Specializing these tableaux to periodic cases leads to some hypergeometric formulas.

Proposition 3.4. Consider Jenga tableaux with period p , arbitrary left sequence $(\ell_i)_{i=0}^p$, and right sequence $(r_i)_{i=0}^p = (0, \dots, 0)$ (see Figure 3). Define $L := \sum_{i=1}^p \ell_i$. Then, the number y_n of such tableaux satisfies

$$y_{kp+m} = y_m \left(\frac{(L+p)^L}{\prod_{i=1}^p \ell_i!} \right)^k \prod_{\substack{j=1 \\ j \neq \ell_1 + \dots + \ell_i + i}}^{L+p} \frac{\Gamma(k + \frac{j+m}{L+p})}{\Gamma(\frac{j+m}{L+p})}.$$

Accordingly, the generating function of such tableaux is the sum of p hypergeometric functions.

It is also possible to consider other shapes, such as skew Young tableaux. Next, we give such an example and thus add walls to a model analysed in [5].

Proposition 3.5. Consider tableaux with periodic walls in a diagonal strip of width w between each column in all but the top cell; see Figure 4. Let $b_{w,n}$ be the number of such tableaux with n columns; one has

$$b_{w,n} = \left(\frac{w^{w-2}}{(w-2)!} \right)^n \prod_{j=1}^{w-2} \frac{\Gamma(n + \frac{j}{w})}{\Gamma(\frac{j}{w})}.$$

Proof. The formula is obtained by a bijection (depicted in Figure 4) between this class and periodic Jenga tableaux of period $p = 2$, $\ell_1 = w - 2$, $\ell_2 = 0$, and $r_i = 0$, such that $b_{w,n} = a_{2n}$. □

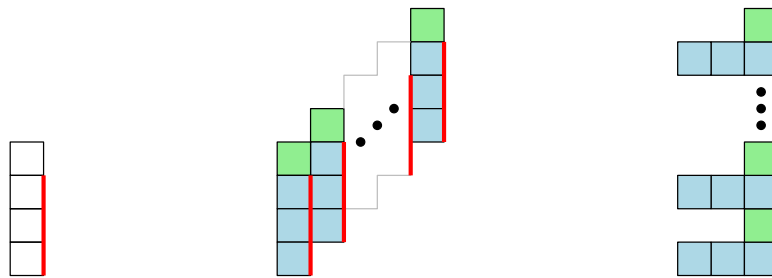


Figure 4: The building block of width 4 (left) is repeated k times and each time shifted up by one cell to form a Young tableau with periodic walls in a diagonal strip (centre). These tableaux are in bijection with periodic Jenga tableaux with period $p = 2$, left sequence $(\ell_i)_{i=1}^2 = (2, 0)$, and right sequence $(r_i)_{i=1}^2 = (0, 0)$ (right).

4 Some unusual asymptotics

The density method can also be used to count and generate objects which do not have simple counting formulas. We now present such a class, which is a priori quite simple, but which however leads to rather surprising asymptotics. Thus, this class illustrates well the non-intuitive asymptotic behaviour of our objects.

6	10	14	15	17	18
3	5	9	12	13	16
2	1	7	4	11	8

	S	Y
R	X	

Figure 5: A $3 \times n$ Young tableau with walls in its first row, and the corresponding building block for each column used in the density method.

Theorem 4.1. *The number a_n of Young tableaux of length n with shape given by Figure 5 has the following asymptotics*

$$a_n = \Theta \left(n! 12^n e^{a_1(3n)^{1/3}} n^{-2/3} \right), \quad (4.1)$$

where $a_1 \approx -2.338$ is the largest root of the Airy function of the first kind.

Proof (sketch). The increasing label constraints encoded in the building block of Figure 5 directly translate to the following densities

$$f_{n+1}(x, y) := x \int_0^x \int_x^y f_n(r, s) ds dr \quad \text{and} \quad f_1(x, y) := x(y - x).$$

Accordingly, as the initial configuration corresponding to f_1 consists of a building block without the cell R , the number of tableaux is

$$a_n = (3n + 1)! \int_0^1 \int_0^y f_n(x, y) dx dy.$$

This gives the sequence [OEIS A213863](#): $\{1, 7, 106, 2575, 87595, 3864040, 210455470, \dots\}$. It also counts words where each letter ℓ of the n -ary alphabet occurs 3 times and for each prefix p one has $|p|_\ell = 0$ or $|p|_\ell \geq |p|_j$ for all $j > \ell$, where $|p|_\ell$ counts the occurrences of ℓ in p . The bijection with our tableaux follows by mapping indices to rows. Formula (4.1) is then obtained by using the methods introduced in [14], i.e., sandwiching a_n between two sequences having the same asymptotics dictated by the first zero of a D-finite function (here, the Airy function satisfying $y'' - xy = 0$; see [16]). \square

5 A classification of 2×2 periodic shapes

We now consider Young tableaux made of the concatenation of 2×2 blocks with walls (see Figure 1 in Section 1). This model is interesting as it leads to rather different natures of generating functions. Indeed, Table 1 hereafter summarizes the main results and groups them into four classes according to their counting sequences: simple products, algebraic, hypergeometric, or D-algebraic. Surprisingly, some of these sequences connect with classical combinatorial objects!

There are 6 possible non-trivial locations for walls in a 2×2 block (due to possible coincidences of the walls on the right when the blocks are concatenated). Thus, there are in total $2^6 = 64$ different types of building blocks. Most of these blocks come in pairs, as rotating a tableau by 180 degrees and reversing the labels gives a bijection.

First, one gets 40 blocks for which the walls create independent regions. This leads to 19 distinct sequences **P1–P19**, all having a simple product formula.

Second, we consider the 4 blocks without vertical walls. They lead to 3 distinct sequences **A1–A3**, which all have an algebraic generating function. For **A1** and **A2** the proof uses a bijection to Dyck paths. For **A3** we decompose at the first wall that cannot be removed and get the recurrence $a_n = \text{Cat}(2n) + \sum_{i=1}^n \text{Cat}(2i-1)a_{n-i}$, which we then solve with generating functions.

Third, we consider 14 blocks with a uniquely determined minimum or maximum. They lead to 7 distinct sequences **H1–H7**, all hypergeometric. The models **H1–H5** are Jenga-like tableaux from Section 3 that satisfy $l_i = 0$ for all i . For the models **H6** and **H7** we use a recursive approach, decomposing with respect to the location of the unique minimum or maximum.

Fourth, there are three blocks which show a zig-zag-like pattern. By analogy to the known zig-zag permutations, we conjecture **Z2** and **Z3** to be non-D-finite. For **Z1** we are able to prove that the exponential generating function is D-algebraic, and not D-finite, i.e., it satisfies a non-linear differential equation and no linear one. For this purpose we use Carlitz' theory [10] of generalized alternating permutations. Let k_1, k_2, \dots, k_m be positive integers such that $k_1 + k_2 + \dots + k_m = n$. Then, a generalized alternating permutation of type (k_1, \dots, k_m) is an n -tuple (a_1, \dots, a_n) such that $a_i \in \{1, \dots, n\}$ and

$$a_1 < \dots < a_{k_1} > a_{k_1+1}, \quad a_{k_1+1} < \dots < a_{k_1+k_2} > a_{k_1+k_2+1}, \quad \dots \quad a_{k_1+\dots+k_{m-1}+1} < \dots < a_n.$$

The type of a classical alternating permutation is thus $k_1 = \dots = k_m = 1$, while the type of a tableau from **Z1** with $m-1$ blocks is $k_1 = 3, k_2 = \dots = k_{m-1} = 4$, and $k_m = 1$. Then, the claimed closed form of $A(t) = \sum_{n \geq 0} a_n \frac{t^n}{n!}$ for **Z1** follows from a generalization of [10, Equation (1.11)] taking into account the different behaviours at the beginning *and* the end of the permutation. Thus, we get

$$A(t) = \frac{F_{4,3}(t)F_{4,1}(t)}{F_{4,0}(t)} + F_{4,0}(t) \quad \text{where} \quad F_{k,r}(t) = \sum_{n \geq 0} (-1)^n \frac{t^{nk+r}}{(nk+r)!}.$$

Class	Shape	Formula	Class	Shape	Formula	Class	Shape	Formula
P1		$4 \frac{(4n)!}{24^n}$	P6		$\frac{(4n)!}{6^n}$	P13		$6 \frac{(4n)!}{3^n}$
P2		$\frac{(4n)!}{12^n}$	P7		$3 \frac{(4n)!}{6^n}$	P14		$\frac{(4n)!}{2^n}$
P3		$3 \frac{(4n)!}{12^n}$	P8		$8 \frac{(4n)!}{5} \left(\frac{5}{24}\right)^n$	P15		$2 \frac{(4n)!}{2^n}$
P4		$\frac{(4n)!}{8^n}$	P9		$\frac{(4n)!}{4^n}$	P16		$\frac{(4n)!}{(2n)!2^n}$
P5		$4 \frac{(4n)!}{8^n}$	P10		$2 \frac{(4n)!}{4^n}$	P17		$2 \frac{(4n)!}{(2n)!2^n}$
			P11		$4 \frac{(4n)!}{4^n}$	P18		$\frac{(4n)!}{(2n)!}$
			P12		$\frac{(4n)!}{3^n}$	P19		$(4n)!$

Class	Shape	Sequence	OEIS
A1		$\text{Cat}(2n) = \frac{1}{2n+1} \binom{4n}{2n}$	A048990
A2		$\binom{4n}{2n}$	A001448
A3		$2^{2n+1} \text{Cat}(n) - \text{Cat}(2n+1)$	A079489
H1		$\prod_{i=1}^n (4i-1)(4i-3)$	A101485
H2		$\prod_{i=1}^n (2i-1)(4i-1)$	A159605
H3		$2^{n+1} n! \prod_{i=1}^n (4i-3)$	$2^{n+1} \cdot$ A084943
H4		$\binom{4n}{n} \prod_{i=1}^n (3i-1)$	$\binom{4n}{n} \cdot$ A008544
H5		$\binom{4n}{n} \prod_{i=1}^n (3i-2)$	$\binom{4n}{n} \cdot$ A007559
H6		$2^n n! \prod_{i=1}^n (4i-3)$	$n! \cdot$ A084948
H7		$\prod_{i=1}^n (2i-1)(4i-1)$	A159605
Z1		$\frac{\cos(t/\sqrt{2})^2 + \cosh(t/\sqrt{2})^2}{2 \cos(t/\sqrt{2}) \cosh(t/\sqrt{2})}$	related to A211212
Z2		?	???
Z3		?	???

Table 1: The 64 different models of 2×2 blocks for tableaux with periodic walls grouped into 4 different classes: (P) simple products, (A) algebraic, (H) hypergeometric, (Z) zig-zag. The length n is equal to the number of repeated blocks. The model **Z1** is D-algebraic and not D-finite, which is what we conjecture for the models **Z2** and **Z3**.

A pleasant feature of the density method approach is that it is automatable. See our [Jenga](#) Maple package dedicated to the enumeration of tableaux with walls, thus allowing our readers to play with the examples of their choice!

In conclusion, we have seen that Young tableaux with walls are a rich model, leading (via the density method) to new varieties of recurrences, interesting *per se*, mixing finite differences and differential operators (challenging the current state of the art in computer algebra and holonomy theory!), and surprising asymptotics (challenging the current state of the art in analytic combinatorics!).

Acknowledgments

We thank the two anonymous referees for their kind feedback.

References

- [1] D. André. “Sur les permutations alternées”. *Journal de mathématiques pures et appliquées* **7** (1881). Long version of several articles by André in 1879, pp. 167–184. [Link](#).
- [2] C. Banderier, M. Bousquet-Mélou, A. Denise, P. Flajolet, D. Gardy, and D. Gouyou-Beauchamps. “Generating functions for generating trees”. *Discrete Math.* **246.1-3** (2002). FPSAC’99 Barcelona, pp. 29–55. [DOI](#).
- [3] C. Banderier, P. Marchal, and M. Wallner. “Rectangular Young tableaux with local decreases and the density method for uniform random generation”. *GASCom 2018, CEUR Workshop Proceedings. Vol. 2113*. 2018, pp. 60–68. [Link](#).
- [4] C. Banderier, P. Marchal, and M. Wallner. “Periodic Pólya urns, the density method and asymptotics of Young tableaux”. *Annals of Probability* **48.4** (2020), pp. 1821–1965. [DOI](#).
- [5] Y. Baryshnikov and D. Romik. “Enumeration formulas for Young tableaux in a diagonal strip”. *Israel J. Math.* **178** (2010), pp. 157–186. [arXiv:0709.0498](#).
- [6] N. Basset. “Counting and generating permutations in regular classes”. *Algorithmica* **76.4** (2016), pp. 989–1034. [Link](#).
- [7] F. Beukers, J. A. C. Kolk, and E. Calabi. “Sums of generalized harmonic series and volumes”. *Nieuw Arch. Wiskd., IV. Ser.* **11.3** (1993), pp. 217–224. [Link](#).
- [8] M. Bóna. *Combinatorics of permutations*. Chapman & Hall/CRC, 2004, p. 383.
- [9] G. Brightwell and P. Winkler. “Counting linear extensions”. *Order* **8.3** (1991). A preliminary version appeared in the proceedings of STOC’91., pp. 225–242. [DOI](#).
- [10] L. Carlitz. “Permutations with prescribed pattern”. *Math. Nachr.* **58** (1973), pp. 31–53. [DOI](#).
- [11] S. Dittmer and I. Pak. “Counting linear extensions of restricted posets” (2018). [arXiv:1802.06312](#).

- [12] P. Duchon, P. Flajolet, G. Louchard, and G. Schaeffer. “Random sampling from Boltzmann principles”. *Automata, languages and programming. Proceedings of ICALP 2002*. Springer, 2002, pp. 501–513. [Link](#).
- [13] N. D. Elkies. “On the sums $\sum_{k=-\infty}^{\infty} (4k+1)^{-n}$ ”. *Amer. Math. Monthly* **110.7** (2003), pp. 561–573. [arXiv:math/0101168](#).
- [14] A. Elvey Price, W. Fang, and M. Wallner. “Compacted binary trees admit a stretched exponential”. *J. Combin. Theory Ser. A* **177** (2021), pp. 105306, 40. [arXiv:1908.11181](#).
- [15] P. Flajolet, P. Zimmermann, and B. van Cutsem. “A calculus for the random generation of labelled combinatorial structures”. *Theor. Comput. Sci.* **132.1-2** (1994), pp. 1–35. [DOI](#).
- [16] M. Fuchs, G.-R. Yu, and L. Zhang. “On the asymptotic growth of the number of tree-child networks”. *Eur. J. Comb.* **93** (2021), pp. 103278, 20. [arXiv:2003.08049](#).
- [17] M. Jerrum. *Counting, Sampling and Integrating: Algorithms and Complexity*. Birkhäuser, 2003, pp. xi + 112. [DOI](#).
- [18] D. E. Knuth. *The Art of Computer Programming. Volume 4A. Combinatorial Algorithms, Part 1*. Addison-Wesley, 2011, xvi+883pp.
- [19] J.-M. Luck. “On the frequencies of patterns of rises and falls”. *Physica A* **407** (2014), pp. 252–275. [arXiv:1309.7764](#).
- [20] P. Marchal. “Rectangular Young tableaux and the Jacobi ensemble”. *Discrete Math. Theor. Comput. Sci. Proceedings* **BC** (2016), pp. 839–850. [arXiv:1510.06598](#).
- [21] P. Marchal. “The density method and permutations with a prescribed descent set”. *GASCom 2018, CEUR Workshop Proceedings. Vol. 2113*. 2018, pp. 179–186. [Link](#).
- [22] A. Nijenhuis and H. S. Wilf. *Combinatorial Algorithms for Computers and Calculators*. Second edition (first edition in 1975). Academic Press, 1978. [Link](#).
- [23] I. Pak. “Hook length formula and geometric combinatorics”. *Sém. Lothar. Combin.* **46** (2001), Art. B46f, 13. [Link](#).
- [24] G.-C. Rota. *Finite Operator Calculus. With the collaboration of P. Doubilet, C. Greene, D. Kahaner, A. Odlyzko and R. Stanley*. Academic Press, 1975.
- [25] R. P. Stanley. *Enumerative Combinatorics. Volume 2*. Cambridge University Press, 1999, pp. xii+581. [Link](#).
- [26] R. P. Stanley. “A survey of alternating permutations”. *Combinatorics and graphs*. American Mathematical Society (AMS), 2010, pp. 165–196. [arXiv:0912.4240](#).

PERIODIC PÓLYA URNS, THE DENSITY METHOD AND ASYMPTOTICS OF YOUNG TABLEAUX

BY CYRIL BANDERIER¹, PHILIPPE MARCHAL² AND MICHAEL WALLNER³

¹LIPN, Université Paris Nord, cyril.banderier@lipn.univ-paris13.fr

²LAGA, Université Paris Nord, marchal@math.univ-paris13.fr

³LaBRI, Université de Bordeaux, michael.wallner@u-bordeaux.fr

Pólya urns are urns where at each unit of time a ball is drawn and replaced with some other balls according to its colour. We introduce a more general model: the replacement rule depends on the colour of the drawn ball and the value of the time (mod p). We extend the work of Flajolet et al. on Pólya urns: the generating function encoding the evolution of the urn is studied by methods of analytic combinatorics. We show that the initial *partial* differential equations lead to *ordinary* linear differential equations which are related to hypergeometric functions (giving the exact state of the urns at time n). When the time goes to infinity, we prove that these *periodic Pólya urns* have asymptotic fluctuations which are described by a product of generalized gamma distributions. With the additional help of what we call the *density method* (a method which offers access to enumeration and random generation of poset structures), we prove that the law of the southeast corner of a triangular Young tableau follows asymptotically a product of generalized gamma distributions. This allows us to tackle some questions related to the continuous limit of random Young tableaux and links with random surfaces.

CONTENTS

1. Introduction	1922
1.1. Periodic Pólya urns	1922
1.2. The generalized gamma product distribution	1923
1.3. Plan of the article	1926
2. A functional equation for periodic Pólya urns	1926
2.1. Urn histories and differential operators	1926
2.2. D-finiteness of history generating functions	1928
3. Moments of periodic Pólya urns	1930
3.1. Number of histories: A hypergeometric closed form	1930
3.2. Mean and critical exponent	1931
3.3. Higher moments	1933
3.4. Limit distribution for periodic Pólya urns	1935
4. Urns, trees and Young tableaux	1937
4.1. The link between Young tableaux and trees	1940
4.2. The density method for Young tableaux	1941
4.3. The density method for trees	1944
4.4. The link between trees and urns	1948
5. Random Young tableaux and random surfaces	1953
5.1. Random surfaces	1953
5.2. From microscopic to macroscopic models: Universality of the tails	1956
5.3. Factorizations of gamma distributions	1958
6. Conclusion and further work	1961
Acknowledgements	1961
References	1962

Received March 2019; revised October 2019.

MSC2010 subject classifications. Primary 60C05; secondary 05A15, 60F05, 60K99.

Key words and phrases. Pólya urn, Young tableau, generating functions, analytic combinatorics, pumping moment, D-finite function, hypergeometric function, generalized gamma distribution, Mittag-Leffler distribution.

1. Introduction.

1.1. *Periodic Pólya urns.* *Pólya urns* were introduced in a simplified version by George Pólya and his PhD student, Florian Eggenberger, in [26, 27, 74], with applications to disease spreading and conflagrations. They constitute a powerful model, which regularly finds new applications; see, for example, Rivest's recent work on auditing elections [78], or the analysis of deanonymization in Bitcoin's peer-to-peer network [29]. They are well-studied objects in combinatorial and probabilistic literature [6, 31, 62], because they offer fascinatingly rich links with numerous objects like random recursive trees, m -ary search trees and branching random walks (see, e.g., [7, 22, 43, 44]). In this paper, we introduce a variation which leads to new links with another important combinatorial structure: Young tableaux. What is more, we solve the enumeration problem of this new Pólya urn model, derive the limit law for the evolution of the urn and give some applications to Young tableaux.

In the *Pólya urn model*, one starts with an urn with b_0 black balls and w_0 white balls at time 0. At every discrete time step, one ball is drawn uniformly at random. After inspecting its colour, this ball is returned to the urn. If the ball is black, a black balls and b white balls are added; if the ball is white, c black balls and d white balls are added (where $a, b, c, d \in \mathbb{N}$ are nonnegative integers). This process can be described by the so-called *replacement matrix*:

$$M = \begin{pmatrix} a & b \\ c & d \end{pmatrix}, \quad a, b, c, d \in \mathbb{N}.$$

We call an urn and its associated replacement matrix *balanced* if $a + b = c + d$. In other words, in every step the same number of balls is added to the urn. This results in a deterministic number of balls after n steps: $b_0 + w_0 + (a + b)n$ balls.

Now, we introduce a more general model which has rich combinatorial, probabilistic and analytic properties.

DEFINITION 1.1. A *periodic Pólya urn* of period p with replacement matrices M_1, M_2, \dots, M_p is a variant of a Pólya urn in which the replacement matrix M_k is used at steps $np + k$. Such a model is called *balanced* if each of its replacement matrices is balanced.

For $p = 1$, this model reduces to the classical Pólya urn model with one replacement matrix. In this article, we illustrate the aforementioned rich properties via the following model.

DEFINITION 1.2. Let $p, \ell \in \mathbb{N}$. We call a *Young–Pólya urn of period p and parameter ℓ* the periodic Pólya urn of period p (with $b_0 \geq 1$ to avoid degenerate cases) and replacement matrices

$$M_1 = M_2 = \dots = M_{p-1} = \begin{pmatrix} 1 & 0 \\ 0 & 1 \end{pmatrix} \quad \text{and} \quad M_p = \begin{pmatrix} 1 & \ell \\ 0 & 1 + \ell \end{pmatrix}.$$

EXAMPLE 1.3. Consider a Young–Pólya urn with parameters $p = 2, \ell = 1$, and initial conditions $b_0 = w_0 = 1$. The replacement matrices are $M_1 := \begin{pmatrix} 1 & 0 \\ 0 & 1 \end{pmatrix}$ for every odd step, and $M_2 := \begin{pmatrix} 1 & 1 \\ 0 & 2 \end{pmatrix}$ for every even step. This case was analysed by the authors in the extended abstract [9]. In the sequel, we will use it as a running example to explain our results.

Let us illustrate the evolution of this urn in Figure 1. Each node of the tree corresponds to the current composition of the urn (number of black balls, number of white balls). One starts with $b_0 = 1$ black ball and $w_0 = 1$ white. In the first step, the matrix M_1 is used and leads to two different compositions. In the second step, matrix M_2 is used, in the third step, matrix M_1 is used again, in the fourth step, matrix M_2 , etc. Thus, the possible compositions are $(2, 1)$ and $(1, 2)$ at time 1, $(3, 2)$, $(2, 3)$ and $(1, 4)$ at time 2, $(4, 2)$, $(3, 3)$, $(2, 4)$ and $(1, 5)$ at time 3.

In fact, each of these states may be reached in different ways, and such a sequence of transitions is called a *history*. (Some authors also call it a *scenario*, an *evolution* or a *trajectory*.) Each history comes with weight one. Implicitly, they induce a probability measure on the states at step n . So, let B_n and W_n be random variables for the number of black and white balls after n steps, respectively. As our model is balanced, $B_n + W_n$ is a deterministic process, reflecting the identity

$$B_n + W_n = b_0 + w_0 + n + \ell \left\lfloor \frac{n}{p} \right\rfloor.$$

So, from now on, we concentrate our analysis on B_n .

1.2. *The generalized gamma product distribution.* For the classical model of a single balanced Pólya urn, the limit law of the random variable B_n is fully known: the possible limit laws include a rich variety of distributions. To name a few, let us mention the uniform distribution [30], the normal distribution [7] and the beta and Mittag-Leffler distributions [43, 45]. Now, periodic Pólya urns (which include the classical model) lead to an even larger variety of distributions involving a product of *generalized gamma distributions* [87].

DEFINITION 1.4. The generalized gamma distribution $\text{GenGamma}(\alpha, \beta)$ with real parameters $\alpha, \beta > 0$ is defined on $(0, +\infty)$ by the density function

$$f(t; \alpha, \beta) := \frac{\beta t^{\alpha-1} \exp(-t^\beta)}{\Gamma(\alpha/\beta)},$$

where Γ is the classical gamma function $\Gamma(z) := \int_0^\infty t^{z-1} \exp(-t) dt$.

The fact that $f(t; \alpha, \beta)$ is indeed a probability density function can be seen by a change of variable $t \mapsto t^\beta$ in the definition of the Γ function, or via the following link.

REMARK 1.5. Let $\Gamma(\alpha)$ be the gamma distribution¹ of parameter $\alpha > 0$, given on $(0, +\infty)$ by

$$g(t; \alpha) = \frac{t^{\alpha-1} \exp(-t)}{\Gamma(\alpha)}.$$

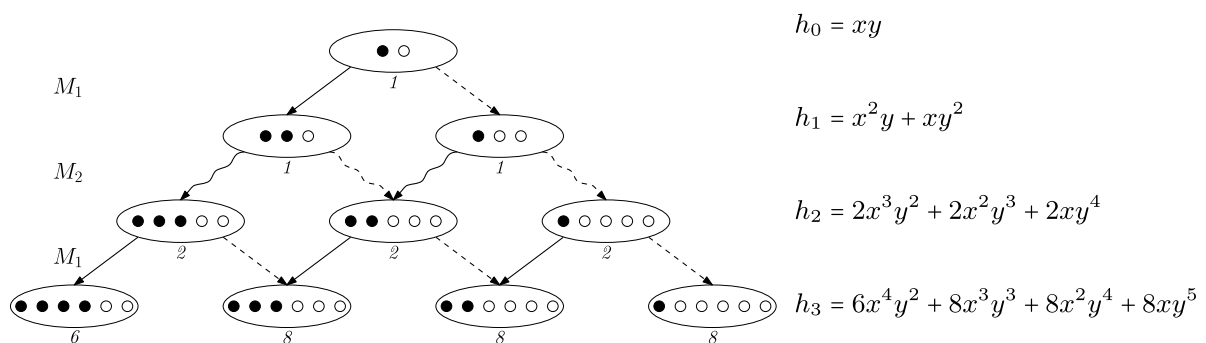


FIG. 1. The evolution of the Young–Pólya urn with period $p = 2$ and parameter $\ell = 1$ with one initial black and one initial white ball. Black arrows mark that a black ball was drawn, dashed arrows mark that a white ball was drawn. Straight arrows indicate that the replacement matrix M_1 was used, curly arrows show that the replacement matrix M_2 was used. The number below each node is the number of possible transitions to reach this state. In this article, we give a formula for h_n (which encodes all the possible states of the urn at time n) and the corresponding asymptotic behaviour.

¹Caveat: it is traditional to use the same letter for both the Γ function and the Γ distribution. Also, some authors add a second parameter to the Γ distribution, which is set to 1 here.

Then one has $\Gamma(\alpha) \stackrel{\mathcal{L}}{=} \text{GenGamma}(\alpha, 1)$, and for $r > 0$, the distribution of the r th power of a random variable distributed according to $\Gamma(\alpha)$ is

$$\Gamma(\alpha)^r \stackrel{\mathcal{L}}{=} \text{GenGamma}(\alpha/r, 1/r).$$

The limit distribution of our urn models is then expressed as a product of such generalized gamma distributions. We prove in Theorem 3.8 a more general version of the following.

THEOREM 1.6 (The generalized gamma product distribution GenGammaProd for Young–Pólya urns). *The renormalized distribution of black balls in a Young–Pólya urn of period p and parameter ℓ is asymptotically for $n \rightarrow \infty$ given by the following product of distributions:*

$$(1) \quad \frac{p^\delta}{p + \ell} \frac{B_n}{n^\delta} \xrightarrow{\mathcal{L}} \text{Beta}(b_0, w_0) \prod_{i=0}^{\ell-1} \text{GenGamma}(b_0 + w_0 + p + i, p + \ell),$$

with $\delta = p/(p + \ell)$, and $\text{Beta}(b_0, w_0) = 1$ when $w_0 = 0$ or $\text{Beta}(b_0, w_0)$ is the beta distribution with support $[0, 1]$ and density $\frac{\Gamma(b_0+w_0)}{\Gamma(b_0)\Gamma(w_0)}x^{b_0-1}(1-x)^{w_0-1}$ otherwise.

In the sequel, we call this distribution the *generalized gamma product distribution* and denote it by $\text{GenGammaProd}(p, \ell, b_0, w_0)$. We will see in Section 3 that this distribution is characterized by its moments, which have a nice factorial shape given in formula (20).

EXAMPLE 1.7. In the case of the Young–Pólya urn with $p = 2$, $\ell = 1$, and $w_0 = b_0 = 1$, one has $\delta = 2/3$. Thus, the previous result shows that the number of black balls converges in law to a generalized gamma distribution:

$$\frac{2^{2/3}}{3} \frac{B_n}{n^{2/3}} \xrightarrow{\mathcal{L}} \text{Unif}(0, 1) \cdot \text{GenGamma}(4, 3) = \text{GenGamma}(1, 3).$$

See Section 5.3 and [24], Proposition 4.2, for more identities of this type.

REMARK 1.8 (Period one). When $p = 1$, our results recover a classical (nonperiodic) urn behaviour. By [45], Theorem 1.3, the renormalization for the limit distribution of B_n in an urn with replacement matrix $\begin{pmatrix} 1 & \ell \\ 0 & 1+\ell \end{pmatrix}$ is equal to $n^{-1/(1+\ell)}$. For $\ell = 0$ the limit distribution is the uniform distribution, whereas for $\ell = 1$ it is a Mittag-Leffler distribution (see [45], Example 3.1, [30], Example 7), and even simplifies to a half-normal distribution² when $b_0 = w_0 = 1$. Thus, the added periodicity by using this replacement matrix only every p th round and otherwise Pólya’s replacement matrix $\begin{pmatrix} 1 & 0 \\ 0 & 1 \end{pmatrix}$ changes the renormalization to $n^{-p/(p+\ell)}$.

The rescaling factor $n^{-\delta}$ with $\delta = p/(p + \ell)$ on the left-hand side of (1) can also be obtained via a martingale computation. The true challenge is to get exact enumeration and the limit law. It is interesting that there exist other families of urn models exhibiting the same rescaling factor, however, these alternative models lead to different limit laws.

- A first natural alternative model consists in averaging the p replacement matrices. This leads to a classical triangular Pólya urn model. The asymptotics is then

$$(2) \quad \frac{B_n}{n^\delta} \xrightarrow{\mathcal{L}} \mathfrak{B},$$

²See [93] for other occurrences of the half-normal distribution in combinatorics.

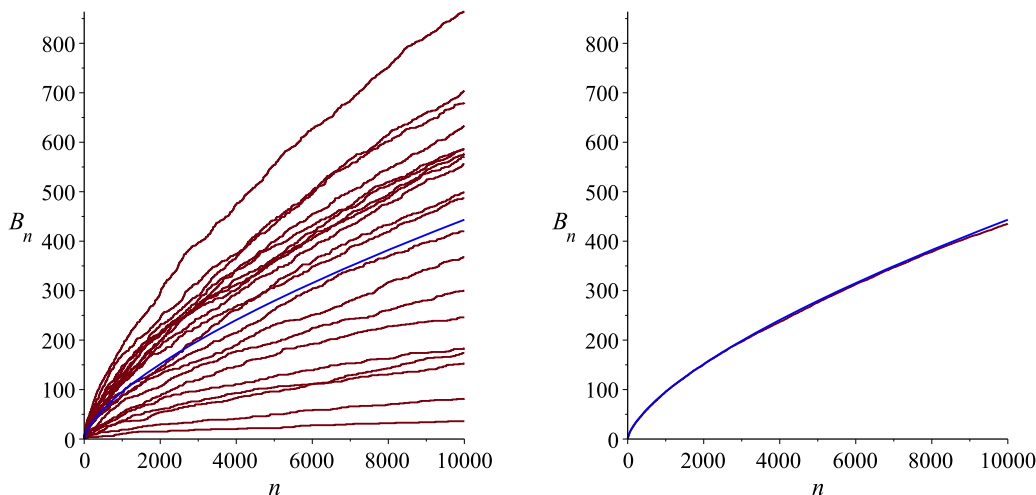


FIG. 2. *Left: 20 simulations (drawn in red) of the evolution of B_n , the number of black balls in the Young–Pólya urn with period $p = 2$ and parameter $\ell = 1$ (first 10,000 steps, with initially $b_0 = 1$ black and $w_0 = 1$ white balls), and the mean $\mathbb{E}(B_n)$ (drawn in blue). Right: the average (in red) of the 20 simulations, fitting neatly (almost indistinguishable!) the limit curve $\mathbb{E}(B_n) = \Theta(n^{2/3})$ (in blue).*

where the distribution of \mathfrak{B} is, for example, analysed by Flajolet et al. [30] via an analytic combinatorics approach, or by Janson [45] and Chauvin et al. [22] via a probabilistic approach relying on a continuous-time embedding introduced by Athreya and Karlin [5]. For example, averaging the Young–Pólya urn with $p = 2$, $\ell = 1$ and $b_0 = w_0 = 1$ leads to the replacement matrix $\begin{pmatrix} 1 & 1/2 \\ 0 & 3/2 \end{pmatrix}$. The corresponding classical urn model leads to a limit distribution with moments given, for example, by Janson in [45], Theorem 1.7:

$$\mathbb{E}(\mathfrak{B}^r) = \frac{\Gamma(4/3)r!}{\Gamma(2r/3 + 4/3)}.$$

Comparing these moments with the moments of our distribution (equation (20) hereafter) proves that these two distributions are distinct. However, it is noteworthy that they have similar tails: we discuss this universality phenomenon in Section 5.2.

- Another interesting alternative model, called multi-drawing Pólya urn model, consists in drawing multiple balls at once; see Lasmar et al. [58] or Kuba and Sulzbach [56]. Grouping p units of time into one drawing leads to a new replacement matrix. For example, for $p = 2$ and $\ell = 1$ we can approximate a Young–Pólya urn by an urn where at each unit of time 2 balls are drawn uniformly at random. If both of them are black we add 2 black balls and 1 white ball, if one is black and one is white we add 1 black and 2 white ball, and if both of them are white we add 3 white balls. Then the same convergence as in equation (2) holds, yet again with a different limit distribution, as can be seen by comparing the means and variances; compare Kuba and Mahmoud [54], Theorem 1, with our Example 3.7.

For all these alternative models, the corresponding histories are inherently different: none of them gives the exact generating function of periodic Pólya urns nor gives the closed form of the underlying distribution. This also motivates the exact and asymptotic analysis of our periodic model, which therefore enriches the urn world with new special functions.

Figure 2 shows that the distribution of B_n is spread; this is consistent with our result that the standard deviation and the mean $\mathbb{E}(B_n)$ (drawn in blue) have the same order of magnitude.³ The fluctuations around this mean are given by the generalized gamma product limit law from equation (1), as proven in Section 3. Let us first mention some articles where this distribution has already appeared before:

³The classical urn models with replacement matrices being either M_1 or M_2 also have such a spread; see [30], Figure 1.

- in Janson [47], as an instance of distributions with moments of gamma type, like the distributions occurring for the area of the supremum process of the Brownian motion;
- in Peköz, Röllin and Ross [70], as distributions of processes on walks, trees, urns and preferential attachments in graphs, where these authors also consider what they call a Pólya urn with immigration, which is a special case of a periodic Pólya urn (other models or random graphs have these distributions as limit laws [19, 84]);
- in Khodabin and Ahmadabadi [53] following a tradition to generalize special functions by adding parameters in order to capture several probability distributions, such as, for example, the normal, Rayleigh and half-normal distribution, as well as the MeijerG function (see also the addendum of [47], mentioning a dozen other generalizations of special functions).

1.3. *Plan of the article.* Our *main results* are the explicit enumeration results and links with hypergeometric functions (Theorems 2.3 and 3.1), and the limit law involving a product of generalized gamma distributions (Theorem 3.8, or the simplified version of it given for readability in Theorem 1.6 above). It is a nice cherry on the cake that this limit law also describes the fluctuations of the southeast⁴ corner of a random triangular Young tableau (as proven in Theorem 4.23). We believe that the methods used, that is, the generating functions for urns (developed in Section 2), the way to access the moments (developed in Section 3), and the density method for Young tableaux (developed in Section 4) are an original combination of tools, which should find many other applications in the future. Finally, Section 5 gives a relation between the southeast and the northwest corners of triangular Young tableaux (Proposition 5.7) and a link with factorizations of gamma distributions. Additionally, we discuss some universality properties of random surfaces, and we show to what extent the tails of our distributions are related to the tails of Mittag-Leffler distributions (Theorem 5.3), and when they are sub-Gaussian (Proposition 5.6).

In the next section, we translate the evolution of the urn into the language of generating functions by encoding the dynamics of this process into partial differential equations.

2. A functional equation for periodic Pólya urns.

2.1. *Urn histories and differential operators.* Let $h_{n,b,w}$ be the number of histories of a periodic Pólya urn after n steps with b black balls and w white balls, with an initial state of b_0 black and w_0 white balls. We define the polynomials

$$h_n(x, y) := \sum_{b,w \geq 0} h_{n,b,w} x^b y^w.$$

Note that these are indeed polynomials as there is just a finite number of histories after n steps. Due to the balanced urn model these polynomials are homogeneous. We collect all these histories in the trivariate exponential generating function

$$H(x, y, z) := \sum_{n \geq 0} h_n(x, y) \frac{z^n}{n!}.$$

EXAMPLE 2.1. For the Young–Pólya urn with $p = 2$, $\ell = 1$, and $b_0 = w_0 = 1$, we get for the first three terms of $H(x, y, z)$ the expansion (compare Figure 1)

$$H(x, y, z) = xy + (xy^2 + x^2y)z + (2xy^4 + 2x^2y^3 + 2x^3y^2) \frac{z^2}{2} + \dots$$

⁴In this article, we use the French convention to draw the Young tableaux; see Section 4 and [61].

In this section, our goal is to derive a partial differential equation describing the evolution of the periodic Pólya urn model.

The periodic nature of the problem motivates to split the number of histories into p residue classes. Let $H_0(x, y, z), H_1(x, y, z), \dots, H_{p-1}(x, y, z)$ be the generating functions of histories after $0, 1, \dots, p - 1$ draws modulo p , respectively. In particular, we have

$$H_i(x, y, z) := \sum_{n \geq 0} h_{pn+i}(x, y) \frac{z^{pn+i}}{(pn+i)!},$$

for $i = 0, 1, \dots, p - 1$ such that

$$H(x, y, z) = H_0(x, y, z) + H_1(x, y, z) + \dots + H_{p-1}(x, y, z).$$

Next, we associate with the two distinct replacement matrices

$$\begin{pmatrix} 1 & 0 \\ 0 & 1 \end{pmatrix} \quad \text{and} \quad \begin{pmatrix} 1 & \ell \\ 0 & 1 + \ell \end{pmatrix}$$

from Definition 1.2 the differential operators \mathcal{D}_1 and \mathcal{D}_2 , respectively. We get

$$\mathcal{D}_1 := x^2 \partial_x + y^2 \partial_y \quad \text{and} \quad \mathcal{D}_2 := y^\ell \mathcal{D}_1,$$

where ∂_x and ∂_y are defined as the partial derivatives $\frac{\partial}{\partial x}$ and $\frac{\partial}{\partial y}$, respectively. This models the evolution of the urn. For example, in the term $x^2 \partial_x$, the derivative ∂_x represents drawing a black ball and the multiplication by x^2 returning this black ball and an additional black ball into the urn. The other terms have analogous interpretations.

With these operators, we are able to link the consecutive drawings with the following system:

$$(3) \quad \begin{cases} \partial_z H_{i+1}(x, y, z) = \mathcal{D}_1 H_i(x, y, z) & \text{for } i = 0, 1, \dots, p - 2, \\ \partial_z H_0(x, y, z) = \mathcal{D}_2 H_{p-1}(x, y, z). \end{cases}$$

Note that the derivative ∂_z models the evolution in time. We see two types of transitions: in the first $p - 1$ rounds the urn behaves like a normal Pólya urn, but in the p th round we additionally add ℓ white balls. The first transition type is modelled by the \mathcal{D}_1 operator and the second type by the \mathcal{D}_2 operator. This system of partial differential equations naturally corresponds to recurrences on the level of coefficients $h_{n,b,w}$, and *vice versa*. This philosophy is well explained in the *symbolic method* part of [33] (see also [30, 31, 42, 67] for examples of applications to urns).

As a next step, we want to eliminate the y variable in these equations. This is possible as the number of balls in each round and the number of black and white balls are connected due to the fact that we are dealing with balanced urns. As observed previously, one has

$$(4) \quad \text{number of balls after } n \text{ steps} = s_0 + n + \ell \left\lfloor \frac{n}{p} \right\rfloor,$$

with $s_0 := b_0 + w_0$ being the number of initial balls. Therefore, for any $x^b y^w z^n$ appearing in $H(x, y, z)$, we have

$$b + w = s_0 + n + \ell \frac{n - i}{p} \quad \text{if } n \equiv i \pmod{p},$$

which directly translates into the following system of equations (for $i = 0, \dots, p - 1$):

$$(5) \quad x \partial_x H_i(x, y, z) + y \partial_y H_i(x, y, z) = \left(1 + \frac{\ell}{p}\right) z \partial_z H_i(x, y, z) + \left(s_0 - \frac{i \ell}{p}\right) H_i(x, y, z).$$

These equations are contractions in the metric space of formal power series in z (see, e.g., [8] or [33], Section A.5), so, given the initial conditions $[z^0]H_i(x, y, z)$, the Banach fixed-point theorem entails that this system has a unique solution: our set of generating functions. Now, because of the deterministic link between the number of black balls and the number of white balls, it is natural to introduce the two shorthands $H(x, z) := H(x, 1, z)$ and $H_i(x, z) := H_i(x, 1, z)$. What is the nature of these functions? This is what we tackle now.

2.2. D-finiteness of history generating functions. Let us first give a formal definition of the fundamental concept of D-finiteness.

DEFINITION 2.2 (D-finiteness). A power series $F(z) = \sum_{n \geq 0} f_n z^n$ with coefficients in some ring \mathbb{A} is called *D-finite* if it satisfies a linear differential equation $L.F(z) = 0$, where $L \neq 0$ is a differential operator, $L \in \mathbb{A}[z, \partial_z]$. Equivalently, the sequence $(f_n)_{n \in \mathbb{N}}$ is called *P-recursive*: it satisfies a linear recurrence with polynomial coefficients in n . Such functions and sequences are also sometimes called *holonomic*.

D-finite functions are ubiquitous in combinatorics, computer science, probability theory, number theory, physics, etc.; see, for example, [1] or [33], Appendix B.4. They possess closure properties galore; this provides an ideal framework for handling (via computer algebra) sums and integrals involving such functions [15, 71]. The same idea applies to a full family of linear operators (differentiations, recurrences, finite differences, q -shifts) and is unified by what is called holonomy theory. This theory leads to a fascinating algorithmic universe to deal with orthogonal polynomials, Laplace and Mellin transforms, and most of the integrals of special functions: it offers powerful tools to prove identities, asymptotic expansions, numerical values, structural properties; see [50, 68, 76].

We have seen in Section 2.1 that the dynamics of urns is intrinsically related to *partial* differential equations (mixing ∂_x , ∂_y , and ∂_z). It is therefore a nice surprise that it is also possible to describe their evolution in many cases with *ordinary* differential equations (i.e., involving only ∂_z).

THEOREM 2.3 (Differential equations for histories). *The generating functions describing a Young–Pólya urn of period p and parameter ℓ with initially $s_0 = b_0 + w_0$ balls, where b_0 are black and w_0 are white, satisfy the following system of p partial differential equations:*

$$(6) \quad \partial_z H_{i+1}(x, z) = x(x-1)\partial_x H_i(x, z) + \left(1 + \frac{\ell}{p}\right)z\partial_z H_i(x, z) + \left(s_0 - \frac{i\ell}{p}\right)H_i(x, z),$$

for $i = 0, \dots, p-1$ with $H_p(x, z) := H_0(x, z)$. Moreover, if any of the corresponding generating functions (ordinary, exponential, ordinary probability or exponential probability) is D-finite in z , then all of them are D-finite in z .

PROOF. First, let us prove the system involving ∂_z and ∂_x only. Combining (3) and (5), we eliminate ∂_y . Then it is legitimate to insert $y = 1$ as there appears no differentiation with respect to y anymore. This gives (6).

Now, assume the ordinary generating function is D-finite. Multiplying a holonomic sequence by $n!$ (or by $1/n!$, or more generally by any holonomic sequence) gives a new sequence, which is also holonomic. In other words, the Hadamard product of two holonomic sequences is still holonomic [89], Chapter 6.4. This proves that the ordinary and exponential versions of our generating functions H and H_i are D-finite in z .

Finally, for the probability generating function defined as

$$\sum_{n,b,w} \mathbb{P}(B_n = b \quad \text{and} \quad W_n = w) x^b y^w z^n = \sum_n \frac{h_n(x, y)}{h_n(1, 1)} z^n,$$

TABLE 1

Size of the D-finite equations for the four types of generating functions of histories (for the urn model of Example 2.4). We use the abbreviations EGF (exponential generating function), OGF (ordinary generating function), EPGF (exponential probability generating function), OPGF (ordinary probability generating function). We omit the degree of the variable y , as, for balanced urns, it is trivially related to the degree in x

Type	Generating function	Order in ∂_z	Degree in z	Degree in x
EGF	$\sum_{n,b,w} h_{n,b,w} x^b y^w \frac{z^n}{n!}$	5	13	16
OGF	$\sum_{n,b,w} h_{n,b,w} x^b y^w z^n$	7	23	20
EPGF	$\sum_{n,b,w} \mathbb{P}(B_n = b \text{ and } W_n = w) x^b y^w \frac{z^n}{n!}$	8	4	15
OPGF	$\sum_{n,b,w} \mathbb{P}(B_n = b \text{ and } W_n = w) x^b y^w z^n$	3	13	14

it is in general not the case that it is holonomic if the initial ordinary generating function is holonomic. But in our case a miracle occurs: in each residue class of $n \pmod p$, the sequence $(h_{pm+i}(1, 1))_{m \in \mathbb{N}}$ is hypergeometric (as shown in Theorem 3.1), therefore, the p subsequences $(1/h_{pm+i}(1, 1))_{m \in \mathbb{N}}$ are also hypergeometric, and thus the above probability generating function (which is the sum of p holonomic functions, each one being the Hadamard product of two holonomic functions) is holonomic. \square

Experimentally, in most cases a few terms suffice to guess a holonomic sequence in z . We believe that this sequence is always holonomic, yet we were not able to prove it in full generality. We plan to comment more on this and other related phenomena in a forthcoming article.

EXAMPLE 2.4. In the case of the Young–Pólya urn with $p = 2$, $\ell = 1$, and $b_0 = w_0 = 1$, the differential equations for histories (6) are

$$\begin{cases} \partial_z H_0(x, z) = x(x - 1)\partial_x H_1(x, z) + \frac{3}{2}z\partial_z H_1(x, z) + \frac{3}{2}H_1(x, z), \\ \partial_z H_1(x, z) = x(x - 1)\partial_x H_0(x, z) + \frac{3}{2}z\partial_z H_0(x, z) + 2H_0(x, z). \end{cases}$$

In addition to this system of *partial* differential equations, there exist also two *ordinary* linear differential equations in z for H_0 and H_1 and, therefore, for their sum $H := H_0 + H_1$, the generating function of all histories.

In Table 1, we compare the size of the D-finite equations⁵ for the different generating functions. For example, for the ordinary probability generating function one has the equation $L.F(x, z) = 0$, where L is the following differential operator of order 3 in ∂_z :

$$\begin{aligned} L = & 9z(z - 1)(z + 1)(15x^{13}z^{10} + \dots + 3)\partial_z^3 + 3(375x^{13}z^{12} + \dots - 21)\partial_z^2 \\ & + 2(1020x^{13}z^{11} + \dots + 42)\partial_z + 600x^{13}z^{10} + \dots + 1. \end{aligned}$$

The singularity at $z = 1$ of the leading coefficient reflects the fact that F is a probability generating function (and thus has radius of convergence equal to 1). It is noteworthy that some roots of the indicial polynomial of L at $z = 1$ differ by an integer, this phenomenon is sometimes called resonance, and often occurs in the world of hypergeometric functions; we will come back to these facts and what they imply for the asymptotics (see also [33], Chapter IX. 7.4).

⁵When we say *the* equation, we mean the linear differential equation of minimal order in ∂_z , and then minimal degrees in z and x , up to a constant factor for its leading term.

Note that the fact to be D-finite has an unexpected consequence: it allows a surprisingly fast computation of h_n in time $O(\sqrt{n} \log^2 n)$ (see [15], Chapter 15, for a refined complexity analysis of the corresponding algorithm). Such efficient computations are, for example, implemented in the Maple package `gfun` (see [83]). This package, together with some packages for differential elimination (see [16, 35]), allows us to compute the different D-finite equations from Table 1, via the union of our Theorem 3.1 on the hypergeometric closed forms and the closure properties mentioned above.

Another important consequence of the D-finiteness is that the type of the singularities that the function can have is constrained. In particular, the following important subclass of D-finite functions can be automatically analysed:

REMARK 2.5. Flajolet and Lafforgue have proven that under some “generic” conditions, such D-finite equations lead to a Gaussian limit law (see [32], Theorem 7, and [33], Chapter IX. 7.4). It is interesting that these generic conditions are not fulfilled in our case: we have a cancellation of the leading coefficient of L at $(x, z) = (1, 1)$, a confluence for the indicial polynomial, and the resonance phenomenon mentioned above! The natural model of periodic Pólya urns thus leads to an original analytic situation, which offers a new (non-Gaussian) limit law.

We thus need another strategy to determine the limit law. In the next section, we use the system of equations (6) to iteratively derive the moments of the distribution of black balls after n steps.

3. Moments of periodic Pólya urns. In this section, we give the proof of Theorem 1.6 and a generalization of it. As it will use the method of moments, let us introduce $m_r(n)$, the r th factorial moment of the distribution of black balls after n steps, that is,

$$m_r(n) := \mathbb{E}(B_n(B_n - 1) \cdots (B_n - r + 1)).$$

Expressing them in terms of the generating function $H(x, z)$, it holds that

$$m_r(n) = \frac{[z^n] \frac{\partial^r}{\partial x^r} H(x, z) \Big|_{x=1}}{[z^n] H(1, z)},$$

where $[z^n] \sum_n f_n z^n := f_n$ is the coefficient extraction operator.

We will compute the sequences of the numerator and denominator separately. We start with the denominators, the total number of histories after n steps.

3.1. Number of histories: A hypergeometric closed form. We prove that $H(1, z)$ satisfies a miraculous property which does not hold for $H(x, z)$: it is a sum of generalized hypergeometric functions (see, e.g., [3] for an introduction to this important class of special functions).

THEOREM 3.1 (Hypergeometric closed forms). *Let $h_n := n![z^n]H(1, z)$ be the number of histories after n steps in a Young–Pólya urn of period p and parameter ℓ with initially $s_0 = b_0 + w_0$ balls, where b_0 are black and w_0 are white. Then, for each i , $(h_{p(m+i)})_{m \in \mathbb{N}}$ is a hypergeometric sequence, satisfying the recurrence*

$$(7) \quad h_{p(m+1)+i} = \prod_{j=0}^{i-1} ((p + \ell)(m + 1) + s_0 + j) \prod_{j=i}^{p-1} ((p + \ell)m + s_0 + j) h_{pm+i}.$$

Equivalent closed forms are given in equations (10), (11) and (12).

PROOF. Substituting $x = 1$ into (6) and extracting the coefficient of z^n for $i = 0, \dots, p - 1$ gives the recurrence

$$(8) \quad h_{n+1} = \left(\left(1 + \frac{\ell}{p} \right) n + b_n \right) h_n \quad \text{with}$$

$$(9) \quad b_n := s_0 - \frac{\ell}{p} (n \bmod p),$$

where $n \bmod p$ gives values in $\{0, 1, \dots, p - 1\}$. Iterating this recurrence relation p times gives (7). This leads to the following equivalent closed forms:

$$(10) \quad h_{pm+i} = \frac{(p + \ell)^{pm+i}}{\prod_{j=0}^{p-1} \Gamma\left(\frac{s_0+j}{p+\ell}\right)} \prod_{j=0}^{i-1} \Gamma\left(m + 1 + \frac{s_0 + j}{p + \ell}\right) \prod_{j=i}^{p-1} \Gamma\left(m + \frac{s_0 + j}{p + \ell}\right),$$

$$(11) \quad h_{pm+i} = (p + \ell)^{pm} \frac{\Gamma(s_0 + (p + \ell)m + i)}{\Gamma(s_0 + (p + \ell)m)} \prod_{j=0}^{p-1} \frac{\Gamma\left(m + \frac{s_0+j}{p+\ell}\right)}{\Gamma\left(\frac{s_0+j}{p+\ell}\right)}.$$

Accordingly, the function $H(1, z)$ is the sum of p generalized hypergeometric functions ${}_pF_{p-1}$:

$$(12) \quad H(1, z) = \sum_{i=0}^{p-1} \binom{s_0 + i - 1}{i} z^i {}_pF_{p-1} \left(L_1(i), L_2(i), \left(\frac{(p + \ell)z}{p} \right)^p \right),$$

where the lists of arguments are given by $L_1(i) := \left[\left(\frac{s_0+j}{p+\ell} + 1 \right)_{j=0, \dots, i-1}, \left(\frac{s_0+j}{p+\ell} \right)_{j=i, \dots, p-1} \right]$ and $L_2(i) := \left[\left(\frac{j}{p} + 1 \right)_{j=1, \dots, i}, \left(\frac{j}{p} \right)_{j=i+1, \dots, p-1} \right]$. \square

EXAMPLE 3.2. In the case of the Young–Pólya urn with $p = 2$, $\ell = 1$, and $b_0 = w_0 = 1$, one has the hypergeometric closed forms for $h_n := n![z^n]H(1, z)$:

$$h_n = \begin{cases} 3^n \frac{\Gamma\left(\frac{n}{2} + 1\right)\Gamma\left(\frac{n}{2} + \frac{2}{3}\right)}{\Gamma(2/3)} & \text{if } n \text{ is even,} \\ 3^n \frac{\Gamma\left(\frac{n}{2} + \frac{1}{2}\right)\Gamma\left(\frac{n}{2} + \frac{7}{6}\right)}{\Gamma(2/3)} & \text{if } n \text{ is odd.} \end{cases}$$

Alternatively, this sequence satisfies $h(n + 2) = \frac{3}{2}h(n + 1) + \frac{1}{4}(9n^2 + 21n + 12)h(n)$. This sequence was not in the On-Line Encyclopedia of Integer Sequences, accessible at <https://oeis.org>. We added it there; it is now [A293653](#), and it starts like this: 1, 2, 6, 30, 180, 1440, 12960, 142560, 1710720, The exponential generating function can be written as the sum of two hypergeometric functions:

$$H(1, z) = {}_2F_1 \left(\left[\frac{2}{3}, 1 \right], \left[\frac{1}{2} \right], \left(\frac{3z}{2} \right)^2 \right) + 2z {}_2F_1 \left(\left[\frac{5}{3}, 1 \right], \left[\frac{3}{2} \right], \left(\frac{3z}{2} \right)^2 \right).$$

3.2. Mean and critical exponent. Let us proceed with the computation of moments. For this purpose, define

$$h_n^{(r)} := n![z^n] \frac{\partial^r}{\partial x^r} H(x, z) \Big|_{x=1},$$

as the coefficient of $\frac{(x-1)^r z^n}{r!n!}$ of $H(x, z)$. Then the r th moment is obviously computed as $m_r(n) = \frac{h_n^{(r)}}{h_n}$. The key idea why to use these quantities comes from the differential equations for histories (6). The derivative of $H_i(x, z)$ with respect to x has a factor $(x - 1)$, which

makes it possible to compute $h_n^{(r)}$ iteratively by taking the r -th derivative with respect to x and substituting $x = 1$. Let us define the auxiliary functions

$$H_i^{(r)}(z) := \frac{\partial^r}{\partial x^r} H_i(x, z) \Big|_{x=1}.$$

We get for $i = 0, \dots, p - 1$ (with b_i as defined in (9)):

$$\partial_z H_{i+1}^{(r)}(z) = \left(1 + \frac{\ell}{p}\right) z \partial_z H_i^{(r)}(z) + (b_i + r) H_i^{(r)}(z) + (r - 1)r H_i^{(r-1)}(z).$$

From this equation we extract the n th coefficient with respect to z and multiply by $n!$ to get

$$(13) \quad h_{n+1}^{(r)} = \left(\left(1 + \frac{\ell}{p}\right)n + b_n + r \right) h_n^{(r)} + (r - 1)r h_n^{(r-1)}.$$

We reveal a perturbed version of (8). In particular, this is a nonhomogeneous linear recurrence relation. Yet, the inhomogeneity only emerges for $r \geq 2$. Thus, the mean is derived directly with the same approach as h_n previously. Note that for $r = 1$, equation (13) is exactly of the same type as (8) after replacing s_0 by $s_0 + r$ and h_0 by b_0 . We get without any further work

$$h_{pm+i}^{(1)} = C_1 (p + \ell)^{pm+i} \prod_{j=0}^{i-1} \Gamma\left(m + 1 + \frac{s_0 + 1 + j}{p + \ell}\right) \prod_{j=i}^{p-1} \Gamma\left(m + \frac{s_0 + 1 + j}{p + \ell}\right),$$

$$C_1 = b_0 \prod_{j=0}^{p-1} \Gamma\left(\frac{s_0 + 1 + j}{p + \ell}\right)^{-1}.$$

Combining the last two results, we get a (surprisingly) simple expression

$$\begin{aligned} \mathbb{E}B_{pm+i} &= \frac{h_{pm+i}^{(1)}}{h_{pm+i}} = \frac{C_1 \prod_{j=0}^{i-1} \Gamma\left(m + 1 + \frac{s_0+1+j}{p+\ell}\right) \prod_{j=i}^{p-1} \Gamma\left(m + \frac{s_0+1+j}{p+\ell}\right)}{C_0 \prod_{j=0}^{i-1} \Gamma\left(m + 1 + \frac{s_0+j}{p+\ell}\right) \prod_{j=i}^{p-1} \Gamma\left(m + \frac{s_0+j}{p+\ell}\right)} \\ &= b_0 \frac{\Gamma\left(\frac{s_0}{p+\ell}\right)}{\Gamma\left(\frac{s_0+p}{p+\ell}\right)} \left(m + \frac{s_0 + i}{p + \ell}\right) \frac{\Gamma\left(m + \frac{s_0+p}{p+\ell}\right)}{\Gamma\left(m + 1 + \frac{s_0}{p+\ell}\right)}. \end{aligned}$$

In particular, it is straightforward to compute an asymptotic expansion for the mean by Stirling’s approximation. For $i = 0, 1, \dots, p - 1$, we get

$$\mathbb{E}B_{pm+i} = b_0 \frac{\Gamma\left(\frac{s_0}{p+\ell}\right)}{\Gamma\left(\frac{s_0+p}{p+\ell}\right)} m^{\frac{p}{p+\ell}} \left(1 + O\left(\frac{1}{m}\right)\right).$$

This leads to the following proposition.

PROPOSITION 3.3 (Formula for the mean of Young–Pólya urns). *The expected number of black balls in a Young–Pólya urn of period p and parameter ℓ with initially $s_0 = b_0 + w_0$ balls, where b_0 are black and w_0 are white, satisfies for large n*

$$\mathbb{E}B_n = b_0 \frac{\Gamma\left(\frac{s_0}{p+\ell}\right)}{\Gamma\left(\frac{s_0+p}{p+\ell}\right)} \left(\frac{n}{p}\right)^{\frac{p}{p+\ell}} \left(1 + O\left(\frac{1}{n}\right)\right).$$

REMARK 3.4 (Critical exponent). As will be more transparent from discussions in the next sections, the exponent $\delta := \frac{p}{p+\ell}$ is here the crucial quantity to keep in mind. It is sometimes called “critical exponent” as such exponents can often be captured by ideas from statistical mechanics, as a signature of a phase transition phenomenon.

EXAMPLE 3.5. For the Young–Pólya urn with $p = 2$, $\ell = 1$, and $b_0 = w_0 = 1$, the expected number of black balls at time n is thus

$$\mathbb{E}B_n = \frac{\Gamma(2/3)}{\Gamma(4/3)} \left(\frac{n}{2}\right)^{\frac{2}{3}} \left(1 + O\left(\frac{1}{n}\right)\right) \approx 0.9552n^{2/3} \left(1 + O\left(\frac{1}{n}\right)\right).$$

This is coherent with the renormalization used for the limit law of B_n in Example 1.7.

3.3. *Higher moments.* When computing higher moments, the first idea is to transform the nonhomogeneous recurrence relation (13) into a homogeneous one. To this aim, one rewrites this equation into

$$(14) \quad y_{n+1} - (an + b_n + r)y_n = (r - 1)rh_n^{(r-1)} \quad \text{and} \quad y_0 = \partial_x^r H(x, 0)|_{x=1}.$$

Note that we have $y_n = h_n^{(r)}$, the r -th moment we want to determine. From now on, we speak of the *homogeneous equation* to refer to the left-hand side of equation (14) set equal to 0, whereas equation (14) itself is called the *nonhomogeneous equation*. In order to get $h_n^{(r)}$, we proceed by induction on r : we assume that the $(r - 1)$ -st moment is known (thus, we know the right-hand side of (14)), and we want to express the r th moment $h_n^{(r)}$ (i.e., we want to solve the recurrence (14) for y_n) in terms of this previously computed quantity.

As for any linear recurrence, its solution is given by a combination of a solution $h_{n,\text{hom}}^{(r)}$ of the homogeneous equation and of a particular solution $h_{n,\text{par}}^{(r)}$ such that

$$(15) \quad h_n^{(r)} = C_r h_{n,\text{hom}}^{(r)} - h_{n,\text{par}}^{(r)},$$

with $C_r \in \mathbb{R}$ such that the initial condition in (14) is satisfied. We will show that asymptotically only the solution $h_{n,\text{hom}}^{(r)}$ of the homogeneous equation is dominant. First of all, this solution is easy to compute, as it is again of the same type as (8). We have

$$(16) \quad h_{pm+i,\text{hom}}^{(r)} = (p + \ell)^{pm+i} \prod_{j=0}^{i-1} \Gamma\left(m + 1 + \frac{s_0 + r + j}{p + \ell}\right) \prod_{j=i}^{p-1} \Gamma\left(m + \frac{s_0 + r + j}{p + \ell}\right).$$

The next idea is to find a particular solution of the nonhomogeneous recurrence relation (14). We will show that the equation exhibits a phenomenon similar to resonance and we will show that the particular solution is

$$(17) \quad h_{n,\text{par}}^{(r)} = \sum_{j=1}^{r-1} d_j h_n^{(j)} \quad \text{for constants } d_j \in \mathbb{R}.$$

We will compute the coefficients d_j by induction from $r - 1$ to 1. First, we observe that the inhomogeneous part in the r th equation is a multiple of the solution $h_n^{(r-1)}$ of the $(r - 1)$ -st equation. This motivates us to set $y_n = h_n^{(r-1)}$ in the homogeneous equation of the r -th equation. Using (14) then leads to

$$h_{n+1}^{(r-1)} - (an + b_n + r)h_n^{(r-1)} = (r - 1)(r - 2)h_n^{(r-2)} - h_n^{(r-1)}.$$

Thus, by linearity we choose $h_{n,\text{par}}^{(r)} = z_n - (r - 1)rh_n^{(r-1)}$, that is, $d_{r-1} = (r - 1)r$, as a first candidate for a particular solution where z_n is (still) an undetermined sequence. Inserting this into (14), we get a recurrence relation for z_n , where we reduced the order of the inhomogeneity by one in r (in comparison with (14)):

$$z_{n+1} - (an + b_n + r)z_n = r(r - 1)^2(r - 2)h_n^{(r-2)}.$$

Continuing this approach, we compute all d_j 's inductively. As the order in r decreases, this approach terminates at $r = 1$. One thus identifies the constants d_j of formula (17):

$$d_j = \prod_{i=j+1}^r \frac{(i-1)i}{r-i+1} = \binom{r-1}{j-1} \frac{r!}{j!} = L(r, j),$$

with $L(r, j)$ being the Lah numbers, which express the rising factorials in terms of falling factorials⁶ (see [57] and [77], page 43):

$$(18) \quad \sum_{j=1}^r L(r, j)x^{\underline{j}} = x^{\bar{r}}.$$

Then, by (15) we get the general solution of the r th moment

$$(19) \quad h_n^{(r)} = C_r h_{n,\text{hom}}^{(r)} - \sum_{j=1}^{r-1} L(r, j)h_n^{(j)}.$$

For $n = 0$, equation (19) becomes

$$h_0^{(r)} = \partial_x^r H(x, 0)|_{x=1} = b_0^{\underline{r}} = C_r h_{0,\text{hom}}^{(r)} - \sum_{j=1}^{r-1} L(r, j)b_0^{\underline{j}},$$

which gives together with (18) that $C_r h_{0,\text{hom}}^{(r)} = b_0^{\bar{r}}$.

Finally, we are now able to compute the asymptotic expansion of the r th (factorial) moment. Using Stirling's approximation, the quotient of the quantities given by (19) and (16) gives that $\frac{h_n^{(j)}}{h_{n,\text{hom}}^{(r)}} = O(n^{-\frac{(r-j)p}{p+\ell}})$, for $j = 1, \dots, r - 1$. Hence, for the r th moment given by (19), we proved that the contribution of $h_{n,\text{hom}}^{(r)}$ is the asymptotically dominant one. This leads to the main result on the asymptotics of the moments.

PROPOSITION 3.6 (Moments of Young–Pólya urns). *The r th (factorial) moment of B_n (the number of black balls in the Young–Pólya urn of period p and parameter ℓ with initially $s_0 = b_0 + w_0$ balls, where b_0 are black and w_0 are white) for large n satisfies⁶*

$$m_r(n) = \gamma_r n^{\delta r} \left(1 + O\left(\frac{1}{n}\right) \right) \quad \text{with } \gamma_r = \frac{b_0^{\bar{r}}}{p^{\delta r}} \prod_{j=0}^{r-1} \frac{\Gamma(\frac{s_0+j}{p+\ell})}{\Gamma(\frac{s_0+r+j}{p+\ell})} \text{ and } \delta = \frac{p}{p+\ell}.$$

EXAMPLE 3.7. For the Young–Pólya urn with $p = 2$, $\ell = 1$, and $b_0 = w_0 = 1$, the variance of the number of black balls at time n is thus

$$\mathbb{V}B_n = \frac{27}{8} \frac{\Gamma(\frac{2}{3})^2 (3\Gamma(\frac{4}{3}) - \Gamma(\frac{2}{3})^2)}{2^{1/3}\pi^2} n^{4/3} \left(1 + O\left(\frac{1}{n}\right) \right) \approx 0.42068n^{4/3} \left(1 + O\left(\frac{1}{n}\right) \right).$$

NOTA BENE. The reasoning following equation (19) shows that these asymptotics are the same for the moments and the factorial moments, so in the sequel we refer to this result indifferently from both points of view.

⁶The falling factorial $x^{\underline{r}}$ is defined by $x^{\underline{r}} := x(x-1)\cdots(x-r+1) = \Gamma(x+1)/\Gamma(x-r+1)$, while the rising factorial $x^{\bar{r}}$ is defined by $x^{\bar{r}} := \Gamma(x+r)/\Gamma(x) = x(x+1)\cdots(x+r-1)$. These two notations were introduced as an alternative to the Pochhammer symbols by Graham, Knuth and Patashnik in [39].

3.4. *Limit distribution for periodic Pólya urns.* We use the method of moments to prove Theorem 1.6 (the generalized gamma product distribution for Young–Pólya urns). The natural factors occurring in the constant γ_r of Proposition 3.6, may they be $1/\Gamma(\frac{s+r+j}{p+\ell})$ or $(b_0^r)^{1/p}/\Gamma(\frac{s+r+j}{p+\ell})$, do not satisfy the determinant/finite difference positivity tests for the Stieltjes/Hamburger/Hausdorff moment problems, therefore, no continuous distribution has such moments (see [92]). However, the full product does correspond to moments of a distribution which is easier to identify if we start by transforming the constant γ_r by the Gauss multiplication formula of the gamma function; this gives

$$\gamma_r = \frac{(p + \ell)^r}{p^{\delta r}} \frac{\Gamma(b_0 + r)\Gamma(s_0)}{\Gamma(b_0)\Gamma(s_0 + r)} \prod_{j=0}^{\ell-1} \frac{\Gamma(\frac{s_0+r+p+j}{p+\ell})}{\Gamma(\frac{s_0+p+j}{p+\ell})}.$$

Combining this result with the r th (factorial) moment $m_r(n)$ from Proposition 3.6, we see that the moments $\mathbb{E}(B_n^{*r})$ of the rescaled random variable $B_n^* := \frac{p^\delta}{p+\ell} \frac{B_n}{n^\delta}$ converge for $n \rightarrow \infty$ to the limit

$$(20) \quad m_r := \frac{\Gamma(b_0 + r)\Gamma(s_0)}{\Gamma(b_0)\Gamma(s_0 + r)} \prod_{j=0}^{\ell-1} \frac{\Gamma(\frac{s_0+r+p+j}{p+\ell})}{\Gamma(\frac{s_0+p+j}{p+\ell})},$$

a simple formula involving the parameters (p, ℓ, b_0, w_0) of the model (with $s_0 := b_0 + w_0$).

Next, note that the following sum diverges (recall that $0 \leq (1 - \delta) < 1$):

$$\sum_{r>0} m_r^{-1/(2r)} = \sum_{r>0} \left(\frac{(p + \ell)e}{r} \right)^{(1-\delta)/2} (1 + o(1)) = +\infty.$$

Therefore, a result by Carleman (see [21], pages 189–220) implies that there exists a unique distribution (let us call it \mathcal{D}) with such moments m_r . Then, by the limit theorem of Fréchet and Shohat [34], page 536,⁷ B_n^* converges to \mathcal{D} .

Finally, we use the shape of the moments in (20) in order to express this distribution \mathcal{D} in terms of the main functions defined in Section 1. First, note that if for some independent random variables X, Y, Z , one has $\mathbb{E}(X^r) = \mathbb{E}(Y^r)\mathbb{E}(Z^r)$ (and if Y and Z are determined by their moments), then $X \stackrel{\mathcal{L}}{=} YZ$. Therefore, we treat the factors independently. The first factor corresponds to a beta distribution $\text{Beta}(b_0, w_0)$. For the other factors, it is easy to check that if $X \sim \text{GenGamma}(\alpha, \beta)$ is a generalized gamma distributed random variable (as defined in Definition 1.4), then it is a distribution determined by its moments, which are given by $\mathbb{E}(X^r) = \frac{\Gamma(\frac{\alpha+r}{\beta})}{\Gamma(\frac{\alpha}{\beta})}$. Therefore, the expression in (20) characterizes the GenGammaProd distribution. This completes the proof of Theorem 1.6.

For reasons which would be clear in Section 4, it was natural to focus first on Young–Pólya urns. However, the method presented in this section allows us to handle more general models. It would have been quite indigestible to present directly the general proof with heavy notation and many variables but now that the reader got the key steps of the method, she should be delighted to recycle all of this for free in the following much more general result.

THEOREM 3.8 (The generalized gamma product distribution for triangular balanced urns). *Let $p \geq 1$ and $\ell_1, \dots, \ell_p \geq 0$ be nonnegative integers. Consider a periodic Pólya urn of period p with replacement matrices M_1, \dots, M_p given by $M_j := \begin{pmatrix} 1 & \ell_j \\ 0 & 1+\ell_j \end{pmatrix}$. Then the renormalized distribution of black balls is asymptotically for $n \rightarrow \infty$ given by the following product*

⁷As a funny coincidence, Fréchet and Shohat mention in [34] that the generalized gamma distribution with parameter $p \geq 1/2$ is uniquely characterized by its moments.

of distributions:

$$\frac{p^\delta}{p + \ell} \frac{B_n}{n^\delta} \xrightarrow{\mathcal{L}} \text{Beta}(b_0, w_0) \prod_{\substack{i=1 \\ i \neq \ell_1 + \dots + \ell_j + j \text{ with } 1 \leq j \leq p-1}}^{p+\ell-1} \text{GenGamma}(b_0 + w_0 + i, p + \ell)$$

with $\ell = \ell_1 + \dots + \ell_p$, $\delta = p/(p + \ell)$, and $\text{Beta}(b_0, w_0) = 1$ when $w_0 = 0$.

In the sequel, we denote this distribution by $\text{GenGammaProd}([\ell_1, \dots, \ell_p]; b_0, w_0)$.

PROOF. The proof relies on the same steps as in Sections 2 and 3 with some minor technical changes, so we only point out the main differences.

The behaviour of the urn is now modeled by the p differential operators $\mathcal{D}_j = y^{\ell_j}(x^2\partial_x + y^2\partial_y)$. As the matrices are balanced, there is (like in equation (4)) a direct link between the number of black balls and the total number of balls. This allows to eliminate the y variable and leads to the following system of partial differential equations (which generalizes equation (6)):

$$\partial_z H_{i+1}(x, z) = x(x - 1)\partial_x H_i(x, z) + \left(1 + \frac{\ell}{p}\right)z\partial_z H_i(x, z) + \left(s_0 - \sum_{j=1}^i \ell_j - \frac{i\ell}{p}\right)H_i(x, z),$$

for $i = 0, \dots, p - 1$ with $H_p(x, z) := H_0(x, z)$. Here, one again applies the method of moments used in this Section 3. In particular, equation (8) remains the same. Only the coefficients b_n in equation (9) change to $s_0 - \sum_{j=1}^i \ell_j - \frac{\ell}{p}(i \bmod p)$.

Hence, we get the following asymptotic result for the moments generalizing Proposition 3.6:

$$(21) \quad m_r(n) = \gamma_r n^{\delta r} \left(1 + O\left(\frac{1}{n}\right)\right) \quad \text{with } \gamma_r = \frac{b_0^{\bar{r}}}{p^{\delta r}} \prod_{j=0}^{p-1} \frac{\Gamma\left(\frac{s_0}{p+\ell} + \frac{j+\sum_{k=1}^j \ell_k}{p+\ell}\right)}{\Gamma\left(\frac{s_0+r}{p+\ell} + \frac{j+\sum_{k=1}^j \ell_k}{p+\ell}\right)}.$$

After rewriting γ_r via the Gauss multiplication formula, we recognize the product of distributions (characterized by their moments) which we wanted to prove. \square

Let us illustrate this theorem with what we call the staircase periodic Pólya urn (this model will reappear later in the article).

EXAMPLE 3.9 (Staircase periodic Pólya urn). For the Pólya urn of period 3 with replacement matrices

$$M_1 := \begin{pmatrix} 1 & 0 \\ 0 & 1 \end{pmatrix}, \quad M_2 := \begin{pmatrix} 1 & 1 \\ 0 & 2 \end{pmatrix} \quad \text{and} \quad M_3 := \begin{pmatrix} 1 & 2 \\ 0 & 3 \end{pmatrix},$$

the number B_n of black balls has the limit law $\text{GenGammaProd}([0, 1, 2]; b_0, w_0)$:

$$\frac{\sqrt{3}}{6} \frac{B_n}{\sqrt{n}} \xrightarrow{\mathcal{L}} \text{Beta}(b_0, w_0) \prod_{i=2,4,5} \text{GenGamma}(b_0 + w_0 + i, 6).$$

In the next section, we will see what are the implications of our results for urns on an apparently unrelated topic: Young tableaux.

4. Urns, trees and Young tableaux. As predicted by Anatoly Vershik in [90], the twenty-first century should see a lot of challenges and advances on the links between probability theory and (algebraic) combinatorics. A key rôle is played here by Young tableaux⁸ because of their ubiquity in representation theory. Many results on their asymptotic shape have been collected, but very few results are known on their asymptotic content when the shape is fixed (see, e.g., the works by Pittel and Romik, Angel et al., Marchal [4, 63, 73, 81], who have studied the distribution of the values of the cells in random rectangular or staircase Young tableaux, while the case of Young tableaux with a more general shape seems to be very intricate). It is therefore pleasant that our work on periodic Pólya urns allows us to get advances on the case of a triangular shape, with any rational slope.

DEFINITION 4.1. For any fixed integers $n, \ell, p \geq 1$, we define a *triangular Young tableau* of parameters (ℓ, p, n) as a classical Young tableau with $N := p\ell n(n + 1)/2$ cells, with length $n\ell$, and height np such that the first ℓ columns have np cells, the next ℓ columns have $(n - 1)p$ cells, and so on (see Figure 3).

For such a tableau, we now study what is the typical value of its southeast corner (with the French convention of drawing tableaux; see [61] but, however, take care that on page 2 therein, Macdonald advises readers preferring the French convention to “read this book upside down in a mirror!” Some French authors quickly propagated the joke that Macdonald was welcome to apply his own advice while reading their articles!).

It could be expected (e.g., via the Greene–Nijenhuis–Wilf hook walk algorithm for generating Young tableaux; see [40]) that the entries near the hypotenuse should be $N - o(N)$. Can we expect a more precise description of these $o(N)$ fluctuations? Our result on periodic urns enables us to exhibit the right critical exponent, and the limit law in the corner.

THEOREM 4.2. Choose a uniform random triangular Young tableau of parameters (ℓ, p, n) and of size $N = p\ell n(n + 1)/2$ and put $\delta = p/(p + \ell)$. Let X_n be the entry of the southeast corner. Then $(N - X_n)/n^{1+\delta}$ converges in law to the same limiting distribution as the number of black balls in the periodic Young–Pólya urn with initial conditions $b_0 = p$, $w_0 = \ell$ and with replacement matrices $M_1 = \dots = M_{p-1} = \begin{pmatrix} 1 & 0 \\ 0 & 1 \end{pmatrix}$ and $M_p = \begin{pmatrix} 1 & \ell \\ 0 & 1+\ell \end{pmatrix}$, that is, we have the convergence in law, as n goes to infinity, towards GenGammaProd (the distribution defined by formula (1), page 1924):

$$\frac{2}{p\ell} \frac{N - X_n}{n^{1+\delta}} \xrightarrow{\mathcal{L}} \text{GenGammaProd}(p, \ell, p, \ell).$$

REMARK 4.3. The case $p = 1$ corresponds to a classical (nonperiodic) urn; see Remark 1.8. The case $p = 2$ and $\ell = 1$ corresponds to our running example of a Young–Pólya urn; see Example 1.7.

REMARK 4.4. If we replace the parameters (ℓ, p, n) by $(K\ell, Kp, n)$ for some integer $K > 1$, we are basically modelling the same triangle, yet the limit law is GenGammaProd($Kp, K\ell, Kp, K\ell$), which differs from GenGammaProd(p, ℓ, p, ℓ). It is noteworthy that one still has some universality: the critical exponent δ remains the same and, besides, the limit laws are closely related in the sense that they have similar tails. We address these questions in Section 5.2.

⁸A Young tableau of size n is an array with columns of (weakly) decreasing height, in which each cell is labelled, and where the labels run from 1 to n and are strictly increasing along rows from left to right and columns from bottom to top; see Figure 3. We refer to [61] for a thorough discussion on these objects.

43	55	61	72									
31	44	60	71									
22	25	32	39									
18	24	27	35	41	58	59	68					
17	19	26	30	40	52	56	63					
12	14	20	29	38	49	51	62					
6	8	10	21	28	46	50	53	57	65	67	70	
3	5	7	13	15	45	47	48	54	64	66	69	
1	2	4	9	11	16	23	33	34	36	37	42	

$\xleftarrow{\ell}$ $\xleftarrow{\ell}$ $\xleftarrow{\ell}$

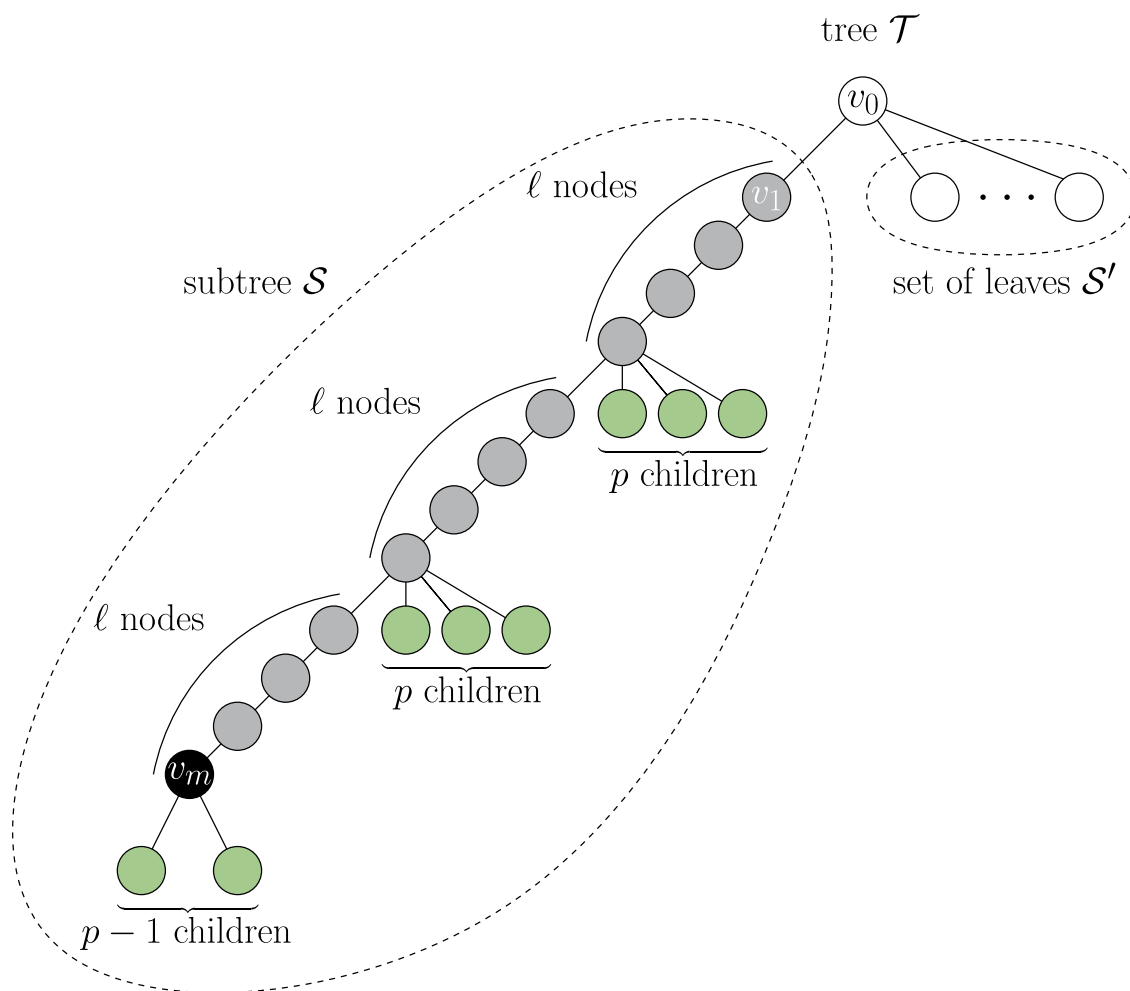


FIG. 3. In this section, we see that there is a relation between Young tableaux with a given periodic shape, some trees and the periodic Young–Pólya urns. The key observation is that the cells (in grey) in the first row of the tableaux have the same hook lengths as the nodes (in grey) in the leftmost branch of the tree. The southeast cell v (in black) of this Young tableau has also the same hook length as the node v_m (in black) in the tree, and is following the same distribution we proved for urns (generalized gamma product distribution).

PROOF. As this proof involves several technical lemmas (which we prove in the next subsections), we first present its structure so that the reader gets a better understanding of the key ideas. Our proof starts by establishing a link between Young tableaux and linear extensions of trees. After that, we will be able to conclude via a second link between these trees and periodic Pólya urns.

Let us begin with Figure 3 which describes the link between the main characters of this proof: the Young tableau \mathcal{Y} and the “big” tree \mathcal{T} (which contains the “small” tree \mathcal{S}). More precisely, we define the rooted planar tree \mathcal{S} as follows:

- The leftmost branch of \mathcal{S} is a sequence of vertices which we call v_1, v_2, \dots .
- Set $m := n\ell$. The vertex v_m (the one in black in Figure 3) has $p - 1$ children.
- For $2 \leq k \leq n - 1$, the vertex $v_{k\ell}$ has $p + 1$ children.
- All other vertices v_j (for $j < m, j \neq k\ell$) have exactly one child.

Now, define \mathcal{T} as the “big” tree obtained from the “small” tree \mathcal{S} by adding a vertex v_0 as the parent of v_1 and adding a set \mathcal{S}' of children to v_0 . The size of \mathcal{S}' is chosen such that $|\mathcal{T}| = 1 + |\mathcal{S}| + |\mathcal{S}'| = 1 + N$, where N is the number of cells of the Young tableau \mathcal{Y} . Moreover, the hook length of each cell (in grey) in the first row of \mathcal{Y} is equal to the hook length⁹ of the corresponding vertex (in grey also) in the leftmost branch of \mathcal{S} .

Let us now introduce a linear extension $E_{\mathcal{T}}$ of \mathcal{T} , that is, a bijection from the set of vertices of \mathcal{T} to $\{1, \dots, N + 1\}$ such that $E_{\mathcal{T}}(u) < E_{\mathcal{T}}(u')$ whenever u is an ancestor of u' . A key result, which we prove hereafter in Proposition 4.9, is the following: if $E_{\mathcal{T}}$ is a uniformly random linear extension of \mathcal{T} , then $E_{\mathcal{Y}}(v)$ (the entry of the southeast corner v in a uniformly random Young tableau \mathcal{Y}) has the same law as $E_{\mathcal{T}}(v_m)$:

$$(22) \quad 1 + E_{\mathcal{Y}}(v) \stackrel{\mathcal{L}}{=} E_{\mathcal{T}}(v_m).$$

Note that in the statement of the theorem, $E_{\mathcal{Y}}(v)$ is denoted by X_n to initially help the reader to follow the dependency on n .

Furthermore, recall that \mathcal{T} was obtained from \mathcal{S} by adding a root and some children to this root. Therefore, one can obtain a linear extension of the “big” tree \mathcal{T} from a linear extension of the “small” tree \mathcal{S} . In Section 4.4, we show that this allows us to construct a uniformly random linear extension $E_{\mathcal{T}}$ of \mathcal{T} and a uniformly random linear extension $E_{\mathcal{S}}$ of \mathcal{S} such that

$$(23) \quad |\mathcal{T}| - E_{\mathcal{T}}(v_m) \stackrel{\mathcal{L}}{=} n(|\mathcal{S}| - E_{\mathcal{S}}(v_m) + \text{smaller order error terms}).$$

The last step, which we prove in Proposition 4.17, is that

$$(24) \quad |\mathcal{S}| - E_{\mathcal{S}}(v_m) \stackrel{\mathcal{L}}{=} \text{distribution of periodic Pólya urn} + \text{deterministic quantity}.$$

Indeed, more precisely $|\mathcal{S}| - E_{\mathcal{S}}(v_m)$ has the same law as the number of black balls in a periodic urn after $(n - 1)p$ steps (an urn with period p , with parameter ℓ , and with initial conditions $b_0 = p$ and $w_0 = \ell$). Thus, our results on periodic urns from Section 3 and the conjunction of equations (22), (23) and (24) give the convergence in law for $E_{\mathcal{Y}}(v)$ which we wanted to prove. \square

The subsequent sections are dedicated to the proofs of the auxiliary propositions that are crucial for the proof of Theorem 4.2. First, we establish a link between our problem on Young tableaux and a related problem on trees. Second, we explain the connection between the related problem on trees and the model of periodic urns.

⁹The hook length of a vertex in a tree is the size of the subtree rooted at this vertex.

4.1. *The link between Young tableaux and trees.* We will need the following definitions.

DEFINITION 4.5 (The shape of a tableau¹⁰). We say that a tableau has *shape* $\lambda_1^{i_1} \cdots \lambda_n^{i_n}$ (with $\lambda_1 > \cdots > \lambda_n$) if it has (from left to right) first i_1 columns of height λ_1 , etc., and ends with i_n columns of height λ_n .

As an illustration, the tableau on the top of Figure 3 has shape $9^4 6^4 3^4$.

DEFINITION 4.6 (The shape of a tree). Consider a rooted planar tree \mathcal{T} with at least two vertices and having the shape of a “comb”: at each level only the leftmost node can have children. It has *shape* $(i_0, j_0; i_1, j_1; \dots; i_n, j_n)$ if

- when $n = 0$, then \mathcal{T} is the tree with j_0 leaves and i_0 internal nodes, all of them unary except for the last one which has j_0 children;
- when $n \geq 1$, then \mathcal{T} is the tree with *shape* $(i_0, j_0; i_1, j_1; \dots; i_{n-1}, j_{n-1})$ to which we attach a tree of shape (i_n, j_n) as a new leftmost subtree to the parent of the leftmost leaf.

Figure 4 illustrates the recursive construction of a tree of shape $(1, 4; 1, 2; 2, 2)$. As another example, the tree \mathcal{T} in Figure 3 has shape $(1, |\mathcal{S}'|; 4, 3; 4, 3; 4, 2)$, where $|\mathcal{S}'|$ stands for the number of leaves in \mathcal{S}' .

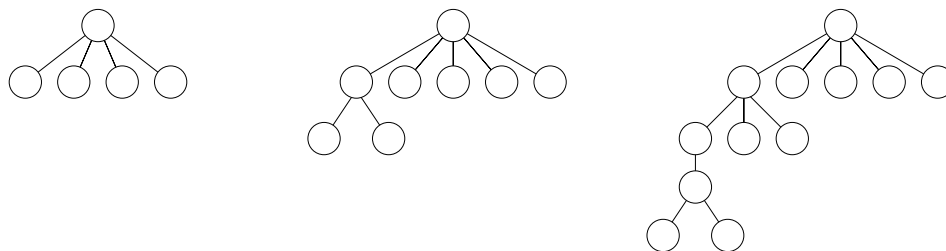


FIG. 4. *The recursive construction of a tree of shape $(1, 4; 1, 2; 2, 2)$. First, a tree of shape $(1, 4)$, second, a tree of shape $(1, 4; 1, 2)$, third, a tree of shape $(1, 4; 1, 2; 2, 2)$.*

Let us end this small collection of definitions with a more classical one.

DEFINITION 4.7 (Linear extension of a poset and of a tree). A *linear extension* E of a poset \mathcal{A} of size N is a bijection between this poset and $\{1, \dots, N\}$ satisfying $E(u) \leq E(v)$ whenever $u \leq v$. Accordingly, a linear extension of a tree \mathcal{A} with N vertices is a bijection E between the vertices of \mathcal{A} and $\{1, \dots, N\}$ satisfying $E(u) \leq E(v)$ whenever u is a child of v .

We denote by $\text{ext}(\mathcal{A})$ the number of linear extensions of \mathcal{A} .

REMARK 4.8. In combinatorics, a linear extension is also called an increasing labelling. In the sequel, we will sometimes say “(increasing) labelling” instead of “linear extension”, hoping that this less precise terminology will help the intuition of the reader.

We are now ready to state the following result.

¹⁰Some authors define the shape of a tableau as its row lengths from bottom to top. In this article, we use the list of column lengths, as it directly gives the natural quantities to state our results in terms of trees and urns.

PROPOSITION 4.9 (Link between the southeast corner of Young tableaux and linear extensions of trees). *Fix a tableau with shape $\lambda_1^{i_1} \cdots \lambda_n^{i_n}$ and consider a random uniform Young tableau \mathcal{Y} with this given shape. Let $E_{\mathcal{Y}}(v)$ be the entry of the southeast corner of this Young tableau. Let \mathcal{T} be a tree with shape $(1, N - m - \lambda_1 + 1; i_1, \lambda_1 - \lambda_2; i_2, \lambda_2 - \lambda_3; \dots; i_n, \lambda_n - 1)$, where $N = \sum \lambda_k i_k$ is the size of the tableau \mathcal{Y} and $m = i_1 + \dots + i_n$ is the number of its columns. Let $E_{\mathcal{T}}$ be a random uniform linear extension of \mathcal{T} , and v_m be the m th vertex in the leftmost branch of this tree \mathcal{T} . Then $E_{\mathcal{T}}(v_m)$ and $1 + E_{\mathcal{Y}}(v)$ have the same law.*

PROOF. The proof will be given on page 1948, as it requires two ingredients, which have their own interest and which are presented in the two next sections (Section 4.2 on the density method for Young tableaux, and Section 4.3 on the density method for trees). \square

EXAMPLE 4.10. Let us apply the previous result to the tree of shape $(1, 4; 1, 2; 2, 2)$ from Figure 4. There we have $n = 2, m = 3$. Then this tree corresponds to a Young tableau of shape $5^1 3^2$ and size $N = 11$.

REMARK 4.11. In the simplest case when the tableau is a rectangle (i.e., it has shape $\lambda_1^{i_1}$), the associated tree has shape $(1, (\lambda_1 - 1)(i_1 - 1); i_1, \lambda_1 - 1)$. In that case, the law of $E_{\mathcal{T}}(v_m)$ is easy to compute and we get an alternative proof of the following formula, first established in [63]:

$$\mathbb{P}(E_{\mathcal{Y}}(v) = k) = \frac{\binom{k-1}{i_1-1} \binom{\lambda_1 i_1 - k}{\lambda_1 - 1}}{\binom{\lambda_1 i_1}{\lambda_1 + i_1 - 1}}.$$

The fact that \mathcal{Y} and \mathcal{T} are related is obvious from the construction of \mathcal{T} , but it is not a priori granted that it will lead to a simple, nice link between the distributions of v and v_m (the two black cells in Figure 3). So, $E_{\mathcal{T}}(v_m) \stackrel{\mathcal{L}}{=} 1 + E_{\mathcal{Y}}(v)$ deserves a detailed proof: it will be the topic of the next subsections. The proof has a nice feature: it uses a generic method, which we call the *density method* and which was introduced in our articles [10, 64]. In fact, *en passant*, these next subsections also illustrate the efficiency of the density method in order to enumerate (and to perform uniform random generation) of combinatorial structures (like we did in the two aforementioned articles for permutations with some given pattern, or rectangular Young tableaux with “local decreases”).

The advantage of Proposition 4.9 is that linear extensions of a tree are easier to study than Young tableaux and can, in fact, be related to our periodic urn models, as shown in Section 4.3.

4.2. *The density method for Young tableaux.* Trees and Young tableaux can be viewed as posets [88]. We will use this point of view to prove Proposition 4.9. We recall here some general facts that will be useful in the sequel.

DEFINITION 4.12 (Order polytope of a poset). Let \mathcal{A} be a general poset with cardinality N and order relation \leq . We can associate with \mathcal{A} a polytope $\mathcal{P} \subset [0, 1]^{\mathcal{A}}$ defined by the condition $(Y_e)_{e \in \mathcal{A}} \in \mathcal{P}$ if and only if $Y_e \leq Y_{e'}$ whenever $e \leq e'$. Then \mathcal{P} is called the *order polytope* of the poset \mathcal{A} .

EXAMPLE 4.13. Let \mathcal{A} be the set of subsets of $\{a, b\}$ ordered by inclusion. Then its order polytope is given by $\mathcal{P} = \{(Y_{\emptyset}, Y_{\{a\}}, Y_{\{b\}}, Y_{\{a,b\}}) \in [0, 1]^4 : Y_{\emptyset} \leq Y_{\{a\}}, Y_{\emptyset} \leq Y_{\{b\}}, Y_{\emptyset} \leq Y_{\{a,b\}}, Y_{\{a\}} \leq Y_{\{a,b\}}, Y_{\{b\}} \leq Y_{\{a,b\}}\}$.

Let $Y = (Y_e)_{e \in \mathcal{A}} \in [0, 1]^{\mathcal{A}}$ be a tuple of random variables¹¹ chosen according to the uniform measure on the polytope \mathcal{P} . Then we consider the function X having integer values, defined by $X_e := k$ if Y_e is the k th smallest real in the set of reals $\{Y_e : e \in \mathcal{A}\}$. It is sometimes called order statistic. Note that X is a random variable, defined almost surely as we have a zero probability that some marginals of Y have the same value, and X is uniformly distributed on the set of all linear extensions of \mathcal{A} . The last claim holds because the wedges of each linear extension have equal size $1/N!$ for $N = |\mathcal{A}|$ being the size of the poset \mathcal{A} .

EXAMPLE 4.14. Continuing Example 4.13, there are two linear extensions of \mathcal{A} : $(X_\emptyset, X_{\{a\}}, X_{\{b\}}, X_{\{a,b\}}) = (1, 2, 3, 4)$ and $(X_\emptyset, X_{\{a\}}, X_{\{b\}}, X_{\{a,b\}}) = (1, 3, 2, 4)$. They correspond to the following two wedges in \mathcal{P} : $Y_\emptyset \leq Y_{\{a\}} \leq Y_{\{b\}} \leq Y_{\{a,b\}}$ and $Y_\emptyset \leq Y_{\{b\}} \leq Y_{\{a\}} \leq Y_{\{a,b\}}$. The volume of each of them is $1/24$, while the volume of \mathcal{P} is $1/12$.

Conversely, if X is a random uniform increasing labelling of \mathcal{A} , one gets a random variable Y on the polytope \mathcal{P} via $Y_e := T_{X_e}$, where T is a random uniform N -tuple from the set $\{(T_1, \dots, T_N) \in [0, 1]^N : T_1 < \dots < T_N\}$. Therefore, Y is uniformly distributed on \mathcal{P} . What is more, T_k is the k th largest uniform random variable among N independent uniform random variables. Thus, it has density $k \binom{N}{k} x^{k-1} (1-x)^{N-k}$. As a consequence, for any $e \in \mathcal{A}$, Y_e has density

$$(25) \quad g_e(x) = \sum_{k=1}^N \mathbb{P}(X_e = k) k \binom{N}{k} x^{k-1} (1-x)^{N-k}.$$

This formula can be read as two different writings of the same polynomial in two different bases; thus, by elementary linear algebra, it implies that $\mathbb{P}(X_e = k)$ can be deduced from the polynomial g_e . In particular, we have the following property.

LEMMA 4.15. *Let $\mathcal{A}, \mathcal{A}'$ be two posets with the same cardinality, and let $\mathcal{P}, \mathcal{P}'$ be their respective order polytopes. Let X (resp., X') be a random linear extension of \mathcal{A} (resp., \mathcal{A}'). Let Y (resp., Y') be a uniform random variable on \mathcal{P} (resp., \mathcal{P}'). Then, for any $e \in \mathcal{A}$ and $e' \in \mathcal{A}'$, such that Y_e and $Y'_{e'}$ have the same density, X_e and $X'_{e'}$ have the same law.*

Let \mathcal{Y} be a tableau with shape $\lambda_1^{i_1} \dots \lambda_n^{i_n}$ and total size $N = \sum_k \lambda_k i_k$. We view \mathcal{Y} as a poset: \mathcal{Y} is a set of N cells equipped with a partial order “ \leq ”, where $c \leq c'$ if one can go from c to c' with only north and east steps. We denote by \mathcal{P} the order polytope of the tableau \mathcal{Y} .

We will introduce an algorithm generating a random element of \mathcal{P} according to the uniform measure. In order to do so, we fill the diagonals one by one. Let us introduce some notation. The tableau \mathcal{Y} can be sliced into $M = \lambda_1 + i_1 + \dots + i_n - 1$ diagonals D_1, \dots, D_M as follows: D_1 is the northwest corner and recursively, D_{k+1} is the set of cells which are adjacent to one of the cells of $D_1 \cup \dots \cup D_k$ and which are not in $D_1 \cup \dots \cup D_k$. In particular, D_M is the southeast corner. For example, Figure 3 has $M = 20$ such diagonals.

Note that between two consecutive diagonals D_k and D_{k+1} (let us denote their cell entries by $y_1 < \dots < y_j$ and $x_1 < \dots < x_{j'}$), there exist four different interlocking relations illustrated by Figure 5. The shape of the tableau implies that for each k we are in one of these four possibilities, each of them thus corresponds to a polytope \mathcal{P}_k defined as:

$$(26) \quad \text{case 1: } \mathcal{P}_k := \{y_1 < x_1 < \dots < y_j < x_{j'}\},$$

$$(27) \quad \text{case 2: } \mathcal{P}_k := \{x_1 < y_1 < \dots < x_j < y_{j'}\},$$

$$(28) \quad \text{case 3: } \mathcal{P}_k := \{y_1 < x_1 < \dots < x_{j-1} < y_{j'}\},$$

$$(29) \quad \text{case 4: } \mathcal{P}_k := \{x_1 < y_1 < \dots < x_j < y_{j'} < x_{j'+1}\}.$$

¹¹When the poset is a Young tableau, this corresponds to what is called a Poissonized Young tableau in [37].

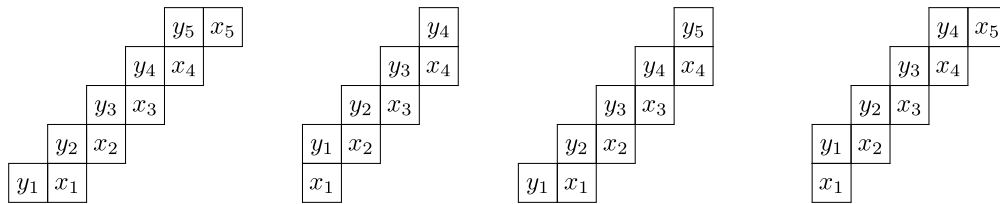


FIG. 5. Young tableaux of any shape can be generated by a sequence of “diagonals,” which interlock according to the four possibilities above.

Our algorithm will make use of conditional densities along the M diagonals of \mathcal{Y} . For this purpose, for every $k \in \{1, \dots, M\}$ we define a polynomial g_k in $|D_k|$ variables as follows. First, one sets $g_1 := 1$; the next polynomials are defined by induction. Suppose that $1 \leq k \leq M - 1$ and $D_k = (y_1 < \dots < y_j)$. The four above-mentioned possibilities for D_{k+1} lead to the definition of the following polynomials:

1. In the first case (interlocking given by (26)), this gives

$$g_{k+1}(x_1, \dots, x_j) := \int_0^{x_1} dy_1 \int_{x_1}^{x_2} dy_2 \cdots \int_{x_{j-1}}^{x_j} dy_j g_k(y_1, \dots, y_j).$$

2. In the second case (interlocking given by (27)), this gives

$$g_{k+1}(x_1, \dots, x_j) := \int_{x_1}^{x_2} dy_1 \int_{x_2}^{x_3} dy_2 \cdots \int_{x_{j-1}}^{x_j} dy_{j-1} \int_{x_j}^1 dy_j g_k(y_1, \dots, y_j).$$

3. In the third case (interlocking given by (28)), this gives

$$g_{k+1}(x_1, \dots, x_{j-1}) := \int_0^{x_1} dy_1 \int_{x_1}^{x_2} dy_2 \cdots \int_{x_{j-1}}^1 dy_j g_k(y_1, \dots, y_j).$$

4. In the fourth case (interlocking given by (29)), this gives

$$g_{k+1}(x_1, \dots, x_{j+1}) := \int_{x_1}^{x_2} dy_1 \int_{x_2}^{x_3} dy_2 \cdots \int_{x_j}^{x_{j+1}} dy_j g_k(y_1, \dots, y_j).$$

Now, we use these polynomials to formulate a random generation algorithm which will also be able to enumerate the corresponding Young tableaux. Note that faster random generation algorithms are known (like the hook walk from [40]), but it is striking that the above polynomials g_k will be the key to relate the distributions of different combinatorial structures, allowing us to capture second order fluctuations in Young tableaux, trees and urns. It is also noteworthy that our density method is in some cases the most efficient way to enumerate and generate combinatorial objects (see [10] for applications on variants of Young tableaux, where the hook length formula is no more available, and see [23] for algorithmic subtleties related to sampling conditional multivariate densities).

Recall that \mathcal{P} is the order polytope of the tableau \mathcal{Y} and that we want to generate a random element of \mathcal{P} according to the uniform measure. The algorithm is the following. We generate by descending induction on k , for each diagonal D_k , a $|D_k|$ -tuple of reals in $[0, 1]$ which will be the entries of the cells of D_k .

First, remark that the functions defined by (30) and (31) in Algorithm 1 are indeed probability densities. That is, they are measurable, positive functions and their integral is equal to 1. To prove this, remark first that these functions are polynomials and, therefore, measurable. Next, by definition, as integrals of positive functions, they are positive. Finally, the fact that the integral is equal to 1 follows from their definition.

ALGORITHM 1 (Output: a random uniform Young tableau \mathcal{Y} , via the density method).

Step 1. Recall that D_M is the southeast corner. Generate the corresponding cell entry at random with probability density

$$(30) \quad \frac{g_M(x)}{\int_0^1 g_M(y) dy}.$$

Step 2. By descending induction on k from $M - 1$ down to 1, generate the diagonal D_k (seen as a tuple of $|D_k|$ reals in $[0, 1]$) according to the density

$$(31) \quad \frac{g_k(x_1, \dots, x_{|D_k|})}{g_{k+1}(D_{k+1})} \mathbf{1}_{\mathcal{P}_k},$$

where g_k and $\mathbf{1}_{\mathcal{P}_k}$ are chosen according to the cases given by (26), (27), (28), (29).

We then claim that Algorithm 1 yields a random element (D_1, \dots, D_M) of \mathcal{P} with the uniform measure. Indeed, by construction, its density is the product of the conditional densities of the diagonals D_1, \dots, D_M . The crucial observation now is that the product of the conditional densities (31) is a telescopic product, so the algorithm generates each Young tableau \mathcal{Y} with the same “probability” (or more rigorously, as we have continuous variables, with the same *density*):

$$(32) \quad \frac{g_M(D_M)}{\int_0^1 g_M(y) dy} \prod_{k=1}^{M-1} \frac{g_k(D_k)}{g_{k+1}(D_{k+1})} \mathbf{1}_{\mathcal{P}_k} = \frac{\mathbf{1}_{\{\mathcal{Y} \in \mathcal{P}\}}}{\int_0^1 g_M(y) dy}.$$

This indeed means that our algorithm yields a uniform random variable on the order polytope \mathcal{P} . Alternatively, one can say that the Young tableau \mathcal{Y} is a random variable on $[0, 1]^N$ with density given by (32), therefore,

$$\int_{[0,1]^N} \mathbf{1}_{\{Z \in \mathcal{P}\}} dZ = \int_0^1 g_M(y) dy.$$

Now, suppose that we pick uniformly at random an element Z' of $[0, 1]^N$. Then one has

$$\mathbb{P}(Z' \in \mathcal{P}) = \int_{[0,1]^N} \mathbf{1}_{\{Z \in \mathcal{P}\}} dZ = \frac{\text{ext}(\mathcal{Y})}{N!},$$

where $\text{ext}(\mathcal{Y})$ is the number of increasing labellings (linear extensions) of the tableau \mathcal{Y} . Thus,

$$\text{ext}(\mathcal{Y}) = N! \int_0^1 g_M(y) dy.$$

In the next section, we turn our attention to the density method for trees.

4.3. *The density method for trees.* Let the tree \mathcal{T} , its subtree \mathcal{S} , and the vertices v_0, \dots, v_m be defined as on page 1939 (see Figure 3). As in Section 4.2, it is possible to construct a random linear extension of \mathcal{S} by using a uniform random variable Y on the order polytope of \mathcal{S} . The vertex v_m has then a random value Y_{v_m} between 0 and 1, and we want to compute its density. To this aim, we associate to each internal node v_k a polynomial f_k (in σ_k variables, where σ_k is the number of siblings of v_k). These polynomials f_k are defined by induction starting with $f_1 := 1$, while f_2, \dots, f_{m-1} are defined by

$$f_k(x_0, \dots, x_{\sigma_k}) := \int_0^{\inf\{x_0, \dots, x_{\sigma_k}\}} dy_0 \int_0^1 dy_1 \cdots \int_0^1 dy_{\sigma_k-1} f_{k-1}(y_0, y_1, \dots, y_{\sigma_k-1}).$$

The last polynomial, f_m , additionally depends on the number j of children of v_m :

$$(33) \quad \begin{aligned} & f_m(x_0, \dots, x_{\sigma_m}) \\ & := (1 - x_0)^j \int_0^{\inf\{x_0, \dots, x_{\sigma_m}\}} dy_0 \int_0^1 dy_1 \cdots \int_0^1 dy_{\sigma_m-1} f_{m-1}(y_0, y_1, \dots, y_{\sigma_m-1}). \end{aligned}$$

We also define h_{v_m} :

$$h_{v_m}(x) := \int_0^1 dx_1 \cdots \int_0^1 dx_{\sigma_m} f_m(x, x_1, \dots, x_{\sigma_m}).$$

We claim that $h_{v_m}(x)$ is (up to a multiplicative constant) the density of Y_{v_m} . This is shown as in Section 4.2 using Algorithm 2, which generates uniformly at random a labelling of \mathcal{S} .

ALGORITHM 2 (Output: a random uniform increasing labelling Y of the tree \mathcal{S}).

Step 1. Generate Y_{v_m} according to the density

$$\frac{h_{v_m}(x)}{\int_0^1 h_{v_m}(x) dx}.$$

Step 2. If v_m has j children s_1, \dots, s_j , then generate $(Y_{s_1}, \dots, Y_{s_j})$ according to the density

$$\frac{\prod_{i=1}^j \mathbf{1}_{\{y_i > Y_{v_m}\}}}{(1 - Y_{v_m})^j}.$$

Step 3. If v_m has j siblings s_1, \dots, s_j , then generate $(Y_{s_1}, \dots, Y_{s_j})$ according to the density

$$\frac{f_m(Y_{v_m}, y_1, \dots, y_j)}{\int_0^1 dy_1 \cdots \int_0^1 dy_j f_m(Y_{v_m}, y_1, \dots, y_j)}.$$

Step 4. By descending induction for k from $m - 1$ down to 1, if v_k has j siblings s_1, \dots, s_j , then generate the tuple $\mathbf{Y}_k = (Y_{v_k}, Y_{s_1}, \dots, Y_{s_j})$ according to the density

$$\frac{f_k(y_0, \dots, y_j)}{f_{k+1}(\mathbf{Y}_{k+1})} \mathbf{1}_{\{y_0 < \min \mathbf{Y}_{k+1}\}}.$$

Indeed, the random tuple Y generated by this algorithm is by construction an element of the order polytope. What is more, we have the uniform distribution, as the probabilities of all Y 's are equal to a telescopic product similar to formula (32). Therefore, $h_m(x)$ is (up to a multiplicative constant) the density of Y_{v_m} and the number $\text{ext}(\mathcal{S})$ of linear extensions of \mathcal{S} is given by

$$\text{ext}(\mathcal{S}) = |\mathcal{S}|! \int_0^1 h_{v_m}(x) dx.$$

It remains to connect the densities of v in \mathcal{Y} and v_m in \mathcal{S} ; we do this in the following lemma.

LEMMA 4.16. *The polynomial $g_M(x)$ (which gives the density of v , the southeast corner of the Young tableau \mathcal{Y}) and the polynomial $h_{v_m}(x)$ (which gives the density of v_m in the tree \mathcal{S}) are equal up to a multiplicative constant:*

$$h_{v_m}(x) = c g_M(x) \quad \text{with } c = \frac{|\mathcal{Y}|! \operatorname{ext}(\mathcal{S})}{|\mathcal{S}|! \operatorname{ext}(\mathcal{Y})}.$$

PROOF. The main idea of the proof consists in adding a filament to the tree and to the tableau, and inspecting the consequences via the density method.

Part 1 (adding a filament to the tableau). Let \mathcal{Y}_L be the tableau obtained by adding to \mathcal{Y} L cells horizontally to the right of its southeast corner v (and denote these new cells by e_1, \dots, e_L). We can generate a random element of the order polytope of \mathcal{Y}_L as follows: remark that \mathcal{Y} is a subtableau of \mathcal{Y}_L and that the first M diagonals D_1, \dots, D_M of \mathcal{Y}_L are the same as the first M diagonals of \mathcal{Y} (recall that the diagonals are lines with positive slope $+1$, starting from each cell of the first column and row). In particular, D_M is the southeast corner cell v . Then we can extend Algorithm 1 in the following way:

ALGORITHM 3 (Output: a random uniform increasing labelling X of the tableau with L added cells).

Step 1. Generate $X_{M,L}$ the entry of the cell v according to the density

$$\frac{g_{M,L}(x)}{\int_0^1 g_{M,L}(y) dy} \quad \text{where } g_{M,L}(x) := \frac{g_M(x)(1-x)^L}{L!}.$$

Step 2. Generate the entries of the diagonals D_{M-1}, \dots, D_1 as in Algorithm 1.

Step 3. Generate the entry X_1 of e_1 with density

$$L \frac{(1-x)^{L-1}}{(1-X_{M,L})^L} \mathbf{1}_{\{x > X_{M,L}\}}.$$

Step 4. For i from 1 to $L-1$, generate the entry X_{i+1} of e_{i+1} with density

$$(L-i) \frac{(1-x)^{L-i-1}}{(1-X_i)^{L-i}} \mathbf{1}_{\{x > X_i\}}.$$

Using the same arguments as for Algorithm 1, we can show that Algorithm 3 yields a uniform random variable on the order polytope of \mathcal{Y}_L and that the number of increasing labellings of \mathcal{Y}_L is

$$\operatorname{ext}(\mathcal{Y}_L) = (N+L)! \int_0^1 g_{M,L}(y) dy = (N+L)! \int_0^1 \frac{g_M(y)(1-y)^L}{L!} dy.$$

On the other hand, using the hook length formula, we see that the hook lengths of \mathcal{Y}_L are the same as those of \mathcal{Y} , except for the first row. A straightforward computation shows that

$$\frac{\operatorname{ext}(\mathcal{Y})}{N!} = \frac{\operatorname{ext}(\mathcal{Y}_L)}{(N+L)!} \times G_L,$$

where, as \mathcal{Y} has shape $\lambda_1^{i_1} \cdots \lambda_n^{i_n}$, the constant G_L is given by

$$(34) \quad G_L = L! \prod_{k=1}^n \frac{(i_1 + \cdots + i_k + L + \lambda_k - 1)^{i_k}}{(i_1 + \cdots + i_k + \lambda_k - 1)^{i_k}},$$

where we reuse the falling factorial notation $a^b = a(a - 1) \cdots (a - b + 1)$. This leads to

$$(35) \quad \int_0^1 g_M(y)(1 - y)^L dy = \frac{L! \operatorname{ext}(\mathcal{Y})}{G_L N!}.$$

Part 2 (adding a filament to the tree). Suppose that we extend the tree \mathcal{S} by adding a filament of length L . Let \mathcal{S}_L be the tree obtained from \mathcal{S} by attaching to v_m a subtree consisting of a line with L vertices. Put

$$f_L(x) := \frac{(1 - x)^L h_{v_m}(x)}{L!}.$$

With the same arguments as for the function h_{v_m} defined in (33), we see that $f_L / \int_0^1 f_L(x) dx$ is the density of $Y_L(v_m)$ where Y_L is a uniform random variable on the order polytope of \mathcal{S}_L . Following the same reasoning, we can show that the number of linear extensions of \mathcal{S}_L is

$$\operatorname{ext}(\mathcal{S}_L) = (|\mathcal{S}| + L)! \int_0^1 f_L(y) dy.$$

On the other hand, recall that a version of the hook length formula holds for trees (see, e.g., [41, 55, 82]): the number of linear extensions of a tree of size N is given by

$$\frac{N!}{\prod_{v \in \mathcal{S}} \operatorname{hook}(v)},$$

where here $\operatorname{hook}(v)$ is the number of descendants of v (including v itself).

Applying this formula to the tree \mathcal{S} yields

$$\frac{\operatorname{ext}(\mathcal{S})}{|\mathcal{S}|!} = \frac{\operatorname{ext}(\mathcal{S}_L)}{(|\mathcal{S}| + L)!} \times G_L,$$

with the same G_L as in (34). Indeed, the most crucial point is that the hook lengths of the Young tableau on the first row are *the same* as the hook lengths of the tree along the leftmost branch. This key construction allows us to connect these two structures. Hence, one has

$$(36) \quad \int_0^1 h_{v_m}(y)(1 - y)^L dy = \frac{L! \operatorname{ext}(\mathcal{S})}{G_L |\mathcal{S}|!}.$$

Part 3 (linking tableaux and trees). Comparing (35) and (36), we get for any integer $L \geq 1$,

$$\int_0^1 h_{v_m}(y)(1 - y)^L dy = c \int_0^1 g_M(y)(1 - y)^L dy,$$

where c is the constant given by

$$c = \frac{|\mathcal{Y}|! \operatorname{ext}(\mathcal{S})}{|\mathcal{S}|! \operatorname{ext}(\mathcal{Y})}.$$

Since $h_{v_m}(x)$ and $g_M(x)$ are polynomials, this implies that $h_{v_m} = c g_M$. \square

Before establishing the final link between Young tableaux and urns, we start by collecting what we got via the density method: this gives the proof of Proposition 4.9, which we now restate.

PROPOSITION 4.9 (Link between the corner of a Young tableau and linear extensions of trees). *Fix a tableau with shape $\lambda_1^{i_1} \cdots \lambda_n^{i_n}$ and consider a random uniform Young tableau \mathcal{Y} with this given shape. Let $E_{\mathcal{Y}}(v)$ be the entry of the southeast corner of this Young tableau. Let \mathcal{T} be a tree with shape $(1, N - m - \lambda_1 + 1; i_1, \lambda_1 - \lambda_2; i_2, \lambda_2 - \lambda_3; \dots; i_n, \lambda_n - 1)$, where $N = \sum \lambda_k i_k$ is the size of the tableau \mathcal{Y} and $m = i_1 + \cdots + i_n$ is the number of its columns. Let $E_{\mathcal{T}}$ be a random uniform linear extension of \mathcal{T} , and v_m be the m th vertex in the leftmost branch of this tree \mathcal{T} . Then $E_{\mathcal{T}}(v_m)$ and $1 + E_{\mathcal{Y}}(v)$ have the same law.*

PROOF. The reader is invited to have a new look on Figure 3 (page 1938), which illustrates for this proof the idea of the trees \mathcal{T} , \mathcal{S} and the set of leaves \mathcal{S}' . We first introduce a forest $\mathcal{T}^* := \mathcal{S} \cup \mathcal{S}'$ obtained by adding $N - m - \lambda_1 + 1$ vertices without any order relation to the tree \mathcal{S} . \mathcal{T}^* has an order relation inherited from the order relation \leq on \mathcal{S} : two nodes x, y of \mathcal{T}^* are comparable if and only if they belong to \mathcal{S} and in that case, the order relation on \mathcal{T}^* is the same as the one on \mathcal{S} .

Let \mathcal{P}' be the order polytope of \mathcal{S} . Then it is clear that the order polytope of \mathcal{T}^* is

$$\mathcal{P} = \mathcal{P}' \times [0, 1]^{N-m-\lambda_1+1}.$$

In particular, if Y' is a uniform random variable on \mathcal{P}' and if Y is a uniform random variable on \mathcal{P} , then Y'_v and Y_v have the same density. This density is proportional to the function h_{v_m} computed in Section 4.3. Next, recall the notation g_M and D_M from Section 4.2. Lemma 4.16 gives that $h_{v_m} = cg_M$. Thus, the density of Y_{v_m} is the same as the density of D_M . Moreover, \mathcal{T}^* and \mathcal{Y} have the same cardinality. Therefore, Lemma 4.15 entails that if $E_{\mathcal{T}^*}$ is a random uniform linear extension of \mathcal{T}^* and if $E_{\mathcal{Y}}(v)$ is the entry of the southeast corner in a random increasing labelling of \mathcal{Y} , then $E_{\mathcal{T}^*}(v_m)$ and $E_{\mathcal{Y}}(v)$ have the same distribution.

Now, it is easy to deduce from $E_{\mathcal{T}^*}$ a random uniform linear extension $E_{\mathcal{T}}$ of \mathcal{T} : set $E_{\mathcal{T}}(u) = 1$ if u is the root of \mathcal{T} , and set $E_{\mathcal{T}}(u) = 1 + E_{\mathcal{T}^*}(u)$ for the other nodes (since any such node u can be identified as a node of \mathcal{T}). Applying this to the vertex v_m completes the proof of Proposition 4.9. \square

4.4. *The link between trees and urns.* In order to end the proof of Theorem 4.2, we need two more propositions.

PROPOSITION 4.17 (Link between trees and urns). *Consider a tree \mathcal{S} with shape $(i_1, j_1; \dots; i_n, j_n)$. Let v be the parent of the leftmost leaf if $j_n \geq 1$, or the leftmost leaf if $j_n = 0$. Let $E_{\mathcal{S}}$ be a random uniform linear extension of \mathcal{S} .*

Let $X = |\mathcal{S}| - E_{\mathcal{S}}(v)$. Then X has the same law as the number of black balls in the following urn process:

- Initialize the urn with $b_0 := j_n + 1$ black balls and $w_0 := i_n$ white balls.
- For k from $n - 1$ to 1, perform the following steps:
 1. Perform $j_k - 1$ times the classical Pólya urn with replacement matrix $\begin{pmatrix} 1 & 0 \\ 0 & 1 \end{pmatrix}$.
 2. Make one transition with the replacement matrix $\begin{pmatrix} 1 & i_k \\ 0 & 1+i_k \end{pmatrix}$.

REMARK 4.18. Note that the urn scheme described in the proposition is precisely the model of periodic Pólya urns covered by Theorem 3.8. For Young–Pólya urns, one has $i_k = \ell$ and $j_k = p$ for $k < n$, and $i_n = \ell$ and $j_n = p - 1$, compare Figure 3.

PROOF OF PROPOSITION 4.17. First, consider the transition probabilities in the classical Pólya urn. At step $i > 0$, the composition (B_i, W_i) is obtained from (B_{i-1}, W_{i-1}) by adding a black ball with probability $\frac{B_{i-1}}{B_{i-1}+W_{i-1}}$ and a white ball with probability $\frac{W_{i-1}}{B_{i-1}+W_{i-1}}$. We will now show that the same transition probabilities are imposed by the linear extension of the tree.

We start with a definition. If $\mathcal{R} \subset \mathcal{S}$ we define $E_{\mathcal{R}} : \mathcal{R} \rightarrow \{1, \dots, |\mathcal{R}|\}$ as the only bijection preserving the order relation induced by $E_{\mathcal{S}}$. That is, $E_{\mathcal{R}}(u) = k$ if and only if $E_{\mathcal{S}}(u)$ is the k th smallest value in the set $\{E_{\mathcal{S}}(r) : r \in \mathcal{R}\}$. It is easy to check that $E_{\mathcal{R}}$ is a uniform linear extension of \mathcal{R} seen as a poset equipped with the order relation inherited from \mathcal{S} .

Let us prove our claim. On the one hand, for every vertex w which is one of the j_n children of v , we have $E_{\mathcal{S}}(w) > E_{\mathcal{S}}(v)$. On the other hand, for every vertex u which is one of the $i_n - 1$

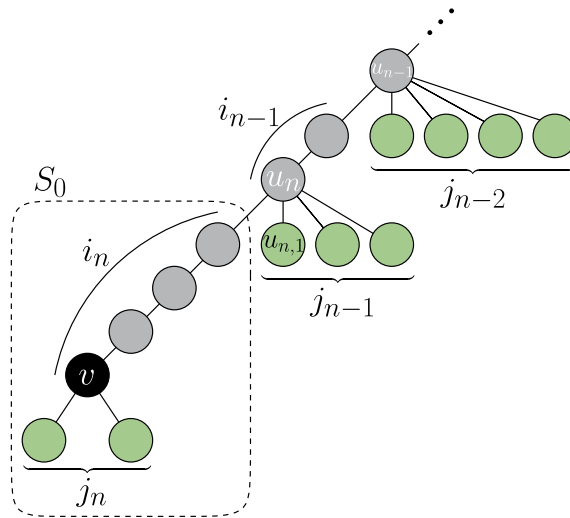


FIG. 6. Proposition 4.17 relates the labels in the tree S with a Pólya urn process. For periodic shapes, it gives a periodic Pólya urn. The initial conditions are given by S_0 . The tree is traversed bottom to top, along vertices not in the leftmost branch, starting at $u_{n,1}$. Each of these nodes corresponds to a classical Pólya urn step, whereas each vertex in the leftmost branch corresponds to an additionally added white ball.

most recent ancestors of v , we have $E_S(u) < E_S(v)$. Let S_0 be the set consisting of v , all its children and its $i_n - 1$ most recent ancestors; see Figure 6.

We will perform two nested inductions. The outer one is decreasing from $k = n - 1$ to 1, and each inner one increasing from 1 to j_k .

We start with $k = n - 1$. First, let u_n be the i_n -th most recent ancestor of v . The node u_n has j_{n-1} children which are not ancestors of v . Call these $u_{n,1}, \dots, u_{n,j_{n-1}}$. Let $S_1 := S_0 \cup \{u_{n,1}\}$, then $E_{S_1}(u_{n,1})$ is uniformly distributed on $\{1, \dots, |S_1|\}$. As a consequence, $E_{S_1}(u_{n,1}) > E_{S_1}(v)$ with probability $(j_n + 1)/(j_n + 1 + i_n)$. This probability can be expressed as $\frac{b_0}{b_0 + w_0}$, where b_0 is the number of vertices u in S_0 such that $E_S(u) \geq E_S(v)$ and w_0 is the number of vertices u in S_0 such that $E_S(u) \leq E_S(v)$. Conditionally on the initial configuration S_0 , this defines two random variables: let B_1 be the number of vertices u in S_1 satisfying $E_S(u) \geq E_S(v)$ and W_1 be the number of vertices u in S_1 satisfying $E_S(u) \leq E_S(v)$.

Next, let $S_2 := S_1 \cup \{u_{n,2}\}$, then $E_{S_2}(u_{n,2})$ is uniformly distributed on $\{1, \dots, |S_2|\}$. Then, conditionally on B_1 and W_1 , one has $E_{S_2}(u_{n,2}) \geq E_{S_2}(v)$, with probability $\frac{B_1}{B_1 + W_1}$. This process is then continued by induction until $S_{j_{n-1}}$. After that i_{n-1} white balls are added.

Continuing this process via a decreasing induction in k from $n - 2$ to 1 completes the proof. \square

Our final proposition requires first the following basic lemma.

LEMMA 4.19 (Order statistics comparisons). *Let $(Z_i, 1 \leq i \leq N - s - 1)$ be independent, uniform random variables on $[0, 1]$ and let Z be a random variable on $[0, 1]$, independent of each Z_i , and distributed like $\text{Beta}(a, s + 1 - a)$. Let I be the number of indices $i \geq 1$ such that $Z_i < Z$. Then one has*

$$(37) \quad \mathbb{E}(I) = \frac{(N - s - 1)a}{s + 1}$$

and

$$(38) \quad \mathbb{E}(I^2) = \frac{a(N - s - 1)((a + 1)N - (s + 2)a)}{(s + 1)(s + 2)}.$$

PROOF. The density of the beta distribution Z was already encountered in Equation (25); Z is thus the a th order statistic of the uniform distribution. It is easily seen that for all $1 \leq i < j \leq N - s - 1$,

$$\mathbb{P}(Z_i < Z) = \frac{a}{s + 1} \quad \text{and} \quad \mathbb{P}(Z_i < Z, Z_j < Z) = \frac{a(a + 1)}{(s + 1)(s + 2)}.$$

Moreover, writing the random variable I as $I = \sum_{i=1}^{N-s-1} \mathbf{1}_{\{Z_i < Z\}}$, we get

$$\begin{aligned} \mathbb{E}(I) &= \sum_{i=1}^{N-s-1} \mathbb{P}(Z_i < Z) = \frac{(N - s - 1)a}{s + 1}, \\ \mathbb{E}(I^2) &= \sum_{1 \leq i \neq j \leq N-s-1} \mathbb{P}(Z_i < Z, Z_j < Z) + \sum_{i=1}^{N-s-1} \mathbb{P}(Z_i < Z) \\ &= (N - s - 1)(N - s - 2) \frac{a(a + 1)}{(s + 1)(s + 2)} + \frac{(N - s - 1)a}{s + 1}. \quad \square \end{aligned}$$

In order to complete the proof of Theorem 4.2, we still have to relate $|\mathcal{S}| - E_{\mathcal{S}}(v_m)$ to the quantity that we are interested in, namely $N - E_{\mathcal{T}}(v_m)$.

PROPOSITION 4.20 (Same asymptotic densities). *The random variables $E_{\mathcal{S}}(v_m)$ and $E_{\mathcal{T}}(v_m)$ satisfy asymptotically the following link: for any $s, t \in \mathbb{R}^+$, one has*

$$(39) \quad \lim_{n \rightarrow \infty} \mathbb{P}\left(s < \frac{|\mathcal{S}| - E_{\mathcal{S}}(v_m)}{n^\delta} < t\right) = \lim_{n \rightarrow \infty} \mathbb{P}\left(s < \frac{2(p + \ell)}{p\ell} \frac{N - E_{\mathcal{T}}(v_m)}{n^{1+\delta}} < t\right).$$

PROOF. Let $\mathcal{T}^* = \mathcal{S} \cup \mathcal{S}'$ be the graph obtained from \mathcal{T} by removing the root. Then \mathcal{T}^* is a poset where there is no order relation between any vertex of \mathcal{S}' and any other vertex from \mathcal{T}^* . Due to this independence, the order polytope of \mathcal{T}^* is the Cartesian product of the order polytope of \mathcal{S} and $[0, 1]^{|\mathcal{S}'|}$. Now, let $a > 0$ be an integer and let F_a be the event that

$$|\mathcal{S}| - E_{\mathcal{S}}(v_m) = a.$$

In other words, a is the number of vertices in \mathcal{S} with a label greater than $E_{\mathcal{S}}(v_m)$. Let I be the random variable counting the number of vertices in \mathcal{S}' with a label greater than $\mathbb{E}_{\mathcal{T}}(v_m)$. Then, conditionally on the event F_a , the random variable $N - E_{\mathcal{T}}(v_m)$ has the same law as $I + a$. Indeed, $N - E_{\mathcal{T}}(v_m)$ counts the number of vertices in \mathcal{T} with a label greater than $E_{\mathcal{T}}(v_m)$. Note that I satisfies the conditions of Lemma 4.19 (with $s := |\mathcal{S}|$ therein), due to the order polytope independence mentioned above.

Recall that $|\mathcal{S}| = \Theta(n)$ while $N = \Theta(n^2)$ (in fact, $|\mathcal{S}| = (p + \ell)n - 1$ and $|\mathcal{T}| = N = \frac{1}{2}p\ell n(n + 1)$). Therefore, if $(a_n)_{n \geq 1}$ is a sequence of integers tending to $+\infty$ and such that $a_n = o(n)$, then thanks to (37), we have the estimates for the conditional expectation

$$(40) \quad \mathbb{E}(I|F_{a_n}) \sim \frac{a_n N}{|\mathcal{S}|} \sim cna_n,$$

with the constant $c = \frac{p\ell}{2(p+\ell)}$ and, thanks to (38), for the conditional variance

$$(41) \quad \text{var}(I|F_{a_n}) = \mathbb{E}(I^2|F_{a_n}) - (\mathbb{E}(I|F_{a_n}))^2 \sim c^2 n^2 a_n.$$

Combining (40) and (41), the Bienaymé–Chebyshev inequality gives that (for any $\kappa > 0$):

$$(42) \quad \mathbb{P}\left(\left|\frac{I}{cna_n} - 1\right| > \kappa \mid F_{a_n}\right) \leq \frac{1 + \varepsilon_n}{\kappa^2 a_n},$$

where ε_n is a sequence converging to 0 as $n \rightarrow \infty$. Since we have

$$\frac{N - E_{\mathcal{T}}(v_m)}{na_n} = \frac{I + a_n}{na_n} = \frac{I}{na_n} + \frac{1}{n},$$

the inequality (42) can be rewritten into

$$(43) \quad \mathbb{P}\left(\left|\frac{N - E_{\mathcal{T}}(v_m)}{cna_n} - 1\right| > \kappa \mid F_{a_n}\right) \leq \frac{1 + \varepsilon'_n}{\kappa^2 a_n},$$

where ε'_n is a sequence converging to 0 as $n \rightarrow \infty$. In particular, for any $t > 0$ and $0 < \delta < 1$, setting $a_n = \lceil tn^\delta \rceil$ in (43) gives

$$(44) \quad \mathbb{P}\left(\left|\frac{N - E_{\mathcal{T}}(v_m)}{cn^{1+\delta}} - t\right| > \kappa t \mid F_{a_n}\right) \leq \frac{1 + o(1)}{\kappa^2 tn^\delta}.$$

Finally, for all reals $0 < s < t$, define the event

$$F_{s,t} = \bigcup_{sn^\delta < a < tn^\delta} F_a = \left\{s < \frac{|\mathcal{S}| - E_{\mathcal{S}}(v_m)}{n^\delta} < t\right\}.$$

According to (44) (set $\kappa = \varepsilon/t$ for any $\varepsilon > 0$), we have for $n \rightarrow \infty$

$$\mathbb{P}\left(\left\{s < \frac{N - E_{\mathcal{T}}(v_m)}{cn^{1+\delta}} < t\right\} \mid F_{s,t}\right) \rightarrow 1.$$

Thus, conditioning on the complementary event $\bar{F}_{s,t}$, we have

$$(45) \quad \lim_{n \rightarrow \infty} \mathbb{P}\left(\left\{s < \frac{N - E_{\mathcal{T}}(v_m)}{cn^{1+\delta}} < t\right\} \cap \bar{F}_{s,t}\right) = 0,$$

whereas conditioning on $F_{s,t}$ gives

$$(46) \quad \lim_{n \rightarrow \infty} \mathbb{P}\left(\left\{s < \frac{N - E_{\mathcal{T}}(v_m)}{cn^{1+\delta}} < t\right\} \cap F_{s,t}\right) = \lim_{n \rightarrow \infty} \mathbb{P}\left(s < \frac{|\mathcal{S}| - E_{\mathcal{S}}(v_m)}{n^\delta} < t\right).$$

Summing (45) and (46) leads to (39). \square

In summary, in this section we have proven that the four following quantities have asymptotically the same distribution:

$$(47) \quad \begin{aligned} \frac{2}{p\ell} \frac{N - E_{\mathcal{Y}}(v)}{n^{1+\delta}} &= \frac{2}{p\ell} \frac{N - E_{\mathcal{T}}(v_m)}{n^{1+\delta}} && \text{Prop. 4.9 (density method)} \\ &\sim \frac{1}{p + \ell} \frac{|\mathcal{S}| - E_{\mathcal{S}}(v_m)}{n^\delta} && \text{Prop. 4.20 (order statistics)} \\ &= \frac{1}{p + \ell} \frac{B_{(n-1)p}}{n^\delta}. && \text{Prop. 4.17 (Pólya urn)} \end{aligned}$$

In conjunction with Theorem 1.6 proven via analytic combinatorics methods, this implies that the four quantities in (47) converge in law to the distribution $\text{GenGammaProd}(p, \ell, b_0, w_0)$, when $\delta = p/(p + \ell)$. This is exactly the statement of Theorem 4.2.

NOTA BENE. It should be stressed that the sequence of transformations in (47) is *not* a bijection between Young tableaux and urns, it is only *asymptotically* that the corresponding distributions are equal.

The perspicacious reader would have noted that in the previous pages, we used several small lemmas and propositions which were stated with slightly more generality than what was a priori needed. In fact, this now allows us to state an even stronger version of Theorem 4.2. (It would have been not unpedagogical to introduce it first: we think it would have been harder for the reader to digest the different key steps/definitions/figures used in the proof.) In order to state this generalization to any Young tableau with a more general periodic shape, we need a slight extension of the shape $\lambda_1^{i_1} \cdots \lambda_n^{i_n}$ introduced in Definition 4.5: we allow some of the indices i_k to be equal to zero, in which case there is no column of height λ_k .

DEFINITION 4.21 (Periodic tableau). For any tuple of nonnegative integers (ℓ_1, \dots, ℓ_p) , a tableau with periodic pattern shape $(\ell_1, \dots, \ell_p; n)$ is a tableau with shape

$$((np)^{\ell_p} (np - 1)^{\ell_{p-1}} \cdots (np - p + 1)^{\ell_1}) \\ \times (((n - 1)p)^{\ell_p} \cdots ((n - 1)p - p + 1)^{\ell_1}) \times \cdots \times (p^{\ell_p} \cdots 1^{\ell_1}).$$

A uniform random Young tableau with periodic pattern shape $(\ell_1, \dots, \ell_p; n)$ is a uniform random filling of a tableau with periodic pattern shape $(\ell_1, \dots, \ell_p; n)$.

Let us put the previous pattern in words: we have a tableau made of n blocks, each of these blocks consisting of p smaller blocks of length ℓ_p, \dots, ℓ_1 , and the height decreases by 1 between each of these smaller blocks. This leads to a tableau length $(\ell_1 + \cdots + \ell_p)n$, which repeats periodically the same subshape along its hypotenuse.

Note that the triangular Young tableau of parameters (ℓ, p, n) from Definition 4.1 corresponds to Definition 4.21 for the $(p + 1)$ -tuple $(0, \dots, 0, \ell; n)$. In order to state our main result in full generality, we extend the above defined Young tableau by additional rows from below.

DEFINITION 4.22. Let $b_0, w_0 > 0$. A tableau of shape $\lambda_1^{i_1} \cdots \lambda_n^{i_n}$ shifted by a block $b_0^{w_0}$ is a tableau of shape $(\lambda_1 + b_0)^{i_1} \cdots (\lambda_n + b_0)^{i_n} b_0^{w_0}$.

We can now state the main theorem of this section.

THEOREM 4.23 (The distribution of the southeast entry in periodic Young tableaux). Choose a uniform random Young tableau with periodic pattern shape $(\ell_1, \dots, \ell_p; n)$ shifted by a block $b_0^{w_0}$. Let N be its size, set $\ell := \ell_1 + \cdots + \ell_p$ and $\delta := p/(p + \ell)$. Let X_n be the entry of the southeast corner. Then $(N - X_n)/n^{1+\delta}$ converges in law to the same limiting distribution as the number of black balls in the periodic Young–Pólya urn with initial conditions (b_0, w_0) and with replacement matrices $M_i = \begin{pmatrix} 1 & \ell_i \\ 0 & 1+\ell_i \end{pmatrix}$:

$$\frac{2}{p\ell} \frac{N - X_n}{n^{1+\delta}} \xrightarrow{\mathcal{L}} \text{Beta}(b_0, w_0) \prod_{\substack{i=1 \\ i \neq \ell_1 + \cdots + \ell_j + j \\ \text{with } 1 \leq j \leq p-1}}^{p+\ell-1} \text{GenGamma}(b_0 + w_0 + i, p + \ell).$$

PROOF. One just follows the same steps as in (47). The final proof holds *verbatim*, only the equality $N = \frac{p\ell}{2}n(n + 1)$ has to be replaced by an asymptotic $N \sim \frac{p\ell}{2}n$, which is anyway the only information that is used. One then concludes via Theorem 3.8. \square

In the next section, we discuss some consequences of our results in the context of limit shapes of random Young tableaux.

5. Random Young tableaux and random surfaces. There is a vast and fascinating literature related to the asymptotics of Young tableaux when their shape is free, but the number of cells is going to infinity: it even originates from the considerations of Erdős, Szekeres and Ulam on longest increasing subsequences in permutations (see [2, 81] for a nice presentation of these fascinating aspects). There algebraic combinatorics and variational calculus appear to play a key rôle, as became obvious with the seminal works of Vershik and Kerov, Logan and Shepp [60, 91]. The asymptotics of Young tableaux when the shape is constrained is harder to handle, and this section tackles some of these aspects.

5.1. *Random surfaces.* Figure 7 illustrates some known results and some conjectures on “the continuous” limit of Young tableaux (see also the notion of continual Young tableaux in [52]). Let us now explain a little bit what is summarized by this figure, which, in fact, refers to different levels of renormalization in order to catch the right fluctuations. It should also be pinpointed that some results are established under the Plancherel distribution, while some others are established under the uniform distribution (like in the present work).

First, our Theorem 4.2 can be seen as a result on random surfaces arising from Young tableaux with a fixed shape. Let us be more specific. Consider a fixed rectangular triangle Tr where the size of the edges meeting at the right angle are p and q , respectively, where p and q are integers. One can approximate Tr by a sequence of tableaux $(\mathcal{Y}_n)_{n \geq 0}$ of the same form as \mathcal{Y} in Section 4 where the size of the sides meeting at the right angle are pn and qn .

For each of these tableaux, one can pick a random standard filling and one can interpret it as a random discretized surface. More precisely, if $0 \leq x \leq p$ and $0 \leq y \leq q$ are two reals and if the entry of the cell $(\lfloor xn \rfloor, \lfloor yn \rfloor)$ is z , then we set $f_n(x, y) := 2z/(pqn^2)$. Thereby, we construct a random function $f_n : \text{Tr} \rightarrow [0, 1]$ which is discontinuous but it is to be expected that, in the limit, the functions f_n converge in probability to a deterministic, continuous function f (see Figure 8). Intuitively, for every point (x, y) on the hypotenuse, one will have $f(x, y) = 1$ and this is the case in particular for the southeast corner, that is, the point $(p, 0)$. Then one can view Theorem 4.2 as a result on the fluctuations of the random quantity $f_n(p, 0)$ away from its deterministic limit, which is 1.

As a matter of fact, the convergence of f_n to f has only been studied when the shape of the tableau is fixed. The convergence toward a limiting surface was first proven when the

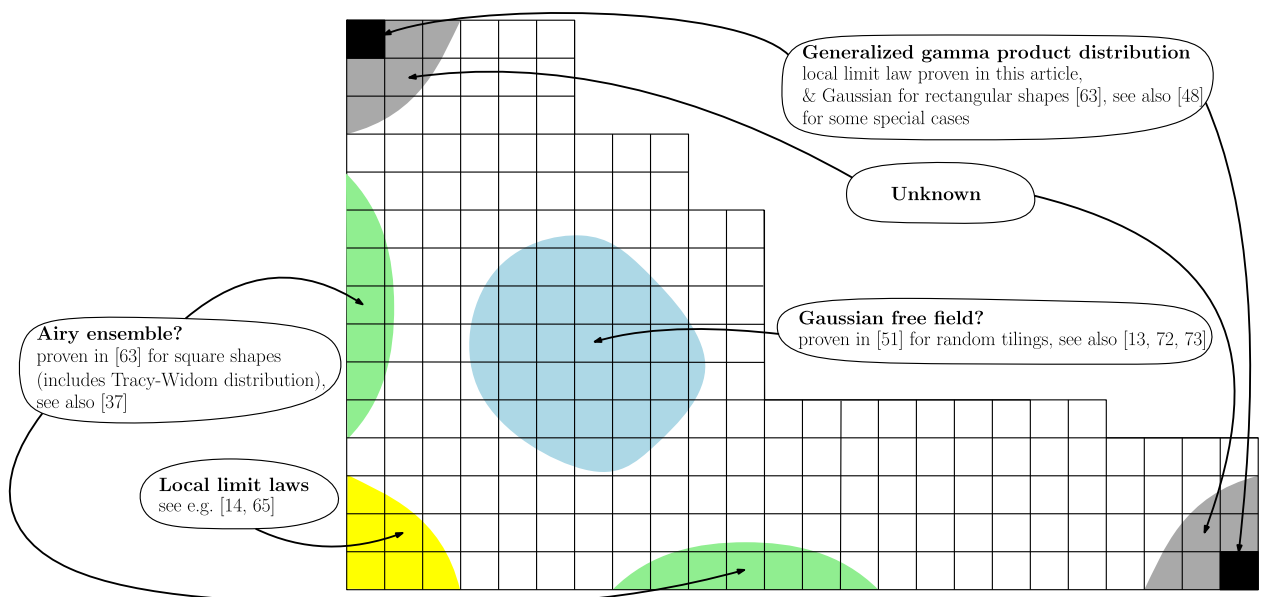


FIG. 7. *Known and conjectured limit laws of random Young tableaux. Would it one day lead to a nice notion of “continuous Young tableau”?*

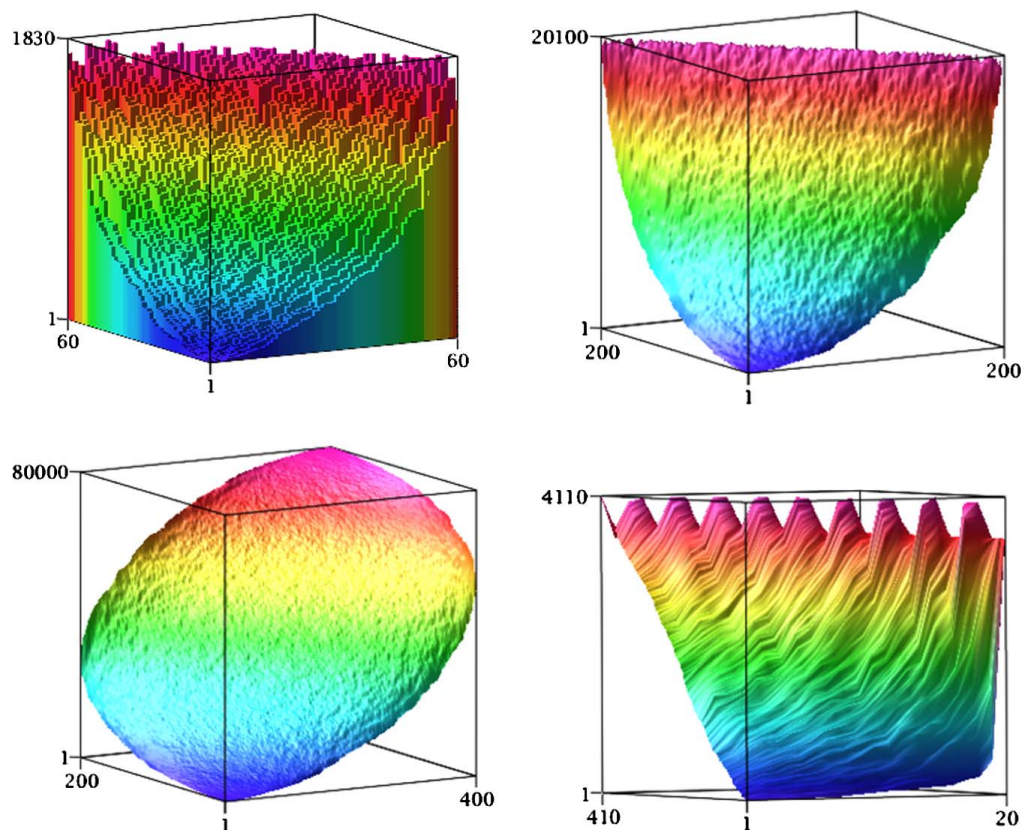


FIG. 8. Random generation of Young tableaux, seen as random surfaces (the colours correspond to level lines):

- top: triangular Young tableaux (size 60×60 , seen as histogram, and 200×200),
- bottom: rectangular and triangular Young tableaux (400×200 and 410×20).

If one watches such surfaces from above, then one sees exactly the triangular/rectangular shapes, but one loses the 3D effect. The images are generated via our own Maple package available at <https://lipn.fr/~cb/YoungTableaux>, relying on a variant of the hook-length walk of [40].

limit shape is a finite union of rectangles; see Biane [13]. There the limiting surface can be interpreted in terms of characters of the symmetric group and free probability but this leads to complicated computations from which it is difficult to extract explicit expressions.

For rectangular Young tableaux, the limiting surface is described more precisely by Pittel and Romik [73]. A limiting surface also exists for staircase tableaux: it can be obtained by taking the limiting surface of a square tableau and cutting it along the diagonal; see [4, 59]. This idea does not work for *rectangular* (nonsquare) Young tableaux: if one cuts such tableaux along the diagonal, one *does not* get the limiting surface of triangular Young tableaux (the hypotenuse would have been the level line 1, but the diagonal is in fact not even a level line, as visible in Figure 8 and proven in [73]).

Apart from the particular cases mentioned above, convergence results for surfaces arising from Young tableau seem to be lacking. There are also very few results about the fluctuations away from the limiting surface. For rectangular shapes, these fluctuations were studied by Marchal [63]: they are Gaussian in the southeast and northwest corner, while the fluctuations on each edge follow a Tracy–Widom limit law, at least when the rectangle is a square (for general rectangles, there remain some technicalities, although the expected behaviour is the same). For staircase triangles, Gorin and Rahman [37] use a sorting network representation to obtain asymptotic formulas using double integrals. In particular, they find the limit law on the edge. Their approach may be generalizable to other triangular shapes. Also, instead of renormalized limits, one may be interested in local limits, there are then nice links with the famous jeu de taquin [86] and characters of symmetric groups [14].

There is another framework where random surfaces naturally arise, namely random tilings and related structures (see, e.g., [85]). Indeed, one can associate a height function with a

tiling: this gives an interpretation as a surface. In this framework, there are results on the fluctuations of these surfaces, which are similar to the ones on Young tableaux. In the case of the Aztec diamond shape, Johansson and Nordenstam [48] proved that the fluctuations of the Artic curve are related to eigenvalues of GUE minors (and are therefore Gaussian near the places where the curve is touching the edges, whereas they are Tracy–Widomian when the curve is far away from the edges). Note that this gives the same limit laws as for the Artic curve of a TASEP jump process associated to rectangular Young tableaux [63, 80]. Similar results were also obtained for pyramid partitions [17, 18]. Moreover, in other models of lozenge tilings, it is proven that for some singular points, other limit laws appear: they are called cusp–Airy distributions, and are related to the Airy kernel [25]. It has to be noticed that, up to our knowledge, the generalized gamma distributions, which appear in our results, have not been found in the framework of random tilings.

A major challenge would be to capture the fluctuations of the surface in the interior of the domain. For Young tableaux, it is reasonable to conjecture that these fluctuations could be similar to those observed for random tilings: in this framework, Kenyon [51] and Petrov [72] proved that the fluctuations are given by the Gaussian free field (see also [20]).

Finally, a dual question would be: in which cell does a given entry lie in a random filling of the tableau? In the case of triangular shapes like ours, if we look at the largest entry, we get the following.

PROPOSITION 5.1 (Limit law for the location of the maximum in a triangular Young tableau). *Choose a uniform random triangular Young tableau of parameters (ℓ, p, n) (see Definition 4.1). Let $\text{Posi}_n \in \{1, \dots, \ell n\}$ be the x -coordinate of the cell containing the largest entry. Then one has*

$$\frac{\text{Posi}_n}{\ell n} \xrightarrow{\mathcal{L}} \text{Arcsine}(\delta) \quad \text{where } \delta := p/(p + \ell).$$

PROOF. Remove from the Young tableau \mathcal{Y} the cell containing its largest entry, and call \mathcal{Y}^* this new tableau. Then, using the hook length formula, the probability that the largest entry of \mathcal{Y} is situated at x -coordinate $k\ell$ is

$$\mathbb{P}(\text{Posi}_n = k\ell) = \frac{\prod_{c \in \mathcal{Y}^*} \text{hook}_{\mathcal{Y}^*}(c)}{\prod_{c \in \mathcal{Y}} \text{hook}_{\mathcal{Y}}(c)} = \prod_{\substack{c \in \mathcal{Y}^* \text{ with } (x\text{-coord of } c) = k\ell \\ \text{or } (y\text{-coord of } c) = (n - k + 1)p}} \frac{\text{hook}_{\mathcal{Y}^*}(c)}{1 + \text{hook}_{\mathcal{Y}^*}(c)}.$$

An easy computation then gives (with $\delta = p/(p + \ell)$):

$$\mathbb{P}(\text{Posi}_n = k\ell) \sim \frac{(k/n)^{\delta-1} (1 - k/n)^{-\delta}}{\Gamma(\delta)\Gamma(1 - \delta)} \frac{1}{n}.$$

Here, one recognizes an instance of the generalized arcsine law on $[0, 1]$ with density

$$\frac{x^{\delta-1} (1 - x)^{-\delta}}{\Gamma(\delta)\Gamma(1 - \delta)}. \quad \square$$

So, if we compare models with different p and ℓ , then the largest entry will have the tendency to be on the top of the hypotenuse when ℓ is much larger than p , while it will be on its bottom if p is much larger than ℓ (and on the bottom or the top with equally high probabilities when $p \approx \ell$); see Figure 8. This is in sharp contrast with the case of an $n \times n$ square tableau where, for $t \in (0, 1)$, the cell containing the entry tn^2 is asymptotically distributed according to the Wigner semicircle law on its level line; see [73]. We also refer to Romik [79] for further discussions on Young tableau landscapes and to Morales, Pak and Panova [66] for recent results on skew-shaped tableaux.

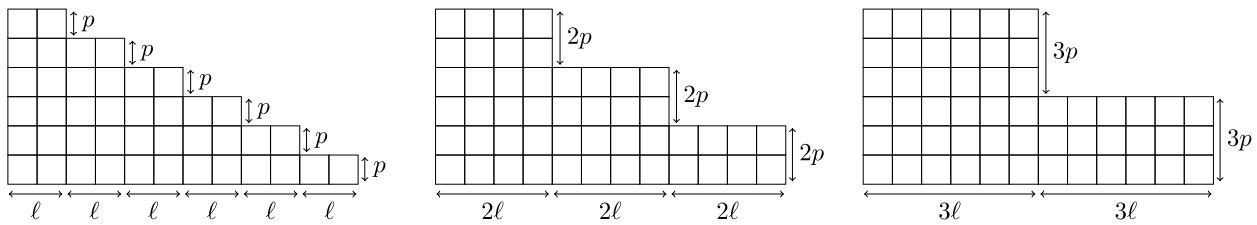


FIG. 9. Different discrete models converge toward a tableau of slope $-p/\ell$. As usual for problems related to urns, many statistics have a sensibility to the initial conditions; it is therefore nice that some universality holds: the distributions (depending on p, ℓ and the “zoom factor” K) of our statistics have similar tails compared to Mittag-Leffler distributions.

5.2. From microscopic to macroscopic models: Universality of the tails. As mentioned in the previous section, we can approximate a triangle of slope $-p/\ell$ by a tableau of parameters (ℓ, p, n) but what happens if we approximate it by a tableau of parameters $(K\ell, Kp, n)$ for any “zoom factor” $K \in \mathbb{N}$? (See Figure 9.) In the first case, we obtain as a limit law in the southeast corner $\text{GenGammaProd}(p, \ell, p, \ell)$ whereas in the second case, we get the law $\text{GenGammaProd}(Kp, K\ell, Kp, K\ell)$ and these two distributions are different.

In fact, we could even imagine more general periodic patterns as in Theorem 4.23 corresponding to the same macroscopic object. All these models lead to different asymptotic distributions. However, we partially have some universal phenomenon in the sense that, although these limit distributions are different, they are closely related by the fact that their tails are similar to the tail of a Mittag-Leffler distribution.

DEFINITION 5.2 (Similar tails). One says that two random variables X and Y have similar tails and one writes $X \asymp Y$ if

$$\frac{\log \frac{\mathbb{E}(X^r)}{\mathbb{E}(Y^r)}}{r} \rightarrow 0 \quad \text{as } r \rightarrow \infty.$$

This definition has the advantage to induce an equivalence relation between random variables which have moments of all orders: if X, Y are in the same equivalence class, then for every $\varepsilon \in (0, 1)$, for r large enough, one has

$$\mathbb{E}(((1 - \varepsilon)X)^r) \leq \mathbb{E}(Y^r) \leq \mathbb{E}(((1 + \varepsilon)X)^r).$$

In the proof of the following theorem, we give much finer asymptotics than the above bounds.

THEOREM 5.3 (Similarity with the tail of a Mittag-Leffler distribution). Let X be a random variable distributed as $\text{GenGammaProd}([\ell_1, \dots, \ell_p]; b_0, w_0)$ and put $\ell = \ell_1 + \dots + \ell_p$, $\delta = p/(p + \ell)$. Let $Y := \text{ML}(\delta, \beta)$ (where ML is the Mittag-Leffler distribution defined as in (48) hereafter, with any $\beta > -\delta$). Then X and $\delta p^{\delta-1} Y$ have similar tails in the sense of Definition 5.2.

PROOF. First, recall from, for example, [36], page 8, that the Mittag-Leffler distribution $\text{ML}(\alpha, \beta)$ (where $0 < \alpha < 1$ and $\beta > -\alpha$) is determined by its moments. Its r th moment has two equally useful closed forms:

$$(48) \quad m_{\text{ML},r} = \frac{\Gamma(\beta)\Gamma(\beta/\alpha + r)}{\Gamma(\beta/\alpha)\Gamma(\beta + \alpha r)} = \frac{\Gamma(\beta + 1)\Gamma(\beta/\alpha + r + 1)}{\Gamma(\beta/\alpha + 1)\Gamma(\beta + \alpha r + 1)}.$$

Now, we prove that, for a fixed α , the Mittag-Leffler distributions have similar tails. From the Stirling’s approximation formula, we have

$$(49) \quad \log \Gamma(\alpha r + \beta) = \alpha r \log(r) + (\alpha \log(\alpha) - \alpha)r + \left(\beta - \frac{1}{2}\right) \log(\alpha r) + \frac{\log(2\pi)}{2} + O\left(\frac{1}{r}\right).$$

Applying this to the moments (48) of the Mittag-Leffler distribution $Y = \text{ML}(\alpha, \beta)$, we get

$$(50) \quad \log \mathbb{E}(Y^r) = (1 - \alpha)r \log(r) + (-\alpha \log(\alpha) + \alpha - 1)r + \left(\frac{\beta}{\alpha} - \beta\right) \log(r) + O(1),$$

and thus if one compares with another distribution $Y' = \text{ML}(\alpha, \beta')$, this leads to $Y \asymp Y'$.

Next, we prove that GenGammaProd distributions with the same δ have similar tails. The moments of $X = \text{GenGammaProd}([\ell_1, \dots, \ell_p]; b_0, w_0)$ are given by formula (21). Using the approximation (49), we get

$$(51) \quad \begin{aligned} \log \mathbb{E}(X^r) = & (1 - \delta)r \log(r) + (1 - \delta) \left(\log\left(\frac{\delta}{p}\right) - 1 \right)r \\ & + \left(b_0 + s_0\delta + \frac{(1 + \delta)(p - 1)}{2} - \frac{\delta}{p} \sum_{j=0}^{p-1} \sum_{k=1}^j \ell_k \right) \log(r) + O(1). \end{aligned}$$

Here, we see that in fact up to order $O(r)$ only the slope δ and the period length p play a rôle; it is only at order $o(r)$ that b_0, s_0 , and the ℓ_k really occur. Thus, if we now also consider $X' = \text{GenGammaProd}([\ell'_1, \dots, \ell'_{p'}]; b'_0, w'_0)$, we directly deduce $X \asymp \left(\frac{p}{p'}\right)^{\delta-1} X'$.

Finally, we can compare the moments of X (any GenGammaProd distribution associated to a slope δ and period p) and Y (any Mittag-Leffler distribution with $\alpha := \delta$) via formulas (50) and (51), this leads to $X \asymp \delta p^{\delta-1} Y$. \square

REMARK 5.4. The tails of this distribution are universal: they depend only on the slope δ and the period length p . They depend neither on the initial conditions b_0 and w_0 , nor on further details of the geometry of the periodic pattern (the ℓ_i 's).

One more universal property which holds for some families of urn distributions is that they possess sub-Gaussian tails, a notion introduced by Kahane in [49] (see also [56] for some urn models exhibiting this behaviour).

DEFINITION 5.5. A random variable X has sub-Gaussian tails if there exist two constants $c, C > 0$, such that

$$\mathbb{P}(|X| \geq t) \leq C e^{-ct^2}, \quad t > 0.$$

PROPOSITION 5.6. The $\text{GenGammaProd}(p, \ell, b_0, w_0)$ distributions have subGaussian tails if and only if $p \geq \ell$.

PROOF. The GenGammaProd distribution, as defined in equation (1), has moments given in equation (20). As derived thereafter, it has moments asymptotically equivalent to

$$(m_r)^{1/r} = ((p + \ell)e)^{(\delta-1)} r^{(1-\delta)} (1 + o(1)).$$

By [49], Proposition 9, a random variable X has sub-Gaussian tails if and only if there exists a constant $K > 0$ such that for all $r > 0$ we have $(\mathbb{E}(X^r))^{1/r} \leq K \sqrt{r}$. As $\delta = \frac{p}{p+\ell}$ the claim follows. \square

Another useful notion which helps to gain insight into the limit of Young tableaux is the notion of a *level line*: let C_v be the curve separating the cells with an entry bigger than v and the cells with an entry smaller than v (and to get a continuous curve, one follows the border of the Young tableau if needed; see Figure 10).

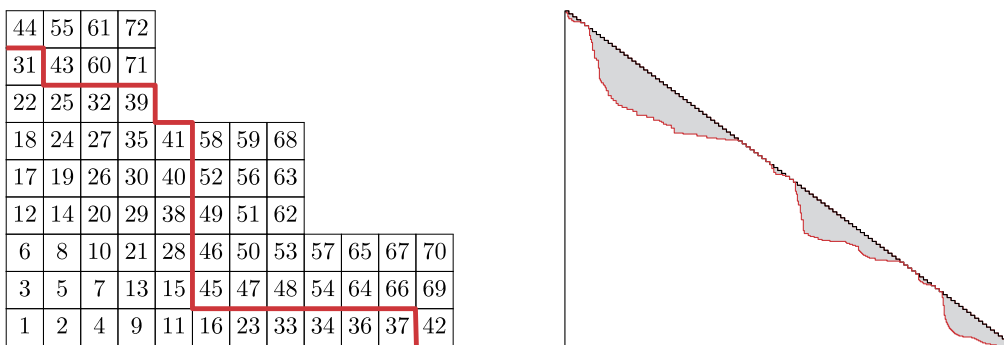


FIG. 10. The level line (in red) of the southeast corner X_n : it separates all the entries smaller than X_n from the other ones. On the left: one example with the level line of $X_n = 42$. On the right: the level line of X_n , for a very large Young tableau of size N of triangular shape. The area between this level line and the hypotenuse is the quantity $N - X_n$ analysed in Section 4.

When $n \rightarrow \infty$, one may ask whether the level line \mathcal{C}_{X_n} converges in distribution to some limiting random curve \mathcal{C} . If so, the limit laws we computed in Theorem 4.2 would give the (renormalized) area between the macroscopic curve \mathcal{C} and the hypotenuse. In particular, the law of \mathcal{C} would depend on the microscopic details of the model, since we find for the renormalized area a whole family of distributions $\text{GenGammaProd}(p, \ell, b_0, w_0)$ depending on 4 parameters. Besides, note that we could imagine even more general microscopic models for the same macroscopic triangle. For instance, for a slope -1 , starting from the southeast corner we could have a periodic pattern (1 step north, 2 steps west, 2 steps north, 1 step west). All shapes leading to the same slope are covered by Theorem 3.8 (see also Example 3.9), and our method then gives similar, but distinct, limit laws. Such models thus yield another limit law for the area, and thus another limiting random curve \mathcal{C} .

Note that the renormalized area between \mathcal{C} and the hypotenuse does not have the same distribution as the area below the positive part of a Brownian meander [46]. Funnily, Brownian motion theory is cocking a snook at us: another one of Janson’s papers [47] studies the area below curves which are related to the Brownian supremum process and, here, one observes more similarities with our problem, as the moments of the corresponding distribution involve the gamma function. However, these moments grow faster than in the limit laws found in Theorem 4.2. It is widely open if there is some framework unifying all these points of view.

5.3. Factorizations of gamma distributions. With respect to the asymptotic landscape of random Young tableaux, let us add one last result: our results on the southeast corner directly imply similar results on the northwest corner. In particular, the critical exponent for the upper left corner is $1 - \delta$. In fact, it is a nice surprise that there is even more structure: any periodic pattern shape is naturally associated with a family of patterns such that the limit laws of the southeast corners of the corresponding Young tableaux are related to each other.

First, let us describe the periodic pattern via a *shape path* $(i_1, j_1; \dots; i_m, j_m)$: it starts at the northwest corner of the tableau described by the pattern with i_1 right steps, followed by j_1 down steps, etc.; see Figure 11. Then its cyclic shift is defined by $(j_m, i_1; \dots; j_{m-1}, i_m)$.

Furthermore, this notion is equivalent to Definition 4.21 of a periodic tableau via the following formula:

$$(\ell_1, \dots, \ell_p) = \underbrace{(0, \dots, 0, j_m)}_{i_m \text{ elements}}, \underbrace{(0, \dots, 0, j_{m-1}, \dots)}_{i_{m-1} \text{ elements}}, \underbrace{(0, \dots, 0, j_1)}_{i_1 \text{ elements}}.$$

Then the *cyclic shift* is given by

$$(\ell'_1, \dots, \ell'_{p'}) := \underbrace{(0, \dots, 0, i_m)}_{j_{m-1} \text{ elements}}, \underbrace{(0, \dots, 0, i_2)}_{j_1 \text{ elements}}, \underbrace{(0, \dots, 0, i_1)}_{j_m \text{ elements}}.$$

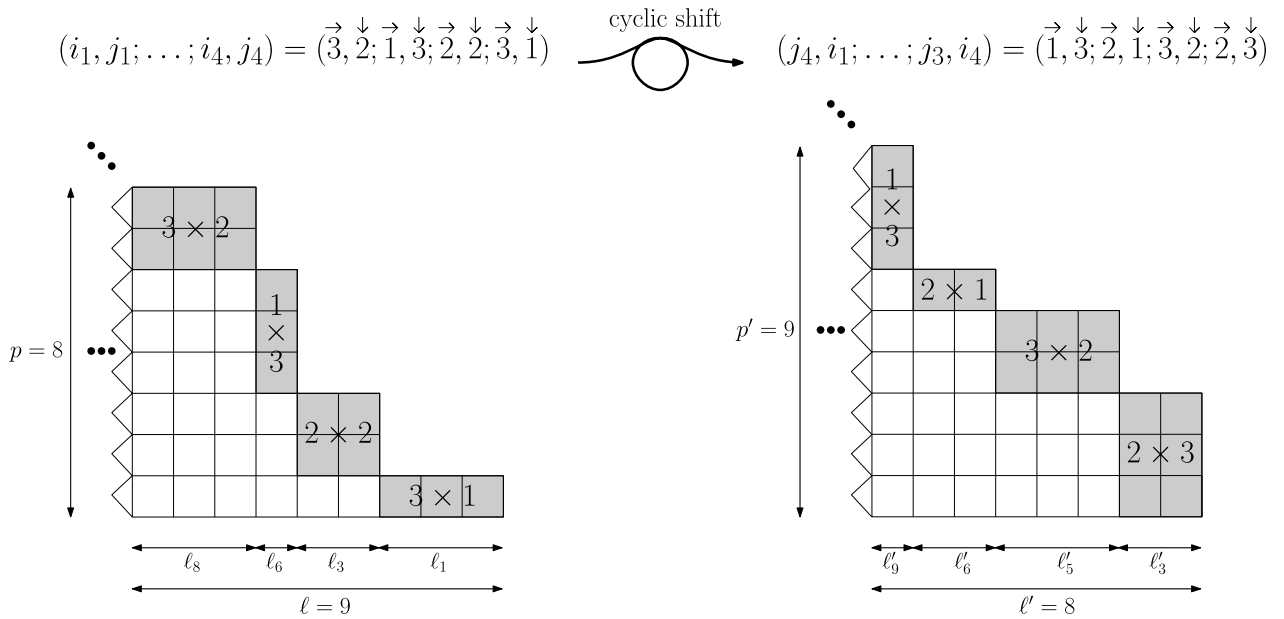


FIG. 11. Example of a cyclic shift on a periodic pattern. On the left: one sees the shape path $(3,2;1,3;2,2;3,1)$, it corresponds to the pattern $(\ell_1, \dots, \ell_8) = (3, 0, 2, 0, 0, 1, 0, 3)$ (as sequence of consecutive heights, from right to left). On the right: one sees its cyclic shift, which corresponds to the pattern $(\ell'_1, \dots, \ell'_9) = (0, 0, 2, 0, 3, 2, 0, 0, 1)$. In grey, we see the size of the subrectangles described by the shape path, that is, the k th rectangle has size $i_k \times j_k$.

In particular, we have $p' = \ell$ and $\ell' = p$.

Appending n copies of the shape path $(i_1, j_1; \dots; i_m, j_m)$ to each other corresponds to n repetitions of the pattern and, therefore, gives a periodic tableau. Note that this new sequence is then equal to the shape of its associated tree, similarly to Figure 3 and in accordance with Definition 4.6.

PROPOSITION 5.7 (Factorization of gamma distributions). *Let two sequences (ℓ_1, \dots, ℓ_p) and $(\ell'_1, \dots, \ell'_{p'})$ be defined as above and let j_m be the smallest index such that $\ell_{j_m} > 0$. Let b_0, w_0 be two positive integers, and Y and Y' be independent random variables with respective distribution $\text{GenGammaProd}([\ell_1, \dots, \ell_p]; b_0, w_0)$ and $\text{GenGammaProd}([\ell'_1, \dots, \ell'_{p'}]; b_0 + w_0, j_m)$ from Theorem 3.8. Then we have the factorization:*

$$(52) \quad YY' \stackrel{\mathcal{L}}{=} \frac{1}{p + \ell} \Gamma(b_0).$$

PROOF. The equality in distribution is obtained by checking the equality of the r th moments and then applying Carleman's theorem: using formula (20) for the moments of GenGammaProd indeed leads (after simplification via the Gauss multiplication formula on the gamma function) to $\mathbb{E}(Y^r)\mathbb{E}((Y')^r) = \frac{1}{(p+\ell)^r} \mathbb{E}(Z^r)$, where Z is a random variable distributed according to $\Gamma(b_0)$. \square

REMARK 5.8 (A duality between corners). One case of special interest is the case of Young tableaux having the mirror symmetry $(\ell_{j_m}, \dots, \ell_p) = (\ell_p, \dots, \ell_{j_m})$, where j_m is again the smallest index such that $\ell_{j_m} > 0$. Indeed, Y and Y' then correspond to the limit laws for the southeast (resp., northwest) corner of the same tableau. In this case, we can think of (52) as expressing a kind of duality between the corners of the tableau.

Similar factorizations of the exponential law, which is a particular case of the gamma distribution, have appeared recently in relation with functionals of Lévy processes, following [12]. These formulas are also some probabilistic echoes of identities satisfied by the gamma function.

We can mention one last result in this direction: indeed, Theorem 4.23 used for the Young tableau with periodic pattern shape $(\ell_1, \dots, \ell_p; 2n)$ and the (same) Young tableau with periodic pattern shape $(\ell_1, \dots, \ell_p, \ell_1, \dots, \ell_p; n)$ leads to two different closed forms of the same limit distribution, and one also gets other closed forms if one repeats m times the pattern (ℓ_1, \dots, ℓ_p) . For example, if one takes all the ℓ_i 's equal to 1, this gives

$$\text{GenGamma}(3, 2) = \sqrt{2} \text{GenGamma}(3, 4) \text{GenGamma}(5, 4),$$

and, more generally,

$$\text{GenGamma}(s_0 + 1, 2) = \sqrt{m} \prod_{k=1}^m \text{GenGamma}(s_0 + 2k - 1, 2m).$$

Using the fact that $\text{GenGamma}(a, 1/b) = \Gamma(ab)^b$, we can rephrase this identity in terms of powers of Γ distributions (the notation Γ , in bold, stands for the distribution, while Γ stands for the function; below, we have only occurrences in bold):

$$\Gamma\left(\frac{s_0 + 1}{2}\right)^{\frac{1}{2}} = \sqrt{m} \prod_{k=1}^m \Gamma\left(\frac{s_0 + 2k - 1}{2m}\right)^{\frac{1}{2m}}.$$

With $x := \frac{s_0 + 1}{2m}$, one gets the following formula equivalent to the Gauss multiplication formula:

$$\Gamma(mx)^m = m^m \prod_{k=1}^m \Gamma\left(x + \frac{k-1}{m}\right).$$

Choosing other values for the ℓ_i 's leads to more identities:

$$\begin{aligned} & \prod_{\substack{i=1 \\ i \neq \ell_1 + \dots + \ell_j + j \\ \text{with } 1 \leq j \leq p-1}}^{p+\ell-1} \text{GenGamma}(s_0 + i, p + \ell) \\ &= m^{1-\delta} \prod_{\substack{i=1 \\ i \neq \ell'_1 + \dots + \ell'_j + j \\ \text{with } 1 \leq j \leq mp-1}}^{m(p+\ell)-1} \text{GenGamma}(s_0 + i, m(p + \ell)). \end{aligned}$$

It is pleasant that it is possible to reverse engineer such identities, and thus obtain a probabilistic proof of the Gauss multiplication formula (see [24]).

This ends our journey in the realm of urns and Young tableaux; in the next final section, we conclude with a few words on possible extensions of the methods used in this article.

A method is a trick used twice.

George Pólya (1887–1985)

After this the reader who wishes to do so will have no difficulty in developing the theory of urns¹² when they are regarded as differential operators.

Alfred Young (1873–1940)

¹²The reader is invited to compare with the original citations of Pólya and Young in [75], page 208, and [38], page 366.

6. Conclusion and further work. In this article, we introduced Pólya urns with periodic replacements and showed that they can be exactly solved with generating function techniques. The initial partial differential equation encoding their dynamics leads to D-finite moment generating functions, which we identify as the signature of a generalized gamma product distribution. It is also pleasant that it finds applications for some statistics of Young tableaux.

Many extensions of this work are possible:

- The *density method* which we introduced in [10, 64] can be used to analyse other combinatorial structures, like we did already on permutations, trees, Young tableaux and Young tableaux with local decreases. In fact, the idea to use integral representations of order polytope volumes in order to enumerate poset structures is quite natural, and was used, for example, in [11, 28, 69]. Our approach, which uses this idea while following at the same time the densities of some parameter, allows us to solve both enumeration and random generation. We hope that some readers will give it a try on their favourite poset structure.
- In [31], Flajolet et al. analyse an urn model which leads to a remarkably simple factorization for the history generating function; see Theorem 1 therein and also Theorem 1 in [30]. This greatly helps them to perform the asymptotic analysis via *analytic combinatorics* tools. Our model does not possess such a factorization; this makes the proofs more involved. It is nice that our new approach remains generic and can be applied to more general periodic urn models (with weights, negative entries, random entries, unbalanced schemes, triangular urns with more colours, multiple drawings, ...). It is a full programme to investigate these variants, in order to get a better characterization of the zoo of special functions (combination of generalized hypergeometric, etc.) and distributions occurring for the different models.
- There exists a theory of elimination for partial differential equations, chiefly developed in the 1920s by Janet, Riquier and Thomas (see, e.g., [16, 35] for modern approaches). In our case, these approaches however fail to get the linear ordinary differential equations satisfied by our generating functions. It is thus an interesting challenge for *computer algebra* to get an efficient algorithm taking as input the PDE and its boundary conditions, and giving as output the D-finite equation (if any). Is it possible to extend holonomy theory beyond its apparent linear frontiers? (See the last part of [71].) Also, as an extension of Remark 2.5, it is natural to ask: is it possible to extend the work of Flajolet and Lafforgue to the full class of D-finite equations, thus exhibiting new universal limit laws like we did here?
- Our approach can also be used to analyse the fluctuations of further cells in a random Young tableau. It remains a challenge to understand the full *asymptotic landscape of surfaces* associated with *random Young tableaux*, even if it could be globally expected that they behave like a Gaussian free field, like many other random surfaces [51]. Understanding the fluctuations and the universality of the critical exponent at the corner could help to get a more global picture. The Arctic circle phenomenon (see [80]) and the study of the level lines \mathcal{C} in random Young tableaux and their possible limits in distribution, as discussed in Section 5.2, seems to be an interesting but very challenging problem.

Acknowledgements. Let us thank Vadim Gorin, Markus Kuba, Cécile Mailler and Henning Sulzbach for kind exchanges on their work [37, 56, 58] and on related questions. We also thank the referees of the preliminary AofA'2018 version [9] and of this *Annals of Probability* version for their careful reading and suggestions which improved the quality of our paper. We also thank the organizers (Igor Pak, Alejandro Morales, Greta Panova and Dan Romik) of the meeting *Asymptotic Algebraic Combinatorics* (Banff, 11–15 March 2019) where we got the opportunity to present this work.

Michael Wallner was supported by a MathStic funding from the University Paris Nord September–December 2017 and the Erwin Schrödinger Fellowship of the Austrian Science Fund (FWF): J 4162-N35.

REFERENCES

- [1] ABRAMOWITZ, M. and STEGUN, I. A., eds. (1984). *Handbook of Mathematical Functions with Formulas, Graphs, and Mathematical Tables. A Wiley-Interscience Publication*. Wiley, New York. Reprint of the 1972 edition, Selected Government Publications. [MR0757537](#)
- [2] ALDOUS, D. and DIACONIS, P. (1999). Longest increasing subsequences: From patience sorting to the Baik–Deift–Johansson theorem. *Bull. Amer. Math. Soc. (N.S.)* **36** 413–432. [MR1694204](#) <https://doi.org/10.1090/S0273-0979-99-00796-X>
- [3] ANDREWS, G. E., ASKEY, R. and ROY, R. (1999). *Special Functions. Encyclopedia of Mathematics and Its Applications* **71**. Cambridge Univ. Press, Cambridge. [MR1688958](#) <https://doi.org/10.1017/CBO9781107325937>
- [4] ANGEL, O., HOLROYD, A. E., ROMIK, D. and VIRÁG, B. (2007). Random sorting networks. *Adv. Math.* **215** 839–868. [MR2355610](#) <https://doi.org/10.1016/j.aim.2007.05.019>
- [5] ATHREYA, K. B. and KARLIN, S. (1968). Embedding of urn schemes into continuous time Markov branching processes and related limit theorems. *Ann. Math. Stat.* **39** 1801–1817. [MR0232455](#) <https://doi.org/10.1214/aoms/1177698013>
- [6] ATHREYA, K. B. and NEY, P. E. (2004). *Branching Processes*. Dover, Mineola, NY. Reprint of the 1972 original [Springer, New York; [MR0373040](#)]. [MR2047480](#)
- [7] BAGCHI, A. and PAL, A. K. (1985). Asymptotic normality in the generalized Pólya–Eggenberger urn model, with an application to computer data structures. *SIAM J. Algebr. Discrete Methods* **6** 394–405. [MR0791169](#) <https://doi.org/10.1137/0606041>
- [8] BANDERIER, C. and DRMOTA, M. (2015). Formulae and asymptotics for coefficients of algebraic functions. *Combin. Probab. Comput.* **24** 1–53. [MR3318039](#) <https://doi.org/10.1017/S0963548314000728>
- [9] BANDERIER, C., MARCHAL, P. and WALLNER, M. (2018). Periodic Pólya urns and an application to Young tableaux. In *29th International Conference on Probabilistic, Combinatorial and Asymptotic Methods for the Analysis of Algorithms. LIPIcs. Leibniz Int. Proc. Inform.* **110** Art. No. 11, 13. Schloss Dagstuhl. Leibniz-Zent. Inform., Wadern. [MR3826130](#)
- [10] BANDERIER, C., MARCHAL, P. and WALLNER, M. (2018). Rectangular Young tableaux with local decreases and the density method for uniform random generation. In *GASCom 2018, CEUR Workshop Proceedings* **2113** 60–68.
- [11] BARYSHNIKOV, Y. and ROMIK, D. (2010). Enumeration formulas for Young tableaux in a diagonal strip. *Israel J. Math.* **178** 157–186. [MR2733067](#) <https://doi.org/10.1007/s11856-010-0061-6>
- [12] BERTOIN, J. and YOR, M. (2001). On subordinators, self-similar Markov processes and some factorizations of the exponential variable. *Electron. Commun. Probab.* **6** 95–106. [MR1871698](#) <https://doi.org/10.1214/ECP.v6-1039>
- [13] BIANE, P. (1998). Representations of symmetric groups and free probability. *Adv. Math.* **138** 126–181. [MR1644993](#) <https://doi.org/10.1006/aima.1998.1745>
- [14] BORODIN, A. and OLSHANSKI, G. (2017). *Representations of the Infinite Symmetric Group. Cambridge Studies in Advanced Mathematics* **160**. Cambridge Univ. Press, Cambridge. [MR3618143](#) <https://doi.org/10.1017/CBO9781316798577>
- [15] BOSTAN, A., CHYZAK, F., GIUSTI, M., LEBRETON, R., LECERF, G., SALVY, B. and SCHOST, É. (2017). *Algorithmes Efficaces en Calcul Formel*. Self-publishing.
- [16] BOULIER, F., LEMAIRE, F., POTEAUX, A. and MORENO MAZA, M. (2019). An equivalence theorem for regular differential chains. *J. Symbolic Comput.* **93** 34–55. [MR3913563](#) <https://doi.org/10.1016/j.jsc.2018.04.011>
- [17] BOUTILLIER, C., BOUTTIER, J., CHAPUY, G., CORTEEL, S. and RAMASSAMY, S. (2017). Dimers on rail yard graphs. *Ann. Inst. Henri Poincaré D* **4** 479–539. [MR3734415](#) <https://doi.org/10.4171/AIHPD/46>
- [18] BOUTTIER, J., CHAPUY, G. and CORTEEL, S. (2017). From Aztec diamonds to pyramids: Steep tilings. *Trans. Amer. Math. Soc.* **369** 5921–5959. [MR3646784](#) <https://doi.org/10.1090/tran/7169>
- [19] BUBECK, S., MOSSEL, E. and RÁ CZ, M. Z. (2015). On the influence of the seed graph in the preferential attachment model. *IEEE Trans. Netw. Sci. Eng.* **2** 30–39. [MR3361606](#) <https://doi.org/10.1109/TNSE.2015.2397592>
- [20] BUFETOV, A. and GORIN, V. (2019). Fourier transform on high-dimensional unitary groups with applications to random tilings. *Duke Math. J.* **168** 2559–2649. [MR4007600](#) <https://doi.org/10.1215/00127094-2019-0023>
- [21] CARLEMAN, T. (1923). *Sur les équations intégrales singulières à noyau réel et symétrique*. Uppsala Universitets Årsskrift.
- [22] CHAUVIN, B., MAILLER, C. and POUYANNE, N. (2015). Smoothing equations for large Pólya urns. *J. Theoret. Probab.* **28** 923–957. [MR3413961](#) <https://doi.org/10.1007/s10959-013-0530-z>

- [23] DEVROYE, L. (1986). *Nonuniform Random Variate Generation*. Springer, New York. MR0836973 <https://doi.org/10.1007/978-1-4613-8643-8>
- [24] DUFRESNE, D. (2010). G distributions and the beta-gamma algebra. *Electron. J. Probab.* **15** 2163–2199. MR2745729 <https://doi.org/10.1214/EJP.v15-845>
- [25] DUSE, E., JOHANSSON, K. and METCALFE, A. (2016). The cusp-Airy process. *Electron. J. Probab.* **21** Paper No. 57, 50. MR3546394 <https://doi.org/10.1214/16-EJP2>
- [26] EGGENBERGER, F. and PÓLYA, G. (1923). Über die Statistik verketteter Vorgänge. *ZAMM Z. Angew. Math. Mech.* **3** 279–290. <https://doi.org/10.1002/zamm.19230030407>
- [27] EGGENBERGER, F. and PÓLYA, G. (1928). Sur l'interprétation de certaines courbes de fréquence. *C. R. Acad. Sci.* **187** 870–872.
- [28] ELKIES, N. D. (2003). On the sums $\sum_{k=-\infty}^{\infty} (4k+1)^{-n}$. *Amer. Math. Monthly* **110** 561–573. MR2001148 <https://doi.org/10.2307/3647742>
- [29] FANTI, G. and VISWANATH, P. (2017). Deanonymization in the Bitcoin P2P network. In *Proceedings of the 31st Conference on Neural Information Processing Systems*.
- [30] FLAJOLET, P., DUMAS, P. and PUYHAUBERT, V. (2006). Some exactly solvable models of urn process theory. In *Fourth Colloquium on Mathematics and Computer Science Algorithms, Trees, Combinatorics and Probabilities*. *Discrete Math. Theor. Comput. Sci. Proc.*, AG 59–118. Assoc. Discrete Math. Theor. Comput. Sci., Nancy. MR2509623
- [31] FLAJOLET, P., GABARRÓ, J. and PEKARI, H. (2005). Analytic urns. *Ann. Probab.* **33** 1200–1233. MR2135318 <https://doi.org/10.1214/009117905000000026>
- [32] FLAJOLET, P. and LAFFORGUE, T. (1994). Search costs in quadrees and singularity perturbation asymptotics. *Discrete Comput. Geom.* **12** 151–175. MR1283884 <https://doi.org/10.1007/BF02574372>
- [33] FLAJOLET, P. and SEDGEWICK, R. (2009). *Analytic Combinatorics*. Cambridge Univ. Press, Cambridge. MR2483235 <https://doi.org/10.1017/CBO9780511801655>
- [34] FRÉCHET, M. and SHOHAT, J. (1931). A proof of the generalized second-limit theorem in the theory of probability. *Trans. Amer. Math. Soc.* **33** 533–543. MR1501604 <https://doi.org/10.2307/1989421>
- [35] GERDT, V. P., LANGE-HEGERMANN, M. and ROBERTZ, D. (2019). The MAPLE package TDDS for computing Thomas decompositions of systems of nonlinear PDEs. *Comput. Phys. Commun.* **234** 202–215. MR3864422 <https://doi.org/10.1016/j.cpc.2018.07.025>
- [36] GOLDSCHMIDT, C. and HAAS, B. (2015). A line-breaking construction of the stable trees. *Electron. J. Probab.* **20** no. 16, 24. MR3317158 <https://doi.org/10.1214/EJP.v20-3690>
- [37] GORIN, V. and RAHMAN, M. (2019). Random sorting networks: Local statistics via random matrix laws. *Probab. Theory Related Fields* **175** 45–96. MR4009705 <https://doi.org/10.1007/s00440-018-0886-1>
- [38] GRACE, J. H. and YOUNG, A. (2010). *The Algebra of Invariants*. *Cambridge Library Collection*. Cambridge Univ. Press, Cambridge. Reprint of the 1903 original. MR2850282 <https://doi.org/10.1017/CBO9780511708534>
- [39] GRAHAM, R. L., KNUTH, D. E. and PATASHNIK, O. (1994). *Concrete Mathematics: A Foundation for Computer Science*, 2nd ed. Addison-Wesley, Reading, MA. MR1397498
- [40] GREENE, C., NIJENHUIS, A. and WILF, H. S. (1984). Another probabilistic method in the theory of Young tableaux. *J. Combin. Theory Ser. A* **37** 127–135. MR0757611 [https://doi.org/10.1016/0097-3165\(84\)90065-7](https://doi.org/10.1016/0097-3165(84)90065-7)
- [41] HAN, G.-N. (2010). New hook length formulas for binary trees. *Combinatorica* **30** 253–256. MR2676840 <https://doi.org/10.1007/s00493-010-2503-5>
- [42] HWANG, H.-K., KUBA, M. and PANHOLZER, A. (2007). Analysis of some exactly solvable diminishing urn models. In *Proceedings of FPSAC'2007 (Formal Power Series and Algebraic Combinatorics)*. Nankai Univ., Tianjin.
- [43] JANSON, S. (2004). Functional limit theorems for multitype branching processes and generalized Pólya urns. *Stochastic Process. Appl.* **110** 177–245. MR2040966 <https://doi.org/10.1016/j.spa.2003.12.002>
- [44] JANSON, S. (2005). Asymptotic degree distribution in random recursive trees. *Random Structures Algorithms* **26** 69–83. MR2116576 <https://doi.org/10.1002/rsa.20046>
- [45] JANSON, S. (2006). Limit theorems for triangular urn schemes. *Probab. Theory Related Fields* **134** 417–452. MR2226887 <https://doi.org/10.1007/s00440-005-0442-7>
- [46] JANSON, S. (2007). Brownian excursion area, Wright's constants in graph enumeration, and other Brownian areas. *Probab. Surv.* **4** 80–145. MR2318402 <https://doi.org/10.1214/07-PS104>
- [47] JANSON, S. (2010). Moments of gamma type and the Brownian supremum process area. *Probab. Surv.* **7** 1–52. MR2645216 <https://doi.org/10.1214/10-PS160>
- [48] JOHANSSON, K. and NORDENSTAM, E. (2006). Eigenvalues of GUE minors. *Electron. J. Probab.* **11** 1342–1371. MR2268547 <https://doi.org/10.1214/EJP.v11-370>
- [49] KAHANE, J.-P. (1960). Propriétés locales des fonctions à séries de Fourier aléatoires. *Studia Math.* **19** 1–25. MR0117506 <https://doi.org/10.4064/sm-19-1-1-25>

- [50] KAUSERS, M. and PAULE, P. (2011). *The Concrete Tetrahedron: Symbolic Sums, Recurrence Equations, Generating Functions, Asymptotic Estimates. Texts and Monographs in Symbolic Computation*. Springer, Vienna. MR2768529 <https://doi.org/10.1007/978-3-7091-0445-3>
- [51] KENYON, R. (2001). Dominos and the Gaussian free field. *Ann. Probab.* **29** 1128–1137. MR1872739 <https://doi.org/10.1214/aop/1015345599>
- [52] KEROV, S. V. (1993). Transition probabilities of continual Young diagrams and the Markov moment problem. *Funct. Anal. Appl.* **27** 104–117. <https://doi.org/10.1007/BF01085981>
- [53] KHODABIN, M. and AHMADABADI, A. (2010). Some properties of generalized gamma distribution. *Math. Sci.* **4** 9–27. MR2673499
- [54] KUBA, M. and MAHMOUD, H. M. (2017). Two-color balanced affine urn models with multiple drawings. *Adv. in Appl. Math.* **90** 1–26. MR3666709 <https://doi.org/10.1016/j.aam.2017.04.004>
- [55] KUBA, M. and PANHOLZER, A. (2016). Combinatorial families of multilabelled increasing trees and hook-length formulas. *Discrete Math.* **339** 227–254. MR3404485 <https://doi.org/10.1016/j.disc.2015.08.010>
- [56] KUBA, M. and SULZBACH, H. (2017). On martingale tail sums in affine two-color urn models with multiple drawings. *J. Appl. Probab.* **54** 96–117. MR3632608 <https://doi.org/10.1017/jpr.2016.89>
- [57] LAH, I. (1954). A new kind of numbers and its application in the actuarial mathematics. *Bol. Inst. Dos Actuár. Portugueses* **9** 7–15.
- [58] LASMAR, N., MAILLER, C. and SELMI, O. (2018). Multiple drawing multi-colour urns by stochastic approximation. *J. Appl. Probab.* **55** 254–281. MR3780393 <https://doi.org/10.1017/jpr.2018.16>
- [59] LINUSSON, S., POTKA, S. and SULZGRUBER, R. (2018). On random shifted standard Young tableaux and 132-avoiding sorting networks. Available at [arXiv:1804.01795](https://arxiv.org/abs/1804.01795).
- [60] LOGAN, B. F. and SHEPP, L. A. (1977). A variational problem for random Young tableaux. *Adv. Math.* **26** 206–222. MR1417317 [https://doi.org/10.1016/0001-8708\(77\)90030-5](https://doi.org/10.1016/0001-8708(77)90030-5)
- [61] MACDONALD, I. G. (2015). *Symmetric Functions and Hall Polynomials*, 2nd ed. *Oxford Classic Texts in the Physical Sciences*. Clarendon, Oxford. With contribution by A. V. Zelevinsky and a foreword by Richard Stanley. Reprint of the 2008 paperback edition [MR1354144]. MR3443860
- [62] MAHMOUD, H. M. (2009). *Pólya Urn Models. Texts in Statistical Science Series*. CRC Press, Boca Raton, FL. MR2435823
- [63] MARCHAL, P. (2016). Rectangular Young tableaux and the Jacobi ensemble. *Discrete Math. Theor. Comput. Sci. Proc.* **BC** 839–850.
- [64] MARCHAL, P. (2018). The density method for permutations with prescribed descents. In *GASCom 2018, CEUR Workshop Proceedings* **2113** 179–186.
- [65] MCKAY, B. D., MORSE, J. and WILF, H. S. (2002). The distributions of the entries of Young tableaux. *J. Combin. Theory Ser. A* **97** 117–128. MR1879130 <https://doi.org/10.1006/jcta.2001.3200>
- [66] MORALES, A. H., PAK, I. and PANOVA, G. (2019). Hook formulas for skew shapes III. Multivariate and product formulas. *Algebraic Combin.* **2** 815–861. MR4023568
- [67] MORCRETTE, B. and MAHMOUD, H. M. (2012). Exactly solvable balanced tenable urns with random entries via the analytic methodology. In *23rd Intern. Meeting on Probabilistic, Combinatorial, and Asymptotic Methods for the Analysis of Algorithms (AofA'12). Discrete Math. Theor. Comput. Sci. Proc., AQ* 219–232. Assoc. Discrete Math. Theor. Comput. Sci., Nancy. MR2957333
- [68] OLVER, F. W. J., LOZIER, D. W., BOISVERT, R. F. and CLARK, C. W., eds. (2010). *NIST Handbook of Mathematical Functions*. U.S. Dept. Commerce, National Institute of Standards and Technology. See also the [NIST Digital Library of Mathematical Functions](https://www.nist.gov/special-publications/nist-sp-480).
- [69] PAK, I. (2001/02). Hook length formula and geometric combinatorics. *Sém. Lothar. Combin.* **46** Art. B46f, 13. MR1877632
- [70] PEKÖZ, E. A., RÖLLIN, A. and ROSS, N. (2016). Generalized gamma approximation with rates for urns, walks and trees. *Ann. Probab.* **44** 1776–1816. MR3502594 <https://doi.org/10.1214/15-AOP1010>
- [71] PETKOVSĚK, M., WILF, H. S. and ZEILBERGER, D. (1996). *A = B*. AK Peters, Wellesley.
- [72] PETROV, L. (2015). Asymptotics of uniformly random lozenge tilings of polygons. Gaussian free field. *Ann. Probab.* **43** 1–43. MR3298467 <https://doi.org/10.1214/12-AOP823>
- [73] PITTEL, B. and ROMIK, D. (2007). Limit shapes for random square Young tableaux. *Adv. in Appl. Math.* **38** 164–209. MR2290809 <https://doi.org/10.1016/j.aam.2005.12.005>
- [74] PÓLYA, G. (1930). Sur quelques points de la théorie des probabilités. *Ann. Inst. Henri Poincaré* **1** 117–161. MR1507985
- [75] POLYA, G. (2014). *How to Solve It: A New Aspect of Mathematical Method. Princeton Science Library*. Princeton Univ. Press, Princeton, NJ. With a foreword by John H. Conway. Reprint of the 1957 second edition [MR2183670]. MR3289212
- [76] PRUDNIKOV, A. P., BRYCHKOV, Y. A. and MARICHEV, O. I. (1992). *Integrals and Series. Vol. 4: Direct Laplace Transforms*. Gordon & Breach, New York.

- [77] RIORDAN, J. (2002). *An Introduction to Combinatorial Analysis*. Dover, Mineola, NY. Reprint of the 1958 original [Wiley, New York; MR0096594 (20 #3077)]. MR1949650
- [78] RIVEST, R. L. (2018). Bayesian tabulation audits: Explained and extended. Available at [arXiv:1801.00528](https://arxiv.org/abs/1801.00528).
- [79] ROMIK, D. (2004). Explicit formulas for hook walks on continual Young diagrams. *Adv. in Appl. Math.* **32** 625–654. MR2053837 [https://doi.org/10.1016/S0196-8858\(03\)00096-4](https://doi.org/10.1016/S0196-8858(03)00096-4)
- [80] ROMIK, D. (2012). Arctic circles, domino tilings and square Young tableaux. *Ann. Probab.* **40** 611–647. MR2952086 <https://doi.org/10.1214/10-AOP628>
- [81] ROMIK, D. (2015). *The Surprising Mathematics of Longest Increasing Subsequences*. Institute of Mathematical Statistics Textbooks **4**. Cambridge Univ. Press, New York. MR3468738
- [82] SAGAN, B. E. and YEH, Y. N. (1989). Probabilistic algorithms for trees. *Fibonacci Quart.* **27** 201–208. MR1002062
- [83] SALVY, B. and ZIMMERMANN, P. (1994). Gfun: A Maple package for the manipulation of generating and holonomic functions in one variable. *ACM Trans. Math. Software* **20** 163–177. <https://doi.org/10.1145/178365.178368>
- [84] SÉNIZERGUES, D. (2019). Geometry of weighted recursive and affine preferential attachment trees. Available at [arXiv:1904.07115](https://arxiv.org/abs/1904.07115).
- [85] SHEFFIELD, S. (2005). Random surfaces. *Astérisque* **304** vi+175. MR2251117
- [86] ŚNIADY, P. (2014). Robinson–Schensted–Knuth algorithm, jeu de taquin, and Kerov–Vershik measures on infinite tableaux. *SIAM J. Discrete Math.* **28** 598–630. MR3190750 <https://doi.org/10.1137/130930169>
- [87] STACY, E. W. (1962). A generalization of the gamma distribution. *Ann. Math. Stat.* **33** 1187–1192. MR0143277 <https://doi.org/10.1214/aoms/1177704481>
- [88] STANLEY, R. P. (1986). Two poset polytopes. *Discrete Comput. Geom.* **1** 9–23. MR0824105 <https://doi.org/10.1007/BF02187680>
- [89] STANLEY, R. P. (1999). *Enumerative Combinatorics. Vol. 2*. Cambridge Studies in Advanced Mathematics **62**. Cambridge Univ. Press, Cambridge. MR1676282 <https://doi.org/10.1017/CBO9780511609589>
- [90] VERSHIK, A. M. (2001). Randomization of algebra and algebraization of probability—an attempt at prediction. In *Mathematics Unlimited—2001 and Beyond* 1157–1166. Springer, Berlin. MR1852209
- [91] VERŠIK, A. M. and KEROV, S. V. (1977). Asymptotic behavior of the Plancherel measure of the symmetric group and the limit form of Young tableaux. *Dokl. Akad. Nauk SSSR* **233** 1024–1027. MR0480398
- [92] WALL, H. S. (1948). *Analytic Theory of Continued Fractions*. Van Nostrand, New York, NY. MR0025596
- [93] WALLNER, M. (2020). A half-normal distribution scheme for generating functions. *European J. Combin.* **87** 103–138. MR4090824 <https://doi.org/10.1016/j.ejc.2020.103138>

Latticepathology and Symmetric Functions (Extended Abstract)

Cyril Banderier 

Université Paris 13, LIPN, UMR CNRS 7030, France

<https://lipn.fr/~banderier>

Marie-Louise Lackner 

Christian Doppler Laboratory for Artificial Intelligence and Optimization for Planning and Scheduling, DBAI, TU Wien, Austria

<http://marielouise.lackner.xyz>

Michael Wallner 

Université de Bordeaux, LaBRI, UMR CNRS 5800, France

Institute for Discrete Mathematics and Geometry, TU Wien, Austria

<https://dmg.tuwien.ac.at/mwallner>

Abstract

In this article, we revisit and extend a list of formulas based on lattice path surgery: cut-and-paste methods, factorizations, the kernel method, etc. For this purpose, we focus on the natural model of directed lattice paths (also called generalized Dyck paths). We introduce the notion of prime walks, which appear to be the key structure to get natural decompositions of excursions, meanders, bridges, directly leading to the associated context-free grammars. This allows us to give bijective proofs of bivariate versions of Spitzer/Sparre Andersen/Wiener–Hopf formulas, thus capturing joint distributions. We also show that each of the fundamental families of symmetric polynomials corresponds to a lattice path generating function, and that these symmetric polynomials are accordingly needed to express the asymptotic enumeration of these paths and some parameters of limit laws. En passant, we give two other small results which have their own interest for folklore conjectures of lattice paths (non-analyticity of the small roots in the kernel method, and universal positivity of the variability condition occurring in many Gaussian limit law schemes).

2012 ACM Subject Classification Mathematics of computing → Generating functions; Mathematics of computing → Distribution functions; Theory of computation → Random walks and Markov chains; Theory of computation → Grammars and context-free languages

Keywords and phrases Lattice path, generating function, symmetric function, algebraic function, kernel method, context-free grammar, Sparre Andersen formula, Spitzer’s identity, Wiener–Hopf factorization

Digital Object Identifier 10.4230/LIPIcs.AofA.2020.2

Funding This work was initiated during the sojourn of Marie-Louise Lackner and Michael Wallner at the University of Paris Nord, via a Franco-Austrian “Amadeus” project and via a MathStic funding. The subsequent part of this collaboration was funded by the Erwin Schrödinger Fellowship of the Austrian Science Fund (FWF): J 4162-N35.

Acknowledgements We thank our referees for their careful reading. In this period of worldwide lockdown due to the COVID19 pandemic, let us also thank Klaus Hulek, Barbara Strazabosco, and the staff from zbMATH who implemented some technical solution so that we can have home access to this wonderful database.



© Cyril Banderier, Marie-Louise Lackner, and Michael Wallner;
licensed under Creative Commons License CC-BY

31st International Conference on Probabilistic, Combinatorial and Asymptotic Methods for the Analysis of Algorithms (AofA 2020).

Editors: Michael Drmota and Clemens Heuberger; Article No. 2; pp. 2:1–2:16



Leibniz International Proceedings in Informatics

Schloss Dagstuhl – Leibniz-Zentrum für Informatik, Dagstuhl Publishing, Germany

1 Introduction and definitions

The recursive nature of lattice paths makes them amenable to context-free grammar techniques; their geometric nature makes them amenable to cut-and-paste bijections; their step-by-step nature makes them amenable to functional equations solvable by the kernel method (see e.g. [3–5, 8–11, 16, 30, 32, 35] for many applications of these ideas). We present in a unified way some consequences of these observations in Section 2 on context-free grammars (where we introduce the fruitful notion of prime walks) and in Section 3 on Spitzer and Wiener–Hopf identities. Additionally, we give new connections with symmetric functions in Section 4, see Table 2. All of this allows us to greatly extend the enumerative formulas and asymptotics given in [4], and gives us access to some limit laws, as shown in Section 5.

► **Definition 1** (Jumps and lattice paths). *A step set \mathcal{S} is a finite subset of \mathbb{Z} . The elements of \mathcal{S} are called steps or jumps. An n -step lattice path or walk ω is a sequence $(j_1, \dots, j_n) \in \mathcal{S}^n$. The length $|\omega|$ of this lattice path is its number n of jumps.*

Such sequences are one-dimensional objects. Geometrically, they can be interpreted as two-dimensional objects which justifies the name *lattice path*. Indeed, (j_1, \dots, j_n) may be seen as a sequence of points $(\omega_0, \omega_1, \dots, \omega_n)$, where ω_0 is the starting point and $\omega_i - \omega_{i-1} = (1, j_i)$ for $i = 1, \dots, n$. Except when mentioned differently, the starting point ω_0 of these lattice paths is $(0, 0)$.

Let $\sigma_k := \sum_{i=1}^k j_i$ be the partial sum of the first k steps of the walk ω . We define the *height* or *maximum* of ω as $\max_k \sigma_k$, and the *final altitude* of ω as σ_n . For example, the first walk in Table 1 has height 3 and final altitude 1. Table 1 and Figure 1 are also illustrating the four following classical types of paths:

► **Definition 2** (Excursions, arches, meanders, bridges).

- *Excursions are paths never going below the x -axis and ending on the x -axis;*
- *Arches are excursions that only touch the x -axis twice: at the beginning and at the end;*
- *Meanders are prefixes of excursions, i.e., paths never going below the x -axis;*
- *Bridges are paths ending on the x -axis (allowed to cross the x -axis any number of times).*

Let $c := -\min \mathcal{S}$ be the maximal negative step, and let $d := \max \mathcal{S}$ be the maximal positive step. To avoid trivial cases we assume $\min \mathcal{S} < 0 < \max \mathcal{S}$. Furthermore we associate to each step $i \in \mathcal{S}$ a weight s_i . These weights s_i are typically real numbers, like probabilities or non-negative integers encoding the multiplicity of each jump. The weight of a lattice path is the product of the weights of its steps. Then we associate to this set of steps the following *step polynomial*:

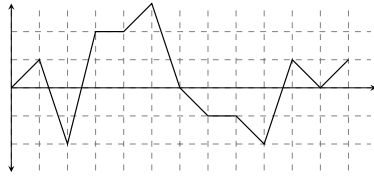
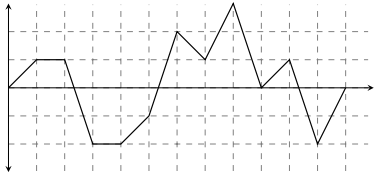
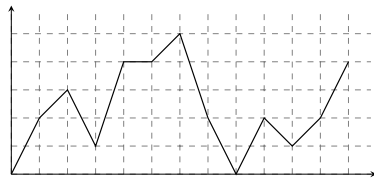
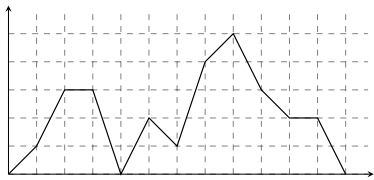
$$S(u) = \sum_{i=-c}^d s_i u^i.$$

The generating functions of directed lattice paths can be expressed in terms of the roots of the *kernel equation*

$$1 - zS(u) = 0. \tag{1}$$

More precisely, this equation has $c + d$ solutions in u . The *small roots* $u_i(z)$, for $i = 1, \dots, c$, are the c solutions with the property $u_i(z) \sim 0$ for $z \sim 0$. The remaining d solutions are called *large roots* as they satisfy $|v_i(z)| \sim +\infty$ for $z \sim 0$. The generating functions of the four classical types of lattice paths introduced above are shown in Table 1.

■ **Table 1** The four types of paths: walks, bridges, meanders and excursions, and the corresponding generating functions for directed lattice paths. The functions $u_i(z)$ for $i = 1, \dots, c$ are the roots of the kernel equation $1 - zS(u) = 0$ such that $\lim_{z \rightarrow 0} u_i(z) = 0$.

	ending anywhere	ending at 0
unconstrained (on \mathbb{Z})	 <p>walk/path (\mathcal{W})</p> $W(z) = \frac{1}{1-zS(1)}$	 <p>bridge (\mathcal{B})</p> $B(z) = z \sum_{i=1}^c \frac{u'_i(z)}{u_i(z)}$
constrained (on \mathbb{Z})	 <p>meander (\mathcal{M})</p> $M(z) = \frac{1}{1-zS(1)} \prod_{i=1}^c (1 - u_i(z))$	 <p>excursion (\mathcal{E})</p> $E(z) = \frac{(-1)^{c-1}}{s-cz} \prod_{i=1}^c u_i(z)$

These results follow from the expression for the bivariate generating function $M(z, u)$ of meanders. Indeed, let $m_{n,k}$ be the number of meanders of length n going from altitude 0 to altitude k , then we have

$$M(z, u) = \sum_k M_k(z) u^k = \sum_{n,k \geq 0} m_{n,k} z^n u^k = \frac{\prod_{i=1}^c (u - u_i(z))}{u^c (1 - zS(u))}. \tag{2}$$

This last formula is obtained by the kernel method: this method starts with the functional equation which mimics the recursive definition of meanders, namely $M(z, u) = 1 + zS(u)M(z, u) - \{u^{<0}\}zS(u)M(z, u)$ (where $\{u^{<0}\}$ extracts the monomials of negative degree in u , as one does not want to allow a jump going below the x -axis). Note that $\{u^{<0}\}S(u)M(z, u)$ is a linear combination (with coefficients in u and z) of c unknowns, namely $M_0(z), \dots, M_{c-1}(z)$. Then, substituting $u = u_i(z)$ (each of the c small roots of (1)) into this system leads to the closed form (2). This also directly gives the generating function of excursions $E(z) := M(z, 0)$ and meanders $M(z) := M(z, 1)$. The generating function for bridges follows from the link given in Theorem 8 hereafter. See [4, 10] for more details.

It should be stressed that the closed forms of Table 1 grant easy access to the asymptotics of all these classes of paths after the localization of the dominant singularities:

► **Theorem 3** (Radius of convergence of excursions, bridges, and meanders [4]). *The radius of convergence of excursions $E(z) := M(z, 0)$ and of bridges $B(z)$ is given by $\rho = 1/S(\tau)$, where τ is the smallest positive real number such that $S'(\tau) = 0$. For meanders $M(z) := M(z, 1)$, the radius depends on the drift $\delta := S'(1)$: It is ρ if $\delta < 0$ and it is $1/S(1)$ if $\delta \geq 0$.*

We shall make use of all these facts in Section 5 on asymptotics and limit laws, but, before to do so, we now present several combinatorial decompositions which will be the key to get these new asymptotic results.

2 Prime walks and context-free grammars

Context-free grammars are a powerful tool to tackle problems related to directed lattice paths (we refer to [27] for a detailed presentation of grammar techniques). In this section, we introduce some key families of lattice paths (generalized arches, prime walks), which will also be used in the next section. Illustrating the philosophy of “latticepathology”, these new families allow short concise visual proofs based on lattice path surgery: we give grammars generating the most fundamental classes of lattice paths (excursions, bridges, meanders); this generalizes and unifies results from [11, 16, 32, 35].

All our grammars are non-ambiguous: there is only one way to generate each lattice path. They require the introduction of two classes of paths: *generalized arches* and *prime walks*.

► **Definition 4** (Generalized arches). *An arch from i to j is a walk starting at altitude i ending at altitude j and staying always strictly above altitude $\max(i, j)$ except for its first and final position; see Figure 1.*

An important consequence of this definition is that generalized arches cannot have an excursion as left or right factor. Note that an arch from i to j can be considered as an arch from 0 to $j - i$. This justifies that we now focus on arches starting at 0. Let \mathcal{A}_k be the class of arches from 0 to k ; see Figure 1. Following the tradition of several authors, we refer to *arches* (omitting the start and end point) as arches from 0 to 0, see e.g. [4]. Thus, an excursion is clearly a sequence of arches.

► **Definition 5** (Prime walks). *Given a set of steps \mathcal{S} , with $d = \max \mathcal{S}$, the set \mathcal{P} of prime walks is defined as the following sets of arches*

$$\mathcal{P} = \bigcup_{k=0}^d \mathcal{A}_k.$$

These prime walks are the key to get short proofs for the decomposition of several constrained classes of paths (Section 3) and for meanders (Theorem 6). Note that these decompositions hold for any set of jumps: it is straightforward to extend them to multiplicities (jumps with different colours) or even to an infinite set of jumps.

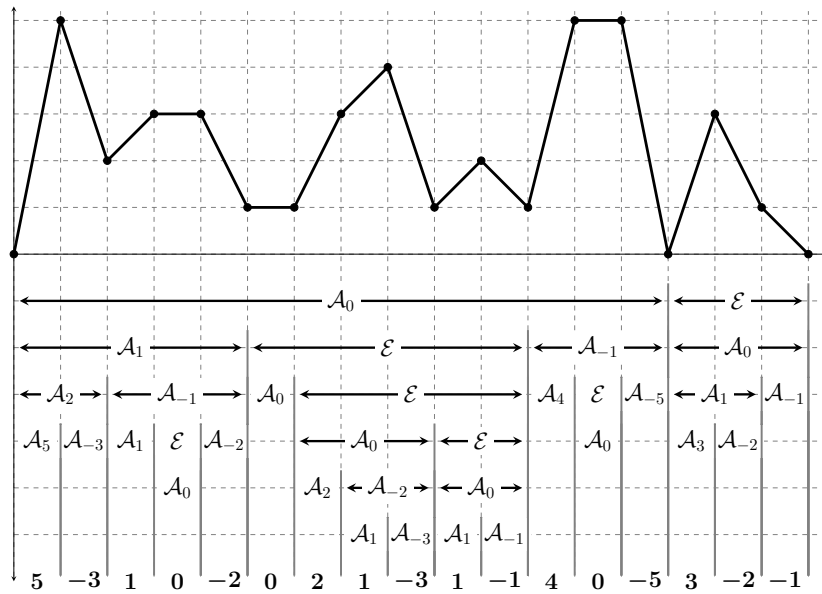
► **Theorem 6** (The universal context-free grammar for directed lattice paths). *Meanders and excursions are generated by the following grammar:*

$$\begin{aligned} \mathcal{M} &\rightarrow \varepsilon + \mathcal{P}\mathcal{M} && \text{(meanders),} \\ \mathcal{E} &\rightarrow \varepsilon + \mathcal{A}_0\mathcal{E} && \text{(excursions),} \end{aligned}$$

which can be rephrased as “meanders are sequences of prime walks”: $\mathcal{M} = \text{Seq}\left(\sum_{k=0}^d \mathcal{A}_k\right)$ and “excursions are sequences of arches”: $\mathcal{E} = \text{Seq}(\mathcal{A}_0)$, where the arches \mathcal{A}_k from 0 to k are generated by

$$\begin{aligned} \mathcal{A}_k &\rightarrow k + \sum_{j=k+1}^d \mathcal{A}_j \mathcal{E} \mathcal{A}_{k-j} && \text{(arches for } k \geq 0), \\ \mathcal{A}_k &\rightarrow k + \sum_{j=-c}^{k-1} \mathcal{A}_{k-j} \mathcal{E} \mathcal{A}_j && \text{(arches for } k < 0), \end{aligned}$$

with the convention that, in these two rules, the part $\mathcal{A}_k \rightarrow k$ is omitted whenever $k \notin \mathcal{S}$.



■ **Figure 1** Example of our non-ambiguous decomposition of an excursion into generalized arches. Similar decompositions hold for the factorization of meanders into prime walks.

Proof. Let us start with arches \mathcal{A}_k from 0 to $k \geq 0$. (The results for \mathcal{A}_{-k} follow analogously.) For such arches of length > 1 , we cut them at the first and the last time their minimal altitude (not taking end points into account) is attained. The first factor goes from 0 to j and stays in-between always strictly above j , and therefore is given by \mathcal{A}_j . The second factor is a (possibly empty) excursion. The last factor is an arch from j to k given by \mathcal{A}_{k-j} . This gives $\mathcal{A}_k = \mathcal{A}_j \mathcal{E} \mathcal{A}_{k-j}$. From this, it is immediate to get the grammar for excursions, as they are a sequence of arches \mathcal{A}_0 ; thus $\mathcal{E} = \varepsilon + \mathcal{A}_0 \mathcal{E}$.

Now take any meander and cut it at the last time it touches altitude 0 . The first part is a (possibly empty) sequence of arches. We cut the second part at the first point where its minimal altitude > 0 is attained. The remaining part is again a meander. This gives the factorization $\mathcal{M} = \mathcal{E} + \sum_{k=1}^d \mathcal{E} \mathcal{A}_k \mathcal{M}$, which is in turn equivalent to $\mathcal{M} = \text{seq}(\mathcal{P})$.

All these decompositions are clearly 1-to-1 correspondences, as exemplified in Figure 1. ◀

We end this section with the grammar of bridges. It uses another class of walks: the negative arches from 0 to k , denoted by $\bar{\mathcal{A}}_k$. These stay always strictly below $\min(0, k)$. Their grammar is just the mirror of the one for \mathcal{A}_k given in Theorem 6.

► **Theorem 7.** *Bridges $\mathcal{B} = \mathcal{B}_0$ are generated by the following grammar:*

$$\mathcal{B}_0 \rightarrow \varepsilon + \sum_{k \in \mathcal{S}} k \mathcal{B}_{-k},$$

where \mathcal{B}_k stands for the “bridges ending at k ”, i.e. walks on \mathbb{Z} from 0 to k , given by

$$\begin{aligned} \mathcal{B}_k &\rightarrow \sum_{j=-c}^0 \mathcal{A}_j \mathcal{B}_{k-j} && (\text{if } k > 0), \\ \mathcal{B}_k &\rightarrow \sum_{j=0}^d \bar{\mathcal{A}}_j \mathcal{B}_{k-j} && (\text{if } k < 0). \end{aligned}$$

In the next section we present some applications of our decompositions (obtained above in the framework of the non-commutative world of words) to famous identities from probability theory (stated below in the framework of the commutative world of generating functions).

3 Latticepathology and surgery of paths

The decompositions of lattice paths mentioned in the previous section find application in the bivariate versions of the Spitzer/Sparre Andersen¹/Wiener–Hopf formulas [2, 25, 26, 34, 37]. It gives for free elegant short proofs for these fundamental results which were definitively missing in [4], neatly illustrating the latticepathology philosophy!

► **Theorem 8** (Bivariate version of Spitzer/Sparre Andersen's identities). *The generating function $W^+(z, u) = \sum_n w_n^+(u)z^n$ of walks on \mathbb{Z} ending at an altitude ≥ 0 and the generating function $M(z, u) = \sum_n m_n(u)z^n$ of meanders (where u encodes the final altitude and z encodes the length of the lattice path) are related by the formulas*

$$W^+(z, u) = 1 + z \frac{M'(z, u)}{M(z, u)} \quad \text{or, equivalently,} \quad (3a)$$

$$M(z, u) = \exp\left(\int_0^z \frac{W^+(t, u) - 1}{t} dt\right) = \exp\left(\sum_{n \geq 1} \frac{w_n^+(u)}{n} t^n\right). \quad (3b)$$

Proof (Sketch). We give a bijective proof. It consists in factorizing any non-empty walk ω ending at an altitude ≥ 0 into 3 factors: $\omega = \phi_1.m.\phi_2$ where m is the longest meander starting at the first minimum of the walk and such that $\phi_2.\phi_1$ is a prime walk (pointed, in order to remember where to split it); see Figure 2. The fact that this factorization exists and is unique follows from the positivity of ω and from the grammar for meanders from Theorem 6. This decomposition directly keeps track of the last altitude of each of its factors:

$$W^+(z, u) - 1 = M(z, u)z \frac{\partial}{\partial z} \left(1 - \frac{1}{M(z, u)}\right). \quad \blacktriangleleft$$

► **Remark 9** (Spitzer/Sparre Andersen's identities for excursions and bridges). Extracting the constant coefficient with respect to u in the above identities leads to the following links between bridges and excursions (these specific identities were also proven in [4]).

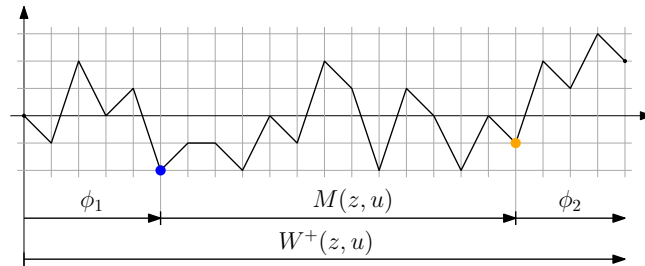
$$B(z) = 1 + E(z)z \frac{\partial}{\partial z} \left(1 - \frac{1}{E(z)}\right) = 1 + z \frac{E'(z)}{E(z)} \quad \text{or, equivalently,} \quad (4a)$$

$$E(z) = \exp\left(\int_0^z \frac{B(t) - 1}{t} dt\right) = \exp\left(\sum_{n \geq 1} \frac{b_n}{n} t^n\right). \quad (4b)$$

Nota bene: Spitzer's formula is often given as a variant of Formula (3b), stated in terms of characteristic functions instead of generating functions, and also keeping track of the height of the path (see e.g. [37, 39, 42]). More generally, in Brownian motion theory, path decompositions are also useful for Vervaat transformations, quantile transforms [13, 33, 40], Ray–Knight theorems for local times and Lamperti, Jeulin, Bougerol, Donati-Martin identities [1, 7, 15, 28].

We now illustrate such approaches with one more important surgery of lattice paths. (This requires the natural classes of positive and negative meanders, see Definition 12 hereafter.)

¹ Funnily, in the literature, this identity of Erik Albrecht Sparre Andersen (Andersen is the family name) is often called the “Sparre Andersen identity”, probably as he was often signing E. Sparre Andersen.



■ **Figure 2** The bijection at the heart of Spitzer/Sparre Andersen identity decomposes a walk $\omega \in \mathcal{W}^+$ into $\omega = \phi_1.m.\phi_2$, where the meander $m \in \mathcal{M}$ starts at the first minimum of ω and ends at the rightmost point such that $\phi_2.\phi_1$ ends at altitude ≥ 0 (and $\phi_2.\phi_1$ is thus a prime walk).

► **Theorem 10** (Bivariate version of Wiener–Hopf formula). *The bivariate generating functions $W_{+h}(z, u)$ and $W_{-h}(z, u)$ of walks on \mathbb{Z} with u marking the positive and negative height (not the altitude!) are related to the bivariate generating functions $M^+(z, u)$ of positive meanders and $M^-(z, u)$ of negative meanders (with u marking the final altitude, see Figure 3):*

$$W_{+h}(z, u) = M^-(z)E(z)M^+(z, u) = -\frac{1}{s_d z} \left(\prod_{j=1}^c \frac{1}{1 - u_j(z)} \right) \left(\prod_{\ell=1}^d \frac{1}{u - v_\ell(z)} \right),$$

$$W_{-h}(z, u) = M^-(z, u)E(z)M^+(z) = -\frac{1}{s_d z} \left(\prod_{j=1}^c \frac{1}{1 - u_j(z)/u} \right) \left(\prod_{\ell=1}^d \frac{1}{1 - v_\ell(z)} \right).$$

This Wiener–Hopf factorization $W = M^-EM^+$ thus gives

$$M^-(z) = \frac{W(z)}{M(z)} = \prod_{j=1}^c \frac{1}{1 - u_j(z)} \quad \text{and} \quad M^+(z) = \frac{M(z)}{E(z)} = \prod_{\ell=1}^d \frac{1}{1 - 1/v_\ell(z)}.$$

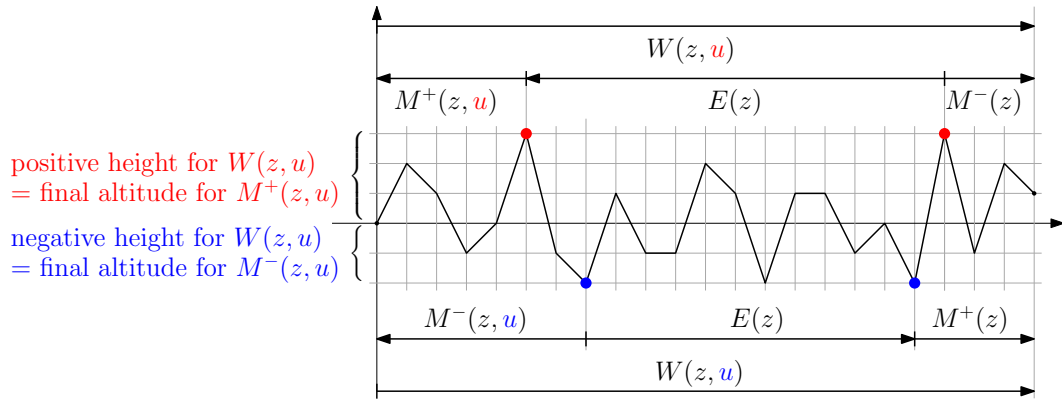
Proof (Sketch). The proof follows from the decomposition illustrated in Figure 3. Cutting at the first and last maxima of the walk gives the factorization $\mathcal{W} = \mathcal{M}^+\mathcal{E}\mathcal{M}^-$, where the positive meander and the excursion are obtained after a 180° rotation, and it is thus clear that the final altitude of this positive meander is the height of the initial walk. Similarly, cutting the walk at its first and last minima gives the factorization $\mathcal{W} = \mathcal{M}^-\mathcal{E}\mathcal{M}^+$. ◀

4 Lattice paths and symmetric functions

Building on the quantities introduced in the previous sections, we now show that three fundamental classes of symmetric polynomials evaluated at the small roots of the kernel have a natural combinatorial interpretation in terms of directed lattice paths. *En passant*, this also gives the generating function of generalized arches. For our main results see Table 2. We first recall the definitions of these symmetric polynomials (see e.g. [38] for more on these objects).

► **Definition 11.** *The complete homogeneous symmetric polynomials h_k of degree k in the d variables x_1, \dots, x_d are defined as*

$$h_k(x_1, \dots, x_d) = \sum_{1 \leq i_1 \leq \dots \leq i_k \leq d} x_{i_1} \cdots x_{i_k}, \quad \text{thus} \quad \sum_{k \geq 0} h_k(x_1, \dots, x_d)u^k = \prod_{i=1}^d \frac{1}{1 - ux_i}. \quad (5)$$



■ **Figure 3** The Wiener–Hopf decomposition of a walk: $\mathcal{W} = \mathcal{M}^- \mathcal{E} \mathcal{M}^+$, a product of a negative meander, an excursion, and a positive meander. See e.g. [25] for the importance of this factorization for lattice path enumeration. It offers a link between two important parameters (height and final altitude): the proof uses a 180° rotation of some of the factors (the ones indicated by a right to left arrow in the picture). The above picture crystallizes the key idea behind the theorems given by Feller in his nice introduction to the Wiener–Hopf factorization [19, Chapter XVIII.3 and XVIII.4]. It also explains why this decomposition holds for Lévy processes, which can be seen as the continuous time and space version of lattice paths, see [31].

The elementary homogeneous symmetric polynomials e_k of degree k in the d variables x_1, \dots, x_d are defined as

$$e_k(x_1, \dots, x_d) = \sum_{1 \leq i_1 < \dots < i_k \leq d} x_{i_1} \cdots x_{i_k}, \quad \text{thus } \sum_{k=0}^c e_k(x_1, \dots, x_d) u^k = \prod_{i=1}^d (1 + ux_i). \quad (6)$$

The power sum homogeneous symmetric polynomials p_k of degree k in the d variables x_1, \dots, x_d are defined as

$$p_k(x_1, \dots, x_d) = \sum_{i=1}^d x_i^k, \quad \text{thus } \sum_{k \geq 0} p_k(x_1, \dots, x_d) u^k = \sum_{i=1}^d \frac{1}{1 - ux_i}. \quad (7)$$

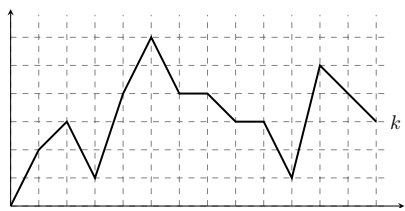
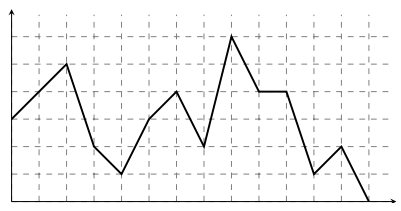
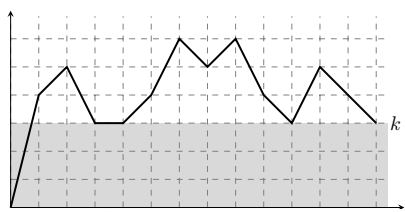
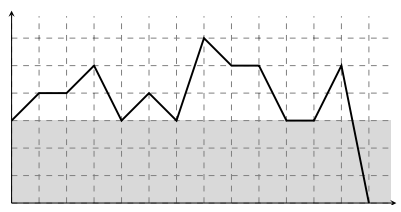
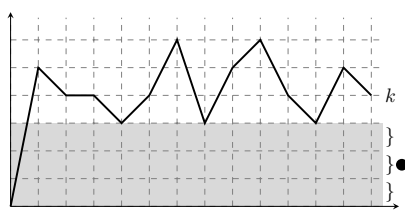
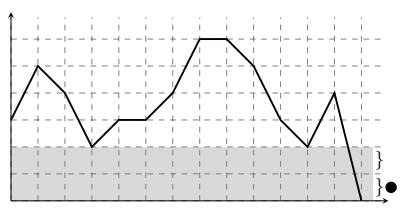
Many variants of directed lattice paths satisfy functional equations which are solvable by the kernel method and lead to formulas involving a quotient of Vandermonde-like determinants, see e.g. [4]. It is thus natural that Schur polynomials intervene, they e.g. play an important role for lattice paths in a strip, see [5, 9]. It is nice that the other symmetric polynomials also have a combinatorial interpretation, as presented in the following table.

Let us now give a more formal definition of the corresponding objects and a proof of the formulas for the associated generating functions.

► **Definition 12.** A positive meander is a path from $\ell \geq 0$ to $k \geq 0$ staying strictly above the x -axis (and possibly touching it at at most one of its end points). The generating function is denoted by $M_{\ell, k}^+(z)$. Negative meanders are defined similarly, with the condition to stay strictly below the x -axis.

In Table 2, we focus on positive meanders from 0 to k and from k to 0. Note that it suffices to consider the paths from 0 to k as by time-reversion they are mapped to each other. In particular, let $u_i(z)$ and $v_j(z)$ be the small and large roots of the initial model. Then, after time-reversion the small roots are $\frac{1}{v_j(z)}$ and the large roots are $\frac{1}{u_i(z)}$. More details are given in the long version.

■ **Table 2** In this article, we show that the fundamental symmetric polynomials (of the complete homogeneous, elementary, and power sum type) are counting families of positive meanders (walks touching the x -axis only at one of the end points and staying always above the x -axis). The functions $v_j(z)$ for $j = 1, \dots, d$ are the roots of the kernel equation $1 - zS(u) = 0$ with $\lim_{z=0} |v_j(z)| = +\infty$, whereas the functions $u_i(z)$ for $i = 1, \dots, c$ are the roots such that $\lim_{z=0} u_i(z) = 0$.

	from 0 to k	from k to 0
positive meander	 $M_{0,k}^+(z) = h_k \left(\frac{1}{v_1(z)}, \dots, \frac{1}{v_d(z)} \right)$	 $M_{k,0}^+(z) = h_k (u_1(z), \dots, u_c(z))$
positive meander avoiding $(0, k)$	 $M_{0,k}^{\geq}(z) = (-1)^{k-1} e_k \left(\frac{1}{v_1(z)}, \dots, \frac{1}{v_d(z)} \right)$	 $M_{k,0}^{\geq}(z) = (-1)^{k-1} e_k (u_1(z), \dots, u_c(z))$
positive meander marked below the minimum	 $M_{0,k}^\bullet(z) = p_k \left(\frac{1}{v_1(z)}, \dots, \frac{1}{v_d(z)} \right)$	 $M_{k,0}^\bullet(z) = p_k (u_1(z), \dots, u_c(z))$

► **Theorem 13** (Generating function of positive meanders).

$$M_{0,k}^+(z) = h_k \left(\frac{1}{v_1(z)}, \dots, \frac{1}{v_d(z)} \right).$$

Proof. Observe that a meander ending at altitude k can be uniquely decomposed into an initial excursion followed by a positive meander from 0 to k . By [4, Theorem 2] their generating function is the coefficient of u^k in $\prod_{j=1}^d \frac{1}{1-u/v_j(z)}$. Consequently, by Equation (5) this is the generating function of the complete homogeneous symmetric polynomials $h_k(1/v_1(z), \dots, 1/v_d(z))$. ◀

This theorem gives a shorter proof of [4, Corollary 3]:

► **Corollary 14.** *The generating function $M_k(z)$ of meanders ending at altitude k are given by*

$$M_k(z) = E(z)h_k \left(\frac{1}{v_1(z)}, \dots, \frac{1}{v_d(z)} \right) = \frac{1}{s_d z} \sum_{\ell=1}^d \left(\prod_{j \neq \ell} \frac{1}{v_j(z) - v_\ell(z)} \right) \frac{1}{v_\ell(z)^{k+1}}.$$

Proof. As in the proof of Theorem 13, we use that positive meanders are classical meanders factored by excursions. Then a partial fraction decomposition of (5) yields the result. ◀

The last class we consider is the one of elementary symmetric polynomials. These are associated to a decorated class of paths.

► **Definition 15.** *A positive meander avoiding a strip of width k is a positive meander from 0 to k that always stays above any point of altitude $j < k$ except for its start point. The generating function is denoted by $M_{0,k}^{\geq}(z)$.*

► **Theorem 16** (Positive meanders avoiding the strip $[0, k]$).

$$M_{0,k}^{\geq}(z) = (-1)^{k-1} e_k \left(\frac{1}{v_1(z)}, \dots, \frac{1}{v_d(z)} \right).$$

Proof. We proceed by induction on k . The base case $k = 1$ holds due to $M_{0,1}^{\geq}(z) = M_{0,1}^+(z) = 1/v_1(z) + \dots + 1/v_d(z)$. Next assume the claim holds for $M_{0,1}^{\geq}(z), \dots, M_{0,k-1}^{\geq}(z)$.

Take an arbitrary positive meander from 0 to k . Either it is a positive meander avoiding the strip of width k , or at least one of its lattice points has an altitude smaller than k .

Let $0 < i < k$ be the altitude of the last step below altitude k . Then the path can be uniquely decomposed into an initial part from altitude 0 to this altitude i and a part from this point to the end. Note that by the construction the initial part starts at altitude 0 and then always stays above the x -axis, whereas the last part avoids a strip of width $k - i$. In terms of generating functions this gives

$$M_{0,k}^{\geq}(z) = M_{0,k}^+(z) - \sum_{i=1}^{k-1} M_{0,i}^+(z) M_{0,k-i}^{\geq}(z).$$

Inserting the known expressions, we get

$$M_{0,k}^{\geq}(z) = \sum_{i=1}^k (-1)^{k-i} e_{k-i} \left(\frac{1}{v_1}, \dots, \frac{1}{v_d} \right) h_i \left(\frac{1}{v_1}, \dots, \frac{1}{v_d} \right) = (-1)^{k-1} e_k \left(\frac{1}{v_1}, \dots, \frac{1}{v_d} \right),$$

thanks to the fundamental involution relation [38, Equation (7.13)] between elementary symmetric polynomials and complete homogeneous symmetric polynomials. ◀

► **Corollary 17.** *The generating functions of generalized arches (as introduced in Definition 4) satisfy (for $k > 0$)*

$$A_k = \frac{(-1)^{k-c} s_{-c} z}{u_1(z) \cdots u_c(z)} e_k \left(\frac{1}{v_1(z)}, \dots, \frac{1}{v_d(z)} \right),$$

$$A_{-k} = \frac{(-1)^{k-c} s_{-c} z}{u_1(z) \cdots u_c(z)} e_k(u_1(z), \dots, u_c(z)).$$

Proof. This follows from $A_k = M_{0,k}^{\geq}/E$ and $A_{-k} = M_{k,0}^{\geq}/E$. ◀

We end our discussion with a third class of positive meanders.

► **Definition 18.** *A positive meanders marked below the minimum is a positive meander with an additional marker in $\{1, \dots, m\}$ where m is its minimal positive altitude. The generating function for such paths from 0 to k is denoted by $M_{0,k}^{\bullet}(z)$.*

For example it is immediate that $M_{0,1}^{\bullet}(z) = M_{0,1}^{\geq}(z) = M_{0,1}^+(z)$ as the only restriction is to avoid the x -axis. Furthermore, $M_{0,0}^{\bullet}(z) = 0$ while $M_{0,0}^{\geq}(z) = M_{0,0}^+(z) = 1$.

► **Theorem 19** (Positive meanders marked below the minimum).

$$M_{0,k}^\bullet(z) = p_k \left(\frac{1}{v_1(z)}, \dots, \frac{1}{v_d(z)} \right).$$

Proof (Sketch). Every path from 0 to k has to touch at least one of the altitudes $1, \dots, d$, as the largest possible up step is $+d$. We decompose any positive meander from 0 to k into two parts by cutting at the unique last positive minimum m . The first part is an arch avoiding the strip of width m , whereas the second part is a positive meander from m to k . Translating this decomposition into generating functions, we get

$$M_{0,k}^\bullet(z) = \sum_{m=1}^d m M_{0,m}^{\geq}(z) M_{0,k-m}^+(z),$$

where the factor m encodes the m possible ways to put a mark below the minimum, see Definition 18. Note that $M_{0,k}^{\geq}(z) = 0$ for $k > d$. Thus, by Theorems 13 and 16 we get

$$\sum_{k \geq 1} M_{0,k}^\bullet(z) u^k = \left(u \frac{\partial}{\partial u} \sum_{j \geq 0} M_{0,j}^{\geq}(z) u^j \right) \left(\sum_{i \geq 0} M_{0,i}^+(z) u^i \right) = \sum_{i=1}^d \frac{u/v_i(z)}{1 - u/v_i(z)}.$$

By Equation (7) this proves the claim. ◀

5 Asymptotics and limit laws

We end the discussion on the symmetric polynomial expressions by deriving their respective asymptotics: this allows us to revisit some limit laws in which the appearance of symmetric polynomials was so far unrecognized.

We only consider *aperiodic* step sets \mathcal{S} , which are defined by $\gcd\{|i - j| : i, j \in \mathcal{S}\} = 1$. For the treatment of periodic step sets see [6]. We only treat paths from k to 0, as the formulas are a bit simpler. The results for paths from 0 to k follow in an analogous fashion. The principal small branch $u_1(z)$ and the principal large branch $v_1(z)$ are defined by the property that they are real positive for near $0+$ and meet at $z = \rho$; see [4].

In the next theorem we give the asymptotics of our three classes of positive meanders.

► **Theorem 20.** *Consider an aperiodic step set \mathcal{S} . Let τ be the structural constant determined by $S'(\tau) = 0$, $\tau > 0$. For the different variants of positive meanders given in Table 2, the number of paths from k to 0 of size n has the following asymptotic expansions*

$$[z^n] M_{k,0}^+(z) = \alpha_1 \frac{S(\tau)^n}{2\sqrt{\pi n^3}} \left(1 + \mathcal{O}\left(\frac{1}{n}\right) \right), \quad \alpha_1 = \frac{\partial e_k}{\partial x_1}(\tau, u_2(\rho), \dots, u_c(\rho)).$$

The number of positive meanders avoiding $(0, k)$ from k to 0 of size n satisfies

$$[z^n] M_{k,0}^{\geq}(z) = \alpha_2 \frac{S(\tau)^n}{2\sqrt{\pi n^3}} \left(1 + \mathcal{O}\left(\frac{1}{n}\right) \right), \quad \alpha_2 = \frac{\partial h_k}{\partial x_1}(\tau, u_2(\rho), \dots, u_c(\rho)).$$

The number of positive meanders marked below the minimum from k to 0 of size n satisfies

$$[z^n] M_{k,0}^\bullet(z) = \alpha_3 \frac{S(\tau)^n}{2\sqrt{\pi n^3}} \left(1 + \mathcal{O}\left(\frac{1}{n}\right) \right), \quad \alpha_3 = \frac{\partial p_k}{\partial x_1}(\tau, u_2(\rho), \dots, u_c(\rho)).$$

Proof. Let $\mathcal{M}_{k,0}^+$, $\mathcal{M}_{k,0}^{\geq}$, and $\mathcal{M}_{k,0}^\bullet$ be the sets of positive meanders, positive meanders avoiding $(0, k)$, and positive meanders marked below the minimum, respectively; see Table 2. Let $\omega_k \in \mathcal{A}_k$ and $\omega_{-k} \in \mathcal{A}_{-k}$ be two generalized arches. Now, define the multiset \mathcal{E}_k that consists of d copies of the set $\{w : \omega_k \cdot w \in \mathcal{E}\}$ of excursions factored by ω_k . Then, the following chain of inclusions holds:

$$\mathcal{E} \cdot \omega_{-k} \subseteq \mathcal{M}_{k,0}^{\geq} \subseteq \mathcal{M}_{k,0}^+ \subseteq \mathcal{M}_{k,0}^\bullet \subseteq \mathcal{E}_k. \tag{8}$$

The first inclusion holds as every walk $e \cdot \omega_{-k}$ with $e \in \mathcal{E}$ is a positive meander avoiding $(0, k)$. The middle inclusions hold by definition (see Table 2). The last inclusion holds since, for every $m \in \mathcal{M}_{k,0}^\bullet$, we have $\omega_k \cdot m \in \mathcal{E}$ after removing the marker from m . Therefore, the exponential growth rates of the counting sequences of $\mathcal{E} \cdot \omega_{-k}$ and \mathcal{E}_k are equal to the one of classical excursions \mathcal{E} , which has been explicitly computed in [4]. Hence, all 3 classes of meanders in (8) have the same asymptotic growth R^n .

Next, we observe that the corresponding generating functions have non-negative coefficients, and whence Pringsheim’s Theorem [22, Theorem IV.6] guarantees the existence of a dominant singularity on the positive real axis \mathbb{R}^+ . By [4] this is the only dominant singularity and we have $\rho = 1/R$. Furthermore, it was shown that on the radius of convergence $|z| = \rho$ only one root $u_1(z)$ is singular and has a square-root singularity, while the other ones are analytic. Then, we combine this result with the explicit shape of the symmetric polynomials from Definition 11. This gives the Puiseux expansion at $z = \rho$ on which we apply singularity analysis to derive the claimed formulas. ◀

Before we continue, let us comment on an often overlooked phenomenon concerning the analyticity of the small branches.

► **Remark 21 (Singularities of the small roots).** The small roots (and, in particular the principal small branch $u_1(z)$) can have a singularity inside the disk of convergence of $E(z)$. For example, for $S(u) = u + 13/u + 6/u^2$, one easily checks that the radius of convergence of $E(z)$ is $\rho = 8/61$ while $u_1(z)$ and $u_2(z)$ are singular at $z = -1/8$. However, their product $u_1 u_2$ is regular for $|z| < \rho$; more generally what is proven in [4] is that the product of the small roots is always regular for $0 < |z| < \rho$, while in general not each single small root is regular for $0 < |z| < \rho$.

Many theorems leading to a Gaussian distribution require that a key quantity (let us call it σ) is nonzero. In [22], this nonzero assumption is called “variability condition”; see therein Theorem IX.8 (Quasi-power theorem), Theorem IX.9 (Meromorphic schema), Theorem IX.10 (Positive rational systems). Now, many lattice path statistics have a variance with an expansion $\sigma n + o(n)$, where σ is defined as in the following lemma, and is therefore nonzero.

► **Lemma 22 (Universal positivity of the variability condition).** *For any Laurent series $S(u) = \sum_{i \geq -c} s_i u^i$, with $s_i \geq 0$ (at least two $s_i > 0$), one has $\sigma := S''(1)S(1) + S'(1)S(1) - S'(1)^2 > 0$.*

Proof. The trick is to introduce $\sigma(u) := uS''(u)S(u) + S'(u)S(u) - uS'(u)^2$. Then, all the monomials of $\sigma(u)$ have positive coefficients: this follows from $[s_i s_j] \sigma(u) = u^{i+j-1} (i-j)^2 \geq 0$, and thus $\sigma(u) > 0$ for $u > 0$. ◀

It is worth noting that an alternative version of this lemma is: « $uS(u)/S'(u) = n$ has no double root for $u > 0$ »; this plays a role in the tuning of Boltzmann random generation [17]. Such considerations are also related to Harald Cramér’s trick of shifting the mean which transforms a problem with drift into a problem with zero drift, via the modification of the weights of the step set $\tilde{S}(u) := S(\tau u)/S(\tau)$ (and choosing τ such that $S'(\tau) = 0$ indeed implies that $\tilde{S}'(1) = 0$). Compare also with the proof of [21, Formula (2.37)].

As a consequence, Lemma 22 guarantees that we can apply the quasi-power theorem [22, Theorem IX.8], and obtain a Gaussian limit theorem. This explains why many statistics related to lattice paths are Gaussian. E.g., for paths with positive or zero drift, it furnishes a Gaussian limit theorem for the final altitude of meanders or for the height of walks. When the drift is negative, one gets some discrete limit laws of parameter given by our symmetric polynomial expressions:

► **Theorem 23** ([4, Theorem 6] and [41, Theorem 4.7]; negative drift cases). *Assume a negative drift $\delta = S'(1) < 0$ and let $\rho = 1/P(\tau)$ and $\rho_1 = 1/P(1)$.*

1. *Let X_n be the random variable of the final altitude of a meander of length n . Then, the limit law is discrete and given by*

$$\lim_{n \rightarrow \infty} \Pr(X_n = k) = (1 - \tau^{-1}) \frac{\sum_{i=0}^k \tau^{i-k} h_i(v_1(\rho)^{-1}, \dots, v_d(\rho)^{-1})}{\sum_{i \geq 0} h_i(v_1(\rho)^{-1}, \dots, v_d(\rho)^{-1})}.$$

2. *Let Y_n be the random variable of the height of a walk of length n . Then, the limit law is discrete and given by*

$$\lim_{n \rightarrow \infty} \Pr(Y_n = k) = \frac{h_k(v_1(\rho_1)^{-1}, \dots, v_d(\rho_1)^{-1})}{\sum_{i \geq 0} h_i(v_1(\rho_1)^{-1}, \dots, v_d(\rho_1)^{-1})}.$$

Proof (Sketch). Recall that for a path represented by a sequence of points $(\omega_0, \omega_1, \dots, \omega_n)$ the final altitude is ω_n and the height is $\max_i \omega_i$. In both cases the limit law follows from a rewriting of the closed form of the discrete probability generating function which basically consists of the generating function of h_k (alternatively, M^+) and proper rescaling. ◀

Note that the second case is an avatar of the Wiener–Hopf decomposition which links the height of walks with the final altitude of meanders; see Theorem 10 and [41].

6 Conclusion and perspectives

In this article we introduced the notion of prime walks, a class of walks which leads to natural decompositions of lattice paths and to concise proofs of several identities in probability theory that we are even able to further generalize by capturing some additional statistics. Moreover, these decompositions can keep track of some additional parameters (e.g. counting the number of occurrences of some given patterns, see [3]), which then gives access to many joint distribution studies, see e.g. [12].

Our work also offers new links with symmetric polynomials, adding to previous fundamental connections with algebraic combinatorics via Vandermonde determinants, the Jacobi–Trudi identity, and Schur functions (see [5, 9]). In [6], we give an interpretation of Schur polynomials (for some appropriate index) in terms of meanders ending at a given altitude. Together with the results of the present work, this extends the table given in [38, Prop. 2.8.3]: therein, Stanley gives some nice combinatorial expressions for the bases of symmetric functions (Definition 11), when they are evaluated at specific values like $x_i = 1$ or $x_i = q^i$. This is what he calls the “principal specializations”. Our work shows that what we could call the “kernel root specialization” of the symmetric function bases (i.e. evaluation at $x_i = u_i(z)$) is leading to the enumeration of fundamental lattice path classes, holding for any set of jumps.

En passant, we illustrate the old Schützenberger philosophy: most of the identities in the commutative world are images of structural identities in the non-commutative world. It is natural to ask how far we can extend the link between lattice paths and the non-commutative symmetric world; note that further non-commutative points of view are developed in [18, 23, 24].

It is striking that astonishingly powerful formulas can be obtained by astonishingly simple tools from symbolic combinatorics. Such formulas, e.g. the Spitzer formula for bridges, have some unexpected avatars. Indeed, bridges of length n can be seen as $[u^0]S(u)^n$ for some Laurent polynomial $S(u)$ and the same holds with multivariate polynomials; this leads to some interesting connections between the non-commutative world, the Laurent phenomenon (i.e. the fact that some expressions which by design are a priori rational functions are in fact some Laurent polynomial), and lattice paths (see [14, 29, 36]).

On the computer algebra side, the so-called “Platypus algorithm” from [4] is a way to get the algebraic equation satisfied by the generating function of excursions. Another nice consequence of our formulas is that they permit a generalization of this “Platypus algorithm”: starting from the generating functions of the symmetric polynomials given in Definition 11, we show in the long version of this article how to get the algebraic equations of the different families of constrained meanders, bridges, etc. This offers an effective alternative to an approach by resultants or Gröbner bases, which are quickly time and memory consuming.

For Motzkin paths (that is, paths with step set $\mathcal{S} = \{-1, 0, +1\}$), the generating functions associated to starting/final altitude constraints can be expressed as continued fractions, and thus as quotients of orthogonal polynomials [20]. Our work, in one sense, gives the generalization of these formulas as soon as one has steps $> +1$ or < -1 . Many combinatorial structures related to the Motzkin paths have some asymptotics in which the “algebra of orthogonal polynomials” plays a role (e.g. the height of binary trees, related to the Mandelbrot fractal equation involves Chebyshev polynomials, see e.g. [22]). It is thus natural to ask if there is a nice “algebra of symmetric polynomials” in which plugging the Puiseux expansions offered by the kernel method could lead to the limit laws of many parameters of lattice paths?

In conclusion, our work largely complements and extends [4], being part of a wider program illustrating how lattice path surgery (which we call *latticepathology*) leads directly to many neat enumerative, probabilistic, computational, and asymptotic formulas.

References

- 1 David Aldous, Grégory Miermont, and Jim Pitman. The exploration process of inhomogeneous continuum random trees, and an extension of Jeulin’s local time identity. *Probab. Theory Related Fields*, 129(2):182–218, 2004. doi:10.1007/s00440-003-0334-7.
- 2 Erik Sparre Andersen. On the number of positive sums of random variables. *Scandinavian Actuarial Journal*, 1949(1):27–36, 1949. doi:10.1080/03461238.1949.10419756.
- 3 Andrei Asinowski, Axel Bacher, Cyril Banderier, and Bernhard Gittenberger. Analytic combinatorics of lattice paths with forbidden patterns: enumerative aspects. In *LATA’18*, volume 10792 of *Lecture Notes in Comput. Sci.*, pages 195–206. Springer, 2018. URL: <https://lipn.univ-paris13.fr/~banderier/Papers/lata2018.pdf>.
- 4 Cyril Banderier and Philippe Flajolet. Basic analytic combinatorics of directed lattice paths. *Theoretical Computer Science*, 281(1-2):37–80, 2002. doi:10.1016/S0304-3975(02)00007-5.
- 5 Cyril Banderier and Pierre Nicodème. Bounded discrete walks. *Discrete Math. Theor. Comput. Sci.*, AM:35–48, 2010. URL: <https://dmtcs.episciences.org/2792/pdf>.
- 6 Cyril Banderier and Michael Wallner. The kernel method for lattice paths below a rational slope. In *Lattice paths combinatorics and applications*, Developments in Mathematics Series, pages 119–154. Springer, 2019. doi:10.1007/978-3-030-11102-1_7.
- 7 Jean Bertoin and Jim Pitman. Path transformations connecting Brownian bridge, excursion and meander. *Bull. Sci. Math.*, 118(2):147–166, 1994. URL: <https://digitalassets.lib.berkeley.edu/sdtr/ucb/text/350.pdf>.

- 8 Olivier Bodini and Yann Ponty. Multi-dimensional Boltzmann sampling of languages. *Discrete Math. Theor. Comput. Sci. Proc.*, AM:49–63, 2010. URL: <https://hal.inria.fr/hal-00450763v4/document>.
- 9 Mireille Bousquet-Mélou. Discrete excursions. *Sém. Lothar. Combin.*, 57:23 pp., 2008. URL: <https://www.mat.univie.ac.at/~slc/wpapers/s57bousquet.pdf>.
- 10 Mireille Bousquet-Mélou and Marko Petkovšek. Linear recurrences with constant coefficients: the multivariate case. *Discrete Mathematics*, 225(1-3):51–75, 2000. doi:10.1016/S0012-365X(00)00147-3.
- 11 Mireille Bousquet-Mélou and Yann Ponty. Culminating paths. *Discrete Math. Theor. Comput. Sci.*, 10(2):125–152, 2008. URL: <https://hal.archives-ouvertes.fr/hal-00151979v2/document>.
- 12 Alan J. Bray, Satya N. Majumdar, and Grégory Schehr. Persistence and first-passage properties in nonequilibrium systems. *Advances in Physics*, 62(3):225–361, 2013. doi:10.1080/00018732.2013.803819.
- 13 Philippe Chassaing and Svante Janson. A Vervaat-like path transformation for the reflected Brownian bridge conditioned on its local time at 0. *Ann. Probab.*, 29(4):1755–1779, 2001. doi:10.1214/aop/1015345771.
- 14 Philippe Di Francesco and Rinat Kedem. Discrete non-commutative integrability: Proof of a conjecture by M. Kontsevich. *International Mathematics Research Notices*, 2010(21):4042–4063, 2010. doi:10.1093/imrn/rnq024.
- 15 Catherine Donati-Martin, Hiroyuki Matsumoto, and Marc Yor. On striking identities about the exponential functionals of the Brownian bridge and Brownian motion. *Period. Math. Hungar.*, 41(1-2):103–119, 2000. doi:10.1023/A:1010308203346.
- 16 Philippe Duchon. On the enumeration and generation of generalized Dyck words. *Discrete Mathematics*, 225(1-3):121–135, 2000. doi:10.1016/S0012-365X(00)00150-3.
- 17 Philippe Duchon, Philippe Flajolet, Guy Louchard, and Gilles Schaeffer. Boltzmann samplers for the random generation of combinatorial structures. *Combinatorics, Probability and Computing*, 13(4-5):577–625, 2004. doi:10.1017/S0963548304006315.
- 18 Kurusch Ebrahimi-Fard, Li Guo, and Dirk Kreimer. Spitzer’s identity and the algebraic Birkhoff decomposition in pQFT. *J. Phys. A*, 37(45):11037–11052, 2004. doi:10.1088/0305-4470/37/45/020.
- 19 William Feller. *An Introduction to Probability Theory and its Applications. Vol. II*. Second edition. John Wiley & Sons, 1971.
- 20 Philippe Flajolet. Combinatorial aspects of continued fractions. *Discrete Mathematics*, 32(2):125–161, 1980. doi:10.1016/0012-365X(80)90050-3.
- 21 Philippe Flajolet and Andrew M. Odlyzko. Limit distributions for coefficients of iterates of polynomials with applications to combinatorial enumerations. *Math. Proc. Cambridge Philos. Soc.*, 96(2):237–253, 1984. doi:10.1017/S0305004100062149.
- 22 Philippe Flajolet and Robert Sedgewick. *Analytic Combinatorics*. Cambridge University Press, 2009. URL: <http://algo.inria.fr/flajolet/Publications/book.pdf>.
- 23 Sergey Fomin and Curtis Greene. Noncommutative Schur functions and their applications. *Discrete Math.*, 193(1-3):179–200, 1998. doi:10.1016/S0012-365X(98)00140-X.
- 24 Israel M. Gelfand, Daniel Krob, Alain Lascoux, Bernard Leclerc, Vladimir S. Retakh, and Jean-Yves Thibon. Noncommutative symmetric functions. *Adv. Math.*, 112(2):218–348, 1995. doi:10.1006/aima.1995.1032.
- 25 Ira M. Gessel. A factorization for formal Laurent series and lattice path enumeration. *Journal of Combinatorial Theory, Series A*, 28(3):321–337, 1980. doi:10.1016/0097-3165(80)90074-6.
- 26 Priscilla Greenwood. Wiener–Hopf methods, decompositions, and factorisation identities for maxima and minima of homogeneous random processes. *Advances in Appl. Probability*, 7(4):767–785, 1975. doi:10.2307/1426398.
- 27 John E. Hopcroft, Raghavan Motwani, and Jeffrey D. Ullman. *Introduction to Automata Theory, Languages, and Computation*. Addison-Wesley, 3rd edition, 2006.

- 28 Thierry Jeulin and Marc Yor. Grossissements de filtrations: exemples et applications. In *Séminaire de Calcul Stochastique 1982/83, Université Paris VI*, volume 1118 of *Lecture Notes in Math*. Springer, 1985. doi:10.1007/BFb0075765.
- 29 Maxim Kontsevich. Noncommutative identities. *arXiv*, pages 1–10, 2011. arXiv:1109.2469v1.
- 30 Christian Krattenthaler. *Lattice Path Enumeration*. CRC Press, 2015. In: *Handbook of Enumerative Combinatorics*, M. Bóna (ed.), *Discrete Math. and Its Appl.* arXiv:1503.05930.
- 31 Alexey Kuznetsov, Andreas E. Kyprianou, and Juan C. Pardo. Meromorphic Lévy processes and their fluctuation identities. *Ann. Appl. Probab.*, 22(3):1101–1135, 2012. doi:10.1214/11-AAP787.
- 32 Jacques Labelle and Yeong N. Yeh. Generalized Dyck paths. *Discrete Mathematics*, 82(1):1–6, 1990. doi:10.1016/0012-365X(90)90039-K.
- 33 Titus Lupu, Jim Pitman, and Wenpin Tang. The Vervaat transform of Brownian bridges and Brownian motion. *Electron. J. Probab.*, 20:no. 51, 31, 2015. doi:10.1214/EJP.v20-3744.
- 34 Philippe Marchal. On a new Wiener–Hopf factorization by Alili and Doney. In *Sém. de Probabilités, XXXV*, *Lecture Notes in Math.* #1755, pages 416–420. Springer, 2001. doi:10.1007/978-3-540-44671-2_28.
- 35 Donatella Merlini, Douglas G. Rogers, Renzo Sprugnoli, and Cecilia Verri. Underdiagonal lattice paths with unrestricted steps. *Discrete Appl. Math.*, 91(1-3):197–213, 1999. doi:10.1016/S0166-218X(98)00126-7.
- 36 Christophe Reutenauer and Marco Robado. On an algebraicity theorem of Kontsevich. *Discrete Math. Theor. Comput. Sci.*, AR:239–246, 2012. 24th International Conference on Formal Power Series and Algebraic Combinatorics (FPSAC 2012). URL: <https://hal.archives-ouvertes.fr/hal-01283155/document>.
- 37 Frank Spitzer. A combinatorial lemma and its application to probability theory. *Trans. Amer. Math. Soc.*, 82:323–339, 1956. doi:10.2307/1993051.
- 38 Richard P. Stanley. *Enumerative Combinatorics. Vol. 2*, volume 62. Cambridge University Press, 1999. doi:10.1017/CB09780511609589.
- 39 J. Michael Steele. The Bohnenblust–Spitzer algorithm and its applications. *J. Comput. Appl. Math.*, 142(1):235–249, 2002. doi:10.1016/S0377-0427(01)00472-1.
- 40 Wim Vervaat. A relation between Brownian bridge and Brownian excursion. *Ann. Probab.*, 7(1):143–149, 1979. URL: <https://www.jstor.org/stable/2242845>.
- 41 Michael Wallner. A half-normal distribution scheme for generating functions. *European J. Combin.*, 87(103138):1–21, 2020. arXiv:1610.00541, doi:10.1016/j.ejc.2020.103138.
- 42 James G. Wendel. Spitzer’s formula: a short proof. *Proc. Amer. Math. Soc.*, 9:905–908, 1958. doi:10.2307/2033326.

Combinatorics of nondeterministic walks of the Dyck and Motzkin type

Élie de Panafieu*

Mohamed Lamine Lamali†

Michael Wallner†

Abstract

This paper introduces *nondeterministic walks*, a new variant of one-dimensional discrete walks. At each step, a nondeterministic walk draws a random set of steps from a predefined set of sets and explores all possible extensions in parallel. We introduce our new model on Dyck steps with the nondeterministic step set $\{\{-1\}, \{1\}, \{-1, 1\}\}$ and Motzkin steps with the nondeterministic step set $\{\{-1\}, \{0\}, \{1\}, \{-1, 0\}, \{-1, 1\}, \{0, 1\}, \{-1, 0, 1\}\}$. For general lists of step sets and a given length, we express the generating function of nondeterministic walks where at least one of the walks explored in parallel is a bridge (ends at the origin). In the particular cases of Dyck and Motzkin steps, we also compute the asymptotic probability that at least one of those parallel walks is a meander (stays nonnegative) or an excursion (stays nonnegative and ends at the origin).

This research is motivated by the study of networks involving encapsulations and decapsulations of protocols. Our results are obtained using generating functions and analytic combinatorics.

Keywords. Random walks, analytic combinatorics, generating functions, networking, encapsulation.

1 Introduction

In recent years lattice paths have received a lot of attention in different fields, such as probability theory, computer science, biology, chemistry, physics, and much more [5, 9, 11]. One reason for that is their versatility as models like *e.g.*, the up-to-date model of certain polymers in chemistry [16]. In this paper we introduce yet another application: the encapsulation of protocols over networks. To achieve this goal we generalize the class of lattice paths to so called *nondeterministic lattice paths*.

1.1 Definitions

Classical walks. We mostly follow terminology from [2]. Given a set S of integers, called the *steps*, a *walk* is a sequence $v = (v_1, \dots, v_n)$ of steps $v_i \in S$. In this paper we will always assume that our walks start at the origin. Its *length* $|v|$ is the number n of its steps, and its *endpoint* is equal to the sum of the steps $\sum_{i=1}^n v_i$. As illustrated in Figure 1a, a walk can be visualized by its *geometric realization*. Starting from the origin, the steps are added one by one to the previous endpoints. This gives a sequence $(y_j)_{0 \leq j \leq n}$ of ordinates at discrete

time steps, such that $y_0 = 0$ and $y_j := \sum_{i=1}^j v_i$. A *bridge* is a walk with endpoint $y_n = 0$. A *meander* is a walk where all points have nonnegative ordinate, *i.e.*, $y_j \geq 0$ for all $j = 0, \dots, n$. An *excursion* is a meander with endpoint $y_n = 0$.

Nondeterministic walks. This paper investigates a new variant of walks, called *nondeterministic walks*, or *N-walks*. In our context, this word does not mean “*random*”. Instead it is understood in the same sense as for automata and Turing machines. A process is nondeterministic if several branches are explored in parallel, and the process is said to end in an accepting state if one of those branches ends in an accepting state. Let us now give a precise definition of these walks.

DEFINITION 1.1. (NONDETERMINISTIC WALKS) *An N -step is a nonempty set of integers. Given an N -step set S , an N -walk w is a sequence of N -steps. Its length $|w|$ is equal to the number of its N -steps.*

As for classical walks we always assume that they start at the origin and we distinguish different types.

DEFINITION 1.2. (TYPES OF N-WALKS) *An N -walk $w = (w_1, \dots, w_n)$ and a classical walk $v = (v_1, \dots, v_n)$ are compatible if they have the same length n , the same starting point, and for each $1 \leq i \leq n$, the i^{th} step is included in the i^{th} N -step, *i.e.*, $v_i \in w_i$. An N -bridge (*resp.* N -meander, *resp.* N -excursion) is an N -walk compatible with at least one bridge (*resp.* meander, *resp.* excursion). Thus, N -excursions are particular cases of N -meanders.*

The endpoints of classical walks are central to the analysis. We define their nondeterministic analogues.

DEFINITION 1.3. (REACHABLE POINTS) *The reachable points of a general N -walk are the endpoints of all walks compatible with it. For N -meanders, the reachable points are defined as the set of endpoints of compatible meanders. In particular, all reachable endpoints of an N -meander are nonnegative. The minimum (*resp.* maximum) reachable point of an N -walk w is denoted by $\min(w)$ (*resp.* $\max(w)$). The minimum (*resp.* maximum) reachable point of an N -meander w is denoted by $\min^+(w)$ (*resp.* $\max^+(w)$).*

*Nokia Bell Labs and Lincs, France

†LaBRI - Université de Bordeaux, France

The geometric realization of an N-walk is the sequence, for j from 0 to n , of its reachable points after j steps. Figure 1 illustrates the geometric realization of a walk $v = (2, -1, 0, 1)$ in (1a), of an N-walk $w = (\{2\}, \{-1, 1\}, \{-2, 0\}, \{0, 1, 2\})$ in (1b), and of the classical meanders compatible with w in (1c). Note that the walk v (highlighted in red) is compatible with the N-walk w .

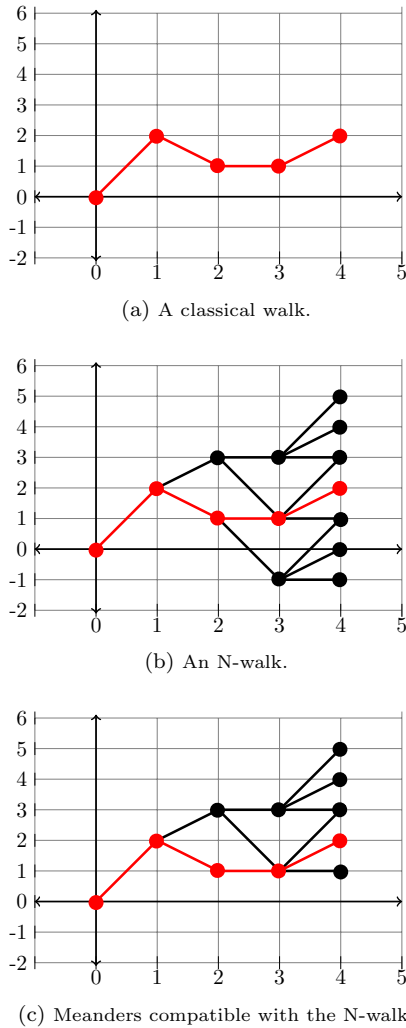


Figure 1: Geometric realization of a walk, an N-walk, and its compatible meanders.

Probabilities. Any set of weights, and in particular any probability distribution on the set of steps or N-steps induces a probability distribution on walks or N-walks. The probability associated to the walk or N-walk $w = (w_1, \dots, w_n)$ is then the product $\prod_{i=1}^n \mathbb{P}(w_i)$ of the probabilities of its steps or N-steps.

1.2 Main results Our main results are the analysis of the asymptotic number of non-deterministic walks of the Dyck and Motzkin type with step sets $\{-1, 1, -1, 1\}$ and $\{-1, 0, 1, -1, 0, -1, 1, 0, 1, -1, 0, 1\}$, respectively. The results for the unweighted case where all weights are set equal to one are summarized in Table 1. These results are derived using generating functions and singularity analysis. The reappearing phenomenon is the one of a simple dominating polar singularity arising from the large redundancy in the steps. The type of N-walk only influences the constant or the proportion among all N-walks. The lower order terms are exponentially smaller and of the square root type. These are much more influenced by the types. From a combinatorial point of view, we see a quite different behavior compared with classical paths. In particular, the limit probabilities for a Dyck N-walk of even length to be an N-bridge, an N-meander, or an N-excursion, are 1, 1/2, or 1/4, and for Motzkin N-walks 1, 3/4, or 9/16.

We also explore general N-steps and prove that the generating function of N-bridges is always algebraic. N-excursions with general N-steps will be investigated in a longer version of this article.

1.3 Motivation and related work Let us start with a vivid motivation of the model using Russian dolls. Suppose we have a set of $n + 1$ people arranged in a line. There are three kinds of people. A person of the first kind is only able to put a received doll in a bigger one. A person of the second kind is only able to extract a smaller doll (if any) from a bigger one. Finally, a person of the third kind can either put a doll in a bigger one or extract a smaller doll if any. We want to know if it is possible for the last person to receive the smallest doll after it has been given to the first person and then, consecutively, handed from person to person while performing their respective operations. This is equivalent to asking if a given N-walk with each N-step $\in \{1, -1, -1, 1\}$ is an N-excursion, *i.e.*, if the N-walk is compatible with at least one excursion. The probabilistic version of this question is: what is the probability that the last person can receive the smallest doll according to some distribution on the set of people over the three kinds?

Networks and encapsulations. The original motivation of this work comes from networking. In a network, some nodes are able to encapsulate protocols (put a packet of a protocol inside a packet of another one), decapsulate protocols (extract a nested packet from another one), or perform any of these two

Type	Dyck N-steps $\mathcal{P}(\{-1, 1\}) \setminus \emptyset$	Motzkin N-steps $\mathcal{P}(\{-1, 0, 1\}) \setminus \emptyset$
N-Walk	3^n	7^n
N-Bridge	$\frac{1+(-1)^n}{2} \left(3^n - \frac{2\sqrt{2}}{\sqrt{\pi}} \frac{8^{n/2}}{\sqrt{n}} + \mathcal{O}\left(\frac{8^{n/2}}{n^{3/2}}\right) \right)$	$7^n - \sqrt{\frac{3}{\pi}} \frac{6^n}{\sqrt{n}} + \mathcal{O}\left(\frac{6^n}{n^{3/2}}\right)$
N-Meander	$\frac{3^n}{2} + \frac{3\sqrt{2}(1+(-1)^n)+4(1-(-1)^n)}{\sqrt{\pi}} \frac{8^{n/2}}{\sqrt{n^3}} + \mathcal{O}\left(\frac{8^{n/2}}{n^{5/2}}\right)$	$\frac{3}{4} 7^n + \frac{3\sqrt{3}}{2\sqrt{\pi}} \frac{6^n}{\sqrt{n^3}} + \mathcal{O}\left(\frac{6^n}{n^{5/2}}\right)$
N-Excursion	$\frac{1+(-1)^n}{2} \left(\frac{3^n}{4} + 4\sqrt{2} \frac{8^{n/2}}{\sqrt{\pi n^3}} + \mathcal{O}\left(\frac{8^{n/2}}{n^{5/2}}\right) \right)$	$\frac{9}{16} 7^n - \gamma \frac{6^n}{\sqrt{\pi n^3}} + \mathcal{O}\left(\frac{6^n}{n^{5/2}}\right)$

Table 1: The asymptotic number of nondeterministic unweighted (all weights equal to 1) Dyck and Motzkin N-walks with n steps obeying different constraints: N-Bridges contain at least one classical bridge ending at 0, N-Meanders contain at least one classical meander staying nonnegative, and N-excursions contain at least one classical excursion staying nonnegative and ending at 0. The constant $\gamma \approx 0.6183$ is an algebraic number defined as the positive real solution of $1024\gamma^4 - 8019\gamma^2 + 2916 = 0$.

operations (albeit most nodes are only able to transmit packets as they receive them). Typically, a tunnel is a subpath starting with an encapsulation and ending with the corresponding decapsulation. Tunnels are very useful for achieving several goals in networking (*e.g.*, interoperability: connecting IPv6 networks across IPv4 ones [19]; security and privacy: securing IP connections [18], establishing Virtual Private Networks [17], etc.). Moreover, tunnels can be nested to achieve several goals. Replacing the Russian dolls by packets, it is easy to see that an encapsulation can be modeled by a $\{1\}$ step and a decapsulation by a $\{-1\}$, while a passive transmission of a packet is modeled by a $\{0\}$ step.

Given a network with some nodes that are able to encapsulate or decapsulate protocols, a path from a sender to a receiver is *feasible* if it allows the latter to retrieve a packet exactly as dispatched by the sender. Computing the shortest feasible path between two nodes is polynomial [12] if cycles are allowed without restriction. In contrast, the problem is NP-hard if cycles are forbidden or arbitrarily limited. In [12], the algorithms are compared through worst-case complexity analysis and simulation. The simulation methodology for a fixed network topology is to make encapsulation (*resp.* decapsulation) capabilities available with some probability p and observe the processing time of the different algorithms. It would be interesting, for simulation purposes, to generate random networks with a given probability of existence of a feasible path between two nodes. This work is the first step towards achieving this goal, since our results give the probability that any path is feasible (*i.e.*, is a N-excursion) according to a probability distribution of encapsulation and decapsulation capabilities over the nodes.

Lattice paths. Nondeterministic walks naturally connect between lattice paths and branching processes. This is underlined by our usage of many well-established

analytic and algebraic tools previously used to study lattice paths. In particular, those are the robustness of D-finite functions with respect to the Hadamard product, and the kernel method [2, 4, 7].

The N-walks are nondeterministic one-dimensional discrete walks. We will see that their generating functions require three variables: one marking the lowest point $\min(w)$ that can be reached by the N-walk w , another one marking the highest point $\max(w)$, and the last one marking its length $|w|$. Hence, they are also closely related to two-dimensional lattice paths, if we interpret $(\min(w), \max(w))$ as coordinates in the plane.

2 Dyck N-walks

The step set of classical Dyck paths is $\{-1, 1\}$. The N-step set of all nonempty subsets is

$$S = \{\{-1\}, \{1\}, \{-1, 1\}\},$$

and we call the corresponding N-walks *Dyck N-walks*. To every step we associate a weight or probability p_{-1}, p_1 , and $p_{-1,1}$, respectively.

EXAMPLE 2.1. (DYCK N-WALKS) *Let us consider the Dyck N-walk $w = (\{1\}, \{-1, 1\}, \{-1, 1\}, \{-1\})$. The sequence of its reachable points is $(\{0\}, \{1\}, \{0, 2\}, \{-1, 1, 3\}, \{-2, 0, 2\})$. There are 4 classical walks compatible with it:*

Classical walk (sequence of steps)	Geometric realization (ordinates)
(1, -1, -1, -1)	(0, 1, 0, -1, -2)
(1, -1, 1, -1)	(0, 1, 0, 1, 0)
(1, 1, -1, -1)	(0, 1, 2, 1, 0)
(1, 1, 1, -1)	(0, 1, 2, 3, 2)

There are two bridges, which happen to be excursions. Thus, w is an N-bridge and an N-excursion.

The set of reachable points of a Dyck N-walk or N-meander has the following particular structure.

LEMMA 2.1. *The reachable points of a Dyck N-walk w are $\{\min(w) + 2i \mid 0 \leq \min(w) + 2i \leq \max(w)\}$, where $\min(w)$, $\max(w)$, and the length of w have the same parity. The same result holds for Dyck N-meanders, with $\min(w)$ and $\max(w)$ replaced by $\min^+(w)$ and $\max^+(w)$ (see Definition 1.3).*

We define the generating functions $D(x, y; t)$, $D^+(x, y; t)$, of Dyck N-walks and Dyck N-meanders as

$$\sum_{\text{Dyck N-walk } w} \left(\prod_{s \in w} p_s \right) x^{\min(w)} y^{\max(w)} t^{|w|},$$

$$\sum_{\text{Dyck N-meander } w} \left(\prod_{s \in w} p_s \right) x^{\min^+(w)} y^{\max^+(w)} t^{|w|}.$$

Note that by construction these are power series in t with Laurent polynomials in x and y , as each of the finitely many N-walks of length n has a finite minimum and maximum reachable point.

REMARK 2.1. *One difference to classical lattice paths is the choice of the catalytic variables x and y . Here, they encode the minimum and the maximum reachable points, while in classical problems one chooses to keep track of the coordinates of the endpoint, (see [2], for example).*

2.1 Dyck N-meanders and N-excursions As a direct corollary of Lemma 2.1, all N-bridges and N-excursions have even length. The total number of Dyck N-bridges and Dyck N-excursions are then, respectively, given by

$$[x^{\leq 0} y^{\geq 0} t^{2n}] D(x, y; t) \quad \text{and} \quad D^+(0, 1; t),$$

where the coefficient extraction operator $[t^k]$ is defined as $[t^k] \sum_{n \geq 0} f_n t^n := f_k$ and the nonpositive part extraction operator $[x^{\leq 0}]$ is defined as $[x^{\leq 0}] \sum_{k \in \mathbb{Z}} g_k x^k := \sum_{k \leq 0} g_k x^k$ (and analogously for $[y^{\geq 0}]$).

PROPOSITION 2.1. *The generating function of Dyck N-meanders is characterized by the relation*

$$\begin{aligned} D^+(x, y; t) &= 1 + t(p_{-1}x^{-1}y^{-1} + p_1xy + p_{-1,1}x^{-1}y) \\ &\quad \times (D^+(x, y; t) - D^+(0, y; t)) \\ &\quad + t(p_{-1}xy^{-1} + (p_1 + p_{-1,1})xy) \\ &\quad \times (D^+(0, y; t) - D^+(0, 0; t)) \\ &\quad + t(p_1 + p_{-1,1})xyD^+(0, 0; t). \end{aligned}$$

Proof. Applying the symbolic method (see [7]), we translate the following combinatorial characterization of N-meanders into the claimed equation. An N-meander is either of length 0, or it can be uniquely decomposed into an N-meander w followed by an N-step. If $\min^+(w)$ is nonzero, then any N-step can be applied. The generating function of N-meanders with positive minimum reachable point is $D^+(x, y; t) - D^+(0, y; t)$. If $\min^+(w)$ vanishes, but $\max^+(w)$ is nonzero (those N-meanders have generating function $D^+(0, y; t) - D^+(0, 0; t)$), then an additional N-step $\{-1\}$ increases $\min^+(w)$ (the path ending at 0 disappears, and the one ending at 2 becomes the minimum) and decreases $\max^+(w)$, while an additional N-step $\{1\}$ or $\{-1, 1\}$ increases both $\min^+(w)$ and $\max^+(w)$. Finally, if $\min^+(w)$ and $\max^+(w)$ vanish, which corresponds to the generating function $D^+(0, 0; t)$, then the N-step $\{-1\}$ is forbidden, and the two other available N-steps both increase $\min^+(w)$ and $\max^+(w)$.

Let us introduce the *min-max-change polynomial* $S(x, y)$ and the *kernel* $K(x, y)$ as

$$S(x, y) := \frac{p_{-1}}{xy} + p_1xy + p_{-1,1} \frac{y}{x},$$

$$K(x, y) := xy(1 - tS(x, y)).$$

The generating function of Dyck N-walks has now the compact form $1/(1 - tS(x, y))$. A key role in the following result on the closed form of Dyck N-meanders is played by $Y(t)$ and $X(y, t)$, the unique power series solutions satisfying $K(1, Y(t)) = 0$, and $K(X(y, t), y) = 0$ which are given by

$$Y(t) = \frac{1 - \sqrt{1 - 4p_{-1}(p_1 + p_{-1,1})t^2}}{2(p_1 + p_{-1,1})t},$$

$$X(y, t) = \frac{1 - \sqrt{1 - 4p_1(p_{-1} + p_{-1,1}y^2)t^2}}{2p_1yt}.$$

THEOREM 2.1. *The generating function $D^+(x, y; t)$ of Dyck N-meanders is algebraic of degree 4, and equal to*

$$\frac{x - X(y, t)}{1 - X(y, t)^2} \frac{y - xY(t) - X(y, t)Y(t) + xyX(y, t)}{xy(1 - tS(x, y))}.$$

The generating function of Dyck N-excursions is symmetric in p_{-1} and p_1 , and equal to

$$D^+(0, 1; t) = \frac{X(1, t)}{1 - X(1, t)^2} \frac{1 - X(1, t)Y(t)}{(p_{-1} + p_{-1,1})t}.$$

Proof (Sketch). Starting from the result of Proposition 2.1 one first substitutes $x = 1$ and finds a closed-form expression for $D^+(0, 0; t)$ using the kernel method. After substituting this expression back into

the initial equation one applies the kernel method again with respect to x and finds a closed-form solution for $D^+(0, y; t)$. Combining these results one proves the claim. Finally, using a computer algebra system a short computation using the closed form of Dyck N-excursions shows the symmetry in p_{-1} and p_1 .

REMARK 2.2. *It would be desirable to find a combinatorial interpretation of the surprising symmetry in p_{-1} and p_1 of Dyck N-excursions (which is clear for Dyck N-bridges).*

With this result, we can easily answer the counting problem in which all weights are set equal to one. Thereby we also solve a conjecture in the OEIS¹ on the asymptotic growth.

COROLLARY 2.1. *For $p_{-1} = p_1 = p_{-1,1} = 1$ the generating function of unweighted Dyck N-meanders is*

$$D^+(1, 1, t) = -\frac{1 - 4t - \sqrt{1 - 8t^2}}{4t(1 - 3t)} = 1 + 2t + 6t^2 + 16t^3 + 48t^4 + \dots$$

The number of unweighted Dyck N-meanders is asymptotically equal to

$$[t^n]D^+(1, 1, t) = \frac{3^n}{2} + \left(3\sqrt{2}(1 + (-1)^n) + 4(1 - (-1)^n)\right) \times \frac{8^{n/2}}{\sqrt{\pi n^3}} + \mathcal{O}\left(\frac{8^{n/2}}{n^{5/2}}\right).$$

These N-walks are in bijection with walks in the first quadrant $\mathbb{Z}_{\geq 0}^2$ starting at $(0, 0)$ and consisting of steps $\{(-1, 0), (1, 0), (1, 1)\}$. The counting sequence is given by OEIS A151281.

For $p_{-1} = p_1 = p_{-1,1} = 1$ the complete generating function of unweighted Dyck N-excursions is

$$D^+(0, 1, t) = \frac{1 - 8t^2 - (1 - 12t^2)\sqrt{1 - 8t^2}}{8t^2(1 - 9t^2)} = 1 + 4t^2 + 28t^4 + 224t^6 + 1888t^8 + \dots$$

The number $[t^n]D^+(0, 1, t)$ of unweighted Dyck N-excursions is asymptotically equal to

$$(1 + (-1)^n) \left(\frac{3^n}{8} + \sqrt{8} \frac{8^{n/2}}{\sqrt{\pi n^3}} + \mathcal{O}\left(\frac{8^{n/2}}{n^{5/2}}\right) \right).$$

Finally, we come back to one of the starting questions from the networking motivation.

¹The on-line encyclopedia of integer sequences: <http://oeis.org/A151281>.

THEOREM 2.2. *The probability for a random Dyck N-walk of length $2n$ to be an N-excursion has for $n \rightarrow \infty$ the following asymptotic form where the roles of p_{-1} and p_1 are interchangeable:*

- $\frac{(1-2p_1)(1-2p_{-1})}{(1-p_1)(1-p_{-1})} + \mathcal{O}\left(\frac{(4p_{-1}(1-p_{-1}))^n}{n^{3/2}}\right)$ if $0 < p_1 \leq p_{-1} < \frac{1}{2}$,
- $\frac{1-2p_1}{(1-p_1)\sqrt{\pi n}} + \mathcal{O}\left(\frac{1}{n^{3/2}}\right)$ if $0 < p_1 < \frac{1}{2}$ and $p_{-1} = \frac{1}{2}$,
- $\frac{1}{\sqrt{\pi n^3}} + \mathcal{O}\left(\frac{1}{n^{5/2}}\right)$ if $p_1 = p_{-1} = \frac{1}{2}$,
- $\mathcal{O}\left(\frac{(4p_{-1}(1-p_{-1}))^n}{n^{3/2}}\right)$ if $0 < p_1 < \frac{1}{2} < p_{-1} < 1$ and $p_{-1} + p_1 \leq 1$.

Proof (Sketch). Starting from the results of Theorem 2.1 we perform a singularity analysis [7]. Thereby different regimes need to be considered, leading to the different cases in the result. In the last case the condition guarantees that p_{-1} is closer to $1/2$ than p_1 .

Note that the (huge) formula for the constant in the last case can be made explicit in terms of p_{-1} and p_1 . However, it is of different shape for $p_{-1} + p_1 = 1$, and $p_{-1} + p_1 < 1$. In Figure 2 we compare the theoretical results with simulations for three different probability distributions. These nicely exemplify three of the four possible regimes of convergence.

2.2 Dyck N-bridges We now turn our attention to Dyck N-bridges. Their generating function is defined as

$$B(x, y, t) = \sum_{n,k,\ell \geq 0} b_{2n,k,\ell} x^{-k} y^\ell t^{2n}.$$

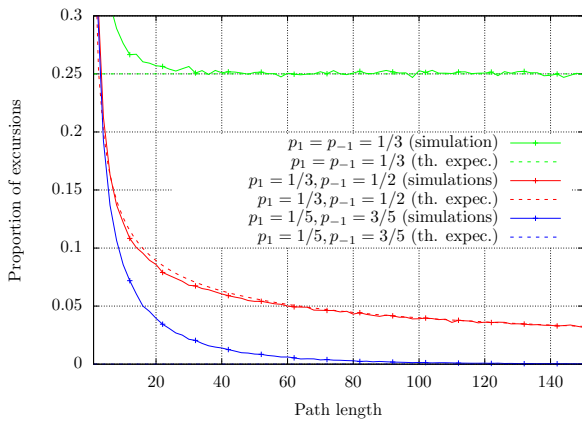
Recall the following relation with all N-walks (note that bridges have to be of even length): $[t^{2n}]B(x, y, t) = [x^{\leq 0} y^{\geq 0} t^{2n}]D(x, y, t)$. In the following theorem we will reveal a great contrast to classical walks: nearly all N-walks are N-bridges.

THEOREM 2.3. *The generating function of Dyck N-bridges $B(x, y, t)$ is algebraic of degree 4. For $p_{-1} = p_1 = p_{-1,1} = 1$ the generating function of unweighted Dyck N-bridges is algebraic of degree 2:*

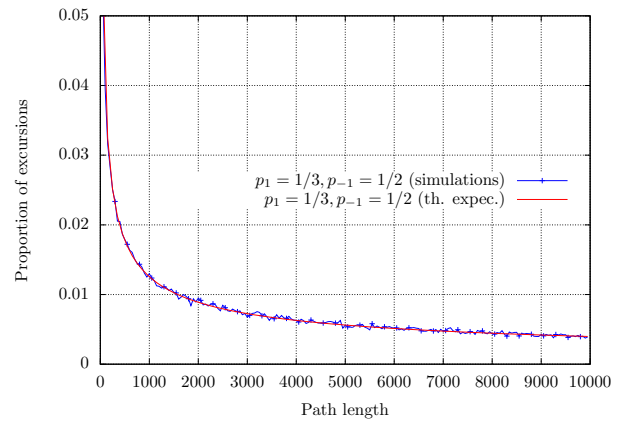
$$B(1, 1, t) = \frac{1 - 6t^2}{\sqrt{1 - 8t^2}(1 - 9t^2)} = 1 + 7t^2 + 63t^4 + 583t^6 + 5407t^8 + \dots$$

The number $[t^n]B(1, 1, t)$ of unweighted Dyck N-bridges is asymptotically equal to

$$\frac{1 + (-1)^n}{2} \left(3^n - \frac{2\sqrt{2}}{\sqrt{\pi}} \frac{8^{n/2}}{\sqrt{n}} + \mathcal{O}\left(\frac{8^{n/2}}{n^{3/2}}\right) \right).$$



(a) Short paths (from 0 to 150)



(b) Long paths (from 0 to 10^4)

Figure 2: Comparison of theoretical expectation and averaged simulation (over 10^5 runs) of the proportion of Dyck N -excursions among Dyck N -walks.

Proof. In order to improve readability we drop the parity condition on t and define

$$B_2(x, y, t) := [x^{\leq 0} y^{\geq 0}] D(x, y, t),$$

such that

$$(2.1) \quad B_2(x, y, t) = D(x, y, t) - [x^{> 0}] D(x, y, t) - [y^{< 0}] D(x, y, t).$$

It is then simple to recover $B(x, y, t)$ from $B_2(x, y, t)$. In words, an N -bridge is an N -walk of even length whose minimum is not strictly positive, nor is its maximum strictly negative².

The change in the x - (minimal reachable point) and y -coordinate (maximal reachable point) can be conveniently encoded in the min-max-change polynomial

$$S(x, y) = \frac{p_{-1}}{xy} + p_1 xy + p_{-1,1} \frac{y}{x}.$$

Then, the construction can be interpreted as the one of two-dimensional walks of length n , starting at $(0, 0)$, with the step set $\{(-1, -1), (1, 1), (-1, 1)\}$, and ending in the fourth quadrant $\{(x, y) : x \geq 0, y \leq 0\}$. A lot is known about these walks, see *e.g.*, [4]. By (2.1) it suffices to find the generating functions $F(x, y, t) := [x^{> 0}] D(x, y, t)$ and $G(x, y, t) := [y^{< 0}] D(x, y, t)$ for $2D$ -walks ending with a positive abscissa (*resp.* negative ordinate). The theory of formal Laurent series with positive coefficients tells us automatically that they are algebraic, which implies that the generating function of

²We thank Mireille Bousquet-Mélou for suggesting us this approach.

bridges is algebraic, see *e.g.*, [8, Section 6] which also gives further historical references.

Due to the symmetry of the step set we have $F(x, y, t) = G(1/y, 1/x, t)$ after additionally interchanging the role of p_{-1} and p_1 . In order to end the proof it remains to compute the roots of the denominator of $D(x, y, t)$ and perform a partial fraction decomposition.

After this detailed discussion of nondeterministic walks derived from Dyck paths, we turn to the probably next most classical lattice paths: Motzkin paths.

3 Motzkin N -walks

The step set of classical Motzkin paths is $\{-1, 0, 1\}$. The N -step set of all nonempty subsets is

$$S = \{\{-1\}, \{0\}, \{1\}, \{-1, 0\}, \{-1, 1\}, \{0, 1\}, \{-1, 0, 1\}\},$$

and we call the corresponding N -walks *Motzkin N -walks*.

A Motzkin N -walk w is said to be

- of type 1 if $\text{reach}(w)$ is equal to $\{\min(w), \min(w) + 2, \min(w) + 4, \dots, \max(w)\}$,
- of type 2 if $\text{reach}(w)$ is equal to $\{\min(w), \min(w) + 1, \min(w) + 2, \dots, \max(w)\}$ and $\max(w) - \min(w) \geq 1$.

The following proposition explains how these two types are sufficient to characterize the structure of Motzkin N -walks.

PROPOSITION 3.1. *A Motzkin N -walk w is of type 1 if and only if it is constructed only from the N -steps $\{-1\}$, $\{0\}$, $\{1\}$, and $\{-1, 1\}$. Otherwise, it is of type 2.*

Proof (Sketch). The proof is based on a recurrence and a case-by-case analysis on the number and type of N -steps.

The set of Motzkin N-walks of type 1 (*resp.* 2) is denoted by M_1 (*resp.* M_2), and their generating functions are defined as

$$M_1(x, y; t) = \sum_{w \in M_1} x^{\min(w)} y^{\max(w)} t^{|w|},$$

$$M_2(x, y; t) = \sum_{w \in M_2} x^{\min(w)} y^{\max(w)-1} t^{|w|}.$$

THEOREM 3.1. *The generating functions of Motzkin N-walks of type 1 and 2 are rational. The generating function of Motzkin N-bridges is algebraic.*

Proof. The first statement is a direct corollary of the previous proposition due to a simple sequence construction. An N-bridge w of type 1 is an M_1 N-walk that satisfies $\min(w) \leq 0$, $\max(w) \geq 0$, and $\min(w)$ is even. Note that in this case this property is not equivalent to an even number of steps. An N-bridge w of type 2 is an M_2 N-walk that satisfies $\min(w) \leq 0$ and $\max(w) \geq 0$. Thus, the generating function of Motzkin N-bridges is equal to

$$[x^{\leq 0} y^{\geq 0}] \left(\frac{M_1(x, y; t) + M_1(-x, y; t)}{2} + M_2(x, y; t) \right).$$

Since the generating functions of M_1 and M_2 are rational, according to [4, Proposition 1] (see also [13]), the generating function of N-bridges is D-finite. Yet the generating function is even algebraic, which can be proved similarly as done the proof of Theorem 2.3.

REMARK 3.1. *Using a computer algebra system it is easy to get closed-form solutions and asymptotics for specific values of the weights. We do not give these closed forms, as they are quite large and do not shed new light on the problem. It is however interesting to compute the asymptotic proportion of N-bridges among all N-walks. For example, when all weights are set to 1, it is equal to*

$$1 - \sqrt{\frac{3}{\pi}} \frac{(6/7)^n}{\sqrt{n}} + \mathcal{O}\left(\frac{(6/7)^n}{n^{3/2}}\right).$$

Hence, nearly all N-walks are N-bridges.

We now turn to the analysis of Motzkin N-meanders and N-excursions.

THEOREM 3.2. *The generating functions of Motzkin N-meanders and N-excursions are algebraic.*

Proof. Without loss of generality we perform all computations here with all weights $p_i = 1$. Let M_1^+ and

M_2^+ denote the Motzkin N-meanders of type 1 and 2. Their generating functions are

$$M_1^+(x, y; t) = \sum_{w \in M_1^+} x^{\min^+(w)} y^{\max^+(w)} t^{|w|},$$

$$M_2^+(x, y; t) = \sum_{w \in M_2^+} x^{\min^+(w)} y^{\max^+(w)-1} t^{|w|}.$$

Let also $M^+(x, y; t)$ denote the column vector $(M_1^+(x, y; t), M_2^+(x, y; t))$. An N-meander is either empty – in which case, it is of type 1 – or it is an N-meander w followed by an N-step s . The type of $w \cdot s$ depends on the type of w , the N-step s , as well as on the case if $\min^+(w) = 0$ or if $\max^+(w) = 0$. Specifically,

- when w has type 1, then $w \cdot s$ has type 1 if $s \in \{-1\}, \{0\}, \{1\}, \{-1, 1\}$, otherwise it has type 2,
- when w has type 2 and $\max^+(w) > 1$ then $w \cdot s$ has type 2 for any s ,
- when w has type 2 and $\max^+(w) = 1$ (i.e. the reachable points are $\{0, 1\}$) then $w \cdot s$ has type 1 if $s = \{-1\}$, and type 2 otherwise.

Applying the Symbolic Method [7] and the same reasoning as in the proof of Proposition 2.1, we obtain the following system of equations characterizing the generating functions from the vector $M^+(x, y; t)$

$$M^+(x, y; t) = e_1 + t \left(A(x, y) (M^+(x, y; t) - M^+(0, y; t)) \right. \\ \left. + B(x, y) (M^+(0, y; t) - M^+(0, 0; t)) \right. \\ \left. + C(x, y) M^+(0, 0; t) \right),$$

where e_1 is the column vector $(1, 0)$, and $A(x, y)$, $B(x, y)$, $C(x, y)$ are two-by-two matrices with Laurent polynomials in x and y given in Figure 3. Observe that the first two matrices are upper-triangular. This equation is rearranged into

$$(3.2) \quad (\text{Id} - tA(x, y)) M^+(x, y; t) = \\ e_1 - t(A(x, y) - B(x, y)) M^+(0, y; t) \\ - t(B(x, y) - C(x, y)) M^+(0, 0; t).$$

Next, we apply the kernel method (see *e.g.*, [2] and [1]) successively on x and y in a two phases to compute the generating function $M^+(x, y; t)$ of Motzkin N-meanders. The small roots in the variable x of the equations

$$1 - tA_{0,0}(x, y) = 0, \\ 1 - tA_{1,1}(x, y) = 0,$$

are denoted by $X_1(y, t)$ and $X_2(y, t)$, and are equal to

$$\frac{1 - t - \sqrt{1 - 4t^2y^2 - 3t^2 - 2t}}{2ty}, \\ \frac{1 - t(y + 1) - \sqrt{1 - 7t^2y^2 - 2t^2y - 3t^2 - 2ty - 2t}}{2ty}.$$

$$A(x, y) = \begin{pmatrix} x^{-1}y^{-1} + 1 + xy + x^{-1}y & 0 \\ x^{-1}y^{-1} + 1 + x^{-1} & x^{-1}y^{-1} + 1 + xy + x^{-1} + y + 2x^{-1}y \end{pmatrix},$$

$$B(x, y) = \begin{pmatrix} xy^{-1} + 1 + 2xy & 0 \\ y^{-1} + 2 & y^{-1} + 2 + xy + 3y \end{pmatrix}, \quad C(x, y) = \begin{pmatrix} 2 + 2xy & 1 \\ 2 & xy + 2 + 3y \end{pmatrix}.$$

Figure 3: Matrices involved in the proof of Theorem 3.2.

We then define the row vectors

$$u_1 = (1, 0),$$

$$u_2(y, t) = (tA_{1,0}(X_2(y, t), y), 1 - tA_{0,0}(X_2(y, t), y)),$$

so that the left-hand side of Equation (3.2) vanishes both when evaluated at $x = X_1(y, t)$ and left-multiplied by u_1 , and also when evaluated at $x = X_2(y, t)$ and left-multiplied by $u_2(y, t)$. Combining the corresponding two right-hand sides, we obtain a new two-by-two system of linear equations

$$(3.3) \quad tD(y, t)M^+(0, y; t) = f(y, t) - E(y, t)M^+(0, 0; t),$$

where the vector $f(y, t)$ of size 2 has its first element equal to 1, and its second element equal to

$$\frac{(ty + t - \sqrt{-7t^2y^2 - 3t^2 - 2(t^2 + t)y - 2t + 1})t}{1 - ty - t - \sqrt{-7t^2y^2 - 3t^2 - 2(t^2 + t)y - 2t + 1}},$$

and the two-by-two matrices $D(y, t)$ and $E(y, t)$ are two large to be shown here. Again, the matrix $D(y, t)$ is upper-triangular. We now define

$$Y_1(t) = \frac{t - 1 + \sqrt{-7t^2 - 2t + 1}}{4t},$$

$$Y_2(t) = \frac{1 - 2t - \sqrt{-12t^2 - 4t + 1}}{8t},$$

and the row vectors

$$v_1 = (1, 0),$$

$$v_2(t) = (-D_{1,0}(Y_2(t), t), D_{0,0}(Y_2(t), t)),$$

to ensure that $Y_1(t)$ and $Y_2(t)$ have series expansions at the origin, and that the left-hand side of Equation (3.3) vanishes both when evaluated at $y = Y_1(t)$ and left-multiplied by v_1 , and also when evaluated at $y = Y_2(t)$ and left-multiplied by $v_2(t)$. The corresponding two right-hand side are combined to form a new two-by-two system of equations

$$h(t) = tF(t)M^+(0, 0; t),$$

where the column vector $h(t)$ and the matrix $F(t)$ are too large to be shown here. The matrix $F(t)$ is

invertible, so the generating function of Motzkin N-meanders with maximum reachable point 0 is equal to

$$M^+(0, 0; t) = \frac{1}{t}F(t)^{-1}h(t).$$

This expression is injected in Equation (3.3) to express the generating function of Motzkin N-meanders with minimum reachable point 0

$$M^+(0, y; t) = \frac{1}{t}D(y, t)^{-1}(f(y, t) - E(y, t)M^+(0, 0; t)).$$

Finally, this expression is injected in Equation (3.2) to express the generating function of Motzkin N-meanders

$$M^+(x, y; t) = (\text{Id} - tA(x, y))^{-1} \\ \times (e_1 - t(A(x, y) - B(x, y))M^+(0, y; t) \\ - t(B(x, y) - C(x, y))M^+(0, 0; t)).$$

The generating function of N-meanders and N-excursions are then, respectively, $M_1^+(1, 1; t) + M_2^+(1, 1; t)$ and $M_1^+(0, 1; t) + M_2^+(0, 1; t)$.

REMARK 3.2. *As before we can use a computer algebra system to get numeric results. After tedious computations one gets that for all p_i 's equal to 1 the generating function of N-meanders is algebraic of degree 2 and given by*

$$\frac{10t - 1 + \sqrt{(1 + 2t)(1 - 6t)}}{8t(1 - 7t)}.$$

The total number of N-meanders is asymptotically equal to

$$\frac{3}{4}7^n + \frac{3\sqrt{3}}{2\sqrt{\pi}} \frac{6^n}{\sqrt{n^3}} + \mathcal{O}\left(\frac{6^n}{n^{5/2}}\right).$$

The generating function of N-excursions is algebraic of degree 4. Their asymptotic number is

$$\frac{9}{16}7^n - \gamma \frac{6^n}{\sqrt{\pi n^3}} + \mathcal{O}\left(\frac{6^n}{n^{5/2}}\right),$$

where $\gamma \approx 0.6183$ is the positive real solution of $1024\gamma^4 - 8019\gamma^2 + 2916 = 0$. This means that for large n approximately 75% of all N-walks are N-meanders and 56.25% of all N-walks are N-excursions.

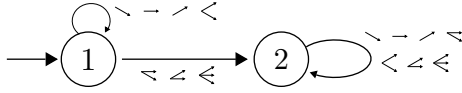


Figure 4: The automaton representing the structure of reachable points of Motzkin N-walks. The types from Theorem 4.1 corresponding to vertex 1 are $A_1 = \{0\}$, $B_1 = \{1\}$, $C_1 = \emptyset$, and for vertex 2, we have $A_2 = \{0\}$, $B_2 = \{0\}$, $C_2 = \{0\}$.

4 N-bridges with general N-steps

The main result of this section is

THEOREM 4.1. *For any N-step set S , the generating function of N-bridges is algebraic.*

A method for computing this generating function is provided by the proof, in Subsection 4.2. In order to establish this result, we first derive Proposition 4.1, which provides a description of the set of reachable points for N-walks on a given N-step set. It is proven in Section 4.1.

Given nonnegative integer sets A, B, C , an N-walk w is of type (A, B, C) when an integer r is reachable if and only if $\max(w) - \min(w) \geq \max(A) + \max(C)$, and at least one of the following conditions holds

- $r - \min(w)$ belongs to A ,
- $\max(w) - r$ belongs to C ,
- $r - \min(w) \geq \max(A)$, $\max(w) - r \geq \max(C)$, and $r - \min(w) - \max(A) - 1 \pmod{\max(B) + 1}$ belongs to B ,

with the convention $\max(\emptyset) = 0$. The set of N-walks of type (A, B, C) is denoted by $W_{A,B,C}$.

PROPOSITION 4.1. *Given an N-step set S , there is a finite set of types $(A_j, B_j, C_j)_{1 \leq j \leq m}$ such that the set of all N-walks on S is equal to the disjoint union $\biguplus_{j=1}^m W_{A_j, B_j, C_j}$. Furthermore, if we consider the N-walks as words on the alphabet S , there are nonempty subsets $(T_{i,j})_{1 \leq i \leq j \leq m}$ of S such that for all $1 \leq j \leq m$, the grammar characterizing the N-walks of type (A_j, B_j, C_j) is*

$$W_{A_j, B_j, C_j} = (\text{empty N-walk if } j = 1) + \sum_{i=1}^j W_{A_i, B_i, C_i} \sum_{s \in T_{i,j}} s.$$

Figure 4 illustrates the previous proposition on the example of Motzkin N-walks.

4.1 Proof of Proposition 4.1 Consider an N-walk w and the N-walk $w \cdot s$ obtained by adding the N-step

s to w . In this section, we will use the observation that the set of reachable points of w and $w \cdot s$ are linked by the relation

$$\text{reach}(w \cdot s) = \bigcup_{h \in s} \{r + h \mid r \in \text{reach}(w)\}.$$

Hence, the set of reachable points of an N-walk does not depend on the order of its N-steps. We start the proof with a description of reachable points as solutions of a linear equation.

LEMMA 4.1. *There exists an N-walk on the N-step set S that reaches the point r if and only if the following equation has a solution*

$$\sum_{s \in S} \sum_{h \in s} h x_{s,h} = r, \quad \forall (s, h), x_{s,h} \in \mathbb{Z}_{\geq 0}.$$

Furthermore, any N-walk that contains exactly $\sum_{h \in s} x_{s,h}$ occurrences of the N-step s reaches r .

Proof. By definition, if the N-walk $w = s_1 \cdot s_2 \cdots s_{|w|}$ on the N-step set S reaches the point r , then there exists a sequence of integers $(h_i)_{1 \leq i \leq |w|}$ such that for all i , we have $h_i \in s_i$, and

$$\sum_{i=1}^{|w|} h_i = r.$$

Let $x_{h,s}$ denote the number of values of $1 \leq i \leq |w|$ such that $(h, s) = (h_i, s_i)$, then the previous equation becomes

$$\sum_{s \in S} \sum_{h \in s} h x_{s,h} = r.$$

The previous lemma translates the study of reachable points into the realm of numerical semigroups. Using the tools of this field (Schur's Theorem and Fröbenius number [15]), we obtain the following lemma, that specializes Proposition 4.1 to N-walks containing sufficiently many occurrences of each N-step.

LEMMA 4.2. *Let p_S denote the gcd of the N-steps from S , shifted so that their minimum is at 0*

$$p_S = \gcd \left(\bigcup_{s \in S} \{h - \min(s) \mid h \in s\} \right).$$

For any N-step set S , there exist an integer m_S and two nonnegative integer sets A and C such that any N-walk w on S that contains at least m_S occurrences of each N-step is in $W_{A, \{p_S\}, C}$.

Proof. Given an N-step set S , the normalized version of the N-step s is defined as $\{(h - \min(s))/p_S \mid h \in s\}$. The normalized version of S is then the set

of its normalized N-steps. If Lemma 4.2 holds for normalized N-step sets, it also holds in the general case. Thus, without loss of generality, we assume S to be normalized. In particular, all its N-steps have minimum 0, so the smallest reachable point is always 0. According to Schur's Theorem, there is an integer f , called the *Fröbenius number*³, such that for any $r > f$, the equation from Lemma 4.1 has a solution. Let w_r denote an N-walk reaching r , and $|w|_s$ the number of occurrences of the N-step s in w . Let us define the integers ℓ , $m_S^{(0)}$ and b as

$$\begin{aligned} \ell &= \max_{s \in S} \max(s), \\ m_S^{(0)} &= \max_{s \in S, f < r \leq f + \ell} |w_r|_s, \\ c &= \max_{\forall s \in S, |w|_s = m_S^{(0)}} (\max(w) - f - \ell). \end{aligned}$$

Those three integers have the following meanings:

- ℓ is the maximum height of any N-step from S ,
- any N-walk containing at least $m_S^{(0)}$ occurrences of each N-step reaches all integers from $[f + 1, f + \ell]$,
- let $W^{=m_S^{(0)}}$ denote the set of N-walks that contain exactly $m_S^{(0)}$ occurrences of each N-step, then for any such N-walk, the distance between the maximal reachable point and $f + \ell$ is at most c .

Since any N-step has minimum 0, and maximum at most ℓ , adding an N-step s to an N-walk w from $W^{=m_S^{(0)}}$ produces an N-walk $w \cdot s$ which reaches all the points from $f + 1$ to $\max(w \cdot s) - c$. By recurrence, for any N-walk w that contains at least $m_S^{(0)}$ occurrences of each N-step, all points from $f + 1$ to $\max(w) - c$ are reachable. Since all N-steps contain 0, we have

$$\text{reach}(w) \subset \text{reach}(w \cdot s).$$

Let $w_{=m}$ denote an N-walk that contains exactly m occurrences of each N-step. Then $([0, f] \cap \text{reach}(w_{=m}))_m$ is an increasing (for the inclusion) sequence of sets included in $[0, f]$. Thus, it reaches for some finite integer $m = n$ its limit A . We set $m_S^{(1)} = \max(m_S^{(0)}, n)$. Any N-walk w containing at least $m_S^{(1)}$ occurrences of each N-step satisfies

$$\begin{aligned} \text{reach}(w) \cap [0, f] &= A, \\ [f + 1, \max(w) - c] &\subset \text{reach}(w). \end{aligned}$$

³Computing the Fröbenius number is NP-hard under Turing reduction if the number of integers $n = |\cup_{s \in S} s|$ is arbitrary [14]. It is an open problem whether it is also NP-hard under Karp reduction. If n is fixed, there is a polynomial algorithm [10] to compute the Fröbenius number but it is unpractical as its complexity is in $O((\log m)^{n^{O(n)}})$ where $m = \max_{s \in S} \max(s)$. However, there are algorithms that perform very well in practice [3, 6].

Finally, let us define the symmetric of an N-step s as the N-step $\{\max(s) - h \mid h \in s\}$, and the symmetric of an N-step set as the set of its symmetric N-steps. Applying the previous proof to the symmetric of S , we obtain the existence of an integer $m_S^{(2)}$, and integer f' and a set C such that for any N-walk w containing at least $m_S^{(2)}$ occurrences of each N-step, we have

$$\text{reach}(w) \cap [\max(w) - f', \max(w)] = C.$$

Defining the integer m_S as $\max(m_S^{(1)}, m_S^{(2)})$ finishes the proof.

We can finally provide the proof of Proposition 4.1.

Proof of Proposition 4.1. Given an N-step set S , we set $q_S = \max_{T \subset S} m_T$, where m_T has been defined in Lemma 4.2. Let $|w|_s$ denote the number of occurrences of the N-step s in the N-walk w . Consider the partial order on N-walks such that $w \leq w'$ if and only if any N-step that has less than q_S occurrences in w' has at least as many occurrences in w as in w' . Let us also define the equivalence relation $w \sim w'$ when the N-steps that occurs at least q_S times in w and w' are the same, and the other N-steps have the same number of occurrences in both N-walks

$$\begin{aligned} w \leq w' &\Leftrightarrow (\forall s \in S, |w'|_s < q_S \Rightarrow |w|_s \leq |w'|_s), \\ w \sim w' &\Leftrightarrow (\forall s \in S, (|w|_s \geq q_S \Rightarrow |w'|_s \geq q_S) \\ &\text{and } (|w|_s < q_S \Rightarrow |w|_s = |w'|_s)). \end{aligned}$$

When the set of all N-walks is factored by the “ \sim ” relation, we obtain a finite number of disjoint subsets, on which the “ \leq ” partial order induces a lattice structure. In the next paragraph, we will prove that each of those subsets V corresponds to a type, such that there are finite nonnegative integer sets A, B, C such that $V = W_{A,B,C}$. This will conclude the proof of the proposition, as the lattice structure ensures the grammar characterization stated in the second part of the proposition.

First, observe that two N-walks that contain the same N-steps with the same multiplicities reach the same set of points. Consider an element V of the lattice. By definition, if an N-walk from V contains less than q_S occurrences of each N-step, then all N-walks in V contain, for each N-step, the same number of occurrences, and thus have the same set R of reachable points. We then define A as the set R shifted by $\min(R)$, and obtain $V = W_{A,\emptyset,\emptyset}$. Otherwise, let $T \subset S$ denote the set of N-steps that occur in the N-walks from V at least q_S times. Let also v denote any N-walk with exactly $|w|_s$ occurrences of each N-step s from $S \setminus T$,

and no other N-step. Let $W_{\geq m_T}$ denote the set of N-walks that contain at least m_T occurrences of each N-step from T , and no other N-step. Since $q_S \geq m_T$, for any N-walk w from V , there is an N-walk w' from $W_{\geq m_T}$ such that the reachable points of w are the same as for $w' \cdot v$, the concatenation of w' and v . Since w' belongs to $W_{\geq m_T}$, according to Lemma 4.2, there are integer sets A', C' and an integer p_T such that w' is in $W_{A', \{p_T\}, C'}$. Adding the N-steps from v to w' changes the set of reachable points, and we obtain integer sets A, B, C such that $w' \cdot v$ belongs to $W_{A, B, C}$.

4.2 Proof of Theorem 4.1 The main idea of the proof is the repeated use of closure properties of algebraic functions, see [7]. Let $W_{A, B, C}(x, y; t) = \sum_{w \in W_{A, B, C}} x^{\min(w)} y^{\max(w)} t^{|w|}$ and $\text{Bridge}_{A, B, C}(t)$ denote the generating functions of N-walks and N-bridges of type (A, B, C) . The first part of Proposition 4.1 implies

$$\text{Bridge}(t) = \sum_{j=1}^m \text{Bridge}_{A_j, B_j, C_j}(t).$$

Hence, the proof is complete once established that each $\text{Bridge}_{A_j, B_j, C_j}(t)$ is algebraic. The grammar characterization from the second part of Proposition 4.1 is translated into the following system of equations: for j from 1 to m , the generating function $W_{A_j, B_j, C_j}(x, y; t)$ is equal to

$$\mathbb{1}_{j=1} + t \sum_{i=1}^j W_{A_i, B_i, C_i}(x, y; t) \sum_{s \in T_{i,j}} x^{\min(s)} y^{\max(s)}.$$

Solving this system, we obtain a rational expression for each $W_{A_j, B_j, C_j}(x, y; t)$, because the sets $T_{i,j}$ are nonempty. In the following, we consider some $1 \leq j \leq m$, set $(A, B, C) = (A_j, B_j, C_j)$, and prove that $\text{Bridge}_{A, B, C}(t)$ is algebraic. We assume that those three sets are nonempty, the other cases being similar.

An N-walk where the minimal reachable point is positive or the maximal reachable point is negative cannot be a bridge. Thus, we distinguish three kinds of N-walks that have the potential to be bridges:

- $w \in W_{A, B, C}^{(1)}$ when $-\max(A) \leq \min(w) \leq 0$,
- $w \in W_{A, B, C}^{(2)}$ when $\min(w) < -\max(A)$ and $\max(C) > \max(w)$,
- $w \in W_{A, B, C}^{(3)}$ when $0 \leq \max(w) \leq \max(C)$.

The corresponding generating functions are expressed as sums of positive parts in x and y of rational function

in t with Laurent polynomials in x and y coefficients

$$W_{A, B, C}^{(1)}(x, y; t) = W_{A, B, C}(x, y; t) - [x^{< -\max(A)}] W_{A, B, C}(x, y; t) - [x^{> 0}] W_{A, B, C}(x, y; t),$$

$$W_{A, B, C}^{(2)}(x, y; t) = W_{A, B, C}(x, y; t) - [x^{\geq -\max(A)}] W_{A, B, C}(x, y; t) - [y^{\leq \max(C)}] W_{A, B, C}(x, y; t),$$

$$W_{A, B, C}^{(3)}(x, y; t) = W_{A, B, C}(x, y; t) - [y^{< 0}] W_{A, B, C}(x, y; t) - [y^{> \max(C)}] W_{A, B, C}(x, y; t).$$

The set of bridges from $W_{A, B, C}^{(1)}$ is denoted by $\text{Bridge}_{A, B, C}^{(1)}$, and the same holds for (2) and (3). By definition of the type, we have

- $w \in \text{Bridge}_{A, B, C}^{(1)}$ if and only if $-\min(w) \in A$,
- $w \in \text{Bridge}_{A, B, C}^{(2)}$ if and only if $-\min(w) - \max(A) - 1 \pmod{\max(B) + 1} \in B$,
- $w \in \text{Bridge}_{A, B, C}^{(3)}$ if and only if $\max(w) \in C$.

Those characterizations imply

$$\text{Bridge}_{A, B, C}^{(1)}(t) = \sum_{a \in A} [x^a] W_{A, B, C}^{(1)}(x^{-1}, 1; t),$$

$$\text{Bridge}_{A, B, C}^{(3)}(t) = \sum_{c \in C} [y^c] W_{A, B, C}^{(3)}(1, y; t),$$

which are algebraic functions because the set A is finite, and $W_{A, B, C}^{(1)}(x^{-1}, 1; t)$ is an algebraic function analytic in x and t at the origin, so

$$[x^a] W_{A, B, C}^{(1)}(x^{-1}, 1; t) = \frac{d^a}{dx^a} W_{A, B, C}^{(1)}(x^{-1}, 1; t)|_{x=0}$$

(the same reasoning applies to (3)). Using the classical relation, $\frac{1}{p} \sum_{k=0}^{p-1} F(e^{2i\pi k/p}) = \sum_{p|n} [z^n] F(z)$, valid for any series $F(z)$ and $p > 0$ we obtain that $\text{Bridge}_{A, B, C}^{(2)}(t)$, equal to

$$\sum_{b \in B} \sum_{(n - \max(A) - 1 - b)} [x^n] W_{A, B, C}^{(2)}(x^{-1}, 1; t),$$

is algebraic as well. We conclude that the generating function of all N-bridges is algebraic, since

$$\begin{aligned} \text{Bridge}(t) &= \sum_{j=1}^m \text{Bridge}_{A_j, B_j, C_j}(t) \\ &= \sum_{j=1}^m \text{Bridge}_{A_j, B_j, C_j}^{(1)}(t) + \text{Bridge}_{A_j, B_j, C_j}^{(2)}(t) \\ &\quad + \text{Bridge}_{A_j, B_j, C_j}^{(3)}(t). \end{aligned}$$

5 Conclusion

In this paper we introduced nondeterministic lattice paths and solved the asymptotic counting problem for such walks of the Dyck and Motzkin type. The strength of our approach relies on the methods of analytic combinatorics, which allowed us to derive not only the asymptotic main terms but also lower order terms (to any order if needed). Furthermore, we showed that for a general step set the generating function of bridges is algebraic. In the long version of this work we will extend this setting to excursions and meanders with general N -steps.

The method of choice is the well-established kernel method. We extended it to a two-phase approach in order to deal with two catalytic variables.

Additionally to the mathematically interesting model, our nondeterministic lattice paths have applications in the encapsulation and decapsulation of protocols over networks. In the long version of this work we want to further explore this interesting bridge between combinatorics and networking.

Acknowledgements: The authors would like to thank Mireille Bousquet-Mélou for her useful comments and suggestions. We also thank the three referees for their feedback. The second author was partially supported by the HÉRA project, funded by The French National Research Agency. Grant no.: ANR-18-CE25-0002. The third author was supported by the Exzellenzstipendium of the Austrian Federal Ministry of Education, Science and Research and the Erwin Schrödinger Fellowship of the Austrian Science Fund (FWF): J 4162-N35.

References

- [1] Andrei Asinowski, Axel Bacher, Cyril Banderier, and Bernhard Gittenberger. Analytic combinatorics of lattice paths with forbidden patterns: Asymptotic aspects and borges's theorem. *LIPICs, Vol. 110 – Aofa 2018*, pages 10:1–10:14, 2018.
- [2] Cyril Banderier and Philippe Flajolet. Basic analytic combinatorics of directed lattice paths. *Theoretical Computer Science*, 281(12):37 – 80, 2002.
- [3] Dale Beihoffer, Jemimah Hendry, Albert Nijenhuis, and Stan Wagon. Faster algorithms for Frobenius numbers. *The Electronic Journal of Combinatorics*, 12(1), 2005.
- [4] Mireille Bousquet-Mélou and Marni Mishna. Walks with small steps in the quarter plane. In *Algorithmic probability and combinatorics*, volume 520 of *Contemp. Math.*, pages 1–39. Amer. Math. Soc., Providence, RI, 2010.
- [5] Mireille Bousquet-Mélou and Yann Ponty. Culminating paths. *Discrete Math. Theor. Comput. Sci.*, 10(2):125–152, 2008.
- [6] David Einstein, Daniel Lichtblau, Adam Strzebonski, and Stan Wagon. Frobenius numbers by lattice point enumeration. *Integers*, 7(1), 2007.
- [7] Philippe Flajolet and Robert Sedgewick. Analytic Combinatorics. *Cambridge University Press*, 2009.
- [8] Ira Martin Gessel. A factorization for formal Laurent series and lattice path enumeration. *J. Combin. Theory Ser. A*, 28(3):321–337, 1980.
- [9] Nils Haug, Adrie Daalhuis, and Thomas Prellberg. Higher-order Airy scaling in deformed Dyck paths. *Journal of Statistical Physics*, 1–16, 2017.
- [10] Ravi Kannan. Lattice translates of a polytope and the Frobenius problem. *Combinatorica*, 12(2):161–177, 1992.
- [11] Donald Ervin Knuth. *The art of computer programming. Vol. 1: Fundamental algorithms*. Addison-Wesley, 1968.
- [12] Mohamed Lamine Lamali, Nasreddine Fergani, Johanne Cohen, and Hélia Pouyllau. Path computation in multi-layer networks: Complexity and algorithms. In *IEEE INFOCOM 2016, San Francisco, CA, USA, April 10-14, 2016*, pages 1–9, 2016.
- [13] Leonard Lipshitz. The diagonal of a D -finite power series is D -finite. *J. Algebra*, 113(2):373–378, 1988.
- [14] Jorge Luis Ramírez Alfonsín. Complexity of the Frobenius problem. *Combinatorica*, 16(1):143–147, 1996.
- [15] Jorge Luis Ramírez Alfonsín. The diophantine Frobenius problem *Oxford Univ. Press*, pages 10:1–10:14, 2009.
- [16] Esaias J. Janse van Rensburg, Thomas Prellberg, and Andrew Rechnitzer. Partially directed paths in a wedge. *J. Combin. Theory Ser. A*, 115(4):623–650, 2008.
- [17] E Rosen, IJ Wijnands, Y Cai, and A Boers. RFC7582 - multicast virtual private network (mvpn): Using bidirectional p-tunnels. 2015.
- [18] Karen Seo and Stephen Kent. RFC4301 - security architecture for the internet protocol. 2005.
- [19] Peng Wu, Yong Cui, Jianping Wu, Jiangchuan Liu, and Chris Metz. Transition from IPv4 to IPv6: A state-of-the-art survey. *IEEE Communications Surveys & Tutorials*, 15(3):1407–1424, 2013.

More Models of Walks Avoiding a Quadrant

Mireille Bousquet-Mélou

CNRS, Université de Bordeaux, Laboratoire Bordelais de Recherche en Informatique, UMR 5800,
351 cours de la Libération, 33405 Talence Cedex, France
<https://www.labri.fr/perso/bousquet/>
mireille.bousquet-melou@u-bordeaux.fr

Michael Wallner 

Université de Bordeaux, Laboratoire Bordelais de Recherche en Informatique, UMR 5800,
351 cours de la Libération, 33405 Talence Cedex, France
TU Wien, Institute for Discrete Mathematics and Geometry,
Wiedner Hauptstraße 8–10, 1040 Wien, Austria
<https://dmg.tuwien.ac.at/mwallner/>
michael.wallner@tuwien.ac.at

Abstract

We continue the enumeration of plane lattice paths avoiding the negative quadrant initiated by the first author in [1]. We solve in detail a new case, the king walks, where all 8 nearest neighbour steps are allowed. As in the two cases solved in [1], the associated generating function is proved to differ from a simple, explicit D-finite series (related to the enumeration of walks confined to the first quadrant) by an algebraic one. The principle of the approach is the same as in [1], but challenging theoretical and computational difficulties arise as we now handle algebraic series of larger degree.

We also explain why we expect the observed algebraicity phenomenon to persist for 4 more models, for which the quadrant problem is solvable using the reflection principle.

2012 ACM Subject Classification Theory of computation → Random walks and Markov chains; Mathematics of computing → Enumeration; Mathematics of computing → Generating functions; Mathematics of computing → Computations on polynomials

Keywords and phrases Enumerative combinatorics, lattice paths, non-convex cones, algebraic series, D-finite series

Digital Object Identifier 10.4230/LIPIcs.AofA.2020.8

Funding *Michael Wallner*: Supported by the Erwin Schrödinger Fellowship of the Austrian Science Fund (FWF): J 4162-N35.

Acknowledgements We thank our referees for their careful reading.

1 Introduction

In this paper we continue the enumeration of plane lattice paths confined to non-convex cones initiated by the first author in [1]. Therein the two most natural models of walks confined to the three-quadrant cone $\mathcal{C} := \{(i, j) : i \geq 0 \text{ or } j \geq 0\}$ were studied: walks with steps $\{\rightarrow, \uparrow, \leftarrow, \downarrow\}$, and those with steps $\{\nearrow, \nwarrow, \swarrow, \searrow\}$. In both cases, the generating function that counts walks starting at the origin was proved to differ (additively) from a simple explicit D-finite series by an algebraic one. The tools essentially involved power series manipulations, coefficient extractions, and polynomial elimination.

Later, Raschel and Trotignon gave in [13] sophisticated integral expressions for 8 models, which imply that 3 additional models ($\{\nearrow, \leftarrow, \downarrow\}$, $\{\rightarrow, \uparrow, \swarrow\}$, and $\{\rightarrow, \nearrow, \uparrow, \leftarrow, \swarrow, \downarrow\}$) are D-finite. Their results use an analytic approach inspired by earlier work on probabilistic and enumerative aspects of quadrant walks [5, 12].

In this paper we first extend the results of [1] to the so-called *king walks*, which take their steps from $\{\rightarrow, \nearrow, \uparrow, \nwarrow, \leftarrow, \swarrow, \downarrow, \searrow\}$. We show that the *algebraicity phenomenon* of [1] persists: if $Q(x, y; t)$ (resp. $C(x, y; t)$) counts walks starting from the origin that are confined



© Mireille Bousquet-Mélou and Michael Wallner;
licensed under Creative Commons License CC-BY

31st International Conference on Probabilistic, Combinatorial and Asymptotic Methods for the Analysis of Algorithms (AofA 2020).

Editors: Michael Drmota and Clemens Heuberger; Article No. 8; pp. 8:1–8:14



Leibniz International Proceedings in Informatics

Schloss Dagstuhl – Leibniz-Zentrum für Informatik, Dagstuhl Publishing, Germany

8:2 More Models of Walks Avoiding a Quadrant

to the non-negative quadrant $\mathcal{Q} := \{(i, j) : i \geq 0 \text{ and } j \geq 0\}$ (resp. to the cone \mathcal{C}) by the length (variable t) and the coordinates of the endpoint (variables x, y), then $C(x, y; t)$ differs from the series

$$\frac{1}{3} (Q(x, y; t) - Q(1/x, y; t)/x^2 - Q(x, 1/y; t)/y^2)$$

by an algebraic series, as detailed in our main theorem below. Moreover, we expect a similar property to hold (with variations on the above linear combination of the series Q) for the 7 step sets of Figure 1, related to reflection groups, and for which the quadrant problem can be solved using the reflection principle [7]. However, we also expect the effective solution of these models to be extremely challenging in computational terms, mostly, because the relevant algebraic series have very large degree. This is illustrated by our main theorem below. There, and in the sequel, we use the shorthand $\bar{x} = 1/x, \bar{y} = 1/y$, and omit in the notation the dependencies on t , writing for instance $Q(x, y)$ instead of $Q(x, y; t)$.

► **Theorem 1.** *Take the step set $\{-1, 0, 1\}^2 \setminus \{(0, 0)\}$ and let $Q(x, y)$ be the generating function of lattice walks starting from $(0, 0)$ that are confined to the first quadrant \mathcal{Q} (this series is D -finite and given in [3]). Then, the generating function of walks starting from $(0, 0)$, confined to \mathcal{C} , and ending in the first quadrant (resp. at a negative abscissa) is*

$$\frac{1}{3}Q(x, y) + P(x, y), \quad (\text{resp. } -\frac{\bar{x}^2}{3}Q(\bar{x}, y) + \bar{x}M(\bar{x}, y)), \tag{1}$$

where $P(x, y)$ and $M(x, y)$ are algebraic of degree 216 over $\mathbb{Q}(x, y, t)$. Of course, the generating function of walks ending at a negative ordinate follows, using the x/y -symmetry.

The series P is expressed in terms of M by:

$$P(x, y) = \bar{x}(M(x, y) - M(0, y)) + \bar{y}(M(y, x) - M(0, x)), \tag{2}$$

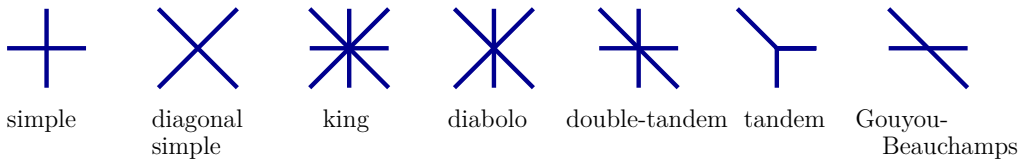
and M is defined by the following equation:

$$K(x, y) (2M(x, y) - M(0, y)) = \frac{2x}{3} - 2t\bar{y}(x + 1 + \bar{x})M(x, 0) + t\bar{y}(y + 1 + \bar{y})M(y, 0) + t(x - \bar{x})(y + 1 + \bar{y})M(0, y) - t(1 + \bar{y}^2 - 2\bar{x}\bar{y})M(0, 0) - t\bar{y}M_x(0, 0), \tag{3}$$

where $K(x, y) = 1 - t(x + xy + y + \bar{x}y + \bar{x} + \bar{x}\bar{y} + \bar{y} + x\bar{y})$. The specializations $M(x, 0)$ and $M(0, y)$ are algebraic each of degree 72 over $\mathbb{Q}(x, t)$ and $\mathbb{Q}(y, t)$, respectively, and $M(0, 0)$ and $M_x(0, 0)$ have degree 24 over $\mathbb{Q}(t)$.

We have moreover a complete algebraic description of all the series needed to reconstruct $P(x, y)$ and $M(x, y)$ from (2) and (3), namely the univariate series $M(0, 0)$ and $M_x(0, 0)$, and the bivariate series $M(x, 0)$ and $M(0, y)$. In particular, both univariate series lie in the extension of $\mathbb{Q}(t)$ (the field of rational functions in t) generated in 3 steps as follows: first, $u = t + t^2 + \mathcal{O}(t^3)$ is the only series in t satisfying

$$(1 - 3u)^3(1 + u)t^2 + (1 + 18u^2 - 27u^4)t - u = 0, \tag{4}$$



■ **Figure 1** The seven step sets to which the strategy of this paper should apply. The first two are solved in [1], the third one in this paper.

then $v = t + 3t^2 + \mathcal{O}(t^3)$ is the only series with constant term zero satisfying

$$(1 + 3v - v^3)u - v(v^2 + v + 1) = 0, \tag{5}$$

and finally

$$w = \sqrt{1 + 4v - 4v^3 - 4v^4} = 1 + 2t + 4t^2 + \mathcal{O}(t^3). \tag{6}$$

Schematically, $\mathbb{Q}(t) \xrightarrow{4} \mathbb{Q}(t, u) \xrightarrow{3} \mathbb{Q}(t, v) \xrightarrow{2} \mathbb{Q}(t, w)$. Of particular interest is the series $M(0, 0)$: by (1), this is also the series $C_{-1,0}$ that counts by the length walks in \mathcal{C} ending at $(-1, 0)$. It is algebraic, as conjectured in [13], and given by

$$M(0, 0) = C_{-1,0} = \frac{1}{2t} \left(\frac{w(1 + 2v)}{1 + 4v - 2v^3} - 1 \right) = t + 2t^2 + 17t^3 + 80t^4 + 536t^5 + \mathcal{O}(t^6). \tag{7}$$

Due to the lack of space, the extensions of $\mathbb{Q}(x, t)$ generated by $M(x, 0)$ and $M(0, x)$ will only be described in the long version of this paper.

Once the series $C(x, y)$ is determined, we can derive detailed asymptotic results, which refine general results of Denisov and Wachtel [4] and Mustapha [11] (who only obtain the following estimates up to a multiplicative factor).

► **Corollary 2.** *The number $c_{0,0}(n)$ of n -step king walks confined to \mathcal{C} and ending at the origin, and the number $c(n)$ of walks of \mathcal{C} ending anywhere satisfy for $n \rightarrow \infty$:*

$$c_{0,0}(n) \sim \left(\frac{2^{29}K}{3^7} \right)^{1/3} \frac{\Gamma(2/3)}{\pi} \frac{8^n}{n^{5/3}},$$

$$c(n) \sim \left(\frac{2^{32}K}{3^7} \right)^{1/6} \frac{1}{\Gamma(2/3)} \frac{8^n}{n^{1/3}},$$

where K is the unique real root of $101^6K^3 - 601275603K^2 + 92811K - 1$.

Outline of the paper

We begin in Section 2 with a general discussion on models of walks with small steps confined to the cone \mathcal{C} , and on the related functional equations. The main part of the paper, Section 3, is devoted to the solution of the king model. We sketch in the final Section 4 what should be the starting point for the 4 rightmost models of Figure 1.

Some definitions and notation

Let \mathbb{A} be a commutative ring and x an indeterminate. We denote by $\mathbb{A}[x]$ (resp. $\mathbb{A}[[x]]$) the ring of polynomials (resp. formal power series) in x with coefficients in \mathbb{A} . If \mathbb{A} is a field, then $\mathbb{A}(x)$ denotes the field of rational functions in x , and $\mathbb{A}((x))$ the field of Laurent series in x , that is, series of the form $\sum_{n \geq n_0} a_n x^n$, with $n_0 \in \mathbb{Z}$ and $a_n \in \mathbb{A}$. The coefficient of x^n in a series $F(x)$ is denoted by $[x^n]F(x)$.

This notation is generalized to polynomials, fractions, and series in several indeterminates. If $F(x, x_1, \dots, x_d)$ is a series in the x_i 's whose coefficients are Laurent series in x , say

$$F(x, x_1, \dots, x_d) = \sum_{i_1, \dots, i_d} x_1^{i_1} \cdots x_d^{i_d} \sum_{n \geq n_0(i_1, \dots, i_d)} a(n, i_1, \dots, i_d) x^n,$$

then the *non-negative part of F in x* is the following formal power series in x, x_1, \dots, x_d :

$$[x^{\geq 0}]F(x, x_1, \dots, x_d) = \sum_{i_1, \dots, i_d} x_1^{i_1} \cdots x_d^{i_d} \sum_{n \geq 0} a(n, i_1, \dots, i_d) x^n.$$

8:4 More Models of Walks Avoiding a Quadrant

We define similarly the negative part of F , its positive part, and so on. We denote with bars the reciprocals of variables: that is, $\bar{x} = 1/x$, so that $\mathbb{A}[x, \bar{x}]$ is the ring of Laurent polynomials in x with coefficients in \mathbb{A} .

If \mathbb{A} is a field, a power series $F(x) \in \mathbb{A}[[x]]$ is *algebraic* (over $\mathbb{A}(x)$) if it satisfies a non-trivial polynomial equation $P(x, F(x)) = 0$ with coefficients in \mathbb{A} . It is *differentially finite* (or *D-finite*) if it satisfies a non-trivial linear differential equation with coefficients in $\mathbb{A}(x)$. For multivariate series, D-finiteness requires the existence of a differential equation *in each variable*. We refer to [8, 9] for general results on D-finite series.

As mentioned above, we usually omit the dependency in t of our series. For a series $F(x, y; t) \in \mathbb{Q}[x, \bar{x}, y, \bar{y}][[t]]$ and two integers i and j , we denote by $F_{i,j}$ the coefficient of $x^i y^j$ in $F(x, y; t)$. This is a series in $\mathbb{Q}[[t]]$.

2 Enumeration in the three-quarter plane

We fix a subset \mathcal{S} of $\{-1, 0, 1\}^2 \setminus \{(0, 0)\}$ and we want to count walks with steps in \mathcal{S} that start from the origin $(0, 0)$ of \mathbb{Z}^2 and remain in the cone $\mathcal{C} := \{(x, y) : x \geq 0 \text{ or } y \geq 0\}$. By this, we mean that not only must every vertex of the walk lie in \mathcal{C} , but also every edge: a walk containing a step from $(-1, 0)$ to $(0, -1)$ (or vice versa) is not considered as lying in \mathcal{C} . We often say for short that our walks *avoid the negative quadrant*. The *step polynomial* of \mathcal{S} is defined by

$$S(x, y) = \sum_{(i,j) \in \mathcal{S}} x^i y^j = \bar{y}H_-(x) + H_0(x) + yH_+(x) = \bar{x}V_-(y) + V_0(y) + xV_+(y),$$

for some Laurent polynomials H_-, H_0, H_+ and V_-, V_0, V_+ (of degree at most 1 and valuation at least -1) recording horizontal and vertical displacements, respectively. We denote by $C(x, y; t) \equiv C(x, y)$ the generating function of walks confined to \mathcal{C} , where the variable t records the length of the walk, and x and y the coordinates of its endpoints:

$$C(x, y) = \sum_{(i,j) \in \mathcal{C}} \sum_{n \geq 0} c_{i,j}(n) x^i y^j t^n = \sum_{(i,j) \in \mathcal{C}} x^i y^j C_{i,j}(t). \quad (8)$$

Here, $c_{i,j}(n)$ is the number of walks of length n that go from $(0, 0)$ to (i, j) and that are confined to \mathcal{C} .

2.1 Interesting step sets

As in the quadrant case [3], we can decrease the number of step sets that are worth being considered (*a priori*, there are 2^8 of them) thanks to a few simple observations:

- Since the cone \mathcal{C} (as well as the quarter plane \mathcal{Q}) is x/y -symmetric, the models defined by \mathcal{S} and by its mirror image $\bar{\mathcal{S}} := \{(j, i) : (i, j) \in \mathcal{S}\}$ are equivalent; the associated generating functions are related by $\bar{C}(x, y) = C(y, x)$.
- If all steps of \mathcal{S} are contained in the right half-plane $\{(x, y) : x \geq 0\}$, then *all* walks with steps in \mathcal{S} lie in \mathcal{C} , and the series $C(x, y) = 1/(1 - tS(x, y))$ is simply rational. The series $Q(x, y)$ is known to be algebraic in this case [6].
- If all steps of \mathcal{S} are contained in the left half-plane $\{(x, y) : x \leq 0\}$, then confining a walk to \mathcal{C} is equivalent to confining it to the upper half-plane: the associated generating function is then algebraic, and so is $Q(x, y)$.
- If all steps of \mathcal{S} lie (weakly) above the first diagonal ($x = y$), then confining a walk to \mathcal{C} is again equivalent to confining it to the upper half-plane: the associated generating function is then algebraic, and so is $Q(x, y)$.

- Finally, if all steps of \mathcal{S} lie (weakly) above the second diagonal ($x + y = 0$), then all walks with steps in \mathcal{C} lie in \mathcal{C} , and $C(x, y) = 1/(1 - tS(x, y))$ is simply rational. In this case however, the series $Q(x, y)$ is not at all trivial [3, 10]. Such step sets are sometimes called *singular* in the framework of quadrant walks.

Symmetric statements allow us to discard step sets that lie in the upper half-plane $\mathbb{Z} \times \mathbb{N}$, in the lower half-plane $\mathbb{Z} \times (-\mathbb{N})$, or weakly below the x/y diagonal.

In conclusion, one finds that there are exactly 51 essentially distinct models of walks avoiding the negative quadrant that are worth studying: the 56 models considered for quadrant walks (see Tables 1–4 in [3]) except the 5 singular models for which all steps of \mathcal{S} lie weakly above the diagonal $x + y = 0$.

2.2 A functional equation

Constructing walks confined to \mathcal{C} step by step gives the following functional equation:

$$C(x, y) = 1 + tS(x, y)C(x, y) - t\bar{y}H_-(x)C_{-,0}(\bar{x}) - t\bar{x}V_-(y)C_{0,-}(\bar{y}) - t\bar{x}\bar{y}C_{0,0}\mathbb{1}_{(-1,-1)\in\mathcal{S}},$$

where the series $C_{-,0}(\bar{x})$ and $C_{0,-}(\bar{y})$ count walks ending on the horizontal and vertical boundaries of \mathcal{C} (but not at $(0, 0)$):

$$C_{-,0}(\bar{x}) = \sum_{\substack{i < 0 \\ n \geq 0}} c_{i,0}(n)x^i t^n \in \bar{x}\mathbb{Q}[\bar{x}][[t]],$$

$$C_{0,-}(\bar{y}) = \sum_{\substack{j < 0 \\ n \geq 0}} c_{0,j}(n)y^j t^n \in \bar{y}\mathbb{Q}[\bar{y}][[t]].$$

On the right-hand side of the above functional equation, the term 1 accounts for the empty walk, the next term describes the extension of a walk in \mathcal{C} by one step of \mathcal{S} , and each of the other three terms correspond to a “bad” move, either starting from the negative x -axis, or from the negative y -axis, or from $(0, 0)$. Equivalently,

$$K(x, y)C(x, y) = 1 - t\bar{y}H_-(x)C_{-,0}(\bar{x}) - t\bar{x}V_-(y)C_{0,-}(\bar{y}) - t\bar{x}\bar{y}C_{0,0}\mathbb{1}_{(-1,-1)\in\mathcal{S}}, \tag{9}$$

where $K(x, y) := 1 - tS(x, y)$ is the *kernel* of the equation.

The case of walks confined to the first (non-negative) quadrant \mathcal{Q} has been much studied in the past 15 years. The associated generating function $Q(x, y) \equiv Q(x, y; t) \in \mathbb{Q}[x, y][[t]]$ is defined similarly to (8) and satisfies a similarly looking equation:

$$K(x, y)Q(x, y) = 1 - t\bar{y}H_-(x)Q_{-,0}(x) - t\bar{x}V_-(y)Q_{0,-}(y) + t\bar{x}\bar{y}Q_{0,0}\mathbb{1}_{(-1,-1)\in\mathcal{S}},$$

where now

$$Q_{-,0}(x) = \sum_{\substack{i \geq 0 \\ n \geq 0}} q_{i,0}(n)x^i t^n = Q(x, 0) \in \mathbb{Q}[x][[t]],$$

$$Q_{0,-}(y) = \sum_{\substack{j \geq 0 \\ n \geq 0}} q_{0,j}(n)y^j t^n = Q(0, y) \in \mathbb{Q}[y][[t]].$$

3 The king walks

In this section we focus on the case where the 8 steps of $\{-1, 0, 1\}^2 \setminus \{(0, 0)\}$ are allowed. That is,

$$S(x, y) = (\bar{x} + 1 + x)(\bar{y} + 1 + y) - 1 = x + xy + y + \bar{x}y + \bar{x} + \bar{x}\bar{y} + \bar{y} + x\bar{y}.$$

8:6 More Models of Walks Avoiding a Quadrant

The functional equation (9) specializes to

$$K(x, y)C(x, y) = 1 - t\bar{y}(x + 1 + \bar{x})C_-(\bar{x}) - t\bar{x}(y + 1 + \bar{y})C_-(\bar{y}) - t\bar{x}\bar{y}C_{0,0}, \quad (10)$$

where we have denoted $C_-(\bar{x}) = C_{-,0}(\bar{x}) = C_{0,-}(\bar{x})$ (by symmetry). Equivalently,

$$xyK(x, y)C(x, y) = xy - t(x^2 + x + 1)C_-(\bar{x}) - t(y^2 + y + 1)C_-(\bar{y}) - tC_{0,0}. \quad (11)$$

The generating function $Q(x, y)$ of quadrant walks satisfies

$$xyK(x, y)Q(x, y) = xy - t(x^2 + x + 1)Q(x, 0) - t(y^2 + y + 1)Q(0, y) + tQ_{0,0}. \quad (12)$$

3.1 Reduction to an equation with orbit sum zero

A key object in the study of walks confined to the first quadrant is a certain group of birational transformations that depends on the step set. For king walks, it is generated by $(x, y) \mapsto (\bar{x}, y)$ and $(x, y) \mapsto (x, \bar{y})$. As in [1], the similarities between the equations for C and Q , combined with the structure of this group, lead us to define a new series $A(x, y)$ by

$$C(x, y) = A(x, y) + \frac{1}{3} (Q(x, y) - \bar{x}^2 Q(\bar{x}, y) - \bar{y}^2 Q(x, \bar{y})). \quad (13)$$

Then the combination of (11) and (12) gives

$$xyK(x, y)A(x, y) = \frac{2xy + \bar{x}y + x\bar{y}}{3} - t(x^2 + x + 1)A_-(\bar{x}) - t(y^2 + y + 1)A_-(\bar{y}) - tA_{0,0},$$

and it follows from this equation that $xyA(x, y)$ has *orbit sum zero*. By this, we mean:

$$xyA(x, y) - \bar{x}yA(\bar{x}, y) + \bar{x}\bar{y}A(\bar{x}, \bar{y}) - x\bar{y}A(x, \bar{y}) = 0. \quad (14)$$

Theorem 1 states that $A(x, y)$ is algebraic. In Section 4 we define an analogous series A for all models of Figure 1 which we expect to be systematically algebraic.

The proof of Theorem 1 starts as in the case of the simple and diagonal walks in [1]. The first objective, achieved in Section 3.5, is to derive an equation that involves a single bivariate series, essentially $A_-(x)$ (and no trivariate series). In principle, the “generalized quadratic method” of [2] then solves it routinely. But in practise, the king model turns out to be much more difficult to solve than the other two, and raises serious computational difficulties. In what follows, we focus on the points of the derivation that differ from [1]. We have performed all computations with the computer algebra system MAPLE. The corresponding sessions will be available on the authors’ webpages with the long version of the paper.

3.2 Reduction to a quadrant-like problem

We separate in $A(x, y)$ the contributions of the three quadrants, again using the x/y -symmetry of the step set:

$$A(x, y) = P(x, y) + \bar{x}M(\bar{x}, y) + \bar{y}M(\bar{y}, x),$$

where $P(x, y)$ and $M(x, y)$ lie in $\mathbb{Q}[x, y][[t]]$. Note that this identity defines P and M uniquely in terms of A . Replacing A by this expression, and extracting the positive part in x and y from the orbit equation (14) relates the series P and M by

$$xyP(x, y) = y(M(x, y) - M(0, y)) + x(M(y, x) - M(0, x)),$$

which is exactly the same as [1, Eq. (22)], and as Eq. (2) in Theorem 1. We then follow the lines of proof of [1, Sec. 2.3] to obtain the functional equation (3) for M .

3.3 An equation between $M(0, x)$, $M(0, \bar{x})$, and $M(x, 0)$

Next we will cancel the kernel K . As a polynomial in y , the kernel admits only one root that is a formal power series in t :

$$Y(x) = \frac{1 - t(x + \bar{x}) - \sqrt{(1 - t(x + \bar{x}))^2 - 4t^2(x + 1 + \bar{x})^2}}{2t(x + 1 + \bar{x})} = (x + 1 + \bar{x})t + \mathcal{O}(t^2).$$

Note that $Y(x) = Y(\bar{x})$. We specialize (3) to the pairs $(x, Y(x))$, $(\bar{x}, Y(x))$, $(Y(x), x)$, and $(Y(x), \bar{x})$ (the left-hand side vanishes for each specialization since $K(x, y) = K(y, x)$), and eliminate $M(0, Y)$, $M(Y, 0)$, and $M(\bar{x}, 0)$ from the four resulting equations. We obtain:

$$\begin{aligned} (x + 1 + \bar{x}) \left(Y(x) - \frac{1}{Y(x)} \right) (xM(0, x) - 2\bar{x}M(0, \bar{x})) + 3(x + 1 + \bar{x})M(x, 0) \\ - \frac{2\bar{x}Y(x)}{t} + 3M_{1,0} + (2Y(x) - x - \bar{x})M_{0,0} = 0. \end{aligned} \tag{15}$$

3.4 An equation between $M(0, x)$ and $M(0, \bar{x})$

Let us denote the discriminant occurring in $Y(x)$ by

$$\Delta(x) := (1 - t(x + \bar{x}))^2 - 4t^2(x + 1 + \bar{x})^2 = (1 - t(3(x + \bar{x}) + 2))(1 + t(x + \bar{x} + 2)) \tag{16}$$

and introduce the notation

$$\begin{aligned} R(x) &:= t^2M(x, 0) = \frac{xt^2}{3} + \left(1 + \frac{x^2}{3}\right)t^3 + \mathcal{O}(t^4), \\ S(x) &:= txM(0, x) = x(1 + x)t^2 + 2x(1 + x + x^2)t^3 + \mathcal{O}(t^4). \end{aligned} \tag{17}$$

Then (15) reads

$$\begin{aligned} \sqrt{\Delta(x)} \left(S(x) - 2S(\bar{x}) + \frac{R(0) - t\bar{x}}{t(x + 1 + \bar{x})} \right) = 3(x + 1 + \bar{x})R(x) + 3R'(0) \\ + \frac{1 - t(x + \bar{x})(x + 2 + \bar{x})}{t(x + 1 + \bar{x})}R(0) - \frac{1 - t(x + \bar{x})}{1 + x + x^2}. \end{aligned} \tag{18}$$

Next, we square this equation and extract the negative part in x . The series $R(x)$ (mostly) disappears as it involves only non-negative powers of x . This gives an expression for the negative part of $\Delta(x)S(x)S(\bar{x})$. Using the symmetry of $\Delta(x)$ in x and \bar{x} , we then reconstruct an expression of $\Delta(x)S(x)S(\bar{x})$ that does not involve $R(x)$, as in [1, Sec. 2.5].

During these calculations, we have to extract the negative and non-negative parts in series of the form $F(x)/(1 + x + \bar{x})^m$, where $F(x)$ is a series in t with coefficients in $\mathbb{Q}[x, \bar{x}]$. Upon performing a partial fraction expansion, and separating in F the negative and non-negative parts, we see that the key question is how to extract and express the non-negative part in series of the form $F(\bar{x})/(1 - \zeta_i x)^m$, where $F(x) \in \mathbb{C}[x][[t]]$ and

$$\zeta_1 := -\frac{1}{2} + \frac{i\sqrt{3}}{2} \quad \text{and} \quad \zeta_2 := -\frac{1}{2} - \frac{i\sqrt{3}}{2}$$

are the primitive cubic roots of unity. A simple calculation establishes the following lemma.

► **Lemma 3** (Non-negative part at pole ρ). *Let $F(x) \in \mathbb{C}[x][[t]]$ and $\rho \in \mathbb{C}$. Then,*

$$\begin{aligned} [x \geq 0] \frac{F(\bar{x})}{1 - \rho x} &= \frac{F(\rho)}{1 - \rho x}, \\ [x \geq 0] \frac{F(\bar{x})}{(1 - \rho x)^2} &= \frac{F(\rho)}{(1 - \rho x)^2} + \frac{\rho F'(\rho)}{1 - \rho x}. \end{aligned}$$

8:8 More Models of Walks Avoiding a Quadrant

One outcome of the extraction procedure is the following identity:

$$S(\zeta_1) = S(\zeta_2) = -\frac{R(0) + 3R'(0)}{1+t} = -t^2 - 11t^4 - 30t^5 + \mathcal{O}(t^6). \quad (19)$$

Using these results, we finally arrive at an equation relating $S(x)$ and $S(\bar{x})$:

$$\begin{aligned} \Delta(x) \left(S(x)^2 + S(\bar{x})^2 - S(x)S(\bar{x}) + \frac{S(x)(xt - R(0)) + \bar{x}S(\bar{x})(\bar{x}t - R(0))}{t(x+1+\bar{x})} \right) = \\ (1+t)S(\zeta_1) \left(2(x+1+\bar{x})R(0) - \frac{(1-t(x+\bar{x}))(t(x+\bar{x}) - 2R(0))}{t(x+1+\bar{x})} \right) \\ + (1+4t)(x+\bar{x})R(0) - (t^2 + tR(0) + R(0)^2)(x^2 + \bar{x}^2) + \Delta_0, \end{aligned} \quad (20)$$

where Δ_0 is the coefficient of x^0 in $\Delta(x)S(x)S(\bar{x})$.

3.5 An equation for $M(0, x)$ only

Equation (20) is almost ready for a positive part extraction, except for the mixed term $S(x)S(\bar{x})$. To eliminate it, we multiply (20) by $S(x) + S(\bar{x}) + \frac{x+\bar{x}-2R(0)/t}{x+1+\bar{x}}$. Then we are able to extract the non-negative terms in x . Hereby we repeatedly apply Lemma 3. Additionally, we use $R(0) = tS'(0)$ and (19). Furthermore, we work with the real and imaginary parts of $\zeta_1 S'(\zeta_1)$ and $\zeta_2 S'(\zeta_2)$. More precisely, we define

$$\begin{aligned} (1+t)^2 \zeta_1 S'(\zeta_1) &= B_1 + i\sqrt{3}B_2, \\ (1+t)^2 \zeta_2 S'(\zeta_2) &= B_1 - i\sqrt{3}B_2. \end{aligned}$$

(Note that B_1 and B_2 here are series in t .) In the end we get a cubic equation in $S(x)$:

$$\text{Pol}(S(x), S'(0), S(\zeta_1), B_1, B_2, t, x) = 0, \quad (21)$$

where the polynomial $\text{Pol}(x_0, x_1, x_2, x_3, x_4, t, x)$ is given in Appendix A.

3.6 The generalized quadratic method

We now use the results of [2] to obtain a system of four polynomial equations relating the series $S'(0)$, $S(\zeta_1)$, B_1 , and B_2 . Combined with a few initial terms, this system characterizes these four series. Unfortunately, it turned out to be too big for us to solve it completely, be it by bare hand elimination or using Gröbner bases: we did obtain a polynomial equation for $S'(0)$ and $S(\zeta_1)$, but not for the other two series. Instead, we have resorted to a guess-and-check approach, consisting in *guessing* such equations (of degree 12 or 24, depending on the series), and then *checking* that they satisfy the system. This guess-and-check approach is detailed in the next subsection. For the moment, let us explain how the system is obtained.

The approach of [2] instructs us to consider the fractional series X (in t), satisfying

$$\text{Pol}_{x_0}(S(X), S'(0), S(\zeta_1), B_1, B_2, t, X) = 0, \quad (22)$$

where Pol_{x_0} stands for the derivative of Pol with respect to its first variable. The number and first terms of such series X depend only on the first terms of the series $S(x)$, $S'(0)$, $S(\zeta_1)$, B_1 , and B_2 (see [2, Thm. 2]). We find that 6 such series exist:

$$\begin{aligned} X_1(t) &= i + 2t^2 + 4t^3 + (36 - 2i)t^4 + \mathcal{O}(t^5), \\ X_2(t) &= -i + 2t^2 + 4t^3 + (36 + 2i)t^4 + \mathcal{O}(t^5), \\ X_3(t) &= \sqrt{t} + t + \frac{3}{2}t^{3/2} + 3t^2 + \frac{51}{8}t^{5/2} + 14t^3 + \mathcal{O}(t^{7/2}), \\ X_4(t) &= -\sqrt{t} + t - \frac{3}{2}t^{3/2} + 3t^2 - \frac{51}{8}t^{5/2} + 14t^3 + \mathcal{O}(t^{7/2}), \\ X_5(t) &= i\sqrt{t} - it^{3/2} + 2it^{5/2} + t^3 - 4it^{7/2} + 2t^4 + \mathcal{O}(t^{9/2}), \\ X_6(t) &= -i\sqrt{t} + it^{3/2} - 2it^{5/2} + t^3 + 4it^{7/2} + 2t^4 + \mathcal{O}(t^{9/2}). \end{aligned}$$

Note that the coefficients of X_1 and X_2 (resp. X_5 and X_6) are conjugates of one another. As discussed in [2], each of these series X also satisfies

$$\text{Pol}_x(S(X), S'(0), S(\zeta_1), B_1, B_2, t, X) = 0, \tag{23}$$

where Pol_x is the derivative with respect to the last variable of Pol , and (of course)

$$\text{Pol}(S(X), S'(0), S(\zeta_1), B_1, B_2, t, X) = 0. \tag{24}$$

Using this, we can easily identify two of the series X_i : indeed, eliminating B_1 and B_2 between the three equations (22), (23), and (24) gives a polynomial equation between $S(X), S'(0), S(\zeta_1), t$, and X , which factors. Remarkably, its simplest non-trivial factor does not involve $S(X)$, nor $S'(0)$ nor $S(\zeta_1)$, and reads

$$X^2 - t(1 + X)^2(1 + X^2). \tag{25}$$

By looking at the first terms of the X_i 's and the other factors, one concludes that the above equation holds for X_3 and X_4 , which are thus explicit.

Let $D(x_1, \dots, x_4, t, x)$ be the discriminant of $\text{Pol}(x_0, \dots, x_4, t, x)$ with respect to x_0 . According to [2, Thm. 14], each X_i is a *double root* of $D(S'(0), S(\zeta_1), B_1, B_2, t, x)$, seen as a polynomial in x . Hence this polynomial, which involves 4 unknown series $S'(0), S(\zeta_1), B_1, B_2$, has (at least) 6 double roots. This seems more information than we need! In principle, 4 double roots should suffice to give 4 conditions relating the 4 unknown series. However, we shall see that there is some redundancy in the 6 series X_i , which comes from the special form of D .

We first observe that D factors as

$$D(S'(0), S(\zeta_1), B_1, B_2, t, x) = 27x^2(1 + x + x^2)^2\Delta(x)D_1(S'(0), S(\zeta_1), B_1, B_2, t, x),$$

where $\Delta(x)$ is defined by (16), and D_1 has degree 24 in x . It is easily checked that none of the X_i 's are roots of the prefactors, so they are double roots of D_1 . But we observe that D_1 is symmetric in x and \bar{x} . More precisely,

$$D_1(S'(0), S(\zeta_1), B_1, B_2, t, x) = x^{12}D_2(S'(0), S(\zeta_1), B_1, B_2, t, x + 1 + \bar{x}),$$

for some polynomial $D_2(x_1, \dots, x_4, t, s) \equiv D_2(s)$ of degree 12 in s . Since each X_i is a double root of D_1 , each series $S_i := X_i + 1 + 1/X_i$, for $1 \leq i \leq 6$, is a double root of D_2 . The series S_i , for $2 \leq i \leq 6$, are easily seen from their first terms to be distinct, but the first terms of S_1 and S_2 suspiciously agree: one suspects (and rightly so), that $X_2 = 1/X_1$, and carefully

8:10 More Models of Walks Avoiding a Quadrant

concludes that D_2 has (at least) 5 double roots in s . Moreover, since X_3 and X_4 satisfy (25), the corresponding series S_3 and S_4 are the roots of $1 + t = tS_i^2$, that is, $S_{3,4} = \pm\sqrt{1 + 1/t}$. The other roots start as follows:

$$S_2 = 1 + 4t^2 + 8t^3 + \mathcal{O}(t^4), \quad S_{5,6} = \mp \frac{i}{\sqrt{t}} + 1 + t^2 \pm it^{5/2} + \mathcal{O}(t^3).$$

But this is not the end of the story: indeed, D_2 appears to be almost symmetric in s and $1/s$. More precisely, we observe that

$$D_2(S'(0), S(\zeta_1), B_1, B_2, s) = s^6 D_3 \left(S'(0), S(\zeta_1), B_1, B_2, ts + \frac{t+1}{s} \right),$$

for some polynomial $D_3(S'(0), S(\zeta_1), B_1, B_2, t, z) \equiv D_3(z)$ of degree 6 in z . It follows that each series $Z_i := tS_i + (1+t)/S_i$, for $2 \leq i \leq 6$, is a root of $D_3(z)$, and even a double root, unless $tS_i^2 = 1+t$, which precisely occurs for $i = 3, 4$. One finds $Z_{3,4} = \pm 2\sqrt{t(1+t)}$,

$$Z_2 = 1 + 2t - 4t^2 + \mathcal{O}(t^3), \quad Z_{5,6} = 2t + 2t^3 + \mathcal{O}(t^4).$$

Since Z_5 and Z_6 seem indistinguishable, we safely conclude that $D_3(z)$ has two double roots Z_2 and Z_5 , and a factor $(z^2 - 4t(1+t))$. Writing

$$D_3(z) = \sum_{i=0}^6 d_i z^i,$$

these properties imply, by matching the three monomials of highest degree, that

$$D_3(z) = \frac{(z^2 - 4t(1+t)) (8z^2 d_6^2 + 4z d_5 d_6 + 16t^2 d_6^2 + 16t d_6^2 + 4d_4 d_6 - d_5^2)^2}{64 d_6^3}.$$

Extracting the coefficients of z^0, \dots, z^3 gives 4 polynomial relations between the coefficients d_i , resulting in 4 polynomial relations between the 4 series $S'(0), S(\zeta_1), B_1, B_2$. One easily checks that this system, combined with the first terms of these series, defines them uniquely.

As explained at the beginning of this subsection, we have at the moment only been able to derive from this system polynomial equations (of degree 24) for $S'(0)$ and $S(\zeta_1)$. For the other two, we had to resort to a guess-and-check approach, which we now describe.

3.7 Guess-and-check

Guessing. Returning to the functional equation (10) it is easy to extract a simple recurrence for the polynomials $c_n(x, y)$ that count walks of length n by the position of their endpoint. We implemented this recurrence in the programming language *C* using modular arithmetic and the Chinese remainder theorem to compute the explicit values of this sequence up to $n = 2000$. Then we were able to guess polynomial equations satisfied by $S'(0)$, $S(\zeta_1)$, B_1 , and B_2 using the `gfun` package in MAPLE [14]. Of course, those obtained for $S'(0)$ and $S(\zeta_1)$ coincide with those that we derived from the system of the previous subsection. Details on the corresponding equations are shown below.

Generating function	Degree in GF	Degree in t	Number of terms
$S'(0)$	24	12	323
$S(\zeta_1)$	24	32	823
B_1	12	26	229
B_2	24	60	477

Checking that the guessed series satisfy the system turns out to be much easier once the algebraic structure of these series is elucidated, which we do below¹. We have not tried a direct check.

The algebraic structure of $S'(0)$, $S(\zeta_1)$, B_1 , and B_2 . We begin with the simplest series, B_1 , of (conjectured) degree 12. Let $P(F, t)$ be its guessed monic minimal polynomial. Using the `Subfields` command of MAPLE for several fixed values of t , one conjectures that the extension $\mathbb{Q}(t, B_1)$ possesses a subfield $\mathbb{Q}(t, u)$ of degree 4 over $\mathbb{Q}(t)$. MAPLE gives a possible generator u for fixed values of t , but how can we choose u for a generic t ? Indeed, the value of u given by MAPLE for fixed t has no reason to be canonical. But the factorisation of $P(F, t)$ over $\mathbb{Q}(t, u)$, of the form $P_3(F)P_9(F)$ (with P_i of degree i), with coefficients in $\mathbb{Q}(t, u)$, is canonical. Hence we will compute this factorisation, first for fixed values of t . We proceed as follows: we factor $P(F, t)$ over $\mathbb{Q}(t, B_1)$, and find, for fixed $t = 3, \dots, 50$, that

$$P(F, t) = (F - B_1)P_2(F, B_1)P_9(F, B_1),$$

where P_2 (resp. P_9) is a monic polynomial of degree 2 (resp. 9) in F . Hence the cubic factor $P_3(F) = F^3 + p_2F^2 + p_1F + p_0$ must be $(F - B_1)P_2(F, B_1)$, and we have just found its coefficients p_i in terms of B_1 (for t fixed). We now compute the minimal polynomial over \mathbb{Q} of each p_i using a resultant or the `evala/Norm` command in MAPLE. If the above factorization persists for all t , as we expect, each p_i should have a minimal polynomial over $\mathbb{Q}(t)$ of degree (at most) 4. Having computed this polynomial for sufficiently many values of t , we reconstruct its generic form by rational reconstruction. We find that all p_i generate the same extension of degree 4 of $\mathbb{Q}(t)$, and we can take any of them as a first candidate for the generator u . We may simplify this generator further to end with the choice (4). Then we factor $P(F, t)$ over $\mathbb{Q}(t, u)$, and check that our guess was correct: the series B_1 is indeed cubic over $\mathbb{Q}(t, u)$. Moreover, it can be written rationally in terms of t and the series v given by (5).

Finally, we factor the guessed minimal polynomials of $S'(0)$, $S(\zeta_1)$, and B_2 over $\mathbb{Q}(t, v)$, and find that these three series all belong to the same quadratic extension of $\mathbb{Q}(t, v)$, generated by the series w given by (6). In particular,

$$S'(0) = \frac{1}{2} \left(\frac{w(1+2v)}{1+4v-2v^3} - 1 \right),$$

which coincides with (7), given the Definition (17) of $S(x)$.

Now that we have guessed rational expressions of $S'(0)$, $S(\zeta_1)$, B_1 , and B_2 in terms of t , v , and w , the 4 equations obtained in Section 3.6 are readily checked to hold, using the minimal polynomials of v and w .

3.8 Back to $S(x)$ and $R(x)$

For $S(x)$ we start with Equation (21), with all one-variable series replaced by their expressions in terms of t , v , and w . We eliminate w and v using resultants to arrive at an equation of degree 72 over $\mathbb{Q}(t, x)$ for $S(x) = txM(0, x)$.

¹ For this section, we have greatly benefited from the help of Mark van Hoeij (<https://www.math.fsu.edu/~hoeij/>), who explained us how to find subextensions of $\mathbb{Q}(t, B_1)$, and “simple” series in these extensions.

8:12 More Models of Walks Avoiding a Quadrant

We can simplify (21) by working with the depressed equation, i.e., removing the quadratic term by a suitable change of variable. Indeed, defining $T(x)$ by

$$S(x) = T(x) + \frac{3xS'(0) - 2x^2 - 1}{3(x^2 + x + 1)},$$

we find that $T(x)$ satisfies a cubic equation with no quadratic term, involving t and v but not w . That is, $T(x)$ has degree 36 over $\mathbb{Q}(t, x)$, instead of 72 for $S(x)$.

Introducing $T(x)$ also helps understanding the algebraic structure of $R(x)$. Returning to (18), we recall that $R(0) = tS'(0)$ and use (19) to express $R'(0)$ in terms of t, v , and w . The left-hand side simply reads $\sqrt{\Delta(x)}(T(x) - 2T(\bar{x}))$, and is found to be an element of $w\mathbb{Q}(t, x, T(x))$. In the end, $R(x)$ has degree 72 and belongs to the same extension of $\mathbb{Q}(t, x)$ as $S(x)$. This ends the proof of our main result, Theorem 1.

4 More models

For each of the 7 step sets \mathcal{S} of Figure 1, we are able to define a series $A(x, y)$ that

- satisfies the same equation as $C(x, y)$ (see (9)), but with a different constant term,
- satisfies an *orbit sum* identity similar to (14).

Explaining where this series comes from would require us to introduce the group associated to a step set. For the sake of conciseness, we simply define $A(x, y)$ without further justification.

For the first four step sets \mathcal{S} of Figure 1, the series $A(x, y)$ is defined by (13) (with $Q(x, y)$ counting quadrant walks with steps in \mathcal{S}) as we have seen. For the next two step sets,

$$C(x, y) = A(x, y) + \frac{1}{5} (Q(x, y) - \bar{x}^2 y Q(\bar{x}y, y) + \bar{x}^3 Q(\bar{x}y, \bar{x}) + \bar{y}^3 Q(\bar{y}, x\bar{y}) - x\bar{y}^2 Q(x, x\bar{y})).$$

Finally, for the seventh one,

$$C(x, y) = A(x, y) + \frac{1}{7} (Q(x, y) - \bar{x}^2 y Q(\bar{x}y, y) + \bar{x}^4 y Q(\bar{x}y, \bar{x}^2 y) - \bar{x}^4 Q(\bar{x}, \bar{x}^2 y) - \bar{y}^3 Q(x\bar{y}, \bar{y}) + x^2 \bar{y}^3 Q(x\bar{y}, x^2 \bar{y}) - x^2 \bar{y}^2 Q(x, x^2 \bar{y})).$$

In all cases, the series $A(x, y)$ satisfies the following variant of (9):

$$K(x, y)A(x, y) = P_0(x, y) - t\bar{y}H_-(x)A_{-,0}(\bar{x}) - t\bar{x}V_-(y)A_{0,-}(\bar{y}) - t\bar{x}\bar{y}A_{0,0}\mathbb{1}_{(-1,-1)\in\mathcal{S}},$$

where $K(x, y) = 1 - tS(x, y)$ as before, and $P_0(x, y)$ is a Laurent polynomial. This equation is easily obtained by combining the equations for $C(x, y)$ and $Q(x, y)$.

Finally, the vanishing orbit sum, which is (14) for the first four models, reads

$$xyA(x, y) - \bar{x}y^2A(\bar{x}y, y) + \bar{x}^2yA(\bar{x}y, \bar{x}) - \bar{x}\bar{y}A(\bar{y}, \bar{x}) + x\bar{y}^2A(\bar{y}, x\bar{y}) - x^2\bar{y}A(x, x\bar{y}) = 0$$

for the next two, and

$$xyA(x, y) - \bar{x}y^2A(\bar{x}y, y) + \bar{x}^3y^2A(\bar{x}y, \bar{x}^2y) - \bar{x}^3yA(\bar{x}, \bar{x}^2y) + \bar{x}\bar{y}A(\bar{x}, \bar{y}) - x\bar{y}^2A(x\bar{y}, \bar{y}) + x^3\bar{y}^2A(x\bar{y}, x^2\bar{y}) - x^3\bar{y}A(x, x^2\bar{y}) = 0$$

for the last one. We conjecture that the series $A(x, y)$ is systematically algebraic (this is now proved for the first three models). To support this conjecture, we have tried to guess (using the `gfun` package [14] in MAPLE), for the 4 models for which it is still open, a polynomial equation for the series $A_{-1,0}$, which, in all cases, coincides with the generating function $C_{-1,0}$

of walks ending at $(-1, 0)$ (for the second model we consider $A_{-2,0}$ instead, since $A_{-1,0} = 0$ due to the periodicity of the model). This series has degree 4 (resp. 8, 24) in the three solved cases. We could not guess anything for the 4th model (using the counting sequence for such walks up to length $n = 4000$), but we discovered equations of degree 24 for each of the next three.

We believe that it would be worth exploring if the guiding principles of the present paper apply to these 4 other models. In all cases, we expect to face a *system* of quadrant-like equations rather than a single one. We plan to investigate at least some of these models.

To conclude, we recall that the 4 small step models that are algebraic for the quadrant problem are conjectured to be algebraic for the three-quadrant cone as well [1, Fig. 5]. In this case, the series $A(x, y)$ simply coincides with $C(x, y)$, as the orbit sum of $xyC(x, y)$ vanishes.

References

- 1 M. Bousquet-Mélou. Square lattice walks avoiding a quadrant. *J. Combin. Theory Ser. A*, 144:37–79, 2016. doi:10.1016/j.jcta.2016.06.010.
- 2 M. Bousquet-Mélou and A. Jehanne. Polynomial equations with one catalytic variable, algebraic series and map enumeration. *J. Combin. Theory Ser. B*, 96:623–672, 2006. doi:10.1016/j.jctb.2005.12.003.
- 3 M. Bousquet-Mélou and M. Mishna. Walks with small steps in the quarter plane. In *Algorithmic probability and combinatorics*, volume 520 of *Contemp. Math.*, pages 1–39. Amer. Math. Soc., Providence, RI, 2010. doi:10.1090/conm/520/10252.
- 4 D. Denisov and V. Wachtel. Random walks in cones. *Ann. Probab.*, 43(3):992–1044, 2015. doi:10.1214/13-AOP867.
- 5 G. Fayolle, R. Iasnogorodski, and V. Malyshev. *Random walks in the quarter-plane: Algebraic methods, boundary value problems and applications*, volume 40 of *Applications of Mathematics*. Springer-Verlag, Berlin, 1999.
- 6 I. Gessel. A factorization for formal Laurent series and lattice path enumeration. *J. Combin. Theory Ser. A*, 28(3):321–337, 1980. doi:10.1016/0097-3165(80)90074-6.
- 7 I. M. Gessel and D. Zeilberger. Random walk in a Weyl chamber. *Proc. Amer. Math. Soc.*, 115(1):27–31, 1992. doi:10.1090/S0002-9939-1992-1092920-8.
- 8 L. Lipshitz. The diagonal of a D -finite power series is D -finite. *J. Algebra*, 113(2):373–378, 1988. doi:10.1016/0021-8693(88)90166-4.
- 9 L. Lipshitz. D -finite power series. *J. Algebra*, 122:353–373, 1989. doi:10.1016/0021-8693(89)90222-6.
- 10 M. Mishna and A. Rechnitzer. Two non-holonomic lattice walks in the quarter plane. *Theoret. Comput. Sci.*, 410(38-40):3616–3630, 2009. doi:10.1016/j.tcs.2009.04.008.
- 11 S. Mustapha. Non- D -finite walks in a three-quadrant cone. *Ann. Comb.*, 23(1):143–158, 2019. doi:10.1007/s00026-019-00413-2.
- 12 K. Raschel. Counting walks in a quadrant: a unified approach via boundary value problems. *J. Eur. Math. Soc. (JEMS)*, 14(3):749–777, 2012. doi:10.4171/JEMS/317.
- 13 K. Raschel and A. Trotignon. On walks avoiding a quadrant. *Electron. J. Combin.*, 26(3):Paper 3.31, 34, 2019. doi:10.37236/8019.
- 14 B. Salvy and P. Zimmermann. Gfun: a Maple package for the manipulation of generating and holonomic functions in one variable. *ACM Transactions on Mathematical Software*, 20(2):163–177, 1994. doi:10.1145/178365.178368.

A Final polynomial equation for $S(x)$ in the king model

The polynomial Pol involved in the cubic Equation (21) defining $S(x)$ is:

$$\begin{aligned}
& \text{Pol}(x_0, x_1, x_2, x_3, x_4, t, x) = \\
& - 3(x^2 + x + 1)^2(x^2t + 2xt + x + t)(3x^2t + 2xt - x + 3t) \mathbf{x}_0^3 \\
& + 3(x^2 + x + 1)(x^2t + 2xt + x + t)(3x^2t + 2xt - x + 3t)(3x_1x - 2x^2 - 1) \mathbf{x}_0^2 \\
& + [3x^2(x^2 + x + 1)^2(2x_4x_1 + x_4 - x_3) - 3x^2(t + 1)^2(x^2 + x + 1)^2x_2^2 \\
& + 6x(t + 1)(x^2 + x + 1)(x^4t + 2x^2t + x^2 + t)x_1x_2 \\
& + 3x(t + 1)(x^2 + x + 1)(x^4t - x^3t - x^3 + x^2t - xt - x + t)x_2 - 3(x^8t^2 + 2x^7t^2 \\
& + 10x^6t^2 + 20x^5t^2 + 4x^5t + 25x^4t^2 + 20x^3t^2 - 2x^4 + 4x^3t + 10x^2t^2 + 2xt^2 + t^2) x_1^2 \\
& - 3(x^8t^2 - 11x^7t^2 - x^7t - 32x^6t^2 - 9x^6t - 53x^5t^2 - 6x^5t - 55x^4t^2 + 3x^5 - 15x^4t \\
& - 39x^3t^2 - 6x^3t - 16x^2t^2 + x^3 - 5x^2t - 5xt^2 - xt + t^2) x_1 - 12x^8t^2 - 30x^7t^2 - 6x^7t \\
& - 51x^6t^2 - 60x^5t^2 + 3x^6 - 12x^5t - 54x^4t^2 - 36x^3t^2 + 3x^4 - 6x^3t - 21x^2t^2 - 6xt^2 \\
& - 3t^2] \mathbf{x}_0 + x^2(x^2 + x + 1) [(2x_3x^2 - 6x_4x - 2x_3)x_1^2 - (x^2 + 2)x_3 + 3x_4x^2 \\
& + (2x - 1)(3x_4x + x_3(x + 2))x_1] + 3x^3(t + 1)^2(x^2 + x + 1)(x_1 - x)x_2^2 \\
& - 3x^2(t + 1)x_2(x_1 - x)((2(x^2 + t(x^2 + 1)^2))x_1 + t(x^4 + x^2 + 1) - (t + 1)x(x^2 + 1)) \\
& + 3xt(x^2 + x + 1)^2(x_1 - x)(t(x^2 - x + 1)x_1^2 + (x^2t - 5xt - x + t)x_1 + t(x^2 - x + 1)).
\end{aligned}$$

COLOPHON

This document was typeset using the typographical look-and-feel classicthesis developed by André Miede and Ivo Pletikosić. The style was inspired by Robert Bringhurst's seminal book on typography "*The Elements of Typographic Style*". classicthesis is available for both L^AT_EX and L^YX:

<https://bitbucket.org/amiede/classicthesis/>

Happy users of classicthesis usually send a real postcard to the author, a collection of postcards received so far is featured here:

<http://postcards.miede.de/>

Thank you very much for your feedback and contribution.

Final Version as of March 8, 2022 (classicthesis).